國立臺灣大學生命科學院生化科學研究所
博士論文

Graduate Institute of Biochemical Sciences
College of Life Science
National Taiwan University
Doctoral Thesis

展以醣質為抗原之HIV-1疫苗：設計、合成、以及免疫評估

Design, Synthesis, and Immunological Evaluation of Carbohydrate-based Immunogens for Development of HIV-1 Vaccine

施沙晉
Sachin S. Shivatare

指導教授：翁啟惠博士 Dr. Chi-Huey Wong
吳宗益博士 Dr. Chung-Yi Wu

中華民國102年10月
October 2013

國立臺灣大學博士學位論文
口試委員會審定書

Design, Synthesis, and Immunological Evaluation of Carbohydrate-based Immunogens for Development of HIV-1 Vaccine

本論文係 Sachin S. Shivatare 君（D97B46019）在國立臺灣大學生化科學研究所完成之博士學位論文，於民國 102 年 10 月 29 日承下列考試委員審查通過及口試及格，特此證明。

口試委員：

_____（簽名）

（召集人）

_____ _____

_____ _____

_____ _____

_____ _____(指導教授)

Abstract

An HIV vaccine continues to be the best hope to end the HIV pandemics. The challenge of HIV vaccine development is to design the immunogens to induce the antibodies that can have broadly neutralizing activities. An effective mechanism that HIV uses to avoid attacks of neutralizing antibodies is to coat envelope gp120 with heterogeneous *N*-linked carbohydrate structures. Recently, a class of broadly neutralizing antibodies (bNAbs), isolated from HIV positive donors, was shown to be potent in neutralizing primary HIV-1 strains across clades by targeting the glycan dependent epitopes on gp120 surface, demonstrating the feasibility of inducing such antibodies. Understanding the molecular mechanism of the HIV-gp120 glycan coat recognition by bNAbs may guide effective immunogen design.

This thesis describes the efficient chemical and enzymatic syntheses of diverse HIV-1 gp120 related high-mannose, hybrid, and complex type *N*-glycans. A well defined library of natural and unnatural *N*-glycan structures was used to develop glycan microarray platform for profiling glycan binding specificities of HIV-1 bNAbs, PG9, PG16, PGTs 121, 128, and 141-145. With the next generation array on aluminium oxide-coated glass (ACG) slide, the critical low affinity antibody-carbohydrate interactions were detected. In addition, we showed that a few highly potent HIV-1 broadly neutralizing antibodies exhibit strong binding to closely spaced hetero-glycans on array surface, suggesting that this phenomenon might be an important adaptation of host immune system to deal with heterogeneously glycosylated HIV-1 spike.

The microarray studies of glycan binding specificities of HIV-1 bNAbs established a structural basis for designs of immunogens based on epitopes recognized by these antibodies. Finally, the immunological evaluation of carbohydrate-based immunogens was performed to investigate whether the synthetic glycoconjugates can induce broadly neutralizing antibodies that can cross react with HIV-gp120.

Keywords HIV-1 vaccine, *N*-linked oligosaccharides, carbohydrate-based immunogens, broadly neutralizing antibodies, glycoconjugates, carbohydrate synthesis.

發展以醣質爲抗原之 HIV-1 疫苗: 設計、合成、以及免疫評估

愛滋病是由於受到人類免疫缺陷病毒（HIV）的感染，導致後天性細胞免疫功能出現缺陷所造成的一種致命性疾病。發展出有效抗 HIV 疫苗，一直被認爲是最有希望控制全球愛滋病毒/愛滋病流行的一種方式。然而疫苗發展主要的挑戰在於如何設計出抗原結構，進而產生出廣泛性中和抗體，有效的殺滅病毒。愛滋病毒用於躲避抗體毒殺的主要機制，乃是以多種不同的 N 型鍵結寡醣來遮蔽其位於病毒表面的醣蛋白 gp120。最近的研究顯示 在愛滋病患體內分離出一種新類型的廣泛性中和抗體，能夠經由辨識醣蛋白 gp120 上的 N 型鍵結寡醣，進而對於 HIV-1 病毒株以及它的各種突變類型皆能有效的加以毒殺。此結果揭示利用特殊結構的寡醣分子作爲疫苗抗原，來產生廣泛性中和抗體治療愛滋病的可行性。若能深入了解抗體與 N 型鍵結寡醣間的辨識機制，將有助於設計出最有效的疫苗抗原。

本論文描述利用化學以及酵素的合成方式，來合成各種與醣蛋白 gp120 相關的 N 型鍵結寡醣結構，包括各種高甘露醣型、混合型、以及複雜型的 N 型鍵結寡醣。這些 N 型鍵結寡醣分子將用於建立醣分子庫，並結合醣晶片的技術，來剖析這些醣分子與各種已知抗 HIV-1 廣泛性中和抗體 (PG9, PG16, PGTs 121, 128, 141-145)間的結合專一性。此研究發現利用氧化鋁包覆玻片的醣晶片的技術，可以偵測到抗體與醣分子間微弱但非常重要的結合作用力。分析結果顯示，有些高效價的抗 HIV-1 廣泛性中和抗體，對於非均質的醣分子混合體 (包含兩種醣分子以不同比例混合)的結合力較對於均質的醣分子更強。這種現象可能是爲了因應病毒表面醣蛋白非均質化的醣化情形，宿主人類的免疫系統所採取的對應手段。

經由以上醣晶片研究結果，提供了設計疫苗所需醣抗原分子的基本結構，依照這些基本結構可用來設計與合成疫苗所需的醣共軛體，繼而用以進行免疫學上的研究，觀察此疫苗是否能誘導產生廣泛性中和抗體，以及抗體是否能與各種 HIV 病毒上的醣蛋白 gp120 作結合，進而消滅病毒。

關鍵詞: HIV-1 疫苗，N 型鍵結寡醣，以醣質爲基礎的疫苗抗原，廣泛性中和抗體，醣共軛體，醣合成。

Dedication

To my wonderful mother, and all family members, with love, and gratitude for all their support, and my teachers who have inspired me, and always been encouraging in everything I have undertaken.

I dedicate this thesis in memory of my father,

Mr. Shankar D. Shivatare

Acknowledgements

This thesis documents my serendipitous journey into the field of synthetic carbohydrate chemistry. There are many who deserve to be acknowledged and I apologize in advance to those I neglect to mention on this page.

Foremost, I would like to express my upmost gratitude to my mentor Prof. Wong, Chi-Huey for giving me an opportunity to work on the very challenging HIV-1 vaccine project and also for his constant support, patience, motivation and immense knowledge. I would also like to thank my co-advisor Prof. Wu, Chung-Yi for his supervision and continuous guidance in every aspect of my PhD life. I could not have imagined better advisors for my PhD study.

I would also like to extend my deepest appreciation to the members of my supervisory committee, Dr. Hung Shang-Cheng, Dr. Lin Chun-Hung, and Dr. Wu Shih-Hsuing for all their support, patience and helpful suggestions. My special thanks to Chemical Biology division of Taiwan International Graduate Program and Genomic Research Center, Academia Sinica for providing graduate research scholarship throughout my PhD study.

Along the way, I met a number of extraordinary people in Dr. Wong's laboratory. I had the pleasure to work in collaboration with several of them, including Cheng Yang-Yu, Chang Shi-Huang, Tsai Tsung-I, Liang Chi-Hui, Cheng Ting-Jen, and Ren Chein-Tai. My sincere thanks also go to Mrs. Huang Yi-Ping for her assistance in NMR analysis and Mass spectrometry group at Genomic Research Center. Many thanks to Mrs. Jennifer Chu for investing her valuable time in critically reading my thesis.

Finally, I would like to express my sincere gratitude to all my family members, who made it possible for me to be here and achieve so much, and my in-laws for their support and encouragement during the last few years, my teacher Mrs. Anita Gokule for always motivating me, my friend Fang Yu-Ting for valuable help, and my wonderful wife and daughter without them much of this endeavor would have been meaningless.

"In my view, all that is necessary for faith is the belief that by doing our best we shall come nearer to success and that success in our aims (the improvement of the lot of mankind, present and future) is worth attaining."

Dr. Rosalind Franklin

(Letter to her father Ellis Franklin, 1940)

List of Abbreviation

Abs	Antibodies
Ac	Acetyl
Ac_2O	Acetic anhydride
ACG	Aluminium oxide coated glass slide
Al	Allyl
Asn	Aspargine
ACN	Acetonitrile
Bn	Benzyl
Bu	Butyl
bNAbs	Broadly neutralizing antibodies
Calc	Calculated
DBU	1,8-Diazabicyclo-undec-7-ene
DDQ	2,3-Dichloro-5,6-dicyno-1,4-benzoquinone
DDT	Dithiothreitol
DMAP	4-(Dimethylamino) pyridine
DMF	*N*,*N*-Dimethylformamide
CH_2Cl_2	Dichloromethane
DTBP	2,6-Di-t-butyl pyridine
ER	Eandoplasmic retuculam
ESI	Electron spray ionization mass spectrometry
EtOAc	Ethyl acetate
EtOH	Ethanol
Eqiv	Equivalents
Fuc	L-Fucose
Gal	D-Galactose
GlcNAc	*N*-Acetyl-D-Glucosamine
GnT	GlcNAc transferases
Glc	D-Glucose
h	Hour (s)
Cp_2HfCl_2	Hafnocene dichloride
HPLC	High performance liquid chromatography
HRMS	High resolution mass spectrometry
HSQC	Heteronuclear single quantum coherence spectroscopy
Hz	Hertz

HIV	Human Immunodefficiency virus
IgG	Immunoglobulin G
IgM	Immunoglobulin M
Lev	Levulinoyl
LCMS	Liquid chromatography and mass spectrometry
m/z	Mass to charge ratio
mmol	Millimole
MeOH	Methanol
PMB	*p*-Methoxy Benzyl
PMP	*p*-Methoxy phenol
STol	p-tolylthiol
SiaT	Sialiyltransferases
Man	Mannose
Min	Minute(s)
MS	Molecular sieves
NMR	Nuclear magnetic resonance
N-	Aspargine linked glycans
NIS	N-Iodosuccinimide
Obsd	Observed
Ph	Phenyl
NPhth	N-Phthaloyl
ppm	Parts per million
s	Second(s)
TBAF	Tetra-n-butylammonium fluoride
TBSCl	tert-Butyldimethylsilyl chloride
TfOH	Trifluoromethanesulfonic acid
TMSOTf	Trimethylsilyl trifluoromethanesulfonate
AgOTf	Silver trifluoromethanesulfonate
TFA	Trifluoroacetic acid
TFAA	Trifluoroacetic anhydride
THF	Tetrahydrofuran
TLC	Thin layer chromatography
TMS	Trimethylsilyl

Table of Contents

Chapter 1

Introduction and Background

1.1. Introduction:

Carbohydrates, responsible for supplying energy to body, are one of the three important components of the human diet alongside fats and proteins. The roots of carbohydrate chemistry can be traced back over a century, to the emerging phase of modern organic chemistry and the pioneering days of Emil Fischer. In current era, it is widely accepted that carbohydrates are among the most structurally diverse and complex biopolymers and play numerous biological functions in living organisms. Carbohydrates are fundamental constituents of every cell surface, where they are involved in vital cellular processes such as cell-cell interactions and adhesion[1], cell signaling[2], cell differentiation[3], immune responses[4], and inflammation[5]. Besides their role in metabolism and as structural building blocks, carbohydrates, in form of oligosaccharides and glycoconjugates, are implicated in viral-host interactions[6], bacterial pathogenecity[7], and signal transduction[8]. "*Glycobiology*", a newly defined concept, devotes entirely to study the structures, biosynthesis and biology of glycans that are widely distributed in nature. Following in the footsteps of genomic and proteomics,"*glycomics*" is poised to join the informatics age of biological study.

Because of their notable occurrence on invasive pathogens[9] and malignant cells[10], carbohydrates are being adopted for use in vaccine design against human pathogens and cancers. Currently, various kinds of carbohydrate-based vaccines against pathogenic bacteria are commercially available while several clinical trials of promising vaccine candidates against human infectious diseases and different types of cancers are underway[11]. *"Glycomimetics",* close structural mimics of naturally occurring carbohydrates are being pursued in an attempt to inhibit the interaction between carbohydrates and glycan-binding proteins in some disease states[10].

The structural diversity and complexity that makes carbohydrates important in various biological processes renders their chemical synthesis difficult. With growing appreciation for glycobiology, there is an increased demand for access to pure and well defined material

for study. Though it is possible to synthesize pure oligosaccharides in the laboratory, the regioselective protection of hydroxyl groups and the stereoselective assembly of glycosidic bonds present perhaps the greatest hurdles for synthetic chemists. Unlike synthesis of proteins and nucleic acids, carbohydrate research is limited by a lack of widely available automated synthesis techniques, sequencing, or technologies analogous to cDNA microarray and siRNA gene silencing. Therefore, the new methodologies/techniques that make oligosaccharide synthesis both faster and less labor intensive is therefore most welcome.

1.2. Glycosylation in Biological Systems:

The post-translational protein glycosylation is acknowledged as one of the important modifications, with significant effect on protein folding[12], conformation[13], distribution[14], stability and activity[15]. In general, there are three important classes of glycosyl modifications of polypeptide backbones: *N*-linked glycosylation at aspargine residue found in Asp-X-Ser/Thr recognition sequence; O-linked glycosylation of serine or threonine residues; and glycosylphosphatidyl inositol (GPI) couplings of carboxy-terminus[16]. Glycosylation encompasses a diverse selection of sugar-moiety additions that ranges from simple monosaccharide units to highly complex branched polysaccharide to a variety of proteins such as secreted proteins, membrane proteins, and proteins targeted to vesicles or certain intracellular organelles. In mammalian cells *N*-linked proteins contained standard branched structures, which are composed of mannose (Man), galactose, *N*-acetylglucosamine (GlcNAc) and neuramic acids. However, O-linked glycoproteins are composed of various numbers of sugars including galactose, *N*-acetylglucosamine, N-acetylgalactosamine, Fucose, and neuramic acids. The nature of *N*-linked glycosylation in insect cells depends on the protein expression systems and the host cell line, which is generally of the high-mannose type[17]. The O-linked glycosylation is similar, although not identical, to mammalian cells, depending on localization and types of protein[18].

1.3. Glycans and Pathogenic Infections:

Easily accessible carbohydrates on surface of mammalian cells represent enticing binding opportunities to wide range of pathogens including molecular toxins to viruses and from primitive bacteria to sophisticated eukaryotic parasites. Some of representative examples are:

1. Ricin, a versatile and durable toxin consists of two peptide chains cross-linked by disulfide bond. One of the protein chains is lectin, which recognizes terminal galactose residues on cell surface glycans and recruits other peptide chain into the lumen of secretary vesicle, which upon translocation into cytosol can kill host cell via catalytic deactivation of ribosome[19].
2. The infection of influenza virus is initiated by attachment of virus to cell-surface sialoside receptors via influenza surface glycoproteins, hemagglutinin (HA) with remarkable discrimination by distinguishing between α-2,3-lniked and α-2,6-linked sialosides as well as deliberately avoiding Neu5Gc form of the sialic acid in preference to Neu5Ac[20].
3. The adherence of *Escherichia coli* to the epithelial cells of gastrointestinal or urinary track mediated by bacterial lectins, which preferentially bind to cell surface mannose containing glycoproteins[21].

1.4. Glycan Biosynthesis Pathway in Secretary System:

Carbohydrates play important roles in many physiological and pathological cellular functions because of their structural diversity and ubiquitous nature. The mystery of structure-function relationship fueled a considerable interest for glycobiologists to study glycan biosynthesis pathways. In contrast to nucleic acids and proteins, the structures of carbohydrate are not template based; moreover, the glycan assembly and modifications take place across several sub-cellular compartments, rendering the glycan biosynthesis a substantial challenge to solve[22].

The N-linked glycosylation takes place in endoplasmic reticulum (ER), where oligosaccharyl transferases (OST) catalyses transfer *N*-linked glycan precursor ($Glc_3Man_9GlcNAc_2$) from a dolichylpyrophosphate carrier to Asn-X-Ser/Thr sequons on polypeptide backbone (Fig. 1.1). After removal of two glucose units by ER resident

glucosidase I, the monoglucosylated glycan ($GlcMan_9GlcNAc_2$) binds to calnexin/calreticulin and promotes the glycoprotein folding[23]. Hydrolysis of final glucose-mannose bond by glucosidase II frees glycoprotein with $Man_9GlcNAc_2$ from calnexin to exit from ER and enter into Golgi, where glycoprotein undergoes further processing to acquire complex architecture. Glycoproteins after prolonged residence in ER get trimmed by ER α-1,2-mannosidase to form $Man_8GlcNAc_2$. As the glycoprotein transported from ER to Golgi, the glycan moieties get trimmed further by mannosidase to form $Man_5GlcNAc_2$, a substrate for various Golgi resident cellular enzymes. N-acetyl glucosamine transferase (GnT) catalyses the transfers of GlcNAc to the D1 arm of $Man_5GlcNAc_2$ substrate, converting it to a hybrid type glycan[24]. This hybrid glycoform is then a substrate for modification into complex glycans, in which the D2 and D3 arm mannoses are cleaved, allowing addition of GlcNAc moieties by a series of GnT family enzymes to form complex type *N*-glycans[25].

1.5. Glycobiology of HIV:

Human immunodeficiency virus (HIV-1) is the causative agent of acquired immune deficiency syndrome (AIDS) belongs to lentivirus family. HIV is mainly transmitted through blood, sexual contact and from mother-to-infant. HIV attacks the immunes system by targeting CD4 positive T-cells, the destruction of which leaves HIV infected patient vulnerable for other infections or diseases.

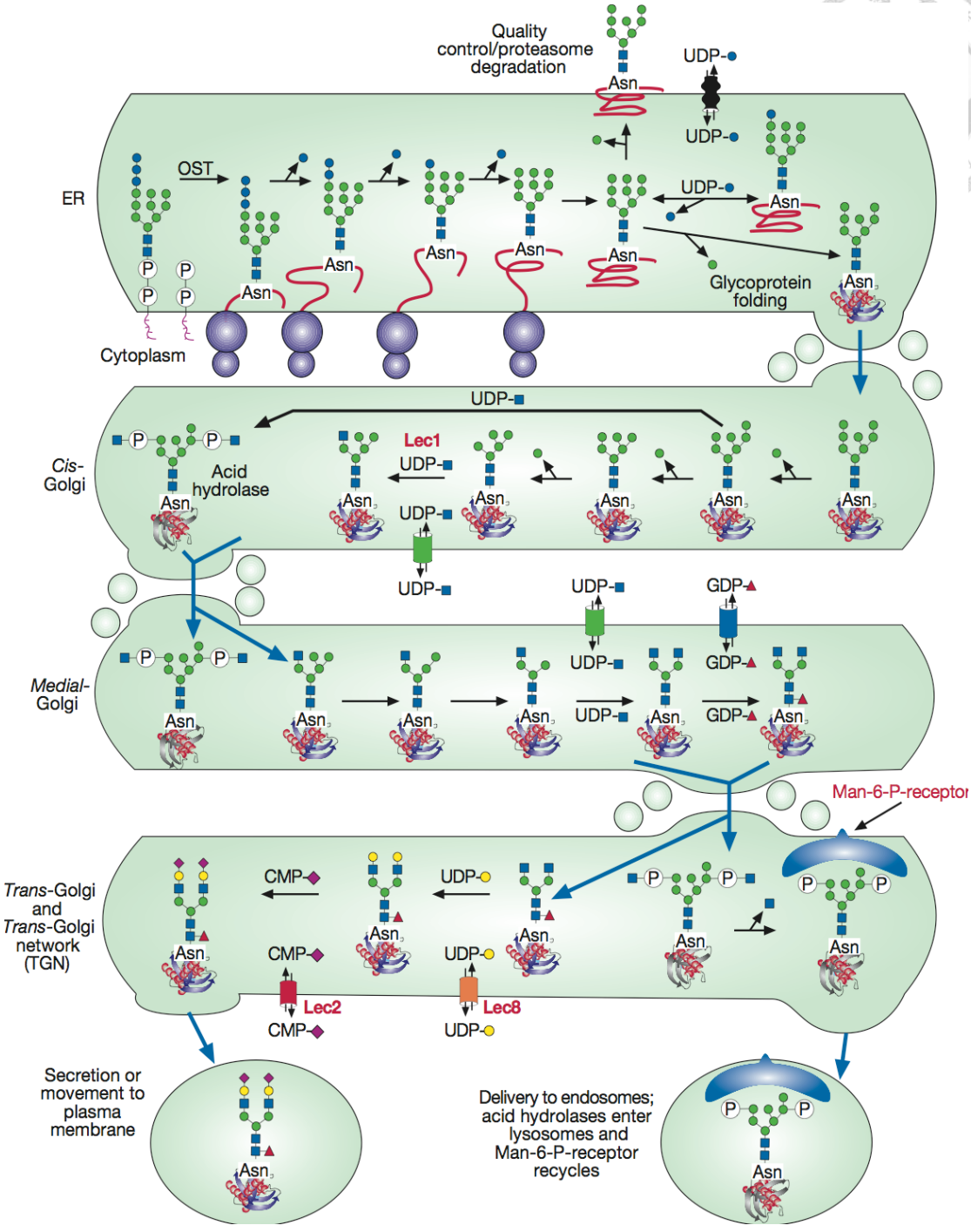

Figure 1.1. Processing and maturation of *N*-glycans in sub-cellular compartments (Adapted from Essentials of Glycobiology- Chapter 8).

1.5.1. Structure of HIV-1 Particle:

HIV particle is spherical in shape and has a diameter of 120 nm (Fig. 1.2). The outer coat, which also known as viral envelop is composed of two layers of lipid chains derived from membrane of host cell when new virus buds from host cells. Within the viral envelop, there is bullet shaped core or capsid which consists of 2000 copies of viral proteins[26]. HIV has three structural genes called gag, pol, and env that contains information required to make structural proteins to form new virus particle.

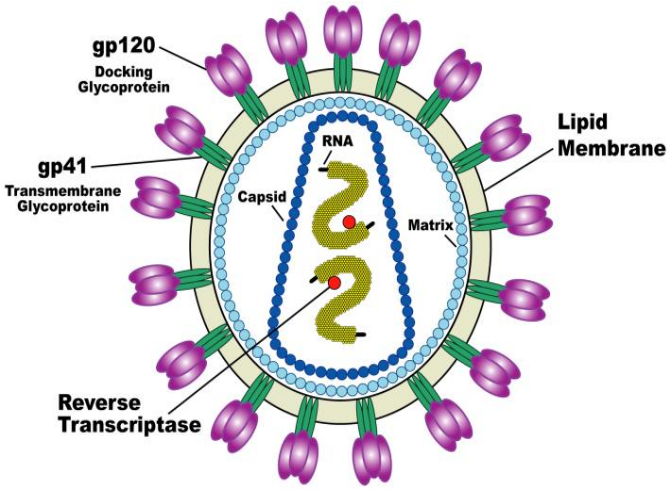

Figure 1.2. Structure of HIV-1 particle (Adapted from www.niaid.nih.gov).

The envelope gene that code for protein called gp160 that is cleaved by a cellular protease, furin in endoplasmic reticulum, to form gp120 and gp41[27]. The gp120 anchored to viral membrane or envelope via non-covalent bond with transmembrane glycoprotein, gp41 (Fig. 1.2). Three gp120s and gp40s combine in a trimer of heterodimers to form the HIV-1 spike, which is responsible for attachment of virus to cell surface CD4 receptor to facilitate its entry into the host cell.

1.5.2. Gycoprotein-120 Mediated HIV-1 Entry into Host Cell:

The first phase of HIV-1 replication cycle begins with attachment of virion to cell surface receptors. HIV binds to CD4 antigens on cells such as T helper lymphocytes or macrophages via envelope glycoprotein, gp120[28]. The interactions of gp120 with CD4 receptors cause conformational rearrangements in V1/V2 and, subsequently, V3 loop of gp120, which allows binding of co-receptors, CCR5 or CXCR4. Recruitment of co-

receptors in stabilizing the gp120-CD4 interactions causes the structural changes in gp41, exposing the hydrophobic region that embeds in the membrane of host cell (Fig. 1.3). Thus, fusion of virus membrane with host cell was initiated, allowing the nucleocapsid to enter into the cytoplasm[29].

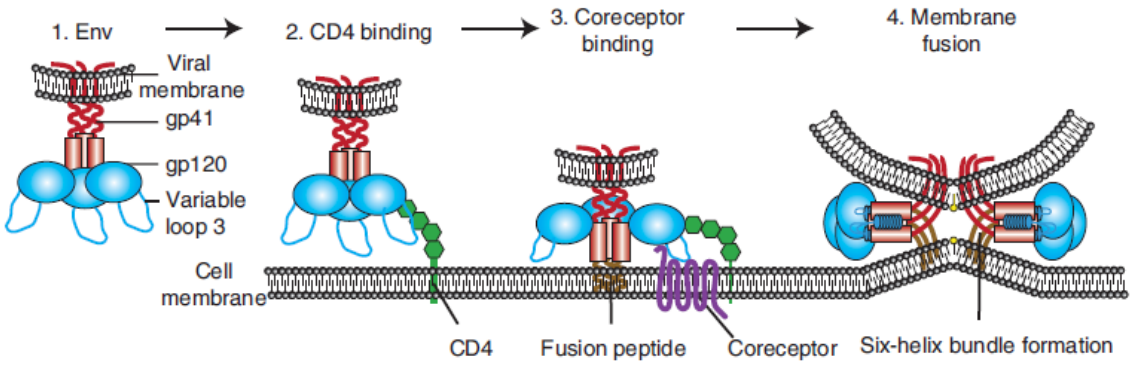

Figure 1.3. Overview of HIV-1 entry

(Adapted from Wilen et al. Perspectives in Medicine).

1.5.3. N-linked Glycosylated gp120 as a Vaccine Target:

Since envelope glycoprotein gp120 is an important part of HIV-1 spike and, thus, a major target of broadly neutralizing antibodies, its evolution is of particular interest. The *N*-linked glycosylation process, which is required for proper folding and conformational stability of gp120, mainly involves attachment of oligosaccharide building units on polypeptide backbone[30]. The process of *N*-linked glycosylation of HIV-1 envelope gp120 and gp41 glycoproteins results in diverse carbohydrate structures, masking the underlying protein domain and, thus, forming a "glycan shield" that can evade immune recognition[31]. The outer envelope glycoprotein gp120 contains 24 glycosylation sites; 13 of those are linked to complex type *N*-glycans, and 11 are occupied by *N*-glycans of high-mannose or hybrid types[32], which in fact account for half of the mass of gp120 (Fig. 1.4).

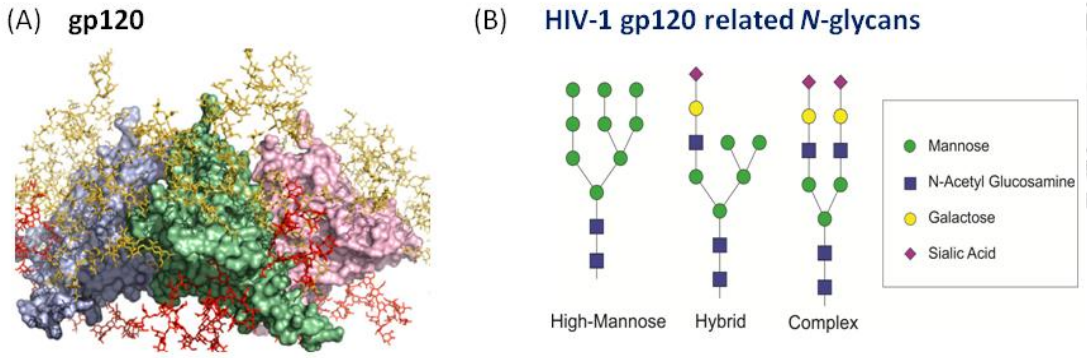

Figure 1.4. (A) Heterogeneously glycosylated envelope glycoprotein, gp120. (B) Schematic representation of diverse *N*-linked oligosaccharides.

N-linked glycans present on gp120 surface are critical for HIV-1 infectivity. In fact, inhibition of *N*-linked glycosylation or enzymatic de-glycosylation has proven to abolish viral infectivity[31]. The prevalence of gp120 on surface of HIV-1 spike renders it an important target of humoral immune response[33]. Furthermore, glycans on gp120 are crucial for virus to escape from immune system recognition. The variability of HIV virus imparted by genome mutation, recombination and glycan reordering could be considered as an important mechanism for virus to stay one step ahead of immune system. These unique features offered by gp120 to HIV, making it a primary target for development of HIV-1 vaccine.

1.6. HIV-1 gp120 and Broadly Neutralizing Antibodies:

Immune response to polypeptide backbones of gp120 in infected individuals does not particularly observed due to extensive coating of conserved peptide epitope by heterogeneous carbohydrate mixtures[34]. Therefore, design of HIV-1 vaccine based on the carbohydrate epitope of gp120 becomes an attractive choice. However, carbohydrate based HIV-1 vaccines face two important issues; first, the glycan exposed on gp120 surface are immunologically self molecules; second, extraordinarily high degree of HIV-1 structural diversity originates from the combination of variable viral genome and micro-heterogeneity of *N*-glycans.

In spite of strategic wrapping of HIV-1 spike by carbohydrates, some HIV-1 infected patients developed broadly neutralizing antibodies (bNAbs) over a period of time.

Recently, a series of bNAbs (2G12, b12, VRCO1, PG9, PG16, and PGT series antibodies) isolated from a pool of B cells of infected individuals were shown to neutralize a wide range of HIV-1 strains in animal models by binding on conserved epitopes on gp120 surface (Fig. 1.5). Some of these glycan binding neutralizing antibodies are:

i. Antibodies 2G12 and recently isolated PGTs 127/128 were shown to bind clusters of oligomannose type glycans (Man_9/$Man_8GlcNAc_2$) as well as a short peptide strand in V3/V4 loop. These results were further supported by various biochemical, glycan array, structural and modeling studies;

ii. Two somatically related antibodies, PG9 and PG16, that neutralize 70-80% of HIV isolates were shown to bind glycosylated epitope in the V1/V2 domain of HIV-1 gp120. Particularly, Peter Kwong et al. reported that antibody PG9 prefers $Man_5GlcNAc2$ at N160 in combination with another glycan either at N156 or N167 and a peptide loop at edge of the sheet[36].

iii. PGTs 141-145 exhibited a strong preference for membrane-bound, trimeric HIV envelop.

iv. Antibody PGT121, a member of neutralizing antibody family, was shown to recognize bi-antennary complex type glycan in V3 loop of gp120[37].

Occurrence of HIV-1 gp120 glycan binding antibodies in sera of HIV infected patients and the neutralization potency exhibited by these bNAbs suggest that these antibodies may provide protection at low serum concentration; therefore, the epitopes recognized by these antibodies are very likely to be good vaccine targets.

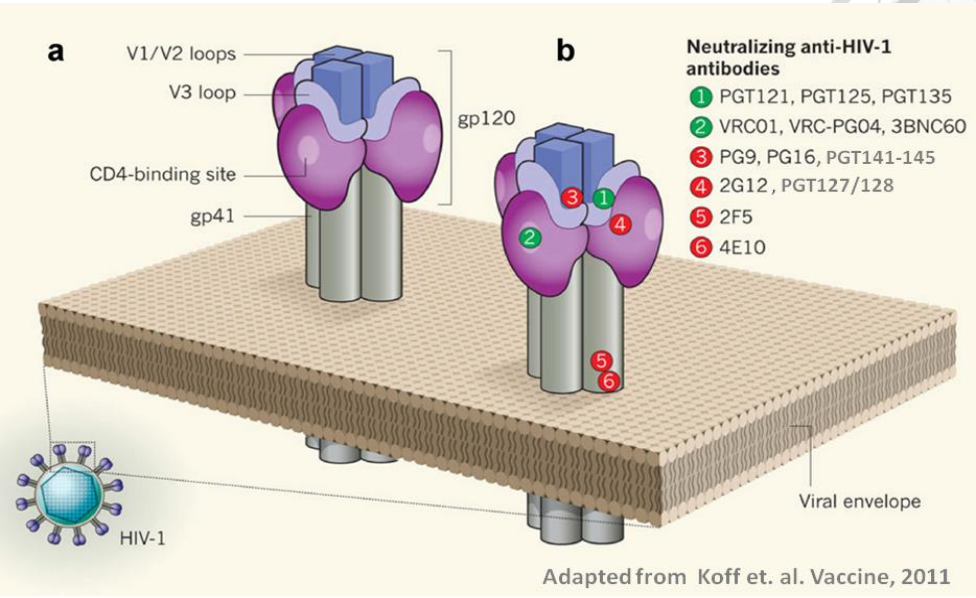

Figure 1.5. The composition of HIV-1 spike (a) Each spike consists of three molecules of surface glycoprotein gp120 and three molecules of transmembrane protein gp41. (b) Highly potent and broadly neutralizing antibodies isolated from HIV-1 infected donors and their binding sites on gp120 surface.

1.7. Carbohydrate Based HIV Vaccines:

In spite of extensive efforts in past two decades, an effective HIV-1 vaccine that can induce broadly neutralizing antibodies is still not on the horizon. The effective mechanisms that HIV uses to escape from host immune response is to coat surface envelope glycoprotein, gp120, with diverse carbohydrate structures, which appears to be a greatest challenge in HIV vaccine development. Furthermore, frequent sequence mutations of neutralizing epitope poses a major hurdle in conventional protein/peptide based vaccine approaches. However, carbohydrate portion of gp120 accounts for half of its molecular mass and could serve as an attractive target for vaccine development.

1.7.1. Oligomannose-Based Vaccines to Mimic 2G12 Epitope:

In the last decade, the characterization of glycan dependent epitopes of some broadly neutralizing antibodies, such as human monoclonal antibody 2G12, provided important clues on rational immunogen design. Several published studies suggested that the epitope

of 2G12 consists of unique oligomannose type oligosaccharides at the glycosylation sites N295, N332 and N339 in V3 loop on gp120 surface. Mutational, biochemical, and structural studies of antibody–antigen complexes revealed that the epitope of 2G12 is mannose dependent with excellent specificity for terminal Man-α-(1-2)-Man moieties of oligomannose type *N*-glycans. In addition, 2G12 exhibits an unusual swapped VH domain structure to generate a multivalent antigen binding surface, which is unique to the bivalent interactions of typical immunoglobulins. These studies on the specificity of 2G12 have provided direction towards the immunogen design, which was mainly based on mimicking the 2G12 epitope, the oligomannose cluster, with an ultimate goal to elicit "2G12-like" antibodies. The representative examples of such studies are;

1. Prof. Danishfesky and coworkers reported the synthesis of $Man_9GlcNAc_2$-based HIV-1 2G12 mimotope. They coupled one to three copies of Man_9 to cyclic peptide scaffold (Fig.1.6a), which was further attached covalently to a powerful immune-stimulating protein carrier, called outer membrane protein complex (OMPC). The immunological evaluation of the glycoconjugate in two animal species revealed that the glycoconjugate can induce high level of carbohydrate specific antibodies; however, these antibodies showed poor recognition of recombinant gp160 and failed to neutralize a panel of viral isolates[38].
2. Prof. Wang Lai-Xi's group demonstrated the synthesis of oligommannose-containing glycoconjugates that contain either a carrier protein (KLH) or a universal T-helper epitope peptide to provide an effective immunogen (Fig.1.6b). Rabbit immunization studies suggest that a very small fraction of antibodies elicited by glycoconjugate was directed towards the carbohydrates, with majority of the IgG type antibodies being directed to the linkers. The anti-sera exhibited very weak cross-reactivity to HIV-1 gp120[39].
3. Recent examples of new immunogens design include the coupling of oligomannose ligands such as Man_4, Man_5, Man_7, Man_8, Man_9 and unnatural Man_4 analogues to various carriers, namely, bacteriophage Qβ[40], bovine serum albumin and dendrimers.

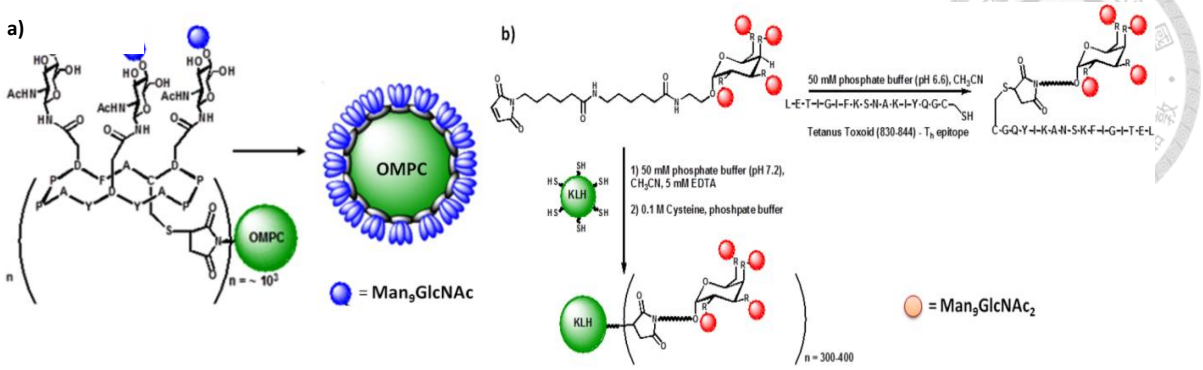

Figure 1.6. Schematic depictions of designed glycoconjugate vaccines. a) Conjugation of trivalent $Man_9GlcNAc_2$ to cyclic peptide scaffold to create multivalency. b) Structures of galactose-based oligomannose clusters conjugates to either KLH or T-helper peptide.

Although the antibody 2G12 isolated from HIV carriers was shown to recognize the oligomannose epitope on the gp120 that lies around C4-V4 region and capable of neutralizing about 30% of the 2000 variants isolated to date, the carbohydrate-specific antibodies induced by the oligomannose-based HIV-1 vaccine (Fig.1.6), unfortunately, fail to neutralize HIV-1 virions, despite the presence of clusters of high-mannose glycans in gp120. One possible reason of this failure is that the synthetic epitope-mimetics did not represent the true 2G12 epitope. In spite of their failure in achieving exact mimicry of gp120 surface, most of the reported studies towards future attempts to improve immunogens design.

1.8. The Chemical Synthesis of *N*-linked Oligosaccharides:

The difficulty associated with isolation of pure carbohydrates or glycoconjugates from natural sources in significant quantity poses a great challenge to produce the material for biological study. The structural diversity, ring size, different anomeric stereochemistry, and existence of branched-architecture contributed to the amazing complexity of carbohydrates. Careful selection of protecting groups to tune reactivity of building blocks, achieving selectivity at anomeric centers, and proper employment of promoter/activator (s) are among the key elements in synthesis of complex oligosaccharides. Chemical and enzymatic

syntheses offer rapid preparation methods for oligosaccharides and neoglycoconjugates[41]. Moreover, chemical synthesis is a reliable way to permit access to the natural and unnatural oligosaccharides in homogeneous form free from unwanted glycoforms.

1.8.1. Isolation of *N*-Glycans From Natural Sources:

N-linked oligosaccharides are covalently bound to side chain nitrogen of asparagines (Asn) residues, which plays important roles in processes such as protein folding, targeting, antigenicity, and lectin interactions with defects leading to cellular dysfunctions[42]. All *N*-glycans share a common core pentasaccharide sugar sequence, Manα1–6(Manα1–3)Manβ1–4GlcNAcβ1–4GlcNAcβ1-Asn-X-Ser/Thr (Scheme 1.1). Depending on modifications, *N*-glycans are divided into three types, namely high mannose, hybrid and complex type (Fig.1.4b). One of the routinely used methods to obtain *N*-glycans from natural sources is to release glycans chemically or enzymatically from glycoprotein of glycolipids followed by introduction of fluorescent tag by reductive amination for HPLC separation and mass spectrometry analysis. However, the major limitations of this process are: a) Introduction of fluorescent tag using reductive amination at reducing end can destroy the native glycan structure and affect its biology; b) this method is not able to provide access to unnatural form of *N*-linked oligosaccharides.

1.8.2. Chemical Methods for Construction of Library of *N*-linked Oligosaccharides:

The chemical synthesis of *N*-linked oligosaccharides has received considerable recognition in recent years because of their growing demand in field of glycobiology. In spite of extensive pioneering work by Ogawa[43] and Paulsen[44] and further developments into modular strategies by Danishefsky[45] and Unverzagt[46], the construction of a library of synthetic *N*-glycans remains a serious challenge. Based on modular approaches, a variety of *N*-glycan core structures have been chemically synthesized and were enzymatically diversified using various glycosyl transferases[41]. Recently, Boons and coworkers developed a general strategy to chemoenzymatically synthesize a library of unsymmetrical multi-antennary *N*-glycans[41]. The key point in the construction of *N*-glycans is to get access to the core trisaccharide, a chitobiose building unit, consisting of reducing end di-GlcNAc linked

to mannose residue by β-1,4 linkage (Scheme 1.1). The presence of amino alkyl linker at reducing end preserves the native glycans structure and also acts as handle for covalent attachment to a N-hydroxysuccinimide activated glass slide for microarray analysis and to carrier protein in vaccine development.

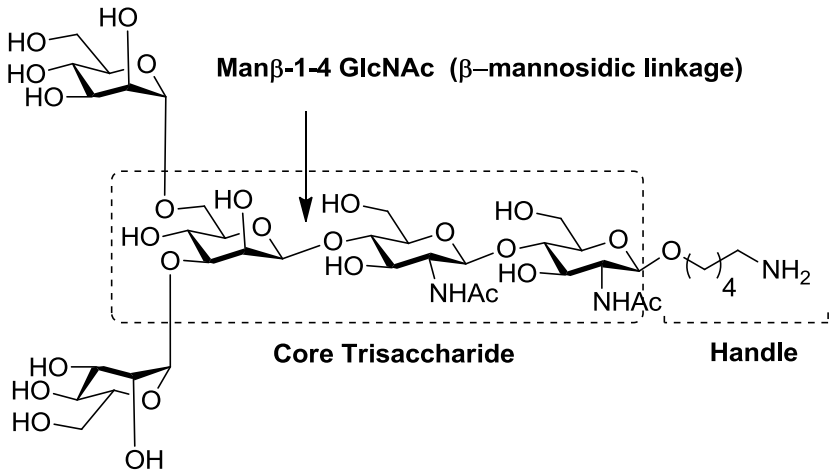

Scheme 1.1. Chemical structure of core pentasaccharide common in all *N*-glycans.

1.8.3. *β*-Mannosylation in Synthesis of Core Trisaccharide:

The *β*-mannoside is ubiquitous in N-linked glycosylation, as it serves as the branching point for core pentasaccharide of *N*-glycans (Scheme 1.1). The biological significance of this structure creates a strong reason for development of effective chemical synthesis methodology. Several methodologies including the pioneering work of David Crich and coworkers[47] have been developed over the years. Some of the few routinely used methods (Schene 1.2) include:

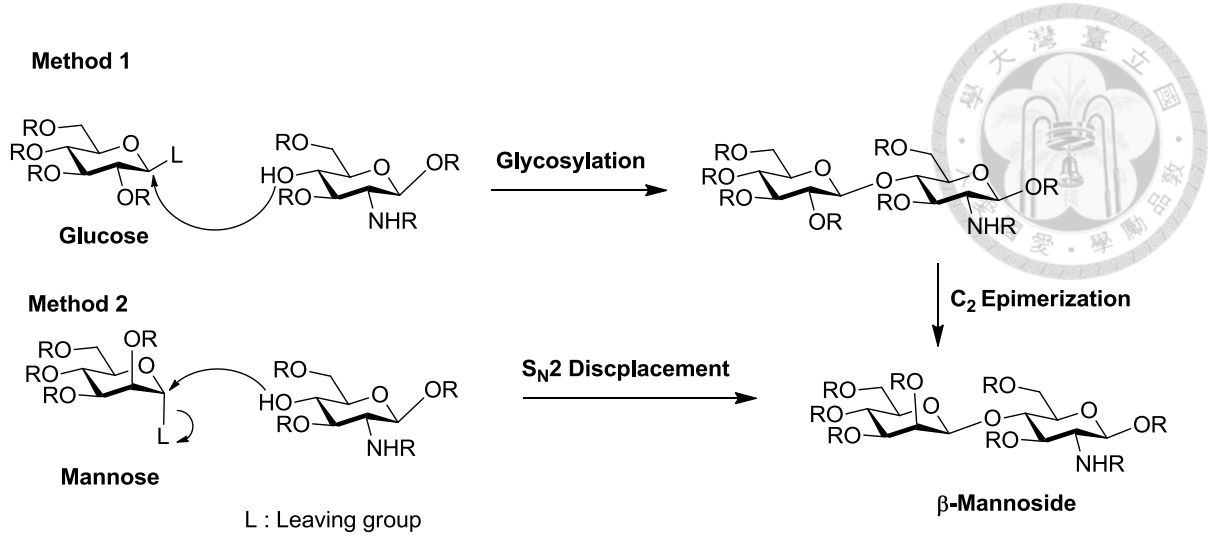

Scheme 1.2. Methods of *β*-mannosylations. Method 1: epimerization of *β*-glucoside to form *β* -mannoside. Method 2: S_N2 displacement of axial leaving group to furnish *β* -mannoside

I. The strategy that uses glucoside to achieve *β*-1,4 linked Man-GlcNAc disaccharide followed by C_2 epimerization to obtained desired *β*-mannoside has been routinely used.

II. Alternatively, the direct S_N2 displacement of anomeric leaving group via in situ generation of anomeric triflate to afford desired *β* -mannoside was developed by David Crich and colleagues.

Ito's group developed a strategy of *p*-methoxybenzyledene-assisted *β*-mannosylation via intramolecular aglycon delivery[58] (Scheme 1.3)

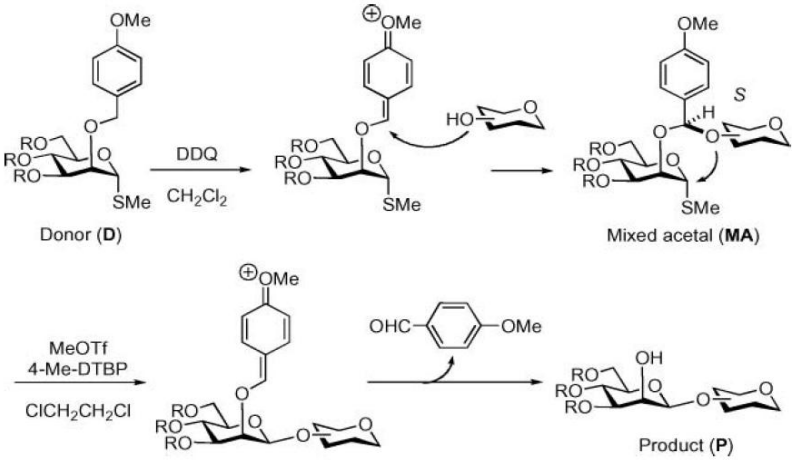

Scheme 1.3. Intramolecular aglycon delivery through 4-methoxy benzyledene-tethered intermediates for desired *β*-mannoside.

1.9. Carbohydrate Microarray: A powerful Tool in Glycobiology:

The invent of glycan microarray offered a new high throughput technology to explore specificity of diverse range of glycan-binding proteins, viruses, bacterial adhesions and toxins, anticarbohydrate antibodies and plant lectins[48]. The systematic glycans arrangement in arrayed chip-based format, aimed at probing problematic low affinity protein-glycan interactions through multivalent presentation, conveniently appear to be an effective mimic of cell-cell interfaces[49]. Various forms of "arrays" have been developed over the years. In 2002, Feizi and coworkers[50] introduced an array of neoglycolipd-based oligosaccharides immobilized noncovalently on nitrocellulose. In the same year, Denong Wang[51] at Columbia University reported an array of underivitized microbial polysaccharides and glycoconjugates efficiently produced on nitrocellulose oxidized polystyrene surface through mixed hydrophobic and hydrophilic interactions. Then, the array of synthetic oligosaccharides in microtiter plate was first introduced by our group in 2002[52]. Thereafter, several research groups including Cummings'[53], Paulson's[49], Blixt's[54] and Gildersleeve's[55] contributed to the field by developing various glycan immobilization strategies. As a result, Consortium of Functional Glycomics (CFG) hold a comprehensive set of more than 600 oligosaccharide covalently attached to N-hydroxysuccinimide and epoxy derivatized glass surface through a variety of linkers or spacers with terminal primary amine group in one spot one glycan manner.

From HIV-1 vaccine perspective, the array of gp120 related N-glycan structures is an invaluable tool for identifying relevant glycan targets of carbohydrate specific antibodies elicited during natural infection. However, the key bottleneck in vaccine research is the access to complex carbohydrate antigens, because the synthetic strategies to obtain these ligands generally require several steps and complicated purification procedures.

1.10. Dissertation Objective:

The Wong laboratory is devoted to advancing the field of glycobiology through development of new chemical and enzymatic strategies and methods for the synthesis of complex carbohydrates and glycoconjugates. Progress towards the goal has been made with development of hemagglutinin-based vaccine against influenza[56], carbohydrate-based vaccine against cancer[57] and oligomannose-based HIV-1 vaccine. In this tradition, this dissertation aims to develop a unified chemical and enzymatic strategy for rapid production of diverse high-mannose, hybrid and complex type *N*-linked oligosaccharides. In addition, the prime goal is to utilize carbohydrate microarray as a platform to investigate the glycan binding specificities of HIV-1 broadly neutralizing antibodies isolated from HIV infected patients and to design carbohydrate-based immunogens for eliciting broad and potent neutralizing antibodies.

Chapters 2 and 3 detail convergent routes for constructing a library of diverse *N*-glycans. This study includes both chemical and enzymatic synthesis, while achieving the desired stereo- and regiospecificity in dealing with branched architecture. Chapter 4 follows the development of high density carbohydrate microarray based on aluminium oxide coated glass slide (ACG) to investigate critical low affinity carbohydrate-antibody interactions. We exploited the newly developed ACG based array to study the heteroglycans binding specificity of several HIV-1 broadly neutralizing antibodies such as PG9, PG16, PGT 121, 128, 130, 141-145. Based on the results of microarray analysis, chapter 5 describes the design and synthesis of carbohydrate based antigens and their immunological evaluation.

Thesis Outline

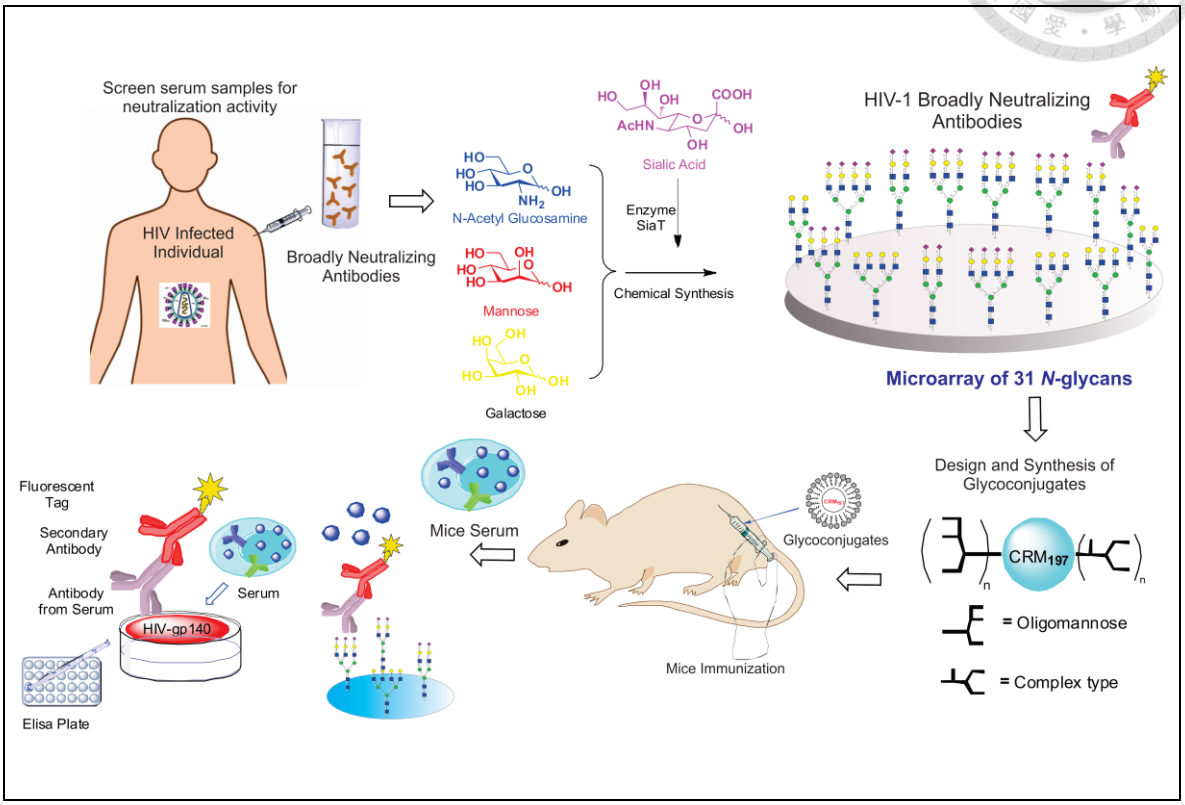

1.11. References:

(1) (a) Geijtenbeek, T. B. H.; Kwon, D. S.; Torensma, R.; van Vliet, S. J.; van Duijnhoven, G. C. F.; Middel, J.; Cornelissen, I. L. M. H. A.; Nottet, H. S. L. M.; KewalRamani, V. N.; Littman, D. R.; Figdor, C. G.; van Kooyk, Y. *Cell* **2000**, *100*, 587; (b) Geijtenbeek, T. B. H.; Torensma, R.; van Vliet, S. J.; van Duijnhoven, G. C. F.; Adema, G. J.; van Kooyk, Y.; Figdor, C. G. *Cell* **2000**, *100*, 575.

(2) Vacquier, V. D.; Moy, G. W. *Dev. Biol.* **1997**, *192*, 125.

(3) Tiemeyer, M.; Goodman, C. S. *Development* **1996**, *122*, 925.

(4) (a) Calarese, D. A.; Scanlan, C. N.; Zwick, M. B.; Deechongkit, S.; Mimura, Y.; Kunert, R.; Zhu, P.; Wormald, M. R.; Stanfield, R. L.; Roux, K. H.; Kelly, J. W.; Rudd, P. M.; Dwek, R. A.; Katinger, H.; Burton, D. R.; Wilson, I. A. *Science* **2003**, *300*, 2065; (b) Scanlan, C. N.; Pantophlet, R.; Wormald, M. R.; Saphire, E. O.; Stanfield, R.; Wilson, I. A.; Katinger, H.; Dwek, R. A.; Rudd, P. M.; Burton, D. R. *J. Virol.* **2002**, *76*, 7306.

(5) Kansas, G. S. *Blood* **1996**, *88*, 3259.

(6) Zinecker, C. F.; Striepen, B.; Geyer, H.; Geyer, R.; Dubremetz, J. F.; Schwarz, R. T. *Mol Biochem Parasit* **2001**, *116*, 127.

(7) Newburg, D. S. *Curr. Med. Chem.* **1999**, *6*, 117.

(8) Sacchettini, J. C.; Baum, L. G.; Brewer, C. F. *Biochemistry* **2001**, *40*, 3009.

(9) (a) Schofield, L.; Hewitt, M. C.; Evans, K.; Siomos, M. A.; Seeberger, P. H. *Nature* **2002**, *418*, 785; (b) Nyame, A. K.; Kawar, Z. S.; Cummings, R. D. *Arch. Biochem. Biophys.* **2004**, *426*, 182.

(10) Ragupathi, G.; Coltart, D. M.; Williams, L. J.; Koide, F.; Kagan, E.; Allen, J.; Harris, C.; Glunz, P. W.; Livingston, P. O.; Danishefsky, S. J. *Proc. Natl. Acad. Sci. U.S.A.* **2002**, *99*, 13699.

(11) (a) Astronomo, R. D.; Burton, D. R. *Nat Rev Drug Discov* **2010**, *9*, 308; (b) Hevey, R.; Ling, C. C. *Future Med. Chem.* **2012**, *4*, 545.

(12) Banks, D. D. *J. Mol. Biol.* **2011**, *412*, 536.

(13) Benyair, R.; Ron, E.; Lederkremer, G. Z. *Int. Rev. Cell. Mol. Biol.* **2011**, *292*, 197.

(14) Shental-Bechor, D.; Levy, Y. *Proc. Natl. Acad. Sci. U.S.A.* **2008**, *105*, 8256.

(15) Bolt, G.; Kristensen, C.; Steenstrup, T. D. *Glycobiology* **2005**, *15*, 541.

(16) (a) Sareneva, T.; Mortz, E.; Tolo, H.; Roepstorff, P.; Julkunen, T. *Eur J Biochem* **1996**, *242*, 191; (b) Sun, Q.; Zhao, L. X.; Song, Q. Q.; Wang, Z.; Qiu, X. S.; Zhang, W. J.; Zhao, M. J.; Zhao, G.; Liu, W. B.; Liu, H. Y.; Li, Y. S.; Liu, X. F. *Glycobiology* **2012**, *22*, 369.

(17) Hsu, T. A.; Takahashi, N.; Tsukamoto, Y.; Kato, K.; Shimada, I.; Masuda, K.; Whiteley, E. M.; Fan, J. Q.; Lee, Y. C.; Betenbaugh, M. J. *J. Biol. Chem.* **1997**, *272*, 9062.

(18) Pallesen, L. T.; Pedersen, L. R. L.; Petersen, T. E.; Rasmussen, J. T. *J. Dairy Sci.* **2007**, *90*, 3143.

(19) Hoshida, S.; Hayashi, T.; Kanamasa, K.; Ishikawa, K.; Naka, M.; Kawarabayashi, T.; Yokoi, Y.; Matsuda, M.; Nagai, Y.; Yamada, Y.; St, S. O. A. C. S. *American Journal of Cardiology* **2004**, *93*, 608.

(20) (a) Kimble, B.; Nieto, G. R.; Perez, D. R. *Virol. J.* **2010**, *7*, *365*; (b) Stevens, J.; Blixt, O.; Tumpey, T. M.; Taubenberger, J. K.; Paulson, J. C.; Wilson, I. A. *Science* **2006**, *312*, 404.

(21) Thomas, W.; Forero, M.; Yakovenko, O.; Nilsson, L.; Vicini, P.; Sokurenko, E.; Vogel, V. *Biophys. J.* **2006**, *90*, 753.

(22) Helenius, A.; Aebi, M. *Annu. Rev. Biochem.* **2004**, *73*, 1019.

(23) Herscovics, A. *Bba-Gen Subjects* **1999**, *1473*, 96.

(24) (a) Takahashi, S.; Sasaki, T.; Manya, H.; Chiba, Y.; Yoshida, A.; Mizuno, M.; Ishida, H. K.; Ito, F.; Inazu, T.; Kotani, N.; Takasaki, S.; Takeuchi, M.; Endo, T. *Glycobiology* **2001**, *11*, 37; (b) Betenbaugh, M. J.; Tomiya, N.; Narang, S.; Hsu, J. T. A.; Lee, Y. C. *Curr. Opin. Struct. Biol.* **2004**, *14*, 601.

(25) Crispin, M.; Harvey, D. J.; Chang, V. T.; Yu, C.; Aricescu, A. R.; Jones, E. Y.; Davis, S. J.; Dwek, R. A.; Rudd, P. M. *Glycobiology* **2006**, *16*, 748.

(26) Matarrese, P.; Malorni, W. *Cell Death Differ.* **2005**, *12*, 932.

(27) Ullrich, C. K.; Groopman, J. E.; Ganju, R. K. *Blood* **2000**, *96*, 1438.

(28) (a) Wilen, C. B.; Tilton, J. C.; Doms, R. W. *Viral Molecular Machines* **2012**, *726*, 223; (b) Wilen, C. B.; Tilton, J. C.; Doms, R. W. *Cold Spring Harbor perspectives in medicine* **2012**, *2*.a006866.

(29) Perdomo, M. F.; Sallberg, M.; Vahlne, A. *Aids. Res. Hum. Retrov.* **2012**, *28*, 852.

(30) Gavazova, R.; Ivanov, D.; Borissov, K.; Genova-Kalou, P.; Raleva, S.; Dundarova, D.; Argirova, R. *Cr. Acad. Bulg. Sci.* **2011**, *64*, 231.

(31) Doores, K. J.; Bonomelli, C.; Harvey, D. J.; Vasiljevic, S.; Dwek, R. A.; Burton, D. R.; Crispin, M.; Scanlan, C. N. *Proc. Natl. Acad. Sci. U. S. A* **2010**, *107*, 13800.

(32) Wang, L. W.; Qin, Y. L.; Ilchenko, S.; Bohon, J.; Shi, W. X.; Cho, M. W.; Takamoto, K.; Chance, M. R. *Biochemistry* **2010**, *49*, 9032.

(33) Pantophlet, R.; Burton, D. R. *Annu. Rev. Immunol.* **2006**, *24*, 739.

(34) Hessell, A. J.; Rakasz, E. G.; Poignard, P.; Hangartner, L.; Landucci, G.; Forthal, D. N.; Koff, W. C.; Watkins, D. I.; Burton, D. R. *PLoS pathogens* **2009**, *5*, e1000433.

(35) (a) Walker, L. M.; Huber, M.; Doores, K. J.; Falkowska, E.; Pejchal, R.; Julien, J. P.; Wang, S. K.; Ramos, A.; Chan-Hui, P. Y.; Moyle, M.; Mitcham, J. L.; Hammond, P. W.; Olsen, O. A.; Phung, P.; Fling, S.; Wong, C. H.; Phogat, S.; Wrin, T.; Simek, M. D.; Koff, W. C.; Wilson, I. A.; Burton, D. R.; Poignard, P.; Investigators, P. G. P. *Nature* **2011**, *477*, 466; (b) Pejchal, R.; Doores, K. J.; Walker, L. M.; Khayat, R.; Huang, P. S.; Wang, S. K.; Stanfield, R. L.; Julien, J. P.; Ramos, A.; Crispin, M.; Depetris, R.; Katpally, U.; Marozsan, A.; Cupo, A.; Maloveste, S.; Liu, Y.; McBride, R.; Ito, Y.; Sanders, R. W.; Ogohara, C.; Paulson, J. C.; Feizi, T.; Scanlan, C. N.; Wong, C. H.; Moore, J. P.; Olson, W. C.; Ward, A. B.; Poignard, P.; Schief, W. R.; Burton, D. R.; Wilson, I. A. *Science* **2011**, *334*, 1097.

(36) McLellan, J. S.; Pancera, M.; Carrico, C.; Gorman, J.; Julien, J. P.; Khayat, R.; Louder, R.; Pejchal, R.; Sastry, M.; Dai, K. F.; O'Dell, S.; Patel, N.; Shahzad-ul-Hussan, S.; Yang, Y. P.; Zhang, B. S.; Zhou, T. Q.; Zhu, J.; Boyington, J. C.; Chuang, G. Y.; Diwanji, D.; Georgiev, I.; Do Kwon, Y.; Lee, D.; Louder, M. K.; Moquin, S.; Schmidt, S. D.; Yang, Z. Y.; Bonsignori, M.; Crump, J. A.; Kapiga, S. H.; Sam, N. E.; Haynes, B. F.; Burton, D. R.; Koff, W. C.; Walker, L. M.; Phogat, S.; Wyatt, R.; Orwenyo, J.; Wang, L. X.; Arthos, J.; Bewley, C. A.; Mascola, J. R.; Nabel, G. J.; Schief, W. R.; Ward, A. B.; Wilson, I. A.; Kwong, P. D. *Nature* **2011**, *480*, 336.

(37) Mouquet, H.; Scharf, L.; Euler, Z.; Liu, Y.; Eden, C.; Scheid, J. F.; Halper-Stromberg, A.; Gnanapragasam, P. N. P.; Spencer, D. I. R.; Seaman, M. S.; Schuitemaker, H.;

Feizi, T.; Nussenzweig, M. C.; Bjorkman, P. J. *Proc. Natl. Acad. Sci. U.S.A* **2012**, *109*, E3268.

(38) (a) Joyce, J. G.; Krauss, I. J.; Song, H. C.; Opalka, D. W.; Grimm, K. M.; Nahas, D. D.; Esser, M. T.; Hrin, R.; Feng, M.; Dudkin, V. Y.; Chastain, M.; Shiver, J. W.; Danishefsky, S. J. *Proc. Natl. Acad. Sci. U.S.A* **2008**, *105*, 15684; (b) Krauss, I. J.; Joyce, J. G.; Finnefrock, A. C.; Song, H. C.; Dudkin, V. Y.; Geng, X.; Warren, J. D.; Chastain, M.; Shiver, J. W.; Danishefsky, S. J. *J Am Chem. Soc.* **2007**, *129*, 11042.

(39) Ni, J.; Song, H.; Wang, Y.; Stamatos, N. M.; Wang, L. X. *Bioconjugate chemistry* **2006**, *17*, 493.

(40) Doores, K. J.; Fulton, Z.; Hong, V.; Patel, M. K.; Scanlan, C. N.; Wormald, M. R.; Finn, M. G.; Burton, D. R.; Wilson, I. A.; Davis, B. G. *Proc. Natl. Acad. Sci. U.S.A* **2010**, *107*, 17107.

(41) (a) Unverzagt, C. *Carbohydrate research* **1997**, *305*, 423. (b) Wang, Z.; Chinoy, Z. S.; Ambre, S. G.; Peng, W.; McBride, R.; de Vries, R. P.; Glushka, J.; Paulson, J. C.; Boons, G. J. *Science* **2013**, *341*, 379.

(42) Thompson, A. J.; Williams, R. J.; Hakki, Z.; Alonzi, D. S.; Wennekes, T.; Gloster, T. M.; Songsrirote, K.; Thomas-Oates, J. E.; Wrodnigg, T. M.; Spreitz, J.; Stutz, A. E.; Butters, T. D.; Williams, S. J.; Davies, G. J. *Proc. Natl. Acad. Sci. U.S.A* **2012**, *109*, 781.

(43) Ogawa, T.; Sugimoto, M.; Kitajima, T.; Sadozai, K. K.; Nukada, T. *Tetrahedron Lett.* **1986**, *27*, 5739.

(44) Paulsen, H.; Heume, M.; Nurnberger, H. *Carbohydrate research* **1990**, *200*, 127.

(45) Wang, P.; Zhu, J. L.; Yuan, Y.; Danishefsky, S. J. *J. Am. Chem. Soc.* **2009**, *131*, 16669.

(46) (a) Unverzagt, C.; Gundel, G.; Eller, S.; Schuberth, R.; Seifert, J.; Weiss, H.; Niemietz, M.; Pischl, M.; Raps, C. *Chemistry* **2009**, *15*, 12292; (b) Unverzagt, C. *Angew. Chem. Int .Ed.* **1997**, *36*, 1989.

(47) (a) Dudkin, V. Y.; Crich, D. *Tetrahedron Lett* **2003**, *44*, 1787; (b) Crich, D.; Dai, Z. M. *Tetrahedron* **1999**, *55*, 1569.

(48) Paulson, J. C.; Blixt, O.; Collins, B. E. *Nat. Chem. Biol.* **2006**, *2*, 238.

(49) Blixt, O.; Head, S.; Mondala, T.; Scanlan, C.; Huflejt, M. E.; Alvarez, R.; Bryan, M. C.; Fazio, F.; Calarese, D.; Stevens, J.; Razi, N.; Stevens, D. J.; Skehel, J. J.; van Die, I.; Burton, D. R.; Wilson, I. A.; Cummings, R.; Bovin, N.; Wong, C. H.; Paulson, J. C. *Proc. Natl. Acad. Sci. U.S.A* **2004**, *101*, 17033.

(50) (a) Feizi, T.; Fazio, F.; Chai, W.; Wong, C. H. *Curr. Opin. Struct. Biol.* **2003**, *13*, 637; (b) Fukui, S.; Feizi, T.; Galustian, C.; Lawson, A. M.; Chai, W. G. *Nat. Biotechnol.* **2002**, *20*, 1011.

(51) (a) Wang, D. N.; Lu, J. H. *Physiol Genomics* **2004**, *18*, 245; (b) Wang, D. N.; Liu, S. Y.; Trummer, B. J.; Deng, C.; Wang, A. L. *Nat. Biotechnol.* **2002**, *20*, 275.

(52) Fazio, F.; Bryan, M. C.; Blixt, O.; Paulson, J. C.; Wong, C. H. *J. Am. Chem. Soc.* **2002**, *124*, 14397.

(53) Song, X. Z.; Xia, B. Y.; Stowell, S. R.; Lasanajak, Y.; Smith, D. F.; Cummings, R. D. *Chem. Biol.* **2009**, *16*, 36.

(54) Bohorov, O.; Andersson-Sand, H.; Hoffmann, J.; Blixt, O. *Glycobiology* **2006**, *16*, 21c.

(55) Oyelaran, O.; Gildersleeve, J. C. *Curr. Opin. Chem. Biol.* **2009**, *13*, 406.

(56) Wang, C. C.; Chen, J. R.; Tseng, Y. C.; Hsu, C. H.; Hung, Y. F.; Chen, S. W.; Chen, C. M.; Khoo, K. H.; Cheng, T. J.; Cheng, Y. S. E.; Jan, J. T.; Wu, C. Y.; Ma, C.; Wong, C. -H. *Proc. Natl. Acad. Sci. U.S.A* **2009**, *106*, 18137.

(57) Spassov, D. S.; Wong, C. H.; Harris, G.; McDonough, S.; Phojanakong, P.; Wang, D.; Hann, B.; Bazarov, A. V.; Yaswen, P.; Khanafshar, E.; Moasser, M. M. *Oncogene* **2012**, *31*, 419.

(58) (a) Ishiwata A.; Lee Y.J.; Ito Y. *Org. Biomol. Chem.* **2010**, *8*, 3596-3608. (b) Matsuo I.; Wada M.; Manabe S.; Yamaguchi Y.; Otake K.; Kato K.; Ito Y. *J. Am. Chem. Soc.* **2003**, *125*, 3403-3403.

Chapter 2

Synthesis of High Mannose Type Oligosaccharides

2.1. Introduction:

Chapter 2 describes efficient convergent synthesis of HIV-1 gp120 related high mannose type oligosaccharides. The syntheses of undecasaccharide ($Man_9GlcNAc_2$) and the related heptasaccharide ($Man_5GlcNAc_2$) and pentasaccharide ($Man_3GlcNAc_2$) demonstrate the facile assembly of branched structures by installation of D1 and D2/D2 arm building units to central core in two glycosylation events with excellent regio- and stereospecificity. A series of oligomannose type structures and their truncated analogues obtained via the described synthetic strategy can serve as ligands for covalent immobilization on carbohydrate microarray platform to study glycan binding specificity of HIV-1 broadly neutralizing antibodies (PG9, PG16, PGTs 121, 127, 128, and 141-145). Biologically important glycans with alkyl amine spacer at reducing end were also conjugated to carrier protein for the HIV-1 antigenicity study.

2.2. Significance of High Mannose Type Glycans for HIV-1:

The specific glycosylation pattern and structural composition of *N*-linked oligosaccharides on HIV-1 spike is highly dependent on host expression systems in which virus was produced[1]. However, mass spectrometric structural analysis indicated that among 24 glycosylation sites on gp120 surface, up to 11 sites are occupied by high mannose type oligosaccharides, ranging from Man_5, Man_6, Man_7, Man_8, to Man_9[2]. Accumulating evidences suggested that HIV-1 surface glycan coat could act as a target for developing anti-HIV strategy. One such example is a potent anti-HIV protein "Cynovirin-N and Scytovirin", which exerts excellent anti-HIV activity through tight binding to high-mannose type oligosaccharides of gp120[3]. In addition, neutralizing antibody 2G12 recognizes an oligosaccharide cluster of high mannose type glycans at the *N*-glycosylation sites N295, N332, N392[4].

Recently, two new broadly neutralizing antibodies, PGT128 and PG9, were shown to be highly potent by neutralizing 70% of HIV-1 isolates across clades by targeting

oligomannose dependent epitopes in variable loops on gp120 surface[5]. The neutralization potency exhibited by these antibodies suggests that they might provide protection at relatively low serum concentrations.

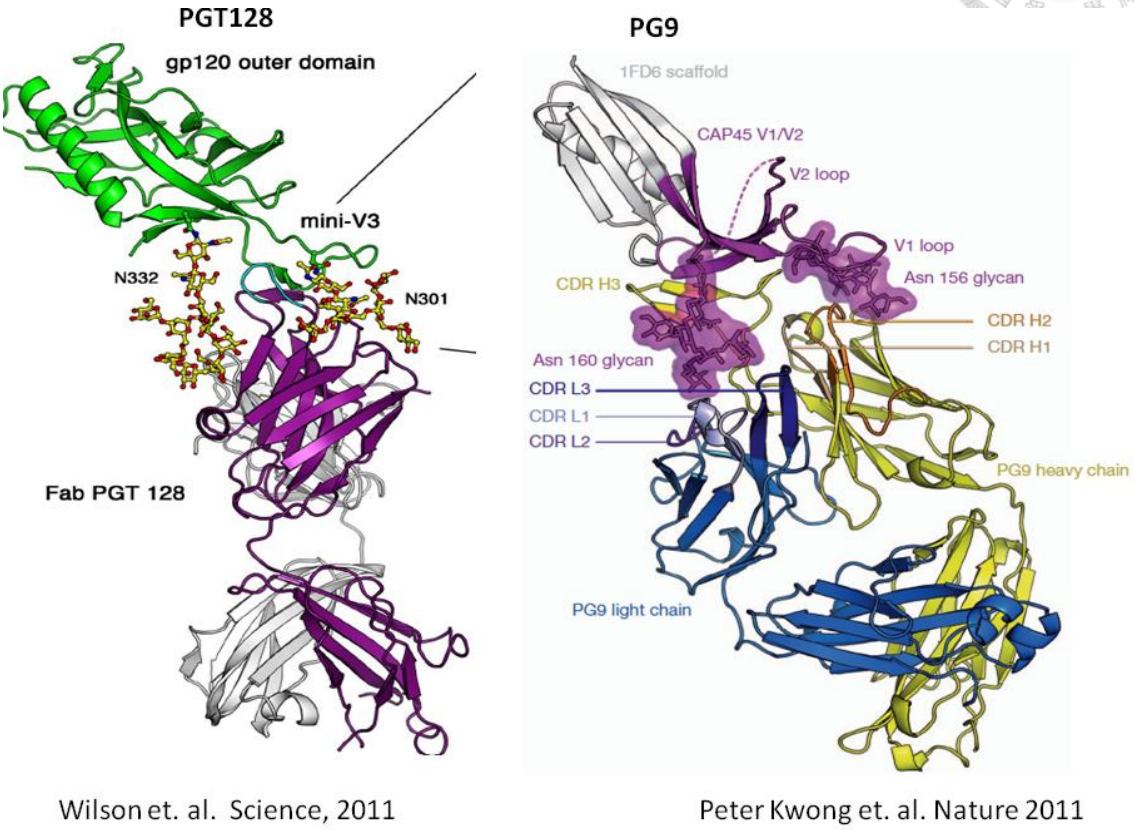

Figure 2.1. Crystal structures of broadly neutralizing antibodies PGT128 and PG9 with recombinant gp120

The crystal structure of Fab PGT128 complexed with Man_9 and fully glycosylated gp120 outer domain reported by Burton and Wilson[6] suggest that antibody penetrates the glycan shield and recognizes two glycans, $Man_9GlcNAc_2$ and short β-strand segment of gp120 V3 loop (Fig. 2.1 left panel) at N332 and N302. The similar phenomenon was documented by Peter Kwong[7] through structure disclosure of HIV-1 gp120 V1/V2 domain with broadly neutralizing antibody PG9. The most prominent interactions between PG9 and V1/V2 loop occur with *N*-linked oligomannose type glycans, more particularly $Man_5GlcNAc_2$ at N160 and N156/167 together with peptide loop. Occurrence of neutralizing antibodies targeting the oligomannose dependent epitope on gp120 surface

suggests that the epitopes recognized by these antibodies may be good vaccine targets if appropriate immunogens can be designed.

2.3. Identification of High Mannose Type Glycan Targets:

The total synthesis of high mannose type viral surface glycans has been explored for the past two decades. Several research groups including Danishfesky[8], Ito[9] and Wang[10] reported the total chemical synthesis of HIV-1 nonamannoside related structures. However, the effective strategy that can minimize number of synthetic steps through full use of shared intermediates could facilitate the assembly of branched oligosaccharides.

Herein, we describe the convergent synthesis of nonamannoside $Man_9GlcNAc_2$ **2-35**, and related pentamannoside $Man_5GlcNAc_2$ **2-30**, and trimannoside $Man_3GlcNAc_2$ **2-27** structures with amino alkyl spacer at reducing end (Scheme 2.1). Using three building units such as chitobiose trisaccharide, D1 arm trimannoside and D2/D3 arm branched pentamannoside, the assembly of undecasaccharide $Man_9GlcNAc_2$ **2-35** was achieved in two glycosylation steps. The synthesis of truncated versions **2-27** and **2-30** was also carried out by sequential installation at 3"-O followed by 6"-O positions of core trisaccharide. The inherent difficulty associated with regio- and stereo specific glycosidic bond formation requires implementation of several glycosylation conditions of which the strategy described in bellow mentioned section was finally adopted because of its robustness and simplicity.

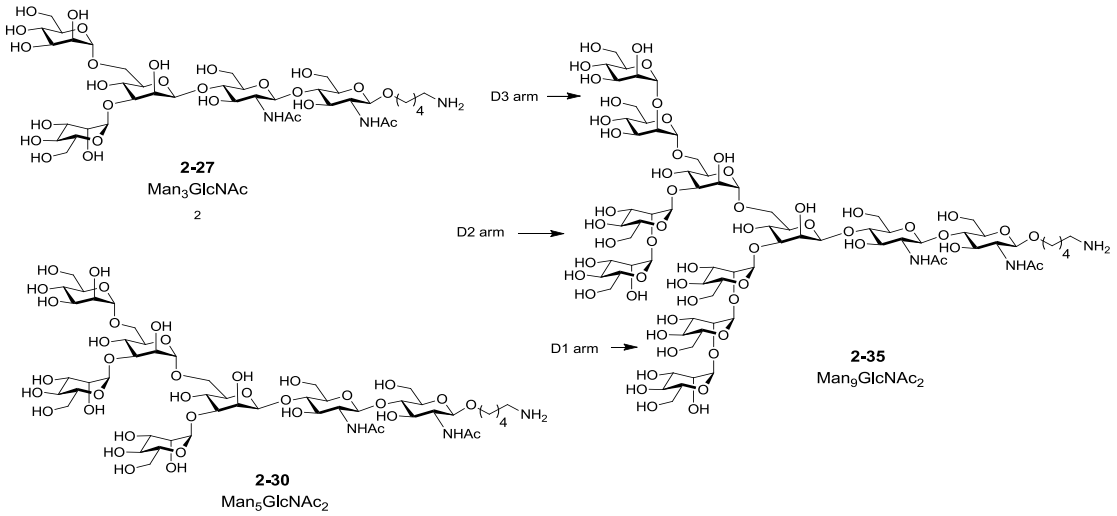

Scheme 2.1. High-Mannose Type oligosaccharides structures.

2.4. Retrosynthesis:

The power of prioritized strategic bond disconnection as a means of guiding synthetic analysis, is well-appreciated by synthetic chemists dealing with construction of complex target systems. The retro synthetic analysis of the amino pentyl $Man_9GlcNAc_2$ suggests that system **2-35** constitutes a significant challenge to chemical synthesis. The undecassacharide **2-35** could be assembled by regioselective installation of branched pentasaccharide **2-21** to hexasaccharide **2-32**. This hexasaccharide would in turn be prepared by the α-mannosylation of chitobiose trisaccharide **2-10** at 3"-O position with trimannosyl fluoride. Diversely protected core trisaccharide could be approached in multigram scale through a sequence featuring coupling of reducing end di-glucosamine acceptor **2-5** with glucose **2-6**. The *β*-Mannoside could be accessed via 2-OTf mediated SN_2 inversion of β-glucoside. Compounds **2-1**, **2-2**, and **2-3** serve as building blocks for preparing reducing end di-GlcNAc.

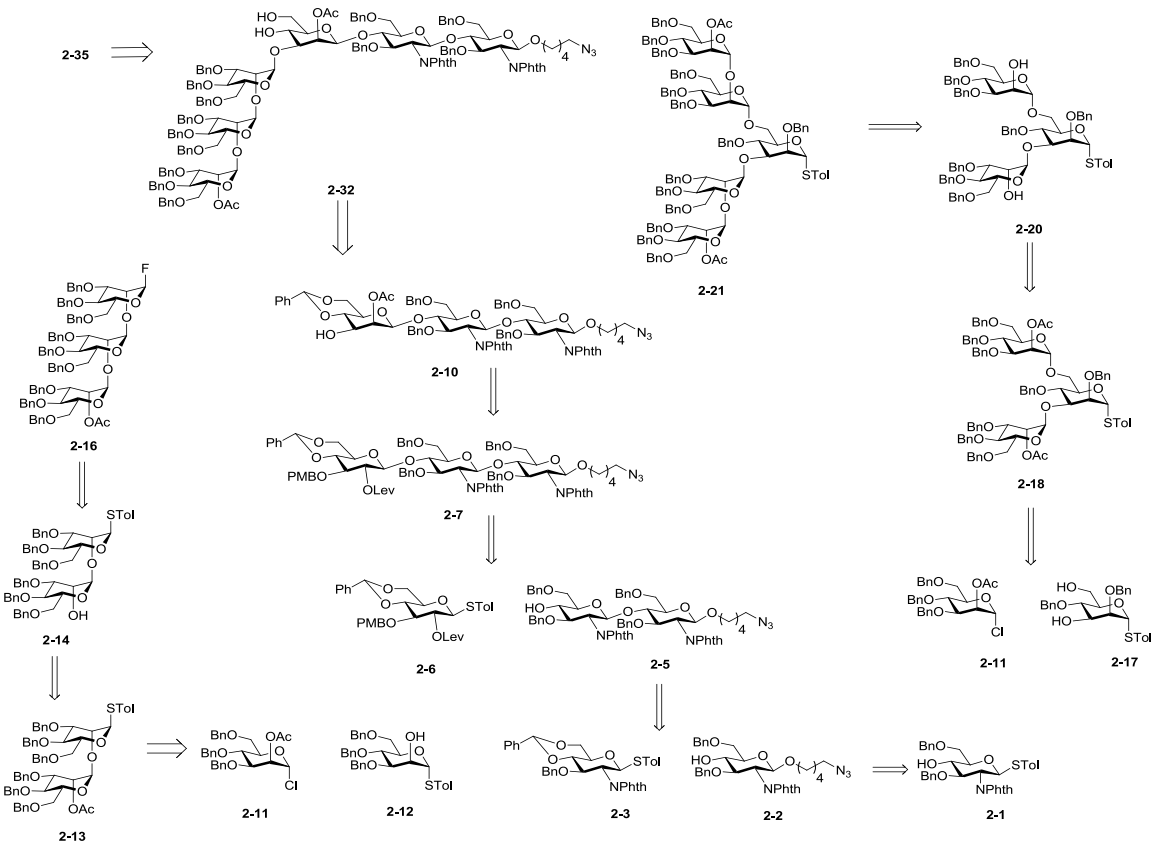

Scheme 2.2. Retrosynthesis of $Man_9GlcNAc_2$.

D1 arm trisaccharide **2-18** could be assembled by condensation of mannosyl thioglycoside **2-12** with mannosyl chloride **2-11**. Removal of 2"-OAc protection of **2-13** followed by addition third mannose unit to **2-14** could afford trimannosyl thioglycoside. Functional group modification at anomeric position could give desired trimannosyl fluoride **2-18**. Similarly D2/D3 arm pentasaccharide can be prepared from sequential double glycosylation of mannosyl chloride **2-11** to thiomannoside acceptor **2-17**. The amino alkyl spacer at reducing end may allow attachment of glycans to carbohydrate microarray platform as well as to carrier protein.

2.5. Synthesis of Core Trisaccharide:

To deal with complex oligosaccharides, the reliable access to monosaccharide building blocks has to be established. The orthogonally protected key core trisaccharide scaffold **2-**

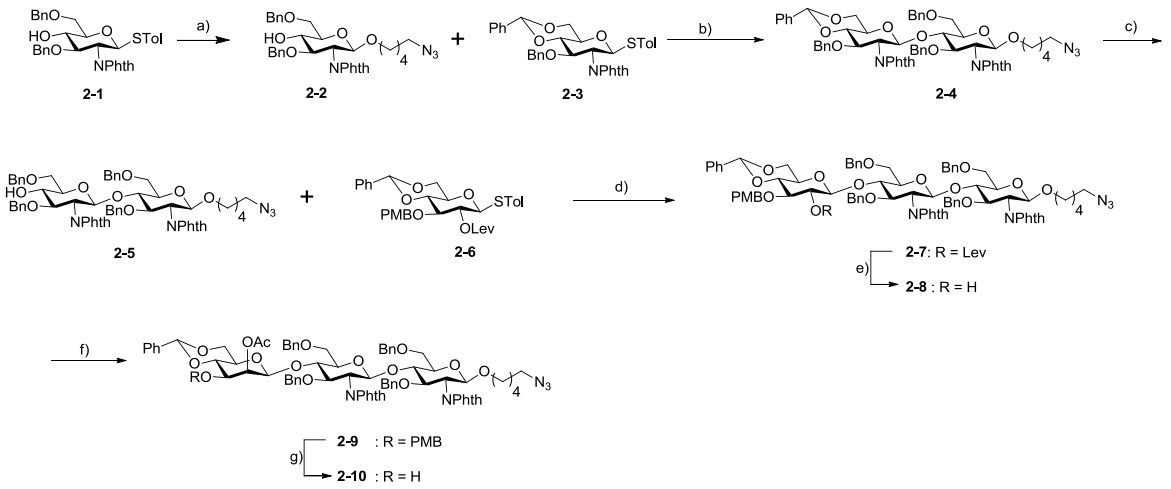

Scheme 2.3: Synthesis of chitobiose trisaccharide. (a) 5-azidopentanol, NIS, TfOH, 4 Å MS, CH_2Cl_2, -20°C, 2h, 70%; (b) NIS, TfOH, 4 Å MS, CH_2Cl_2, -40°C, 1h, 75%; (c) Triethyl silane, TFA, CH_2Cl_2, 0°C, 67%; (d) NIS, TfOH, 4 Å MS, CH_2Cl_2, -20°C, 2h, 76%; (e) Hydrazine acetate, THF, overnight, 80% ; (f) (1) Tf_2O, pyridine, -15°C, overnight; (2) Tetrabutyl ammonium acetate (Bu_4NOAc), toluene, sonication, 16 h, 86% over 2 steps; (g) DDQ, CH_2Cl_2:H_2O=10/1, 4 h, 70%. NIS: N-iodosuccinimide; DDQ: 2,3-Dichloro-5,6-dicyano-1,4-benzoquinone.

10 is the most synthetically challenging due to the presence of *β*-mannosyl linkage. The synthesis of **2-10** commenced with installation of azido alkyl spacer at reducing end via

glycosylation of **2-1** with 1-azido pentanol. Condensation of thioglycoside **2-3** and the acceptor **2-2** mediated by NIS and TfOH supplied the disaccharide **2-4.** The selective benzylidine opening of **2-4** afforded 4"-alcohol, which underwent further glycosylation by orthogonally protected glucose thioglycoside **2-6** to form the trisaccharide **2-7.**

Here, the Lev group situated at C-2 hydroxyl position of donor assisted in generating exclusive *β*-linkage and its selective removal using hydrazine acetate followed by two step epimerization via 2"-OTf intermediate provided us desired *β*-mannoside **2-9**. Treatment of **2-9** with 2,3-dichloro-5,6-dicyano-1,4-benzoquinone (DDQ) to cleave the *p*-methoxybenzyl group (PMB) while leaving acetal untouched afforded 3"-OH**,** which becomes a new installation site to get more complex oligosaccharides.

2.6. Synthesis of D1 and D2/D3 Arm Building Blocks:

The preparation of D1 arm trisaccharide of $Man_9GlcNAc_2$ began by glycosylation of mannosyl chloride **2-11** and thioglycoside acceptor **2-12** under the treatment of 2,6-di-*tert*-butylpyridine (DTBP) and silver triflate (AgOTf) to obtain disaccharide **2-13** (Scheme 2.4). Zemplén de-acetylation of **2-13** at 2-O position followed by α-mannosylation with **2-11** by employing DTBP and AgOTf gave desired trisaccharide **2-15** in 93% yield. The leaving group modification of **2-15** from thioglycoside to glycosyl fluoride **2-16** was performed in presense of *N*-bromo succinamide (NBS) and diethylaminosulfur trifluoride (DAST). The fluoride transformation provided us better results in terms of α-selectivity and excellent yield during glycosylation with chitobiose trisaccharide **2-10.** Under the activation of AgOTf, the condensation of donor **2-11** and acceptor **2-17** was performed to afford trimannose **2-18,** which was subsequently de-acetylated and further di-glycosylated with **2-11** to afford D2/D3 arm pentasaccharide **2-21** in 71% yield. Compound **2-18** was next subjected to leaving group modification using NBS and DAST to trimannosyl fluoride **2-19** in 68% yield. Careful observation of the strategy revealed that using a single mannosyl chloride donor **2-11** in a unique DTBP/AgOTf mediated glycosylation condition affordedt D1, D2/D3 arm tri- and pentasaccharide intermediates in excellent yield.

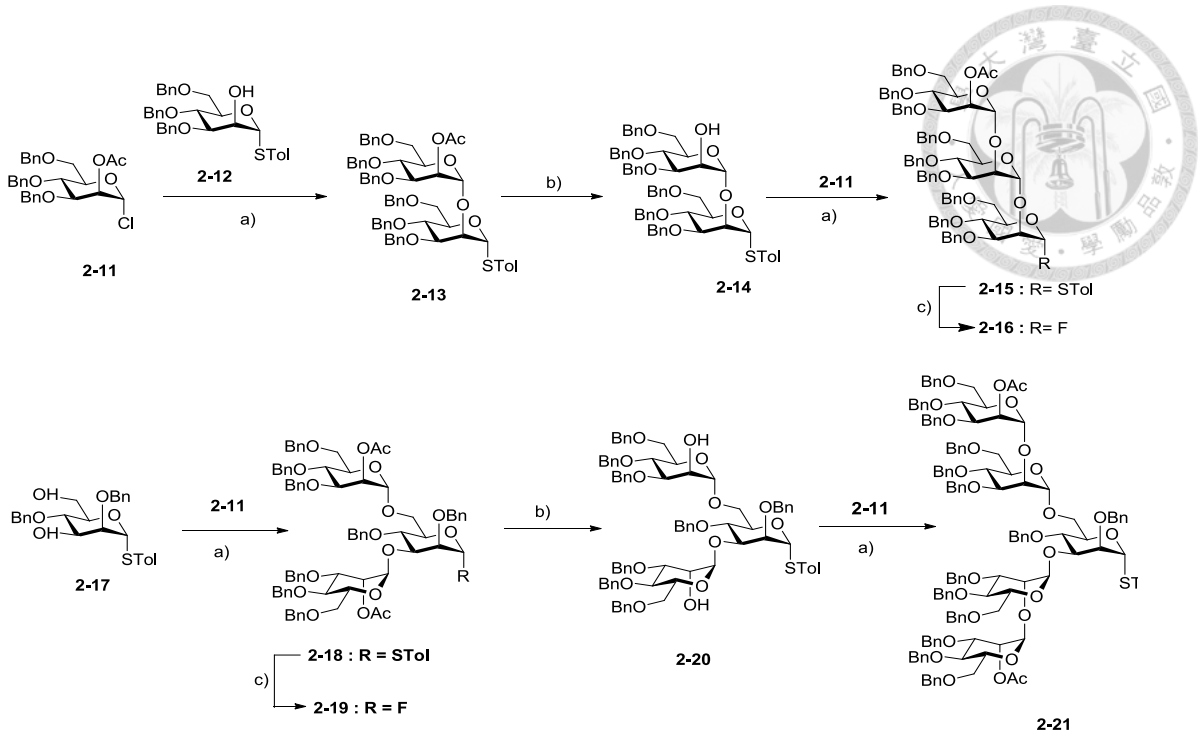

Scheme 2.4 : Synthesis of D1, D2/D3 arm building blocks. a) DTBP, AgOTf, 4 Å MS, CH_2Cl_2, -30°C to RT, overnight; **2-13:** 93%, **2-15:** 91%, **2-18:** 66%, **2-21:** 74%. b) NaOMe, MeOH:CH_2Cl_2 =1/1; **2-14:** 89%, **2-20:** 90%. c) N-bromosuccinamide (NBS), DAST, CH_2Cl_2, -30°C to -10°C; **2-16:** 58%, **2-19:** 61%. DTBP = 2,6-di-tert-butylpyridine; DAST= Diethylaminosulfur trifluoride.

2.7. Assembly of Man3/Man5GlcNAc2:

With the modular set of building blocks in hand, we next proceed to assemble the target oligosaccharide structures. We first focused on preparation of core pentasaccharide $Man_3GlcNAc_2$ and $Man_5GlcNAc_2$. Scheme 2.5 depicted the detailed chemical synthesis of high mannose type glycan **2-27** and **2-30**.

The glycosylation of **2-10** with known mannosyl imidate donor **2-23**[11] afforded tetrasaccharide **2-24** in 70% yield. After selective benzilidine ring opening of **2-24,** the resulting 6"-OH **2-25** was glycosylated with **2-23** to afford the desired fully protected $Man_3GlcNAc_2$ pentasaccharide **2-26,** an early intermediate in *N*-Glycan biosynthesis and thus a conserved motif in all *N*-glycans, in 60% yield. In another pathway, benzilidine reductive opening of **2-24** resulted in diol **2-28**, which was further condensed with

trimannosyl fluoride **2-19** by using Cp_2HfCl_2 and AgOTf to get heptasaccharide **2-29,** an intermediate in GlcNAc mediated branching in the Golgi apparatus, in 52% yield.

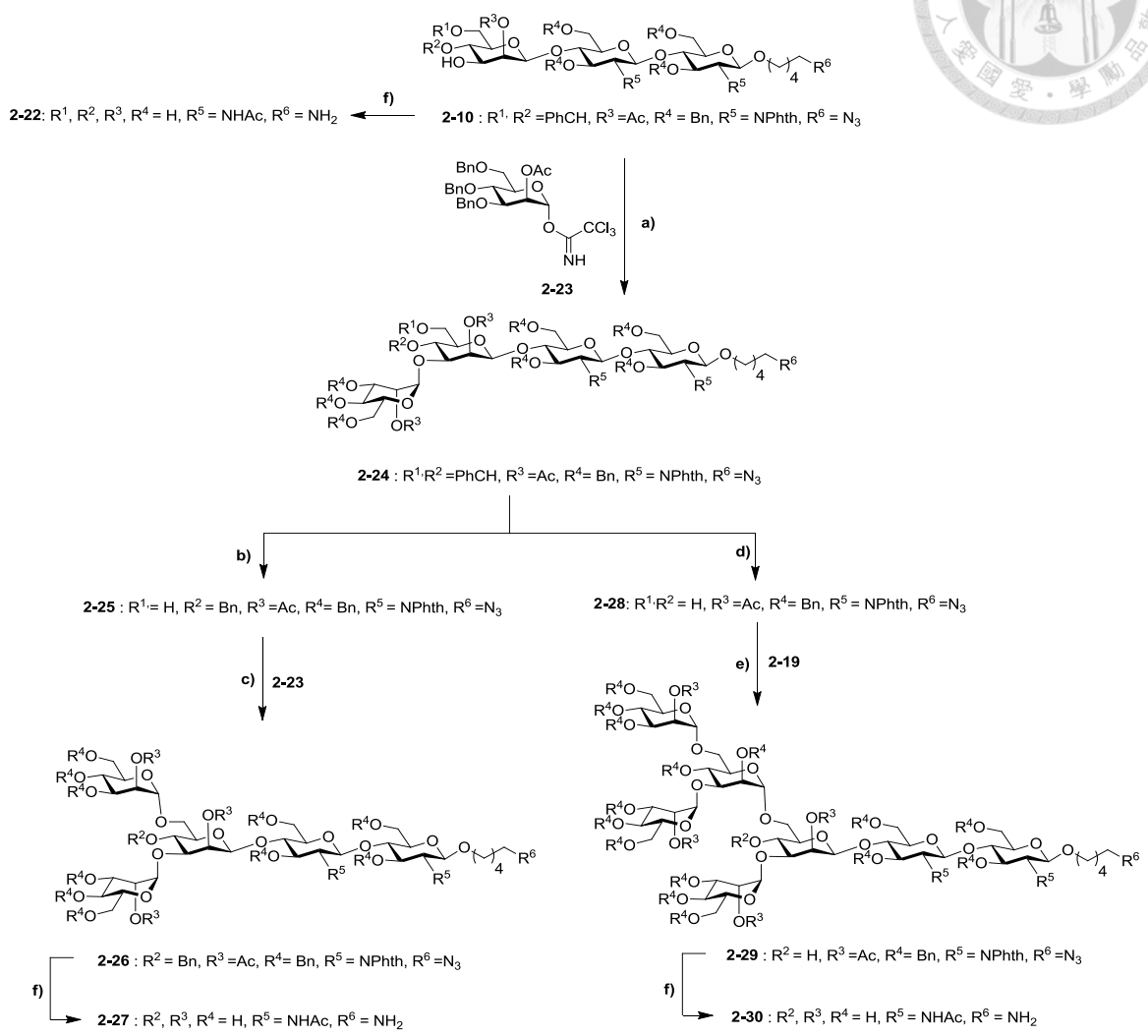

Scheme 2.5. Synthesis of Man_3 and $Man_5GlcNAc_2$. a) $BF_3.OEt_2$, CH_2Cl_2, 4 Å MS, -40°C, 2 h, 70%; b)Triethyl silane, $PhBCl_2$, CH_2Cl_2, 4 Å MS, -78°C ,1 h, 82%; c) $BF_3.OEt_2$, CH_2Cl_2, 4 Å MS, -60°C to -20°C, 2 h, 60%; d) *p*TsOH, CH_3CN, 66%; e) AgOTf, Cp_2HfCl_2, Toluene, 4 Å MS, -40°C, 2 h, 52%; f) i) $NH_2CH_2CH_2NH_2$, nBuOH, 90°C, overnight; ii) Ac_2O, pyridine, overnight; iii) NaOMe, MeOH, overnight; iv) $Pd(OH)_2$, MeOH:H_2O:HCOOH (5:3:2), H_2; **2-27**: 45%; **2-30**: 52%; Cp_2HfCl_2 = Bis (cyclopentadienyl) hafnium Dichloride.

Deprotection of fully protected oligosaccharides **2-10**, **2-26**, and **2-29** started with removal of phthalimide protection by using *n*-butyl alcohol and ethylene diamine at 90°C. Acetylation of free amine followed by complete deacetylation was performed by using sodium methoxide. Finally, the compounds were subjected to hydrogenolysis to supply **2-22, 2-27** and **2-30**, respectively, in good yield and high purity. The structures of these synthetic ligands were confirmed by NMR and mass spectrometric analysis (Appendix A).

2.8. Assembly of Man9GlcNAc2:

To synthesize $Man_9GlcNAc_2$, a major glycoform found on HIV-1 gp120 surface and an important component of epitope recognized by broadly neutralizing antibodies[12], compound **2-10** was subjected to 3"-O glycosylation with fluoride **2-16** under the promotion of Cp_2HfCl_2 /AgOTf to get hexasaccharide **2-31** in 58% yield. The *p*-toluene sulfonic acid mediated reductive ring opening of **2-31** provided diol **2-32.** Exploiting the higher reactivity of primary hydroxyl, **2-32** was further underwent glycosylated at 6"-O position with pentamannosyl thioglycoside **2-21** activated by the stable radical cation tris(4-bromophenyl) ammoniumyl hexachloroantimonate in a one electron transfer reaction as introduced by Sinay[13] and recently used by Danishfesky[8b] to afford undecasaccharide **2-34** (Scheme 2.6). This activation protocol proved to be sufficiently mild to cleanly conjugate the hindered acceptor **2-32** with branched thioglycoside donor **2-21.** Finally, four step global deprotection of **2-31** and **2-34** afforded desired fully Man_4 **2-33** and $Man_9GlcNAc_2$ **2-35**, respectively.

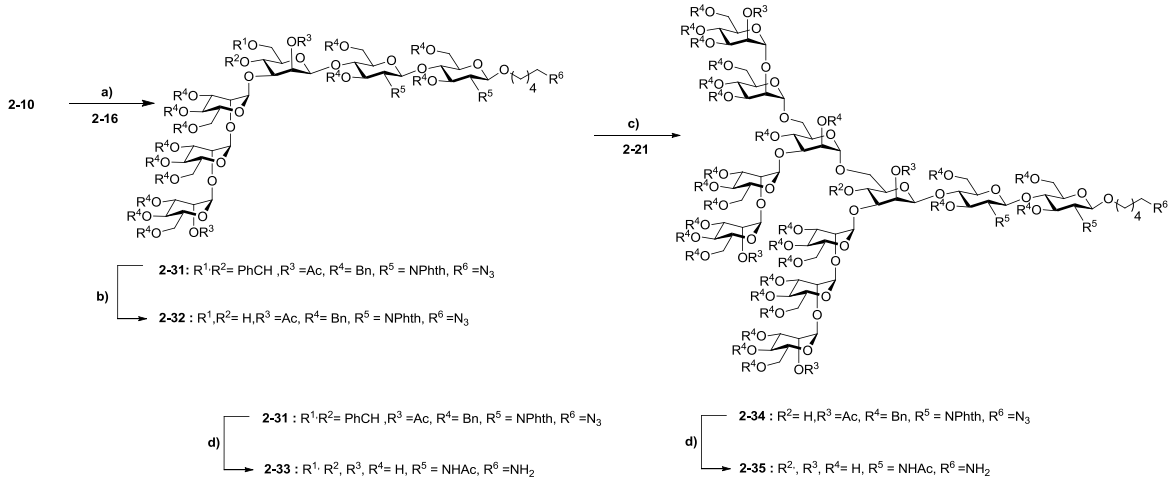

Scheme 2.6. Synthesis of $Man_9GlcNAc_2$. a) AgOTf, Cp_2HfCl_2, Toluene, 4 Å MS, -40°C, 2 h, 58%; b) *p*TsOH, CH_3CN, 60%; c) $(BrC_6H_4)_3NSbCl_6$, CH_3CN, 4 Å MS, -10°C to RT, 4 h, 52%; d) i) $NH_2CH_2CH_2NH_2$, nBuOH, 90°C, overnight; ii) Ac_2O, pyridine, overnight; iii) NaOMe, MeOH, overnight; iv) $Pd(OH)_2$, MeOH:H_2O:HCOOH (5:3:2), H_2 ; **2-33**: 42%; **2-35**: 26%; $(BrC_6H_4)_3NSbCl_6$ = Tris (4-bromophenyl) ammoniumyl hexachloroantimonate.

2.9. Synthesis of Paucimannose Type Oligosaccharides:

Last in this series, the pauci mannose type structure bearing core fucose **2-48** was assembled from reducing end disaccharide **2-46** through fucosylation of diol acceptor **2-45** by donor **2-44** (scheme 2.7). The *α*-selectivity was enhanced by in situ anomarization protocol ($CuBr_2$, tetrabutyl ammonium bromide), which was first developed by Lemieux and co-workers[13], to get disaccharide **2-46** in 76% yield with its regio- and stereo-chemistry confirmed by NMR analysis. The formation of the key *β*-mannosyl linkage using sulfoxide donor **2-36** and acceptor **2-37** was performed using DTBP and Tf_2O to get disaccharide **2-38** in 67% yield with α/β ratio of 1:7. The *p*-methoxy benzyl ether protection at 3" was removed by using DDQ to afford 3"-OH **2-39**, which was further subjected to 3"-O α-mannosylation by using imidate **2-23** under the promotion of $BF_3.OEt_2$ to obtained trisaccharide **2-40**. Selective benzilidine opening of **2-40** produced **2-41**, which further underwent α-mannosylation at 6"-O position to get tetrasaccharide **2-42**. Compound **2-42** was then converted into glycosyl imidate **2-43** by treatment with $PdCl_2$ and then trichloroacetimidate and DBU. Finally the condensation of imidate **2-43** and disaccharide **2-46** under the agency of $BF_3.OEt_2$ obtained desired hexasaccharide **2-47**. The global deprotection afforded the paucimannose type oligosaccharide **2-48**.

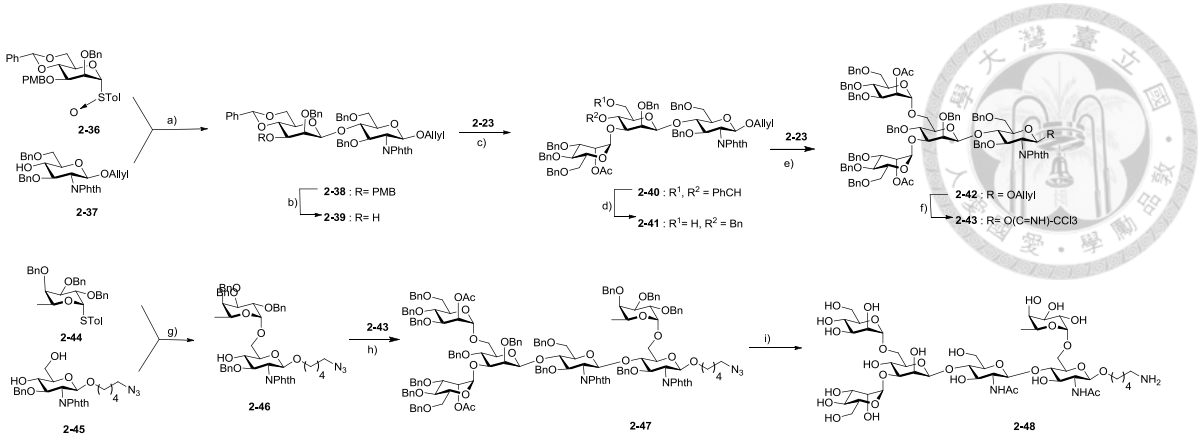

Scheme 2.7. Preparation of Paucimannose type oligosaccharides. a) DTBP, Tf_2O, CH_2Cl_2, -60°C, 3 h, 67% (α/β 1:7); b) DDQ, CH_2Cl_2:H_20 = 10/1, 3 h, 70%; c) $BF_3.OEt_2$, CH_2Cl_2, 4 Å MS, -40°C, 1 h, 81%; d) Triethyl sillane, $PhBCl_2$, CH_2Cl_2, 1 h, 73%; e) $BF_3.OEt_2$, CH_2Cl_2, 4 Å MS , -20°C, 2 h, 65%; f) i) $PdCl_2$, MeOH:CH_2Cl_2, rt, 6 h, ii) DBU, trichloroacetonitrile, CH_2Cl_2 , 63% over 2 steps; g) $CuBr_2$, TBAB, DMF:CH_2Cl_2, 4 Å MS ,0°C to rt, overnight, 76%; h) $BF_3.OEt_2$, CH_2Cl_2, 4 Å MS ,-70°C, 2 h, 45%; i) 1) $NH_2CH_2CH_2NH_2$, nBuOH, 100°C; 2) Ac_2O, pyridine, 0°C to RT; 3) NaOMe, MeOH; 4) $Pd(OH)_2$, MeOH:H_2O:HCOOH (5:3:2), H_2, 22% over 4 steps. TBAB = Tetrabutyl ammonium bromide.

2.10. Applications to Biology:

A panel of high mannose type oligosaccharides including **2-27**, **2-30**, **2-35**, **2-48**, and the truncated analogues **2-22**, and **2-33** were printed on carbohydrate microarray for profiling glycan binding specificity of newly discovered HIV-1 bNAbs. Based on their biological significance, the structures were further conjugated to carrier protein for immunization study (chapter 4).

2.11. References:

(1) (a) Zhu, X. G.; Borchers, C.; Bienstock, R. J.; Tomer, K. B. *Biochemistry* **2000**, *39*, 11194; (b) Cutalo, J. M.; Deterding, L. J.; Tomer, K. B. *J. Am. Soc. Mass Spectr.* **2004**, *15*, 1545.

(2) (a) Doores, K. J.; Bonomcelli, C.; Harvey, D. J.; Vasiljevic, S.; Dwek, R. A.; Burton, D. R.; Crispin, M.; Scanlan, C. N. *Proc. Natl. Acad. Sci. U.S.A* **2010**, *107*, 13800; (b) Bonomelli, C.; Doores, K. J.; Dunlop, D. C.; Thaney, V.; Dwek, R. A.; Burton, D. R.; Crispin, M.; Scanlan, C. N. *PloS One* **2011**, *6*, e23521.

(3) (a) Keeffe, J. R.; Gnanapragasam, P. N. P.; Gillespie, S. K.; Yong, J.; Bjorkman, P. J.; Mayo, S. L. *Proc. Natl. Acad. Sci. U.S.A.* **2011**, *108*, 14079; (b) Buffa, V.; Stieh, D.; Mamhood, N.; Hu, Q. X.; Fletcher, P.; Shattock, R. J. *J. Gen. Virol.* **2009**, *90*, 234.

(4) Calarese, D. A.; Scanlan, C. N.; Zwick, M. B.; Deechongkit, S.; Mimura, Y.; Kunert, R.; Zhu, P.; Wormald, M. R.; Stanfield, R. L.; Roux, K. H.; Kelly, J. W.; Rudd, P. M.; Dwek, R. A.; Katinger, H.; Burton, D. R.; Wilson, I. A. *Science* **2003**, *300*, 2065.

(5) Walker, L. M.; Huber, M.; Doores, K. J.; Falkowska, E.; Pejchal, R.; Julien, J. P.; Wang, S. K.; Ramos, A.; Chan-Hui, P. Y.; Moyle, M.; Mitcham, J. L.; Hammond, P. W.; Olsen, O. A.; Phung, P.; Fling, S.; Wong, C. H.; Phogat, S.; Wrin, T.; Simek, M. D.; Koff, W. C.; Wilson, I. A.; Burton, D. R.; Poignard, P. *Nature* **2011**, *477*, 466.

(6) Pejchal, R.; Doores, K. J.; Walker, L. M.; Khayat, R.; Huang, P. S.; Wang, S. K.; Stanfield, R. L.; Julien, J. P.; Ramos, A.; Crispin, M.; Depetris, R.; Katpally, U.; Marozsan, A.; Cupo, A.; Maloveste, S.; Liu, Y.; McBride, R.; Ito, Y.; Sanders, R. W.; Ogohara, C.; Paulson, J. C.; Feizi, T.; Scanlan, C. N.; Wong, C. H.; Moore, J. P.; Olson, W. C.; Ward, A. B.; Poignard, P.; Schief, W. R.; Burton, D. R.; Wilson, I. A. *Science* **2011**, *334*, 1097.

(7) McLellan, J. S.; Pancera, M.; Carrico, C.; Gorman, J.; Julien, J. P.; Khayat, R.; Louder, R.; Pejchal, R.; Sastry, M.; Dai, K.; O'Dell, S.; Patel, N.; Shahzad-ul-Hussan, S.; Yang, Y.; Zhang, B.; Zhou, T.; Zhu, J.; Boyington, J. C.; Chuang, G. Y.; Diwanji, D.; Georgiev, I.; Kwon, Y. D.; Lee, D.; Louder, M. K.; Moquin, S.; Schmidt, S. D.; Yang, Z. Y.; Bonsignori, M.; Crump, J. A.; Kapiga, S. H.; Sam, N. E.; Haynes, B. F.; Burton, D. R.; Koff, W. C.; Walker, L. M.; Phogat, S.; Wyatt, R.; Orwenyo, J.; Wang, L. X.;

Arthos, J.; Bewley, C. A.; Mascola, J. R.; Nabel, G. J.; Schief, W. R.; Ward, A. B.; Wilson, I. A.; Kwong, P. D. *Nature* **2011**, *480*, 336.

(8) (a) Mandal, M.; Dudkin, V. Y.; Geng, X.; Danishefsky, S. J. *Angew. Chem. Int. Ed.* **2004**, *43*, 2557; (b) Geng, X.; Dudkin, V. Y.; Mandal, M.; Danishefsky, S. J. *Angew. Chem. Int. Ed.* **2004**, *43*, 2562.

(9) Matsuo, I.; Wada, M.; Manabe, S.; Yamaguchi, Y.; Otake, K.; Kato, K.; Ito, Y. *J. Am. Chem. Soc.* **2003**, *125*, 3402.

(10) Amin, M. N.; Huang, W.; Mizanur, R. M.; Wang, L. X. *J. Am. Chem. Soc.* **2011**, *133*, 14404.

(11) Doores, K. J.; Fulton, Z.; Hong, V.; Patel, M. K.; Scanlan, C. N.; Wormald, M. R.; Finn, M. G.; Burton, D. R.; Wilson, I. A.; Davis, B. G. *Proc. Natl. Acad. Sci. U.S.A.* **2010**, *107*, 17107.

(12) Calarese, D. A.; Lee, H. K.; Huang, C. Y.; Best, M. D.; Astronomo, R. D.; Stanfield, R. L.; Katinger, H.; Burton, D. R.; Wong, C. H.; Wilson, I. A. *Proc. Natl. Acad. Sci. U.S.A.* **2005**, *102*, 13372.

(13) Lemieux, R. U.; Hendriks, K. B.; Stick, R. V.; James, K. *J. Am. Chem. Soc.* **1975**, *97*, 4056.

Chapter 3

Synthesis of Hybrid and Complex Type Glycans

3.1. Introduction:

Co-translational modification of newly synthesized polypeptides in the endoplasmic reticulum includes three classes of *N*-linked oligosaccharides: high mannose, hybrid and complex type glycans. Carbohydrate binding agents bind to the variety of *N*-glycans of HIV-1 envelope gp120 and prevent viral entry. The binding study of 13 different types of lectins to gp120 purified from HIV-1 and HIV-2 isolates suggests that lectins could target various kind of glycans on gp120 surface[1]. Based on the lectin-glycan recognition pattern, the gp120 carbohydrates are divided into four types: a high mannose type glycan, a bisected hybrid or complex type glycan, a biantennary fucosylated complex type glycan and a triantennary bisected complex type glycan. Only lectins, which bound at least one of the four types of glycans, were capable to inhibit fusion of HIV-infected cells with CD4 cells by a carbohydrate-specific interaction with the HIV-infected cells. Thus, several different glycan structures may be implicated in CD4-gp120 binding. Chemical and enzymatic syntheses offer rapid and reliable access to these branched hybrid and complex type oligosaccharides to facilitate further investigation in biological functions of these glycoconjugates and their potential application as carbohydrate-based vaccines.

Described here is the highly efficient convergent synthesis of hybrid and complex type *N*-linked oligosaccharides. The structures with terminal galactose were further elaborated by sialyl transferases (SiaT) mediated enzymatic sialic acid transfer by taking advantage of their tremendous specificity. The strategy provided rapid access not only to naturally occurring complex glycans but also unnatural hybrid type glycoforms and their truncated analogues.

3.2. Significance of Hybrid and Complex Type Oligosaccharides for HIV-1:

Leonard *et al.* demonstrated that gp120 of HIV-1_{IIIB}, expressed in CHO cells, contained 24 *N*-linked glycans, of which 11 are high mannose or hybrid type and 13 are complex type[2] (Fig. 3.1). These host-derived carbohydrate structures comprise half the

mass of gp120 and thus shield the underlying protein surface from neutralizing antibody attacks.

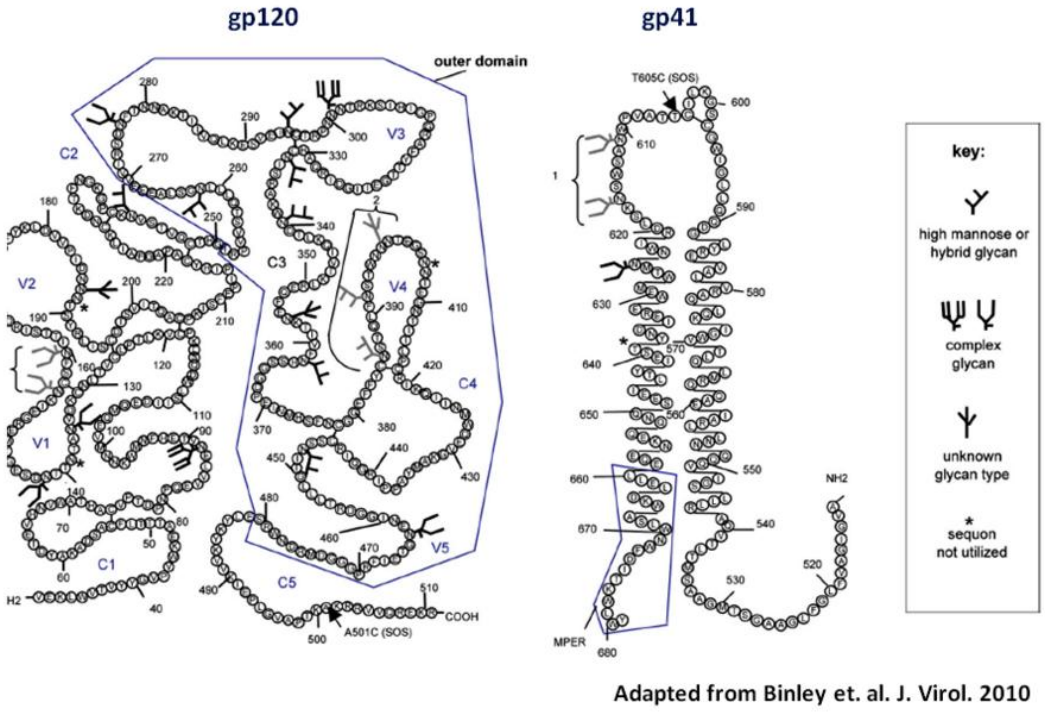

Figure 3.1. The putative carbohydrate modifications on gp120 and gp41 secondary structures

Binley et. al. reported that the antennae of complex type *N*-glycans present on gp120 serve to protect the V3 loop and CD4 binding site, while *N*-glycan stems regulate native trimer conformation. Removal of such complex glycan structures using various endoglycosidases can lead to global changes in neutralization sensitivity and an inability to complete the conformational rearrangements necessary for infections[3]. Apart from their role in regulating gp120 trimer conformation essential for HIV-1 infection, complex type glycans have been targeted by broadly neutralizing antibodies.

Mouquet et. al. reported the first example of broadly neutralizing HIV-1 antibody PGT121, which can recognize bi-antennary complex type glycans on gp120 surface[4]. One interpretation of their finding is that PGT121-like antibodies exhibit promiscuous carbohydrate recognition properties such that they could accommodate either a complex-type or a high-mannose *N*-glycan attached to N332 gp120[5]. However, this N332

glycosylation site is generally assumed to carry high-mannose *N*-glycans based on mass spectrometry data[6] and the fact that it forms a critical part of the epitope recognized by the highmannose–specific antibody 2G12[7]. Nonetheless, the possibility of complex-type glycan at this position under some circumstances remains open given that the N332gp120-linked *N*-glycan has been reported to be a mixture of high mannose and complex type in gp140s from some viral strains[8].

Recently, Peter Kwong et. al. reported the crystal structure of the antigen-binding fragment (Fab) of the PG16 antibody in complex with the V1–V2 domain of HIV-1 gp120 from strain ZM109 along with NMR characterization of glycan recognition by PG16 and PG9. The structure of antibody PG16 to scaffolded V1-V2 showed that the epitope consists of both high mannose and complex type oligosaccharides at N160 and N156 or N173[9]. Accumulating evidences on hybrid and complex type glycans targeting neutralizing antibodies such as PGT121 and PG16 suggest that design effort for carbohydrate based immunogens will probably need to take into account the specific hybrid and complex type glycans.

3.3. Identification of Hybrid and Complex Type Glycan Targets:

In contrast to the classic model of cell-directed post-translational glycosylation, a small number of glycoproteins exhibit the phenomenon of protein-directed glycosylation. In these cases, glycan processing may be enhanced by the recruitment of glycosyl transferases or may be limited by subcellular trafficking of the protein, thus preventing exposure of glycans to the full range of glycosylation enzymes. One such glycoprotein is gp120, which contains a number of unprocessed oligomannose glycans ($Man_{8/9}$) on its heavily glycosylated outer domain. However, the glycans around the variable loops and the receptor binding site are fully processed into cell type-specific complex glycans on recombinant gp120.

During glycan biosynthesis pathway, as the glycoprotein transported through Golgi, accessible glycan moieties get trimmed by α-1,2 mannosidase to form $Man_5GlcNAc_2$, a substrate for various Golgi resident cellular enzymes[10]. *N*-acetyl glucosamine transferase (GnT) transfers a GlcNAc moiety to D1 arm of $Man_5GlcNAc_2$ substrate, followed by actions of galactosyl and sialyl transferases to convert it into hybrid type glycan (VIII). The

hybrid glycoform (II) would act as a substrate for modification into complex glycans, in which D2 and D3 arm mannose get cleaved, allowing addition of GlcNAc moieties by series of GnT family enzymes to form multiantennary mature oligosaccharides as depicted in Figure 3.2. Existence of bi-, tri-, and tetra-antennary structures with varying degrees of sialylations on gp120 surface was characterized by several mass spectrometric analysis reports [2,11].

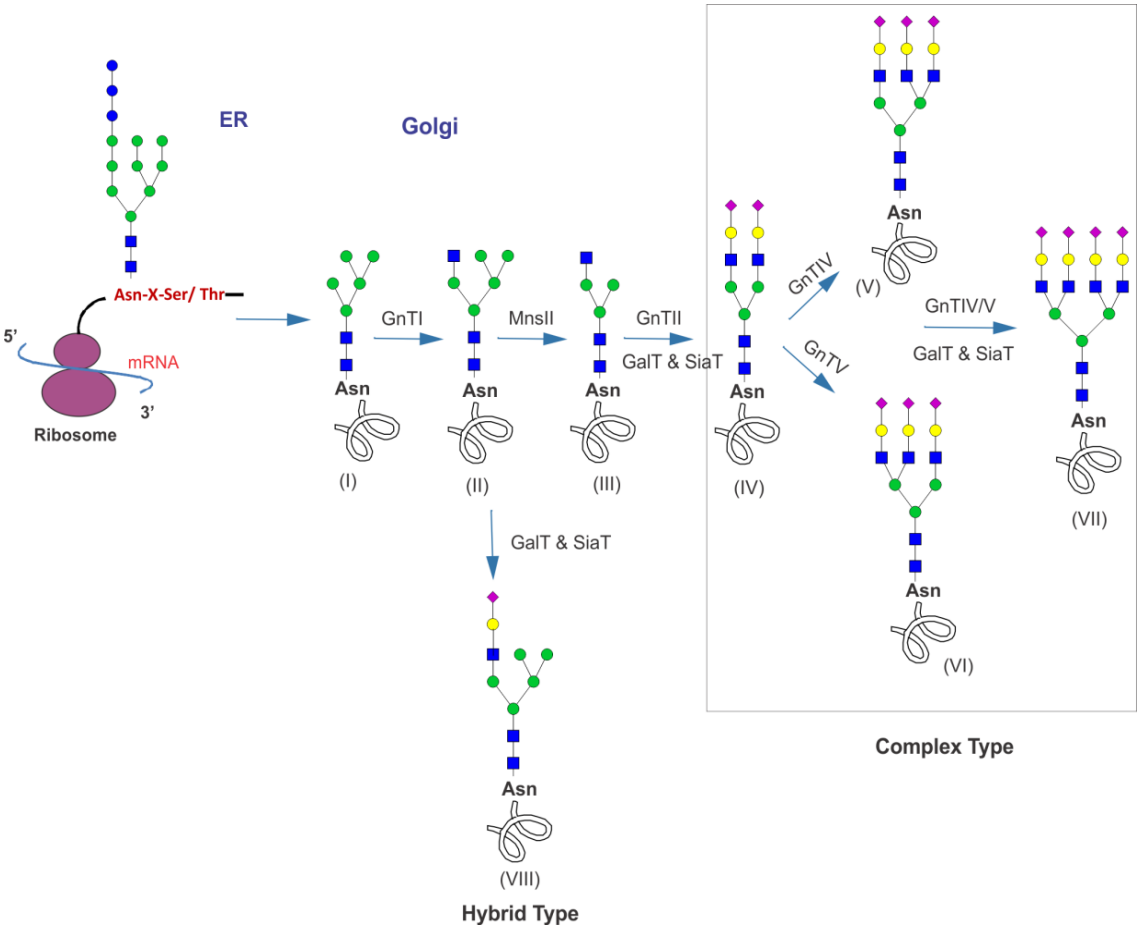

Figure 3.2. Golgi dependent glycan biosynthesis pathway.

Herein we described the efficient chemical and enzymatic syntheses of various hybrid, bi-, tri- and tentraantennary complex type glycans (Fig. 3.3).

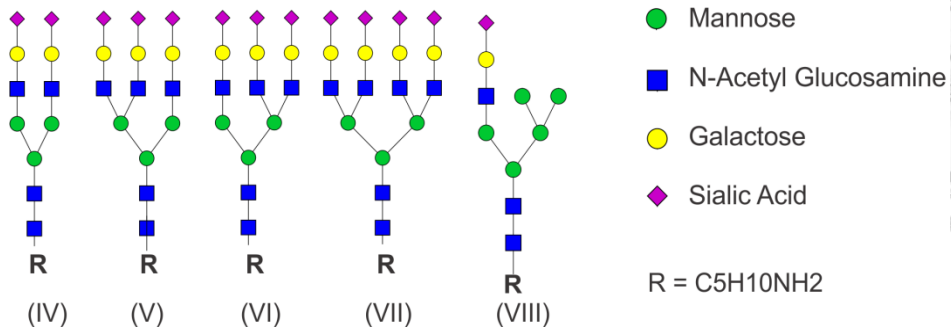

Figure 3.3. Synthetic glycan targets

3.4. Retrosynthesis:

Depicted in Figure 3.3, bi-, tri- and tetra antennary complex and hybrid type glycans are composed of a central trisaccharide core and equipped with one, two, three and four antennae, respectively, with varying degrees of sialylation. The prioritized strategic bond disconnection as means of guiding total chemical synthesis suggested that structure **IV-VIII** could be assembled by conjugation of three building units in two glycosylation events followed by enzymatic sialic acid transfer. Our general synthetic strategy envisioned the double regio- and streoselective glycosylation at 3-O and 6-O positions of core chitobiose trisaccharide with strategically protected D1/D2 arm tri-/pentasaccharide donors. The resultant galactose terminated systems would be then further elaborated by sialyl transferases mediated enzymatic extension to recruit diverse complex structures to our library. Amino pentyl linker at reducing end, aimed at preserving native glycan structure, could also be chemically manipulated for various purpose.

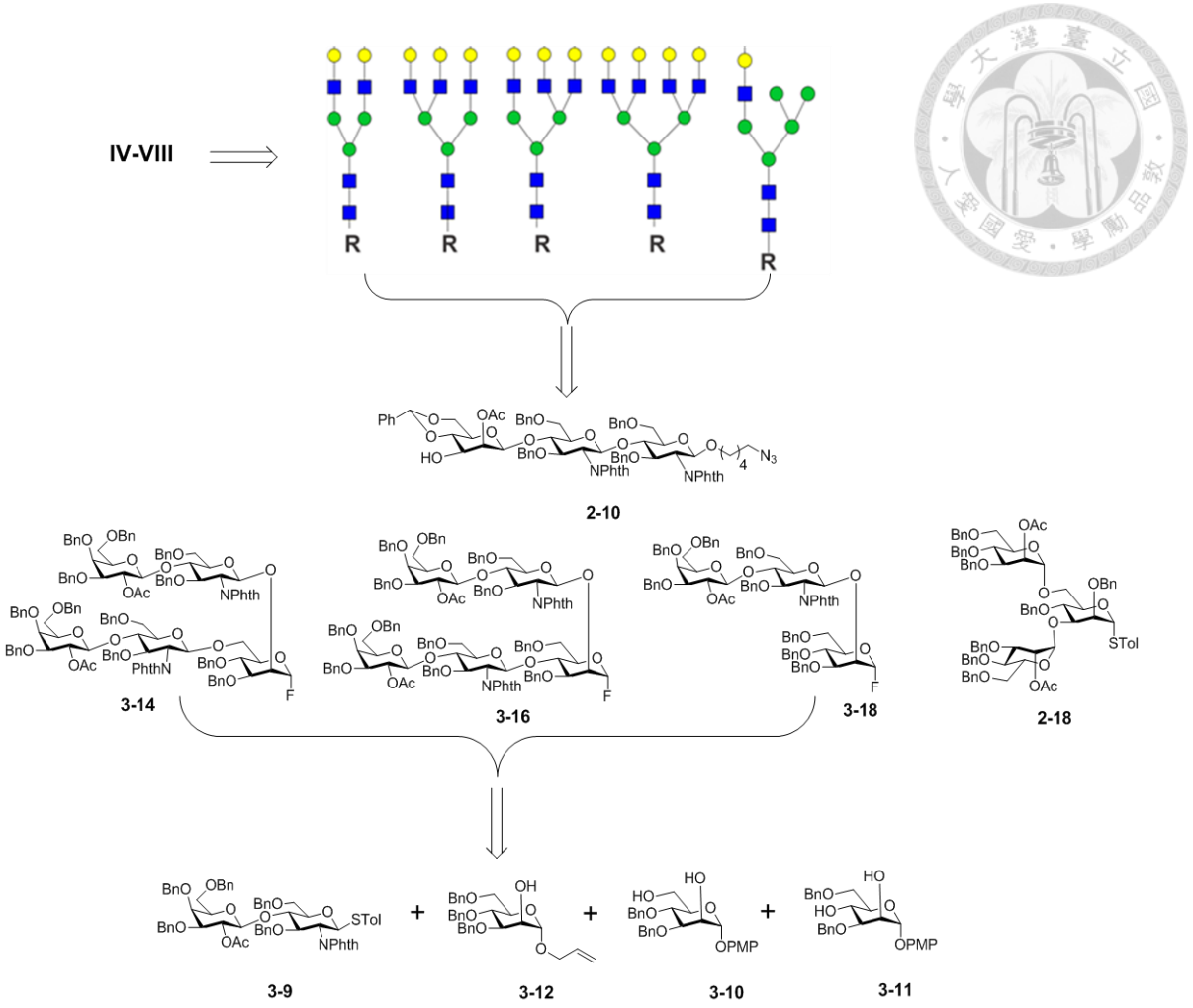

Scheme 3.1. Retro synthetic analysis of hybrid and complex type *N*-glycans.

3.5. Synthesis of D1/D2 Arm Building Blocks:

Building a comprehensive library of synthetic *N*-glycan ligands with each structure obtained from individual steps would be a huge endeavor. Based on the concept of modularizing building blocks for constructing antennae of branched complex type oligosaccharides, a robust and scalable synthesis for the donors was developed. We next tested compatibility of these branched oligosaccharide donors with the double regio- and stereoselective glycosylation with core trisaccharide. The key intermediates were flexibly used to chemically synthesize the most frequent patterns of branched complex type oligosaccharides.

3.5.1. Synthesis of D1/D2 Disaccharides:

Before creating diverse complex type structures, we first focused on truncated versions of hybrid and complex series glycans bearing terminal GlcNAc residues. The inherent difficulty associated with synthesis of complex sugars prompted us to try several approaches. The strategy described in the following section has been adopted because of its robustness and simplicity.

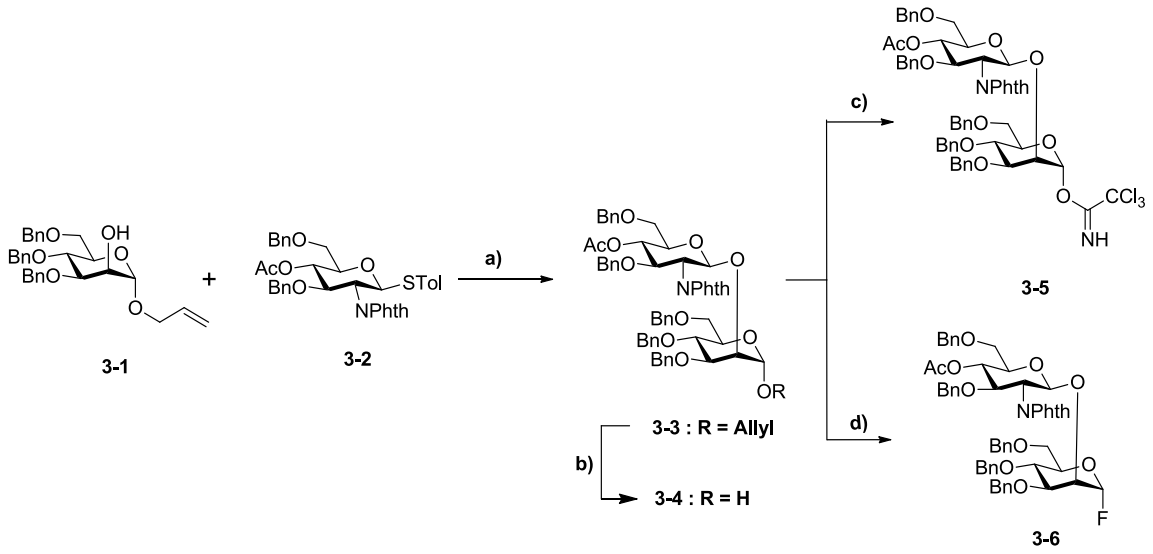

Scheme 3.2 Synthesis of D1/D2 arm disaccharides. a) NIS, TfOH, CH_2Cl_2, 4 Å MS, -40°C, 2 h, 68%; b) $PdCl_2$, MeOH:CH_2Cl_2=1/1, rt, 5 h, 77%; c) DBU, trichloroacetonitrile, CH_2Cl_2 , O°C to RT, 85%; d) DAST, CH_2Cl_2, -30°C to -10°C, 8 h, 61% **.** DBU = 1,8-Diazabicyclo[5.4.0]undec-7-ene

The synthesis of D1/D2 arm disaccharide donors (Scheme 3.2) was commenced with condensation of allyl acceptor **3-1** and thioglycoside donor **3-2** in the presence of NIS/TfOH to obtained desired disaccharide **3-3.** Subsequently, disaccharide **3-3** was de-allylated with $PdCl_2$ in CH_2Cl_2:MeOH. Compound **3-4** was next strategically modified to trichloroacetaimidate **3-5** using trichloroacetonitrile in the presence of DBU and to fluoride **3-6** using DAST**,** depending on the requirements in assembly of more complex sugars.

3.5.2. Synthesis of D1/D2 Tri- and Pentasaccharide:

Based on earlier literature reports, the most challenging phase of complex oligosaccharide synthesis involves installation of highly branched tri- or pentacaccharide antennae at sterically hindered sites on central core. Recently accomplished total synthesis of fully sialylated triantennary *N*-glycan by Danishefsky and coworkers elaborated the intricacy of its assembly. Because of their branched architecture, we first sought to gain

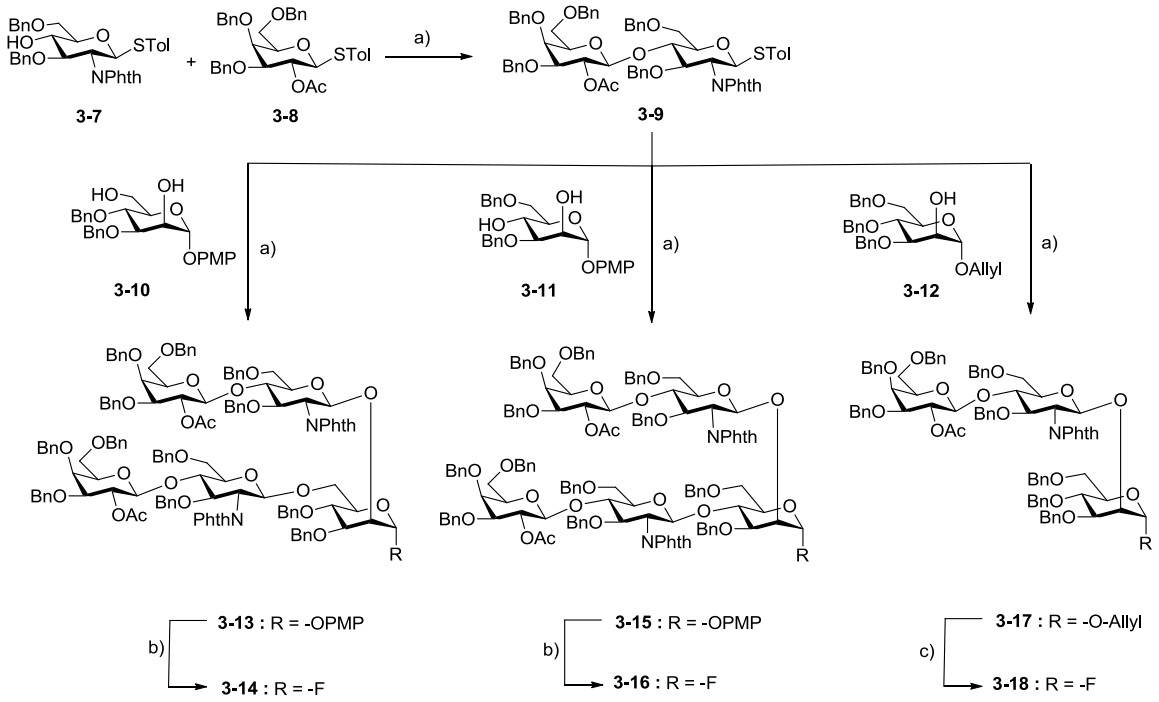

Scheme 3.3 Synthesis of D1/D2 tri- and pentasaccharide. (a) NIS, TMSOTf, 4 Å MS, CH_2Cl_2, -50°C, **3-9**: 82%, **3-13**: 85%, **3-15**: 76%, **3-17**: 72%; (b) (1) CAN, ACN:toluene:H_2O (4:2:1), 1 h, (2) DAST, CH_2Cl_2, -10°C, 1 h, **3-14**: 72%, **3-16**: 69%, over 2 steps; (c) (1) $PdCl_2$, CH_2Cl_2:MeOH (1/1), 3 h; (2) DAST, CH_2Cl_2, -10°C, 1 h , 76% over 2 steps. NIS: N-iodosuccinimide; TMSOTf: trimethylsilyl trifluoromethanesulfonate; CAN: cerium ammonium nitrate; DBU: 1,8-Diazabicyclo[5.4.0]undec-7-ene; CCl_3CN: trichloroacetonitrile; DAST: diethylaminosulfur trifluoride.

access to antennae **3-14**, **3-16,** and **3-18**. The synthesis of key intermediate **3-9**, commenced with NIS/TMSOTf catalyzed coupling of glucosamine **3-7** and properly functionalized

galactosyl thioglycoside donor **3-8,** requisite for the complete *β*-selectivity (Scheme 3.3). Condensation of disaccharide donor **3-9** with **3-10**, **3-11,** and **3-12** under the promotion of NIS and TMSOTf provided pentasaccharides **3-13**, **3-15** and trisaccharide **3-17**, respectively, in excellent yields. It is noteworthy that the disaccharide **3-9**, without further manipulation, can directly act as a donor for single or double glycosylations to facilitate the assembly of antennae in just two glycosylation events starting from desired monosaccharide building blocks. Anticipating upcoming difficulties associated with imidate donors while incorporation of antennae to core, D1/D2 arm building blocks **3-13**, **3-15** and **3-17** were transformed into anomeric fluorides. The syntheses of glycosyl fluorides **3-14**, **3-16** and **3-18** were approached through exposure of anomeric -OH to DAST.

3.6. Assembly of Hybrid and Complex Type Oligosaccharides:

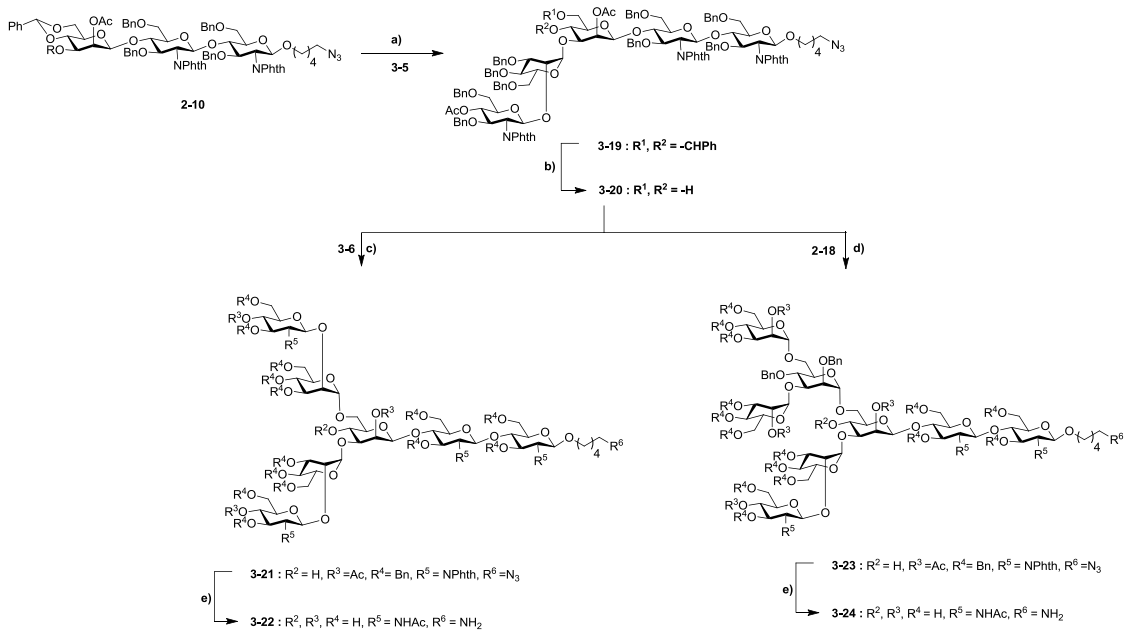

Scheme 3.4: Reagents and Conditions. a) $BF_3.OEt_2$, CH_2Cl_2, 4 Å MS, -40^oC, 2 h, 63%; b) *p*TsOH, CH_3CN, 5 h, 78%; c) AgOTf, Cp_2HfCl_2, Toluene, 4 Å MS, -40°C, 4 h, 55%; d) $(BrC_6H_4)_3NSbCl_6$, CH_3CN, 4 Å MS, -10^oC to RT, 4 h, 55%; e) i) $NH_2CH_2CH_2NH_2$, nBuOH, 90^oC, overnight; ii) Ac_2O, pyridine, overnight; iii) NaOMe, MeOH, overnight; iv) $Pd(OH)_2$, MeOH:H_2O:HCOOH (5:3:2), H_2; **3-22**: 29%; **3-24** : 26%.

The analysis of recombinant gp120 suggested the existence of oligomannose together with hybrid and complex type glycans, which are proposed to exist in discrete domain on protein surface. In an attempt to obtain the access to all naturally occurring and unnatural forms of hybrid and complex type structures, we developed a unified strategy by using shared building blocks to reduce synthetic efforts.

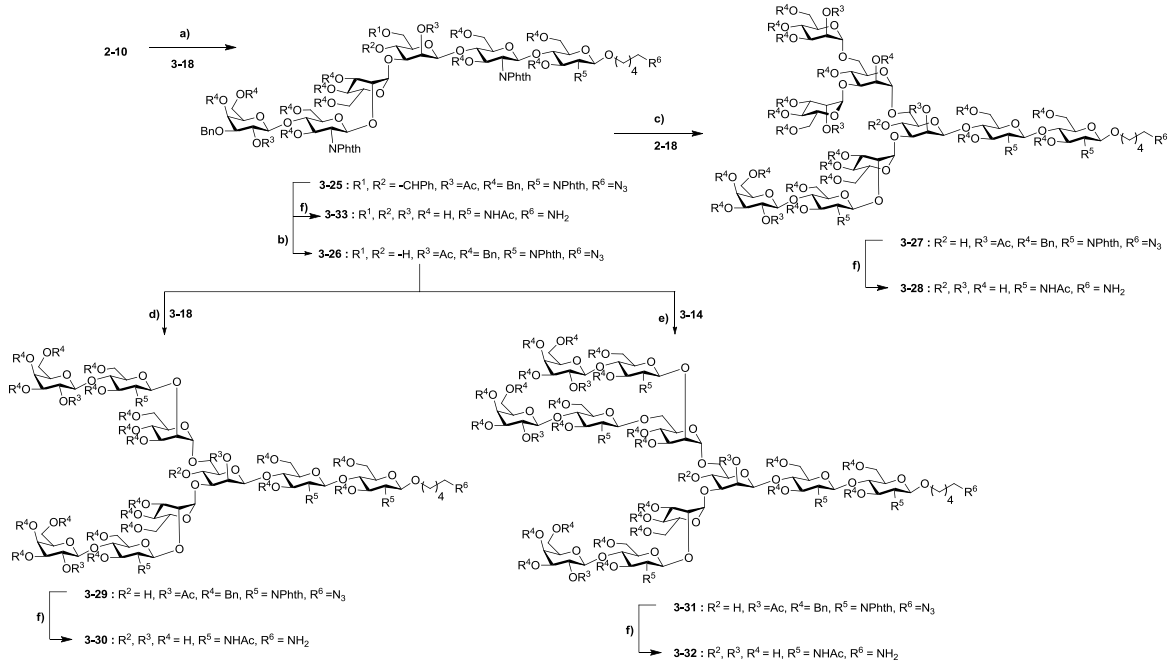

Scheme 3.5. Reagents and Conditions. a) AgOTf, Cp_2HfCl_2, Toluene, 4 Å MS, -40°C, 4 h, 63%; b) *p*TsOH, CH_3CN, 5 h, 78%; c) $(BrC_6H_4)_3NSbCl_6$, CH_3CN, 4 Å MS, -10°C to RT, 4 h, 55%; d) AgOTf, Cp_2HfCl_2, 4 Å MS, toluene, -40°C, 3 h, 69%; e) AgOTf, Cp_2HfCl_2, 4 Å MS, toluene, -40°C, 2 h, 51%; f) (1) $NH_2CH_2CH_2NH_2$, nBuOH, 90°C, overnight; (2) Ac_2O, pyridine, overnight; (3) NaOMe, MeOH, overnight; (4) $Pd(OH)_2$, MeOH:H_2O:HCOOH (5:3:2), H_2, **3-28**: 62%; **3-30**: 60%; **3-32**: 39%; **3-33**: 50%.

The synthesis begins with truncated versions containing GlcNAc residue at the termini. Condensation of core acceptor **2-10** with imidate **3-5** catalyzed by $BF_3.OEt_2$ afforded pentasaccharide **3-19** in 65% yield (Scheme 3.4). Reductive benzilidine opening using p-toluene sulfonic acid resulted in diol **3-20,** which acted as a common precursor for further glycosylation with two different glycosyl donors. For complex series glycan, diol **3-20** was selectively glycosylated at 6'-O position with fluoride **3-6** in presence of

$AgOTf/Cp_2HfCl_2$. Similarly for hybrid series glycans, trimannosyl thioglycoside donor **2-18** was condensed with **3-20** to afford octasaccharide **3-23** in a respectable yield. Final deprotection of **3-21** and **3-23** provided fully deprotected sugars **3-22** and **3-24**, respectively. The synthesis of galactose terminated hybrid series **3-28** and related complex series bi- **3-30**, and triantennary **3-31** type structures has been shown in scheme 3.5.

Stereoselective installation of trisaccharide antenna **3-18** at 3-O position of chitobiose acceptor **2-10** was performed under the promotion of $AgOTf/Cp_2HfCl_2$ to afford hexasaccharide **3-25**. The *p*-toluene sulfonic acid mediated reductive ring opening of **3-25** provided diol **3-26.** Considering the higher reactivity of primary hydroxyl**, 3-25** was further glycosylated at 6-O position with trimannosyl thioglycoside **2-18** and activated by the stable radical cation tris(4-bromophenyl) ammoniumyl hexachloroantimonate to afford nonasaccharide **3-27**. With compounds **3-27** and **3-25** in hand, a series of functional group transformations were carried out to afford desired fully deprotected glycan **3-28** and **3-33**. Next, diol **3-26** was subjected to regioselective glycosylation at 6'-O position with tri- **2-18** and pentasaccharide **2-14** donors to afford corresponding glycans **3-29** and **3-31**, which upon global deprotection provided nonasaccharide **3-30** and tri-undecasaccharide **3-31**. The stereochemistry of all the glycosidic linkages was confirmed by careful NMR analysis.

After establishing effectiveness of the strategy, we turned our attention to highly branched tetra-antennary glycans. The preparative routes for undeca- and tri-decasaccharide derivatives are depicted in scheme 3.6. Regioselective 3-O glycosylation of **2-10** with **3-16** was catalyzed by Cp_2HfCl_2 /AgOTf to furnish desired octasaccharide **3-34** in 68% yield. Compound **3-34** was undergone reductive ring opening in the presence of *p*-toluene sulfonic acid to afford diol **3-36**. Exploiting higher reactivity of secondary -OH, compound **3-36** was condensed with **D2** arm tri- **3-18** and pentasaccharide **3-14** under the agency of Cp_2HfCl_2 /AgOTf to afford the triantennary **3-37** and tetra-antennary **3-39** glycans in satisfactory yields. Final deprotection of compounds **3-37** and **3-39** afforded glycans **3-38** and **3-40**. Throughout the above-mentioned protocols, we effectively reduced the synthetic efforts by utilizing a versatile glycosyl fluoride donor and exclusive glycosylation condition (Cp_2HfCl_2 /AgOTf) to prepare multiple target products.

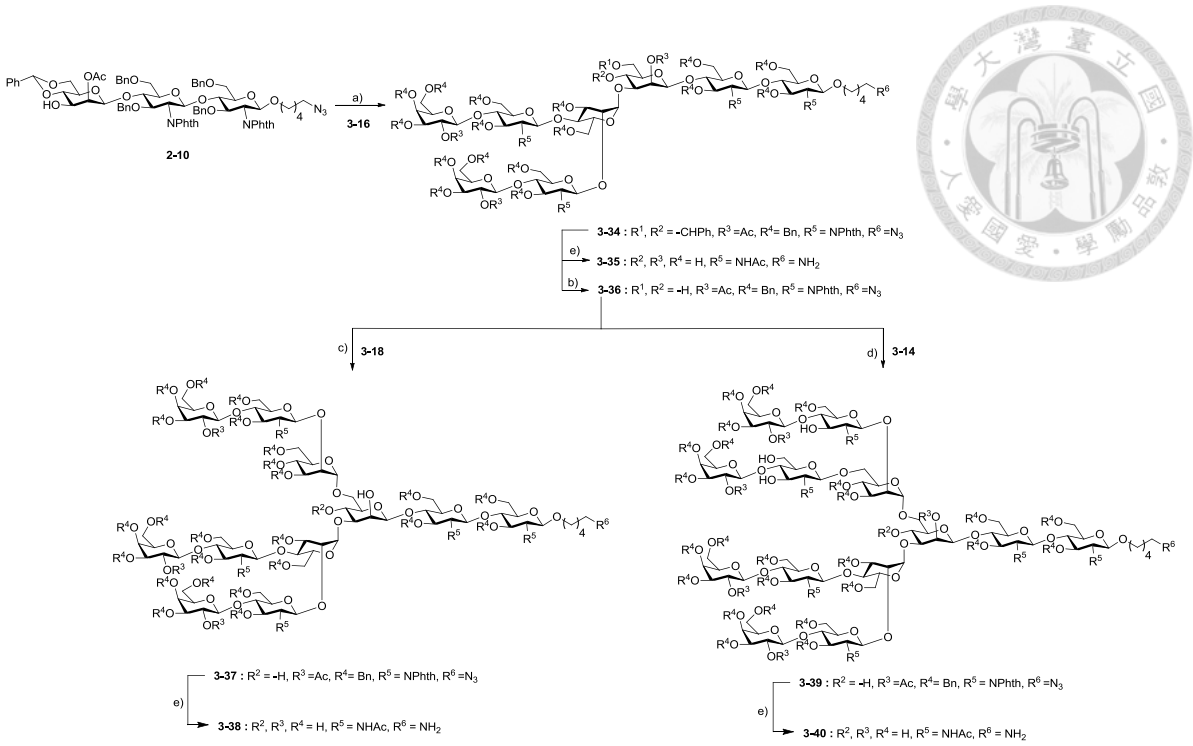

Scheme 3.6.: Reagents and Conditions: (a) AgOTf, Cp_2HfCl_2, 4 Å MS, toluene, -50° to -30°C, 2 h, 68%; (b) *p*-TSA, acetonotrile, rt, 8 h, 72%; (c) AgOTf, Cp_2HfCl_2, 4 Å MS, toluene, -40°C, 3 h, 64%; (d) AgOTf, Cp_2HfCl_2, 4 Å MS, toluene, -50°C to -30°C, 2 h, 73%; (e) (1) $NH_2CH_2CH_2NH_2$, nBuOH, 90°C, overnight; (2) Ac_2O, pyridine, overnight; (3) NaOMe, MeOH, overnight; (4) $Pd(OH)_2$, MeOH:H_2O:HCOOH (5:3:2), H_2, **3-35**: 51%; **3-38**: 37%; **3-40**: 27%.

3.7. Enzymatic Sialylation of Hybrid and Complex Type Glycans:

Sialic acids are important components of carbohydrate chains and are usually found on the terminal position of the carbohydrate moiety of glycoconjugates, including glycoproteins and glycolipids. The chemical installation of sialic acid-containing antennae in assembly of complex oligosaccharides is particularly challenging due to the presence of hindered and charged anomeric center and lack of participating group to achieve desired stereochemistry[12]. As a result, chemoenzymatic methods of sialylation, well demonstrated by Paulson, Wong and coworkers[13] through landmark enzymatic synthesis of sLe^x, are particularly important[14]. Sialyltransferases transfer *N*-acetylneuraminic acid (Neu5Ac) from the common donor substrate, cytidine 5'-monophospho-*N*-acetylneuraminic acid (CMP-

Neu5Ac), to acceptor substrates. Thus, sialyltransferases are considered to be important enzymes in the field of glycobiology.

To date, a list of sialyltransferases have been isolated from various sources including mammalian, bacterial and viral sources. In general, bacterial enzymes are more stable and productive in *Escherichia coli* protein expression system, and bacterial glycosyltransferases have broader acceptor-substrate specificity than mammalian-derived enzymes. Yamamoto and coworkers have reported that α-2,3-sialyltransferase from Vibrio sp. bacterium JT-FAJ-16[15] and α-2,6-sialyltransferase from photobacterium sp. JT-ISH-224[16] has very broad acceptor specificity, excellent productivity, high specific activity and no intrinsic sialidase activity. The unique properties of these sialyltranferases present a powerful tool to construct the library of α-2,3/2,6 sialosides.

3.7.1. Synthesis of Sialylated Hybrid Type Glycans:

Hybrid Glycans **3-33** and **3-28** with galactose terminal were subjected to sialylation using α–2,6-sialyltransferase for 2 days and α–2,6-sialyltransferase for 4 days to afford the desired fully sialylated glycans.

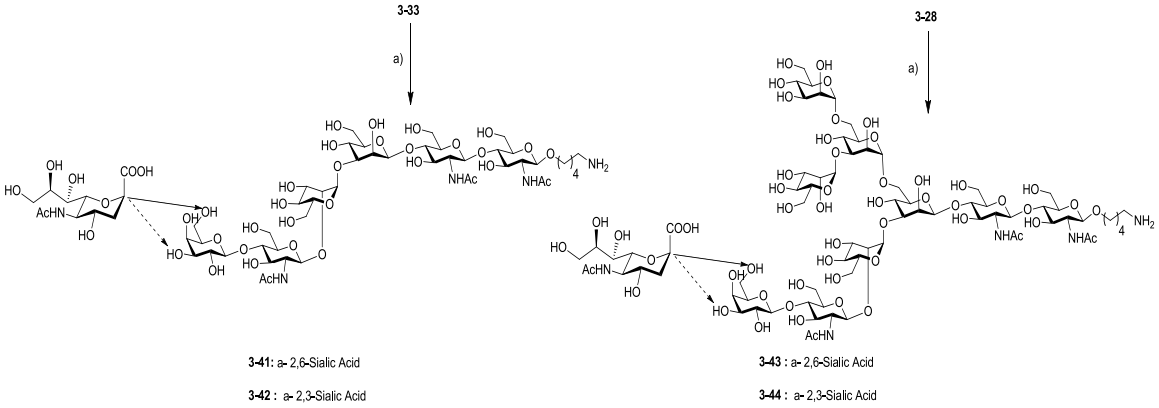

Scheme 3.7. Reagents and Conditions. a) CMP-*β*-D-Sialic acid, α-2,6/2,3-sialyltransferase, alkaline phosphatase, **3-41**: 71%; **3-42**: 68%; **3-43** : 60%; **3-44**: 56%.

3.7.2. Synthesis of Sialylated Bi-antennary Complex Type Glycans:

Bi-antennary complex series glycans **3-30** and its unnatural form **3-35** were treated with α–2,6-sialyltransferase for 2 days and α–2,3-sialyltransferase for 8 days to afford the

desired fully sialylated glycans. However, glycan **3-30** also provided mono sialylated glycans **3-47** and **3-48** on one of the two antennae.

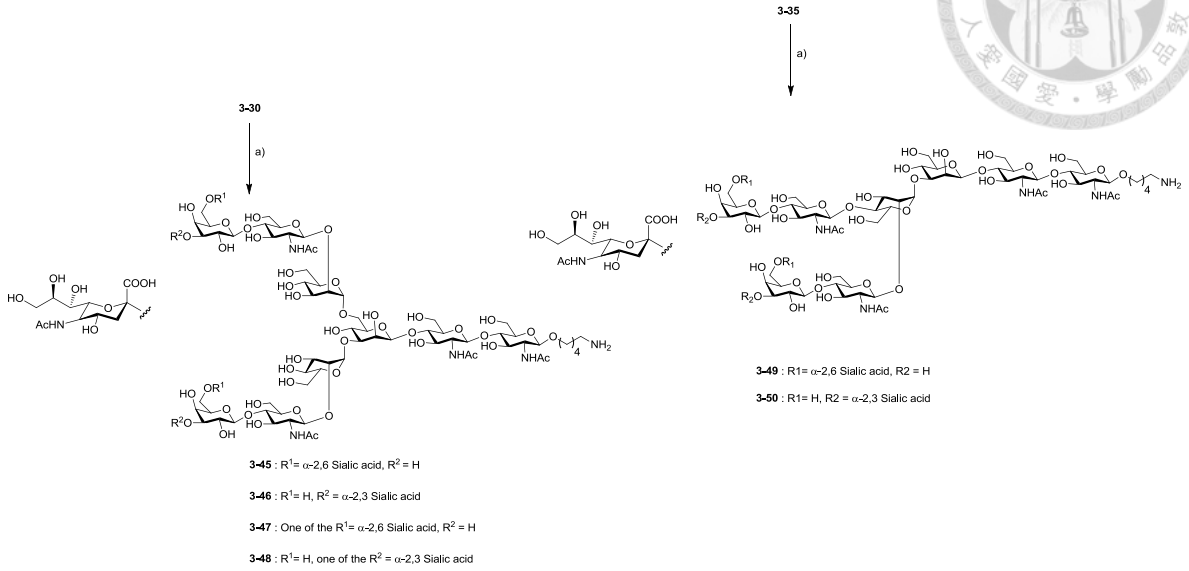

Scheme 3.8 Reagents and Conditions. a) CMP-*β*-D-Sialic acid, α-2,6/2,3-sialyltransferase, alkaline phosphatase, **3-45**: 72%; **3-46**: 75%; **3-47**: 45%; **3-48**: 30%; **3-49** : 55%; **3-50**: 70%.

3.7.3. Synthesis of Sialylated Tri-Antennary Complex Type Glycans:

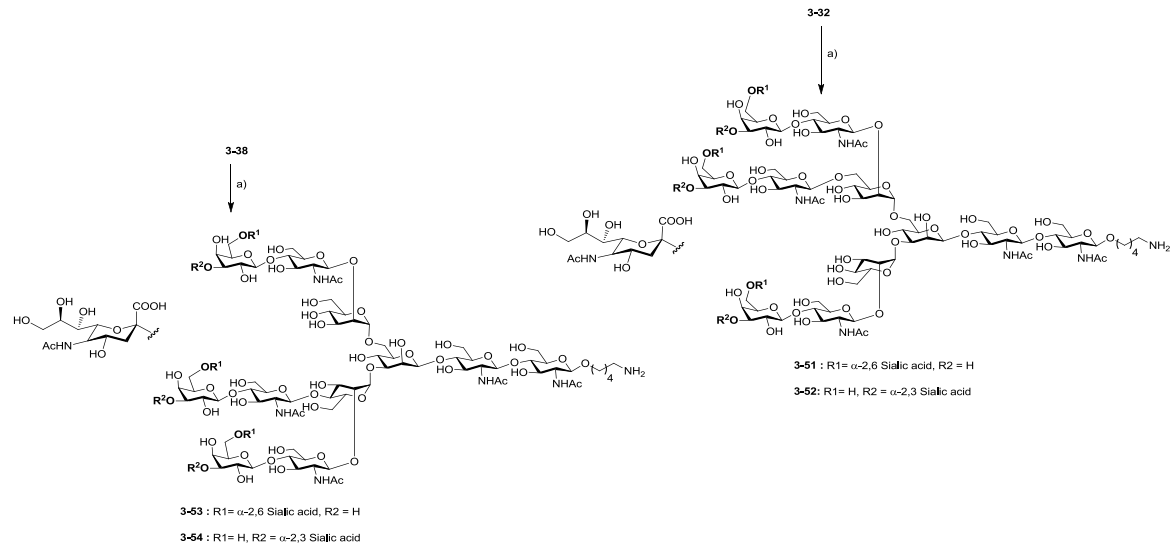

Scheme 3.9 : Reagents and Conditions. a) CMP-*β*-D-Sialic acid, α-2,6/2,3-sialyltransferase, alkaline phosphatase, **3-50**: 66%; **3-51** : 67%; **3-52**: 64%; **3-53**: 66%.

Two glycoforms of tri-antennary complex series glycans **3-32** and **3-38** were treated with α–2,6-sialyltransferase for 2 days and α–2,3-sialyltransferase for 8 days to obtain desired glycans **3-51**, **3-52**, **3-53** and **3-54**, respectively.

3.7.4. Synthesis of Sialylated Tetra-Antennary Complex Type Glycans:

Tetra-antennary complex series glycan **3-40** was treated with α–2,6-sialyltransferase for 2 days and 2,3-sialyltransferase for 8 days to obtain desired glycans **3-55** and **3-56**, respectively.

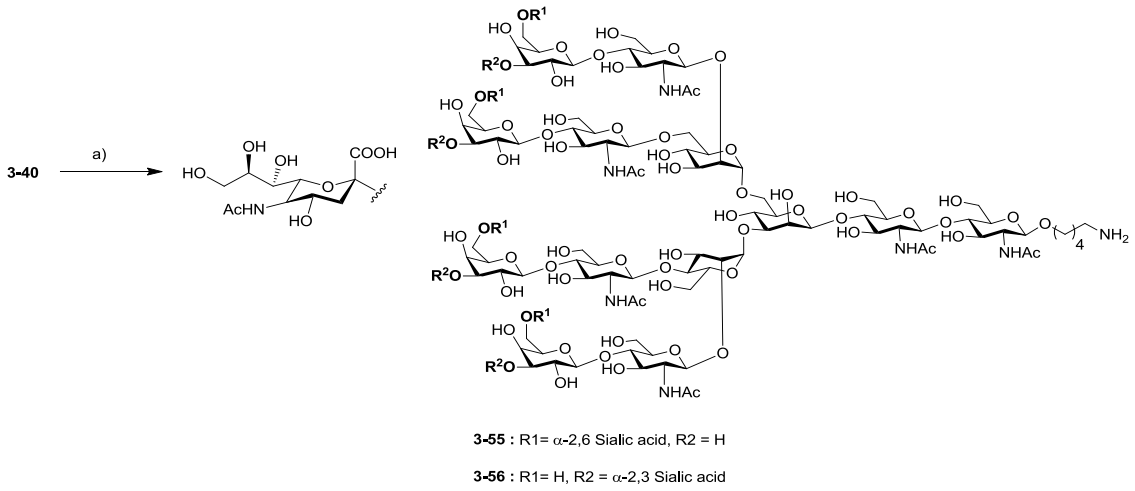

Scheme 3.10. Reagents and Conditions. a) CMP-*β*-D-Sialic acid, α-2,6/2,3-sialyltransferase, alkaline phosphatase, **3-55**: 66%; **3-56**: 67%.

3.8. Applications to Biology:

A series of hybrid **3-28**, **3-42**, **3-43**, bi-antennary complex **3-30**, **3-44**, **3-45, 3-46, 3-47,** tri-antennary **3-32**, **3-50**, **3-51**, **3-38**, **3-52**, **3-53**, tetra-antennary **3-40**, **3-55**, **3-56,** and unnatural forms **3-33**, **3-40**, **3-41, 3-35**, **3-48**, **3-49** were used for covalent immobilization on NHS coated glass slide to study glycan binding specificity of HIV-1 broadly neutralizing antibodies. The glycans were also used to conjugate carrier protein to study their immune response.

3.9. References :

(1) Hansen, J. E. S.; Nielsen, C. M.; Nielsen, C.; Heegaard, P.; Mathiesen, L. R.; Nielsen, J. O. *AIDS (London, England)* **1989**, *3*, 635.

(2) Leonard, C. K.; Spellman, M. W.; Riddle, L.; Harris, R. J.; Thomas, J. N.; Gregory, T. J. *J. Biol. Chem.* **1990**, *265*, 10373.

(3) Binley, J. M.; Ban, Y. E. A.; Crooks, E. T.; Eggink, D.; Osawa, K.; Schief, W. R.; Sanders, R. W. *J. Virol*. **2010**, *84*, 5637.

(4) Mouquet, H.; Scharf, L.; Euler, Z.; Liu, Y.; Eden, C.; Scheid, J. F.; Halper-Stromberg, A.; Gnanapragasam, P. N. P.; Spencer, D. I. R.; Seaman, M. S.; Schuitemaker, H.; Feizi, T.; Nussenzweig, M. C.; Bjorkman, P. J. *Proc. Natl. Acad. Sci. U.S.A.* **2012**, *109*, E3268.

(5) Pancera, M.; Yang, Y. P.; Louder, M. K.; Gorman, J.; Lu, G.; McLellan, J. S.; Stuckey, J.; Zhu, J.; Burton, D. R.; Koff, W. C.; Mascola, J. R.; Kwong, P. D. *PloS one.* **2013**, *8*.

(6) Zhu, X. G.; Borchers, C.; Bienstock, R. J.; Tomer, K. B. *Biochemistry.* **2000**, *39*, 11194.

(7) Calarese, D. A.; Scanlan, C. N.; Zwick, M. B.; Deechongkit, S.; Mimura, Y.; Kunert, R.; Zhu, P.; Wormald, M. R.; Stanfield, R. L.; Roux, K. H.; Kelly, J. W.; Rudd, P. M.; Dwek, R. A.; Katinger, H.; Burton, D. R.; Wilson, I. A. *Science.* **2003**, *300*, 2065.

(8) Julien, J. P.; Sok, D.; Khayat, R.; Lee, J. H.; Doores, K. J.; Walker, L. M.; Ramos, A.; Diwanji, D. C.; Pejchal, R.; Cupo, A.; Katpally, U.; Depetris, R. S.; Stanfield, R. L.; McBride, R.; Marozsan, A. J.; Paulson, J. C.; Sanders, R. W.; Moore, J. P.; Burton, D. R.; Poignard, P.; Ward, A. B.; Wilson, I. A. *PLoS Pathogens.* **2013**, *9*, e1003342.

(9) Pancera, M.; Shahzad-Ul-Hussan, S.; Doria-Rose, N. A.; McLellan, J. S.; Bailer, R. T.; Dai, K.; Loesgen, S.; Louder, M. K.; Staupe, R. P.; Yang, Y.; Zhang, B.; Parks, R.; Eudailey, J.; Lloyd, K. E.; Blinn, J.; Alam, S. M.; Haynes, B. F.; Amin, M. N.; Wang, L. X.; Burton, D. R.; Koff, W. C.; Nabel, G. J.; Mascola, J. R.; Bewley, C. A.; Kwong, P. D. *Nat. Struct Mol. Biol.* **2013.**

(10) (a) Wyatt, R.; Kwong, P. D.; Desjardins, E.; Sweet, R. W.; Robinson, J.; Hendrickson, W. A.; Sodroski, J. G. *Nature.* **1998**, *393*, 705; (b) Choi, B. K.; Bobrowicz, P.; Davidson, R. C.; Hamilton, S. R.; Kung, D. H.; Li, H. J.; Miele, R. G.; Nett, J. H.; Wildt, S.; Gerngross, T. U. *Proc. Natl. Acad. Sci. U.S.A.* **2003**, *100*, 5022.

(11) (a) Mizuochi, T.; Spellman, M. W.; Larkin, M.; Solomon, J.; Basa, L. J.; Feizi, T. *Biochem.* **1988**, *254*, 599; (b) Pabst, M.; Chang, M.; Stadlmann, J.; Altmann, F. *Biol. Chem.* **2012**, *393*, 719.

(12) (a) Schwardt, O.; Visekruna, T.; Rabbani, S.; Ernst, B. *Chimia* **2006**, *60*, 234; (b) Rabbani, S.; Schwardt, O.; Ernst, B. *Chimia.* **2006**, *60*, 23.

(13) Ichikawa, Y.; Lin, Y. C.; Dumas, D. P.; Shen, G. J.; Garciajunceda, E.; Williams, M. A.; Bayer, R.; Ketcham, C.; Walker, L. E.; Paulson, J. C.; Wong, C. H. *J. Am. Chem. Soc.* **1992**, *114*, 9283.

(14) (a) Wong, C. H.; Ichikawa, Y.; Look, G. *Abstr. Pap. Am. Chem. Soc.* 1992, *204*, 1; (b) Yu, H.; Huang, S. S.; Chokhawala, H.; Sun, M. C.; Zheng, H. J.; Chen, X. *Angew. Chem. Int. Ed.* **2006**, *45*, 3938.

(15) Takakura, Y.; Tsukamoto, H.; Yamamoto, T. *J. Biochem.* **2007**, *142*, 403.

(16) Tsukamoto, H.; Takakura, Y.; Mine, T.; Yamamoto, T. *J. Biochem.* **2008**, *143*, 187.

Chapter 4

Carbohydrate Microarray: Synthetic Tools for Glycobiology

After establishing efficient strategy for synthesizing a library of diverse *N*-linked oligosaccharides in chapter 2 and 3, this chapter describes the development of carbohydrate microarray-based platform for profiling glycan binding specificities of HIV-1 broadly neutralizing antibodies isolated from HIV infected donors. The specificity study of HIV-gp120 carbohydrates with bNAbs is important for the development of new therapeutics. Glycan microarray offers a way to determine low affinity protein-carbohydrate interactions through multivalent glycan presentation on its surface.

4.1. Introduction:

In last decade, carbohydrate microarrays have gained considerable recognition for analyzing carbohydrate mediated interactions in a high-throughput fashion[1] (Fig. 4.1). A variety of methods have been utilized to prepare carbohydrate microarrays, including a) technologies that directly utilize underivatized carbohydrates in microarray construction; b) technologies that require chemical modification of carbohydrates before microarray fabrications; c) methods of non-covalent immobilization of carbohydrates; and d) methods of covalent coupling of saccharides on array substrates. There are also technologies that are designed to display saccharides in defined orientations or specific cluster configurations in order to resemble the native configuration of functional carbohydrate ligands.

The birth of modern carbohydrate microarrays in 2002 brought in new high-throughput tools to explore biological information content in glycome through first appearance of three major research articles in scientific literature, including polysaccharide and glycoconjugate microarray by Denong Wang[2], array of synthetic and natural neoglycolipids by Ten Feizi[3] and array of synthetic oligosaccharides in micro titer plate by Wong Chi-Huey[4]. Since then, many elegant methods for the covalent and non-covalent immobilization of glycans and the detection of binding events between carbohydrate and their binding partners on the microarrays have been exploited[5].

Nowadays, carbohydrate microarrays have become the leading tools for functional studies of glycans and glycan binding proteins, because the microarray-based technology has the advantage of a simultaneous assessment of many glycan–protein interactions using small amounts of samples than that was required for a conventional molecular or immunological assay[6]. Moreover, carbohydrate microarrays posses higher detection sensitivity than most traditional carbohydrate analytic tools, such as carbohydrate-specific ELISA and the glycolipid-based "Eastern blot" assays. Another important feature of carbohydrate microarrays is that glycans attached to the solid surface are displayed in a multivalent fashion to form multivalent interactions, which can facilitate the determination of problematic low affinity protein-carbohydrate interactions[7].

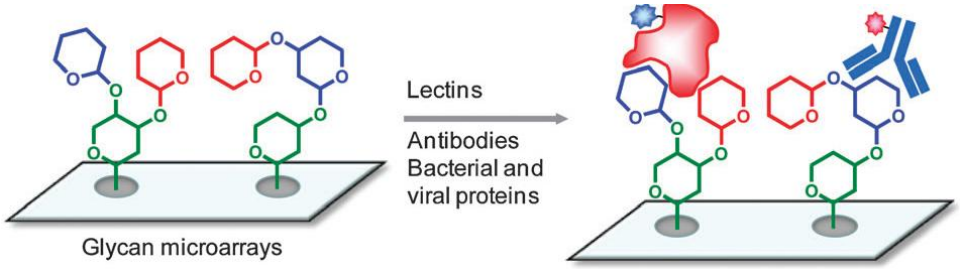

Figure 4.1. Glycan microarray for high-throughput analysis of glycan-protein interactions**.**

4.2. Design and Construction of Glycan Microarray:

One of the key aspects of successful glycan microarrays is the availability of large and diverse oligosaccharide libraries. Because of their intrinsic physiochemical properties, carbohydrates are capable of generating huge structural diversity in a multitude of ways. In addition, depending on the source of glycans (e.g. synthetic or naturally isolated), proper functionalization at reducing end and efficient immobilization on surface are particularly important factors. Although a variety of immobilization methods have been reported over the past decade, there are many practical issues to take into consideration when constructing glycan microarrays, and one approach might not be superior to another[7].

One of the routinely used strategies for covalent glycan immobilization on the array surface is to install a small chain spacer bearing reactive groups (-NH_2 or -SH) at the anomeric position of oligosaccharides. In particular, the Consortium of Functional Glycomics (CFG) hold a comprensive set of more than 600 oligosaccharides with primary

amine functionality at reducing end covalently attached to N-hydroxysuccinimde derivatized glass surface (Fig. 4.2).

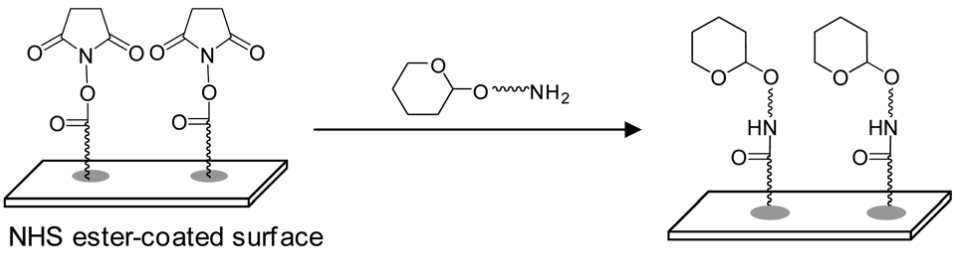

Figure 4.2. Covalent attachment of amine-linked sugars to the NHS ester-coated surface.

Based on glycan microarrays, experimental characterization of the binding events between glycans and glycans binding proteins (GBPs), anti-carbohydrate antibodies, and lectins etc typically involves (1) labeling GBPs directly with fluorescent reagents before incubation with the microarrays, (2) labeling GBPs with biotin before the incubation and detecting the captured GBPs after the incubation using fluorescently labeled streptavidin, or (3) detecting the captured GBPs after the incubation using fluorescently labeled antibodies raised against the GBPs. However, the most common approach involves detection of fluorophore-labeled proteins/antibody directly or indirectly bound to glycans on the surface by using a fluorescence scanner (Fig. 4.3).

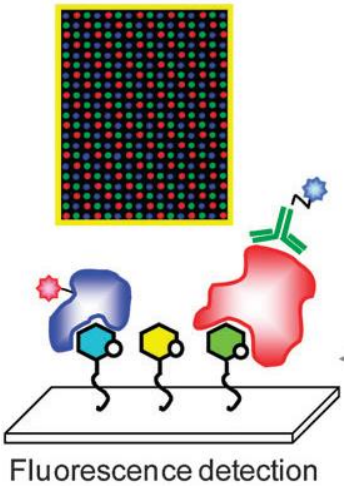

Figure 4.3. Detection of binding events of fluorophore-labeled proteins to glycans on microarrays can be monitored by using a fluorescence scanner.

4.3. Next Generation Array on Aluminum Oxide Coated Glass Slide:

A fundamental problem of carbohydrate microarray technology is the characterization and quantification of the oligosaccharides that are covalently bound to the surface. Effective immobilization of sugars on the surface is essential for surviving consecutive substrate washing when evaluating sugar–protein binding. Mass spectrometry (MS) has been reported to be a useful analytical method for the high-throughput characterization of immobilized sugars on porous glass slides. Most commercially available substrates for glycan arrays, including glass and polyethylene terephthalate (PET) coated with amine, carboxylate, N-hydroxysuccinimide (NHS), avidin, epoxy, aldehyde, and chelating nickel groups etc., are not suitable for direct mass spectrometric analysis[8].

Our group has demonstrated the aluminum oxide coated-glass slide (ACG) microarray, to be very efficient for covalent immobilization of phosphonic acid ended glycans in very short incubation time[9]. ACG seemed advantageous over known array platforms in terms of signal intensity and sensitivity, perhaps due to the surface properties, surface morphologies, and binding site architecture between antibody and immobilized glycan[9]. The unique properties of ACG slides include :

- The metal oxide layer on the surface can be activated for grafting organic compounds such as oligosaccharides modified with phosphonic acid liner;
- The surface remains electrically conductive, and the grafted oligosaccharides can be simultaneously characterized by mass spectrometry and carbohydrate-binding assay; and
- The slides are more sensitive than transparent glass slides in binding analysis.

For HIV-1 vaccine perspective, several neutralizing antibodies such as PG9, PG16, and some PGT series antibodies such as PGTs141-145 were shown to interact with carbohydrates on HIV-1 spike; however, their exact glycan specificities using microarray have not been reported yet. To investigate these unknown specificities, we utilized a improved version of an array of ***N***-glycans on aluminium oxide coated glass.

4.4. Synthetic Oligosaccharides for Microarray Studies:

The synthetic *N*-linked oligosaccharides **1-31** (Fig. 4.4), effectively produced by using the chemo/enzymatic methods as described in chapter 2 and 3 were used for covalent immobilization on N-hydroxy succinimide coated glass slide through amide bond formation. To demonstrate the efficiency of ACG slide, oligosaccharides needs to undergo functional group transformation from amine to phosphonic acid for covalent attachment on aluminium oxide coated glass slide through phosphonate chemistry. Due to limited supply of oligosaccharides structures, we selected 11 representative examples of high mannose, hybrid and complex type. As described in scheme 4.1, two-step conversion of sugars **2-22**, **2-27**, **2-30**, **2-32**, **2-35**, **2-48**, **3-33**, **3-28**, **3-41**, **3-44**, **3-45** with amine tail into phosphonic acid tail was performed to obtain a set of 11 oligosaccharides for microarray studies (Fig. 4.5).

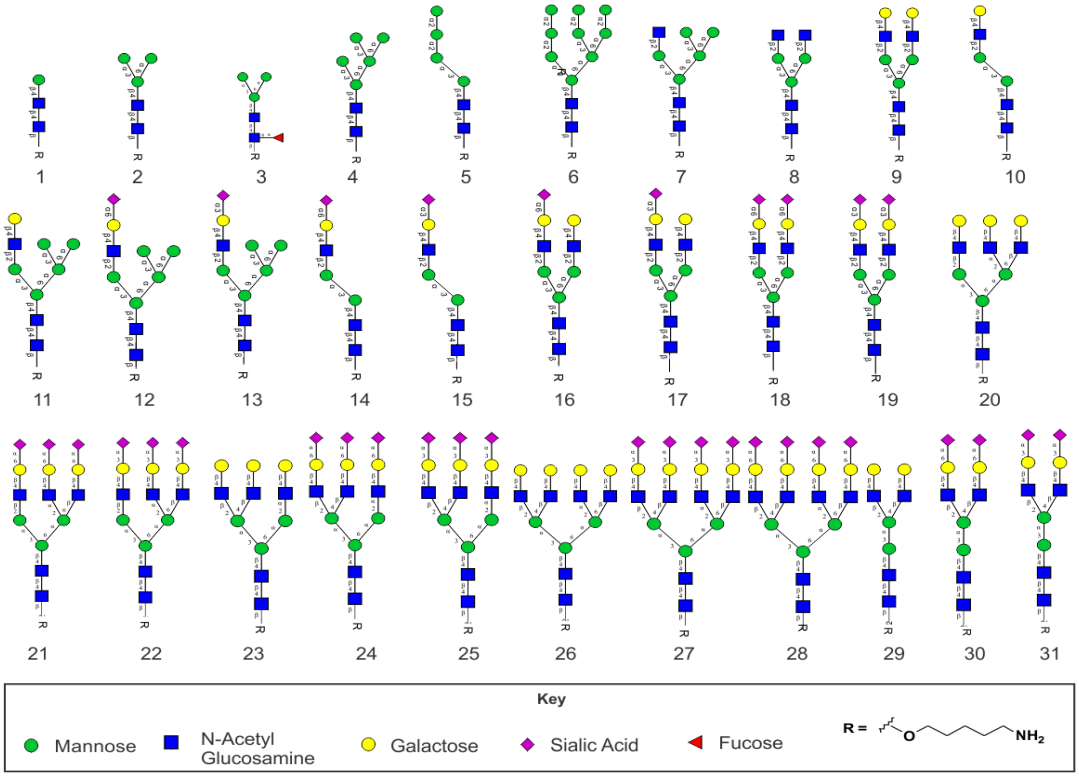

Figure 4.4. Pictorial presentations of *N*-linked oligosaccharides used for covalent immobilization on NHS coated glass slide.

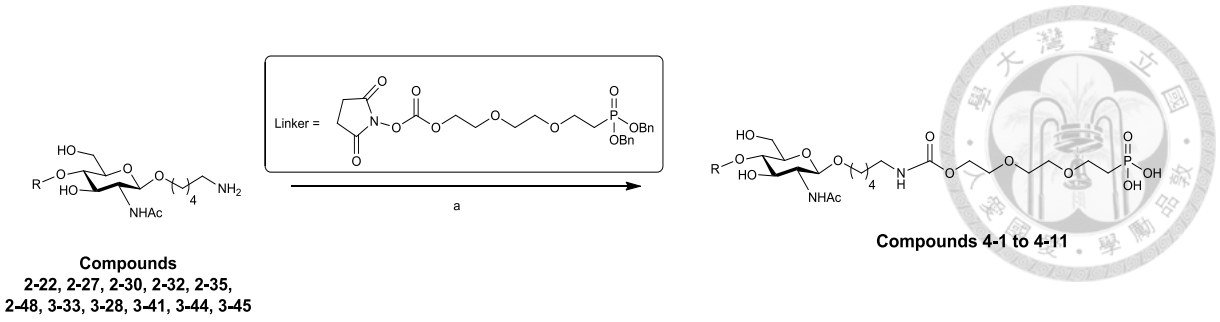

Scheme 4.1. Preparation of sugars with phosphonic acid linker. a, (1) Linker, DMF, r t, 5h; (2) $Pd(OH)_2$, H_2O, room temperature, overnight.

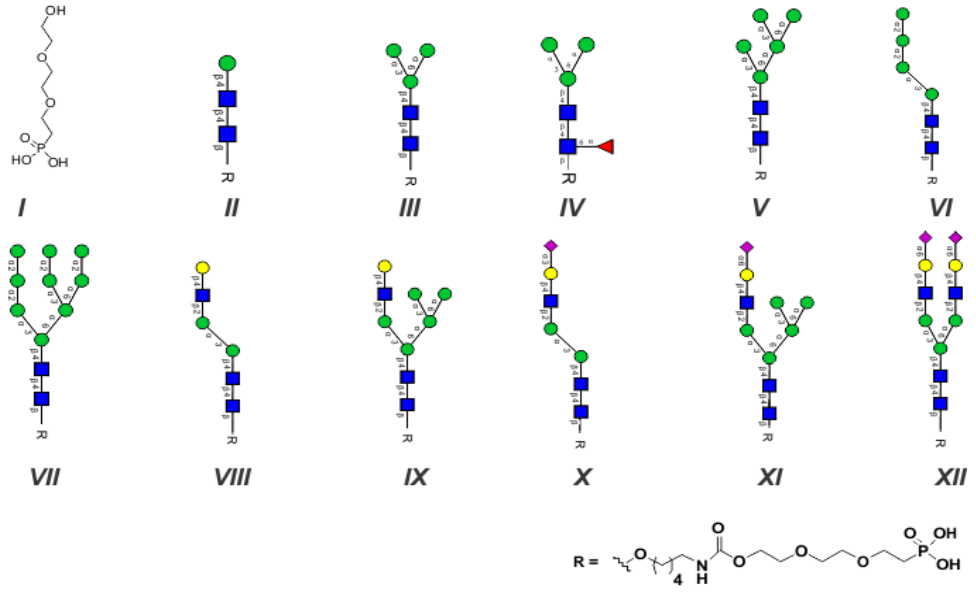

Figure 4.5. Pictorial representation of *N*-glycan structures used for microarray study of aluminium oxide coated glass slide.

4.5. Microarray Analysis

4.5.1. Fabrication:

Figure 4.6 shows a schematic drawing of the fabrication of anodized aluminum oxide (AAO) glass substrate. Approximately 300 nm of aluminum has been coated on glass slide (1 x 75.5 x 24.5 mm) using E-Beam VDP coater by the Thin Film Technology Division, Instrument Technology Research Center at National Applied Research Laboratories, (Hsinchu Science Park, Hsinchu, Taiwan, R.O.C.). Right after coating, the Al-coated slides were immediately packed (one slide per container) and vacuum sealed in air-tight laminated

foil pouches until the moment for surface anodization. Surface anodization of the aluminum coated glass slide has been conducted in-house via electrochemical reaction in 0.3 M oxalic acid aqueous solution in a 4^{o}C chamber. Anodization reaction was controlled by voltage and reaction time. Under proper reaction conditions, a layer of approximately 50 to 65 nm (in thickness) of smooth anodized aluminum oxide (AAO) can be grown consistently on top of aluminum coated glass slide.

All monovalent glycans were prepared in 10mM concentration individually and served as mother solutions, which are to be diluted with printing buffer to prepare working solutions. Microarrays were printed (BioDot Cartesian Technologies) by robotic pin (SMP3: TeleChem International) deposition of ~ 0.6nL of 100 µM concentration of amine-containing glycans **1-31** (Fig. 4.4) in printing buffer from a 384 well plate onto NHS-coated glass slides purchased from SCHOTT (Nexterion H) and of phosphonic acid containing glycans **I-XII** (Fig. 4.5) onto ACG slide (preparation as described above). Printed slides were allowed to react in an atmosphere of 80% humidity for an hour followed by desiccation overnight. These slides were designed for 16 grids in one slides, and stored at room temperature in a desiccator prior to use. Before the binding assay, these slides were blocked with blocking solution for 3h (blocking is not necessary for ACG slides). The slides were then washed with PBST-BSA buffer prior to use. Unless otherwise stated, reagents were obtained from commercial suppliers and used without purification. All aqueous solutions were prepared from distilled de-ionized water filtered with a Milli-Q purification system and sterile filtered through a 0.2µm filter. Buffers used in the experiment include the printing buffer (pH 8.5, 300mM phosphate buffer containing 0.05% (v/v) Tween-20), the blocking buffer (superblock blocking buffer in PBS, Pierce), the washing buffer (PBST buffer; PBS and 0.05% Tween-20) and the binding buffer (PBST-BSA Buffer; PBST buffer and 3% BSA). Printing buffer, blocking buffer, and binding buffer were prepared freshly before use.

4.5.2. Antibody Binding Assay :

Antibodies PG9, PG16 and PGTs 121, 128, 141-145 were diluted by binding buffer to 100ug/mL prior to use. DyLight649-conjugated Donkey Anti-Human IgG antibody was then pre-complexed with primary antibodies. Final concentration of the precomplexed

solution was adjusted to 50ug/mL with binding buffer. The printed glass slide was assembled into FAST® frame slide holder (Whatman®), and 80uL of precomplexed antibody solution was applied to each well accordingly. The antibody binding process was maintained in 4^0C with gentle shaking and then antibody solutions were carefully pipetted out after 6 hours incubation. The slides were gently washed by 100uL PBST washing buffer and then spin-dried for 3 minutes.

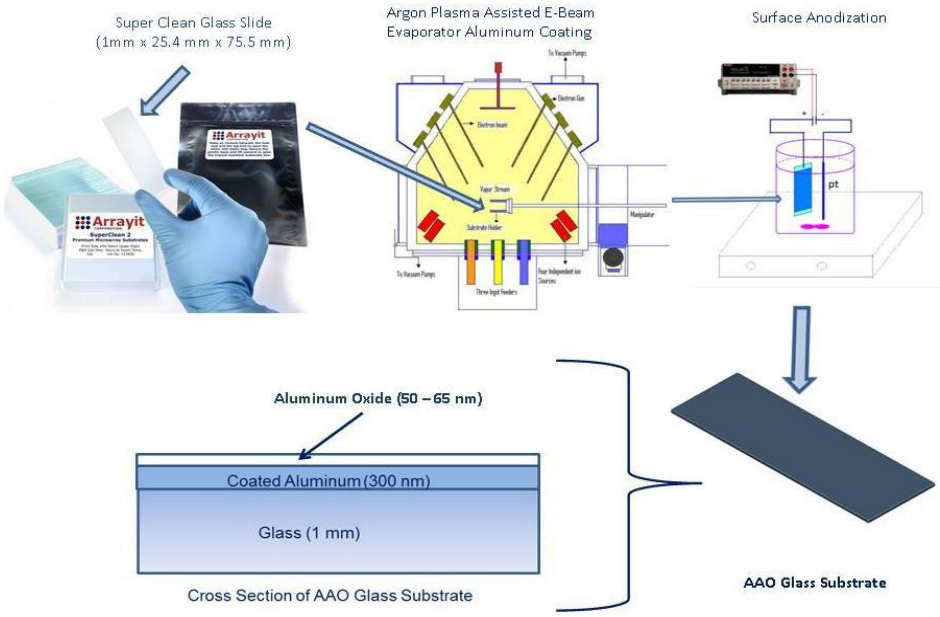

Figure 4.6. Schematic drawing of the fabrication of anodized aluminum oxide (AAO) glass substrate

4.5.3 Image Processing and Data Analysis:

The slides were scanned at 635 nm with a microarray fluorescence chip reader (Genepix® 4300A, Molecular Devices Corporation). Scanned images were analyzed with Genepix Pro 6.0 analysis software (Molecular Devices Corporation,). The image resolution was set to 5μm per pixel. Spots were defined as circular features with defined diameter of 100μm. The values of total intensity were chosen for data processing performed with Graphpad Prism® 6.0. Total intensities for duplicate spots were calculated and averaged. Error bars represent the standard deviation for all data points reported.

4.6. Glycan Binding Specificities Profiling of HIV-1 bNAbs:

4.6.1. Glycan Microarray on NHS-Coated Glass Slide:

Recently isolated HIV-1 bNABs, PG9, PG16, PGTs 121, 127/128, 141-145, were shown to be both broad and potent by neutralizing 70-80% of circulating HIV-1 isolates, suggesting that the targeted epitope(s) are highly conserved among variants of the entire group M[10]. Crystal structures of Fabs PGT 127 and 128 with Man_9 reported by Wilson et al. revealed the origin of their specificity for $Man_{8/9}$ glycans, which was further supported by glycan microarray experiment[11]. Moreover, Peter Kwong et. al. reported that the epitopes of PG9 and PG16 were dependent on the presence of *N*-linked glycosylation sites on certain positions, more particularly N160, in the V1/V2 or V3 variable loop[12]. Furthermore, PGT121 was shown to target bi-antennary complex type N-glycans on gp120 spike[13]. In sum, the glycan composition on gp120 surface could be affecting the neutralization potency of HIV-1 bNAbs; thus, recognizing the optimum epitope sought by these antibodies could guide the designing of appropriate immunogen.

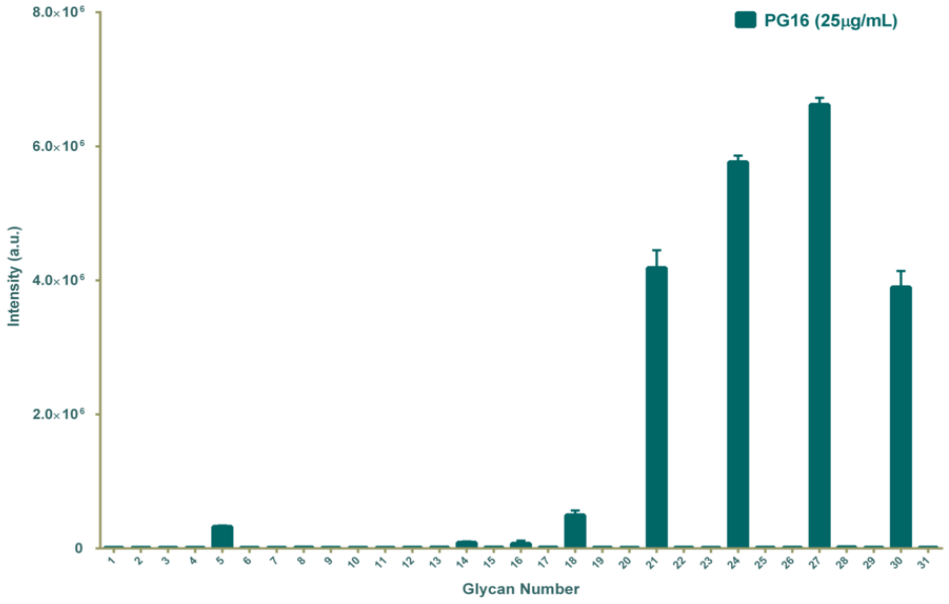

Figure 4.7. Binding of PG16 to a panel of *N*-glycans represented in bar chart. Signal for glycan **5** is due to non-specific binding from secondary antibody.

To gain insight into their glycan specificity, we employed a library of *N*-glycans for glycan array-based ligand profiling. The slides were spotted with 100μm of individual ligands **1-31** (Fig. 4.4). Each sample was printed with 10 replicates horizontally to form

arrays of 10x31 spots in each sub array. The slide images were obtained from a fluorescence scan after DyLight649-conjugated donkey anti-Human IgG antibody incubation and their fluorescent intensities have been compared in bar chart for each of the antibodies.

4.6.1.1. Glycan Binding Specificity of Antibody PG16:

Our study commenced with screening of antibody PG16 against a set of 31 glycans (Fig. 4.4) robotically printed on NHS glass slide. For PG16 at 25μg/mL concentration, we observed PG16 binding to only α-2,6-linked sialic acid terminated complex oligosaccharides, implying significant structural specificity. Furthermore, comparing to biantennary glycan **18**, a major complex type glycoform observed on gp120, we observed that PG16 exhibit high affinity binding to tri-antennary glycans **21**, **24**, and tetra-antennary glycan **27**, probably due to the increase in number of antennae would offers additional binding sites for PG16.

Determination of Surface Dissociation Constants ($K_{d.surf}$):

The determination of dissociation constants of α-2,6-sialylated complex glycans **18**, **21**, **24**, **27**, and **30**, which are multivalently presented on array surface interacting with PG16, was performed by using various concentrations of PG16 (1.25-0.039 μM) and printed sugars (100-12.5 μM). The Langmuir isotherm was then used to analyze binding curves in order to generate dissociation constants on surface ($K_{D, surf.}$). The binding curves provided a quick assessment of the affinity of these glycans for PG16. To calculate K_D for glycan **27**, we plotted PG16 concentrations against the fluorescence intensities at various printing concentrations. The relative binding affinity of PG16 for additional carbohydrate structures were calculated by using the same method and dissociation constants (K_D) values are summarized in Table 1. Our data revealed that tetra-antennary **27** (K_D = 0.1 μM) and tri-antennary **24** (K_D = 0.093 μM) structures exhibits highest binding affinity in comparison with other glycans printed on array. Interestingly, unnatural glycan **30** (K_D = 0.117 μM)**,** a truncated version of tetra-antennary **27**, showed at list three-fold higher affinity compared to its structural surrogate, bi-antennary glycans **24** (K_D = 0.327 μM).

Table 1. $K_{D,surf}$ (μM) values of antibody PG16 and sialylated complex type glycans.

Glycan no.	K D,surf (μM) ± SD (μM)
18	0.327 ± 0.087
21	0.120 ± 0.003
24	0.117 ± 0.003
27	0.093 ± 0.019
30	0.1 ± 0.006

Careful structural observation of **30** revealed that, deletion of one mannose residue (in comparison with naturally occurring bi-antennary complex type structure) might impose restriction on the flexibility of antennae. Such restricted orientation may project two antennae at appropriate distance necessary for strong PG16 binding. Further studies are needed to understand the exact mode of binding of unnatural form **30** to PG16 in comparison with natural form **18**. A detailed survey of structures and binding constants (K_D), suggest that glycan **30** could be considered as an important unnatural glycan ligand of HIV-1 bNAb PG16 in relation to $Man_4GlcNAc_2$ (an important unnatural ligand of HIV-1 bNAb 2G12). In principle, glycan **30** is structurally simpler and its synthesis could be approached in less number of steps as compared to other multiantennary series glycans. Theoretically, immunization with vaccine constructs bearing different copies of unnatural glycan **30** would induce antibodies that may not target the host glycoproteins with natural glycoforms on their surfaces. For these reasons, glycan **30** was selected as a potential candidate for development of carbohydrate-based HIV-1 vaccine and to study its immune response.

4.6.1.2. Glycan Binding Specificity of Antibodies PG9 and PGTs 141-145:

We next sought to gain information on the epitope recognized by newly identified HIV-1 bNAbs PGTs 141-145, exhibiting a strong preference for membrane-bound trimeric gp120. These antibodies were shown to neutralize 40-80% circulating isolates by targeting glycan-dependent epitope in V1/V2 loop[14]. For this reason, we studied glycan binding behavior of PG9 and PGTs 141-145 against a panel of 31 glycans. Our glycan array

analysis did not show any detectable binding of these antibodies towards any of the glycans **1-31**, probably due to their weak glycan binding affinities and inability of NHS coated glass slide to offer high density glycan distribution on array surface because of hydrolyzing activity of N-hydroxysuccinimide functionality.

4.6.1.3. Glycan Binding Specificity of Antibodies PGT121:

Recently isolated members of PGT121 family of antibodies from an African donor were shown to be highly broad and potent in neutralizing 70% of circulating isolates with median IC_{50} less than 0.05 mg/mL. Research articles published by Mouquet et.al. and Wilson et.al. suggested the binding of PGT121 to complex type oligosaccharides rather than high mannose type glycans; however, the absence of a PGT121–gp120 structure has

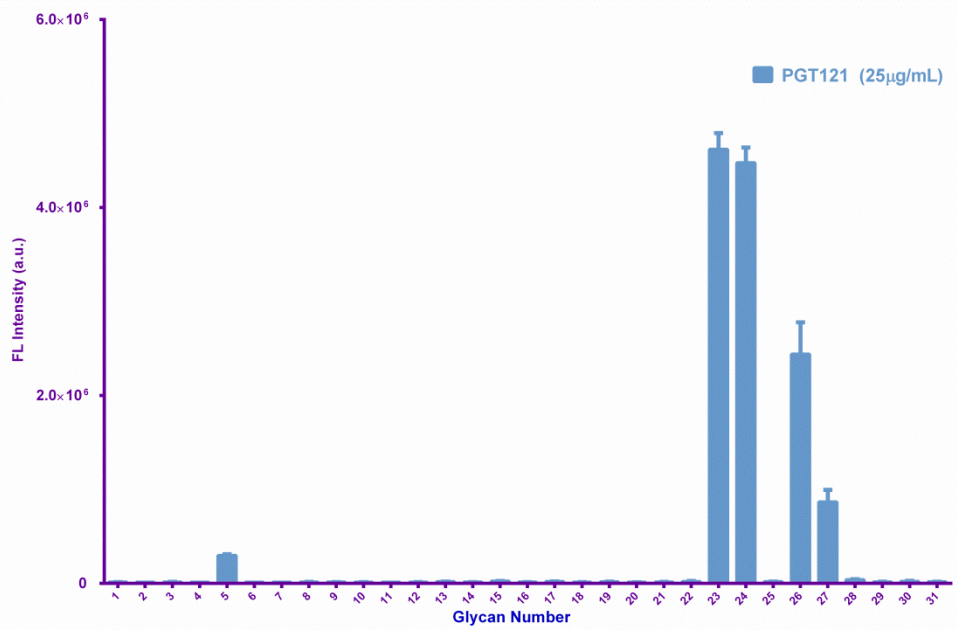

Figure 4.8. Binding of PGT121 to a panel of *N*-glycans represented in bar chart. Signal for glycan **5** is due to non-specific binding from secondary antibody

made it difficult to understand the context of this recognition[13,15]. To address these questions, we utilized our microarray of synthetic *N*-glycan structures to determine the glycan binding specificity.

The binding of PGT121 based on fluorescent intensities suggest that antibody exhibits distinct glycan binding specificity. We observed that antibody binds more specifically to

glycans **23**, **24**, **26**, and **27** with terminal galactose and α-2,6-linked sialic acid. Among different glycoforms of triantennary glycans (**20-25**), PGT121 recognizes only glycans **23** and **24**. Surprisingly, the PGT121 showed almost no reactivity to high mannose sugars on the glycan array in contrast to bNAbs of the PGT128 family. Based on the binding study, we concluded that structures **23** and **24** might constitute a PGT121 epitope and should be considered for immunological evaluation.

4.6.1.4. Glycan Binding Specificity of Antibodies PGT127/128:

Glycan binding analysis of PGTs 127/128 towards 31 glycans showed binding towards only to structure **6**, $Man_9GlcNAc_2$, which is in well agreement with previously reported glycan array data by Wilson et al.[10]. The terminal mannose residues of both the D1 and D3 arms, which are only present on $Man_9GlcNAc_2$ glycans, are heavily contacted through hydrogen bonding interactions with the antibodies[11].

4.6.2. Glycan Microarray on Aluminium Oxide-Coated Glass Slide (ACG):

For NHS coated glass slide, the hydrolyzing activity of NHS group might be a limiting factor to create homogenous glycan distribution on the array surface, resulting in lack of binding for antibodies PG9 and PGTs141-145 in our previous experiments. Therefore, an array that can facilitate the determination of such interactions is urgently needed. Accordingly, we utilized our improved array on aluminium oxide coated glass slide to investigate unknown binding specificities of PG9 and PGTs141-145.

Structures **I-XII** with phosphonic acid tail were dissolved in ethylene glycol and covalently attached on array surface through phosphonate chemistry. Structure **I** is phosphonic acid linker, which acts as control. The slides were spotted with 100μm of individual ligands **I-XII** (Fig. 4.5). Each sample was printed with 10 replicates horizontally to form arrays of 10 x 12 spots in each sub array, and slide images were obtained from a fluorescence scan after DyLight649-conjugated donkey anti-Human IgG antibody incubation and their fluorescent intensities have been compared in bar chart.

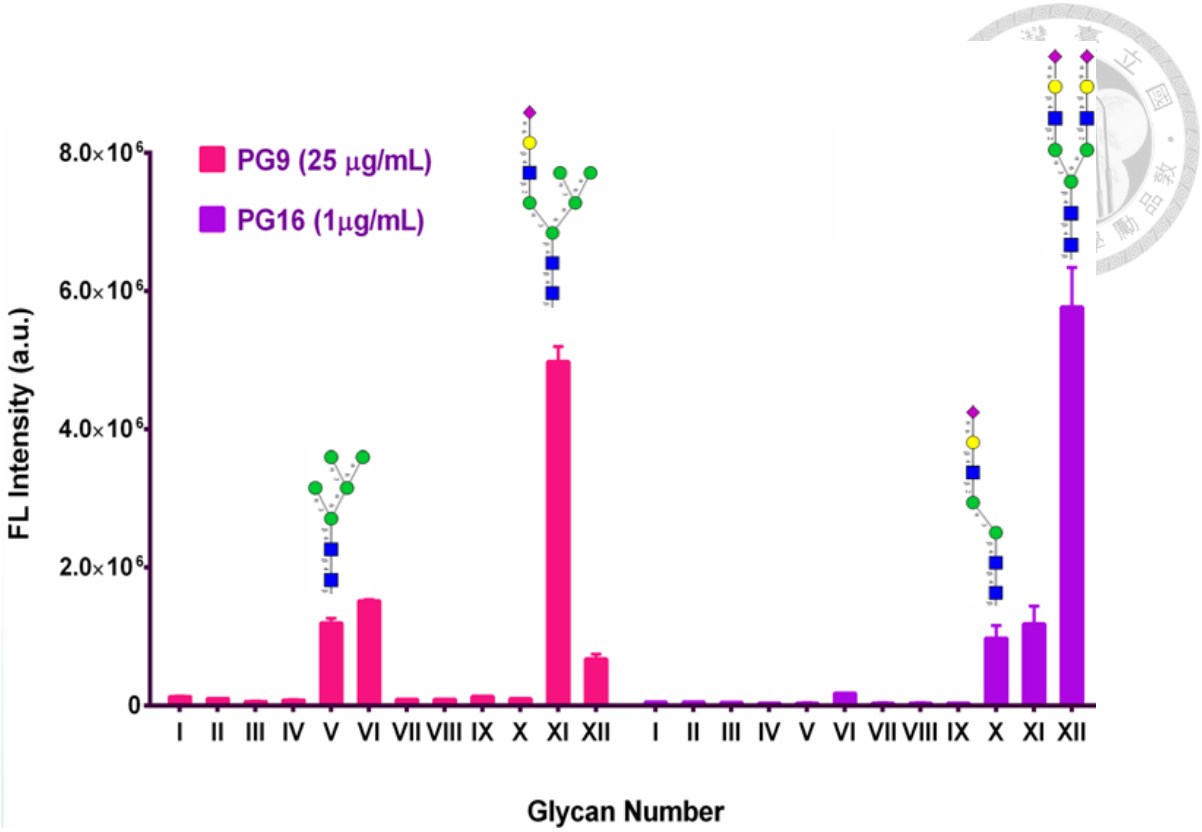

Figure 4.9. Binding of PG9 and PG16 to structures **I-XII** printed on aluminium oxide coated glass slide. Signal for glycan VI is non-specific binding. The concentration in μm for PG9 and PG16 is given in the legend.

Consistent with binding study of PG16 using NHS coated glass slide (Fig. 4.7), we observed that PG16 retained its binding specificity towards α-2,6 linked sialic acid containing glycans, **X**, **XI** and **XII** (Fig. 4.9 right hand panel). But the concentration of PG16 required for ACG slide based assay is dramatically reduced to 1μg/mL compared to NHS slide based assay (25μg/mL), highlighting the excellent sensitivity of ACG slide. Moreover, binding of PG9 towards structures **I-XII** showed that PG9 binds more specifically to sialylated hybrid series glycan X**I**. A detectable binding towards $Man_5GlcNAc_2$ (**V**) or bi-antennary complex type glycan (**XII**) was also observed (Fig. 4.9 left hand panel). ACG array since we could not observed detectable binding using NHS array.

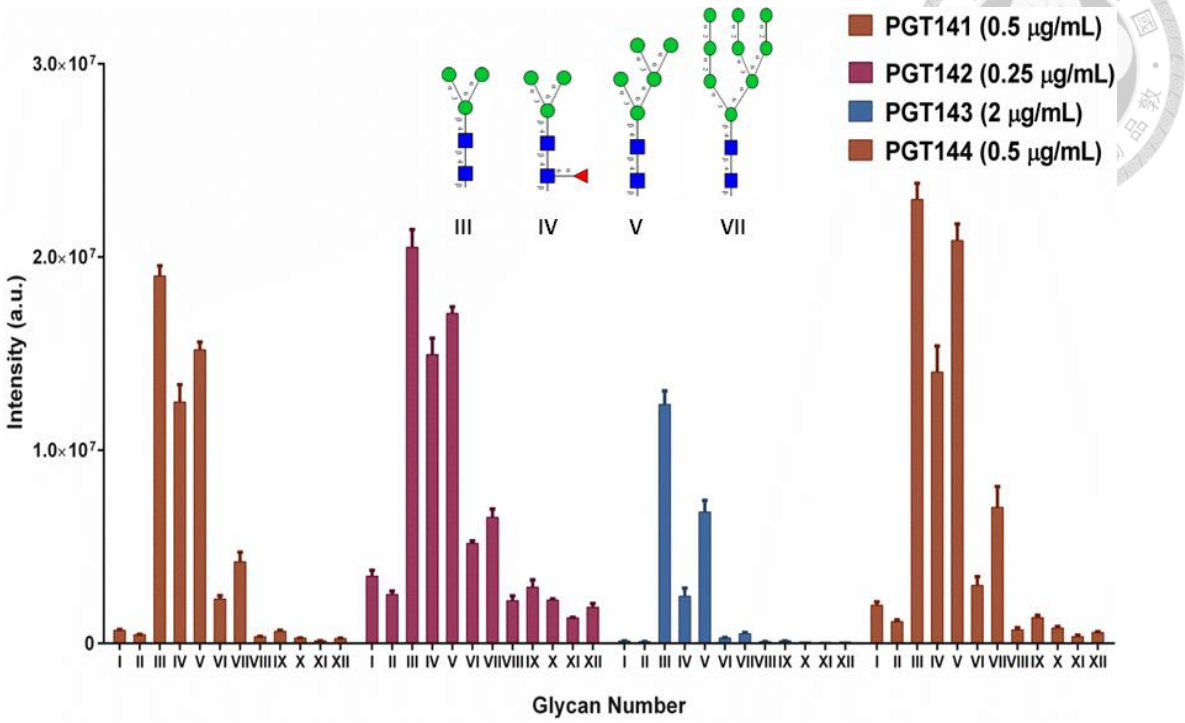

Figure 4.10. Bindings of PGTs 141-144 towards panel of I-XII structures represented in bar charts. The concentration in μm for PGTs 141-144 is given in the legend.

As depicted in Fig. 4.10, PGTs 141-144 at various concentrations showed excellent specificity towards high mannose type but not to the hybrid or complex type oligosaccharides. The relative binding strength, based on fluorescent intensities, was $Man_3GlcNAc_2$ > $Man_5GlcNAc_2$ > $FucMan_3GlcNAc_2$ > $Man_9GlcNAc_2$. Antibody PGT145 did not show detectable binding to any of the glycans printed on both NHS-coated and aluminium oxide-coated glass slide. This is the first example of recognition of core pentasaccharide ($Man_3GlcNAc_2$), which is common in all *N*-linked oligosaccharides by HIV-1 bNAbs. PGTs 141-144 exhibits nearly equivalent binding to $Man_5GlcNAc_2$; however, for core fucosylated Man_3 **IV**, slightly decrease in binding was observed. Interestingly, highly branched version of oligomannoses, $Man_9GlcNAc_2$ **VII**, dramatically lost the binding by PGTs141-144, probably due to effective shielding of core pentasaccharide by terminal mannose residues.

4.7. Analyzing Hetero-Glycans Binding Specificity of HIV-1 bNAbs:

Heterogeneous posttranslational glycosylation of HIV-1 spike raise the possibility that the gp120 glycan recognition by HIV antibodies might involve mixture of high mannose, hybrid and complex type glycans. This might be an important adaptation of host immune system to deal with diversely glycosylated HIV-1 spike. To test this hypothesis, we utilized ACG array to print heterogeneous glycan mixtures to study the binding behavior of HIV antibodies towards each of these mixtures on the slide.

4.7.1. Antibody PG9:

The structure of V1/V2 region in complex with PG9 reported by Peter Kwong showed that the epitope recognized by PG9 consists primarily of $Man_5GlcNAc_2$ at N160 and another glycan either at N156 or N173 together with short peptide strand. Several reports thereafter highlighted importance of $Man_5GlcNAc_2$ as a major component of epitope recognized by PG9 on gp120 surface[12a]. However, in our preliminary study, we showed that PG9 could recognize hybrid type glycan **XI** strongly but weak affinity to Man5 **V** (Fig. 4.9 left hand panel). Structural features of glycan **XI** suggested that it composed of complex type D1 arm and high mannose type D2/D3 arm linked to central trisaccharide core. The specificity of PG9 to glycan **XI** and necessity of $Man_5GlcNAc_2$ at N160 in PG9 epitope prompted us to hypothesize that epitope of PG9 in V1/V2 loop might consist of mixture of high mannose with hybrid and complex type glycans.

To uncover the molecular mechanism of gp120 glycan recognition by PG9, we utilized ACG array of closely spaced heteroglycans, prepared by printing a mixtures of phosphonic acid modified structures **I-XII** with $Man_5GlcNAc_2$ **V**, and bi-antennary complex type structure **XII** in 1:1 mole ratio. We found that when complex type glycan was mixed with structures **I-XII,** PG9 bound more strongly to a mixture containing V+XII (Fig. 4.11). The similar binding trend was observed when $Man_5GlcNAc_2$ was mixed with structures I-**XII.** Our results showed that a combination of $Man_5GlcNAc_2$ and complex type glycan (V+XII or XII+V) achieved strong PG9 binding among the mixtures printed on array. Furthermore, we also observed comparable bindings towards mixtures V+X and V+XI, suggesting that $Man_5GlcNAc_2$, a glycan at Asn160 is critical at primary binding site while structures X, XI, and XII contributed complex type D1 arm for binding at secondary

binding site. Based on binding affinities of PG9, it appears that $Man_5GlcNAc_2$ or complex type glycan alone did not seem to provide sufficient affinity but hybrid type glycan, with inbuilt features of complex and oligomannose type structures, showed significant enhancement in binding affinity. In mixed glycans study, a combination Man_5: complex type was found to be the best followed by a combination of Man_5: hybrid type in achieving much tighter interactions with PG9, since both complex and hybrid type glycans contain complex type D1 arm.

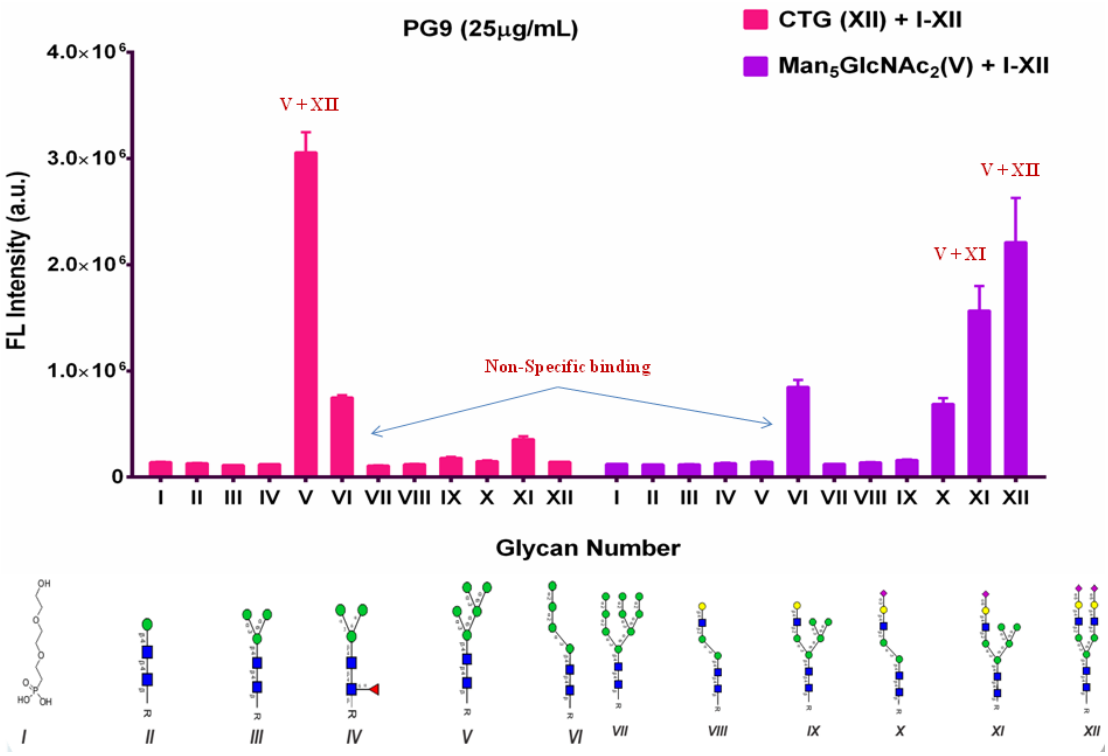

Figure 4.11. Binding of PG9 (25μg/mL) to each of the mixtures was evaluated to determine the effect of adjacent glycans on binding affinity.

4.7.2. Antibody PG16 :

Recently reported crystal structure of the antigen-binding fragment (Fab) of the PG16 antibody in complex with the V1–V2 domain of HIV-1 gp120 from strain ZM109 revealed epitope comprising of both high mannose type *N*-linked glycan at N160 and hybrid/complex type glycans at N173[12b]. The results were supported by crystal structure, NMR and mutagenesis analysis. In order to determine best glycan combination for PG16

binding, we printed mixtures of glycan **V** and **XII** with structures **I-XII** and studied their binding pattern against PG16 (Fig. 4.12). For mixtures containing half of $Man_5GlcNAc_2$, we observed highest PG16 binding towards a mixture containing $Man_5GlcNAc_2$ and complex type glycan (V+XII), which is in well agreement with previous structural and biochemical studies[12]. When complex type glycan was printed with structures I-XII, the binding trend of PG16 to each of the mixtures was found to be XII+XII > XII+X > XII+XI, implicating the importance of sialylated antennae in PG16 binding site. A combination of complex and hybrid type glycans indeed contributed to binding, however, the binding strength was observed to be weak compared to complex type glycan alone. Taken together, these data suggest that PG16 might target a epitope containing sialylated bi-antennary complex type glycans in V1/V2 loop.

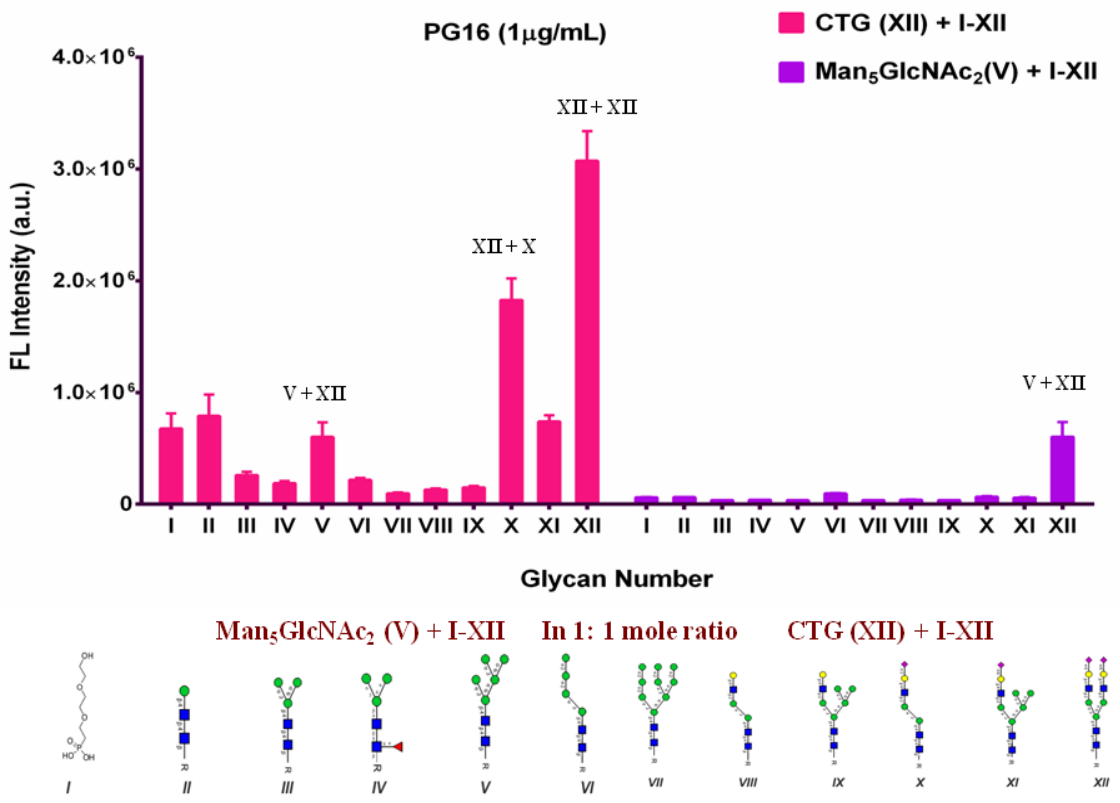

Figure 4.12. Binding of PG16 to mixtures of glycans **V** and **XII** with structures **I-XII**

4.7.3. Antibody PGT128:

Crystal structures of Fabs PGT 127 and 128 with Man_9 reported by Wilson et al. suggested the origin of their specificity for $Man_{8/9}$ glycans. Antibody PGT128 bound to N332 glycan ($Man_9GlcNAc_2$) in the primary binding site, whereas the secondary glycan binding site recognized the N301 glycan involving only core pentasaccharide, a portion common in all *N*-glycans[11]. The PGT 128 requirement for two closely spaced *N*-linked glycans likely accounts for its lack of reactivity with self-glycoproteins displaying single $Man_{8/9}GlcNAc_2$ and for resistance of HIV-2 and SIV viruses to neutralization. Notably, N332 and N301 glycans are highly conserved among HIV isolates, accounting for the broader neutralization potency exhibited by PGT128[14]. However, $N301_{gp102}$ attached carbohydrate appears to be a complex type *N*-glycan in gp120s in by mass spectrometry analysis, but not in the gp120 outer domain which was produced in $GnTI^{-/-}$ cells. By analogy, although PGT128-like antibodies may prefer interactions with $Man_{8/9}GlcNAc_2$ as suggested by glycan microarray results and liganded PGT128 structure construct, the possibility that these antibodies may be able to accommodate $Man_9GlcNAc_2$ together with other high mannose, hybrid or complex type *N*-glycans in secondary binding site cannot be excluded.

To gain detail insights of this mechanism, we mixed $Man_9GlcNAc_2$ **VII** with structures **I-XII** to study binding specificity towards each of the mixtures.

Glycan array analysis of PGT128 binding to structures **I-XII** showed strong binding affinity for $Man_9GlcNAc_2$. However, among the mixtures of $Man_9GlcNAc_2$ with structures **I-XII**, PGT128 exhibited stronger binding to mixture containing $Man_9GlcNAc_2$ alone. No significant enhancement in binding was observed for a combination of Man_9 with structures **I-XII**. These results indicate that PGT128 prefers to bind $Man_9GlcNAc_2$ in both primary and secondary binding sites.

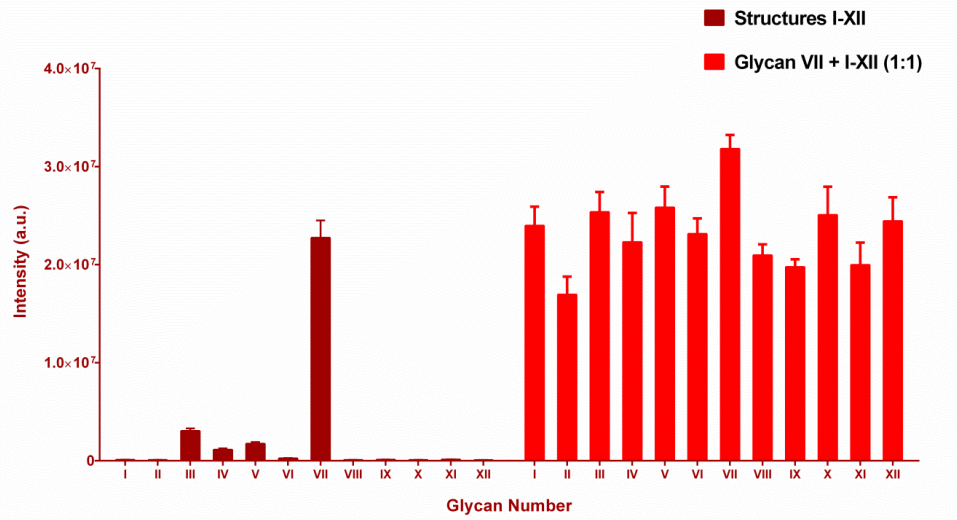

Figure 4.13. Binding of PGT128 to structures **I-XII** and mixtures of glycan **VII** with structures **I-XII.**

4.8. Summary and Conclusion:

In conclusion, we have successfully developed a library of *N*-linked oligosaccharides to employ NHS and ACG based glycan array platform to determine unknown glycan specificities of newly discovered HIV-1 bNAbs. Introduction of an array on aluminum oxide coated glass slide facilitated the determination of critical low affinity interactions between PG9 and PGTs141-144 and also the discovery of heteroglycan binding by HIV-1 bNAb PG9. The binding specificity of PG9, PG16, and PGTs 121, 128, 141-144 to various kind of *N*-glycans on array surface is a step towards better understanding of essential component of epitope recognized by these antibodies in V1/V2 or V3 loop of gp120 for the design of carbohydrate based immunogens to elicit HIV-1 bNAbs.

4.9. References:

(1) (a) Paulson, J. C.; Blixt, O.; Collins, B. E. *Nature chemical biology*. **2006**, *2*, 238; (b) Rillahan, C. D.; Paulson, J. C. *Annu. Rev. Biochem. Vol 80* **2011**, *80*, 797.

(2) Wang, D. N.; Liu, S. Y.; Trummer, B. J.; Deng, C.; Wang, A. L. *Nat. Biotechnol.* **2002**, *20*, 275.

(3) Fukui, S.; Feizi, T.; Galustian, C.; Lawson, A. M.; Chai, W. G. *Nat. Biotechnol.* **2002**, *20*, 1011.

(4) Fazio, F.; Bryan, M. C.; Blixt, O.; Paulson, J. C.; Wong, C. -H. *J. Am. Chem. Soc.* **2002**, *124*, 14397.

(5) (a) Oyelaran, O.; Gildersleeve, J. C. *Curr. Opin. Chem. Biol.* **2009**, *13*, 406; (b) Song, X. Z.; Xia, B. Y.; Stowell, S. R.; Lasanajak, Y.; Smith, D. F.; Cummings, R. D. *Chem. Biol*. **2009**, *16*, 36.

(6) Bohorov, O.; Andersson-Sand, H.; Hoffmann, J.; Blixt, O. *Glycobiology*. **2006**, *16*, 21c.

(7) Park, S.; Gildersleeve, J. C.; Blixt, O.; Shin, I. *Chem. Soc. Rev.* **2013**, *42*, 4310.

(8) Blixt, O.; Head, S.; Mondala, T.; Scanlan, C.; Huflejt, M. E.; Alvarez, R.; Bryan, M. C.; Fazio, F.; Calarese, D.; Stevens, J.; Razi, N.; Stevens, D. J.; Skehel, J. J.; van Die, I.; Burton, D. R.; Wilson, I. A.; Cummings, R.; Bovin, N.; Wong, C. H.; Paulson, J. C. *Proc. Natl. Acad. Sci. U. S. A.* **2004**, *101*, 17033.

(9) (a) Tseng, S. Y.; Wang, C. C.; Lin, C. W.; Chen, C. L.; Yu, W. Y.; Chen, C. H.; Wu, C. Y.; Wong, C. -H. *Chemistry, an Asian journal.* **2008**, *3*, 1395; (b) Chang, S. H.; Han, J. L.; Tseng, S. Y.; Lee, H. Y.; Lin, C. W.; Lin, Y. C.; Jeng, W. Y.; Wang, A. H.; Wu, C. Y.; Wong, C. -H. *J. Am. Chem. Soc.* **2010**, *132*, 13371.

(10) (a) Walker, L. M.; Huber, M.; Doores, K. J.; Falkowska, E.; Pejchal, R.; Julien, J. P.; Wang, S. K.; Ramos, A.; Chan-Hui, P. Y.; Moyle, M.; Mitcham, J. L.; Hammond, P. W.; Olsen, O. A.; Phung, P.; Fling, S.; Wong, C. H.; Phogat, S.; Wrin, T.; Simek, M. D.; Koff, W. C.; Wilson, I. A.; Burton, D. R.; Poignard, P.; Investigators, P. G. P. *Nature.* **2011**, *477*, 466; (b) Walker, L. M.; Phogat, S. K.; Chan-Hui, P. Y.; Wagner, D.; Phung, P.; Goss, J. L.; Wrin, T.; Simek, M. D.; Fling, S.; Mitcham, J. L.; Lehrman, J. K.; Priddy, F. H.; Olsen, O. A.; Frey, S. M.; Hammond, P. W.; Kaminsky, S.; Zamb, T.; Moyle, M.; Koff, W. C.; Poignard, P.; Burton, D. R.; Investigators, P. G. P. *Science.* **2009**, *326*, 285.

(11) Pejchal, R.; Doores, K. J.; Walker, L. M.; Khayat, R.; Huang, P. S.; Wang, S. K.; Stanfield, R. L.; Julien, J. P.; Ramos, A.; Crispin, M.; Depetris, R.; Katpally, U.; Marozsan, A.; Cupo, A.; Maloveste, S.; Liu, Y.; McBride, R.; Ito, Y.; Sanders, R. W.; Ogohara, C.; Paulson, J. C.; Feizi, T.; Scanlan, C. N.; Wong, C. H.; Moore, J. P.; Olson, W. C.; Ward, A. B.; Poignard, P.; Schief, W. R.; Burton, D. R.; Wilson, I. A. *Science*. **2011**, *334*, 1097.

(12) (a) McLellan, J. S.; Pancera, M.; Carrico, C.; Gorman, J.; Julien, J. P.; Khayat, R.; Louder, R.; Pejchal, R.; Sastry, M.; Dai, K.; O'Dell, S.; Patel, N.; Shahzad-ul-Hussan, S.; Yang, Y.; Zhang, B.; Zhou, T.; Zhu, J.; Boyington, J. C.; Chuang, G. Y.; Diwanji, D.; Georgiev, I.; Kwon, Y. D.; Lee, D.; Louder, M. K.; Moquin, S.; Schmidt, S. D.; Yang, Z. Y.; Bonsignori, M.; Crump, J. A.; Kapiga, S. H.; Sam, N. E.; Haynes, B. F.; Burton, D. R.; Koff, W. C.; Walker, L. M.; Phogat, S.; Wyatt, R.; Orwenyo, J.; Wang, L. X.; Arthos, J.; Bewley, C. A.; Mascola, J. R.; Nabel, G. J.; Schief, W. R.; Ward, A. B.; Wilson, I. A.; Kwong, P. D. *Nature*. **2011**, *480*, 336; (b) Pancera, M.; Shahzad-Ul-Hussan, S.; Doria-Rose, N. A.; McLellan, J. S.; Bailer, R. T.; Dai, K.; Loesgen, S.; Louder, M. K.; Staupe, R. P.; Yang, Y.; Zhang, B.; Parks, R.; Eudailey, J.; Lloyd, K. E.; Blinn, J.; Alam, S. M.; Haynes, B. F.; Amin, M. N.; Wang, L. X.; Burton, D. R.; Koff, W. C.; Nabel, G. J.; Mascola, J. R.; Bewley, C. A.; Kwong, P. D. *Nat .Struct. Mol. Biol.* **2013**.

(13) Mouquet, H.; Scharf, L.; Euler, Z.; Liu, Y.; Eden, C.; Scheid, J. F.; Halper-Stromberg, A.; Gnanapragasam, P. N. P.; Spencer, D. I. R.; Seaman, M. S.; Schuitemaker, H.; Feizi, T.; Nussenzweig, M. C.; Bjorkman, P. J. *Proc. Natl. Acad. Sci. U. S. A.* **2012**, *109*, E3268.

(14) Walker, L. M.; Huber, M.; Doores, K. J.; Falkowska, E.; Pejchal, R.; Julien, J. P.; Wang, S. K.; Ramos, A.; Chan-Hui, P. Y.; Moyle, M.; Mitcham, J. L.; Hammond, P. W.; Olsen, O. A.; Phung, P.; Fling, S.; Wong, C. H.; Phogat, S.; Wrin, T.; Simek, M. D.; Koff, W. C.; Wilson, I. A.; Burton, D. R.; Poignard, P. *Nature.* **2011**, *477*, 466.

(15) Julien, J. P.; Sok, D.; Khayat, R.; Lee, J. H.; Doores, K. J.; Walker, L. M.; Ramos, A.; Diwanji, D. C.; Pejchal, R.; Cupo, A.; Katpally, U.; Depetris, R. S.; Stanfield, R. L.; McBride, R.; Marozsan, A. J.; Paulson, J. C.; Sanders, R. W.; Moore, J. P.; Burton, D. R.; Poignard, P.; Ward, A. B.; Wilson, I. A. *PLoS Pathogens.* **2013**, *9*, e1003342.

Chapter 5

Design and Synthesis and Immunological Evaluation of Carbohydrate-based Antigens

In chapter 4, we described the glycan microarray based glycan specificity profiling of HIV-1 broadly neutralizing antibodies to identify relevant glycan targets. This chapter describes conjugation of potential carbohydrate antigens to carrier proteins and their immunological evaluation to investigate whether these carbohydrate-based immunogens could induce HIV-1 broadly neutralizing antibodies and T-cell response.

5.1. Introduction:

Approximately 30 million people are infected with human immunodeficiency virus (HIV), and new infections continue at a high rate. Despite the remarkable achievements in development of antiretroviral therapies against HIV and the recent advances in new prevention technologies, the rate of new HIV infections continue to outpace efforts on HIV prevention and control[1]. The development of an effective prophylactic vaccine remains an unrealized goal in the effort to contain the current pandemic. Such a vaccine should be capable of eliciting broadly neutralizing antibodies against multiple virus isolates and T-cell response[2]. The natural immune response to HIV is generally characterized by titers of NAbs against a narrow range of isolates; however, the bNAbs develops only in few individuals over a time. Virtually most of the vaccine initiatives to elicit NAbs are focused on the external envelope glycoproteins, gp120 and gp41[3]. Numerous defense mechanism helps HIV to escape from host immune attacks directed against HIV envelope (Env) neutralization epitopes by means of frequent mutations and heavy glycosylation immunogenic polypeptide backbone[4].

Since the discovery of AIDS virus, there have been only three vaccine approaches that have completed human efficacy trials: a) a gp120 monomeric protein in alum, and this candidate failed to prevent or control HIV infection, b) a recombinant adenovirus type 5 vaccine, containing HIV gag, pol and nef genes, and this candidate also failed to provide any benefit, and c) lastly, in 2009, a prime-boost strategy (RV-144) utilizing a canarypox

vector prime + monomeric gp120 boost provided the first signal for prevention of HIV infection in humans with 30% efficacy.

Apart from protein-based vaccine candidates, several carbohydrate dependent vaccines have been evaluated. In all immunization studies performed to date, the oligomannose containing glycoconjugates designed based on the logic of 2G12 epitopes have failed to elicit broadly neutralizing antibodies[5]. The reasonable explanation behind the failure are: i) the glycoproteins exist as numerous glycoforms in which different glycans can exist at a single site, thereby providing a heterogeneous array of antigens and diluting out the antiglycan immune response to any single glycoform; ii) the protein-glycan interactions are typically weaker than protein-protein interactions, potentially restricting the production of anti-carbohydrate antibodies; and iii) the presentation of glycans on carrier protein surface fails to achieve exact mimicry of 2G12 epitope.

Studies of HIV infected individuals have revealed that between 10% and 30% of HIV infected individuals developed bNAbs, though it usually takes three or more years of post infection for such antibodies to develop[6]. However, only 1% of HIV infected individuals could develop antibodies with outstanding breadth and potency. Recently, a panel of broadly NAbs has been isolated from HIV-1-infected individuals (PG9, PG16, and PGT series antibodies) and shown to provide protection against viral challenge in animal models by targeting glycan dependent epitopes on gp120 surface[7]. The epitopes of these Abs may serve as targets for vaccine design.

5.2. Identification of Carbohydrate Dependent Antigenic Epitopes:

Based on our glycan microarray analysis described in chapter 4, we identified several potential carbohydrate antigens, which are specifically recognized by different HIV-1 bNAbs. The chemical structures of all these oligosaccharides are shown in scheme 5.1 and 5.2. Among oligomannose series structures, $Man_3GlcNAc_2$ **5-1** and $Man_5GlcNAc_2$ **5-2** were shown to exhibit specificity towards PGTs141-144, while $Man_9GlcNAc_2$ **5-3** is well known ligand of antibodies 2G12, PGTs127/128. Hybrid type glycan **5-4** has also been targeted by PG9 on aluminium oxide coated glass slide. We also demonstrated the importance of bi- and triantennary complex type glycans in forming epitopes of HIV-1 bNAbs. In particular, bi-antennary complex type glycan **5-5** in combination with $Man_5GlcNAc_2$ **5-2** showed

excellent binding specificity towards PG9 in mixed glycan study. Moreover, PG16 can binds to both α-2,6-sialylated triantennary type glycan **5-8** and unnatural form **5-6**. Furthermore, PGT121 showed significant structural specificity towards glycans **5-7** and **5-8**. For these reasons, oligosaccharides **5-1** to **5-8** were prepared in sufficient amount for conjugation to carrier proteins and further studies.

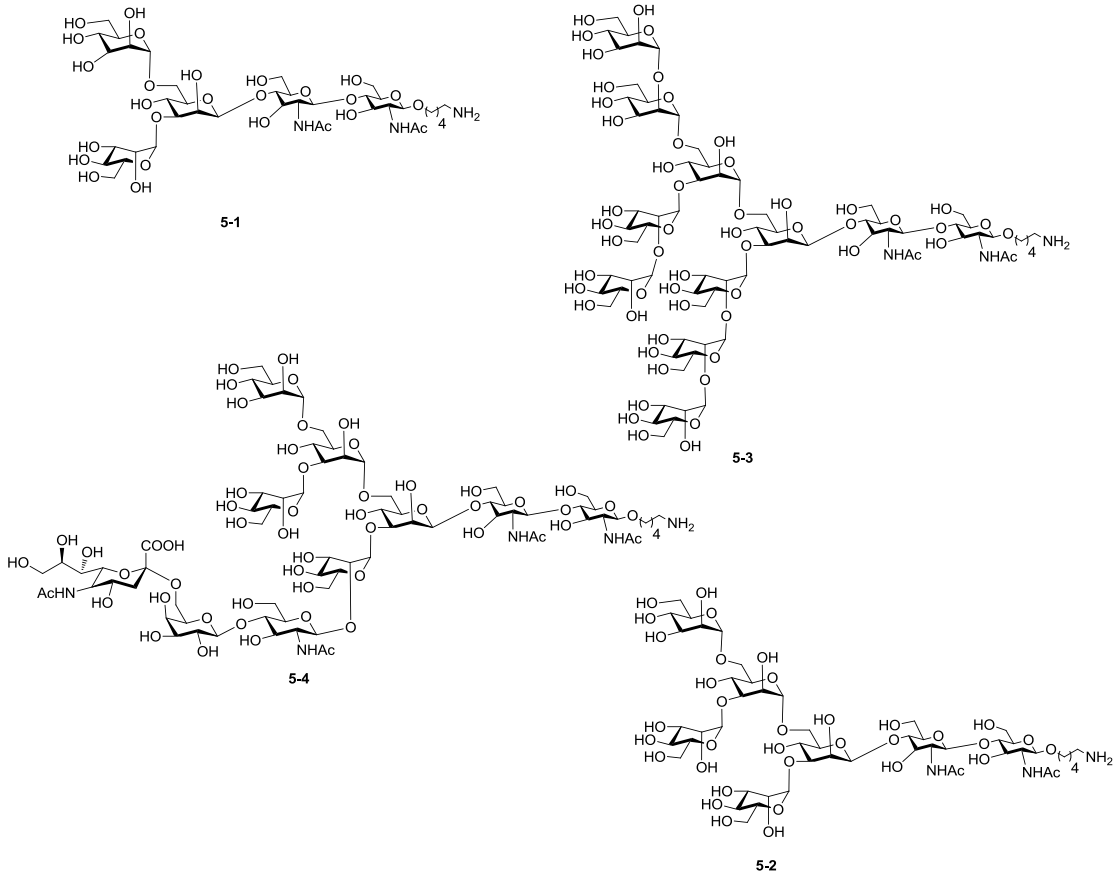

Scheme 5.1. Structures of high mannose and hybrid type glycans subjected to immunological evaluation.

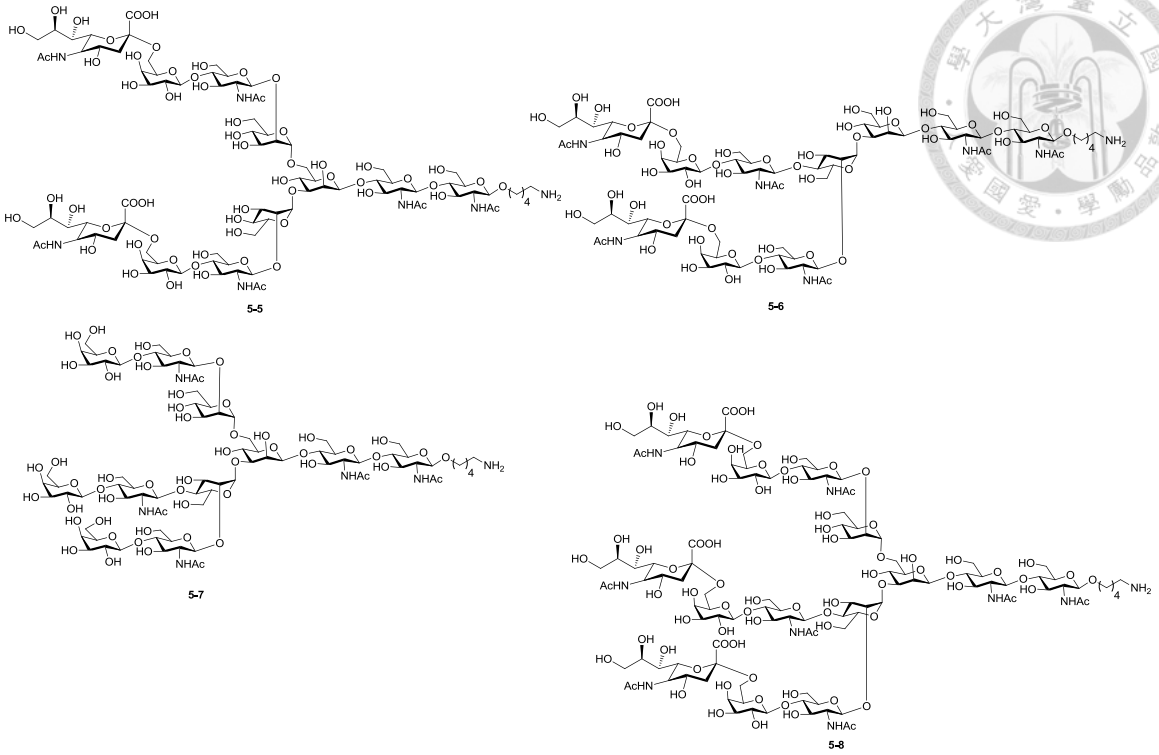

Scheme 5.2. Structures of complex type N-linked oligosaccharides selected for immunological evaluation.

5.3. Synthesis of Glycoconjugates:

Currently, several kinds of capsular polysaccharide based antibacterial glycoconjugate vaccines are commercially available, and many clinical trials of promising vaccine candidates against human infectious diseases and various types of cancers are underway[8]. The advent of new efficient, sensitive, analytical, and synthetic methods in carbohydrate chemistry together with increased understanding of glycobiology and immunology fascilitate the development of carbohydrate-based vaccines. There are two important classes of commercially available carbohydrate-based vaccines, namely oligosaccharide vaccine and conjugate vaccines. Because polysaccharides are usually T-cell-independent antigens that are unable to elicit a T-cell-assisted immune response, the "oligosaccharide vaccines" usually elicit short-lasting antibody and cannot provide adequate protections for high-risk groups, such as infants and children under two years old. Moreover, carbohydrates generally exhibit poor immunogenicity; therefore, many issues need to be resolved before practically using carbohydrate-based immunogens as vaccines.

Carbohydrate immunogenicity can be enhanced by their covalent attachment to antigenic carrier proteins such as Tetanus Toxoid (TT), Diphtheria Toxoid (DT) and Keyhole Lympet hemocyanin (KLH), etc. in the presence of suitable adjuvant. Moreover, the α-galactosylceramide (α-GalCer or C1) isolated from marine sponges and analogs exhibit antitumor activity are considered as possible adjuvant candidates[9]. For Globo H (GH) based cancer vaccine[10], our group has recently shown that combination of GH-DT adjuvanted with the α-glactosylceramide C34 has the highest enhancement of anti-GH IgG, prompting us to consider DT (CRM_{197}) as a potential carrier protein and C34 as adjuvant for immunization study.

5.3.1. Design of Glycoconjugates Based on PG9 Epitope:

The structure of gp120-V1/V2 loop with PG9 suggest the presence in PG9 epitope of $Man_5GlcNAc_2$ at N-linked glycosylation sites Asn160 and/or Asn156/173 and short peptide strand[14]. In the same report, the PG9 binding to $Man_5GlcNAc_2$ was accessed by saturation transfer difference NMR, where, the binding affinity was found to be very weak (K_d = 1.6 mM)[15]. Later in 2013, it has been shown that PG9 prefers to bind $Man_5GlcNAc_2$ at Asn160 with another glycan of bi-antennary complex type at Asn156/173 on gp120 peptide scaffold[15]. In the course of investigation, we showed that the PG9 binding affinity for $Man_5GlcNAc_2$ and bi-antennary complex type glycan without protein/peptide domain is extremely weak; however, PG9 could recognize hybrid type glycan printed on array surface. Moreover, we also observed that binding affinity of PG9 was significantly enhances when $Man_5GlcNAc_2$ was printed in combination with bi-antennary complex type glycan, which is in well agreement with published reports.

A systematic immunological investigation was commenced with preparation of glycoconjugate based on hybrid type recognition motif. Conjugation of hybrid type oligosaccharides **5-4** to carrier protein was performed via amide bond formation between activated oligosaccharides and lysine residues on protein surface. Initially, oligosaccharides with five carbon amino linker at reducing end were converted into *p*-nitro phenyl half ester by reaction with ten-fold molar excess of homo bifunctional linker, so that formation of dimer could be avoided (Scheme 5.1). After purification from the excess of bi-functional inker by P2-Gel (Bio-rad) column chromatography using water as eluent, the activated

oligosaccharides were lyophilized and incubated with DT (CRM_{197}) at pH 8.1 to provide desired glycoconjugates **1**, which further underwent MALDI-TOF MS analysis to determine average number of glycan epitope on carrier protein.

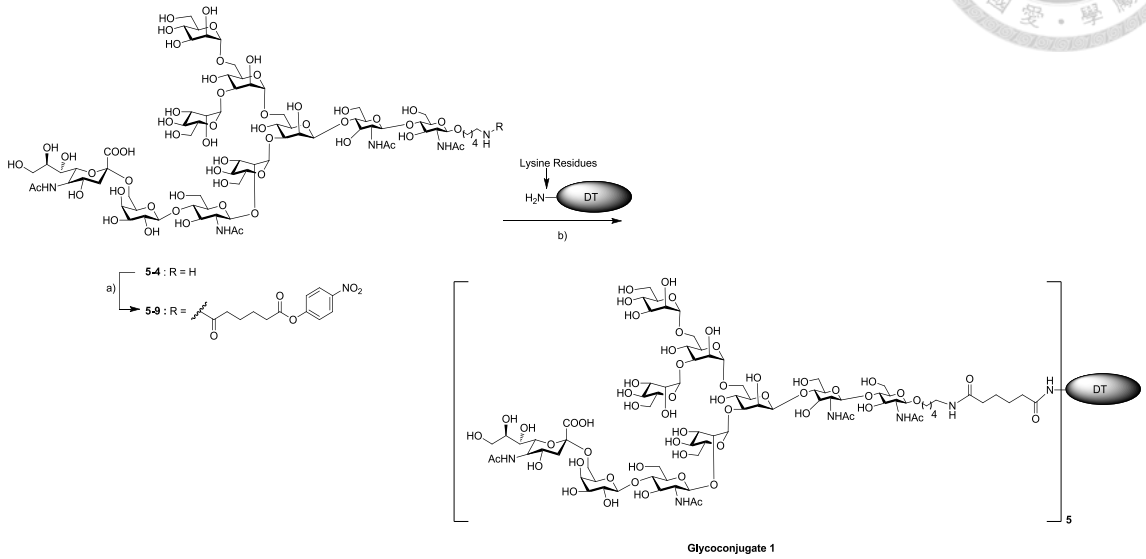

Scheme 5.3 Synthesis of glycoconjugate 1. Reagents and conditions**:** (a) *p*-nitrophenyl ester (linker), DMF, rt, 5 h, 61%; (b) 10 mM PBS, pH 8.1, rt, overnight.

An alternate way to constitute a PG9 epitopes is heterogeneous chemical glycosylation of carrier protein DT with $Man_5GlcNAc_2$ **5-2** and bi-antennary complex type glycan **5-5**. The strategy of using homo bi-functional linker for preparation of such glycoconjugates resulted in low yield, prompting us to explore another conjugation chemistry. Conjugate addition of thiol to Michael acceptors is a reliable way for selective modification of proteins. Because of its excellent reaction efficiency, we utilized maleimide as a Michael acceptor for selective modification of lysine residues on DT-CRM_{197}. Reaction of DT with Sulfo-EMCS at pH 6.4 resulted in attachment of 20-25 copies of maleimide linkers on protein surface (Scheme 5.2 and detailed protocol described in chapter 6).

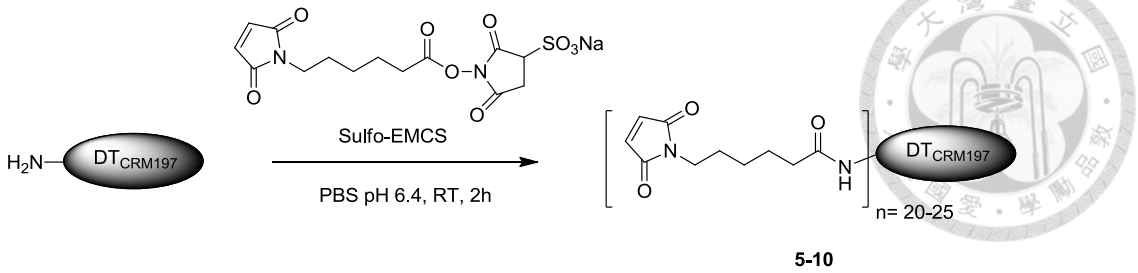

Scheme 5.4. Modification of carrier protein with maleimide linker.

We next proceed to modification of amino group into thiol at reducing end of glycans selected for glycoconjugate synthesis. The amino linker at reducing of **5-2**, **5-3**, **5-5**, **5-7**, and **5-8** aimed at preserving native glycan structures, was modified by reaction with 2 equivalents of 3,3'- Dithiobis (sulfosuccimidylpropionate) (DTSSP) in phosphate buffer (pH 7.2) followed by DTT mediated disulfide bond cleavage to afford thiolated glycans **5-11-5-15** (Scheme 5.3).

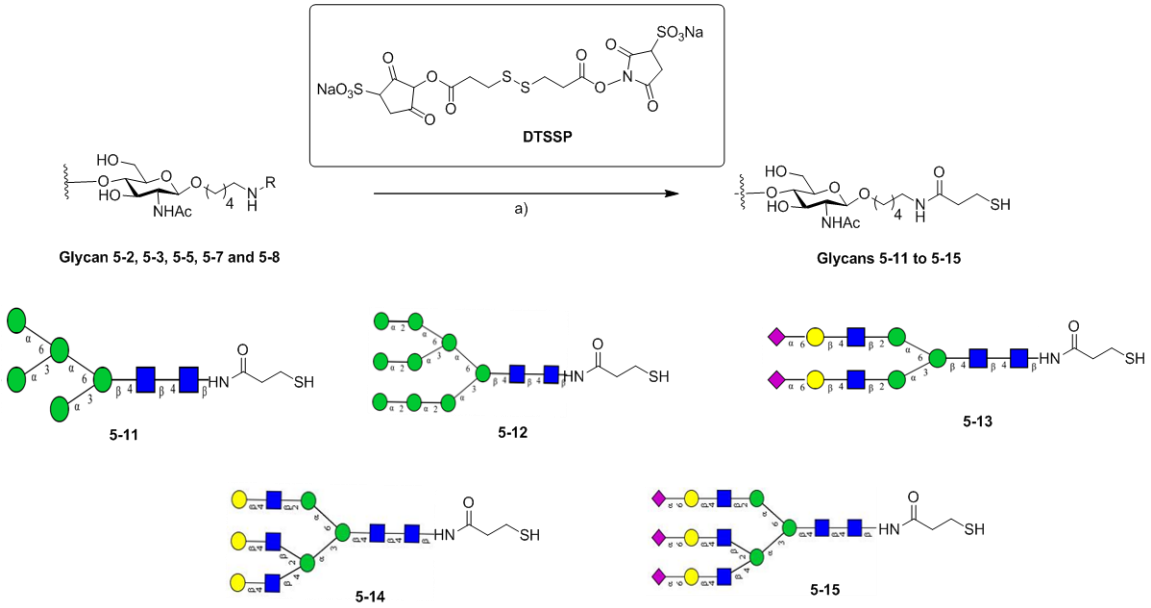

Scheme 5.5. Thiol modification at reducing end of glycans. a) i) DTSSP, PBS buffer pH 7.4, overnight; ii. DTT, 40°C, 2hr.

Maleimide modified DT-CRM_{197} **5-10** was incubated with **5-11** at room temperature overnight, excess of glycan was removed by dialysis, and glycan incorporation was checked by MALDI TOF (Scheme 5.4). Intermediate **5-16** was next subjected to reaction

with **5-13** overnight. Intact maleimide functional groups on protein surface were capped by mercaptoethanaol. Finally, glycoconjugate **2** was purified, carbohydrate loading was confirmed by MS (Appendix A), and protein quantification was done by bicinchoninic acid (BCA) assay.

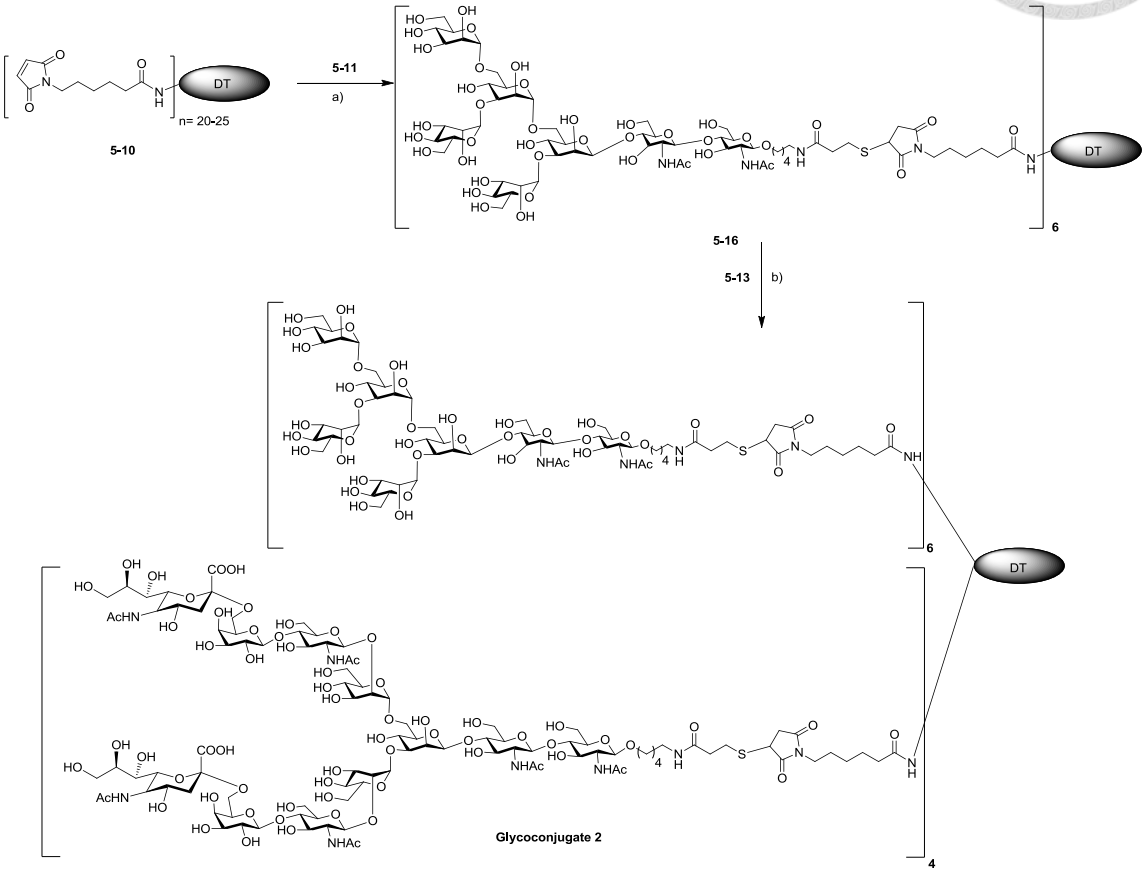

Scheme 5.6. Synthesis of glycoconjugate 2. a) PBS buffer pH 7.4, rt, overnight; b) i. PBS buffer pH 7.4, rt, overnight; ii. mercaptoethanol, PBS buffer pH 7.4, overnight.

5.3.2. Design of Glycoconjugates Based on PGT121 Epitope:

Recently, three primary members of PGT121 family (PGT121, 122 and 123) identified from African donor were found to be the most potent anti-HIV bNAbs beside PGT128. This family of bNAbs neutralizes 65-70% of HIV-1 isolates at an $IC_{50} < 50$ μg/mL and also recognizes N332-sensitive epitope[16]. A previous report investigating putative epitope has suggested that the PGT121 family antibodies involves protein component of the V3 base in addition to multiple surrounding glycans[18]. As a part of our interest in development of HIV-

1 vaccine, we performed a glycan specificity profiling of PGT121 using our in-house version of glycan microarray consisting of diverse high-mannose, hybrid and complex type *N*-linked oligosaccharides. Interestingly, we found that PGT121 showed significant enhancement in binding to tri-antennary complex type structure with and without terminal α-2,6-linked sialic acid, which has never been revealed before.

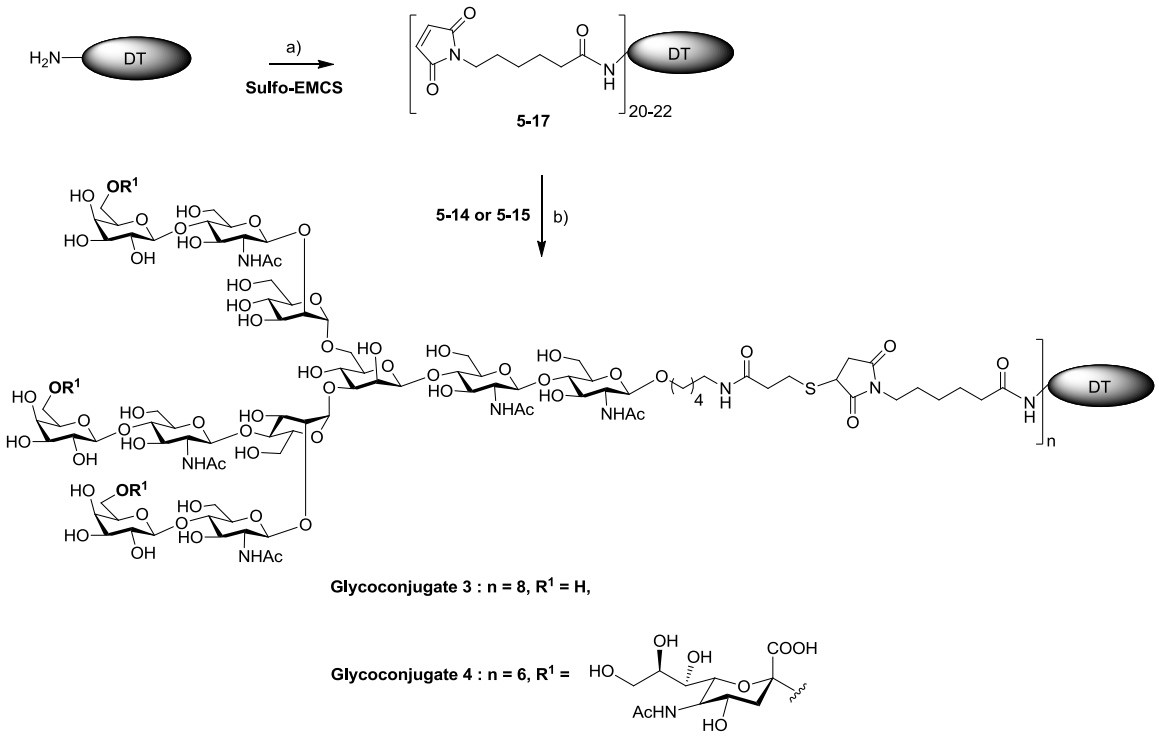

Scheme 5.7. Synthesis of glycoconjugate 3 and 4. a) PBS buffer pH 7.4, rt, overnight; b) i. PBS buffer pH 7.4, rt, overnight; ii. mercaptoethanol, PBS buffer pH 7.4, overnight.

To evaluate the HIV-1 immunogenicity of carbohydrate epitopes recognized by PGT121, the conjugate addition of compounds **5-14** and **5-15** to modified DT **5-17** was performed in phosphate buffer (pH 7.2) at room temperature for 2 h. Deactivation of the unreacted maleimides on DT was accomplished by excess of thioethanol. The synthetic constructs were underwent MALDI-TOF mass analysis to determine carbohydrate epitope ratio on DT. The average numbers of glycan copies were found to be eight for construct **3** and six for construct **4**.

5.3.3. Design of Glycoconjugates Based on Asn332 and Asn301 Sensitive PGT128 Epitope:

Antibody PGT128, the most potent HIV-1 broadly neutralizing antibody identified to date, shown to bind the N332 glycan ($Man_9GlcNAc_2$) in the primary binding site whereas, the secondary glycan binding site recognizes the N301 glycan involve only core pentasaccharide, a portion common in all *N*-glycans[11,12]. Notably, N332 and N301glycans are highly conserved among HIV isolates, which accounts for the broader neutralization potency exhibited by PGT128. However, $N301_{gp102}$ attached carbohydrates appears to be a complex type *N*-glycan in gp120s that were analyzed by mass spectrometry, but not in the gp120 outer domain construct used for structural studies[13,17].

To construct the predicted epitope of PGT128, we used similar conjugation chemistry as used for synthesis of glycoconjugate **2**. Depicted in Scheme 5.6, thiolated $Man_9GlcNAc_2$ **5-12** was conjugated to maleimide activated DT to afford five copies of glycans attached on DT surface. Next, the intermediate **5-18** was again conjugated with thiolated complex type glycan **5-13,** followed by quenching of residual maleimides on DT. The resultant glycoconjugate **5** was subjected to MALDI-TOF analysis to determine the average carbohydrate loadings.

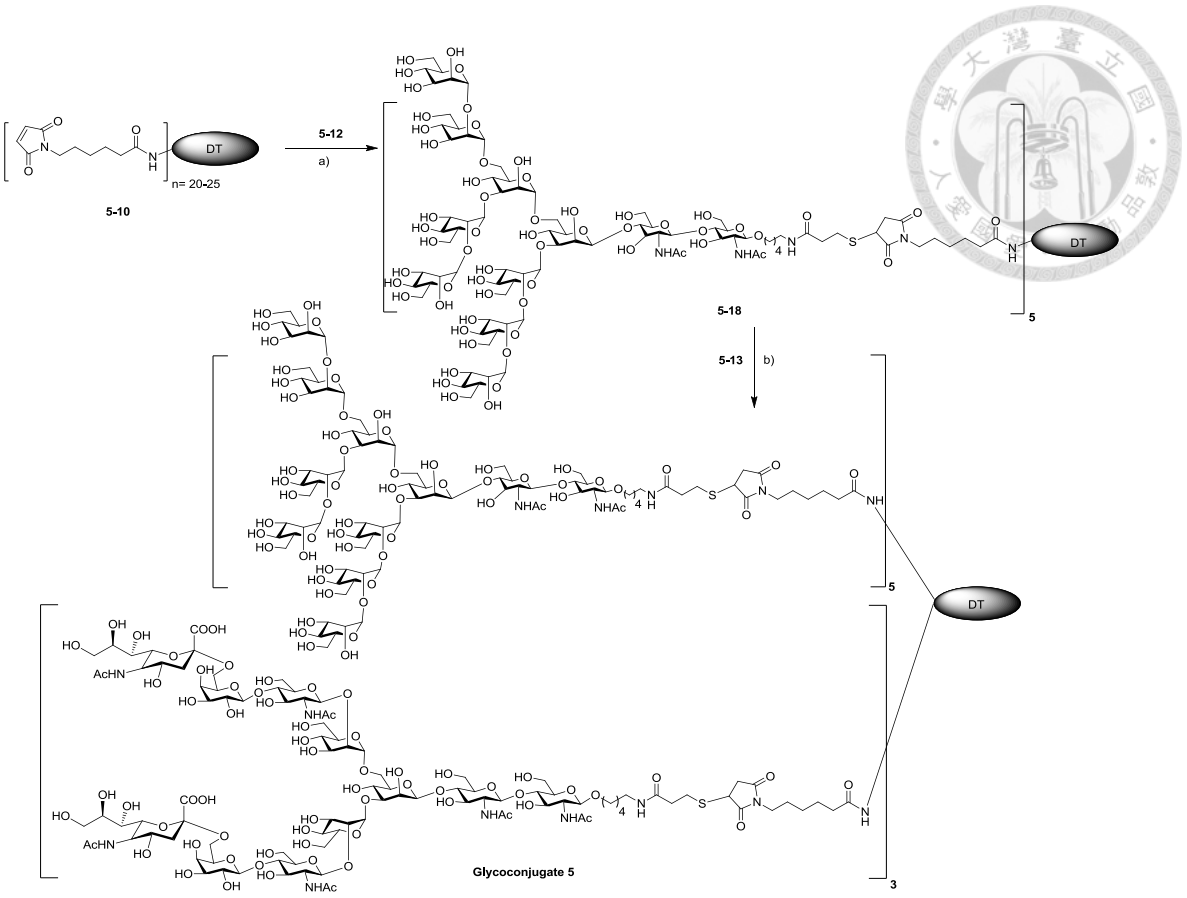

Scheme 5.8. Synthesis of glycoconjugate 5. a) PBS buffer pH 7.4, rt, overnight; b) i. PBS buffer pH 7.4, rt, overnight; ii. mercaptoethanol, PBS buffer pH 7.4, overnight.

5.3.4. MALDI TOF Analysis of Glycan Incorporation on Carrier Protein:

Glycoconjugates **1-5** with different copies of various carbohydrate structures were analyzed by bicinchoninic acid (BCA) assay for protein quantification. Based on average glycans incorporation and protein quantification, the carbohydrate content on protein was determined. The detailed analysis of conjugates **1-5** is shown in table 5.1.

Table 5.1. The carbohydrate content on carrier protein.

Glyco-conjugate	Protein mol. wt	After glycosylation	Average Incorporation (n)	Carbohydrate on protein (μg)	Protein quantity (μg)
1	58284.03	68914.93	5.0	186	1050
2	63598.22	82177.99	10.0	466	1430
3	62410.87	83466.97	8.0	92	310
4	62410.87	83169.54	6.5	96	328
5	63598.22	82994.56	8.0	473	1550

5.4. Mice Immunization Studies:

To evaluate the immunogenicity of synthetic constructs, a group of five mice were immunized intramuscularly with glycoconjugates **1-5** (2 μg of sugars) in presence of α-galactosylceramide C34 as a adjuvant, since our previous report showed that glycoconjugate vaccine combined with α-galactosylceramide C34 could induce higher IgG titer. Three injections were performed at two -week interval and serum was collected two weeks after third injection (Figure 5.1). All mice remained healthy for the duration of the study and no adverse reactions were observed.

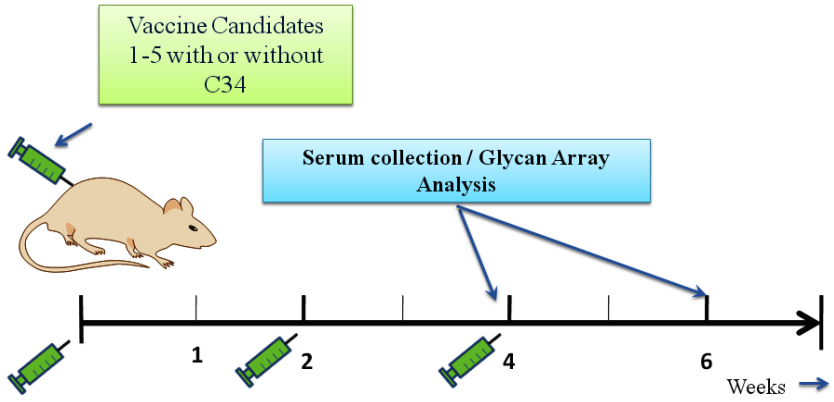

Figure 5.1. Mice Immunization Schedule.

The serum binding titer was determined against a wider panel of related *N*-linked oligosaccharides on printed glycan array (Figure 5.2). Serum was assayed at a 1 : 100

dilution to facilitate the detection of low affinity interactions while minimizing nonspecific background binding.

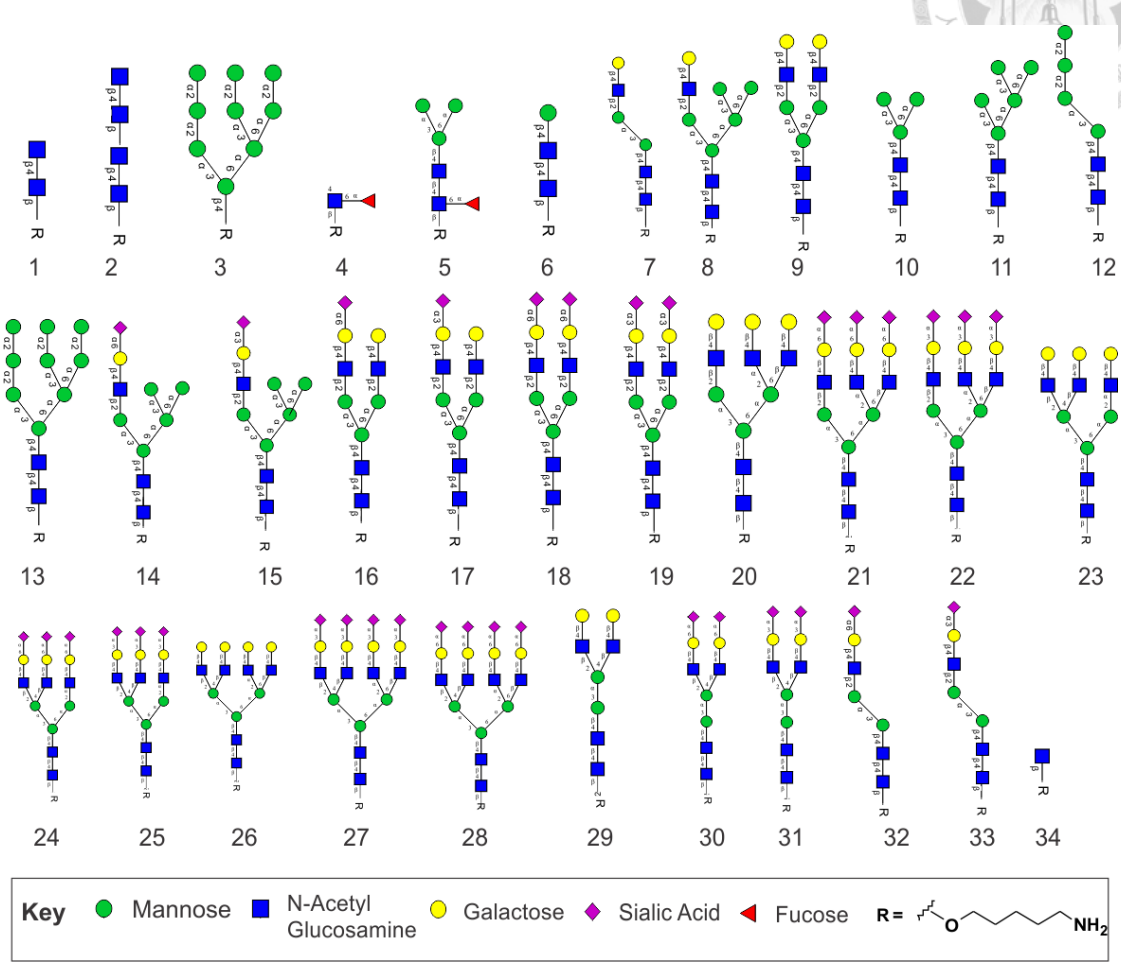

Figure 5.2. Pictorial presentation of set of 34 *N*-linked oligosaccharides printed N-hydroxy succinimide activated glass surface through amide bond formation.

The binding of serum IgG/IgM from mice immunized with construct **1-5** to *N*-glycan structures is shown in Figure 5.3-5.4. Mice immunized with all the constructs generated high titer of IgG antibodies compared to IgM, demonstrating that immunoglobulin class switching was induced.

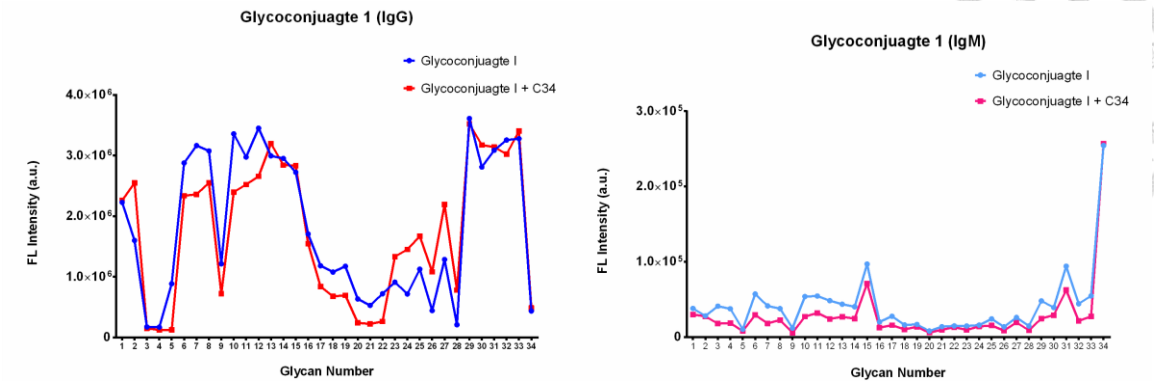

Figure 5.3. The glycan binding profile of IgG (left panel)and IgM (right panel) collected from glycoconjugate **1** immunized mice. Female BALB/c mice were immunized with 2 µg of glycoconjugate **1** in combination with or without C34. Mouse serum was collected two weeks after the final vaccination, and the generation of IgG and IgM against a panel of *N*-linked glycan was done after 100 fold dilution. Data represent total intensity of five mice ± the SEM.

Immunization with glycoconjugate **1** with or without C34, we observed that induced IgG antibodies recognized a series of *N*-linked glycans printed on array, however, IgM response was specifically directed towards N-Acetyl glucosamine (Figure 5.3). The major difference between IgG and IgM antibodies induced my glycoconjugate **1** is their titer and specificity towards reducing end di-GlcNAc and GlcNAc respectively. The similar IgG response was generated for antibodies induced by mice immunized with glycoconjugates 2-5 in presence of C34 (Figure 5.4), however, IgM titer for glycoconjugates 2 and 5 was very low. Despite, the structural diversity of immunogenic epitopes, the induction of immune response was observed to be non-specific through recognition of structures with di-GlcNAc motif.

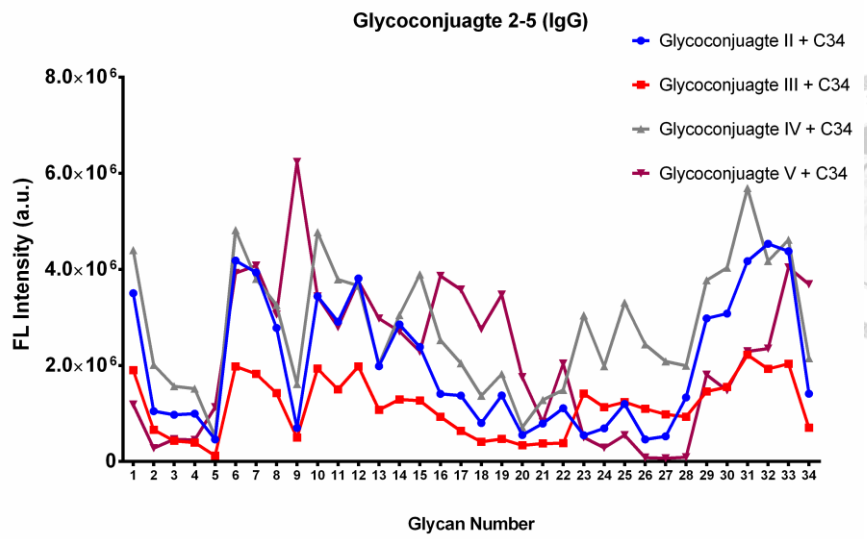

Figure 5.4. The glycan binding profile of IgG collected from glycoconjugate **2-5** immunized mice. Female BALB/c mice were immunized with 2 μg of glycoconjugate **2-5** in combination with C34. Mouse serum was collected two weeks after the final vaccination, and the generation of IgG against a panel of *N*-linked glycan was done after 100 fold dilution. Data represent total intensity of five mice ± the SEM.

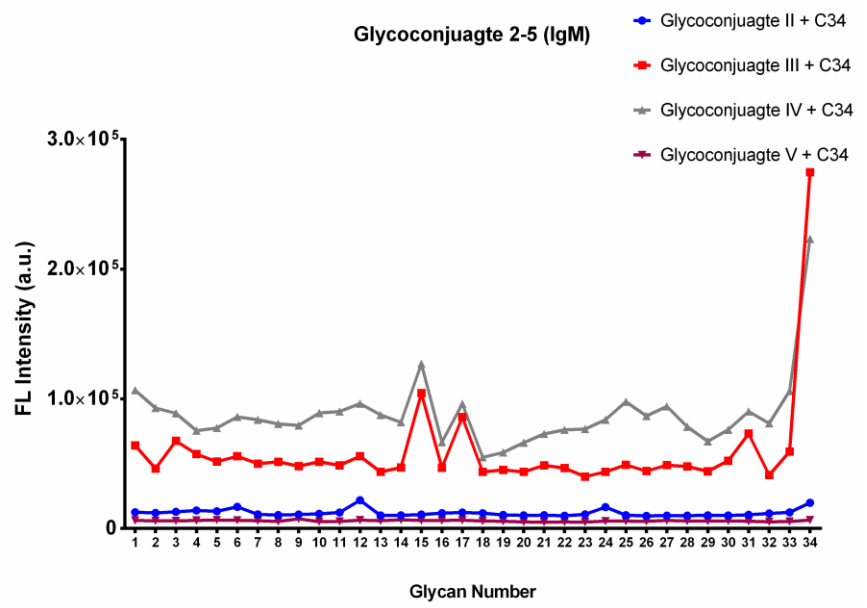

Figure 5.5. The glycan binding profile of IgM collected from glycoconjugate **2-5** immunized mice. Female BALB/c mice were immunized with 2 μg of glycoconjugate **2-5** in combination with C34.

5.5. Binding of Pooled Mice Antisera to HIV-1 gp120 Glycoproteins:

We next tested the cross reactivity of the antisera pooled form mice immunized with glycoconjugates 1-5 towards HIV-1 gp120 ($HXBc_2$ and YU_2 strains). Microtiter plates were coated with HIV-1 gp120 ($HXBc_2$ and YU_2 strains) overnight at 4°C. After plates were washed, the nonspecific bindings are blocked with 3% BAS in PBS for 1h at room temperature. 1:100 diluted mice serum samples were added to each well and incubated at 37°C for 1h and washed with washing buffer. Finally, the binding was detected by adding 100µL of HRP-conjugated anti-mice IgG and optical density was measured at 450 nm.

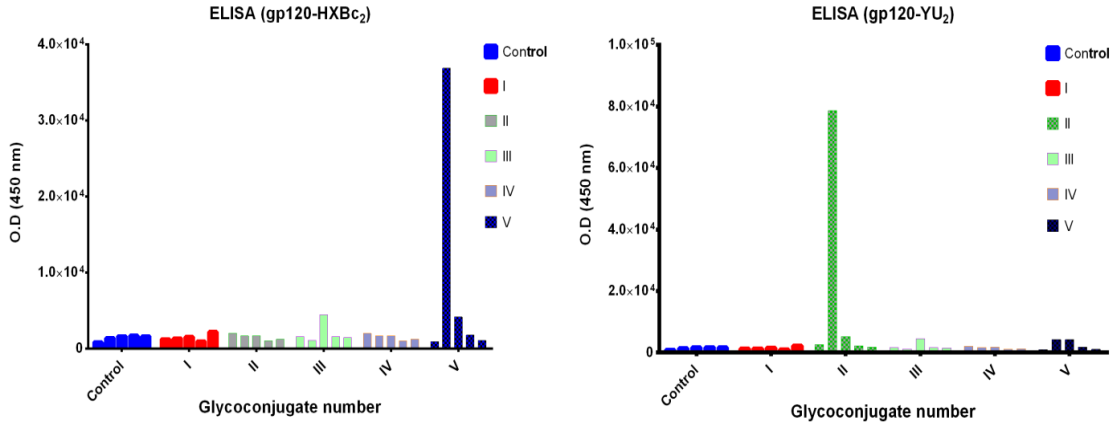

Figure 5.6. Antisera cross reactivity to HIV-1 gp120 assessment using ELISA.

It was found that the mice pre-sera showed a significant background of cross-reactivity to the HIV-1gp120. Glycoconjugates **1**, **3**, and **4** failed to induced gp120 cross reactive antibodies. Nevertheless, the anti-sera of mice number 2 immunized with glycoconjugates **2** clearly showed an enhanced reactivity to HIV-1 gp120 $HXBC_2$, however, mice number 2 from glycoconjugate 5 to gp120 YU_2 strain. The observed cross reactivity might be contributed from the oligomannose and complex type glycans specific antibodies in the anti-sera.

5.6. Summary and Conclusion:

Taken together, our immunological study led us to conclude that immunization of mice with glycoconjugates 1-5 designed based on PG9 and PGT121 epitope, induced high titer of IgG antibodies specific towards di-GlcNAc but not to the glycans which are specifically incorporated in synthetic construct. The possible reasons behind induction of non-specific antibodies could be; (i) the multivalency of conjugated glycans on carrier protein was not enough to mimic the native carbohydrate epitope; (ii) strong immunogenicity of reducing end di-GlcNAc motif which was never been addressed before. Failure in achieving desired specificity raised an important question whether the success of *N*-linked oligosaccharides based conjugate vaccines could be hampered by strong immune response towards di-GlcNAc at reducing end of *N*-glycans. To the end, some of our synthetic constructs induced gp120 cross reactive antibodies in one out of five used for immunization study.

5.7. References:

(1) Sax, P. E.; Baden, L. R. *N. Engl. J. Med.* **2009**, *360*, 1897.

(2) Excler, J. L.; Tomaras, G. D.; Russell, N. D. *Curr. Opin. Hiv. Aids.* **2013**.

(3) (a) Pantaleo, G.; Esteban, M.; Jacobs, B.; Tartaglia, J. *Curr. Opin. Hiv. Aids.* **2010**, *5*, 391; (b) Schief, W. R.; Ban, Y. E.; Stamatatos, L. *Curr. Opin. Hiv. Aids.* **2009**, *4*, 431; (c) Pantophlet, R.; Burton, D. R. *Annu. Rev. Immunol.* **2006**, *24*, 739.

(4) Koff, W. C. *Vaccine* **2012**, *30*, 4310.

(5) (a) Joyce, J. G.; Krauss, I. J.; Song, H. C.; Opalka, D. W.; Grimm, K. M.; Nahas, D. D.; Esser, M. T.; Hrin, R.; Feng, M.; Dudkin, V. Y.; Chastain, M.; Shiver, J. W.; Danishefsky, S. J. *Proc. Natl. Acad. Sci. U.S.A* **2008**, *105*, 15684; (b) Wang, L. X. *Curr. Opin. Drug Disco. Develop.***2006**, *9*, 194.

(6) Simek, M. D.; Rida, W.; Priddy, F. H.; Pung, P.; Carrow, E.; Laufer, D. S.; Lehrman, J. K.; Boaz, M.; Tarragona-Fiol, T.; Miiro, G.; Birungi, J.; Pozniak, A.; McPhee, D. A.; Manigart, O.; Karita, E.; Inwoley, A.; Jaoko, W.; Dehovitz, J.; Bekker, L. G.; Pitisuttithum, P.; Paris, R.; Walker, L. M.; Poignard, P.; Wrin, T.; Fast, P. E.; Burton, D. R.; Koff, W. C. *J. Virol.* **2009**, *83*, 7337.

(7) Walker, L. M.; Huber, M.; Doores, K. J.; Falkowska, E.; Pejchal, R.; Julien, J. P.; Wang, S. K.; Ramos, A.; Chan-Hui, P. Y.; Moyle, M.; Mitcham, J. L.; Hammond, P. W.; Olsen, O. A.; Phung, P.; Fling, S.; Wong, C. H.; Phogat, S.; Wrin, T.; Simek, M. D.; Koff, W. C.; Wilson, I. A.; Burton, D. R.; Poignard, P. *Nature* **2011**, *477*, 466.

(8) Hevey, R.; Ling, C. C. *Future Med. Chem.* **2012**, *4*, 545.

(9) (a) Godfrey, D. I.; Rossjohn, J. *The Journal of experimental medicine* **2011**, *208*, 1121; (b) Van Kaer, L.; Parekh, V. V.; Wu, L. *Immunotherapy-Uk* **2011**, *3*, 59.

(10) Huang, Y. L.; Hung, J. T.; Cheung, S. K.; Lee, H. Y.; Chu, K. C.; Li, S. T.; Lin, Y. C.; Ren, C. T.; Cheng, T. J.; Hsu, T. L.; Yu, A. L.; Wu, C. Y.; Wong, C. H. *Proc. Natl. Acad. Sci. U. S. A.* **2013**, *110*, 2517.

(11) Walker, L. M.; Huber, M.; Doores, K. J.; Falkowska, E.; Pejchal, R.; Julien, J. P.; Wang, S. K.; Ramos, A.; Chan-Hui, P. Y.; Moyle, M.; Mitcham, J. L.; Hammond, P. W.; Olsen, O. A.; Phung, P.; Fling, S.; Wong, C. H.; Phogat, S.; Wrin, T.; Simek, M. D.; Koff, W. C.; Wilson, I. A.; Burton, D. R.; Poignard, P.; Investigators, P. G. P. *Nature* **2011**, *477*, 466;

(12) Walker, L. M.; Phogat, S. K.; Chan-Hui, P. Y.; Wagner, D.; Phung, P.; Goss, J. L.; Wrin, T.; Simek, M. D.; Fling, S.; Mitcham, J. L.; Lehrman, J. K.; Priddy, F. H.; Olsen, O. A.; Frey, S. M.; Hammond, P. W.; Kaminsky, S.; Zamb, T.; Moyle, M.; Koff, W. C.; Poignard, P.; Burton, D. R.; Investigators, P. G. P. *Science* **2009**, *326*, 285.

(13) Pejchal, R.; Doores, K. J.; Walker, L. M.; Khayat, R.; Huang, P. S.; Wang, S. K.; Stanfield, R. L.; Julien, J. P.; Ramos, A.; Crispin, M.; Depetris, R.; Katpally, U.; Marozsan, A.; Cupo, A.; Maloveste, S.; Liu, Y.; McBride, R.; Ito, Y.; Sanders, R. W.; Ogohara, C.; Paulson, J. C.; Feizi, T.; Scanlan, C. N.; Wong, C. H.; Moore, J. P.; Olson, W. C.; Ward, A. B.; Poignard, P.; Schief, W. R.; Burton, D. R.; Wilson, I. A. *Science* **2011**, *334*, 1097.

(14) McLellan, J. S.; Pancera, M.; Carrico, C.; Gorman, J.; Julien, J. P.; Khayat, R.; Louder, R.; Pejchal, R.; Sastry, M.; Dai, K.; O'Dell, S.; Patel, N.; Shahzad-ul-Hussan, S.; Yang, Y.; Zhang, B.; Zhou, T.; Zhu, J.; Boyington, J. C.; Chuang, G. Y.; Diwanji, D.; Georgiev, I.; Kwon, Y. D.; Lee, D.; Louder, M. K.; Moquin, S.; Schmidt, S. D.; Yang, Z. Y.; Bonsignori, M.; Crump, J. A.; Kapiga, S. H.; Sam, N. E.; Haynes, B. F.; Burton, D. R.; Koff, W. C.; Walker, L. M.; Phogat, S.; Wyatt, R.; Orwenyo, J.; Wang, L. X.; Arthos, J.; Bewley, C. A.; Mascola, J. R.; Nabel, G. J.; Schief, W. R.; Ward, A. B.; Wilson, I. A.; Kwong, P. D. *Nature* **2011**, *480*, 336;

(15) Pancera, M.; Shahzad-Ul-Hussan, S.; Doria-Rose, N. A.; McLellan, J. S.; Bailer, R. T.; Dai, K.; Loesgen, S.; Louder, M. K.; Staupe, R. P.; Yang, Y.; Zhang, B.; Parks, R.; Eudailey, J.; Lloyd, K. E.; Blinn, J.; Alam, S. M.; Haynes, B. F.; Amin, M. N.; Wang, L. X.; Burton, D. R.; Koff, W. C.; Nabel, G. J.; Mascola, J. R.; Bewley, C. A.; Kwong, P. D. *Nat. Struct. Mol. Biol* .**2013**.

(16) Mouquet, H.; Scharf, L.; Euler, Z.; Liu, Y.; Eden, C.; Scheid, J. F.; Halper-Stromberg, A.; Gnanapragasam, P. N. P.; Spencer, D. I. R.; Seaman, M. S.; Schuitemaker, H.; Feizi, T.; Nussenzweig, M. C.; Bjorkman, P. J. *Proc. Natl. Acad. Sci. U. S. A.* **2012**, *109*, E3268.

(17) Walker, L. M.; Huber, M.; Doores, K. J.; Falkowska, E.; Pejchal, R.; Julien, J. P.; Wang, S. K.; Ramos, A.; Chan-Hui, P. Y.; Moyle, M.; Mitcham, J. L.; Hammond, P. W.; Olsen, O. A.; Phung, P.; Fling, S.; Wong, C. H.; Phogat, S.; Wrin, T.; Simek, M. D.; Koff, W. C.; Wilson, I. A.; Burton, D. R.; Poignard, P. *Nature* **2011**, *477*, 466.

(18) Julien, J. P.; Sok, D.; Khayat, R.; Lee, J. H.; Doores, K. J.; Walker, L. M.; Ramos, A.; Diwanji, D. C.; Pejchal, R.; Cupo, A.; Katpally, U.; Depetris, R. S.; Stanfield, R. L.; McBride, R.; Marozsan, A. J.; Paulson, J. C.; Sanders, R. W.; Moore, J. P.; Burton, D. R.; Poignard, P.; Ward, A. B.; Wilson, I. A. *PLoS pathogens* **2013**, *9*, e1003342.

Chapter 6

Experimental

6.1. General Methods:

NHS coated glass slides were purchased from SCHOTT (Nexterion H), bNAbs PG9, PG16 and PGTs 141-145 were kindly gifted by Prof. Peter Kwong, NIH (PG9/PG16 also purchased from Polymun, Vienna Austria), PGTs 121, 128 were obtained from Prof. Dennis Burton, The Scripps Research Institute. Secondary antibody DyLight649-conjugated donkey anti-Human IgG was purchased from Jackson Immuno Research. Cytidine 5'-triphosphate (CTP), N-Acetylneuraminic acid (Neu5Ac) and Phospho (enol) pyruvic acid (PEP) were purchase from Sigma-Aldrich. The α-2,3-sialyltransferase JT-FAJ-16 and α-2,6-sialyltransferase JT-ISH-224 pst6-224 were DNA synthesized and optimized for E.coli. Cytidine monophosphate kinase (CMK), pyruvate kinase (PK) and pyrophosphatase (PPA) were cloned from E.coli MG1655 (ATCC700926).

All chemicals were purchased as reagent grade and used without further purification. Anhydrous dichloromethane (CH_2Cl_2), acetonitrile (CH_3CN), tetrahydrofuran (THF), N,N-Dimethyl formamide (DMF), toluene, methanol (MeOH) were purchased from a commercial source without further distillation. Pulverized Molecular Sieves MS-4Å (Aldrich) for glycosylation was activated by heating at 350^{o}C for 3 h. Reactions were monitored by analytical thin-layer chromatography (TLC) in EM silica gel 60 F254 plates and visualized under UV (254 nm) and/or by staining with acidic ceric ammonium molybdate or *p*-anisadehyde. Flash chromatography was performed on silica gel (Merck) of 40-63 μm particle size. ^{1}H NMR spectra were recorded on a Bruker AVANCE 600 (600 MHz) spectrometer at 25 ºC. Chemical shifts (in ppm) were assigned according to $CDCl_3$ (δ = 7.24ppm) and D_2O (δ = 4.80ppm). ^{13}C NMR spectra were obtained with Bruker AVANCE 600 spectrometer and were calibrated with $CDCl_3$ (δ = 77.00ppm). Coupling constants (*J*) are reported in hertz (Hz). Splitting patterns are described by using the following abbreviations: s, singlet; brs, broad singlet; d doublet; brd, broad doublet; t, triplet; q, quartet; dt, triplet of doublet; tt, triplet of triplet; qt, triplet of quartet; m, multiplet. ^{1}H NMR spectra are reported in the following order: chemical shift, multiplicity, number(s) of protons and cou-

pling constant(s). High resolution ESI mass spectra were recorded on a Bruker Daltonics spectrometer.

6.1.1. General Procedures:

1: Global Deprotection of Oligosaccharides:

A mixture of protected oligosaccharides (50 mmol) and 10 mL of ethylene diamine:nBuOH (1:4) was stirred at 90^0C overnight. Volatiles were then evaporated, and crude was reacted with 10 mL Ac_2O/pyridine (1:2) overnight. The solvents were removed using high vacuum, and product was purified by flash column chromatography (acetone: toluene, 2/8,v/v). Product was de-acetylated using sodium methoxide in MeOH (10 mL) overnight. Reaction was neutralized by using IR-120 filtered and concentrated in *vacuo.* The residue was purified by flash column chromatography (acetone: toluene, 3/7,v/v). Product was dissolved in 10mL MeOH:H_2O:HCOOH (6:3:1), $Pd(OH)_2$ (50% by weight) was added, and reaction was hydrogenated overnight. Reaction mixture was filtered through celite and concentrated in *vacuo.* The residue was purified by Bio-Gel P-2 (BIO-RAD) column chromatography using water as eluent. Product was then lypholysed to get desired oligosaccharides as a white color powder.

2: Enzymatic Sialylation of Hybrid and Complex Type Oligosaccharides.

Galactose terminated oligosaccharides (5 µmol), CTP (1 µmol), Neu5Ac (9.5 µmol), PEP (10 µmol), α-2,6/α-2,3 sialyltransferase (200 µL, estimated concentration of 2 mg/L), CMK (80 units), PK (40 units) and PPA (40 units) were dissolved in 50 µmol sodium cacodylate (pH 7.4) containing 1% BSA (130 µl). The reaction was incubated at 37°C with gentle agitation for 2d for α-2,6-linked and 8d for α-2,3-linked sialylated glycans. The total consumption of starting material was confirmed my mass spectormetric analysis. Product was purified by using Bio-Gel P-2 chromatography (eluent H_2O) to afford their sialylated analogues as white solid after lyophilization.

6.2. Experimental for Chapter 2.

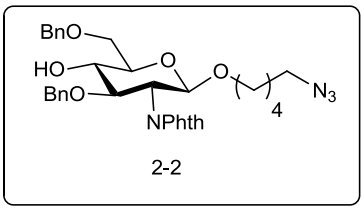

2-2

5-Azidopentyl-O-3,6-di-O-benzyl-2-deoxy-2-phthalimido-β-D-glucopyranoside (2-2): Activated 4Å molecular sieves (5 g) was added to a solution of **2-1** (4.50 g, 7.56 mmol) and 5-azido pentanol (1.95 g, 15.2 mmol) in anhydrous CH_2Cl_2 (50 mL). The mixture was stirred for 1 h at room temperature. The reaction was cooled to -20^{o}C. NIS (4.25 g, 18.9 mmol) and then TfOH (167.7 μL, 1.89 mmol) were added slowly, and the resulting reaction mixture was stirred for 2 h. When TLC (ethyl acetate: toluene, 2/8) indicated formation of product with consumption of starting material, reaction was quenched by adding Et_3N and then filtered through celite. Filtrate was washed with aqueous $NaHCO_3$ (2 x 50mL), aqueous $Na_2S_2O_3$ (2 x 50 mL) and brine (50 mL) solution. The organic layer was dried over Na_2SO_4 and concentrated in *vacuo*. The residue was purified by flash column chromatography to afford **2-2** (3.6 g, 70%) as clear foam. TLC (ethyl acetate:toluene =2/8, v/v): R_f =0.44; ^{1}HNMR (600 MHz, $CDCl_3$): δ 7.69-7.35 (m, 4H), 7.35-7.30 (m, 5H), 7.70-7.03 (m, 2H), 6.95-6.05 (m, 3H,), 5.11 (d, *J*=10.2 Hz, 1H), 4.73 (d, *J*=11.3 Hz, 1H), 4.63 (d, *J*=12.6 Hz, 1H), 4.57 (d, *J*=12 Hz, 1H), 4.52 (d, *J*=12 Hz, 1H), 4.22-4.18 (m, 1H), 4.12-4.10 (m, 1H), 3.80-3.78 (m, 4H), 3.77-3.74 (m, 1H), 3.64-3.610 (m, 1H), 3.36-3.32 (m, 2H); ^{13}CNMR (150 MHz, $CDCl_3$) : δ 168.38, 167.61, 138.40, 138.27, 137.94, 134.23, 134.10, 133.51, 131.97, 131.90, 129.98, 129.85, 128.78, 128.63, 128.45, 128.41, 128.23, 128.15, 128.08, 127.76, 123,81, 123,67, 84.09, 79.95, 78.01, 74.80, 74.43, 74.08, 71.01, 55.77; ESI-MS: *m/z* calcd for $C_{33}H_{36}N_4O_7Na$: 623.2476; found 623.2485 $(M + Na)^+$.

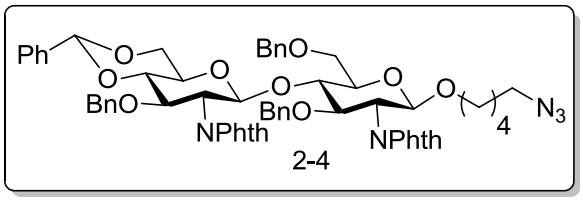

2-4

5-Azidopentyl-O-3-O-benzyl-4,6-O-benzylidene-2-deoxy-2-phthalimido-β-D-glucopyranos-yl-(1→4)-O-3,6-di-O-benzyl-2-deoxy-2-phthalimido-β-D-glucopyranoside (2-4):

Activated 4Å molecular sieves (5 g) was added to a solution of acceptor **2-2** (2.5 g, 4.1 mmol) and donor **2-3** (2.92 g, 4.9 mmol) in anhydrous CH_2Cl_2 (50 mL). The mixture was stirred for 1 h at room temperature. The reaction was cooled to -40^oC; NIS (2.30 g, 10.2 mmol) and then TfOH (90.5 µL, 1.0 mmol) were added slowly, and the resulting reaction mixture was stirred for 2 h. When TLC (ethyl acetate:hexane, 2/8) indicated formation of product with consumption of starting material, reaction was quenched by adding Et_3N and then filtered through celite. Filtrate was washed with aqueous $NaHCO_3$ (2 x 50 mL), aqueous $Na_2S_2O_3$ (2 x 50 mL) and brine (50 mL) solutions. The organic layer was dried over Na_2SO_4 and concentrated in *vacuo*. The residue was purified by flash column chromatography to afford **2-4** (3.15 g, 75%) as clear foam. TLC (ethyl acetate:hexane =2/8 v/v): R_f =0.34; ^{1}HNMR (600 MHz, $CDCl_3$): δ 7.65-7.48 (m, 8H), 7.47-7.46 (m, 2H), 7.35-7.33 (m, 8H), 7.27-7.26 (m, 2H), 7.25-6.89 (m, 8H), 5.49 (s, 1H), 5.36 (d, *J* = 12 Hz, 1H), 4.92 (d, *J* = 8.3 Hz, 1H), 4.80-4.75 (q, 2H), 4.47-4.39 (m, 5H), 4.38-4.20 (m, 2H), 4.18-4.12 (m, 2H), 4.07-4.04 (m, 1H), 3.71-3.68 (t, *J* = 9.6 Hz, 1H), 3.64-3.63 (m, 1H), 3.53 (t, *J* = 10.5Hz, 1H) 3.46 (d, *J* = 12.2 Hz, 1H), 3.38-3.32 (m, 3H), 3.30-3.21 (m, 1H), 2.87-2.76 (m, 2H), 1.76-1.50 (m, 4H) , 1.26-1.04 (m, 2H); ^{13}CNMR (150 MHz, $CDCl_3$): δ 138.20, 137.65, 134.48, 134.24, 134.10, 134.0, 132.07, 131.90, 130.65, 130.35, 129.25 ,128.52, 128.51, 128.43, 128.30, 128.24, 128.16, 128.06, 127.89, 127.85, 127.77, 127.65, 127.56, 127.32, 127.28, 126.35, 126.26, 123.95, 123.53, 101.48, 98.33, 98.01, 83.44, 74.80, 74.78, 74.62, 74.37, 74.25, 73.04, 72.97, 69.01, 68.36, 66.15, 66.02, 56.83, 55.92, 55.79. 51.44, 51.35, 29.03, 28.92, 28.84, 28.60, 28.52, 23.31, 23.25, 21.62; ESI-MS: *m/z* calcd for $C_{54}H_{53}N_5O_{13}Na$: 1002.3532; found 1002.3552 $(M + Na)^+$.

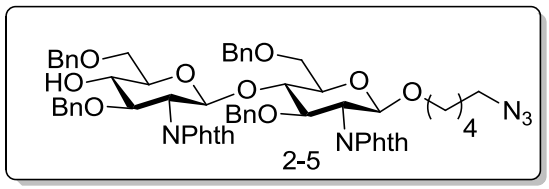

2-5

5-Azidopentyl-O-3,6-di-O-benzyl-2-deoxy-2-phthalimido-β-D-glucopyranosyl)-(1→4)-O-3, 6-di-O-benzyl-2-deoxy-2-phthalimido-β-D-glucopyranoside (2-5): A mixture of **2-4** (1.0 g, 0.93 mmol) and activated 4Å molecular sieves (1 g) in anhydrous CH_2Cl_2 (15 mL) was stirred at room temperature for 1 h. Reaction mixture was cooled to 0^oC; then, triethyl silane (2.90 mL, 18.1 mmol) and then trifluroacetic acid (1.37 mL, 18.2 mmol) were added,

and the resulting reaction mixture was stirred at room temperature for 1 h until TLC (ethyl acetate: hexane, 3/7) indicated product formation with consumption of starting material. The reaction mixture was quenched in ice cooled water and then extracted with CH_2Cl_2 (3 x 50 mL). Organic layer was washed with $NaHCO_3$ (2 x 50 mL). The aqueous layer was further extracted with CH_2Cl_2 (3 x 50 mL). The combined organic layers were washed with brine solution (50 mL), dried over Na_2SO_4, filtered and concentrated in *vacuo*. The residue was purified by flash column chromatography to afford **2-5** (0.670 g, 67%) as colorless foam. TLC (ethyl acetate:hexane =3/7 v/v): R_f =0.24; ^{1}HNMR (600 MHz, $CDCl_3$): δ 7.86-7.57 (m, 8H), 7.35-7.22 (m, 10H), 7.17-6.92 (m, 7H), 6.88-6.82 (m, 3H), 4.90 (d, *J* = 12 Hz, 1H), 4.76 (d, *J* = 12.3 Hz, 2H), 4.51-4.44 (m, 6H), 4.43-4.14 (m, 1H), 4.14-4.04 (m, 4H), 3.81-3.78 (t, *J* =10.2 Hz, 1H), 3.69-3.63 (m, 2H), 3.54-3.50 (m, 2H), 3.41 (dd, *J* = 6.2, 12.1 Hz, 1H), 3.37-3.35 (m, 1H), 3.28 (dd, *J* = 6.4 & 11.8Hz, 1H), 3.23-3.21 (m, 2H), 2.87-2.28 (m, 2H), 1.22-1.27 (m, 4H), 1.25-1.04 (m, 2H); ^{13}CNMR (150 MHz, $CDCl_3$) : δ 168.71, 168.29, 167.95, 138.91, 138.66, 138.59, 137.78, 134.27, 134.13, 133.97, 132.07, 131.92, 131.78 ,128.81, 128.75, 128.56, 128.50, 128.36, 128.20, 128.13, 128.04, 128.01, 127.79, 127.66, 127.58, 127.52, 127.18, 123.91, 123.43, 98.34, 97.43, 78.58, 76.99, 76.09, 75.94, 75.74, 74.84, 74.60, 74.47, 73.98, 73.05, 72.94, 71.27, 69.12, 68.50, 56.39, 55.95, 51.36, 28.93, 28.53, 13.26; ESI-MS: *m/z* calcd for $C_{54}H_{55}N_5O_{13}Na$: 1004.3689; found 1004.3726 $(M + Na)^+$.

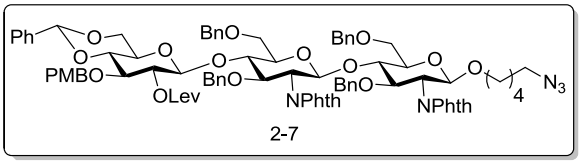

2-7

5-Azidopentyl-O-2-O-levulinoil-3-O-p-methoxy-benzyl-4,6-O-benzylidine-β-D-glucopyranosyl-(1→4)-O-(3,6-di-O-benzyl-2-deoxy-2-phthalimido-β-D-glucopyranosyl)-(1→4)-O-3,6-di-O-benzyl-2-deoxy-2-phthalimido-β-D-glucopyranoside (2-7): A mixture of disaccharide acceptor **2-5** (0.7 g, 0.712 mmol), thioglycoside donor **2-6** (0.633 g, 1.06 mmol) and activated 4Å molecular sieves (2 g) in anhydrous CH_2Cl_2 (15 mL) was stirred at room temperature for 1 h. The reaction was cooled to -20^{o}C, NIS (0.405 g, 1.78 mmol); then, TfOH (15.6 μL, 0.178 mmol) was added, and the resulting reaction mixture was stirred for 2 h. The reaction was quenched by adding Et_3N and then filtered through celite.

The filtrate was washed with aqueous $NaHCO_3$ (2 x 50 mL), aqueous $Na_2S_2O_3$ (2 x 50 mL) and brine (50 mL) solution. The organic layer was dried over Na_2SO_4 filtered and concentrated in *vacuo*. The residue was purified by flash column chromatography to afford trisaccharide **2-7** (0.680 g, 66%) as a white solid. TLC (ethyl acetate toluene =2/8 v/v): R_f = 0.44; ^{1}H NMR (600 MHz, $CDCl_3$): δ 7.83-7.64 (m, 8H), 7.53-7.37 (m, 5H), 7.37-7.27 (m, 12H), 7.24-7.18 (m, 4H), 6.99-6.85 (m, 5H), 6.83-6.73 (m, 3H), 5.42 (s, 1H), 5.26 (d, *J* = 12.2 Hz, 1H), 4.91 (m, 2H), 4.86 (d, *J* =2.2 Hz, 1H), 4.75 (t, *J* =10.2 Hz, 2H), 4.63-4.57 (m, 3H), 4.51-4.43 (m, 5H), 4.36-4.25 (t, *J* =11.0 Hz, 1H), 4.20-4.18 (m, 2H), 4.17-4.07 (m, 4H), 3.83 (s, 3H), 3.77-3.69 (m, 2H), 3.64-3.58 (m, 1H), 3.58-3.54 (m, 1H), 3.48 (d, *J* = 9.1 Hz, 1H), 3.40-3.36 (m, 3H), 3.17 (dd, *J* =3.5, 8.1 Hz, 1H), 3.22-3.19 (m, 2H), 2.87-2.70 (m, 2H), 2.68 (t, *J* = 8.6 Hz, 1H), 2.46-2.39 (m, 1H), 2.38-2.15 (m, 1H), 1.69 (s, 3H), 1.35-1.27 (m, 4H), 1.24-1.02 (m, 2H); ^{13}C NMR (150 MHz, $CDCl_3$): δ 206.14, 171.48, 168.56, 167.85, 159.47, 139.00, 138.92, 138.66, 138.28, 137.50, 134.18, 134.01, 133.83, 132.02, 131.68, 130.62, 129.79, 129.22, 128.76, 128.47, 128.38, 128.29, 128.15, 128.11, 128.10, 128.02, 127.99, 127.82, 127.59, 127.49, 127,24, 127.03, 126.25, 123.81, 123.39, 113.91, 101.37, 100.90, 98.18, 97.31, 81.92, 78.32, 78.18, 77.24, 76.93, 76.36, 74.97, 74.85, 74.78, 74.73, 73.97, 73.90, 73.53, 72.87, 69.06, 68.80, 68.37, 67.37, 66.11, 56.81, 55.96, 55.50, 51.31, 38.00, 30.07, 28.90, 28.48, 28.11, 23.22; ESI-MS: *m/z* calcd for $C_{87}H_{89}N_5O_{21}Na$: 1562.5942; found 1562.5965 $(M + Na)^+$.

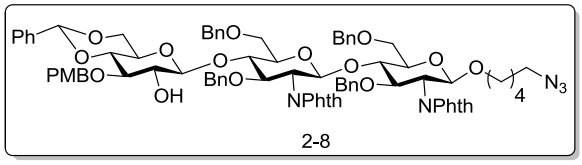

2-8

5-Azidopentyl-O-3-O-p-methoxy-benzyl-4,6-O-benzylidine-β-D-glucopyranosyl-(1→4)-O-(3,6-di-O-benzyl-2-deoxy-2-phthalimido-β-D-glucopyranosyl)-(1→4)-O-3,6-di-O-benzyl-2-deoxy-2-phthalimido-β-D-glucopyranoside (2-8): To a solution of **2-7** (0.650 g, 0.422 mmol) in THF (15 mL) was added hydrazine acetate (0.058 g, 0.632 mmol), stirred for overnight until TLC (ethyl acetate: toluene, 3/7) indicated formation of product with complete consumption of starting material. The reaction was concentrated in *vacuo*. The residue was suspended in ethyl acetate (100 mL) and washed with water (2 x 50 mL). The aqueous layer was further extracted with ethyl acetate (2 x 50 mL). The combined organic

layers were washed with brine solution (100 mL), dried over Na_2SO_4, and concentrated in *vacuo*. The residue was purified by flash column chromatography to afford **2-8** (0.489 g, 80%) as white solid. TLC (ethyl acetate : toluene =3/7 v/v) : R_f = 0.40; ^{1}H NMR (600 MHz, $CDCl_3$) : δ 7.66-7.50 (m, 7H), 7.42-7.48 (m, 2H), 7.23-7.39 (m, 16H), 6.99 (d, *J* = 6.5 Hz, 2H), 6.96 (m, 2H), 6.92 (t, *J* = 11.1 Hz, 2H), 6.88-6.84 (m, 3H), 6.78-6.75 (m, 5H), 5.44 (s, 1H), 5.26 (d, *J* = 12.5 Hz, 1H), 4.92-4.91 (m, 1H), 4.85 (d, *J* = 6.1 Hz, 1H), 4.83 (d, *J* = 6.3 Hz, 1H), 4.78 (d, *J* = 12.3 Hz, 1H), 4.70 (d, *J* = 12.3 Hz, 1H), 4.64 (d, *J* = 12.4 Hz, 1H), 4.59 (d, *J* = 12.8 Hz, 1H), 4.54-4.44 (m, 4H), 4.39 (d, *J* = 12.9 Hz, 1H), 4.36 (d, *J* = 12.2 Hz, 1H), 4.22-4.22 (m, 2H), 4.19-4.09 (m, 4H), 3.85-3.89 (m, 1H), 3.77 (s, 3H), 3.65-3.70 (m, 2H), 3.59-3.45 (m, 5H), 3.40 (dd, *J* = 6.2, 12.3 Hz, 1H), 3.32-3.31 (m, 1H), 3.29-3.28 (m, 1H), 3.25-3.20 (m, 1H), 3.19-3.15 (m, 1H) ,2.90-2.80 (m, 2H); ^{13}CNMR (125 MHz, $CDCl_3$) : δ 168.71, 168.20, 167.76, 159.57, 138.88, 138.72, 138.61, 138.11, 138.00, 137.58, 134.23, 134.07, 133.88, 132.01, 131.92, 131.67, 130.78, 129.95, 129.29, 129.19, 128.73, 128.48, 128.46, 128.35, 128.24, 128.21, 128.07, 128.00, 127.75, 127.63, 127.58, 127.53, 127.38, 127.12, 126.28, 125.55, 123.91, 123.38, 114.09, 103.65, 101.41, 98.36, 97.21, 81.58, 80.20, 78.88, 78.17, 76.94, 75.87,7 5.42, 74.90, 74.85, 74.76, 74.63, 74.50, 73.46, 72.89, 69.09, 68.90 ,68.46, 67.59, 66.51, 56.88, 55.97, 55.53, 51.33, 28.91, 28.51, 23.24, 21.71; ESI-MS: *m/z* calcd for $C_{82}H_{83}N_5O_{19}Na$: 1464.5574; found 1464.5594 $(M + Na)^+$.

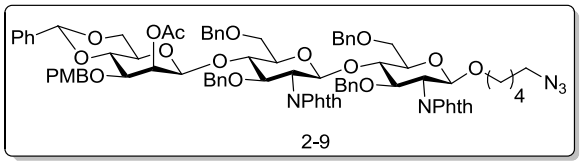

2-9

5-Azidopentyl-O-2-O-acetyl-3-O-p-methoxy-benzyl-4,6-O-benzylidine-β-D-mannopyranosyl-(1→4)-O-(3,6-di-O-benzyl-2-deoxy-2-phthalimido-β-D-glucopyranosyl)-(1→4)-O-3,6-di -O-benzyl-2-deoxy-2-phthalimido-β-D-glucopyranoside (2-9): Compound **2-8 (**1.90 g, 1.32 mmol**)** was concentrated from toluene (30 mL) 2 times. After it was placed under high vacuum for 1 h, freshly distilled CH_2Cl_2 (20 mL) was then added. Strictly anhydrous pyridine (600 μL, 6.69 mmol) was subsequently added and reaction was cooled to -15^{o}C. Tf_2O (350 μL, 1.51 mmol) was added drop wise over 2 min and the reaction mixture was stirred at -15°C for overnight. At this time, the reaction was concentrated under high vacuum and Bu_4NOAc (0.805 g, 2.64 mmol) was added. The resulting syrup was concen-

trated from toluene (30 mL) 2 times, placed under vacuum for 30 min. Freshly distilled toluene (20 mL) was added and reaction was sonicated for 16 h. Reaction was diluted with ethyl acetate (100mL) and washed with H_2O (2 x 50 mL) followed by brine (2 x 30 mL). The organic layer dried over Na_2SO_4, filtered, concentrated in *vacuo*, The residue was purified by silica gel column to afford compound **2-9** (1.69 g, 86%) as pale yellow solid. TLC (ethyl acetate : toluene =2/8 v/v) : R_f = 0.34; ^{1}H NMR (600 MHz, $CDCl_3$) : δ 7.80-7.43 (m, 8H), 7.39-7.38 (m, 2H), 7.32-7.19 (m, 13H), 6.95-6.79 (m, 9H), 6.75-6.79 (d, *J* = 8.2 Hz, 2H), 6.72-6.60 (m, 3H), 5.39 (s, 1H), 5.37 (d, *J* = 6.5 Hz, 1H), 5.16 (d, *J* = 12.3 Hz, 1H), 4.84-4.83 (m, 1H), 4.72 (t, *J* = 9.5 0Hz, 2H) ,4.70 (d, *J* = 3.5 Hz, 1H), 4.69 (dd, *J* = 6.3, 12.8 Hz, 1H), 4.51 (s, 1H), 4.49 (d, 3H), 3.39 (d, *J* = 12.5 Hz, 1H) ,4.32 (t, 2H), 4.17 (t, *J* = 11.2, 1H), 4.15-4.10 (m, 2H), 4.09-4.00 (m, 4H), 3.78-3.70 (m, 1H), 3.69 (s, 3H), 3.61-3.51 (m, 3H), 3.48-3.40 (m, 1H), 3.39 (dd, *J* = 6.3, 12.3Hz, 1H), 3.31 (dd, *J* = 6.5, 12.1Hz, 1H), 3.21 (dd, *J* = 6.9, 12.3Hz, 1H), 3.19-3.10 (m, 2H), 3.05-3.01 (m, 1H), 2.80-2.75 (m, 2H), 2.09 (s, 3H), 1.25-1.00 (m, 4H), 0.99-0.80 (m, 2H); ^{13}CNMR (150 MHz, $CDCl_3$) : δ 170.35, 168.65, 167.74 ,159.49, 138.84, 138.53, 128.09, 137.62,124.20, 134.00, 133.80, 131.96, 131.86, 131.62, 130.22, 129.98, 129.50, 129.08, 128.74, 128.67, 128.46, 128.40, 128.33, 128.26, 128.14, 128.00, 127.90, 127.81, 127.71, 127.68, 127.36, 127.06, 126.28, 123.86, 123.32, 114.00, 101.58, 99.61, 98.28, 97.22, 79.18, 77.97, 76.05, 75.78, 74.77, 74.73, 74.57, 74.40, 73.38, 72.96, 71.57, 69.33, 69.03, 68.61, 68.42, 68.04, 67.19, 56.76, 55.89, 55.45, 51.28, 28.85, 28.45, 23.18, 21.12 ; ESI-MS : *m/z* calcd for $C_{84}H_{85}N_5O_{20}Na$: 1506.5680; found 1506.5714 $(M + Na)^+$.

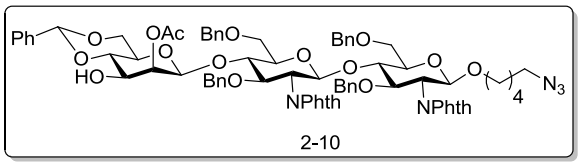

2-10

5-Azidopentyl-O-2-O-acetyl-4,6-O-benzylidine-β-D-mannopyranosyl-(1→4)-O-(3,6-di-O-benzyl-2-deoxy-2-phthalimido-β-D-glucopyranosyl)-(1→4)-O-3,6-di-O-benzyl-2-deoxy-2-phthalimido-β-D-glucopyranoside (2-10) : To a solution of **2-9** (1.0 g, 0.673 mmol) in 10 mL (CH_2Cl_2 : H_2O, 10/1) was added DDQ (0.183 g, 0.808 mmol) at 0°C and resulting reaction mixture was stirred until TLC (ethyl acetate: toluene, 2/8) indicated formation of a product with consumption of the starting material. Reaction mixture was

then filtered, organic layer washed with H_2O (2 x 30 mL). The aqueous layer was further extracted with CH_2Cl_2 (2 x 50 mL). The combined organic layers were washed with brine solution (40 mL), dried over Na_2SO_4, and concentrated in *vacuo.* The residue was purified by flash column chromatography to afford **2-10** (0.652 g, 70%) as colorless foam. TLC (ethyl acetate : toluene =2/8 v/v) : R_f = 0.24; ^{1}HNMR (600MHz, $CDCl_3$) : δ 7.84-7.51 (m, 8H), 7.42-7.10 (m, 14H), 7.00-6.89 (m, 8H), 6.80-6.79 (m, 3H), 5.44 (s, 1H), 5.28 (d, *J* = 6.5 Hz, 1H), 5.23 (d, *J* = 8.4 Hz, 1H), 4.91 (m, 1H), 4.86 (d, *J* = 12.3 Hz, 1H), 4.75 (s, 1H), 4.61 (d, *J* = 12.1 Hz, 1H), 4.51-4.35 (m, 5H), 4.28-4.08 (m, 7H), 3.70-3.54 (m, 5H), 3.50 (t, *J* = 10.6 Hz, 2H), 3.38 (dd, *J* = 6.2, 12.3 Hz, 1H), 3.28 (dd, *J* = 6.4, 12.8 Hz, 1H), 3.25-3.15 (m, 2H), 3.14-3.09 (m, 1H), 2.90-2.75 (m, 1H), 2.16 (s, 3H), 1.45-1.25 (m, 4H), 1.20-0.99 (m, 2H); ^{13}CNMR (150 MHz, $CDCl_3$) : δ 170.50, 168.46, 167.60, 138.67, 138.64, 138.38, 138.32, 137.92, 137.88, 137.05, 134.02, 133.82, 133.63, 131.77, 131.71, 131.45, 129.28, 129.06, 128.59, 128.52, 128.34, 128.22, 128.24, 128.07, 127.98, 127.87, 127.83, 127.64, 127.54, 127.50, 127.32, 127.29, 127.26, 127.20, 126.88 ,126.24 ,125.31, 123.66, 123.13, 101.15, 102.07, 99.17, 98.10, 97.01, 79.13, 78.55, 78.05, 75.82, 74.57, 74.37, 74.27,73.25, 73.30, 72.78, 71.26, 69.89, 68.85, 69,43, 68.25, 67.73, 66.67, 56.57, 55.71, 51.10, 28.67, 28.27, 23.00, 21.47, 21.02; ESI-MS : *m/z* calcd for $C_{76}H_{77}N_5O_{19}Na$: 1386.5105; found 1386.5135 $(M + Na)^+$.

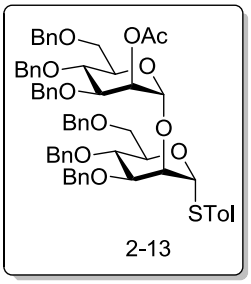

2-13

p-Tolyl-2-O-acetyl-3,4,6-tri-O-benzyl-α-D-mannopyranosyl-(1→2)-3,4,6-tri-O-benzyl-1-thio-α-D-mannopyranoside (2-13) : To a solution of acceptor **2-10** (1.70 g, 3.05 mmol) and donor **2-11**(2.34 g, 4.58 mmol) in 20 mL CH_2Cl_2 was added activated 4 Å molecular sieves and stirred for 1 h at room temperature. In a separate flask, AgOTf (1.19 g, 4.58 mmol) and DTBP (1.03 mL, 4.58 mmol) in 10 mL of CH_2Cl_2 were stirred with 4 Å MS for 1 h. The flask containing the AgOTf/DTBP was cooled to -30°C and solution containing mixture of donor and acceptor was added over 5 min. The solution was stirred with gradual

warming up to room temperature over 24 h. TLC (ethyl acetate: hexane, 2/8) indicated formation of product with consumption of starting material, reaction was quenched with Et_3N, filtered through celite, filtrate was washed with aqueous $NaHCO_3$ (2 x 50 mL) and a brine (50 mL) solution. The organic layer was dried over Na_2SO_4, and concentrated in *vacuo*. The residue was purified by silica gel column chromatography to afford **2-13** (2.90 g, 93%) as colorless foam**.** TLC (ethyl acetate : hexane = 2/8 v/v) : R_f = 0.35; ^{1}H NMR (600 MHz, $CDCl_3$) : δ 7.38-7.16 (m, 30H), 7.11-7.09 (m, 2H), 7.00 (d, *J* = 8.4 Hz, 2H), 5.59 (s, 1H), 5.51 (d, *J* = 2.4 Hz, 1H), 5.06 (s, 1H), 4.88 (d, *J* = 11.8 Hz, 1H), 4.81 (d, *J* = 11.2 Hz, 1H), 4.73-4.37 (m, 10H), 4.29 (t, *J* = 8.9 Hz, 1H), 4.22 (s, 1H), 3.96-3.88 (m, 4H), 3.83-3.71 (m, 2H), 3.69-3.63 (m, 2H), 3.55 (d, *J* = 12.1 Hz, 1H), 2.26 (s, 3H), 2.13 (s, 3H); ^{13}CNMR (150 MHz, $CDCl_3$) : δ 170.49, 138.75, 138.67, 138.62, 138.42, 138.32, 138.24, 137.87, 132.55, 130.51, 128.77, 128.64, 128.61, 128.56, 128.52, 128.39, 128.29, 128.20, 128.15, 128.03, 127.99, 127.94, 127.78, 127.63, 99.99, 87.78, 80.19, 78.35, 76.88, 75.48, 75.32, 75.03, 74.56, 73.46, 73.08, 72.47, 72.21, 72.18, 68.48, 69.02, 68.85, 21.42, 21.36; ESI-MS: *m/z* calcd for $C_{63}H_{66}O_{11}SNa$: 1053.4218; found 1053.4228 $(M + Na)^+$.

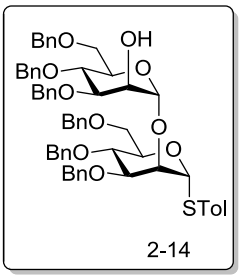

2-14

p-Tolyl-3,4,6-tri-O-benzyl-α-D-mannopyranosyl-(1→2)-3,4,6-tri-O-benzyl-1-thio-α-D-mannopyranoside (2-14): To as solution of compound **2-13** (1.01 g, 0.970 mmol) in 20 mL of methanol : CH_2Cl_2 (1/1) was added Sodium methoxide (0.024 g, 0.42 mmol), stirred at room temperature until TLC (ethyl acetate: hexane, 3/7) indicated formation of a product with consumption of the starting material. The reaction mixture was neutralized with IR-120, filtered and concentrated *in vacuo* and residue was purified by silica gel column chromatography to afford **2-14** (0.859 g, 89%) as a colorless oil. TLC (ethyl acetate: hexane =3/7 v/v) : R_f = 0.29; ^{1}HNMR (600 MHz, $CDCl_3$) : δ 7.33-7.10 (m, 32H), 6.96 (d, *J* = 7.8 Hz, 1H), 5.56 (s, 1H), 5.11 (s, 1H), 4.85 (d, *J* = 10.8 Hz, 1H), 4.75 (d, *J* = 10.8 Hz, 1H), 4.69-4.62 (m, 3H), 4.52-4.38 (m, 6H), 4.37 (d, *J* = 12.1 Hz, 1H), 4.25 (d, *J* = 12 Hz, 2H),

4.09 (s, 1H), 3.90-3.77 (m, 4H), 3.70 (d, *J* = 10.8 Hz, 1H), 3.62 (dd, *J* = 4.8, 8.2 Hz, 1H), 3.54 (d, *J* = 10.2 Hz, 1H), 2.23 (s, 3H); ^{13}CNMR (150 MHz, $CDCl_3$) : δ 138.61, 138.42, 138.33, 138.24, 137.97, 137.51, 132.18, 130.38, 129.73, 128.55, 128.47, 128.38, 128.29, 128.24, 127.93, 127.91, 127.89, 127.86, 127.85, 127.78, 127.68, 127.57, 127.48, 127.45, 127.33, 101.23, 87.62, 80.06, 79.99, 76.52, 75.18, 75.01, 74.95, 94.35, 73.21, 73.18, 72.87, 72.38, 72.18, 71.69, 69.28, 68.70, 68.56, 19.45; ESI-MS: *m/z* calcd for $C_{61}H_{64}O_{10}SNa$: 1011.4112; found 1011.4125 $(M + Na)^+$.

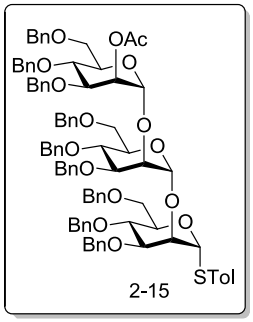

p-Tolyl-2-O-acetyl-3,4,6-tri-O-benzyl-α-D-mannopyranosyl-(1→2)-3,4,6-tri-O-benzyl-α-D-mannopyranosyl-(1→2)-3,4,6-tri-O-benzyl-1-thio-α-D-mannopyranoside (2-15): To a solution of acceptor **2-14** (2.6 g, 2.62 mmol) and donor **2-11** (2.01 g, 3.94 mmol) in 10 mL CH_2Cl_2 was added activated 4 Å molecular sieves and stirred for 1 h at room temp. In a separate flask, AgOTf (1.02 g, 3.94 mmol) and DTBP (893 µL, 3.94 mmol) in 30 mL of CH_2Cl_2 were stirred with activated 4 Å molecular sieves for 1 h. The mixture of AgOTf /DTBP was cooled to -30°C and solution of donor and acceptor was added over 5 min. The solution was stirred with gradual warming up to room temperature over 24 h until TLC (ethyl acetate: hexane, 2/8) indicated formation of product with consumption of starting material, reaction was quenched with Et_3N, filtered through celite. The filtrate was washed with aqueous $NaHCO_3$ (2 x 50 mL) and a brine (50 mL) solution. The organic layer was dried over Na_2SO_4, filtered and concentrated in *vacuo*. The residue was purified by silica gel column chromatography to afford **2-15** (3.50 g, 91%) as colorless foam. TLC (ethyl acetate : hexane = 2/8 v/v) : R_f = 0.41; ^{1}H NMR (600 MHz, $CDCl_3$) : δ 7.34-7.11 (m, 45H), 7.05-7.03 (m, 2H), 7.93 (d, *J* = 7.2 Hz, 1H), 5.65 (s, 1H), 5.50 (d, *J* = 3.0 Hz, 1H), 5.10 (d, *J* = 3.2 Hz, 1H), 4.82 (dd, *J* = 3.1, 10.2Hz, 2H), 4.75 (d, *J* = 12.1 Hz, 1H), 4.68 (s, 2H), 4.60-4.54 (m, 8H), 4.35-4.19 (m, 9H), 3.90-3.84 (m, 5H), 3.78-3.72 (m, 2H), 3.66-

3.63 (m, 3H), 3.55-3.52 (m, 1H), 3.46 (d, *J* = 4.2 Hz, 1H), 3.41 (dd, *J* = 3.4, 9.2Hz, 1H), 3.31 (d, *J* = 9.8 Hz, 1H), 2.20 (s, 3H), 2.05 (s, 3H); ^{13}C NMR (150 MHz, $CDCl_3$) : δ 170.84, 139.12, 138.85, 138.79, 138.65, 138.60, 138.52, 138.37, 138.25, 137.94, 137.60, 132.30, 130.75, 129.97, 129.90, 128.98, 128.63, 128.52, 128.33, 128.20, 128.03, 127.88, 127.64, 100.79, 96.52, 88.06, 80.83, 80.45, 76.45, 76.42, 76.04, 75.65, 75.21. 75.14, 74.69, 73.63, 73.05, 73.01, 72.95, 71.99, 71.87, 71.43, 69.66, 69.51, 69.35, 68.40, 68.34, 21.40, 21.36, 21.31 ;ESI-MS: *m/z* calcd for $C_{90}H_{94}O_{16}SNa$: 1485.6155; found 1485.6190 $(M + Na)^+$.

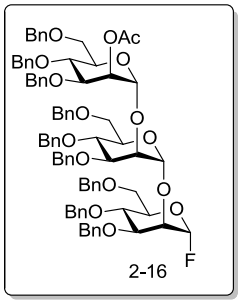

2-O-acetyl-3,4,6-tri-O-benzyl-α-D-mannopyranosyl-(1→2)-3,4,6-tri-O-benzyl-α-D-mannopyranosyl-(1→2)-3,4,6-tri-O-benzyl-1-α-D-mannopyranosyl fluoride (2-16): To a solution of trisaccharide **2-15** (0.600 g, 0.410 mmol) in CH_2Cl_2 (10 mL) at -30^{o}C was added NBS (0.218 mg, 1.23 mmol), stirred for 10 minutes. DAST (324 µL, 2.46 mmol) was added slowly and resulting reaction mixture was stirred at -10°C for 6 h. TLC (ethyl acetate: hexane, 3/7) indicated formation of product with consumption of starting material, reaction was quenched with aq.$NaHCO_3$, filtrate was washed with aqueous $NaHCO_3$ (2 x 50mL) and a brine (50 mL) solution. The organic layer was dried over Na_2SO_4, filtered and concentrated in *vacuo*. The residue was purified by silica gel column chromatography to afford fluoride **2-16** (0.320 g, 58%) as white foam and 0.200 g alcohol (anomeric-OH) as side product. TLC (ethyl acetate : hexane =3/7, v/v) : R_f = 0.31; ^{1}HNMR (600 MHz, $CHCl_3$) : δ 7.32-7.12 (m, 45H), 5.67 (d, *J* = 50.4 Hz, 1H), 5.49 (s, 1H), 5.16 (s, 1H), 4.99 (s, 1H), 4.82-4.77 (m, 3H), 4.65-4.38 (m, 15H), 4.30 (d, *J* = 12.1 Hz, 1H), 4.03 (s, 1H), 3.97-3.94 (m, 3H), 3.90-3.64 (m, 11H), 3.54 (d, *J* = 10.2 Hz, 1H), 2.11 (s, 3H); ^{13}CNMR (150 MHz, $CDCl_3$) : δ 170.44, 138.77, 138.64, 138.60, 138.54, 138.46, 138.41, 138.28, 128.76, 128.64, 128.61, 128.54, 128.44, 128.31, 128.19, 128.13, 128.09, 128.04, 128.01, 127.95, 127.90, 127.87, 127.84, 127.79, 127.73, 107.65, 106.19, 101.04, 99.72, 78.56, 78.31, 75.45,

75.41, 75.31, 74.86, 74.59, 74.31, 74.10, 73.86, 73.68, 73.65, 73.57, 72.69, 72.49, 72.38, 72.17, 69.51, 69.31, 69.01, 68.95, 21.44; ESI-MS: *m/z* calcd for $C_{83}H_{87}FO_{16}Na$: 1381.5870; found 1381.5891 $(M + Na)^+$.

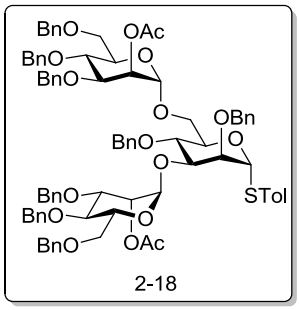

2-18

p-Tolyl-2-O-acetyl-3,4,6-tri-O-benzyl-α-D-mannopyranosyl-(1→3)-2-O-acetyl-3,4,6-tri-O-benzyl-α-D-mannopyranosyl-(1→6)-2,4-di-O-benzyl-1-thio-α-D-mannopyranoside (2-18): To a solution of acceptor **2-17** (0.545 g, 1.23 mmol) and donor **2-11** (1.57 g, 3.07 mmol) in CH_2Cl_2 (10 mL) was added 4 Å activated MS and stirred for 1 h at room temperature. In a separate flask, AgOTf (0.787 g, 3.07 mmol) and DTBP (690 µL, 3.07 mmol) in 10 mL of CH_2Cl_2 were stirred with MS 4 Å. After stirring for 1 h, the flask containing the AgOTf /DTBP was cooled to -30°C and solution containing mixture of donor and acceptor was added over 5 min. The solution was stirred with gradual warming up to room temperature over 24 h. TLC (ethyl acetate: hexane, 2/8) indicated formation of product with consumption of starting material, reaction was quenched with Et_3N, filtered through celite, filtrate was washed with aqueous $NaHCO_3$ (2 x 50 mL) and a brine (50 mL) solution. The organic layer was dried over Na_2SO_4, filtered and concentrated in *vacuo*. The residue was purified by silica gel column chromatography to afford **2-18** (1.10 g, 66%) as colorless foam. TLC (ethyl acetate: hexane =2/8, v/v) : R_f = 0.36; ^{1}H NMR (600 MHz, $CDCl_3$) : δ 7.35-7.10 (m, 32H), 7.05 (d, *J* = 8.0 Hz, 2H), 5.51 (s, 1H), 5.47 (s, 1H), 5.45 (dd, *J* = 2.0, 2.8 Hz, 1H), 5.21 (s, 1H), 4.91 (d, *J* = 1.5 Hz, 1H), 4.86 (t, 2H), 4.75 (d, *J* = 11.2Hz, 1H), 4.67-4.58 (m, 5H), 4.54-4.36 (m, 8H), 4.23 (dd, *J* = 3.9, 9.6 Hz, 1H), 4.12-4.06 (m, 2H), 4.01 (dd, *J* = 3.2, 9.2Hz, 1H), 3.97-3.86 (m, 5H), 3.82 (t, *J* = 9.2 Hz, 1H) 3.79-3.75 (m, 1H), 3.72 (dd, *J* = 3.9, 10.7 Hz, 1H), 3.70-3.56 (m, 4H), 2.17 (s, 3H), 2.13 (s, 3H), 2.09 (s, 3H); ^{13}C NMR (150 MHz, $CDCl_3$) : δ 170.27, 170.10, 138.57, 138.53, 138.18, 138.16, 137.81, 137.77, 137.42, 131.46, 130.85, 129.83, 128.44, 128.42, 128.36, 128.27, 128.21, 128.06, 127.81, 127.72, 127.68, 127.63, 127.53, 127.48, 99.83, 98.17, 85.23, 78.98,

78.08, 77.76, 75.15, 74.98, 74.89, 74.32, 74.15, 73.52, 73.30, 72.23, 72.05, 71.85, 71.48, 71.43, 71.36, 69.05, 68.72, 68.60, 68.41, 66.60, 60.39, 21.15, 21.00, 20.94; ESI-MS: *m/z* calcd for $C_{85}H_{90}O_{17}SNa$: 1437.5791; found 1437.5821 $(M + Na)^+$.

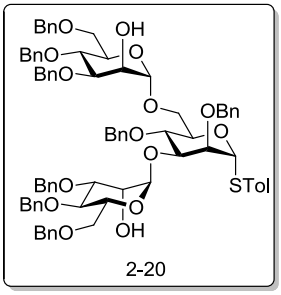

2-20

p-Tolyl-3,4,6-tri-O-benzyl-α-D-mannopyranosyl-(1→3)-3,4,6-tri-O-benzyl-α-D-mannopyranosyl-(1→6)]-2,4-di-O-benzyl-1-thio-α-D-mannopyranoside (2-20): To a solution of trisaccharide **2-19** (1.30 g, 0.918 mmol) in 10 mL methanol : CH_2Cl_2 (1/1) was added sodium methoxide (0.024 g, 0.459 mmol), stirred at room temperature until TLC (ethyl acetate: hexane, 3/7) indicated formation of a product with consumption of the starting material. The reaction mixture was neutralized with IR-120, filtered and concentrated *in vacuo* and residue was purified by silica gel column chromatography to afford **2-20** (1.10 g, 90%) as a colorless oil. TLC (ethyl acetate: hexane =3/7, v/v) : R_f = 0.26; ^{1}H NMR (600 MHz, $CDCl_3$) : δ 7.36-7.12 (m, 42H), 7.06 (d, *J* = 8.0 Hz, 2H), 5.46 (s, 1H), 5.24 (s, 1H), 5.01 (d, *J* = 1.1 Hz, 1H), 4.82 (t, *J* = 11.1 Hz, 2H), 4.69 (d, *J* = 11.1 Hz, 1H), 4.65-4.44 (m, 13H), 4.23 (dd, *J* = 4.1, 9.6Hz, 1H), 4.16 (s, 1H), 4.07 (dd, *J* = 2.8, 9.4 Hz, 1H), 4.03 (d, *J* = 10.1 Hz, 1H), 3.96-3.88 (m, 4H), 3.87-3.81 (m, 3H), 3.80-3.75 (m, 1H), 3.73-3.64 (m, 4H), 3.62 (dd, *J* = 1.6, 10.8 Hz, 1H), 2.38 (s, 1H), 2.34 (s, 1H), 2.19 (s, 3H); ^{13}C NMR (150 MHz, $CDCl_3$) : δ 138.12, 138.11, 137.69, 131.75, 130.12, 128.82, 128.76, 128.73, 128.67, 128.63, 128.57, 128.54, 128.53, 128.41, 128.35, 128.29, 128.19, 128.12, 128.08, 128.03, 127.95, 128.92, 127.82, 124.43, 99.90, 85.55, 80.32, 80.00, 78.49, 79.46, 75.46, 75.41, 75.27, 75.19, 75.13, 74.66, 74.50, 74.39, 73.85, 73.81, 73.62, 72.32, 72.24, 71.85, 71.71, 71.40, 71.33, 69.48, 69.00, 68.96, 68.90, 68.32, 66.51, 21.15; ESI-MS: *m/z* calcd for $C_{81}H_{86}O_{15}SNa$: 1353.5580; found 1353.5614 $(M + Na)^+$.

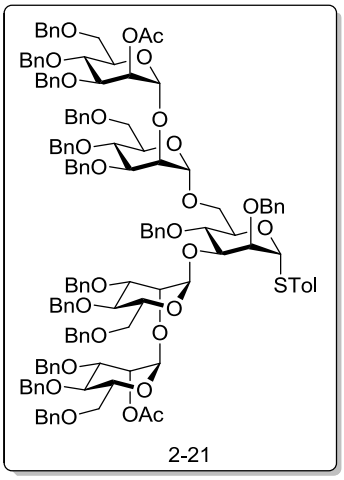

p-Tolyl-2-O-acetyl-3,4,6-tri-O-benzyl-α-D-mannopyranosyl-(1→2)-3,4,6-tri-O-benzyl-α-D-mannopyranosyl-(1→3)-[2-O-acetyl-3,4,6-tri-O-benzyl-α-D-mannopyranosyl-(1→2)-3,4,6-tri-O-benzyl-α-D-mannopyranosyl-(1→6)]-2,4-di-O-benzyl-1-thio-α-D-mannopyranoside (2-21): To a solution of acceptor **2-20** (1.01 g, 0.739 mmol) and donor **2-11** (0.947 g, 1.84 mmol) in 20 mL CH_2Cl_2 was added 4 Å activated MS and stirred for 1 h at room temperature. In a separate flask, AgOTf (0.472 g, 1.85 mmol) and DTBP (415 µL, 1.85 mmol) in 10 mL of CH_2Cl_2 were stirred with MS 4 Å. After stirring for 1 h, the flask containing the AgOTf /DTBP was cooled to -30°C and solution containing mixture of donor and acceptor in CH_2Cl_2 was added over 5 min. The solution was stirred with gradual warming up to room temperature over 24 h. TLC (ethyl acetate: hexane, 3/7) indicated formation of product with consumption of starting material, reaction was quenched with Et_3N, filtered through celite, filtrate was washed with aqueous $NaHCO_3$ (2 x 50 mL) and a brine (50 mL) solution. The organic layer was dried over Na_2SO_4, filtered and concentrated in *vacuo*. The residue was purified by silica gel column chromatography to afford **2-21** (1.25 g, 74%) as white solid. TLC (ethyl acetate: hexane =3/7, v/v) : R_f = 0.33; ^{1}H NMR (600 MHz, $CDCl_3$) : δ 7.27-7.04 (m, 72 H), 7.02 (d, *J* = 8.0 Hz, 2H), 5.52 (d, *J* = 1.5 Hz, 2H), 5.46 (s, 1H), 5.18 (s, 1H), 5.04 (d, *J* = 16.2 Hz, 1H), 4.85 (t, *J* = 11.0 Hz, 2H), 4.78 (t, *J* = 11.1 Hz, 2H), 4.72-4.44 (m, 18H), 4.41-4.30 (m, 8H), 4.27 (d, *J* = 12.3 Hz, 2H), 4.20 (s, 2H), 4.05-3.92 (m, 6H), 3.91-3.73 (m, 8H), 3.68-3.56 (m, 6H), 3.48 (d, *J* = 10.1 Hz, 1H), 3.40 (d, *J* = 10.3 Hz, 1H), 3.34 (d, *J* = 10.5 Hz, 1H), 2.10 (s, 6H), 2.01 (s, 3H); ^{13}C NMR (150 MHz, $CDCl_3$) : δ 170.22, 152.99, 152.78, 152.57, 138.43, 138.38, 138.24, 138.05, 138.02, 137.86, 137.81, 131.15, 129.80, 128.44, 128.30, 128.20, 128.05, 127.95, 127.85,

127.72, 127.70, 127.62, 127.55, 127.53, 127.47, 127.41, 127.38, 127.35, 127.23, 126.94, 101.16, 99.37, 98.86, 84.97, 79.24, 78.07, 78.02, 75.22, 74.99, 74.87, 74.77, 74.55, 74.47, 74.29, 74.17, 73.94, 73.82, 73.38, 73.24, 73.18, 73.01, 72.58, 71.93, 71.85, 71.77, 71.60, 71.55, 71.47, 70.99, 69.41, 68.64, 68.57, 68.46, 68.01, 29.69, 21.22, 20.91; ESI-MS: *m/z* calcd for $C_{139}H_{146}O_{27}SNa$: 2302.9698; found 2302.9747 $(M + Na)^+$.

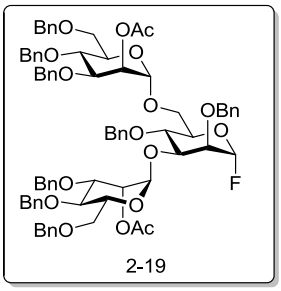

2-19

2-O-acetyl-3,4,6-tri-O-benzyl-α-D-mannopyranosyl-(1→3)-2-O-acetyl-3,4,6-tri-O-benzyl-α-D-mannopyranosyl-(1→6)-2,4-di-O-benzyl-α-D-mannopyranosyl fluoride (2-19): To a solution of compound **2-18** (0.270 g, 0.197 mmol) in CH_2Cl_2 (10 mL) at -30°C was added NBS (0.052 g, 0.296 mmol), stirred for 10 min. DAST (52 µL, 0.395 mmol) was then added slowly and resulting reaction mixture was stirred for 4 h at -10°C. TLC (ethyl acetate: hexane, 3/7) indicated formation of product with consumption of starting material, reaction was quenched with aq.$NaHCO_3$, filtrate was washed with aqueous $NaHCO_3$ (2 x 50 mL) and a brine (50 mL) solution. The organic layer was dried over Na_2SO_4 and concentrated in *vacuo*. The residue was purified by silica gel column chromatography to afford **2-19** (0.150 g, 61%) as white foam. TLC (ethyl acetate : toluene =1/9, v/v) : R_f = 0.19; ^{1}HNMR (600 MHz, $CHCl_3$) : δ 7.29-7.10 (m, 40H), 5.50 (s, 1H), 5.47 (d, *J* = 50 Hz, 1H), 5.46 (s, 1H), 5.18 (s, 1H), 4.92 (s, 1H), 4.86 (d, *J* = 11.2 Hz, 1H), 4.83 (d, *J* = 10.8 Hz, 1H), 4.72 (d, *J* = 10.8 Hz, 1H), 4.72-4.56 (m, 6H), 4.48-4.40 (m, 7H), 4.10 (d, *J* = 8.9 Hz, 1H), 4.00-3.92 (m, 4H), 4.90-3.77 (m, 5H), 3.71-3.64 (m, 5H), 3.57 (d, *J* = 9.2 Hz, 1H), 2.13 (s, 3H), 2.06 (s, 3H); ^{13}CNMR (150 MHz, $CHCl_3$) : δ 170.56, 170.36, 138.80, 138.74, 138.50, 138.39, 138.11, 138.04, 137.89, 137.88, 129.70, 128.81, 128.70, 128.68, 128.65, 128.58, 128.56, 128.54, 128.43, 128.27, 128.18, 128.12, 128.07, 128.04, 128.00, 127.97, 127.89, 127.82, 126.55, 106.66, 105.18, 100.02, 98.84, 98.81, 78.31, 77.70, 76.31, 76.03, 75.42, 75.37, 75.23, 74.62, 74.41, 74.27, 73.90, 73.80, 73.65, 73.16, 72.66, 72.14, 71.92, 71.58, 69.42, 68.96, 68.70, 68.61, 66.53, 42.20, 32.21, 29.98, 29.65, 22.98, 21.63, 21.44, 21.27,

14.71, 14.41; ESI-MS: *m/z* calcd for $C_{78}H_{83}O_{17}FNa$: 1333.5507; found 1333.5536 $(M + Na)^+$.

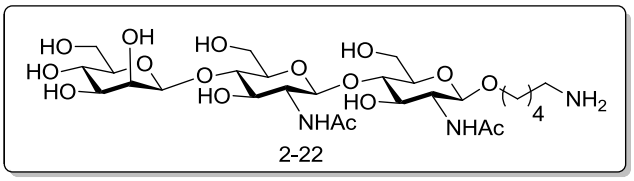

2-22

β-D-mannopyranosyl-(1→4)-2-acetamido-2-deoxy-β-D-glucopyranosyl-(1→4)-2-acetamido -2-deoxy-β-D-glucopyranoside (2-22): Compound **2-10** (0.150 g, 0.110 mmol) was deprotected by following general procedure 1 to yield desired trisaccharide **2-22** (0.045 g, 65%) as a white solid. ^{1}HNMR (600 MHz, D_2O) : δ 4.60 (d, *J* = 7.8 Hz, 1H), 4.49 (d, *J* = 7.8 Hz, 1H), 4.06 (d, *J* = 3 Hz, 1H), 3.94-3.89 (m, 4H), 3.86-3.58 (m, 14H), 3.50-3.49 (m, 1H), 3.42-3.42 (m, 1H), 2.97 (t, *J* = 10.8 Hz, 2H), 2.07 (s, 3H), 2.03 (s, 3H), 1.68-1.65 (m, 2H), 1.60-1.58 (m, 2H), 1.40-1.39 (m, 2H); ^{13}CNMR (150 MHz, D_2O) : δ 177.32, 177.17, 173.76, 104.12, 103.80, 102.80, 82.07, 81.35, 79.15, 77.31, 77.25, 75.49, 75.13, 74.68, 73.23, 72.84, 69.34, 63.65, 62.83, 62.77, 57.75, 57.72, 42.05, 30.78, 29.10, 24.86, 24.84, 24.83; ESI-MS: *m/z* calcd for $C_{27}H_{49}N_3O_{16}Na$: 694.3005; found 694.3115 $(M + Na)^+$.

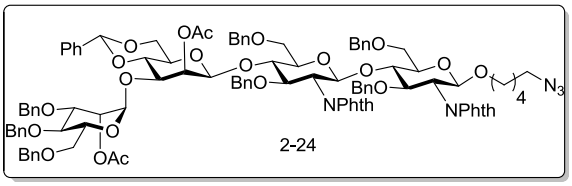

2-24

5-Azidopentyl-O-(2-O-acetyl-3,4,6-tri-O-benzyl-α-D-mannopyranosyl-(1→3)-2-O-acetyl-4, 6-O-benzylidine-β-D-mannopyranosyl-(1→4)-O-(3,6-di-O-benzyl-2-deoxy-2-phthalimido-β -D-glucopyranosyl)-(1→4)-O-3,6-di-O-benzyl-2-deoxy-2-phthalimido-β-D-glucopyranoside (2-24): A mixture of trichloroacetimidate **2-23** (0.278 g, 0.437 mmol), chitobiose acceptor **2-10** (0.300 g, 0.219 mmol) and activated 4 Å molecular sieves in dry CH_2Cl_2 (10 mL) was stirred at room temperature for 1 h. The reaction was cooled to -40^{o}C, boron trifluoride ethyl etherate (12 µL, 0.109 mmol) was then added slowly and resulting reaction mixture was stirred for 2 h. The reaction was quenched by adding Et_3N, diluted with CH_2Cl_2, filtered through celite and concentrated in *vacuo*. The residue was purified by flash column chromatography to afford **2-24** (0.310 g, 70%) as white foam. TLC

(ethyl acetate : toluene =2/8, v/v) : R_f = 0.46; ^{1}HNMR (600 MHz,$CDCl_3$) : δ 7.84-7.65 (m, 8H), 7.38-7.31 (m, 2H), 7.30-7.18 (m, 28H), 6.98-6.90 (m, 7H), 6.75-6.71 (m, 3H), 5.45 (s, 1H), 5.43-5.40 (m, 1H), 5.34 (d, *J* = 3.1 Hz, 1H), 5.21 (d, *J* = 8.1 Hz, 1H), 5.19 (d, *J* = 2.1Hz, 1H), 4.90-4.89 (m, 1H), 4.83-4.81 (m, 3H), 4.67 (s, 1H), 4.67-4.61 (m, 2H), 4.53-4.43 (m, 7H), 4.38-4.23 (q, 2H), 4.22-4.16 (m, 1H), 4.13-4.06 (m, 6H), 3.87-3.75 (m, 6H), 3.66-3.60 (m, 3H), 3.53-3.45 (m, 3H), 3.38 (dd, *J* = 4.2, 12Hz, 1H), 3.26-3.17 (m, 3H), 3.09-3.07 (m, 1H), 2.87-2.82 (m, 2H), 2.06 (s, 3H), 2.03 (s, 3H), 1.35-1.23 (m, 4H), 1.07-1.01 (m, 2H); ^{13}CNMR (150 MHz, $CDCl_3$) : δ 169.87, 168.75, 167.83, 138.97, 138.47, 138.17, 137.36, 134.30, 134.10, 131.72, 129.12, 128.90, 128.64, 128.55, 128.51, 128.32, 128.23, 128.09, 127.84, 127.46, 128.14, 126.24, 123.40, 101.44, 99.38, 98.90, 98.37, 97.31, 79.05, 78.84, 77.89, 76.14,7 5.02, 74.78, 73.70, 73.40, 73.06, 73.04, 72.37, 72.03, 71.00, 69.11, 69.85, 69.11, 68.85, 68.59. 68.50, 67.84, 66.70, 56.85, 55.99, 51.38, 28.95, 28.55, 23.28, 21.33, 21.16; ESI-MS: *m/z* calcd for $C_{105}H_{107}N_5O_{25}Na$: 1861.7180; found 1861.7223 $(M + Na)^+$.

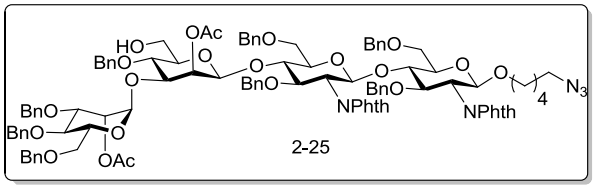

2-25

5-Azidopentyl-O-(2-O-acetyl-3,4,6-tri-O-benzyl-α-D-mannopyranosyl-(1→3)-2-O-acetyl-4-O-benzyl-β-D-mannopyranosyl-(1→4)-O-(3,6-di-O-benzyl-2-deoxy-2-phthalimido-β-D-gl-ucopyranosyl)-(1→4)-O-3,6-di-O-benzyl-2-deoxy-2-phthalimido-β-D-glucopyranoside (2-25): A mixture of tetrasaccharide **2-24** (0.280 g, 0.152 mmol) and 4Å activated molecular sieves in CH_2Cl_2 (10 mL) was stirred at room temperature for 1 h. Reaction was cooled to -78^{o}C, triethyl silane (73 µl, 0.456 mmol) followed by dichlorophenyl borane (69 µl, 0.532 mmol) was added and stirred for 1 h. Reaction was quenched by adding Et_3N, filtered through celite and concentrated in *vacuo.* The residue was co-distilled with methanol 2-3 times before being purified by flash column chromatography to afford 6''-OH **2-25** (0.230 g, 82%). TLC: (ethyl acetate : toluene =2/8, v/v) : R_f = 0.36; ^{1}H NMR (600 MHz, $CDCl_3$) : δ 7.85-7.52 (m, 8H), 7.52-7.12 (m, 29H), 7.00-6.88 (m, 9H), 6.74-6.70 (m, 3H), 5.39 (t, *J* = 1.8 Hz, 1H), 5.32 (d, *J* = 3.6 Hz, 1H), 5.21 (d, *J* = 8.4 Hz, 1H), 5.10 (s, 1H), 4.90-4.81 (m, 4H), 4.67-4.61 (m, 2H), 4.59 (s, 1H), 4.59-4.44 (m,

9H), 4.37(d, *J* = 12 Hz, 2H), 4.24-4.12 (m, 3H), 4.10-4.05 (m, 3H), 3.90-3.77 (m, 4H), 3.69-3.58 (m, 7H), 3.49 (t, *J* = 11.5 Hz, 2H), 3.41-3.36 (dd, *J* = 6.1, 11.2 Hz, 2H), 3.26 (dd, *J* = 6, 9.2 Hz, 1H), 3.26-3.18 (m, 2H), 3.06-2.98 (m, 1H), 2.88-2.81 (m, 2H), 2.06 (s, 3H), 2.04 (s, 3H), 1.37-1.22 (m, 4H), 1.07 -1.00 (m, 2H); ^{13}CNMR (150 MHz, $CDCl_3$) : δ 170.45, 169.88, 168.78, 168.24, 167.86, 138.95, 138.92, 138.77, 138.58, 138.21, 138.11, 137.95, 137.37, 134.35, 134.16, 133.89, 132.09, 131.70, 128.90, 128.76, 128.71, 128.64, 128.58, 128.51, 128.41, 128.31, 128.08, 127.96, 127.81, 127.64, 127.13, 123.97, 123.46, 100.14, 98.40, 98.36, 97.36, 76.24, 75.52, 75.30, 74.96, 74.71, 74.51, 74.29, 73.41, 73.09, 72.55, 72.12, 69.41,69.20, 68.85, 68.48, 67.93, 67.71, 61.87, 56.78, 56.00, 51.38, 28.96, 28.55, 23.28, 21.37; ESI-MS: *m/z* calcd for $C_{105}H_{109}N_5O_{25}Na$: 1863.7337; found 1863.7383 $(M + Na)^+$.

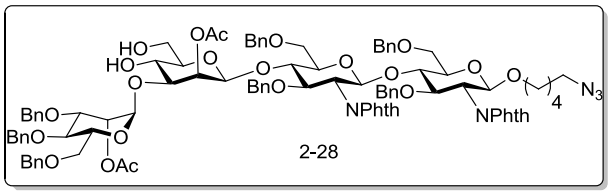

5-Azidopentyl-O-(2-O-acetyl-3,4,6-tri-O-benzyl-α-D-mannopyranosyl-(1→3)-2-O-acetyl-β-D-mannopyranosyl-(1→4)-O-(3,6-di-O-benzyl-2-deoxy-2-phthalimido-β-D-glucopyranos-yl)-(1→4)-O-3,6-di-O-benzyl-2-deoxy-2-phthalimido-β-D-glucopyranoside (2-28): *p*-Toluenesulfonic acid monohydrate (0.045 g, 0.239 mmol) was added to a stirred solution of tetrasaccharide **2-24** (0.220 g, 0.119 mmol) in acetonitrile (10 mL) at room temperature. After 8 h, the reaction mixture was quenched with Et_3N and concentrated in *vacuo*. The residue was purified by flash column chromatography to give the title diol **2-28** (0.140 g, 66%) as white solid. TLC: (ethyl acetate: toluene =2/8, v/v) : R_f = 0.26; ^{1}HNMR (600 MHz, $CDCl_3$) : δ 7.85-7.52 (m, 8H), 7.32-7.17 (m, 25H), 6.98-6.91 (m, 7H), 6.75-6.71 (m, 3H), 6.30 (d, *J* = 3.6 Hz, 1H), 5.21-5.20 (m, 3H), 4.89 (d, *J* = 8.4Hz, 1H), 4.85-4.82 (m, 3H), 4.64-4.60 (m, 3H), 4.54-4.46 (m, 7H), 4.38 (d, *J* = 12 Hz, 1H), 4.34 (d, *J* = 12.2 Hz, 1H), 4.21-4.04 (m, 5H), 3.92 (m, 1H), 3.87-3.79 (m, 3H), 3.70-3.59 (m, 5H), 3.52-3.43 (m, 4H), 3.39 (dd, *J* = 3.2, 8.3Hz, 1H), 3.28 (dd, *J* = 3.2, 8.2Hz, 1H), 3.29-3.19 (m, 2H), 2.29 (m, 1H), 2.86-2.83 (m, 3H), 2.11 (s, 3H), 2.03 (s, 3H), 1.35-1.23 (m, 4H), 1.06-1.01 (m, 2H); ^{13}CNMR (150 MHz, $CDCl_3$) : δ 170.76, 169.88, 138.92, 138.70, 138.62, 138.52, 138.12, 138.06, 134.27, 134.07, 133.81, 131.95, 131.64, 128.82,

128.64, 128.59, 128.52, 128.50, 128.39, 138.33, 128.20, 128.09, 128.06, 128.03, 128.01, 127.94, 127.81, 127.75, 127.54, 127.42, 127.29, 127.06, 123.90, 123.36, 98.51, 98.30, 98.24, 97.30, 79.07, 78.38, 77.60, 76.10, 75.52, 75.03, 74.79, 74.71, 74.59, 74.51, 73.39, 73.03, 72.07, 72.01, 71.30, 69.53, 69.27, 69.05, 68.44, 67.70, 67.17, 62.44, 56.74, 55.94, 51.32, 28.89, 28.49, 23.22, 21.31, 21.22; ESI-MS: *m/z* calcd for $C_{98}H_{103}N_5O_{25}Na$: 1773.6868; found 1773.6913 $(M + Na)^+$.

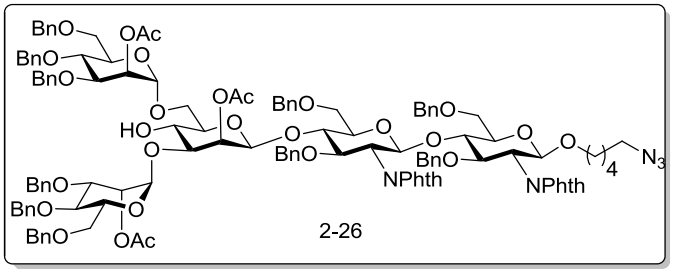

2-26

5-Azidopentyl-O-di-(2-O-acetyl-3,4,6-tri-O-benzyl-α-D-mannopyranosyl-(1→3), (1→6)-2-O-acetyl-4-O-benzyl-β-D-mannopyranosyl-(1→4)-O-(3,6-di-O-benzyl-2-deoxy-2-phthalim-ido-β-D-glucopyranosyl)-(1→4)-O-3,6-di-O-benzyl-2-deoxy-2-phthalimido-β-D-glucopyra-noside (2-26): A mixture of donor **2-23** (0.113 g, 0.178 mmol), acceptor **2-25** (0.220 g, 0.119 mmol) and activated 4 Å molecular sieves in dry CH_2Cl_2 (10 mL) was stirred at room temperature for 1 h. The reaction was cooled to -60^{o}C, boron trifluoride ethyl etherate (12 µL, 0.109 mmol) was added slowly and resulting reaction mixture was stirred for 2 h at -20°C. The reaction was quenched by adding Et_3N, diluted with CH_2Cl_2, filtered through celite and concentrated in *vacuo*. The residue was purified by flash column chromatography to afford **2-26** (0.170 g, 60%) as colorless foam. TLC: (ethyl acetate: hexane =3/7, v/v) : R_f = 0.46; ^{1}HNMR (600 MHz, $CDCl_3$) : δ 7.77-7.59 (m, 8H), 7.32-7.16 (m, 43H), 7.14-7.08 (m, 2H), 6.91-6.89 (m, 4H), 6.73-6.67 (m, 6H), 5.45 (s, 1H), 5.34 (d, *J* = 3.1 Hz, 1H), 5.32 (s, 1H) ,5.17 (d, *J* = 8.4 Hz, 1H), 5.09 (s, 1H), 4.87 (d, *J* = 8.4 Hz, 1H), 4.83-4.78 (q, 2H), 4.74-4.71 (q, 2H), 4.65-4.61 (m, 4H), 4.56-4.42 (m, 15H), 4.31 (d, *J* = 9.2 Hz, 1H), 4.12-4.03 (m, 5H), 4.03-3.76 (m, 9H), 3.68-3.43 (m, 9H), 3.30 (dd, *J* = 3.2, 9.1Hz, 1H), 3.21-3.15 (m, 2H), 3.13 (d, *J* = 9.2 Hz, 1H), 3.09 (d, *J* = 8.4 Hz, 1H), 2.89-2.79 (m, 2H), 2.12 (s, 3H), 2.07 (s, 3H), 1.69 (s, 3H), 1.37-1.12 (m, 4H), 1.07-1.01 (m, 2H); ^{13}CNMR (150 MHz, $CDCl_3$) : δ 170.45, 170.22, 170.18, 168.21, 167.71, 138.93, 138.72, 138.68, 138.50, 138.24, 138.22, 138.07, 133.83, 133.75, 128.87, 128.79,

128.67, 128.63, 128.58, 128.42, 128.21, 128.06, 127.99, 127.96, 127.81, 127.76, 127.70, 127.46, 127.08, 123.36, 100.13, 99.39, 98.35, 98.31, 97.16, 76.20, 76.05, 75.58, 75.21, 74.97, 74.89, 74.70, 74.47, 74.28, 73.94, 73.72, 73.00, 72.25,72.20, 71.70,71.50, 69.15,69.07, 69.04,68.99, 68.50, 68.45, 67.80, 65.45, 56.83, 51.37, 29.94, 23.27, 21.31, 21.28, 20.83; ESI-MS: *m/z* calcd for $C_{134}H_{139}N_5O_{31}Na$: 2337.9379; found 2337.9461 $(M + Na)^+$.

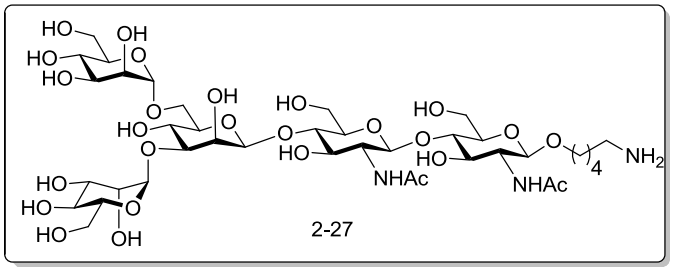

2-27

5-Aminopentyl-di-(α-D-mannopyranosyl)-(1→3),(1→6)-β-D-mannopyranosyl-(1→4)-2-ace-tamido-2-deoxy-β-D-glucopyranosyl-(1→4)-2-acetamido-2-deoxy-β-D-glucopyranoside (2-27): Pentasaccharide **2-26** (0.090 g, 0.038 mmol) was deprotected by following the general procedure 1 to afford compound **2-27** (0.020 g, 45%) as a white powder. ^{1}HNMR (600 MHz, D_2O) : δ 5.10 (d, *J* = 1.3 Hz, 1H), 5.09 (d, *J* = 1.5 Hz, 1H), 4.59 (d, *J* = 8.4 Hz, 1H), 4.49 (d, *J* = 7.8 Hz, 1H), 4.25 (s, 1H), 4.01 (d, *J* = 1.5 Hz, 1H), 4.00 (d, *J* = 1.3 Hz, 1H), 3.97-3.77 (m, 8H), 3.75-3.65 (m, 20H), 3.52-3.48 (m, 2H), 2.98 (t, *J* = 11.2 Hz, 2H), 2.06 (s, 3H),2.02 (s, 3H), 1.68-1.65 (m, 2H), 1.60-1.57 (m, 2H), 1.49-1.40 (m, 2H); ^{13}CNMR (150 MHz, D_2O) : δ 181.17, 174.69, 174.42, 102.51, 101.34, 101.04, 100.35, 99.60, 80.48, 79.61, 79.30, 74.49, 74.36, 74.16, 73.43, 72.66, 72.37, 71.93, 70.39, 70.31, 70.13, 70.09, 69.98, 69.85, 66.84, 66.76, 65.80, 61.12, 90.93, 60.07, 59.97, 54.97, 54.85, 39.30, 28.03, 26.35, 23.07, 22.17, 22.07; ESI-MS: *m/z* calcd for $C_{39}H_{69}N_3O_{26}Na$: 1018.4067; found 1018.4106 $(M + Na)^+$.

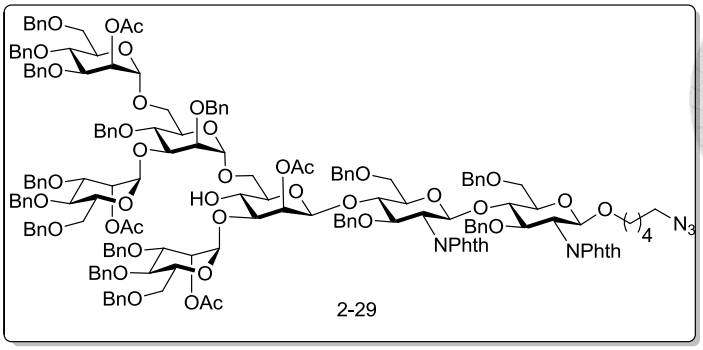

5-Azidopentyl-O-(2-O-acetyl-3,4,6-tri-O-benzyl-α-D-mannopyranosyl-(1→3)-{2-O-acetyl-3,4,6-tri-O-benzyl-α-D-mannopyranosyl-(1→3)}-[2-O-acetyl-3,4,6-tri-O-benzyl-α-D-mannopyranosyl-(1→6)]-2,4-di-O-benzyl-α-D-mannopyranosyl-(1→6)}-2-O-acetyl-β-D-mannopy-ranosyl-(1→4)-O-(3,6-di-O-benzyl-2-deoxy-2-phthalimido-β-D-glucopyranosyl)-(1→4)-O-3,6-di-O-benzyl-2-deoxy-2-phthalimido-β-D-glucopyranos ide (2-29): A mixture of Silver triflate (0.127 g, 0.497 mmol), Bis(cyclopentadienyl) hafnium dichloride (0.121 g, 0.319 mmol) and 4 Å activated molecular sieves in dry toluene (10 mL) was stirred at room temperature for 1 h. The reaction mixture was then cooled to -40°C, a solution of donor **2-19** (0.103 g, 0.085 mmol) and acceptor **2-28** (0.125 g, 0.071 mmol) in 5 mL toluene was added. The mixture was stirred for 2 h, quenched with Et_3N, diluted with CH_2Cl_2 and filtered through celite. The filtrate was washed with aqueous $NaHCO_3$ (2 x 50 mL), and a brine (50 mL) solution. The organic layer was dried over Na_2SO_4 and concentrated in *vacuo*. The residue was purified by flash column chromatography to afford **2-29** (0.110 g, 52%) as colorless foam. TLC: (acetone : toluene = 2/8, v/v) : R_f = 0.36; ^{1}H NMR (600 MHz, CDCl3) : δ 7.77-7.40 (m, 8H), 7.32-7.07 (m, 85H), 6.99-6.88 (m, 4H), 6.79-6.68 (m, 6H), 5.456 (s, 1H), 5.43 (d, *J* = 3.1 Hz, 1H), 5.41 (s, 1H), 5.29 (d, *J* = 6.4 Hz, 1H), 5.09 (s, 1H), 5.00 (s, 1H), 4.83-4.78 (q, 1H), 4.84-4.73 (m, 6H), 4.65-4.61 (m, 2H), 4.60-4.57 (m, 5H), 4.52-4.35 (m, 17H), 4.27 (d, *J* = 12.3 Hz, 1H), 4.20-4.19 (m, 1H), 4.10-3.99 (m, 6H), 3.97-3.70 (m, 13H), 3.69-3.57 (m, 8H), 3.56-3.31 (m, 6H), 3.30 (dd, *J* = 3.2, 9.2 Hz, 1H), 3.30-3.18 (m, 5H), 2.97-2.96 (m, 1H), 2.89-2.79 (m, 2H), 2.12 (s, 3H), 2.07 (s, 3H), 2.01 (s, 6H), 1.33-1.23 (m, 4H), 1.06-0.99 (m, 2H); ^{13}CNMR (150 MHz, $CDCl_3$) : δ 170.56, 170.42, 170.26, 170.02, 168.45, 168.69, 138.95, 138.93, 138.72, 138.68, 138.58, 138.24, 138.22, 138.07, 133.83, 132.09, 131.76, 128.87, 128.79, 128.67, 128.63, 128.61, 128.58, 128.52, 128.42, 128.13, 128.06, 127.99, 127.92, 127.81,

127.76, 127.74, 127.46, 127.08, 123.71, 123.36, 100.13, 99.39, 98.35, 98.31, 97.16, 76.20, 76.05, 75.42, 74.97, 74.89, 74.80, 74.70, 74.65, 74.47, 74.28, 73.94 ,73.68, 73.26, 72.60, 72.25, 72.20, 71.70, 71.50, 69.15, 69.07, 69.04, 68.99, 68.50, 68.45, 67.80, 65.54, 56.73, 55.90, 51.29,31.14, 29.91, 28.87, 28.47, 23.19, 21.33, 21.27, 21.19l; HRMS (MALDI-TOF) : *m/z* calcd for $C_{176}H_{185}N5O_{42}Na$: 3065.2400; found 3065.2210 $(M + Na)^+$.

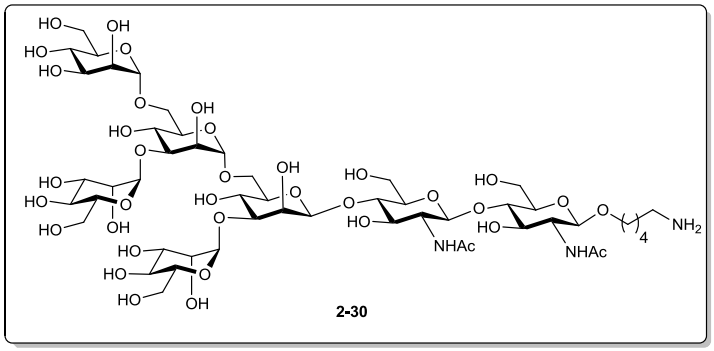

5-Aminopentyl-α-D-mannopyranosyl(1→3),[di-(α-D-mannopyranosyl)-(1→3), (1→6)-α-D-mannopyranosyl](1→6)-β-D-mannopyranosyl-(1→4)-2-acetamido-2-deoxy-β-D-glucopyranosyl-(1→4)-2-acetamido-2-deoxy-β-D-glucopyranoside(2-30):- Heptasaccharide 2-29 (0.140 g, 0.024 mmoles), was deprotected by following the general procedure 1 to obtain title compound **2-30** (0.039 g, 52%) as a white solid. ^{1}H NMR (600 MHz, D_2O): δ 5.09 – 4.89 (m, 2H), 4.86 (d, *J* = 1.5 Hz, 1H), 4.75 (d, *J* = 1.5 Hz, 1H), 4.69 (bs,1 H), 4.50 (dd, *J* = 5.0, 2.9 Hz, 1H), 4.35 (d, *J* = 7.9 Hz, 1H), 4.17 (d, *J* = 1.7 Hz, 1H), 4.07 – 4.05 (m, 1H), 4.00–3.97 (m, 2H), 3.94–3.37 (m, 40H), 2.90 – 2.85 (m, 2H), 1.98 (s, 3H), 1.94 (s, 3H), 1.61–1.46 (m, 4H), 1.35–1.26 (m, 2H); ^{13}C NMR (150 MHz, D_2O) : δ 102.44, 101.44, 101.01, 100.37, 99.85, 99.25, 80.54, 79.49, 79.28, 78.58, 74.45, 74.43,72.50, 71.93, 70.64, 70.24, 70.15, 70.04, 70.01, 69.87, 69.46, 69.39, 66.69, 66.66, 65.94,65.91, 65.56, 65.13, 65.12, 60.93, 60.91, 60.43, 60.13, 60.04, 59.97, 54.90, 54.86, 39.28,27.98, 26.48, 22.08, 22.02, 21.99; ESI-MS: *m/z* calcd for $C_{51}H_{89}N_3O_{36}Na$: 1342.5123; found 1342.5165 $(M + Na)^+$.

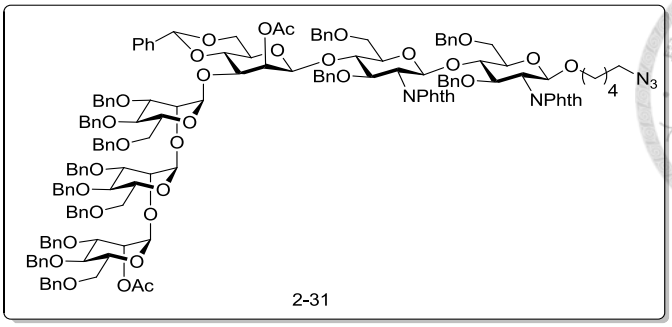

2-31

5-Azidopentyl-O-(2-O-acetyl-3,4,6-tri-O-benzyl-α-D-mannopyranosyl-(1→2)-3,4,6-tri-O-benzyl-α-D-mannopyranosyl-(1→2)-3,4,6-tri-O-benzyl-α-D-mannopyranosyl-(1→3)-2-O-acetyl-4,6-O-benzylidene-β-D-mannopyranosyl-(1→4)-O-(3,6-di-O-benzyl-2-deoxy-2-phth-alimido-β-D-glucopyranosyl)-(1→4)-O-3,6-di-O-benzyl-2-deoxy-2-phthalimido-β-D-gluco-pyranoside (2-31): A mixture of Silver triflate (0.328 g, 1.28 mmol), Bis(cyclopentadienyl) hafnium dichloride (0.340 g, 0.897 mmol) and 4 Å activated molecular sieves in dry toluene (10 mL) was stirred at room temperature for 1 h. The reaction mixture was then cooled to -40°C, a solution of donor **2-16** (0.383 g, 0.282 mmol) and acceptor **2-10** (0.350 g, 0.256 mmol) in 5 mL toluene was added. The mixture was stirred for 2 h, quenched with Et_3N, diluted with CH_2Cl_2 and filtered through celite. The filtrate was washed with aqueous $NaHCO_3$ (2 x 50mL), and a brine (50 mL) solution. The organic layer was dried over Na_2SO_4 and concentrated in *vacuo*. The residue was purified by flash column chromatography to afford **2-31** (0.405 g, 58%) as colorless foam. TLC: (ethyl acetate : toluene = 2/8, v/v) : R_f = 0.46; ^{1}H NMR (600 MHz, $CDCl_3$) : δ 7.89-7.35 (m, 8H), 7.38-7.12 (m, 56H), 7.12-7.08 (m, 3H), 7.03-6.88 (m, 7H), 6.78-6.69 (m, 4H), 5.50 (s, 1H), 5.37 (d, *J* = 3.4 Hz, 1H), 5.25 (s, 1H), 5.23-5.17 (m, 3H), 4.98 (s, 1H), 4.91-4.53 (m, 5H), 4.69-4.58 (m, 3H), 4.55-4.28 (m, 16H), 4.25-4.00 (m, 13H), 3.95-3.91 (m, 1H), 3.91-3.60 (m, 14H), 3.58 (d, *J* = 12 Hz, 1H), 3.51-3.45 (m, 4H), 3.42-3.38 (m, 3H), 3.29-3.10 (m, 3H), 2.98-2.78 (m, 3H), 2.08 (s, 3H), 1.99 (s, 3H), 1.35-1.23 (m, 4H), 1.07-1.00 (m, 2H); ^{13}C NMR (150 MHz, $CDCl_3$) : δ 170.38, 169.81, 168.76, 168.26, 139.06, 138.95, 138.92, 138.87, 138.60, 137.36, 128.85, 128.66, 128.64, 128.58, 128.55, 128.48, 128.43, 128.39, 128.35, 128.26, 128.10, 128.02, 127.82, 127.71, 101.48, 100.08, 99.75, 99.39, 98.36, 97.27, 77.80, 78.75, 76.10, 75.38, 74.93, 74.82, 74.70, 73.58, 73.28, 73.21, 73.06, 72.79, 72.65, 72.57, 72.17, 71.01, 69.60, 69.10, 68.96, 68.63, 66.74, 56.85, 55.97,

51.37, 28.95, 28.54, 23.27, 21.43, 21.09; ESI-MS: *m/z* calcd for $C_{159}H_{163}N_5O_{35}Na$: 2726.1054 ; found 2726.1214 $(M + Na)^+$.

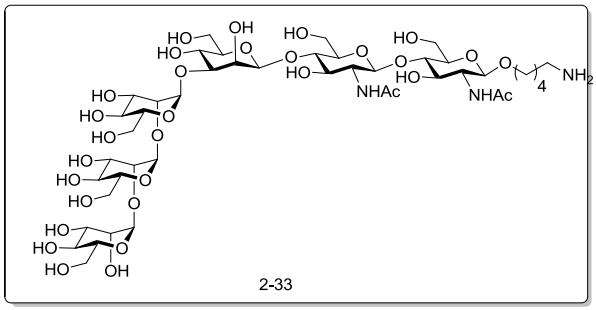

2-33

5-Aminopentyl-α-D-mannopyranosyl-(1→2)-α-D-mannopyranosyl-(1→2)-α-D-mannopyra-nosyl-(1→3)-β-D-mannopyranosyl-(1→4)-2-acetamido-2-deoxy-β-D-glucopyranosyl-(1→4)-2-acetamido-2-deoxy-β-D-glucopyranoside (2-33): Hexasaccharide **2-31** (0.140 g, 0.051 mmoles) was deprotected by following general procedure 1 to get title compound **2-33** (0.025 g, 42%) as white solid. ^{1}HNMR (600 MHz, D_2O) : δ 5.32 (s, 1H), 5.27 (s, 1H), 5.01 (s, 1H), 4.74 (s, 1H), 4.56 (d, *J* = 7.8 Hz, 1H), 4.43 (d, *J* = 7.8 Hz, 1H) ,4.18 (d, *J* = 3.3 Hz, 1H), 4.07 (s, 1H), 4.04 (d, *J* = 3.2 Hz, 1H), 4.03 (d, *J* = 3.1 Hz, 1H), 3.32-3.33 (m, 35H), 2.05 (t, *J* = 11.2 Hz, 2H), 2.03 (s, 3H), 2.00 (s, 3H), 1.64 (m, 2H), 1.50 (m, 2H), 1.36 (m, 2H); ^{13}CNMR (150 MHz, D_2O) : δ 181.64, 174.54, 174.38, 102.17, 101.34, 101.014, 100.70, 100.56, 99.85, 80.50, 79.25, 78.66, 78.55, 78.47, 76.12, 74.48, 73.37, 73.13, 72.33, 71.88, 70.24, 70.17, 70.05, 69.95, 69.89, 66.95, 66.81 ,66.71, 65.81, 61.01, 60.97, 60.88, 60.76, 60.02, 59.92, 54.92, 39.25, 27.99, 26.32, 23.19, 22.06, 22.04; ESI-MS: *m/z* calcd for $C_{45}H_{79}N_3O_{31}Na$: 1180.4590 ; found 1180.4591 $(M + Na)^+$.

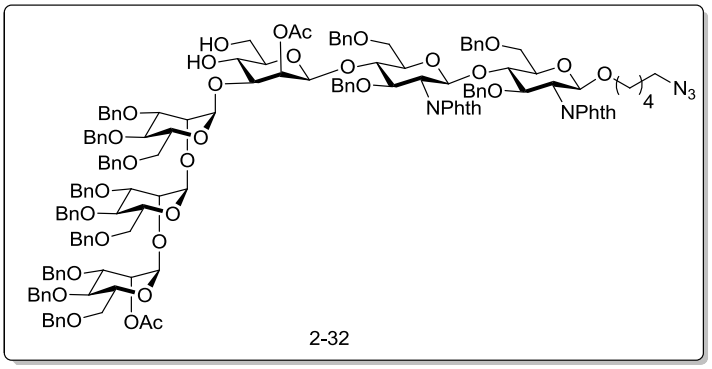

2-32

5-Azidopentyl-O-(2-O-acetyl-3,4,6-tri-O-benzyl-α-D-mannopyranosyl-(1→2)-3,4,6-tri-O-benzyl-α-D-mannopyranosyl-(1→2)-3,4,6-tri-O-benzyl-α-D-mannopyranosyl-(1→3)-2-O-acetyl-β-D-mannopyranosyl-(1→4)-O-(3,6-di-O-benzyl-2-deoxy-2-phthalimido

β-D-gluco-pyranosyl)-(1→4)-O-3,6-di-O-benzyl-2-deoxy-2-phthalimido-β-D-glucopyranoside (2-32):- To a solution of **2-31** (0.205 g, 0.075 mmol) in 10 mL acetonitrile was added *p*-toluene sulfonic acid monohydrate (0.020 g, 0.113 mmol), stirred at room temperature for 9 h. Reaction was quenched with Et_3N and concentrated in *vacuo.* The residue was purified by flash column chromatography to give diol **2-32** (0.120 g, 60%). TLC: (acetone : toluene =2/8, v/v) : R_f = 0.26; ^{1}H NMR (600 MHz, $CDCl_3$) : δ 7.83-7.62 (m, 8H), 7.41-7.06 (m, 57H), 6.95-6.89 (m, 6H), 6.73-6.71 (m, 2H), 5.50 (t, *J* = 4.8 Hz, 1H), 5.23 (d, *J* = 1.8 Hz, 1H), 5.22 (d, *J* = 3.8 Hz, 1H), 5.19 (d, *J* = 3.2 Hz, 1H), 5.18 (s, 1H), 5.03 (d, *J* = 1.8 Hz, 1H), 4.88 (t, *J* = 7.8 Hz, 1H), 4.82-4.74 (m, 5H), 4.68-4.38 (m, 21H), 4.33 (d, *J* = 7.8 Hz, 1H), 4.29 (d, *J* = 7.9 Hz, 1H), 4.20-4.00 (m, 8H), 3.95-3.71 (m, 9H), 3.69-3.53 (m, 6H), 3.52-3.33 (m, 8H), 3.29-3.15 (m, 5H), 2.90-2.79 (m, 2H), 2.08 (s, 3H), 1.92 (s, 3H), 1.35-1.20 (m, 4H), 1.08-1.01 (m, 2H); ^{13}C NMR (150 MHz, $CDCl_3$) : δ 170.40, 169.88, 168.68, 138.20, 138.94, 138.78, 138.71, 138.56, 138.48, 138.38, 138.21, 138.02, 134.30, 133.84, 132.02, 128.78, 128.65, 128.63, 128.43, 128.40, 128.38, 128.25, 128.15, 128.06, 127.94, 127.88, 127.84, 127.77, 127.69, 127.65, 127.56, 127.10, 123.90, 123.41, 100.98, 99.83, 98.34, 97.32, 78.31, 78.17, 78.11, 78.00, 76.22, 75.52, 75.28, 75.05, 74.82, 74.40, 73.98, 73.67, 73.58, 73.36, 73.06, 72.59, 72.48, 72.42, 72.09, 71.32, 70.52, 69.46, 69.09, 68.83, 68.72, 68.42, 68.20, 67..61, 62.57, 56.77, 55.98, 51.37, 29.99, 29.65, 28.94, 28.54, 23.27, 21.44, 21.13, 14.41; ESI-MS: *m/z* calcd for $C_{152}H_{159}N_5O_{35}Na$: 1638.0741 ; found 2638.0754 $(M + Na)^+$.

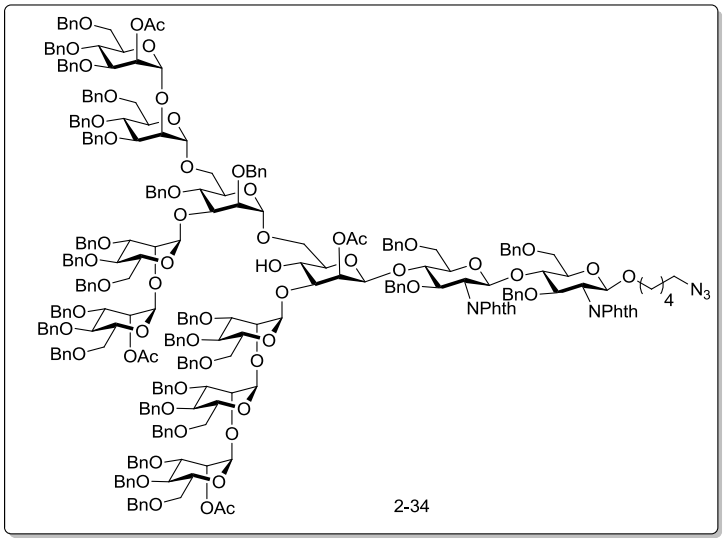

5-Azidopentyl-O-(2-O-acetyl-3,4,6-tri-O-benzyl-α-D-mannopyranosyl-(1→2)-3,4,6-tri-O-benzyl-α-D-mannopyranosyl-(1→2)-3,4,6-tri-O-benzyl-α-D-mannopyranosyl-(1→3)-{2-O-acetyl-3,4,6-tri-O-benzyl-α-D-mannopyranosyl-(1→2)-3,4,6-tri-O-benzyl-α-D-mannopyra-nosyl-(1→3)-[2-O-acetyl-3,4,6-tri-O-benzyl-α-D-mannopyranosyl-(1→2)-3,4,6-tri-O-benzyl -α-D-mannopyranosyl-(1→6)]-2,4-di-O-benzyl-α-D-mannopyranosyl-(1→6)}-2-O-acetyl-β-D-mannopyranosyl-(1→4)-O-(3,6-di-O-benzyl-2-deoxy-2-phthalimido-β-D-glucopyranosyl)-(1→4)-O-3,6-di-O-benzyl-2-deoxy-2-phthalimido-β-D -glucopyranoside (2-34*)*: A mixture of hexasaccharide acceptor **2-32** (0.100 g, 0.038 mmol), thiomannoside donor **2-21** (0.104 g, 0.045 mmol) and activated 4 Å molecular sieves (0.500 g) in CH_3CN (10 mL) was stirred at room temperature for 1 h. The resulting mixture was cooled to -10°C , tris(4-bromophenyl)aminium hexachloroantimonate (0.096 g, 0.114 mmol) was added and stirred at room temperature for 6 h. TLC (ethyl acetate : toluene, 2/8) indicated formation of product with consumption of starting material, reaction was quenched by Et_3N. The reaction mixture was diluted with CH_2Cl_2 and filtered through celite. The filtrate was washed with aqueous $NaHCO_3$ (2x50mL), and a brine (50 mL) solution. The organic layer was dried over Na_2SO_4 and concentrated in *vacuo*. The residue was purified by flash column chromatography to afford **2-34** (0.095gm, 52%) as colorless foam. TLC: (acetone : toluene =2/8, v/v) : R_f = 0.41; ^{1}H NMR (600 MHz, $CDCl_3$) : δ 7.77-7.50 (m, 8H), 7.29-6.98 (m, 126H), 6.95-6.89 (m, 4H), 6.74-6.64 (m, 5H), 5.56 (s, 1H), 5.53 (s, 1H), 5.51 (s, 1H), 5.34 (s, 1H), 5.32 (d, *J* = 12.2 Hz, 2H), 5.18 (d, *J* = 7.8 Hz, 1H), 5.12 (s, 1H), 5.08 (s, 1H), 5.04 (s, 2H), 4.59-3.75 (m, 116H), 3.26-3.16 (m, 4H), 3.08-3.02 (m, 2H), 2.93-2.83 (m, 2H), 2.12 (s, 3H) , 2.06 (s, 3H), 2.06 (s, 3H), 1.97 (s, 3H),1.39-1.26 (m, 4H), 1.07-1.05 (m, 2H); ^{13}CNMR (150 MHz, $CDCl_3$) : δ 170.12, 170.03, 169.76, 168.14, 167.36, 138.64, 138.54, 138.45, 138.41, 138.27, 138.07, 133.68, 133.57, 131.74, 129.05, 128.62, 128.57, 128.51, 128.33, 128.23, 128.14, 128.06, 127.99, 127.94, 127.81, 127.78, 127.73, 127.45, 101.24, 99.81, 99.59, 99.48, 99.34, 99.24, 99.05, 98.02, 96.95, 79.82, 79.23, 78.33, 78.24, 78.14, 75.86, 75.22, 75.12, 75.02, 74.93, 74.77, 74.57, 74.47, 74.38, 74.30, 74.17, 73.29, 73.11, 72.50, 72.20, 71.94, 71.35, 71.25, 69.13, 69.03, 68.79, 68.53, 68.48, 68.35, 68.17, 67.40, 56.56, 55.69, 51.09, 28.66, 28.26, 22.99, 21.17, 21.12; HRMS (MALDI-TOF) : *m/z* calcd for $C_{284}H_{297}N_5O_{62}Na$: 4795.0232 ; found 4794.9783 $(M + Na)^+$.

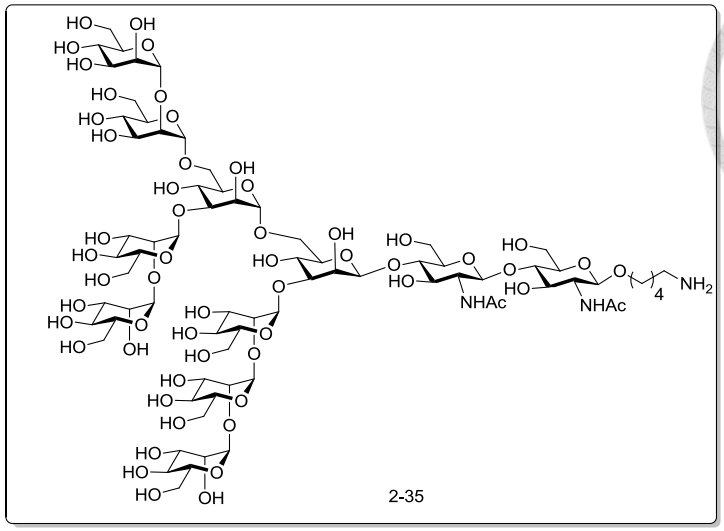

5-Aminopentyl-α-D-mannopyranosyl-(1→2)-α-D-mannopyranosyl-(1→2)-α-D-manno-pyr-anosyl-(1→3)-{α-D-mannopyranosyl-(1→2)-α-D-mannopyranosyl-(1→3)-[α-D-manno-pyr-anosyl-(1→2)-α-D-mannopyranosyl-(1→6)]-α-D-mannopyranosyl-(1→6)}-β-D-manno-pyr-anosyl-(1→4)-2-acetamido-2-deoxy-β-D-glucopyranosyl-(1→4)-2-acetamido-2-deoxy-β-D-glucopyranoside (2-35): Compound **2-34** (0.120 g, 0.024 mmol) was deprotected by following general procedure 1 to get $Man_9GlcNAc_2$ **2-35** (0.012 g, 26%) as a white solid. ^{1}HNMR (600 MHz, D_2O) : δ 5.40 (s, 1H), 5.33 (s, 1H), 5.30 (s, 1H), 5.14 (s, 1H), 5.05 (s, 1H), 5.03 (d, *J* =2.4 Hz, 2H), 4.86 (s, 1H), 4.58 (d, *J* = 7.8 Hz, 1H), 4.48 (d, *J* = 7.8 Hz, 1H), 4.22 (d, *J* = 2.4 Hz, 1H), 4.14 (s, 1H), 4.13-3.95 (m, 12H), 3.94-3.59 (m, 54H), 3.50-3.48 (m, 1H), 3.02 (t, *J* = 9.2 Hz, 2H), 2.06 (s, 3H), 2.02 (s, 3H), 1.68-1.63 (m, 2H), 1.59-1.56 (m, 2H), 1.41-1.37 (m, 2H); ^{13}CNMR (150 MHz, D2O) : δ 174.47, 171.01, 102.24, 102.21, 102.19, 101.43, 101.03, 100.82, 100.59, 100.21, 99.61, 97.97, 81.86, 79.32, 78.88, 78.63, 78.45, 74.50, 74.48, 74.14, 73.39, 73.27, 73.20, 73.17, 72.69, 72.36, 71.90, 71.61, 70.21, 70.03, 69.93, 69.37, 67.01, 66.94, 66.90, 66.85, 66.81, 66.76, 65.42, 65.40, 65.07, 64.90, 61.11, 61.06, 61.01, 60.91, 60.06, 59.94, 54.95, 39.29, 38.61, 28.02, 26.34, 22.16, 22.10, 22.06; ESI-MS: *m/z* calcd for $C_{75}H_{129}N_3O_{56}Na$: 1990.7231; found 1990.7279 $(M+Na)^+$.

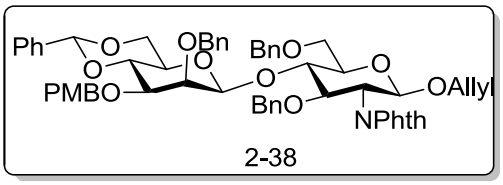

Allyl-O-2-O-benzyl-3-O-*p*-methoxy-benzyl-4,6-O-benzylidine-β-D-mannopyranosyl-(1→4)-O-(3,6-di-O-benzyl-2-deoxy-2-phthalimido-β-D-glucopyranoside (2-38): A mixture of donor **2-36** (0.272 g, 0.483 mmol) and activated 4Å molecular sieves (0.5 g) in CH_2Cl_2 (10 mL) was stirred at room temperature for 1 h. Mixture was cooled to -60^oC, 2,6-di-ter-butyl pyridine (268 µl, 1.24 mmol) followed by Tf_2O (79 µl, 0.483 mmol) was added and stirred for 40 minutes. A solution of acceptor **2-37** (0.2 g, 0.378 mmol) in CH_2Cl_2 (5 mL) was added slowly and resulting reaction was stirred for 1h until TLC (ethyl acetate: toluene, 1/9) indicated formation of a product with consumption of the starting material. Reaction mixture was quenched with Et_3N, diluted with CH_2Cl_2, filtered through celite and concentrated in *vacuo*. The residue was purified by flash column chromatography to afford **2-38** (0.230 g, 67%) as white solid. TLC: (ethyl acetate : toluene =1/9, v/v) : R_f = 0.52; ^{1}H NMR (600 MHz, $CDCl_3$) : δ 7.65-7.45 (m, 8H), 7.35-7.21 (m, 13 H), 6.91-6.90 (m, 2H), 6.90-6.81 (m, 5H), 5.67-5.65 (m, 1H), 5.49 (s, 1H), 5.13 (d, *J* = 8.4 Hz, 1H), 5.07 (d, *J* = 10.8Hz, 1H), 4.99 (d, *J*= 10.4 Hz, 1H), 4.87-4.82 (m, 3H), 4.65 (d, *J* = 5.4Hz, 1H), 4.63 (d, *J* = 5.4 Hz, 1H), 4.53 (s, 1H), 4.50 (d, *J* = 12 Hz, 1H), 4.41 (d, *J* = 6 Hz, 1H), 4.39 (d, *J* = 6 Hz, 1H), 4.24-4.21 (m, 2H), 4.05-3.96 (m, 3H), 3.81 (s, 3H), 3.711 (d, *J* = 3 Hz, 1H), 3.64 (d, *J* = 10.8 Hz, 1H), 3.56-3.52 (m, 2H), 3.45-3.47 (d, *J* = 10 Hz, 1H), 3.40 (dd, *J* = 3, 6.6Hz, 1H), 3.13-3.12 (m, 1H); ^{13}CNMR (150 MHz, $CDCl_3$) : δ 159.46, 139.08, 138.99, 138.12, 138.00, 134.05 ,130.93, 129.37, 129.22, 128.84, 128.60, 128.54, 128.47, 128.45, 128.26, 128.12, 128.09, 128.07, 127.83, 127.21, 126.41, 117.60, 114.04, 102.28, 101.63, 97.70, 79.85, 78.99, 78.33, 77.44, 75.29, 75.03, 74.95, 73.86, 72.61, 69.99, 68.86, 68.84, 67.66, 55.96, 55.58; ESI-MS: *m/z* calcd for $C_{59}H_{59}NO_{13}Na$: 1012.3879; found 1012.3888 $(M + Na)^+$.

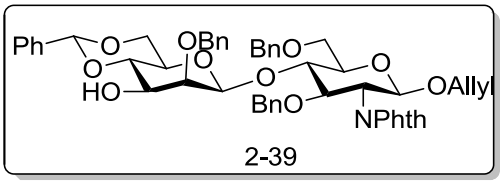

2-39

Allyl-O-2-O-benzyl-4,6-O-benzylidine-β-D-mannopyranosyl-(1→4)-O-(3,6-di-O-benzyl-2-deoxy-2-phthalimido-β-D-glucopyranoside (2-39): To a solution of **2-38** (0.5 g, 0.505 mmol) in 10mL CH_2Cl_2:H_2O (10:1) was added DDQ (0.219 g, 1.01 mmol) at 0°C

and resulting reaction mixture was stirred for 3 h. Reaction mixture was then filtered, organic layer washed with H_2O (2 x 30 mL). The aqueous layer was further extracted with CH_2Cl_2 (2 x 50 mL). The combined organic layer were washed with brine solution (40mL), dried over Na_2SO_4 and concentrated in *vacuo.* The residue was purified by flash column chromatography to afford **2-39** (0.308 g, 70%) as colorless foam. TLC: (ethyl acetate : toluene =2/8, v/v) : R_f = 0.42; ^{1}HNMR (600 MHz, $CDCl_3$) : δ 7.65-7.44 (m, 6H), 7.43-7.28 (m, 13H), 6.92-6.90 (m, 2H), 6.83-6.81 (m, 3H), 5.68-5.64 (m, 1H), 5.42 (s, 1H), 5.14 (d, *J* = 8.4 Hz, 1H), 5.08 (d, *J* = 12.8 Hz, 1H), 5.01-4.98 (m, 2H), 4.85 (d, *J* = 12.6 Hz, 1H), 4.74 (d, *J* = 12 Hz, 1H), 4.65 (d, *J* = 12 Hz, 1H*)*, 4.62 (s, 1H), 4.84 (d, *J* = 12Hz, 1H), 4.40 (d, *J* = 12 Hz, 1H), 4.25-4.16 (t, *J* = 9.6 Hz, 1H), 3.99 (dd, *J* =13, 6.3 Hz, 1H), 3.73-3.65 (m, 4H), 3.54-3.47 (m, 3H), 3.13-3.09 (m, 1H) ; ^{13}CNMR (150 MHz, $CDCl_3$) : 138.97, 138.44 ,137.93, 137.56, 133.98, 129.37, 128.92, 128.79, 128.53, 128.43, 128.35, 128.26, 128.21, 128.10, 127.99, 127.27, 126.58, 117.64, 102.33, 102.25, 97.66, 79.91, 79.42, 79.15, 77.43, 76.00, 75.03, 74.89, 74.01, 71.24, 69.99, 68.78, 68.67, 67.17, 55.90; ESI-MS: *m/z* calcd for $C_{51}H_{51}NO_{12}Na$: 892.3303; found 892.3314 $(M + Na)^+$.

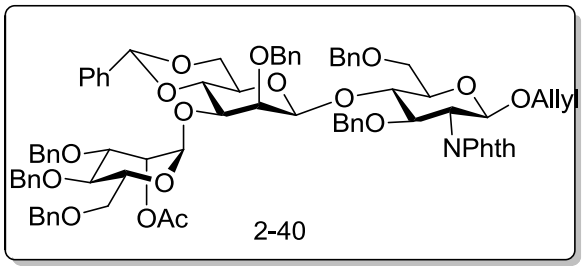

2-40

Ally-O-(2-O-acetyl-3,4,6-tri-O-benzyl-α-D-mannopyranosyl-(1→3)-2-O-benzyl-4,6-O-ben-zylidine-β-D-mannopyranosyl-(1→4)-O-(3,6-di-O-benzyl-2-deoxy-2-phthalimido-β-D-glu-copyranoside (2-40):- A mixture of donor **2-23** (0.537g, 0.863 mmol), acceptor **2-39** (0.500 g, 0.574 mmol) and activated 4Å molecular sieves in dry CH_2Cl_2 (10 mL) was stirred at room temperature for 30 minutes. The reaction was cooled to -40^{o}C, boron trifluoride ethyl etherate (32 µL, 0.288 mmol) was then added slowly and resulting reaction mixture was stirred for 1 h. The reaction was quenched by adding Et_3N, diluted with CH_2Cl_2, filtered through celite and concentrated in *vacuo*. The residue was purified by flash column

chromatography to afford **2-40** (0.630 g, 81%) as colorless oil. TLC: (ethyl acetate : hexane =3/7, v/v) : R_f = 0.62; ^{1}HNMR (600 MHz, $CDCl_3$) : δ 7.41-7.39 (m, 4H), 7.39-7.25 (m, 30H), 7.16-6.82 (m, 5H), 5.57-5.51 (m, 1H), 5.50 (d, *J* = 3 Hz, 1H), 5.47 (s, 1H), 7.29 (d, *J* = 2.1 Hz, 1H), 5.13 (d, *J* = 8.4 Hz, 1H), 5.08 (dd, *J* = 6 , 12.2 Hz, 1H), 5.00 (dd, *J* = 6 , 10.2 Hz, 1H), 4.87-4.82 (m, 2H), 4.79-4.78 (m, 2H), 4.66-4.59 (m, 3H), 4.54 (s, 1H), 4.46-4.44 (m, 3H), 4.22-4.20 (m, 2H), 4.17-4.14 (m, 2H), 4.03-3.93 (m, 4H), 3.82-3.71 (m, 5H), 3.64-3.62 (m, 2H), 3.60-3.52 (m, 2H), 3.50 (d, *J* = 8.2 Hz, 1H), 3.19 (m, 1H), 2.34 (s, 3H); ^{13}CNMR (150 MHz, $CDCl_3$) : δ 170.26, 163.58, 162.83, 138.98, 138.77, 138.60, 138.40, 138.09, 138.04, 137.58, 133.97, 131.97, 129.01, 128.79, 128.71, 128.64, 128.62, 128.56, 128.52, 128.38, 128.32, 128.24, 128.12, 128.05, 127.97, 127.94, 127.84, 127.18, 126.26, 123.57, 117.58, 101.76, 101.35, 98.96, 97.63, 79.24, 78.91, 78.56, 78.22, 75.76, 75.62, 75.03, 74.77, 74.44, 73.75, 72.55, 71.83, 69.94, 69.32, 68.64, 68.54, 68.39, 67.16, 55.88, 36.75, 31.70, 21.27; ESI-MS : *m/z* calcd for $C_{80}H_{81}NO_{18}Na$: 1366.5346; found 1366.5369 $(M + Na)^+$.

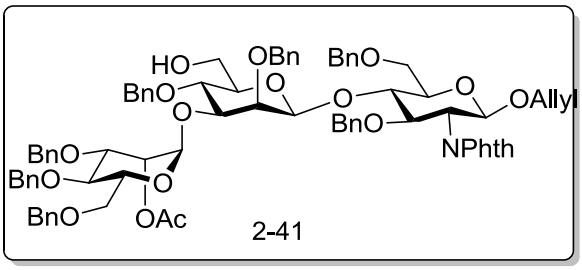

2-41

Ally-O-(2-O-acetyl-3,4,6-tri-O-benzyl-α-D-mannopyranosyl-(1→3)-2,4-O-di-benzyl-β-D-mannopyranosyl-(1→4)-O-(3,6-di-O-benzyl-2-deoxy-2-phthalimido-β-D-glucopyranoside (2-41):- A mixture of compound **2-40** (0.630 g, 0.468 mmol) and activated 4Å molecular sieves in 20 mL CH_2Cl_2 was stirred for 1 h at room temperature. The reaction mixture was cooled to -78^{o}C, triethyl silane (148 µl, 0.946 mmol) followed by dichlorophenyl borane (146 µl, 1.18 mmol) was added and stirred for 1 h. Reaction was quenched by Et_3N, methanol , filtered through celite and concentrated in *vacuo.* The residue was co-distilled with methanol 2-3 times before being purified by flash column chromatography to give alcohol **2-41** (0.460 g, 73%)**.** TLC: (ethyl acetate : toluene =2/8, v/v) : R_f = 0.42; ^{1}HNMR (600 MHz, $CDCl_3$) : δ 7.73-7.57 (m, 4H), 7.50-7.08 (m, 31H), 6.83-6.81 (m, 4H), 5.76-5.69 (m, 1H), 5.44 (t, *J* = 3 Hz, 1H), 5.13 (s, 1H), 5.12 (s, 1H), 5.08 (d, *J* = 11.2

Hz, 1H), 5.01 (d, *J* = 11Hz, 1H), 4.93 (d, *J* = 11 Hz, 1H), 4.87 (d, *J* = 8.6 Hz, 1H), 4.834 (d, *J* = 8.2 Hz, 1H), 4.76 (d, *J* = 12.2 Hz, 1H), 4.69 (d, *J* = 11 Hz, 1H), 4.62 (t, *J* = 8.6 Hz, 1H), 4.57 (t, *J* = 7.8 Hz, 2H), 4.50 (d, *J* = 10.8 Hz, 1H), 4.44 (d, *J* = 2.5 Hz, 1H), 4.42 (s, 1H), 4.40 (d, *J* = 8 Hz, 1H), 4.35 (d, *J* = 12 Hz, 1H), 4.22-4.181 (m, 3H), 4.00-3.99 (m, 2H), 4.90-3.91 (s, 1H), 3.83-3.82 (m,1H), 3.83 (d, *J* = 2.4 Hz, 1H), 3.77-3.78 (m, 2H), 3.64-3.54 (m, 6H), 3.41-3.39 (m, 2H), 3.19-3.18 (m, 1H), 2.08 (s, 3H); ^{13}CNMR (150 MHz, $CDCl_3$) : δ170.34, 138.90, 138.77, 138.73, 138.36, 138.14, 138.07, 138.03, 135.91, 134.50, 134.03, 133.86, 132.97, 131.94, 131.40, 129.31, 128.86, 128.68, 128.66, 128.61, 128.57, 128.50, 128.45, 128.38, 128.26, 128.20, 128.12, 128.11, 128.03, 127.97, 127.94, 127.79, 127.76, 127.72, 127.47, 127.35, 123.50, 117.59, 101.04, 99.89, 97.61, 80.92, 78.64, 78.48, 78.41, 78.21, 75.93, 75.26, 75.20, 75.19, 75.16, 74.82, 74.59, 74.52, 73.78, 73.75, 72.61, 72.11, 69.91, 69.50, 68.99, 68.43, 62.25, 55.86, 21.29; ESI-MS: *m/z* calcd for $C_{80}H_{83}NO_{18}Na$: 1368.5502; found 1368.5527 $(M + Na)^+$.

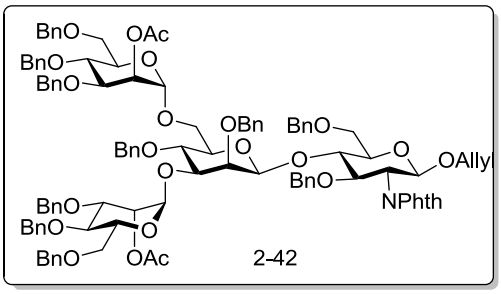

2-42

Allyl-O-di-(2-O-acetyl-3,4,6-tri-O-benzyl-α-D-mannopyranosyl-(1→3), (1→6)-2,4-O-di-benzyl-β-D-mannopyranosyl-(1→4)-O-(3,6-di-O-benzyl-2-deoxy-2-phthalimido-β-D-gluco-pyranoside (2-42): A mixture of donor **2-23** (0.429 g, 0.690 mmol), acceptor **2-41** (0.460 g, 0.345 mmol) and activated 4Å molecular sieves in dry CH_2Cl_2 (10 mL) was stirred at room temperature for 30 minutes. The reaction was cooled to -20^{o}C, boron trifluoride ethyl etherate (19 μL, 0.173 mmol) was then added slowly and resulting reaction mixture was stirred for 2 h. The reaction was quenched by adding Et_3N, diluted with CH_2Cl_2, filtered through celite and concentrated in *vacuo*. The residue was purified by flash column chromatography (ethyl acetate: hexane, 3/7) to afford **2-42** (0.380 g, 65%) as colorless foam. TLC: (ethyl acetate : hexane =3/7, v/v) : R_f = 0.56; ^{1}HNMR (600 MHz, $CDCl_3$) :δ 7.60-7.29 (m, 4H), 7.28-7.08 (m, 37H), 7.08-7.01 (m, 8H), 7.00-6.93 (d, *J* = 8.3 Hz, 1H),

6.82-6.59 (m, 3H), 5.61-5.59 (m, 1H), 5.43 (d, *J* = 6.2 Hz, 1H), 5.31 (d, *J* = 6 Hz, 1H), 5.10 (d, *J* = 3.5 Hz, 1H), 5.06 (d, *J* = 8.2 Hz, 1H), 4.99 (d, *J* = 10.2 Hz, 1H), 4.85 (d, *J* = 8.5 Hz, 1H), 4.83 (s, 1H), 4.67 (d, *J* = 8.3 Hz, 1H), 4.64-4.62 (q, 4H), 4.56 (d, *J* = 9.5 Hz, 1H), 4.55-4.45 (m, 8H), 4.45-4.39 (m, 9H), 4.38 (d, *J* = 10 Hz, 1H), 4.21 (d, *J* = 9 Hz, 1H), 4.19-4.10 (m, 2H), 4.08-3.70 (m, 10H), 3.69-3.49 (m, 7H), 3.39 (d, *J* = 9.1 Hz, 1H), 3.19 (d, *J* = 9.1 Hz, 1H), 2.07 (s, 3H), 1.82 (s, 3H) ; ^{13}CNMR (150 MHz, $CDCl_3$) : δ 170.31, 170.11, 163.43, 139.07, 138.93, 138.83, 138.80, 138.65, 138.35, 138.32, 138.21, 138.09, 134.08, 133.77, 132.00, 128.87, 128.76, 128.66, 128.56, 128.43, 128.37, 128.16, 127.99, 127.91, 127.82, 127.73, 127.13, 123.46, 117.45, 102.07, 99.92, 99.74, 98.62, 97.55, 81.40, 79.81, 78.31, 78.23, 76.84, 75.87, 75.77, 75.66, 74.87, 74.65, 74.44, 74.38, 31.21, 21.29, 21.23;ESI-MS: *m/z* calcd for $C_{109}H_{113}NO_{24}Na$: 1843.7578; found 1843.7676 $(M + Na)^+$.

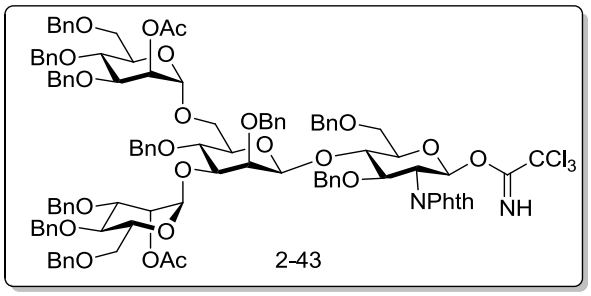

2-43

Di-(2-O-acetyl-3,4,6-tri-O-benzyl-α-D-mannopyranosyl-(1→3),(1→6)-2,4-O-di-benzyl-β-D-mannopyranosyl-(1→4)-O-(3,6-di-O-benzyl-2-deoxy-2-phthalimido-β-D-glucopyranosyl trichloroacetimidate (2-43): To a solution of **2-42** (0.2 g, 0.109 mmol) in 10 mL CH_2Cl_2:MeOH (1/1) was added $PdCl_2$ (20 mg) and stirred at room temperature for 6 h until TLC (ethyl acetate : toluene, 2/8) indicated formation of a product with consumption of the starting material. Reaction mixture was then concentrated in *vacuo.* The residue was purified by flash column chromatography to afford alcohol (0.140gm, 60%) as colorless foam. To a solution of alcohol (0.150 g, 0.084 mmol) in CH_2Cl_2 (10 mL) was added trichloroacetamidate (33 µl, 0.336 mmol) followed by DBU (12 µl, 0.033 mmol) at 0^{o}C and stirred at room temperature for 8 h. Reaction was quenched with Et_3N and concentrated in *vacuo.* The residue was purified by flash column chromatography to afford **2-43** (0.121 g, 67%) as colorless oil. TLC: (ethyl acetate : toluene =2/8, v/v) : R_f = 0.47; ^{1}HNMR (600MHz, $CDCl_3$): δ 8.51 (s,1H), 7.53-7.42 (m, 4H), 7.40-7.00 (m, 49H), 6.58 (d, *J* = 6.6

Hz, 2H), 6.52-6.50 (m, 3H), 5.43 (s, 1H), 5.32 (s, 1H), 5.03 (s, 1H), 5.01 (t, *J* = 7.8Hz, 1H), 4.90-4.78 (m, 6H), 4.67-4.45 (m, 7H), 4.43-4.30 (m, 9H), 4.28-4.20 (m, 2H), 4.10 (t, *J* = 7.8Hz, 1H), 3.39-3.42 (m, 18H), 3.19 (d, *J* = 9.3Hz, 1H), 2.09 (s, 3H), 1.83 (s, 3H).

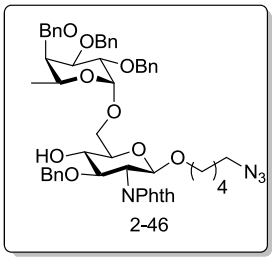

2-46

5-Azidopentyl-O- 2,3,4-tri-O-benzyl-α-L-fucopyranosyl-(1→6)-3-O-benzyl-2-deoxy -2-phthalimido-β-D-glucopyranoside (2-46): A mixture of $CuBr_2$ (0.450 g, 2.01 mmol), Bu_4NBr (0.655 g, 2.03 mmol) and activated 4Å molecular sieves in 10mL of CH_2Cl_2:DMF (2/1) was stirred and cooled over an ice water bath. A solution of donor **2-44** (0.5 g, 0.925 mmol) and acceptor **2-45** (0.450 g, 0.882 mmol) in CH_2Cl_2(10 mL) was added drop wise and resulting reaction mixture was stirred at room temperature for overnight. TLC (ethyl acetate: hexane, 4/6) indicated formation of a product with consumption of the starting material. Reaction was quenched with aq.$NaHCO_3$, diluted with ethyl acetate (50mL) and filtered through celite. The filtrate was washed with aq.$NaHCO_3$, brine (50mL), dried over sodium sulfate. The organic layer was concentrated in *vacuo.* The residue was purified by flash column chromatography to afford **2-46** (0.604 g, 76%) as colorless oil. TLC: (ethyl acetate : hexane =4/6, v/v) : R_f = 0.47; ^{1}HNMR (600 MHz, $CDCl_3$) : δ 7.80-7.64 (m, 4H), 7.41-7.23 (m, 15H), 7.00-6.98 (m, 2H), 6.90-6.87 (m, 3H), 5.06 (d, *J* = 8.4 Hz, 1H), 4.96 (d, *J* = 11.4 Hz, 1H), 4.86 (d, *J* = 11.4 Hz, 1H), 4.82-4.72 (m, 4H), 4.67 (d, *J* = 12.2 Hz, 1H), 4.64 (d, *J* = 12.5 Hz, 1H), 4.48 (d, *J* = 12.6 Hz, 1H), 4.16-4.13 (m, 1H), 4.08-4.05 (m, 2H), 3.39-3.95 (m, 2H), 3.90-3.83 (m, 3H), 3.78 (m, 1H), 3.73-3.69 (m, 2H), 3.56-3.53 (m, 1H), 3.35-3.21 (m, 1H), 2.00-2.03 (m, 2H), 1.38-1.30 (m, 4H), 1.12 (d, *J* = 8.4 Hz, 2H), 1.00-0.96 (m, 2H); ^{13}CNMR (150, MHz, $CDCl_3$) : δ 138.83, 138.77, 138.36, 134.13, 128.90, 128.77, 128.67, 128.60, 128.52, 128.31, 128.26, 128.17, 127.93, 127.88, 127.52, 123.64, 98.81, 98.59, 79.60, 78.07, 77.77, 76.67, 75.22, 74.54, 74.51, 74.24, 73.35, 73.20, 69.37, 68.79, 67.15, 55.88, 51.39, 29.00, 28.58, 23.30, 16.89; ESI-MS: *m/z* calcd for $C_{53}H_{58}N_4O_{11}Na$: 949.3994; found 949.3998 $(M + Na)^+$.

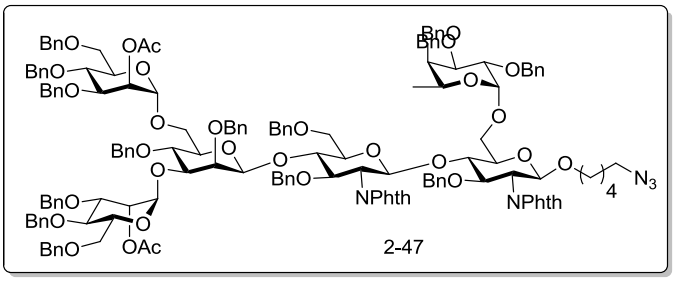

5-Azidopentyl-O-2-O-acetyl-3,4,6-tri-O-benzyl-α-D-mannopyranosyl-(1→6)-(2-O-acetyl-3,4,6-tri-O-benzyl-α-D-mannopyranosyl-(1→3))-2,4-di-O-benzyl-β-mannopyranosyl-(1→4) -O-3,6-di-O-benzyl-2-deoxy-2-phthalimido-β-D-glucopyranosyl-(1→4)-(2,3,4-tri-O-benzyl-α-L-fuco pyranosyl-(1→6))-3-O-benzyl-2-deoxy-2-phthalimido-β-D-glucopyranoside (2-47): A mixture of donor **2-43** (0.050 g, 0.025 mmol), acceptor **2-46** (0.028 g, 0.031 mmol) and activated 4Å molecular sieves in dry CH_2Cl_2 (10 mL) was stirred at room temperature for 30 minutes. The reaction was cooled to -70^oC, boron trifluoride ethyl etherate (0.725 μL, 0.0062 mmol) was then added slowly and resulting reaction mixture was stirred for 2 h. The reaction was quenched by adding Et_3N, diluted with CH_2Cl_2, filtered through celite and concentrated in *vacuo*. The residue was purified by flash column chromatography to afford **2-47** (0.027 g, 45%) as a white foam. TLC: (ethyl acetate : hexane =3/7, v/v) : R_f = 0.50; ^{1}HNMR (600MHz, $CDCl_3$) : δ 7.83-7.62 (m, 7H), 7.49-7.30 (m, 8H), 7.30-7.10 (m, 47H), 7.09-7.03 (m, 10H), 7.03-6.99 (m, 1H), 6.93 (d, *J* = 8.9 Hz, 2H), 6.79-6.63 (m, 6H), 6.55 (t, *J* = 7.8 Hz, 2H), 5.40 (m, 1H), 5.40 (m, 1H), 5.29-5.29 (m, 1H), 5.09 (d, *J* = 1.3 Hz, 1H), 4.88-4.76 (m, 13H), 4.67-4.65 (m, 2H), 4.58-5.48 (m, 9H), 4.42-4.40 (m, 3H), 4.36-4.30 (m, 5H), 4.20-4.10 (m, 5H), 4.05-4.00 (m, 2H), 3.92-3.80 (m, 7H), 3.79-3.60 (m, 7H), 3.62-3.41 (m, 10H), 3.25(dd, *J* = 3.2 & 8.2Hz, 1H), 3.18-3.17 (m, 2H), 2.85-2.79 (m, 2H), 2.06 (s, 3H), 1.76 (s, 3H), 1.42-1.34 (m, 4H), 1.03-0.99 (m, 5H); ^{13}CNMR (150 MHz, $CDCl_3$) : δ 170.30, 169.91, 168.15, 167.76, 139.16, 138.99, 138.88, 138.82, 138.77, 138.54, 138.28, 138.21, 138.10, 138.08, 138.05, 133.86, 132.02, 131.72, 128.80, 128.62, 128.60, 128.57, 128.55, 128.33, 128.23, 128.40, 127.98, 127.92, 127.70, 127.55, 127.26, 127.06, 123.33, 101.97, 99.62, 98.41, 97.95, 97.09, 97.05, 81.42, 79.71, 78.36, 74.98, 74.75, 74.68, 73.65, 72.57, 72.51, 72.03, 71.38, 68.93, 68.86, 68.12, 66.63, 66.12, 56.76, 56.01, 51.26,

28.82, 28.56, 23.20, 21.23, 20.91; ESI-MS: *m/z* calcd for $C_{159}H_{165}N_5O_{34}Na$: 2712.1261; found 2712.1338 $(M + Na)^+$.

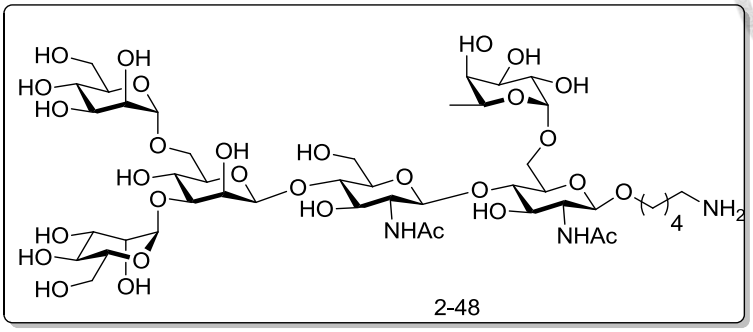

2-48

5-Aminopentyl-di-(α-D-mannopyranosyl)-(1→3),(1→6)-β-D-mannopyranosyl-(1→4)-2-acetamido-2-deoxy-β-D-glucopyranosyl-(1→4)-(α-L-fucopyranosyl-(1→6)-2-acetamido-2-deoxy-β-D-glucopyranoside) (2-48): Compound **2-47** (0.030 g, 0.011 mmol) was deprotected by following general procedure A to get title compound **S63** (0.007 g, 22%) as a white powder. ^{1}HNMR (600 MHz, D_2O) : δ 5.09 (s, 1H), 4.91 (s, 1H), 4.89 (d, *J* = 3.2 Hz, 1H), 4.65 (d, *J* = 7.8 HZ, 1H), 4.49 (d, *J* = 7.8 Hz, 1H), 4.25 (s, 1H), 4.15-4.10 (m, 1H), 4.05 (s, 1H), 3.95 (s, 1H), 3.95-3.80 (m, 8H), 3.80-3.50 (m, 23H), 3.00 (m, 2H), 2.10 (s, 3H), 2.09 (s, 3H), 1.67-1.60 (m, 2H), 1.60-1.57 (m, 2H), 1.41-1.37 (m, 2H), 1.25 (d, *J* = 7.8 Hz, 3H); ^{13}CNMR (150 MHz, D_2O) : δ 174.67, 174.39, 170.97, 102.51, 101.10, 101.04, 100.38, 99.60, 99.39, 80.46, 79.72, 78.60, 74.33, 74.15, 73.42, 72.65, 72.30, 71.95, 71.85, 70.29, 70.12, 70.00, 69.97, 69.85, 69.45, 68.15, 66.77, 66.14, 65.85, 65.80, 61.11, 60.92, 59.97, 55.05, 54.86, 46.66, 39.28, 38.61, 28.05, 26.36, 22.27, 22.15, 21.08, 21.50, 15.37, 15.34; ESI-MS: *m/z* calcd for $C_{45}H_{80}N_3O_{30}$: 1141.4821; found 1142.4827 $(M + H)^+$.

6.3. Experimental for Chapter 3

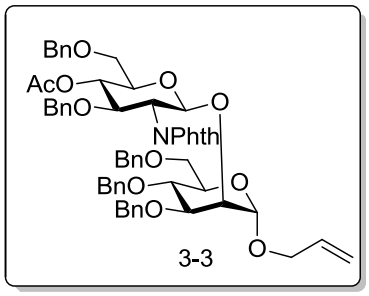

Allyl-O-4-O-acetyl-3,6-O-di-benzyl-2-deoxy-2-phthalimido-β-D-glucopyranosyl-(1→2) -O-3,4, 6-tri-O-benzyl-α-D-mannopyranoside (3-3): A mixture of thioglycoside donor **3-2** (2.33 g, 3.65 mmol), acceptor **3-1** (1.50 g, 3.05 mmol) and activated 4 Å molecular sieves (3 g) in 30 mL dry CH_2Cl_2 was stirred for 1 h at room temperature. NIS (1.35 g, 6.01 mmol) followed by TfOH (66.2 µL, 0.75 mmol) were added slowly at -40^oC and stirred for 2 h until TLC (ethyl acetate: toluene, 1/9) indicated formation of product with consumption of starting material. Reaction was quenched with Et_3N, filtered through celite, filtrate was washed with aq. $NaHCO_3$ (2 x 50mL), aq.$Na_2S_2O_3$ (2 x 50mL) and finally with brine (50 mL) solution. The organic layer was dried over Na_2SO_4 and concentrated in *vacuo*. The residue was purified by flash column chromatography to afford **3-3** (2.10 g, 68%) as white solid. TLC (ethyl acetate : toluene =1/9, v/v) : R_f = 0.29; ^{1}H NMR (600 MHz, $CDCl_3$) : δ 7.52-7.50 (m, 4H), 7.33-7.10 (m, 16H), 7.10-7.09 (m, 4H), 7.00-6.90 (m, 2H), 6.89-6.81 (m, 3H), 5.73-5.71 (m, 1H), 5.26 (d, *J* = 5.4 Hz, 1H), 5.14-5.06 (m, 3H), 4.71 (t, *J* = 7.8 Hz, 2H), 4.58 (d, *J* = 12.1 Hz, 1H), 4.50-4.39 (m, 6H), 4.34 (d, *J* = 4.8 Hz, 1H), 4.32 (d, *J* = 6.6 Hz, 1H), 4.10 (t, *J* = 8.6 Hz, 1H), 4.07-4.00 (q, 2H), 3.78 (dd, *J* = 3.2, 6.1 Hz, 1H), 3.81-3.78 (m, 2H), 3.71-3.70 (dd, *J* =3.2, 6.3 Hz, 1H), 3.65-3.60 (m, 1H), 3.58 (dd, *J* = 3.1, 6.5 Hz, 1H), 3.56 (t, *J* = 8.9 Hz, 1H), 3.480 (t, *J* = 10.2 Hz 1H), 3.392 (d, *J* = 8.4 Hz, 1H), 2.97-2.96 (m, 1H), 1.934 (s, 3H); ^{13}C NMR (150 MHz, $CDCl_3$) : δ 169.94, 138.69, 138.65, 138.53, 137.96, 137.91, 134.06, 133.84, 133.73, 131.91, 130.30, 128.59, 128.45, 128.40, 128.31, 128.23, 128.08, 127.94, 127.78, 127.72, 127.66, 127.59, 127.53, 123.35, 117.56, 97.17, 96.41, 77.90, 76.93, 75.13, 74.87, 73.92, 73.88, 73.82, 73.05, 72.82, 71.97, 71.01, 70.47, 70.19, 68.12, 55.55, 28.79, 21.57, 21.13; ESI-MS: *m/z* calcd for $C_{60}H_{61}NO_{13}Na$; 1026.4035 found 1026.4043 $(M + Na)^+$.

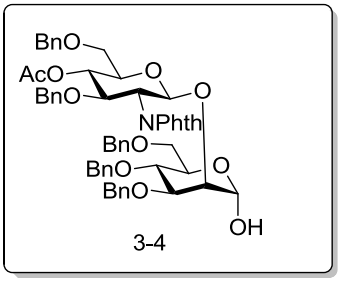

3-4

Allyl-O-3,6-O-di-benzyl-2-deoxy-2-phthalimido-β-D-glucopyranosyl-(1→2)-O-3,4,6-tri-O-benzyl-α-D-mannopyranoside (3-4): To a solution of **3-3** (0.750 g, 0.747 mmol) in 10 mL CH_2Cl_2 : MeOH (1/1) was added $PdCl_2$ (0.020 g) and stirred at room temperature for overnight until TLC (ethyl acetate: toluene, 2/8) indicated formation of a product with consumption of the starting material. Reaction mixture was then concentrated in *vacuo.* The residue was purified by flash column chromatography to afford alcohol **(**0.6 g, 80%) as colorless foam. TLC (ethyl acetate: toluene = 2/8, v/v) : R_f = 0.22; ^{1}H NMR (600MHz, $CDCl_3$) : δ 7.62-7.53 (m, 4H), 7.34-7.20 (m, 16H), 7.11-7.04 (m, 6H), 6.95-6.93 (m, 3H), 5.79-5.70 (m, 1H), 5.24 (d, *J* = 8.4 Hz, 1H), 5.09-5.06 (d, *J* = 10.5 Hz, 2H), 4.76 (d, *J* = 10.8 Hz, 1H), 4.71 (d, *J* = 12.2 Hz, 1H), 4.58-4.48 (m, 5H), 4.35-4.28 (m, 2H), 4.24-4.22 (m, 1H), 4.07-3.99 (m, 3H), 9.26 (dd, *J* = 3.2, 6.1Hz, 1H), 3.82-3.79 (m, 3H), 3.79-3.67 (m, 2H), 3.51-3.48 (m, 2H), 3.39 (d, *J* = 10.2 Hz, 1H), 2.98-2.95 (m, 2H); ^{13}C NMR (150 MHz, $CDCl_3$) : δ 138.74, 138.71, 138.66, 138.45, 137.71, 133.87, 133.81, 132.04, 128.83, 128.52, 128.48, 128.47, 128.44, 128.36, 128.28, 128.10, 127.97, 127.76, 127.74, 127.68, 127.59, 123.39, 117.60, 97.32, 96.50, 78.76, 78.15, 76.00, 75.20, 74.98, 74.44, 74.15, 74.04, 73.72, 73.12, 72.06, 71.29, 70.22, 68.19, 55.45; ESI-MS: *m/z* calcd for $C_{58}H_{59}Cl_3NO_{12}Na$; 985.0886 found 985.0895 $(M + Na)^+$.

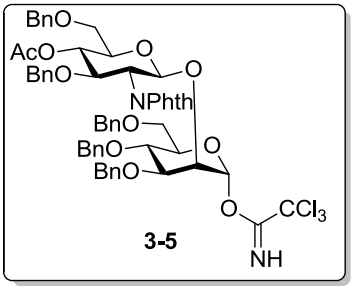

3-5

4-O-acetyl-3,6-O-di-benzyl-2-deoxy-2-phthalimido-β-D-glucopyranosyl-(1→2)-O-3,4,6-tri-O-benzyl-α-D-mannopyranosyl trichloroacetimidate (3-5): Compound **3-4**

(0.6 g, 0.655 mmol) was dissolved in CH_2Cl_2 (10 mL), added trichloroacetamidate (249 µl, 2.49 mmol) followed by DBU (36 µl, 0.249 mmol) at 0°C. Reaction mixture was stirred at room temperature for 5 h until TLC indicated formation of a product with consumption of the starting material. Reaction was quenched with Et_3N and concentrated in *vacuo*. The residue was purified by flash column chromatography to afford **3-5** (0.610 g, 85%) as white foam. TLC (ethyl acetate: toluene =2/8, v/v) : R_f = 0.65; ^{1}HNMR (600 MHz, $CHCl_3$) : δ 8.46 (s, 1H), 7.57-7.52 (m, 4H), 7.36-7.23 (m, 11H), 7.16-6.99 (m, 6H), 6.87-6.81 (m, 3H), 6.00 (s, 1H), 5.41 (d, *J* = 7.8 Hz, 1H), 4.89 (d, *J* = 10.8 Hz, 1H), 4.80 (dd, *J* = 4.2, 11.4 Hz, 2H), 4.72 (d, *J* = 12.2 Hz, 1H), 4.67 (d, *J* = 12 Hz, 1H), 4.54 (d, *J* = 12 Hz, 1H), 5.40 (d, *J* = 12.1 Hz, 1H), 4.445 (d, *J* = 12.4 Hz, 1H), 4.38-4.35 (m, 3H), 4.23 (dd, *J* = 4.1, 7.8 Hz, 1H), 4.17 (bs, 1H), 3.00 (d, *J* = 12.2 Hz, 1H), 3.91 (d, *J* = 12.2 Hz, 1H), 3.80-3.64 (m, 5H), 3.33 (d, *J* = 11.4 Hz, 1H), 3.00 (dd, *J* = 5.4, 11.4 Hz, 1H), 2.03 (s, 3H) ; ^{13}C NMR (150 MHz, $CDCl_3$) : δ 171.01, 160.41, 138.48, 138.44, 138.10, 137.96, 137.82, 131.90, 128.87, 128.60, 128.51, 128.46, 128.43, 128.38, 128.31, 128.20, 128.02, 127.93, 127.86, 127.74, 127.67,127.65, 123.47, 97.28, 95.71, 91.03, 79.59, 79.46, 75.47, 75.35, 75.21, 74.83, 74.07, 73.60, 73.10, 72.32, 71.29, 69.36, 63.29, 55.80, 31.21, 21.14.

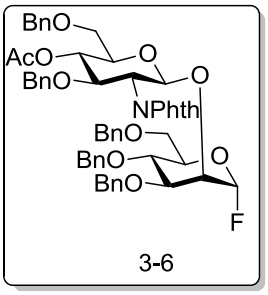

3-6

4-O-acetyl-3,6-O-di-benzyl-2-deoxy-2-phthalimido-β-D-glucopyranosyl-(1→2)-O-3,4,6-tri-O-benzyl-α-D-mannopyranosyl fluoride (3-6): To a solution of alcohol **3-4** (0.270 g, 0.197 mmol) in CH_2Cl_2 (10 mL) at -30°C was DAST (52 µL, 0.395 mmol) and resulting reaction mixture was stirred at -10°C for 8 h until TLC indicated formation of product with consumption of starting material. Reaction was quenched with aq.$NaHCO_3$, filtrate was washed with aqueous $NaHCO_3$ (2 x 50 mL) and a brine (50 mL) solution. The organic layer was dried over Na_2SO_4 and concentrated in *vacuo*. The residue was purified by silica gel column chromatography to afford **3-6** (0.150 g, 61%) as white foam. TLC (ethyl acetate:

hexane =3/7, v/v) : R_f = 0.45; ^{1}HNMR (600 MHz, $CDCl_3$) : δ 7.57-7.55 (m, 4H), 7.35-7.21 (m, 11H), 7.07 (d, *J* = 6.4 Hz, 4H), 6.99 (d, *J* = 7.2 Hz, 2H), 6.88-6.82 (m, 3H), 5.30 (d, *J* = 50.4 Hz, 1H), 5.20 (d, *J* = 12.2 Hz, 1H), 4.88 (d, *J* = 11.2 Hz, 1H), 4.80-4.71 (m, 3H), 4.64 (d, *J* = 11.3 Hz, 1H), 4.49-4.46 (m, 2H), 4.43 (d, *J* = 11.8 Hz, 2H), 4.34-4.28 (m, 3H), 4.23 (dd, *J* = 6.1, 11.3 Hz, 1H), 4.16 (s, 1H), 4.09 (d, *J* = 12.1 Hz, 1H), 4.06 (d, *J* = 12.3 Hz, 1H), 3.76-3.57 (m, 5H), 3.32 (d, *J* = 10.8 Hz, 1H), 3.02 (dd, *J* = 4.2, 11.3 Hz, 1H), 1.979 (s, 3H); ^{13}CNMR (150 MHz, $CDCl_3$) : δ 170.99, 138.40, 138.28, 138.16, 137.94, 137.70, 133.94, 131.82, 128.90, 128.63, 128.57, 128.47, 128.40, 128.31, 128.27, 128.04, 127.89, 127.89, 127.76, 123.54, 106.33, 104.85, 97.45, 79.55, 78.48, 75.43, 75.23, 74.09, 73.84, 73.70, 73.16, 72.78, 72.54, 71.36, 69.18, 63.40, 55.80, 31.21, 29.98, 21.11; ESI-MS: *m/z* calcd for $C_{57}H_{56}FNO_{12}Na$; 988.3679 found 988.3690 $(M + Na)^+$.

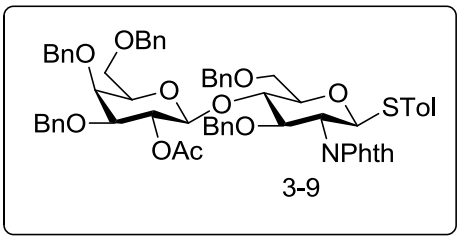

3-9

p-Tolyl-2-O-acetyl-3,4,6-O-tri-benzyl-β-D-galactopyranosyl-(1→4)-O-3,6-O-di-benzyl-2-deoxy-2-phthalimido-β-D-glucopyranoside (3-9): Activated 4Å molecular sieves (10 g) were added to a solution of acceptor **3-7** (5.0 g, 8.4 mmol) and donor **3-8** (6.03 g, 10.03 mmol) in anhydrous CH_2Cl_2 (100 mL) . The mixture was stirred for 1 h at room temperature. The reaction was cooled to -50 ^{o}C. NIS (1.89 g, 8.43 mmol) and, then, TMSOTf (152 µL, 0.84 mmol) were added slowly. The resulting reaction mixture was stirred for 2 h. When TLC (ethyl acetate : toluene, 1/9) indicated formation of product with consumption of starting material, the reaction was quenched by adding Et_3N and filtered through celite. Filtrate was washed with aqueous $NaHCO_3$ (2 x 50 mL), aqueous $Na_2S_2O_3$ (2 x 50 mL), and brine (50 mL) solution. The organic layer was dried over Na_2SO_4 and concentrated in *vacuo*. The residue was purified by flash column chromatography to afford **3-9** (7.40 g, 82%) as clear foam. TLC (ethyl acetate: toluene = 1/9, v/v): R_f = 0.54; ^{1}HNMR (600 MHz, $CDCl_3$) : δ 7.74-7.58 (m, 4H), 7.29-7.10 (m, 22H), 6.90 (d, *J* = 7.8 Hz, 1H), 6.86 (d, *J* = 7.2 Hz, 1H), 6.77-6.72 (m, 5H), 5.36 (d, *J* = 9.6 Hz, 1H), 5.27 (t, *J* = 8.4 Hz, 1H), 4.83 (d, *J* =

11.4 Hz, 1H), 4.76 (d, *J* = 12.6 Hz, 1H), 4.61-4.57 (m, 2H), 4.43-4.33 (m, 5H), 4.24 (d, *J* = 10.2 Hz, 1H), 4.19-4.15 (m, 3H), 3.90-3.84 (m, 2H), 3.73-3.68 (m, 2H), 3.51-3.48 (m, 1H), 3.38-3.29 (m, 4H), 2.18 (s, 3H), 1.93 (s, 3H); ^{13}CNMR (150 MHz, $CDCl_3$) : δ 169.5, 168.2, 167.6, 138.0, 138.9, 138.5, 138.3, 138.2, 134.0, 133.9, 133.5, 131.9, 129.7, 128.6, 128.4, 128.1, 128.0, 127.9, 127.8, 127.5, 127.0, 123.6, 123.5, 101.0, 83.8, 80.6, 79.7, 78.30, 77.9, 75.0, 74.6, 73.5, 72.9, 71.9, 68.3, 68.2, 55.17, 21.36, 21.32; ESI-MS: *m/z* calcd for $C_{64}H_{63}NO_{12}SNa$ 1092.3963; found 1092.3993 $(M + Na)^+$.

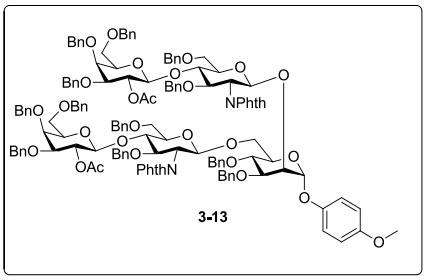

p-methoxyphenyl-O-2-O-acetyl-3,4,6-O-tri-benzyl-β-D-galactopyranosyl-(1→4)-O-3,6-O-di-benzyl-2-deoxy-2-phthalimido-β-D-glucopyranosyl-(1→2)-[2-O-acetyl-3,4,6-O-tri-benz-yl-β-D-galactopyrano-syl-(1→4)-O-3,6-O-di-benzyl-2-deoxy-2-phthalimido-β-D-glucopyr-anosyl-(1→6)]-3,4-O-di-benzyl-α-D-mannopyranoside (3-13): Activated 4Å molecular sieves (1 g) was added to a solution of acceptor **3-10** (0.140 g, 0.298 mmol) and donor **3-9** (0.783 g, 0.722 mmol) in anhydrous CH_2Cl_2 (10 mL). The mixture was stirred for 1 h at room temperature. The reaction was cooled to -50^{o}C. NIS (0.268 g, 1.19 mmol) and, then, by TMSOTf (13.11 µL, 0.074 mmol) were added slowly. The resulting reaction mixture was stirred for 40 mins. When TLC (ethyl acetate : toluene, 2/8) indicated formation of product with consumption of starting material, the reaction was quenched by adding Et_3N and filtered through celite. Filtrate was washed with aqueous $NaHCO_3$ (2 x 50 mL), aqueous $Na_2S_2O_3$ (2 x 50 mL), and brine (50 mL) solution. The organic layer was dried over Na_2SO_4 and concentrated in *vacuo*. The residue was purified by flash column chromatography to afford **3-13** (0.648 g, 85%) as clear foam. TLC (ethyl acetate : toluene = 2/8, v/v): R_f = 0.48; ^{1}HNMR (600 MHz, $CDCl_3$): δ 7.73-7.52 (m, 8H), 7.42-7.02 (m, 50H), 6.98-6.75 (m, 10H), 6.55-6.49 (m, 4H), 5.33-5.28 (m, 2H), 5.15 (d, *J* = 8.4 Hz, 1H), 4.88-4.86 (m, 3H), 4.67-4.55 (m, 4H), 4.46-4.40 (m, 10H), 4.34-4.20 (m, 12H), 4.00-4.05 (m, 2H) 3.95-3.85 (m, 3H), 3.81-3.78 (m, 1H), 3.72-3.62 (m, 6H), 3.41-3.23 (m, 14H), 2.90-

2.89 (m, 1H), 1.05 (s, 3H), 1.93 (s, 3H); ^{13}CNMR (150 MHz, $CDCl_3$) : δ 169.6, 169.56, 155.0, 150.8, 139.1, 139.0, 138.6, 138.5, 138.3, 138.2, 133.8, 131.8, 128.6, 128.5, 128.4, 128.3, 128.2, 128.0, 127.9, 127.6, 127.5, 127.0, 126.9, 123.3, 118.5, 114.6, 101.0, 100.9, 99.2, 97.2, 80.6, 78.2, 78.0, 75.4, 75.3, 73.7, 73.6, 73.4, 72.9, 72.8, 72.1, 71.9, 71.3, 70.3, 68.7, 68.3, 68.2, 68.14, 55.93, 55.86, 31.22, 21.32; ESI-MS: *m/z* calcd for $C_{141}H_{140}N_2O_{31}Na$ 2380.9366; found 2380.9425 $(M + Na)^+$.

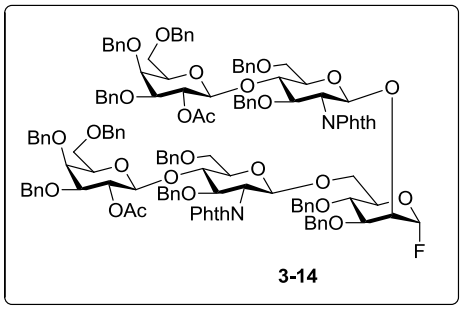

3-14

2-O-acetyl-3,4,6-O-tri-benzyl-β-D-galactopyranosyl-(1→4)-O-3,6-O-di-benzyl-2-deoxy-2-phthalimido-β-D-glucopyranosyl-(1→2)-[2-O-acetyl-3,4,6-O-tri-benzyl-β-D-galactopyran-osyl-(1→4)-O-3,6-O-di-benzyl-2-deoxy-2-phthalimido-β-D-glucopyranosyl-(1→6)]- 3,4-O-di-benzyl-α-D-mannopyranosyl fluoride (3-14): Cerium ammonium nitrate (0.440 g, 0.801 mmol) was added to a solution of pentasaccharide **3-13** (0.640 g, 0.267 mmol) in 7 mL of acetonitrile : toluene : H_2O (4 : 2 : 1). The resulting reaction mixture was stirred at 0 °C for 1 h. The reaction was diluted with EtOAc (100 mL) and washed with H_2O (30 x 2 mL) and brine (30 mL). The organic layer was dried over Na_2SO_4 and concentrated in *vacuo*. The product was purified by flash column chromatography to afford 1-**OH** compound (0.370 g, 62%) as clear foam. The residue (0.250 g, 0.113 mmol) was dissolved in CH_2Cl_2 (10 mL) at -30 ^oC. Then, DAST (30 μL, 0.227 mmol) was added slowly. The resulting reaction mixture was stirred for 1 h. When TLC (ethyl acetate : toluene, 2/8) indicated formation of product with consumption of starting material, the reaction was quenched with aq. $NaHCO_3$, and the filtrate was washed with aqueous $NaHCO_3$ (2 x 50 mL) and brine (50mL) solution. The organic layer was dried over Na_2SO_4 and concentrated in *vacuo*. The residue was purified by silica gel column chromatography to afford **3-14** (0.180 g, 72%) as white foam. TLC (ethyl acetate : toluene = 2/8, v/v): R_f = 0.59; ^{1}H NMR (600 MHz, $CDCl_3$): δ 7.61-7.42 (m, 8H), 7.38-7.05 (m, 50H), 6.95-6.79 (m, 10H), 5.36-

5.30 (m, 2H), 5.14-5.13 (dd, *J* = 5.4, 3.0 Hz, 1H), 4.90-4.83 (m, 2H), 4.83-4.79 (m, 2H), 4.68-4.60 (m, 4H), 4.57 (t, *J* = 9.8 Hz, 2H), 4.49-4.39 (m, 10H), 4.38-4.23 (m, 6H), 4.22-4.19 (m, 4H), 4.01 (t, *J* = 3.6 Hz, 1H), 4.98-4.89 (m, 5H), 3.83 (t, *J* = 8.4 Hz, 1H), 3.77 (d, *J* = 9.4 Hz, 1H), 3.77-3.60 (m, 4H), 3.52-3.30 (m, 11H), 3.18-3.20 (m, 2H), 2.88-2.85 (m, 1H), 2.02 (s, 3H), 1.95 (s, 3H); ^{13}CNMR (150 MHz, $CDCl_3$): δ 169.7, 169.5, 167.8, 139.2, 139.0, 138.99, 138.9, 138.5, 138.3, 138.3, 138.2, 134.2, 133.6, 132.0, 131.7, 128.7, 128.6, 128.5, 128.4, 128.2, 128.1, 128.0, 127.9, 127.8, 127.6, 127.6, 127.1, 126,9, 101.0, 100.1, 97.5, 80.6, 80.5, 78.1, 78.0, 76.7, 75.4, 75.0, 74.8, 74.7, 74.6, 73.9, 73.8, 73.7, 73.6, 73.4, 72.9, 72.8, 72.4, 72.3, 71.9, 71.0, 68.7, 68.4, 68.3, 68.0, 55.7, 55.6, 31.2, 21.4, 21.3; ESI-MS: *m/z* calcd for $C_{134}H_{133}FN_2O_{29}Na$ 2276.8904; found 2276.8752 $(M + Na)^+$.

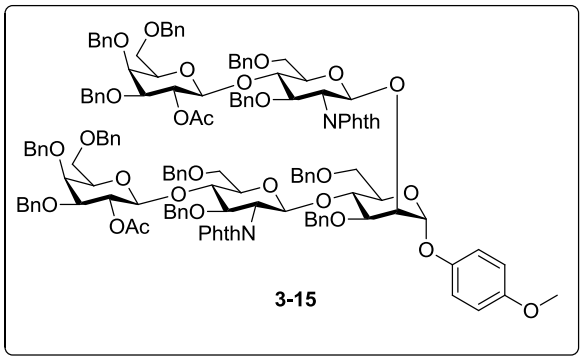

p-methoxyphenyl-O-2-O-acetyl-3,4,6-O-tri-benzyl-β-D-galactopyranosyl-(1→4)-O-3,6-O-di-benzyl-2-deoxy-2-phthalimido-β-D-glucopyranosyl-(1→2)-[2-O-acetyl-3,4,6-O-tri-ben zyl-β-D-galactopyranosyl-(1→4)-O-3,6-O-di-benzyl-2-deoxy-2-phthalimido-β-D-glucopyr-anosyl-(1→4)]-3,6-O-di-benzyl-α-D-mannopyranoside (3-15): Activated 4Å molecular sieves (1 g) was added to a solution of acceptor 3-**11** (0.250 g, 0.536 mmol) and donor **3-09** (1.27 gm, 1.34 mmol) in anhydrous CH_2Cl_2 (10 mL). The reaction mixture was stirred for 1 h at room temperature then cooled to -50^{o}C. NIS (0.482 g, 2.14 mmol) and TMSOTf (25.52 µL, 0.134 mmol) were added slowly, and the resulting reaction mixture was stirred for 60 minute. When TLC (ethyl acetate: toluene, 2/8) indicated formation of product with consumption of starting material, the reaction was quenched by adding Et_3N then filtered through celite. The filtrate was washed with aqueous $NaHCO_3$ (2 x 50 mL), aqueous $Na_2S_2O_3$ (2 x 50 mL), and brine (50 mL) solution. The organic layer was dried over Na_2SO_4 and concentrated in *vacuo*. The residue was purified by flash column chroma-

tography to afford **3-15** (0.970 g, 76%) as clear foam. TLC (ethyl acetate : toluene = 2/8, v/v): R_f =0.49; ^{1}HNMR (600 MHz, $CDCl_3$): δ 7.74-7.35 (m, 8H), 7.40-7.08 (m, 50H), 6.92-6.72 (m, 10H), 6.63-6.53 (m, 4H), 5.31-5.24 (m, 2H), 5.22 (t, *J* = 4.2 Hz, 1H), 5.15 (d, *J* = 8.4 Hz, 1H), 4.94 (d, *J* = 3.2 Hz, 1H), 4.88 (d, *J* = 3.6 Hz, 1H), 4.86 (d, *J* = 3.6 Hz, 1H), 4.80-4.71 (m, 3H), 4.64-4.56 (m, 3H), 4.49-4.44 (m, 10H), 4.39-4.10 (m, 14H), 4.15-4.05 (m, 2H), 4.03 (t, *J* = 8.4 Hz, 1H), 3.98-3.86 (m, 3H), 3.79-3.72 (m, 1H), 3.69 (s, 3H), 3.58-3.56 (m, 1H), 3.49-3.25 (m, 13H), 3.08 (d, *J* = 8.4 Hz, 1H), 3.05 (d, *J* = 8.9 Hz, 1H), 2.90 (bs, 1H), 1.93 (s, 3H), 1.92 (s, 3H); ^{13}CNMR (150 MHz, $CDCl_3$): δ 169.5, 169.4, 168.3, 167.8, 154.8, 150.3, 139.2, 139.1, 139.0, 138.9, 138.8, 138.5, 138.3, 138.2, 138.0, 134.0, 133.6, 132.1, 131.9, 131.7, 129.2, 128.6, 128.5, 128.3, 128.2, 128.1, 128.0, 127.9, 127.9, 127.8, 127.7, 127.6, 127.5, 127.4, 127.4, 127.3, 127.1, 127.0, 126.8, 123.5, 123.4, 123.3, 118.1, 114.4, 108.9, 100.9, 100.7, 100.4, 98.5, 97.6, 97.1, 80.5, 50.5, 79.7, 77.9, 77.8, 77.7, 77.4, 77.2, 75.4, 74.9, 74.6, 74.5, 73.7, 73.6, 73.6, 73.4, 73.3, 73.0, 72.8, 72.7, 72.2, 71.9, 71.8, 71.7, 71.2, 69.2, 68.5, 68.3, 68.2, 67.6, 67.3, 56.4, 55.9, 55.7, 21.3, 21.2, 21.2; ESI-MS: *m/z* calcd for $C_{141}H_{140}N_2O_{31}Na$ 2380.9366; found 2380.9114 $(M + Na)^+$.

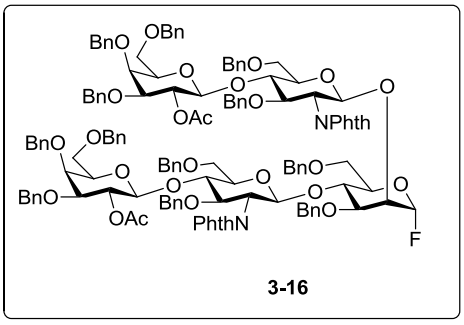

3-16

2-O-acetyl-3,4,6-O-tri-benzyl-β-D-galactopyranosyl-(1→4)-O-3,6-O-di-benzyl-2-deoxy-2-phthalimido-β-D-glucopyranosyl-(1→2)-[2-O-acetyl-3,4,6-O-tri-benzyl-β-D-galactopyran-osyl-(1→4)-O-3,6-O-di-benzyl-2-deoxy-2-phthalimido-β-D-glucopyranosyl-(1→4)]- 3,6-O-di-benzyl-α-D-mannopyranosyl fluoride (3-16): Cerium ammonium nitrate (0.5220 gm, 0.954 mmol) was added to a solution of pentasaccharide **3-15** (0.750 g, 0.318 mmol) in 10 mL of acetonitrile : toluene : H_2O (4 : 2 : 1). The resulting reaction mixture was stirred at 0 °C for 2 h. The reaction was diluted with EtOAc (100 mL) and washed with H_2O (30 x 2 mL) and brine (30 mL). The organic layer was dried over Na_2SO_4 and concentrated in *vacuo*. The product was purified by flash column chromatog-

raphy to afford 1-**OH** compound (0.480 g, 67%) as clear foam. The residue (0.360 g, 0.159 mmol) was dissolved in CH_2Cl_2 (10 mL) at -30 ^oC. Then, DAST (42 μL, 0.318 mmol) was added slowly, and the resulting reaction mixture was stirred for 2 h. When TLC (ethyl acetate: toluene, 2/8) indicated formation of product with consumption of starting material, the reaction was quenched with aq. $NaHCO_3$. The filtrate was washed with aqueous $NaHCO_3$ (2 x 50 mL) and brine (50 mL) solution. The organic layer was dried over Na_2SO_4 and concentrated in *vacuo*. The residue was purified by silica gel column chromatography to afford **3-16** (0.255 g, 69%) as white foam. TLC (ethyl acetate : toluene =2/8, v/v): R_f = 0.54; ^1H NMR (600 MHz, $CDCl_3$): δ 7.68 (m, 8H), 7.38-7.10 (m, 50H), 6.90-6.73 (m, 10H), 5.30-5.25 (m, 2H), 5.24 (t, *J* = 8.9 Hz, 1H), 5.13 (d, *J* = 7.8 Hz, 1H), 4.86 (dd, *J* = 8.5, 2.8 Hz, 2H), 4.78 (d, *J* = 4.8 Hz, 1H), 4.77 (d, *J* = 6.0 Hz, 1H), 4.64-4.56 (m, 3H), 4.53-4.43 (m,10H), 4.33-4.27 (m, 6H), 4.23-4.07 (m, 6H), 4.03 (t, *J* = 8.4 Hz, 1H), 3.95-3.86 (m, 4H), 3.82-3.76 (m, 4H), 3.16-3.61 (m, 2H), 3.53-3.51 (m, 1H), 3.48-3.47 (m, 1H), 3.43-3.21 (m, 10H), 3.06 (dt, J = 3.1 Hz, *J* = 7.8 Hz, 2H), 2.97-3.94 (m, 1H), 1.93 (s, 3H), 1.92 (s, 3H); $^{13}CNMR$ (150 MHz, $CDCl_3$) : δ 169.4, 169.3, 168.2, 167.9, 167.4, 139.0, 138.9, 138.9, 138.4, 138.3, 138.2, 138.1, 138.0, 133.7, 131.9, 131.7, 131.5, 128.6, 128.4, 128.3, 128.2, 128.2, 128.1, 128.0, 127.9, 127.8, 127.8, 127.6, 127.5, 127.3, 127.2, 127.1, 126.9, 126.8, 125.5, 123.3, 100.8, 100.7, 98.8, 97.2, 80.5, 80.5, 77.4, 77.2, 77.0, 74.9, 74.7, 74.6, 74.5, 73.6, 73.4, 73.3, 73.0, 72.8, 72.6, 72.0, 71.8, 71.4, 68.5, 68.3, 68.2, 68.1, 67.2, 56.3, 55.7, 31.1, 21.6, 21.3, 21.2; ESI-MS: *m/z* calcd for $C_{134}H_{133}FN_2O_{29}Na$ 2276.8904; found 2276.8561 $(M + Na)^+$.

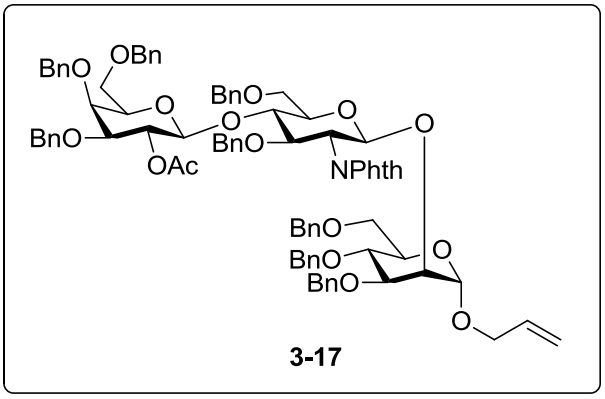

3-17

Allyl-O-2-O-acetyl-3,4,6-O-tri-benzyl-β-D-galactopyranosyl-(1→4)-O-3,6-O-di-benzyl-2-deoxy-2-phthalimido-β-D-glucopyranosyl-(1→2)-O-3,4,6-tri-O-benzyl-α-D-

mannopyrano-side (3-17): Activated 4Å molecular sieves (1 gm) was added to a solution of acceptor **3-12** (0.500 g, 1.02 mmol) and donor **3-09** (1.15 g, 1.22 mmol) in anhydrous CH_2Cl_2 (10 mL). The reaction mixture was stirred for 1 h at room temperature. The reaction was cooled to -50^oC; then, NIS (0.275 g, 1.22 mmol) and TMSOTf (37.18 µL, 0.244 mmol) were added slowly. The resulting reaction mixture was stirred for 2 h. When TLC (ethyl acetate : toluene, 2/8) indicated formation of product with consumption of starting material, the reaction was quenched by adding Et_3N and filtered through celite. Filtrate was washed with aqueous $NaHCO_3$ (2 x 50 mL), aqueous $Na_2S_2O_3$ (2 x 50 mL), and brine (50 mL) solution. The organic layer was dried over Na_2SO_4 and concentrated in *vacuo*. The residue was purified by flash column chromatography to afford **3-17** (1.05 g, 72%) as clear foam. TLC (ethyl acetate : toluene =2/8, v/v): R_f =0.41; NMR (600 MHz, $CDCl_3$): δ 7.63-7.53 (m, 4H), 7.35-7.17 (m, 27H), 7.18-7.09 (m, 5H), 6.95-6.94 (m, 3H), 6.83-6.79 (m, 5H), 5.75-5.72 (m, 1H), 5.36-5.33 (t, *J* = 10.5 Hz, 1H), 5.22 (d, *J* = 7.8 Hz, 1H), 5.10-5.07 (m, 2H), 4.90 (d, *J* = 12.2 Hz, 1H), 4.83-4.74 (m, 3H), 4.65 (d, *J* = 4.8 Hz, 1H), 4.63 (d, *J* = 4.2 Hz, 1H), 5.55 (d, *J* = 1.8 Hz, 1H), 4.51-4.49 (m, 2H), 4.46-4.43 (m, 3H), 4.28-4.26 (m, 3H), 4.10-4.06 (m, 2H), 4.06 (s, 1H), 4.00-3.99 (m, 1H), 3.94 (q, *J* = 3.2, 6.1Hz, 1H), 3.91 (d, *J* = 3.1 Hz, 1H), 3.81 (dd, *J* = 3.6 Hz, *J* = 9 Hz, 1H), 3.76-3.72 (m, 3H), 3.58-3.52 (m, 5H), 3.37 (dd, *J* = 3.3 Hz, *J* = 10.2 Hz, 1H), 2.98-2.90 (m, 1H), 1.98 (s, 3H); ^{13}C NMR (150 MHz, $CDCl_3$): δ 169.5, 162.7, 139.0, 138.9, 138.7, 138.6, 138.3, 138.2, 138.1, 133.8, 133.7, 132.0, 128.6, 128.6, 128.6, 128.4, 128.4, 128.3, 128.2, 128.1, 128.0, 127.9, 127.9, 127.9, 127.6, 127.5, 127.5, 127.0, 123.3, 117.5, 101.0, 97.1, 96.4, 80.5, 78.2, 78.0, 77.1, 75.4, 75.0, 74.9, 74.7, 74.6, 73.8, 73.7, 73.6, 73.5, 73.0, 72.8, 72.2, 71.9, 71.9, 70.8, 68.8, 68.3, 68.1, 55.8, 46.4, 36.7, 31.6, 21.2; ESI-MS: *m/z* calcd for $C_{87}H_{89}NO_{18}Na$ 1458.5972; found 1458.6012 $(M + Na)^+$.

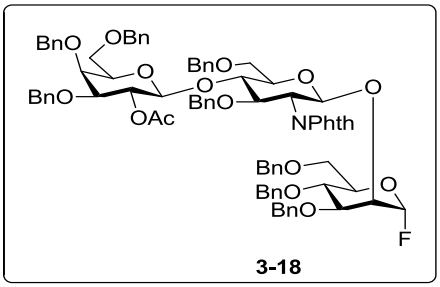

3-18

2-O-acetyl-3,4,6-O-tri-benzyl-β-D-galactopyranosyl-(1→4)-O-3,6-O-di-benzyl-2-deoxy-2-phthalimido-β-D-glucopyranosyl-(1→2)-O-3,4,6-tri-O-benzyl-α-D-mannopyranosyl fluori-de (3-18): $PdCl_2$ (0.020 g) was added to a solution of **3-17** (0.550 g, 0.383 mmol) in 10 mL of CH_2Cl_2 : MeOH (1 : 1). The reaction mixture was stirred at room temperature for 2 h until TLC (ethyl acetate : toluene, 2/8) indicated formation of product with consumption of the starting material. Reaction mixture was then filtered through celite and concentrated in *vacuo*. The residue was purified by flash column chromatography to afford 1-OH compound (0.480 g, 89%) as white color foam. The residue (0.850 g, 0.608 mmol) was dissolved in CH_2Cl_2 (10 mL) at -30 ^oC; then DAST (160 μL, 1.21 mmol) was added slowly. And the resulting reaction mixture was stirred for 1 h. When TLC (ethyl acetate: toluene, 2/8) indicated formation of product with consumption of starting material, the reaction was quenched with aq. $NaHCO_3$. The filtrate was washed with aqueous $NaHCO_3$ (2 x 50 mL) and brine (50 mL) solution. The organic layer was dried over Na_2SO_4 and concentrated in *vacuo*. The residue was purified by silica gel column chromatography to afford **3-18** (0.650 g, 76%) as white foam. TLC (ethyl acetate : toluene = 2/8, v/v): R_f = 0.64; ^1H NMR (600 MHz, $CDCl_3$): δ 7.60-7.48 (m, 4H), 7.38-7.12 (m, 31H), 7.10-7.03 (m, 4H), 6.94-6.96 (m, 2H), 6.85-6.75 (m, 3H), 5.35 (t, *J* = 7.8 Hz, 1H), 5.32 (d, *J* = 51 Hz, 1H), 5.26 (d, *J* = 8.4 Hz, 1H), 4.89 (d, *J* = 11.4 Hz, 1H), 4.82-4.72 (m, 3H), 4.65-4.61 (m, 2H), 4.50-4.42 (m, 5H), 4.37-4.31 (m, 3H), 4.29-4.26 (m, 2H), 4.25-4.16 (m, 2H), 4.09 (d, *J* = 12 Hz, 1H), 4.02-3.98 (d, *J* = 3 Hz, 1H), 3.78-3.74 (m, 3H), 3.67-3.65 (m, 1H), 3.48-3.33 (m, 5H), 3.05-3.03 (m, 1H); ^{13}C NMR (150 MHz, $CDCl_3$) : δ 169.5, 168.7, 167.6, 138.9, 138.9, 138.3, 138.2, 138.1, 131.8, 129.30, 128.7, 128.6, 128.5, 128.3, 128.1, 128.0, 127.9, 127.8, 127.8, 127.6, 127.5, 127.0, 123.5, 123.3, 106.4, 105.0, 101.0, 97.4, 80.5, 78.1, 77.2, 76.8, 75.5, 75.0, 74.8, 74.6, 74.0, 73.8, 73.5, 72.3, 72.2, 71.9, 71.1, 69.2, 68.8, 68.4, 55.7, 21.3; ESI-MS: *m/z* calcd for $C_{84}H_{84}FNO_{17}Na$ 1420.5615; found 1420.5616 $(M + Na)^+$.

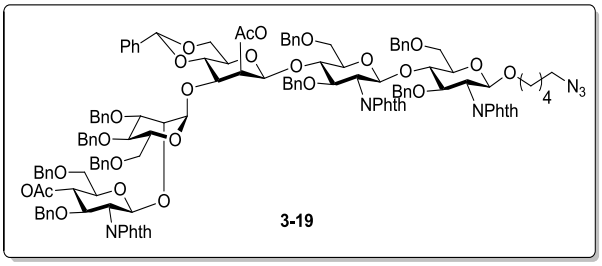

5-Azidopentyl-O-2-O-acetyl-3,6-O-di-benzyl-2-deoxy-2-phthalimido-β-D-gluco-pyranosyl-(1→2)-O-(3,4,6-tri-O-benzyl-α-D-mannopyranosyl-(1→3)-2-O-acetyl-4,6-O-benzylidine-β-D-mannopyranosyl-(1→4)-O-(3,6-di-O-benzyl-2-deoxy-2-phthalimido-β-D-glucopyranosyl) -(1→4)-O-3,6-di-O-benzyl-2-deoxy-2-phthalimido-β-D-glucopyranoside (3-19): A mixture of trichloroacetimidate donor **3-5** (0.341 g, 0.308 mmol), acceptor **2-10** (0.350 g, 0.256 mmol) and activated 4 Å molecular sieves in dry CH_2Cl_2 (10 mL) was stirred at room temperature for 1 h. The reaction was cooled to -40^oC, boron trifluoride ethyl etherate (14.8 µL, 0.129 mmol) was then added slowly and resulting reaction mixture was stirred for 2 h. The reaction was quenched by adding Et_3N, diluted with CH_2Cl_2, filtered through celite and concentrated in *vacuo*. The residue was purified by flash column chromatography to afford **3-19** (0.360 g, 63%) as white foam. TLC: (ethyl acetate : toluene = 2/8, v/v) : R_f = 0.56; ^{1}HNMR (600 MHz, $CDCl_3$) : δ 7.84-7.55 (m, 12H), 7.45-7.10 (m, 28H), 7.06-6.90 (m, 18H), 6.75-6.71 (m, 4H), 5.37 (d, *J* = 8.4 Hz, 1H), 5.21 (d, *J* = 8.4 Hz, 1H), 5.19 (s, 1H), 5.09 (t, *J* = 9.0 Hz, 1H), 4.93-4.76 (m, 6H), 4.57 (s, 1H), 4.54 (d, *J* = 12 Hz, 1H), 4.45-4.07 (m, 20H), 3.69-3.15 (m, 22H), 3.02-3.00 (m, 1H), 2.86-2.81 (m, 2H), 2.25 (s, 3H), 1.84 (s, 3H), 1.35-1.23 (m, 4H), 1.07-1.02 (m, 2H); ^{13}CNMR (150 MHz, $CDCl_3$) : δ 170.68, 170.05, 167.88, 138.98, 138.89, 138.85, 138.71, 138.63, 138.14, 138.07, 137.78, 134.08, 133.90, 133.46, 132.06, 131.81, 129.32, 128.90, 128.83, 128.67, 128.55, 128.50, 128.34, 128.27, 127.95, 127.79, 127.70, 127.60, 101.00, 99.41, 98.38, 97.91, 97.29, 80.38, 79.02, 76.82, 76.76, 76.52, 76.14, 75.25, 74.90, 74.83, 74.67, 74.51, 74.44, 73.68, 73.52, 73.38, 73.06, 73.02, 72.93, 71.46, 70.65, 70.40, 70.03, 69.66, 69.14, 68.52, 67.56, 56.83, 55.98, 55.85, 51.37, 29.99, 28.95, 28.55, 23.28, 21.67, 21.19; ESI-MS: *m/z* calcd for $C_{133}H_{132}N_6O_{31}Na$: 2332.8862; found 2332.8861 $(M+Na)^+$.

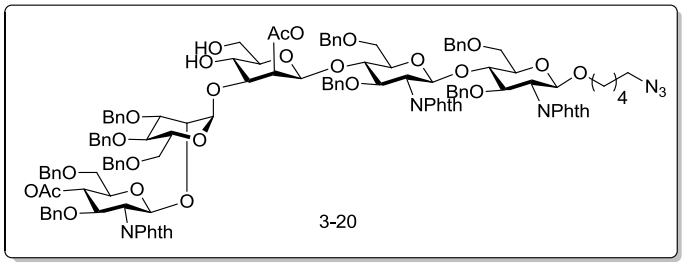

5-Azidopentyl-O-2-O-acetyl-3,6-O-di-benzyl-2-deoxy-2-phthalimido-β-D-gluco-pyranosyl-(1→2)-O-(3,4,6-tri-O-benzyl-α-D-mannopyranosyl-(1→3)-2-O-acetyl-β-D-mannopyranosyl-(1→4)-O-(3,6-di-O-benzyl-2-deoxy-2-phthalimido-β-D-glucopyranosyl)-(1→4)-O-3,6-di-O-benzyl-2-deoxy-2-phthalimido-β-D-glucopyranoside (3-20) : *p*-Toluene sulfonic acid monohydrate (0.020 g, 0.143 mmol) was added to a solution of **3-19** (0.220 g, 0.095 mmol) in acetonitrile (20 mL) and resulting reaction mixture was stirred at room temperature for 5 h. Reaction was quenched by adding Et_3N and concentrated in *vacuo*. The residue was purified by flash column chromatography to give diol **3-20** (0.165 g, 78%). TLC: (ethyl acetate : toluene =2/8, v/v) : R_f = 0.32; ^{1}HNMR (600 MHz, $CDCl_3$) : δ 7.89-7.43 (m, 12H), 7.35-7.16 (m, 28H), 7.09-7.05 (m, 5H), 7.03-6.89 (m, 9H), 6.75-6.72 (m, 3H), 5.30 (d, *J* = 8.4 Hz, 1H), 5.23 (d, *J* = 8.4 Hz, 1H), 5.12 (d, *J* = 9.00 Hz, 1H), 5.09 (t, *J* = 9.8 Hz, 1H), 4.95 (d, *J* = 12 Hz, 1H), 4.90 (d, *J* = 8.4 Hz, 1H), 4.87-4.80 (m, 2H), 4.58-4.55 (m, 2H), 4.50-4.41 (m, 10H), 4.37-4.34 (m, 3H), 4.27-4.24 (m, 2H), 4.18-4.15 (m, 2H), 4.10-3.92 (m, 5H), 3.73-3.70 (m, 2H), 3.65-3.61 (m, 2H), 3.59-3.51 (m, 5H), 3.47-3.38 (m, 6H), 3.23-3.17 (m, 4H), 3.04 (dd, *J* = 3.6, 9 Hz, 1H), 3.01-3.98 (m, 1H), 2.83-2.78 (m, 3H), 2.38 (s, 3H), 1.90 (s, 3H), 1.36-1.22 (m, 4H), 1.06-1.01 (m, 2H) ; ^{13}CNMR (150 MHz, $CDCl_3$) : δ 170.93, 170.05, 168.77, 167.86, 167.69, 138.90, 138.83, 138.65, 138.47, 138.23, 138.14, 138.07, 138.04, 134.35, 134.13, 133.91, 132.04, 131.84, 131.72, 128.81, 128.65, 128.64, 128.62, 128.54, 128.53, 128.48, 128.46, 128.36, 128.17, 128.09, 128.02, 127.99, 127.97, 127.92, 127.91, 127.83, 127.77, 127.74, 127.63, 127.13, 124.73, 123.97, 123.43, 123.08, 118.73, 100.25, 98.37, 98.21, 97.86, 97.30, 82.86, 80.05, 78.38, 76.92, 76.15, 75.72, 75.60, 75.45, 74.86, 74.83, 74.70, 74.42, 74.24, 73.75, 73.42, 73.38, 72.82, 70.81, 70.60, 70.27, 69.99, 69.50, 69.15, 69.13, 68.53, 67.88, 66.28, 62.98, 56.78, 55.99, 55.88, 51.37, 32.21, 29.98, 28.94, 28.54, 23.27, 21.69, 21.18; ESI-MS: *m/z* calcd for $C_{126}H_{128}N_6O_{31}Na$: 2244.8549; found 2244.8529 $(M+Na)^+$.

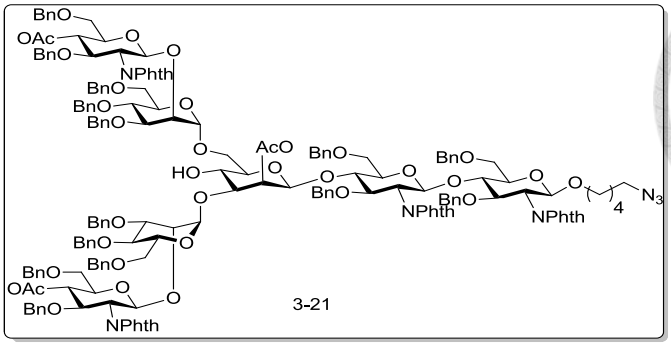

5-Azidopentyl-O-di-[{4-O-acetyl-3,6-O-di-benzyl-2-deoxy-2-phthalimido-β-D-gluco-pyra-nosy-(1→2)}-O-{3,4,6-tri-O-benzyl-α-D-mannopyranosyl}]-(1→3),(1→6)-2-O-acetyl-β-D-mannopyranosyl-(1→4)-O-(3,6-di-O-benzyl-2-deoxy-2-phthalimido-β-D-glucopyranosyl)-(1→4)-O-3,6-di-O-benzyl-2-deoxy-2-phthalimido-β-D-glucopyranoside(3-21): A mixture of Silver triflate (0.080 g, 0.315 mmol), Bis(cyclopentadienyl)hafnium dichloride (0.084 g, 0.220 mmol) and 4 Å activated molecular sieves in dry toluene (10 mL) was stirred at room temperature for 1 h. The reaction mixture was then cooled to -40°C, a solution of donor **3-6** (0.091 g, 0.094 mmol) and acceptor **3-20** (0.140 g, 0.063 mmol) in 5 mL toluene was added. The mixture was stirred for 4 h, quenched with Et_3N, diluted with CH_2Cl_2 and filtered through celite. The filtrate was washed with aqueous $NaHCO_3$ (2 x 50 mL), and a brine (50 mL) solution. The organic layer was dried over Na_2SO_4 and concentrated in *vacuo*. The residue was purified by flash column chromatography to afford **3-21** (0.110 g, 58%) as colorless foam. TLC: (acetone : toluene =2/8, v/v) : R_f = 0.39; ^{1}HNMR (600 MHz, $CDCl_3$) : δ 7.62-7.32 (m, 16H), 7.27-6.87 (m, 41H), 6.85-6.59 (m, 29H), 5.27 (d, *J* = 8.4 Hz, 1H), 5.16 (s, 1H), 5.14 (d, *J* = 3.6 Hz, 1H), 5.10 (d, *J* = 1.8 Hz, 1H), 4.98 (d, *J* = 3.6 Hz, 1H), 4.89-4.68 (m, 10H), 4.59-4.21 (m, 21H), 4.19-3.87 (m, 7H), 3.80 (dd, *J* = 3.2, 1.8Hz, 1H), 3.70-3.52 (m, 7H), 3.51-3.28 (m, 8H), 3.27-3.18 (m, 5H), 3.15-3.03 (m, 3H), 3.01 (dd, *J* = 3.2, 1.8 Hz, 1H), 2.91-2.75 (m, 5H), 2.73-2.69 (m, 1H), 2.27 (s, 3H), 1.98 (s, 3H), 1.86 (s, 3H), 1.32-1.23 (m, 4H), 1.03-0.99 (m, 2H); ^{13}CNMR (150 MHz, $CDCl_3$) : δ 171.09, 171.04, 170094, 167.91, 167.57, 139.19, 138.86, 138.63, 138.54, 138.42, 138.31, 138.21, 138.14, 137.93, 133.84, 133.71, 132.04, 131.80, 131.69, 128.80, 128.64, 128.39, 128.32, 128.13, 128.08, 127.79, 127.70, 127.60, 100.18, 100.00, 98.36, 97.88, 97.61, 97.30, 97.22, 80.14, 79.97, 79.31, 75.85, 75.56, 75.39, 75.30, 75.04, 74.71, 74.59, 73.95, 73.64, 73.24, 72.86, 72.14, 71.55,

71.37, 71.04, 70.53, 70.40, 70.15, 69.71, 69.12, 68.12, 65.40, 63.29, 56.34, 55.92, 51.45, 51.37, 51.27, 28.95, 28.54, 23.26, 21.13, 21.02; HRMS (MALDI-TOF) : *m/z* calcd for $C_{183}H_{183}N_7O_{43}Na$; 3191.2306 found 3191.2375 $(M+Na)^+$.

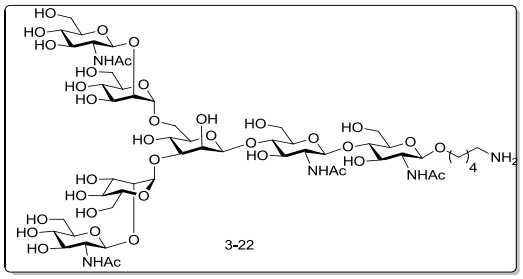

5-Aminopentyl-di-[2-acetamido-2-deoxy-β-D-glucopyranosyl-(1→2)-α-D-manno-pyranosyl]-(1→3),(1→6)-β-D-mannopyranosyl-(1→4)-2-acetamido-2-deoxy-β-D-gluco-pyranosyl-(1→4)-2-acetamido-2-deoxy-β-D-glucopyranoside (3-22): Compound **3-21** (0.130 g, 0.041 mmol) was deprotected by following general procedure 1 to get desired heptasaccharide **3-22** (0.015 g, 29%) as a white solid. ^{1}HNMR (600 MHz, D_2O) : δ 5.99 (d, *J* = 8.5 Hz, 1H), 4.93 (s, 3H), 4.83 (s, 1H), 4.76 (s, 1H), 4.60 (d, *J* = 7.8 Hz, 1H), 4.56 (d, *J* = 7.9 Hz, 1H), 4.49 (d, *J* = 7.9 Hz, 1H), 4.27 (s, 2H), 4.11 (d, *J* = 1.8 Hz, 1H), 3.96-3.41 (m, 41H), 2.98 (t, *J* = 8.9 Hz, 2H), 2.13 (s, 3H), 2.09 (s, 3H), 2.06 (s, 3H), 2.01 (s, 3H), 1.69-1.64 (m, 2H), 1.60-1.57 (m, 2H), 1.42-1.38 (m, 2H); ^{13}CNMR (150 MHz, D_2O) : δ 174.88, 174.78, 174.65, 174.42, 171.0, 101.39, 101.05, 100.61, 100.39, 99.55, 97.60, 97.20, 79.41, 79.28, 78.92, 76.63, 76.25, 75.79, 74.50, 73.64, 72.84, 71.95, 70.09, 69.89, 69.48, 67.39, 67.35, 66.20, 65.39, 61.66, 61.61, 60.75, 60.61, 59.96, 55.68, 54.98, 54.94, 39.30, 28.04, 26.35, 22.55, 22.31, 22.21, 22.12, 22.08; ESI-MS: *m/z* calcd for $C_{55}H_{95}N_5O_{36}$; 1402.5830 ; found 1403.5862 $(M+H)^+$ **.**

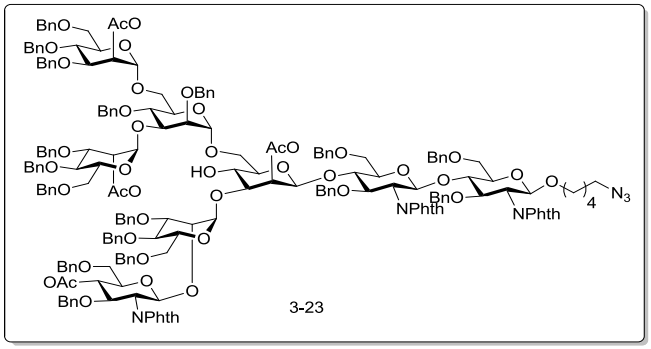

5-Azidopentyl-O-{4-O-acetyl-3,6-O-di-benzyl-2-deoxy-2-phthalimido-β-D-gluco-pyranosyl -(1→2)}-O-{3,4,6-tri-O-benzyl-α-D-mannopyranosyl-(1→3)-{2-O-acetyl-3,4,6-tri-O-benzyl-α-D-mannopyranosyl-(1→3)}-[2-O-acetyl-3,4,6-tri-O-benzyl-α-D-manno-pyranosyl-(1→6)] -2,4-di-O-benzyl-α-D-mannopyranosyl-(1→6)}-2-O-acetyl-β-D-manno-pyranosyl-(1→4)-O -(3,6-di-O-benzyl-2-deoxy-2-phthalimido-β-D-glucopyranosyl)-(1→4)-O-3,6-di-O-benzyl-2 -deoxy-2-phthalimido-β-D-glucopyranoside (3-23): A mixture of pentasaccharide acceptor **3-20** (0.150 g, 0.067 mmol), thiomannoside donor **2-18** (0.110 g, 0.080 mmol) and activated 4Å molecular sieves (0.500 g) in CH_3CN (10mL) was stirred at room temperature for 1h. The resulting mixture was cooled to -10°C , tris(4-bromophenyl) aminium hexachloroantimonate (0.170 g, 0.201 mmol) was added and resulting reaction was stirred at room temperature for 4 h. TLC (ethyl acetate: toluene, 2/8) indicated formation of product with consumption of starting material, reaction was quenched by Et_3N. The reaction mixture was diluted with CH_2Cl_2 and filtered through celite. The filtrate was washed with aqueous $NaHCO_3$ (2 x 50 mL), and a brine (50 mL) solution. The organic layer was dried over Na_2SO_4 and concentrated in *vacuo*. The residue was purified by flash column chromatography to afford **3-23** (0.130 gm, 55%) as colorless foam. TLC: (ethyl acetate : toluene =1/9, v/v) : R_f = 0.42; ^{1}HNMR (600 MHz, $CDCl_3$) : δ 7.71-7.30 (m, 8H), 7.28-7.10 (m, 70H), 7.97-6.86 (m, 12H), 6.69 (m, 7H), 5.47 (t, *J* = 2.4 Hz, 1H), 5.44 (s, 1H), 5.32 (d, *J* = 8.4 Hz, 1H), 5.15 (d, *J* = 8.4 Hz, 1H), 5.13-5.10 (m, 2H), 5.00 (s, 1H), 4.95 (s, 1H), 4.91 (s, 1H), 4.87-4.73 (m, 8H), 4.62 (d, *J* = 8.7 Hz, 1H), 4.57-4.28 (m, 26H), 4.15-3.70 (m, 20H), 3.68-3.40 (m, 15H), 3.38-3.25 (m, 6H), 3.24-3.09 (m, 5H), 2.98 (dd, *J* = 2.3, 7.8Hz, 1H), 2.89-2.79 (m, 2H), 2.73-2.71 (m, 1H), 2.27 (s, 3H), 2.05 (s, 3H), 1.99 (s, 3H), 1.88 (s, 3H), 1.32-1.28 (m, 4H), 1.07-0.98 (m, 2H); ^{13}CNMR (150 MHz, $CDCl_3$) : δ 170.26, 168.89, 138.38, 128.47, 128.37, 128.32, 128.30, 128.26, 128.24, 128.19, 128.08, 128.04, 127.91, 127.86, 127.73, 127.56, 127.49, 127.39, 127.26, 100.35, 100.23, 99.89, 99.56, 99.23, 98.54, 98.33, 98.23, 78.43, 76.09, 75.37, 75.07, 74.08, 74.44, 74.04, 73.47, 73.31, 72.63, 68.81, 51.08, 29.71, 29.37, 28.66, 28.25, 22.98; HRMS (MALDI-TOF) : *m/z* calcd for $C_{204}H_{210}N_6O_{48}Na$; 3536.4134 found 3536.4050 $(M+Na)^+$.

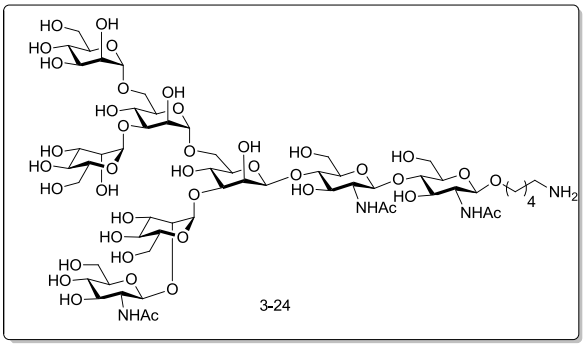

5-Aminopentyl-2-acetamido-2-deoxy-β-D-glucopyranosyl-(1→2)-α-D-mannopyranosyl -(1→3),[di-(α-D-mannopyranosyl)-(1→3),(1→6)-α-D-mannopyranosyl](1→6)-β-D-mannopy-ranosyl-(1→4)-2-acetamido-2-deoxy-β-D-glucopyranosyl-(1→4)-2-acetamido-2-deoxy-β-D-glucopyranoside (3-24) : Compound **3-23** (0.105 g, 0.030 mmole) was deprotected by following general procedure 1 to get title compound **3-24** (0.012 g, 26%) as a white solid. ^{1}H NMR (600 MHz, D_2O) : δ 5.09 (d, *J* = 1.2 Hz, 1H), 5.02 (d, *J* = 8.4 Hz, 1H), 4.93 (d, *J* = 7.8 Hz, 1H), 4.91 (d, *J* = 1.2 Hz, 1H), 4.85 (s, 1H), 4.61 (t, *J* = 7.8 Hz, 1H), 4.51 (d, *J* = 7.8 Hz, 1H), 4.22 (t, *J* = 10.2 Hz, 2H), 4.18 (dd, *J* = 1.8, 3.0Hz, 1H), 4.10 (dd, *J* = 1.8, 3.1 Hz, 1H), 4.08-3.38 (m, 47H), 3.03 (t, *J* = 8.2 Hz, 2H), 2.09 (s, 3H), 2.08 (s, 3H), 2.01 (s, 3H), 1.71-1.66 (m, 2H), 1.62-1.59 (m, 2H), 1.44-1.40 (m, 2H); ^{13}C NMR (150 MHz, D_2O) : δ 174.91, 174.42, 171.02, 110.64, 102.32, 101.48, 100.51, 100.44, 100.15, 99.26, 97.58, 79.48, 78.86, 78.72, 76.64, 76.04, 75.72, 74.65, 74.51, 74.42, 73.31, 72.69, 72.35, 72.09, 71.96, 70.86, 70.57, 70.34, 70.12, 70.09, 69.94, 69.42, 67.39, 66.70, 66.36, 65.54, 65.14, 61.68, 61.02, 60.93, 39.31, 38.62, 28,03, 26.39, 22.58, 22.20, 22.11, 22.08, 21.82; ESI-MS: *m/z* calcd for $C_{59}H_{102}N_4O_{41}$; 1522.6092 found 1523.6148 $(M+H)^+$.

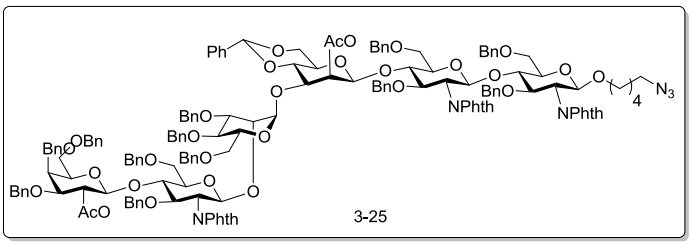

5-Azidopentyl-O-2-O-acetyl-3,4,6-O-tri-benzyl-β-D-galactopyranosyl-(1→4)-O-3,6-O-dibe-nzyl-2-deoxy-2-phthalimido-β-D-glucopyranosyl-(1→2)-O-(3,4,6-tri-O-benzyl-α-D-manno-pyranosyl-(1→3)-2-O-acetyl-4,6-O-benzylidine-β-D-mannopyranosyl-

(1→4)-O-(3,6-di-O –benzyl-2-deoxy-2-phthalimido-β-D-glucopyranosyl)-(1→4)-O-3,6-di-O-benzyl-2-deoxy-2-phthalimido-β-D-glucopyranoside (3-25): A mixture of silver triflate (0.327 g, 1.28 mmol), bis (cyclopentadienyl) hafnium dichloride (0.339 g, 0.896 mmol) and 4Å activated molecular sieves in dry toluene (10 mL) was stirred at room temperature for 1 h. The reaction mixture was then cooled to -40°C, a solution of donor **3-18** (0.430 g, 0.307 mmol) and acceptor chitobiose trisaccharide **2-10** (0.350 g, 0.256 mmol) in 5mL toluene was added. The mixture was stirred for 2 h, quenched with Et_3N, diluted with EtOAc and filtered through celite. The filtrate was washed with aqueous $NaHCO_3$ (2 x 50 mL), and a brine (50 mL) solution. The organic layer was dried over Na_2SO_4 and concentrated in *vacuo*. The residue was purified by flash column chromatography to afford **3-25** (0.500 g, 71%) as white foam. TLC: (ethyl acetate : toluene =2/8, v/v) : R_f = 0.62; ^{1}H NMR (600MHz, $CDCl_3$) : δ 7.85-7.49 (m, 8H), 7.02-7.39 (m, 44H), 7.19-7.02 (m, 11H), 6.99-6.90 (m, 6H), 6.83-6.78 (m, 3H), 6.75-6.70 (m, 5H), 5.310 (t, 1H), 5.27 (dd, *J* = 2.2, 3.1Hz, 1H), 5.25 (d, *J* = 8.4 Hz, 1H), 5.15 (d, *J* = 2.3 Hz, 1H), 5.01 (s, 1H), 4.90-4.80 (m, 7H), 4.62 (d, *J* = 8.5 Hz, 1H), 4.58-4.53 (m, 3H), 4.52-4.38 (m, 10H), 4.32-4.13 (m, 11H), 4.12-4.05 (m, 5H), 4.02 (m, 1H), 3.89 (d, *J* = 3.2 Hz, 1H), 3.75-3.73 (m, 2H), 3.72-3.49 (m, 8H), 3.48-3.37 (m, 5H), 3.34-3.29 (m, 4H), 3.29-3.18 (m, 4H), 2.98 (m, 1H), 2.89-2.79 (m, 2H), 2.29 (s, 3H), 1.99 (s, 3H), 1.49-1.30 (m, 4H), 1.10-1.00 (m, 2H); ^{13}C NMR (150 MHz, $CDCl_3$) : δ 170.8, 169.4, 168.7, 167.7, 139.1, 139.9, 138.9, 138.8, 138.8, 138.5, 138.2, 138.2, 138.1, 137.9, 137.6, 134.2, 133.8, 133.1, 131.9, 131.8, 131.6, 129.1, 128.8, 128.6, 128.5, 128.4, 128.4, 128.4, 128.3, 128.3, 128.2, 128.1, 128.0, 128.0, 127.9, 127.8, 127.8, 127.7, 127.7, 127.5, 127.5, 127.4, 127.3, 127.0, 126.7, 126.1, 123.8, 123.3, 122.8, 100.88, 100.83, 99.94, 99.38, 98.43, 98.30, 97.26, 80.31, 79.00, 78.05, 77.61, 76.42, 76.31, 76.1,. 75.1, 74.8, 74.7, 74.6, 74.6, 74.4, 74.4, 74.2, 73.6, 73.4, 73.3, 72.9, 72.8, 72.2, 71.8, 71.7, 70.4, 70.0, 69.8, 69.0, 68.8, 68.4, 68.2, 67.7, 67.6, 56.7 56.0, 55.9, 51.3, 28.8, 28.4, 23.2, 21.7, 21.2; ESI-MS: *m/z* calcd for $C_{160}H_{160}N_6O_{36}Na$; 2765.0799 found 2765.0952 $(M+Na)^+$.

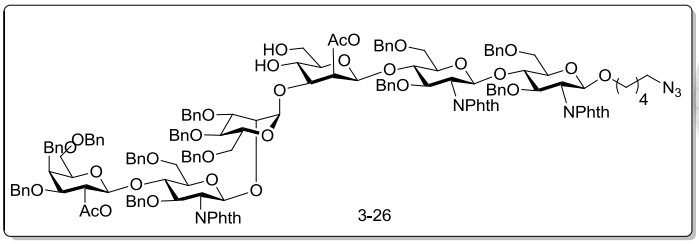

5-Azidopentyl-O-2-O-acetyl-3,4,6-O-tri-benzyl-β-D-galactopyranosyl-(1→4)-O-3,6-O-dibe-nzyl-2-deoxy-2-phthalimido-β-D-glucopyranosyl-(1→2)-O-(3,4,6-tri-O-benzyl-α-D-manno-pyranosyl-(1→3)-2-O-acetyl-β-D-mannopyranosyl-(1→4)-O-(3,6-di-O-benzyl-2-deoxy-2-phthalimido-β-D-glucopyranosyl)-(1→4)-O-3,6-di-O-benzyl-2-deoxy-2-phthalimido-β-D-glucopyranoside (3-26): To a solution of **3-25** (0.601 g, 0.219 mmol) in acetonitrile (10 mL) was added *p*-toluene sulfonic acid monohydrate (0.046 g, 0.328 mmol), stirred at room temperature for 2 h. Reaction was quenched with Et_3N and concentrated in *vacuo*. The residue was purified by flash column chromatography to afford diol **3-26** (0.460 g, 78%). TLC: (acetone : toluene =2/8, v/v) : R_f = 0.32; ^{1}H NMR (600 MHz, $CDCl_3$) : δ 7.91-7.42 (m, 12H), 7.39-7.12 (m, 41H), 7.10-6.93 (m, 13H), 6.85-6.81 (m, 3H), 6.78-6.73 (m, 3H), 5.34-5.31 (t, *J* = 7.8 Hz, 1H), 5.23 (t, *J* = 8.4 Hz, 2H), 5.08 (d, *J* = 6.2 Hz, 1H), 4.97 (d, *J* = 12.2 Hz, 1H), 4.94-4.80 (m, 5H), 4.64-4.60 (m, 2H), 4.49-4.21 (m, 21H), 4.19-4.15 (m, 2H), 4.15-3.89 (m, 8H), 3.89 (d, *J* = 6.2 Hz, 1H), 3.78 (d, *J* = 5.8 Hz, 1H), 3.69 (dd, *J* = 6.3, 12.1 Hz, 1H), 3.65-3.64 (m, 1H), 3.56-3.32 (m, 15H), 3.29 (dd, *J* = 6.6, 12.5 Hz, 1H), 3.29-3.23 (m, 3H), 3.00-2.99 (m, 2H), 2.87-2.82 (m, 2H), 2.74 (t, *J* = 9.5 Hz, 1H), 2.28 (s, 3H), 1.98 (s, 3H), 1.37-1.22 (m, 4H), 1.07-1.00 (m, 2H); ^{13}C NMR (150 MHz, $CDCl_3$) : δ 171.29, 169.57, 168.78, 168.58, 168.03, 167.90, 139.01, 138.92, 138.84, 138.68, 138.45, 138.39, 138.36, 138.22, 138.14, 137.98, 134.35, 134.15, 134.02, 133.89, 132.04, 131.95, 131.68, 130.10, 129.54, 129.46, 128.80, 128.70, 128.66, 128.62, 128.60, 128.52, 128.47, 128.46, 128.39, 128.30, 128.15, 128.07, 128.01, 127.98, 127.94, 127.91, 127.83, 127.72, 127.60, 127.39, 127.20, 126.96, 123.90, 123.46, 122.88, 101.11, 100.87, 98.87, 98.33, 83.75, 80.57, 80.14, 78.58, 78.29, 76.15, 75.78, 75.45, 74.11, 74.96, 74.83, 74.70, 74.61, 74.44, 74.10, 73.77, 73.73, 73.59, 73.43, 73.38, 73.03, 72.30, 71.97, 70.61, 70.29, 69.82, 69.14, 69.08, 68.54, 68.38, 67.94, 66.94, 66.47, 63.21, 56.80, 56.09, 56.01, 51.37, 31.71, 31.21, 30.97, 30.59, 29.99, 29.65, 28.55, 27.87, 27.29, 26.96, 26.24, 25.59, 25.36, 24.26, 23.27, 22.98, 21.86, 21.32, 20.80, 20.49, 18.94, 16.76, 15.95, 15.44,

15.10, 14.40, 14.07, 13.67, 13.47; ESI-MS: *m/z* calcd for $C_{153}H_{156}N_6O_{36}Na$; 1350.0189; found 1350.0207 $(M+Na)^+$.

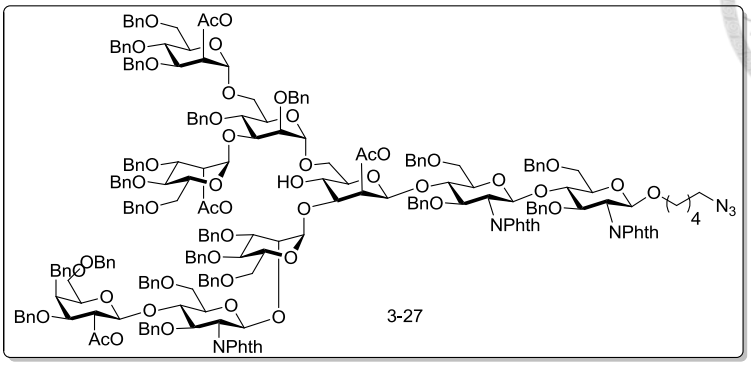

5-Azidopentyl-O-{2-O-acetyl-3,4,6-O-tri-benzyl-β-D-galactopyranosyl-(1→4)}-O-{3,6-O-di -benzyl-2-deoxy-2-phthalimido-β-D-glucopyranosyl-(1→2)}-O-{3,4,6-tri-O-benzyl-α-D-mannopyranosyl-(1→3)-{2-O-acetyl-3,4,6-tri-O-benzyl-α-D-mannopyranosyl-(1→3)}-[2-O-acetyl-3,4,6-tri-O-benzyl-α-D-mannopyranosyl-(1→6)]-2,4-di-O-benzyl-α-D-manno-pyran-osyl-(1→6)}-2-O-acetyl-β-D-mannopyranosyl-(1→4)-O-(3,6-di-O-benzyl-2-deoxy-2-phthal-imido-β-D-glucopyranosyl)-(1→4)-O-3,6-di-O-benzyl-2-deoxy-2-phthalimido-β-D-glucop-yranoside (3-27): A mixture of hexasaccharide acceptor **3-26** (0.400 g, 0.150 mmol), thiomannoside donor **2-18** (0.229 g, 0.226 mmol) and activated 4 Å molecular sieves (0.500 g) in CH_3CN (10 mL) was stirred at room temperature for 1 h. The resulting mixture was cooled to -10°C , tris(4-bromophenyl)aminium hexachloroantimonate (0.254 g, 0.300 mmol) was added and stirred at room temperature for 3 h. TLC indicated formation of product with consumption of starting material, reaction was quenched by Et_3N. The reaction mixture was diluted with CH_2Cl_2 and filtered through celite. The filtrate was washed with aqueous $NaHCO_3$ (2 x 50 mL), and a brine (50 mL) solution. The organic layer was dried over Na_2SO_4 and concentrated in *vacuo*. The residue was purified by flash column chromatography to afford **3-27** (0.335gm, 55%) as colorless foam and acceptor 9 (0.103 g). TLC: (ethyl acetate : toluene =1/9, v/v) : R_f = 0.46; ^1H NMR (600 MHz, $CDCl_3$) : δ 7.72-7.45 (m, 11H), 7.37-7.28 (m, 5H), 7.28-7.12 (m, 67H), 7.09-7.02 (m, 12H), 6.94-6.90 (m, 7H), 6.80-6.78 (m, 4H), 6.69-6.68 (m, 3H), 6.62-6.61 (m, 3H), 5.49 (s, 1H), 5.48 (s, 1H), 5.35 (t, *J* = 8.4 Hz, 1H), 5.28 (d, *J* = 8.4 Hz, 1H), 5.17 (d, *J* = 8.4 Hz, 1H), 5.09 (d, *J* = 6.2 Hz, 1H), 5.00 (s, 1H), 4.92 (d, *J* = 3.1 Hz, 1H), 4.90-4.72 (m, 12H), 4.69-4.72 (m, 23H), 4.26-4.17 (m, 5H), 4.13-3.97 (m,

12H), 3.89-3.82 (m, 12H), 3.72 (t, 1H), 3.68-3.62 (m, 1H), 3.65-3.55 (m, 7H), 3.54-3.45 (m, 4H), 3.43-3.40 (m, 4H), 3.40-3.29 (m, 9H), 3.23-3.19 (m, 3H), 3.17-3.09 (m, 2H), 2.91-2.79 (m, 3H), 2.68 (t, 1H), 2.28 (s, 3H), 2.05 (s, 3H), 2.01 (s, 3H), 1.99 (s, 3H), 1.34-1.22 (m, 4H), 1.06-1.00 (m, 2H); ^{13}C NMR (150 MHz, $CDCl_3$) : δ 171.37, 170.38, 170.29, 169.54, 168.49, 168.23, 167.97, 167.53, 139.28, 139.11, 139.03, 138.97, 138.94, 138.67, 138.63, 138.58, 138.53, 138.41, 138.38, 138.25, 138.10, 128.74, 128.70, 128.67, 128.63, 128.58, 128.55, 128.53, 128.51, 128.48, 128.44, 128.40, 128.37, 128.34, 128.30, 128.15, 128.03, 128.00, 127.95, 127.92, 127.84, 127.77, 127.75, 127.70, 127.64, 127.61, 101.17, 100.92, 98.84, 98.28, 97.71, 97.45, 75.49, 75.36, 75.26, 75.17, 75.06, 74.96, 74.82, 74.75, 74.65, 74.60, 74.38, 74.30, 73.99, 73.77, 73.73, 73.59, 73.25, 73.25, 73.06, 72.99, 72.91, 72.26, 72.18, 71.98, 71.82, 71.57, 71.45, 70.52, 70.03, 69.92, 69.56, 69.10, 68.90, 68.85, 68.57, 68.48, 68.37, 66.64, 66.06, 56.75, 56.09, 55.99, 51.37, 34.25, 29.99, 28.94, 28.54, 25.90, 23.27, 21.86, 21.42, 21.33; HRMS (MALDI-TOF) : *m/z* calcd for $C_{231}H_{238}N_6O_{53}Na$; 3968.6071; found 3968.6006 $(M+Na)^+$.

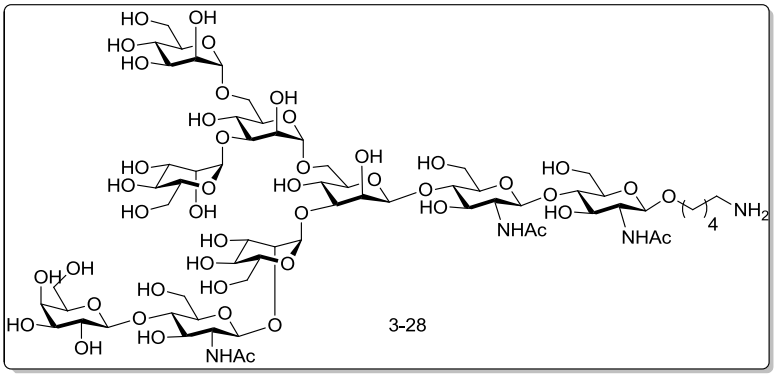

3-28

5-Aminopentyl-β-D-galactopyranosyl-(1→4)-[2-acetamido-2-deoxy-β-D-glucopyranosyl-(1→2)-α-D-mannopyranosyl-(1→3),[di-(α-D-mannopyranosyl)-(1→3),(1→6)-α-D-manno-pyranosyl](1→6)-β-D-mannopyranosyl-(1→4)-2-acetamido-2-deoxy-β-D-glucopyranosyl-(1→4)-2-acetamido-2-deoxy-β-D-glucopyranoside (3-28): Compound **3-27** (0.160 g, 0.048 mmol) was deprotected by following general procedure 1 to afford desired nonasaccharide **3-28** (0.052 g, 62%). ^{1}HNMR (600 MHz, D_2O) : δ 5.10 (s, 1H), 5.07 (d, *J* =9.5Hz, 1H), 4.91 (s, 2H), 4.84 (s,1 H), 4.61-4.60 (m, 1H), 4.50 (d, *J* = 9.2 Hz, 1H), 4.49 (d, *J* = 8.1 Hz, 1H), 4.31 (s, 2H), 4.19 (bs, 1H), 4.07 (bs, 1H), 4.02-3.51 (m, 53H), 3.40-3.40 (m, 2H) 2.99 (t, *J* = 11.2 Hz, 2H), 2.08 (s, 3H), 2.07 (s, 3H), 2.04 (s,

3H), 1.70–1.65 (m, 2H), 1.62-1.58 (m, 2H), 1.48–1.38 (m, 2H); ^{13}CNMR (150 MHz, D_2O) : δ 177.60, 177.17, 105.68, 105.05, 104.23, 104.04, 103.79, 103.37, 103.18, 102.88, 102.23, 102.03, 100.24, 82.20, 82.06, 82.01, 81.58, 81.51, 81.40, 79.38, 78.70, 78.08, 77.43, 77.37, 77.18, 77.03, 76.07, 75.66, 75.43, 75.23, 75.11, 75.06, 74.96, 74.83, 74.71, 73.72, 73.65, 73.33, 73.20, 73.11, 72.95, 72.89, 72.84, 72.69, 72.18, 71.28, 70.15, 68.50, 69.46, 69.36, 69.01, 68.31, 67.90, 67.86, 64.45, 63.75, 63.69, 63.61, 62.87, 62.82, 62.75, 57.94, 57.72, 42.06, 30.78, 29.10, 25.35, 25.30, 24.96, 24.87, 24.83; ESI-MS : *m/z* calcd for $C_{65}H_{112}N_4O_{46}$; 1684.6620 found 1685.6968 $(M+H)^+$.

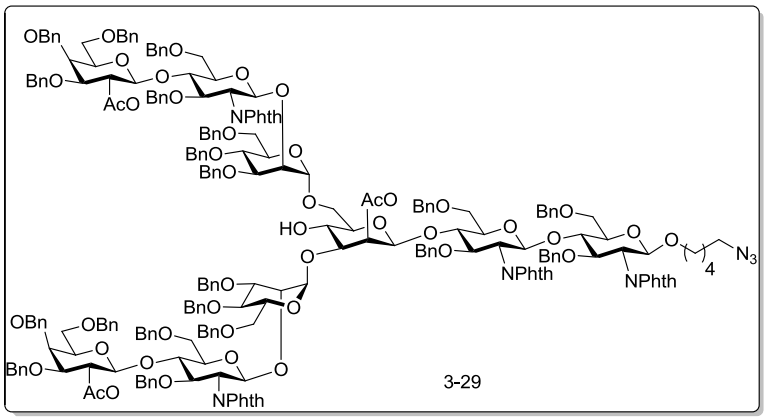

5-Azidopentyl-O-di-[{2-O-acetyl-3,4,6-O-tri-benzyl-β-D-galactopyranosyl-(1→4)}-O-{3,6-O-di-benzyl-2-deoxy-2-phthalimido-β-D-glucopyranosyl-(1→2)}-O-{3,4,6-tri-O-benzyl -α-D-mannopyranosyl]-(1→3),(1→6)-2-O-acetyl-β-D-mannopyranosyl-(1→4)-O-(3,6-di-O-benzyl-2-deoxy-2-phthalimido-β-D-glucopyranosyl)-(1→4)-O-3,6-di-O-benzyl-2-deoxy-2-phthalimido-β-D-glucopyranoside (3-29): A mixture of silver triflate (0.085 g, 0.335 mmol), bis (cyclopentadienyl) hafnium dichloride (0.088 g, 0.234 mmol) and 4Å activated molecular sieves in dry toluene (10 mL) was stirred at room temperature for 1 h. The reaction mixture was then cooled to -40°C, a solution of donor **3-18** (0.123 g , 0.088 mmol) and acceptor **3-26** (0.180 g, 0.067 mmol) in 5 mL toluene was added. The mixture was stirred for 3 h, quenched with Et_3N, diluted with EtOAc and filtered through celite. The filtrate was washed with aqueous $NaHCO_3$ (2 x 50 mL), and a brine (50 mL) solution. The organic layer was dried over Na_2SO_4 and concentrated in *vacuo*. The residue was purified by flash column chromatography to afford **3-29** (0.190 g, 69%) as colorless foam. TLC: (acetone : toluene =1/9, v/v) : R_f = 0.46; ^{1}H NMR (600 MHz, CDCl3) : δ 7.62-

7.42 (m, 12H), 7.38-7.05 (m, 81H), 6.95-6.90 (m, 8H), 6.86-6.69 (m, 15H), 5.37 (d, *J* = 9.3 Hz, 1H), 5.31 (t, *J* =10.4 Hz, 2H), 5.27 (d, *J* = 9.2 Hz, 2H), 4.91-4.90 (m, 2H), 4.89-4.81 (m, 9H), 4.75 (d, *J*=12.1 Hz, 1H), 4.68-4.53 (m, 5H), 4.52-4.29 (m, 23H), 4.28-4.02 (m, 21H), 3.88 (d, *J* = 3.1 Hz, 1H), 3.83 (d, *J* = 3.2 Hz, 1H), 3.77-3.69 (m, 3H), 3.62-3.55 (m, 3H), 3.52-3.33 (m, 21H), 3.28-3.19 (m, 5H), 3.18-3.02 (m, 4H), 2.97-2.90 (m, 2H), 2.89-2.79 (m, 2H), 2.14 (s, 3H), 1.98 (s, 3H), 1.93 (s, 3H), 1.39-1.20 (m, 4H), 1.03-1.00 (m, 2H); ^{13}CNMR (150 MHz, $CDCl_3$) : δ 171.1, 169.6, 168.6, 168.2, 167.8, 167.5, 139.7, 139.6, 139.4, 139.3, 139.1, 138.9, 138.8, 138.6, 138.5, 138.4, 138.3, 138.3, 138.2, 137.9, 133.9, 133.2, 132.4, 131.8, 131.6, 129.0, 128.8, 128.8, 128.7, 128.6, 128.6, 128.5, 128.4, 128.4, 128.3, 128.3, 128.1, 128.0, 128.0, 127.9, 127.8, 127.6, 127.5, 127.5, 127.3, 123.3, 122.9, 80.8, 80.6, 80.2, 75.3, 75.1, 74.9, 74.8, 74.7, 74.6, 74.4, 74.2, 73.9, 73.8, 73.7, 73.6, 73.5, 73.4, 73.3, 73.2, 73.1, 72.9, 72.6, 72.2, 72.1, 71.96, 71.8, 71.0, 69.9, 69.8, 69.6, 69.2, 69.1, 68.8, 68.3, 68.1, 66.1, 56.8, 56.2, 56.1, 55.9, 31.2, 29.9, 28.9, 28.5, 23.2, 21.6, 21.5, 21.3; ESI-MS: *m/z* calcd for $C_{237}H_{239}N_7O_{53}$; 4055.6180 found 4056.6075 $(M+H)^+$.

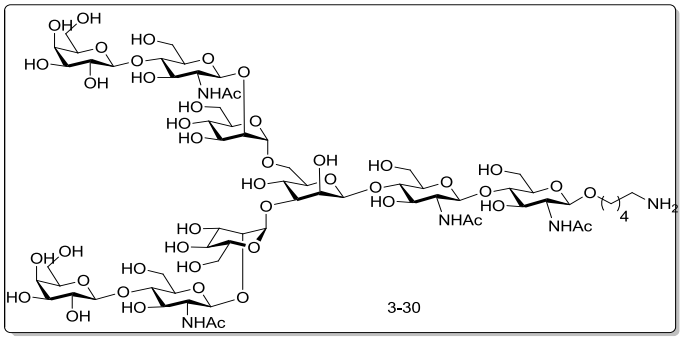

5-Aminopentyl-di-[β-D-galactopyranosyl-(1→4)-2-acetamido-2-deoxy-β-D-glucopyranosyl -(1→2)-α-D-mannopyranosyl]-(1→3),(1→6)-β-D-mannopyranosyl-(1→4)-2-acetamido-2-deoxy-β-D-glucopyranosyl-(1→4)-2-acetamido-2-deoxy-β-D-glucopyranoside (3-30): Compound **3-29** (0.120 g, 0.029 mmol) was deprotected by following general procedure 1 to obtain title compound **3-30** (0.015 g, 32%) as a white solid. ^{1}HNMR (600 MHz, D_2O) : δ 4.03 (d, *J* = 2.2 Hz, 1H), 4.82 (s, 2H), 4.72 (s, 1H), 4.70 (d, *J* = 6.4 Hz, 1H), 4.50-4.46 (m, 3H), 4.30-4.24 (m, 4H), 4.00-3.53 (m, 49H), 3.44-3.34 (m, 4H) 2.97 (t, *J* = 10.6 Hz, 1H), 2.07 (s, 3H), 2.06 (s, 3H), 2.06 (s, 3H), 2.03 (s, 3H) 1.68–1.65 (m, 2H), 1.60-1.595 (m, 2H), 1.58–1.39 (m, 2H); ^{13}CNMR (150 MHz, D_2O) : δ 177.55, 177.48, 177.17, 177.14, 173.76, 105.84, 105.65, 104.06, 103.91, 103.79, 103.24,

103.00, 99.68, 81.50, 81.48, 80.53, 79.42, 79.13, 79.07, 79.01, 78.17, 78.09, 77.98, 77.44, 77.34, 77.23, 77.09, 75.25, 75.14, 75.10, 74.94, 74.83, 74.74, 73.71, 72.85, 71.28, 70.71, 70.18, 70.15, 69.51, 67.49, 64.49, 64.41, 63.76, 62.89, 62.85, 62.71, 57.96, 57.93, 57.85, 57.73, 42.06, 33.62, 31.02, 30.97, 30.79, 30.10, 29.10, 25.40, 25.36, 24.88, 24.83, 24.36, 24.19, 16.09; ESI-MS: *m/z* calcd for $C_{67}H_{115}N_5O_{46}$; 1725.6886 found 1726.7457 $(M+H)^+$.

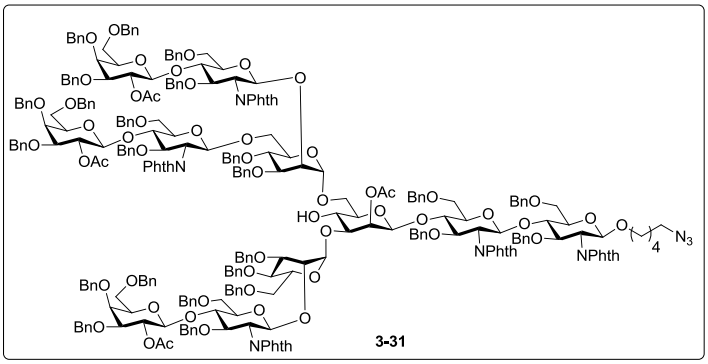

5-Azidopentyl-O-{(2-O-acetyl-3,4,6-O-tri-benzyl-β-D-galactopyranosyl-(1→4)}-O-{(3,6-O-dibenzyl-2-deoxy-2-phthalimido-β-D-glucopyranosyl-(1→2)}-O-(3,4,6-tri-O-benzyl-α-D-mannopyranosyl)-(1→3),{2-O-acetyl-3,4,6-O-tri-benzyl-β-D-galactopyranosyl-(1→4)-O-3,6 -O-di-benzyl-2-deoxy-2-phthalimido-β-D-glucopyranosyl-(1→2)-[2-O-acetyl-3,4,6-O-tri-benzyl-β-D-galactopyranosyl-(1→4)-O-3,6-O-di-benzyl-2-deoxy-2-phthalimido-β-D-glucop yranosyl-(1→6)]-3,4-O-di-benzyl-α-D-mannopyranosyl-(1→6)}-2-O-acetyl-β-D-mannopyr-anosyl-(1→4)-O-(3,6-di-O-benzyl-2-deoxy-2-phthalimido-β-D-glucopyranosyl)-(1→4)-O-3, 6-di-O-benzyl-2-deoxy-2-phthalimido-β-D-glucopyranoside (3-31): A mixture of silver triflate (0.079 g, 0.310 mmol), bis (cyclopentadienyl) hafnium dichloride (0.082 g, 0.217 mmol), and 4Å activated molecular sieves in dry toluene (10 mL) was stirred at room temperature for 1 h. The reaction mixture was then cooled to -40 °C. A solution of donor **3-14** (0.150 g, 0.068 mmol) and acceptor **3-26** (0.165 g, 0.062 mmol) in 5 mL toluene was added. The mixture was stirred for 2 h, quenched with Et_3N, diluted with EtOAc, and filtered through celite. The filtrate was washed with aqueous $NaHCO_3$ (2 x 50mL) and brine (50mL) solution. The organic layer was dried over Na_2SO_4 and concentrated in *vacuo*. The residue was purified by flash column chromatography to afford **3-31** (0.132 g, 51% and 80% based on acceptor recovery) as colorless foam. TLC: (acetone : toluene = 1/9, v/v): R_f = 0.39; ^1H NMR (600 MHz,

$CDCl_3$): δ 7.62-7.41 (m,20H), 7.39-7.08 (m, 100H), 6.91-6.64 (m, 20H), 4.87-4.79 (m, 7H), 4.48-4.45 (m, 14H), 4.43-3.45 (m, 65H), 3.40-3.02 (m, 40H), 2.92-2.75 (m, 5H), 2.02 (s, 3H), 1.97 (s, 3H), 1.94 (s, 3H), 1.91 (s, 3H), 1.35-1.18 (m, 4H), 1.06-1.00 (m, 2H); ^{13}CNMR (150 MHz, $CDCl_3$) : δ 169.5, 168.0, 139.2, 139.0, 138.7, 138.5, 138.4, 138.3, 138.2, 133.8, 132.0, 131.9, 131.0, 129.3, 128.8, 128.7, 128.6, 128.5, 128.4, 128.3, 128.2, 128.2, 128.0, 127.9, 127.7, 127.5, 127.3, 127.0, 126.9, 123.6, 100.9, 100.7, 98.3, 97.1, 94.4, 80.7, 79.2, 78.4, 76.3, 75.4, 75.1, 74.8, 74.6, 73.7, 73.4, 73.0, 72.6, 72.2, 71.9, 71.1, 70.9, 69.0, 68.4, 68.2, 67.5, 55.9, 51.3, 39.0, 30.6, 29.9, 29.2, 28.9, 28.5, 24.0, 23.2, 21.3, 21.2, 20.9, 14.3, 11.2; ESI-MS: *m/z* calcd for $C_{287}H_{288}N_8O_{65}$ 4885.9477; found 4885.7245 $(M+H)^+$.

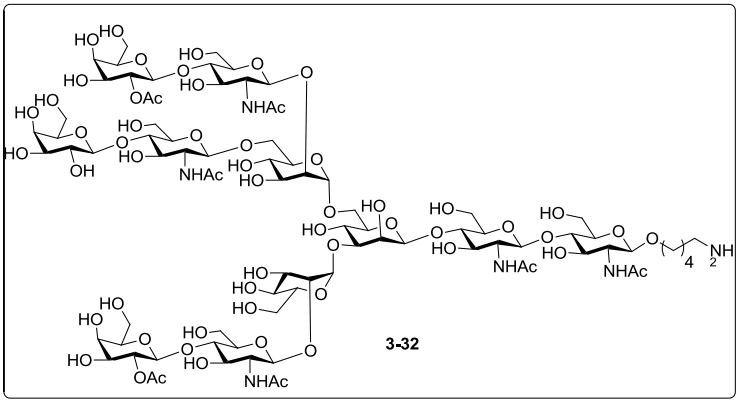

5-Aminopentyl-β-D-galactopyranosyl-(1→4)-2-acetamido-2-deoxy-β-D-glucopyranosyl-(1→2)-α-D-mannopyranosyl]-(1→3),[di-(β-D-galactopyranosyl-(1→4)-2-acetamido-2-deoxy-β-D-glucopyranosyl)-(1→2),(1→6)-α-D-mannopyranosyl](1→6)-β-D-mannopyranosyl(1→4)-2-acetamido-2-deoxy-β-D-glucopyranosyl-(1→4)-2-acetamido-2-deoxy-β-D-glucop-yranoside (3-32): Compound **3-31** (0.090 g, 0.018 mmol) was deprotected by following general procedure 1 to obtain title compound **3-32** (0.015 g, 39%) as a white solid. ^{1}HNMR (600 MHz, D_2O): δ 5.08 (d, *J* = 8.4 Hz, 1H), 4.82 (d, *J* = 7.8 Hz, 1H), 4.87 (d, *J* = 13.2 Hz, 2H), 4.69 (s, 1H), 4.64 (d, *J* = 7.8 Hz, 1H), 4.59 (d, *J* = 8.4 Hz, 1H), 4.53-4.49 (m, 5H), 4.34 (d, *J* = 3Hz, 1H), 4.31 (d, *J* = 3 Hz, 1H), 4.28-4.26 (m, 2H), 4.20 (d, *J* = 9.6 Hz, 1H), 4.02-3.43 (m, 62H), 3.01 (t, *J* = 7.2 Hz, 2H), 2.16 (s, 3H), 2.15 (s, 3H), 2.10 (s, 3H), 2.07 (s, 3H), 2.06 (s, 3H), 1.72-1.67 (m, 2H), 1.63-1.60 (m, 2H), 1.45-1.41 (m, 2H); ^{13}CNMR (150 MHz, D_2O): δ 177.5, 177.2, 177.1, 177.0, 176.7, 173.7, 105.7,

105.6, 104.4, 104.0, 103.8, 103.7, 103.1, 102.8, 99.7, 82.1, 81.8, 81.4, 80.6, 79.3, 79.0, 78.6, 78.1, 78.0, 77.7, 77.6, 77.4, 77.3, 77.2, 77.1, 75.2, 75.0, 75.0, 74.8, 74.6, 73.7, 72.8, 71.4, 72.2, 71.2, 70.5, 70.3, 70.1, 69.4, 67.1, 64.4, 63.7, 62.8, 62.7, 58.0, 57.8, 57.7, 57.6, 42.0, 30.7, 29.1, 25.4, 25.3, 25.1, 24.9, 24.8, 24.8; ESI-MS: *m/z* calcd for $C_{81}H_{138}N_6O_{56}$ 2091.8208; found 2091.8230 $(M+H)^+$; 1046.41$(M+H)^{2+}$.

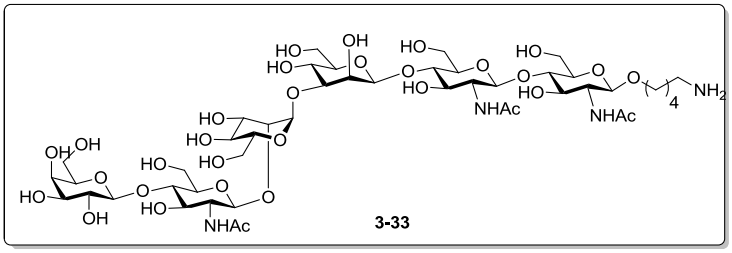

5-Aminopentyl-β-D-galactopyranosyl-(1→4)-2-acetamido-2-deoxy-β-D-glucopyranosyl-(1→2)-α-D-mannopyranosyl]-(1→3)-β-D-mannopyranosyl-(1→4)-2-acetamido-2-deoxy-β-D-glucopyranosyl-(1→4)-2-acetamido-2-deoxy-β-D-glucopyranoside(3-33):
Hexasaccharide **3-25** (0.110 g, 0.041 mmol) was deprotected following general procedure 1 to get desired compound **3-33** (0.025 g, 51%) as white solid. ^{1}H NMR (600 MHz, D_2O) : δ 5.04 (d, *J* = 8.4 Hz, 1H), 4.84 (s, 1H), 4.60 (d, *J* = 8.2 Hz, 1H), 4.51 (d, *J* = 8.1Hz, 1H), 4.46 (d, *J* = 7.8 Hz, 1H), 4.28 (d, *J* = 3.3 Hz, 1H), 4.26 (d, *J* = 3.6 Hz, 1H), 4.10-3.82 (m, 9H), 3.82-3.56 (m, 23H), 3.52-3.38 (m, 5H), 2.97 (t, *J* = 7.8 Hz, 2H), 2.07 (s, 3H), 2.05 (s, 3H), 2.03 (s, 3H), 1.70-1.65 (m, 2H), 1.62-1.58 (m, 2H), 1.48-1.41 (m, 2H); ^{13}C NMR (150 MHz, D_2O) : δ 177.64, 177.32, 177.17, 173.74, 105.65, 104.13, 103.80, 103.18, 102.70, 100.08, 82.05, 81.50, 81.37, 79.38, 79.04, 78.85, 78.09, 77.42, 77.28, 77.24, 75.23, 75.13, 75.06, 74.80, 74.67, 73.69, 72.84, 71.27, 70.14, 70.07, 68.12, 64.43, 63.74, 63.61, 62.85, 62.82, 62.75, 57.91, 57.78, 57.73, 42.05, 30.78, 29.10, 25.27, 24.87, 24.85, 24.83; ESI-MS: *m/z* calcd for $C_{47}H_{82}N_4O_3Na$; 1221.4855 found 1221.5223 $(M+Na)^+$.

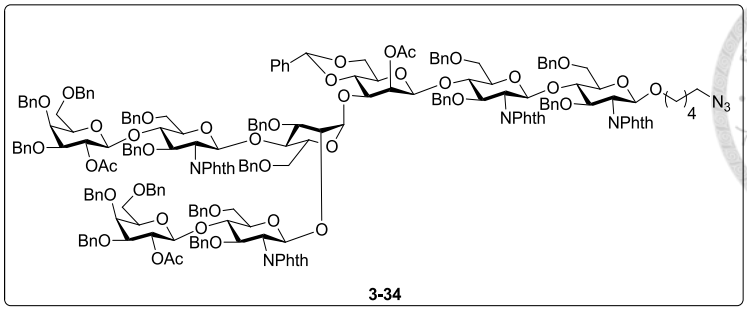

5-Azidopentyl-O-{2-O-acetyl-3,4,6-O-tri-benzyl-β-D-galactopyranosyl-(1→4)-O-3,6-O-di-benzyl-2-deoxy-2-phthalimido-β-D-glucopyranosyl-(1→2)-[2-O-acetyl-3,4,6-O-tri-benzyl-β-D-galactopyranosyl-(1→4)-O-3,6-O-di-benzyl-2-deoxy-2-phthalimido-β-D-glucopyrano-syl-(1→4)]-3,6-O-di-benzyl-α-D-mannopyranosyl-(1→3)}-2-O-acetyl-4,6-O-benzyl-idine-β-D-mannopyranosyl-(1→4)-O-(3,6-di-O-benzyl-2-deoxy-2-phthalimido-β-D-glucopyranosyl)-(1→4)-O-3,6-di-O-benzyl-2-deoxy-2-phthalimido-β-D-glucopyranoside (3-34): A mixture of silver triflate (0.135 g, 0.530 mmol), bis (cyclopentadienyl) hafnium dichloride (0.140 g, 0.371 mmol), and 4Å activated molecular sieves in dry toluene (10 mL) was stirred at room temperature for 1 h. The reaction mixture was then cooled to -50 °C, a solution of donor **3-16** (0.240 g, 0.106 mmol) and chitobiose trisaccharide **2-10** acceptor (0.174 g, 0.127 mmol) in 5 mL toluene was added. The mixture was stirred for 2 h at -30 ^{o}C, quenched with Et_3N, diluted with EtOAc, and filtered through celite. The filtrate was washed with aqueous $NaHCO_3$ (2 x 50 mL), and brine (50 mL) solution. The organic layer was dried over Na_2SO_4 and concentrated in *vacuo*. The residue was purified by flash column chromatography to afford **3-34** (0.258 gm, 68%) as colorless foam. TLC: (acetone : toluene = 1/9, v/v): R_f = 0.20; ^{1}H NMR (600 MHz, $CDCl_3$): δ 7.85-7.36 (m, 16H), 7.30-7.12 (m, 60H), 7.08-6.72 (m, 25H), 5.39 (t, *J* = 10.2 Hz, 1H), 5.29 (t, *J* = 10.3 Hz, 1H), 5.16 (d, *J* = 7.2 Hz, 1H), 5.09 (d, *J* = 8.4 Hz, 2H), 4.91-4.72 (m, 10H), 4.63-4.56 (m, 5H), 4.01-4.80 (m, 30H), 3.80-3.95 (m, 10H), 3.60-3.75 (m, 4H), 3.52-3.48 (m, 6H), 3.41-3.15 (m, 20H), 2.98 (d, *J* = 9.6 Hz, 1H), 2.90-2.76 (m, 3H), 2.66-2.62 (m, 1H), 1.95 (s, 3H), 1.93 (s, 3H), 1.87 (s, 3H), 1.38-1.23 (m, 4H), 1.08-1.01 (m, 2H);); ^{13}CNMR (150 MHz, $CDCl_3$) : δ 169.5, 169.3, 169.2, 168.6, 168.5, 168.3, 167.9, 139.5, 139.1, 139.0, 138.9, 138.8, 138.6, 138.3, 138.2, 137.8, 137.2, 134.2, 133.9, 133.8, 133.6, 133.4, 132.1, 131.9, 131.7, 131.6, 129.2, 129.1, 128.7, 128.6, 128.5, 128.4, 128.2, 128.1, 127.9, 127.8, 127.7, 127.6, 127.5, 127.4, 127.3, 127.2, 126.8, 126.7, 126.4, 125.5, 123.8,

123.3, 75.1, 74.7, 74.6, 74.4, 74.2, 73.6, 73.5, 73.3, 72.7, 72.3, 72.0, 69.86, 69.0, 68.7, 68.5, 68.3, 68.2, 67.5, 67.4, 66.1, 56.6, 56.4, 55.7, 51.3, 29.9, 28.8, 28.4, 23.2, 21.6, 21.4; ESI-MS: *m/z* calcd for $C_{210}H_{209}N_7O_{48}Na$ 3621.4086; found 3621.3714 $(M+Na)^+$.

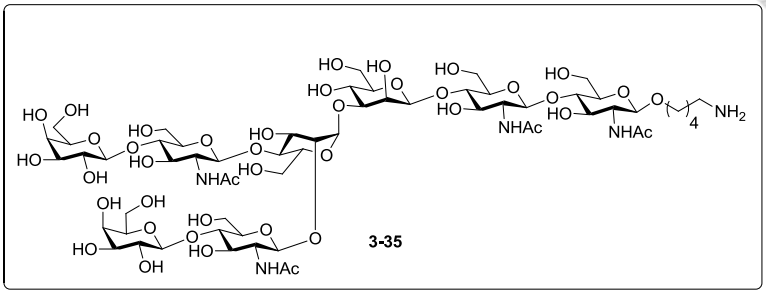

5-Aminopentyl-[di-(β-D-galactopyranosyl-(1→4)-2-acetamido-2-deoxy-β-D-glucopyranosyl)-(1→2), (1→4)- α-D-mannopyranosyl](1→3)-β-D-mannopyranosyl-(1→4)-2-acetamido-2-deoxy-β-D-glucopyranosyl-(1→4)-2-acetamido-2-deoxy-β-D-glucopyranoside (3-35): Compound **3-34** (0.135 g, 0.037 mmol) was deprotected by following general procedure 1 to obtain the title compound **3-35** (0.030 g, 51%) as white solid. ^{1}HNMR (600 MHz, D_2O): δ 5.11 (s, 1H), 4.58 (d, *J* = 7.2Hz, 1H), 4.52 (t, *J* = 8.4 Hz, 2H), 4.49-4.45 (m, 3H), 4.18 (d, *J* = 8.4 Hz, 2H), 4.08-3.50 (m, 49H), 2.97 (t, *J* = 7.8 Hz, 2H), 2.09 (s, 3H), 2.07 (s, 3H), 2.05 (s, 3H), 2.04 (s, 3H), 1.67-1.64 (m, 2H), 1.59-1.57 (m, 2H), 1.39-1.37 (m, 2H); ^{13}CNMR (150 MHz, D_2O) : δ 174.6, 174.5, 174.4, 174.3, 102.9, 102.8, 101.5, 101.3, 101.0, 99.9, 99.5, 99.0, 80.2, 79.2, 78.6, 78.4, 78.1, 78.0, 76.1, 75.9, 74.7, 74.4, 72.4, 74.3, 72.1, 71.9, 70.9, 70.2, 70.0, 68.5, 68.0, 65.9, 61.2, 61.0, 60.9, 60.7, 60.0, 59.9, 59.8, 55.1, 54.9, 54.7, 39.2, 38.6, 28.0, 22.3, 22.1, 22.0; ESI-MS: *m/z* calcd for $C_{61}H_{105}N_5O_{41}$ 1564.6358; found 1564.6380 $(M+H)^+$.

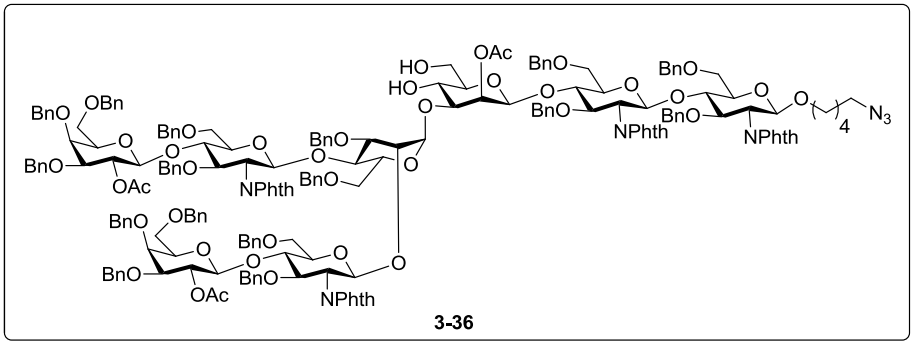

5-Azidopentyl-O-{2-O-acetyl-3,4,6-O-tri-benzyl-β-D-galactopyranosyl-(1→4)-O-3,6-O-di-benzyl-2-deoxy-2-phthalimido-β-D-glucopyranosyl-(1→2)-[2-O-acetyl-3,4,6-O-

tri-benzyl-β-D-galactopyranosyl-(1→4)-O-3,6-O-di-benzyl-2-deoxy-2-phthalimido-β-D-glucopyranos-yl-(1→4)]-3,6-O-di-benzyl-α-D-mannopyranosyl-(1→3)}-2-O-acetyl-β-D-mannopyranosyl-(1→4)-O-(3,6-di-O-benzyl-2-deoxy-2-phthalimido-β-D-glucopyranosyl)-(1→4)-O-3,6-di-O-benzyl-2-deoxy-2-phthalimido-β-D-glucopyranoside (3-36) : *p*-Toluene sulfonic acid monohydrate (0.020 g, 0.142mmol) was added to a solution of **3-34** (0.258 g, 0.071 mmol) in acetonitrile (10 mL). The reaction mixture was stirred at room temperature for 8 h. Then, the reaction was quenched with Et_3N and concentrated in *vacuo*. The residue was purified by flash column chromatography to afford diol **3-36** (0.180 g, 72%). TLC: (acetone : toluene = 2/8, v/v): R_f = 0.42; ^{1}H NMR (600 MHz, $CDCl_3$): δ 7.70-7.38 (m, 16H), 7.35-7.08 (m, 60H), 7.01-6.68 (m, 20H), 5.29-5.25 (m, 3H), 5.15 (d, *J* = 7.8 Hz, 1H), 5.07 (d, *J* = 7.8 Hz, 1H), 5.05 (d, *J* = 3.6 Hz, 1H), 4.90-4.76 (m, 9H), 4.62-3.56 (m, 50H), 3.53-3.05 (m, 25H), 3.0 (d, *J* = 7.8 Hz, 1H), 2.89-2.80 (m, 3H), 1.93 (s, 3H), 1.91 (s, 3H), 1.87 (s, 3H), 1.36-1.23 (m, 4H), 1.07-1.02 (m, 2H); ^{13}CNMR (150 MHz, $CDCl_3$): δ 169.6, 469.5, 169.4, 142.1, 139.3, 139.1, 138.9, 138.9, 138.8, 138.5, 138.5, 138.3, 138.2, 138.0, 134.5, 133.2, 132.6, 131.0, 129.2, 128.8, 128.6, 128.6, 128.5, 128.4, 128.3, 128.0, 127.9, 127.8, 127.8, 127.7, 127.6, 127.5, 127.4, 127.3, 126.9, 123.4, 101.0, 100.8, 99.4, 98.3, 98.2, 97.3, 96.5, 76.3, 75.8, 75.5, 75.1, 74.7, 73.8, 73.6, 73.5, 73.4, 73.2, 73.1, 73.0, 72.9, 72.2, 72.1, 71.9, 71.7, 71.6, 70.6, 70.1, 69.1, 68.4, 68.3, 68.2, 67.5, 64.8, 62.7, 56.7, 56.3, 56.0, 51.3, 38.1, 28.9, 28.5, 23.2, 21.3, 21.2, 21.1; ESI-MS: *m/z* calcd for $C_{203}H_{205}N_7O_{48}Na$ 3533.3773; found 3533.457 $(M+Na)^+$.

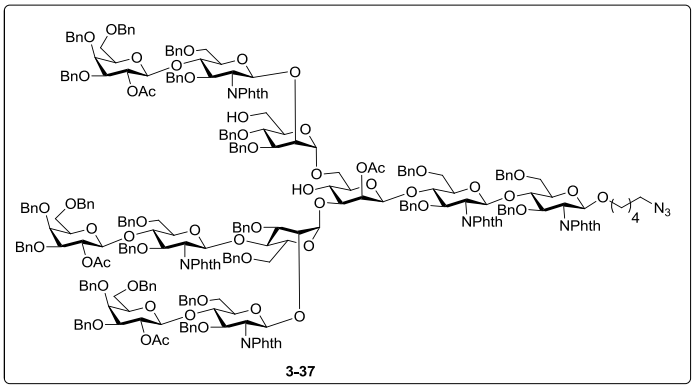

5-Azidopentyl-O-{2-O-acetyl-3,4,6-O-tri-benzyl-β-D-galactopyranosyl-(1→4)-O-3,6-O-di-benzyl-2-deoxy-2-phthalimido-β-D-glucopyranosyl-(1→2)-[2-O-acetyl-3,4,6-O-tri-benzyl-β-D-galactopyranosyl-(1→4)-O-3,6-O-di-benzyl-2-deoxy-2-phthalimido-β-

D-glucopyranos-yl-(1→4)]-3,6-O-di-benzyl-α-D-mannopyranosyl-(1→3)}-[2-O-acetyl-3,4,6-O-tri-benzyl-β-D-galactopyranosyl-(1→4)-O-3,6-O-di-benzyl-2-deoxy-2-phthalimido-β-D-glucopyranosyl-(1→2)]-3,4,6-O-tri-benzyl-α-D-mannopyranosyl-(1→6)}-2-O-acetyl-β-D-mannopyranosyl-(1→4)-O-(3,6-di-O-benzyl-2-deoxy-2-phthalimido-β-D-glucopyranosyl)-(1→4)-O-3,6-di-O-benzyl-2-deoxy-2-phthalimido-β-D-glucopyranoside (3-37): A mixture of silver triflate (0.054 gm, 0.210 mmol), bis (cyclopentadienyl) hafnium dichloride (0.056 g, 0.147 mmol) and 4Å activated molecular sieves in dry toluene (10 mL) was stirred at room temperature for 1 h. The reaction mixture was then cooled to -50 °C. A solution of donor **3-18** (0.089 g, 0.064 mmol) and acceptor **3-36** (0.150 g, 0.042 mmol) in 5mL toluene was added. The mixture was stirred for 3 h at -30^{o}C, quenched with Et_3N, diluted with EtOAc, and filtered through celite. The filtrate was washed with aqueous $NaHCO_3$ (2 x 50 mL) and brine (50mL) solution. The organic layer was dried over Na_2SO_4 and concentrated in *vacuo*. The residue was purified by flash column chromatography to afford **3-37** (0.135 gm, 64%) as colorless foam. TLC: (acetone : toluene = 1/9, v/v): R_f = 0.40; 7.64-7.43 (m, 20H), 7.38-7.69 (m, 100H), 7.68-6.58 (m, 20H), 5.33-5.24 (m, 3H), 5.13 (d, *J* = 8.4 Hz, 2H), 5.09 (d, *J* = 7.8 Hz, 1H), 5.05 (d, *J* = 8.4 Hz, 1H), 4.95 (d, *J* = 2.4 Hz, 1H), 4.89-4.83 (m, 7H), 4.80 (d, *J* = 7.4 Hz, 1H), 4.78 (d, *J* = 7.8 Hz, 1H), 4.76 (d, *J* = 2.8Hz, 1H), 4.74 (d, *J* = 3.5 Hz, 2H), 4.73-4.69 (m, 2H), 4.48-3.95 (m, 51H), 3.90-3.80 (m, 14H), 3.60-2.50 (m, 40H), 2.40-2.37 (m, 5H), 1.98 (s, 3H), 1.97 (s, 3H), 1.91 (s, 3H), 1.78 (s, 3H), 1.35-1.18 (m, 4H), 1.06-1.00 (m, 2H); ^{13}CNMR (150 MHz, $CDCl_3$): δ 169.5, 168.0, 139.2, 139.0, 138.7, 138.5, 138.4, 138.3, 138.2, 133.8, 132.0, 131.9, 131.0, 129.3, 128.8, 128.7, 128.6, 128.5, 128.4, 128.3, 128.2, 128.2, 128.0, 127.9, 127.7, 127.5, 127.3, 127.0, 126.9, 123.6, 100.9, 100.7, 98.3, 97.1, 94.4, 80.7, 79.2, 78.4, 76.3, 75.4, 75.1, 74.8, 74.6, 73.7, 73.4, 73.0, 72.6, 72.2, 71.9, 71.1, 70.9, 69.0, 68.4, 68.2, 67.5, 55.9, 51.3, 39.0, 30.6, 29.9, 29.2, 28.9, 28.5, 24.0, 23.2, 21.3, 21.2, 20.9, 14.3, 11.2; ESI-MS: *m/z* calcd for $C_{287}H_{288}N_8O_{65}$ 4885.9477; found 4885.7032 $(M+H)^+$.

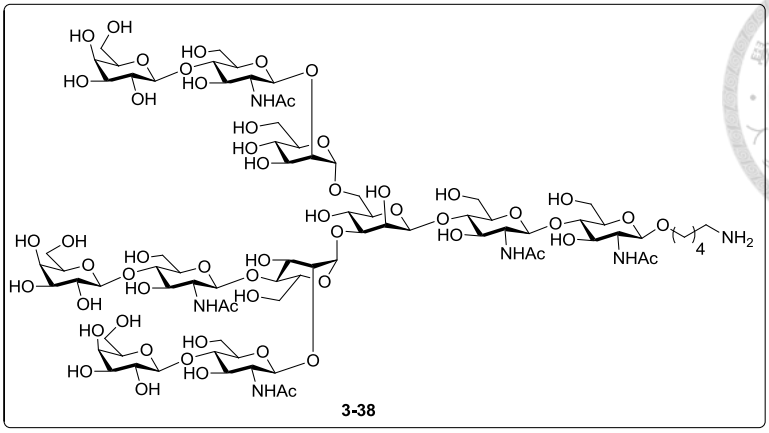

5-Aminopentyl-[di-(β-D-galactopyranosyl-(1→4)-2-acetamido-2-deoxy-β-D-glucopyranos-yl)-(1→2), (1→4)- α-D-mannopyranosyl](1→3)-[β-D-galactopyranosyl-(1→4)-2-acetamido-2-deoxy-β-D-glucopyranosyl)-(1→2)-α-D-mannopyranosyl](1→6)-β-D-mannopyranosyl-(1→4)-2-acetamido-2-deoxy-β-D-glucopyranosyl-(1→4)-2-acetamido-2-deoxy-β-D-glucop-yranoside (3-38): Compound **3-37** (0.125 g, 0.025 mmol) was deprotected by following general procedure 1 to obtain the title compound **3-38** (0.020 g, 37%) as white solid. ^{1}HNMR (600 MHz, D_2O): δ 5.14 (s, 1H), 4.94 (s, 1H), 4.75 (s, 1H), 4.62-4.56 (m, 4H), 4.23 (bs, 2H), 4.13 (d, *J* = 3.6 Hz, 1H), 4.08-3.48 (m, 65H), 3.01 (d, *J* = 8.4 Hz, 2H), 2.11 (s, 3H), 2.10 (s, 3H), 2.09 (s, 3H), 2.07 (s, 3H), 2.05 (s, 3H), 1.70-1.66 (m, 2H), 1.62-1.59 (m, 2H), 1.42-1.39 (m, 2H); ^{13}CNMR (150 MHz, D_2O): δ 177.4, 177.3, 177.2, 177.4, 173.7, 105.6, 105.5, 104.3, 104.2, 103.7, 103.6, 103.1, 102.2, 102.1, 101.8, 99.7, 83.0, 82.1, 82.0, 81.2, 80.9, 80.8, 79.0, 78.3, 77.5, 77.4, 77.3, 77.3, 77.2, 77.1, 75.5, 75.2, 75.1, 74.8, 74.7, 74.6, 73.6, 72.8, 72.1, 70.8, 70.0, 68.5, 68.4, 64.3, 64.0, 63.7, 62.8, 62.7, 62.7, 62.6, 57.8, 57.7, 57.6, 57.5, 57.4, 42.0, 30.7, 29.0; ESI-MS: *m/z* calcd for $C_{81}H_{138}N_6O_{56}Na$ 2136.7982; found 1068.3973 $(M+Na)^{2+}$; 1046.4156 $(M+H)^{2+}$.

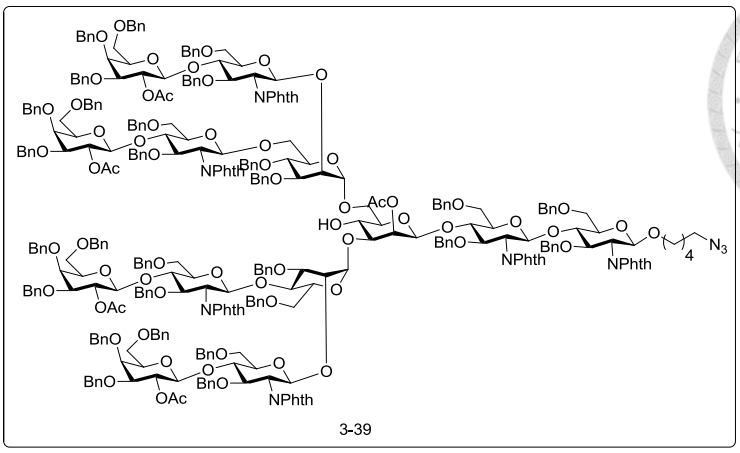

3-39

5-Azidopentyl-O-{2-O-acetyl-3,4,6-O-tri-benzyl-β-D-galactopyranosyl-(1→4)-O-3,6-O-di-benzyl-2-deoxy-2-phthalimido-β-D-glucopyranosyl-(1→2)-[2-O-acetyl-3,4,6-O-tri-benzyl-β-D-galactopyranosyl-(1→4)-O-3,6-O-di-benzyl-2-deoxy-2-phthalimido-β-D-glucopyrano-syl-(1→4)]-3,6-O-di-benzyl-α-D-mannopyranosyl-(1→3)}-{2-O-acetyl-3,4,6-O-tri-benzyl-β-D-galactopyranosyl-(1→4)-O-3,6-O-di-benzyl-2-deoxy-2-phthalimido-β-D-glucopyranosyl-(1→2)-[2-O-acetyl-3,4,6-O-tri-benzyl-β-D-galactopyranosyl-(1→4)-O-3,6-O-di-benzyl-2-deoxy-2-phthalimido-β-D-glucopyranosyl-(1→6)]-3,4-O-di-benzyl-α-D-mannopyranosyl-(1→6)}-2-O-acetyl-β-D-mannopyranosyl-(1→4)-O-(3,6-di-O-benzyl-2-deoxy-2-phthalimido-β-D-glucopyranosyl)-(1→4)-O-3,6-di-O-benzyl-2-deoxy-2-phthalimido-β-D-glucopyrano-side (3-39): A mixture of silver triflate (0.041 g, 0.160 mmol), bis (cyclopentadienyl) hafnium dichloride (0.042 g, 0.112 mmol), and 4Å activated molecular sieves in dry toluene (10 mL) was stirred at room temperature for 1 h. The reaction mixture was then cooled to -50 °C. A solution of donor **3-14** (0.089 g, 0.039 mmol) and acceptor **3-36** (0.115 g, 0.032 mmol) in 5 mL toluene was added. The mixture was stirred for 2 h at -30 ^{o}C, quenched with Et_3N, diluted with EtOAc, and filtered through celite. The filtrate was washed with aqueous $NaHCO_3$ (2 x 50 mL), and brine (50 mL) solution. The organic layer was dried over Na_2SO_4 and concentrated in *vacuo*. The residue was purified by flash column chromatography to afford **3-39** (0.139 g, 73%) as colorless foam. TLC: (ethyl acetate : toluene = 2/8, v/v): R_f = 0.43; ^{1}H NMR (600 MHz, $CDCl_3$): δ 7.64-7.34 (m, 30H), 7.29-7.01 (m, 100H), 7.00-6.52 (m, 40H), 5.55-5.33 (m, 4H), 5.20 (d, *J* = 7.2 Hz, 2H), 5.10 (d, *J* = 3.2 Hz, 2H), 4.92-3.85 (m, 100H), 3.01-3.58 (m, 39H), 2.57-2.90 (m, 4H), 2.02 (s, 3H), 1.98 (s, 3H), 1.96 (s, 3H), 1.85 (s, 3H), 1.72 (s, 3H), 1.36-1.24 (m,

4H), 1.06-1.00 (m, 2H); ^{13}CNMR (150 MHz, $CDCl_3$): δ 169.6, 169.4, 169.3, 169.2, 168.4, 167.9, 167.7, 167.6, 139.4, 139.1, 139.0, 138.9, 138.8, 138.7, 138.6, 138.5, 138.4, 138.0, 134.2, 134.0, 133.7, 133.5, 132.1, 131.9, 131.8, 131.7, 131.6, 129.2, 129.0, 128.9, 128.6, 128.5, 128.4, 128.4, 128.3, 128.3, 128.2, 128.1, 127.9, 127.8, 127.8, 127.7, 127.6, 127.5, 127.4, 127.4, 127.3, 127.3, 127.3, 127.0, 126.9, 126.8, 125.5, 125.3, 125.2, 125.0, 123.3, 123.2, 100.9, 100.8, 100.6, 99.8, 99.2, 98.2, 97.4, 97.2, 96.3, 80.7, 80.6, 80.5, 80.10, 77.9, 77.8, 77.6, 77.5, 77.2, 77.1, 75.3, 75.0, 74.6, 74.5, 74.3, 73.6, 73.5, 73.2, 72.9, 72.8, 72.7, 72.6, 72.5, 71.8, 71.6, 70.9, 70.3, 69.9, 69.0, 68.3, 68.1, 67.8, 67.6, 66.1, 56.8, 56.5, 56.0, 55.9, 55.7, 21.3, 28.4, 28.3, 23.2, 21.6, 21.3, 21.2, 21.1, 20.8; ESI-MS: *m/z* calcd for $C_{337}H_{337}N_9O_{77}$ 5741.2731; found 5741.6082 $(M+H)^+$.

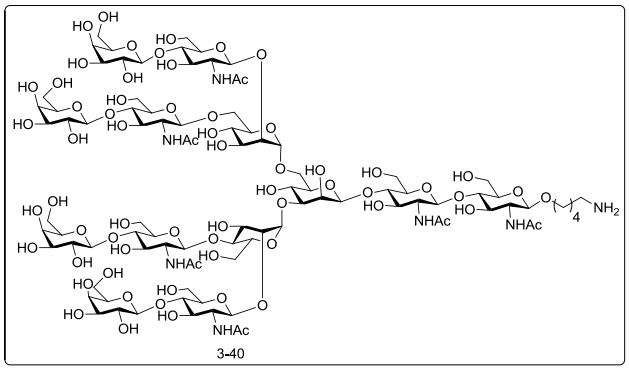

5-Aminopentyl-[di-(β-D-galactopyranosyl-(1→4)-2-acetamido-2-deoxy-β-D-glucopyranosyl)-(1→2),(1→4)-α-D-mannopyranosyl](1→3)-[di-(β-D-galactopyranosyl-(1→4)-2-acetami-do-2-deoxy-β-D-glucopyranosyl)-(1→2), (1→6)- α-D-mannopyranosyl]-(1→6)-β-D-mannopyranosyl-(1→4)-2-acetamido-2-deoxy-β-D-glucopyranosyl-(1→4)-2-acetamido-2-deoxy-β-D-glucopyranoside (3-40): Compound **3-39** (0.130 g, 0.022 mmol) was deprotected by following general procedure 1 to obtain the title compound **3-40** (0.015 g, 27%) as a white solid. ^{1}HNMR (600 MHz, D_2O): δ 5.15 (s, 1H), 4.82 (s, 1H), 4.65 (d, *J* = 7.8 Hz, 1H), 4.63 (d, *J* = 7.2Hz, 1H), 4.62 (dd, *J* = 3.5 Hz, *J* = 7.8 Hz, 3H), 4.51-4.48 (m, 5H), 4.24-4.21 (m, 3H), 4.20-3.70 (m, 78H), 3.00 (t, *J* = 7.8 Hz, 2H), 2.15 (s, 3H), 2.14 (s, 3H), 2.12 (s, 3H), 2.10 (s, 3H), 2.05 (s, 3H), 1.93 (s, 3H), 1.71-1.66 (m, 2H), 1.62 (m, 2H), 1.44-1.39 (m, 2H); ^{13}CNMR (150 MHz, D_2O) : δ 177.4, 177.3, 177.2, 177.1, 177.0, 176.8, 105.6, 105.5, 104.3, 104.1, 103.7, 103.0, 102.3, 101.8, 99.9, 82.9, 82.0, 81.9, 81.3, 81.2, 81.0, 80.0, 79.2, 78.5, 78.3, 77.5, 77.4, 77.3, 77.2, 77.1, 75.2, 75.1, 74.9, 74.8,

74.6, 74.2, 73.6, 73.0, 72.8, 72.7, 72.1, 71.0, 70.8, 70.2, 68.3, 67.9, 64.0, 63.7, 62.8, 62.7, 62.6, 62.5, 57.8, 57.7, 57.6, 57.5, 42.0, 32.9, 30.7, 29.0, 25.4, 25.6, 25.1, 24.9, 24.8, 24.7, 24.7; MS: *m/z* calcd for $C_{95}H_{161}N_7O_{66}Na$; 2480.3021 found 1240.4748 $(M+Na)^{2+}$.

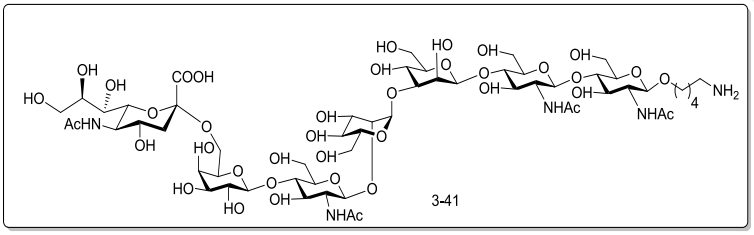

5-Aminopentyl-[5-Acetamido-3,5-dideoxy-D-glycero-α-D-galacto-2-nonulopyranosylonate-(2→6)-β-D-galactopyranosyl-(1→4)-2-acetamido-2-deoxy-β-D-glucopyranosyl-(1→2)-α-D-mannopyranosyl]-(1→3)-β-D-mannopyranosyl-(1→4)-2-acetamido-2-deoxy-β-D-gluco-pyr-anosyl-(1→4)-2-acetamido-2-deoxy-β-D-glucopyranoside (3-41): Compound **3-33** (10 mg, 0.0083 mmol) was sialylated with α-2,6-sialyltransferase for 2 d by following general procedure 2 to get desired title compound **3-41** (9.5 mg, 77%) as white solid. ^{1}HNMR (600 MHz, D_2O) : δ 5.06 (d, *J* = 7.8 Hz, 1H), 4.60 (d, *J* = 7.8 Hz, 1H), 4.49 (d, *J* = 7.8 Hz, 1H), 4.43 (d, *J* = 7.8 Hz, 1H), 4.27 (d, *J* = 3.6 Hz, 1H), 4.25 (d, *J* = 3.6 Hz, 1H), 4.08-3.38 (m, 45H), 2.98 (t, *J* =11.2 Hz, 2H), 2.60 (dd, *J* = 4.8, 12.00 Hz, 1H), 2.08 (s, 6H) 2.05 (s, 3H), 2.03 (s, 3H), 1.71 (t, *J* = 7.8 Hz, 1H), 1.69-1.69 (m, 2H), 1.61-1.56 (m, 2H), 1.41-1.37 (m, 2H); ^{13}CNMR (150 MHz, D_2O) : δ 174.94, 174.83, 174.56, 174.40, 103.50, 101,37, 101.03, 100.31, 100.12, 99.92, 97.31, 80.99, 79.28, 78.63, 78.59, 76.61, 76.32, 76.07, 74.51, 74.48, 74.38, 73.67, 72.52, 72.38, 72.36, 72.08, 71.90, 71.66, 70.70, 70.06, 68.37, 68.34, 67.33, 63.35, 62.63, 61.67, 60.88, 60.09, 59.98, 54.99, 54.87, 51.85, 40.02, 39.30, 28.01, 26.36, 22.56, 22.10, 22.08, 21.99; ESI-MS (negative mode) : *m/z* calcd for $C_{58}H_{99}N_5O_{39}$; 1489.5833 found 1488.5949 $(M-H)^-$.

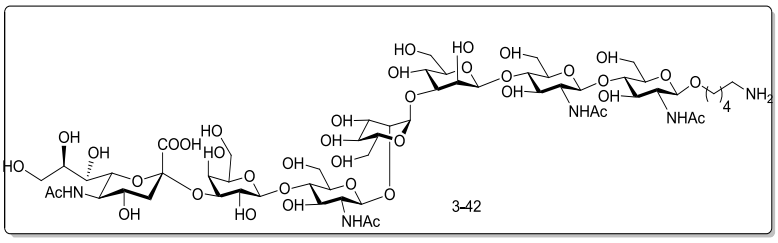

***5*-Aminopentyl-[5-Acetamido-3,5-dideoxy-D-glycero-α-D-galacto-2-nonulopyranosylonate-(2→3)-β-D-galactopyranosyl-(1→4)-2-acetamido-2-deoxy-β-D-glucopyrano**

syl-(1→2)-α-D-mannopyranosyl]-(1→3)-β-D-mannopyranosyl-(1→4)-2-acetamido-2-deoxy-β-D-gluco-pyr-anosyl-(1→4)-2-acetamido-2-deoxy-β-D-glucopyranoside (3-42): Compound **3-33** (7 mg, 0.0058mmol) was sialylated with α-2,3-sialyltransferase for 8 d by following general procedure 2 to get desired title compound **3-42** (4.6 mg, 52%) as white solid. ^{1}HNMR (600 MHz, D_2O) : δ 5.06 (d, *J* = 8.4 Hz, 1H), 4.62 (d, *J* = 6.6 Hz, 1H), 4.56 (d, *J* = 7.8 Hz, 1H), 4.51 (d, *J* = 7.8 Hz, 1H), 4.28 (d, *J* = 14.4 Hz, 2H), 4.13 (d, *J* = 9.6 Hz, 1H), 3.99-3.83 (m, 12H), 3.82-3.57 (m, 27H), 3.53-3.39 (m, 4H), 2.99 (t, *J* = 7.8 Hz, 2H), 2.77 (dd, *J* = 4.8, 2.00 Hz, 1H), 2.12 (s, 3H) 2.09 (s, 3H), 2.05 (s, 3H), 2.03 (s, 3H), 1.80 (t, *J* = 7.8 Hz, 1H), 1.71-1.66 (m, 2H), 1.62-1.59 (m, 2H), 1.44-1.41 (m, 2H); ^{13}CNMR (150 MHz, D_2O) : δ 174.88, 174.53, 174.46, 174.40, 102.50, 102,37, 101.65, 101.31, 100.12, 99.86, 98.31, 80.32, 79.67, 78.78, 78.56, 76.66, 75.32, 75.07, 74.51, 74.48, 74.38, 73.67, 72.52, 72.38, 72.36, 72.08, 71.90, 71.66, 70.70, 70.06, 68.37, 68.34, 67.33, 63.35, 62.63, 61.67, 60.88, 60.09, 59.98, 54.99, 54.87, 51.85, 40.02, 39.30, 28.01, 26.36, 22.56, 22.10, 22.08, 21.27 20.27; ESI-MS (negative mode) : *m/z* calcd for $C_{58}H_{99}N_5O_{39}$; 1489.5833 found 1488.5944(M - H)$^-$.

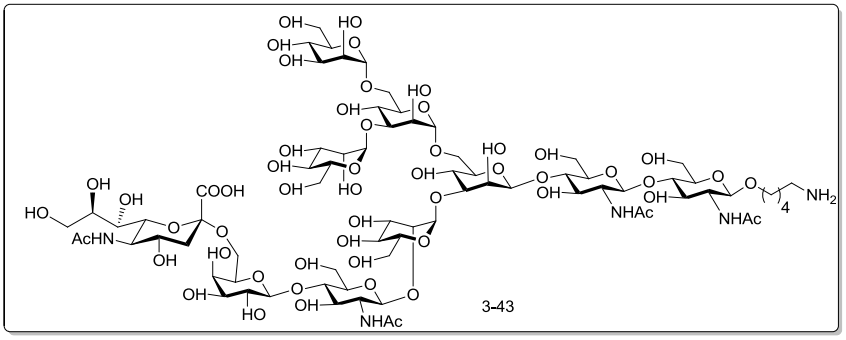

5-Aminopentyl-5-Acetamido-3,5-dideoxy-D-glycero-α-D-galacto-2-nonulopyranosylonate-(2→6)-β-D-galactopyranosyl-(1→4)-[2-acetamido-2-deoxy-β-D-glucopyranosyl-(1→2)-α-D -mannopyranosyl-(1→3),[di-(α-D-mannopyranosyl)-(1→3),(1→6)-α-D-manno-pyranosyl] (1→6)-β-D-mannopyranosyl-(1→4)-2-acetamido-2-deoxy-β-D-glucopyranosyl-(1→4)-2-acetamido-2-deoxy-β-D-glucopyranoside (3-43): Compound **3-28** (5 mg, 0.0029 mmol) was sialylated with α-2,6-sialyltransferase for 2 d by following general procedure 2 to get desired title compound **3-43** (3.5 mg, 60%) as white solid. ^{1}H NMR (600 MHz, D_2O) : δ 5.02 (d, *J* = 9.6 Hz, 1H), 4.88 (d, *J* = 13.8 Hz, 1H), 4.56-4.55 (m, 1H), 4.46 (d, *J* = 7.8 Hz, 1H), 4.41 (d, *J* = 8.4 Hz, 1H), 4.25-4.24 (m, 2H), 4.12 (s, 1H),

4.04 (d, *J* = 4.7 Hz, 1H), 4.04-3.42 (m, 61H), 3.40 (t, *J* = 10.8 Hz, 1H), 3.39-3.35 (m, 1H), 2.95 (t, *J* = 10.9 Hz, 2H), 2.64 (dd, *J* = 4.2, 12.2 Hz, 1H), 2.04 (s, 3H), 2.04 (s, 3H), 2.00 (s, 3H), 2.00 (s, 3H), 1.71-1.61 (m, 3H), 1.58-1.54 (m, 2H), 1.39-1.35 (m, 2H); ^{13}C NMR (150 MHz, D_2O) : δ 174.90, 174.79, 174.38, 173.47, 103.42, 102.29, 101.48, 101.01, 100.41, 100.18, 100.15, 99.24, 97.87, 97.27, 80.78, 79.59, 79.20, 78.72, 78.36, 76.61, 75.81, 74.79, 74.48, 74.36, 73.63, 73.28, 72.63, 72.52, 72.35, 72.30, 72.09, 71.94, 71.65, 70.82, 70.69, 70.53, 70.31, 70.12, 70.05, 69.89, 69.41, 68.33, 68.17, 67.32, 67.17, 66.66, 65.47, 65.09, 63.30, 62.62, 61.66, 60.98, 60.89, 60.32, 60.02, 59.94, 57.95, 54.91, 51.81, 40.01, 39.27, 28.00, 26.37, 23.62, 23.19, 22.59, 22.17, 22.05, 22.00; ESI-MS (negative mode) : *m/z* calcd for $C_{76}H_{129}N_5O_{54}$; 1975.7418 found 1974.7600 $(M-H)^-$.

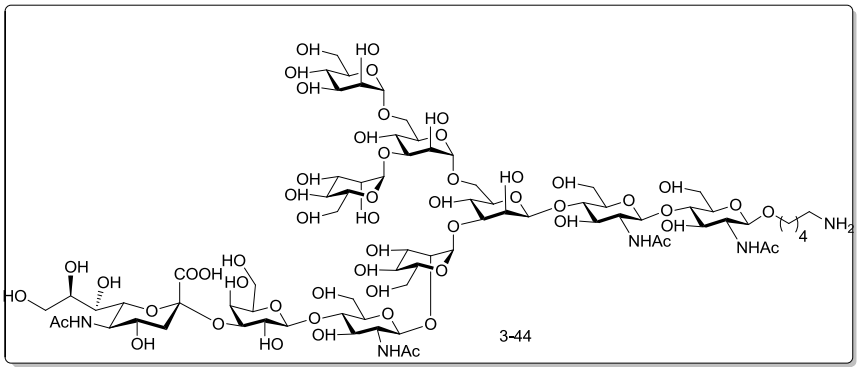

5-Aminopentyl-5-Acetamido-3,5-dideoxy-D-glycero-α-D-galacto-2-nonulopyranosylonate-(2→3)-β-D-galactopyranosyl-(1→4)-[2-acetamido-2-deoxy-β-D-glucopyranosyl-(1→2)-α-D -mannopyranosyl-(1→3),[di-(α-D-mannopyranosyl)-(1→3),(1→6)-α-D-manno-pyranosyl] (1→6)-β-D-mannopyranosyl-(1→4)-2-acetamido-2-deoxy-β-D-glucopyranosyl-(1→4)-2-acetamido-2-deoxy-β-D-glucopyranoside (3-44*)*: Compound **3-28** (5 mg, 0.0029 mmol) was sialylated with α-2,3-sialyltransferase for 8 d by following general procedure 2 to get desired title compound **3-44** (3.1 mg, 56%) as white solid. ^{1}H NMR (600 MHz, D_2O) : δ 5.01 (s, 1H), 4.97 (dd, *J* = 1.8, 3.2 Hz, 1H), 4.82 (d, *J* = 8.4 Hz, 1H), 4.52 (d, *J* = 7.8 Hz, 1H), 4.97 (d, *J* = 9.2 Hz, 1H), 4.42 (d, *J* = 8.3 Hz, 1H), 4.39 (d, *J* = 8.3 Hz, 1H), 4.22 (t, *J* = 7.8 Hz, 2H), 4.09 (s, 1H), 4.06 (d, *J* = 7.4 Hz, 1H), 4.035 (d, *J* = 7.3 Hz, 1H), 4.00 (d, *J* = 3.2 Hz, 1H), 3.96-3.85 (m, 10H), 3.85-3.71 (m, 19H), 3.72-3.52 (m, 26H), 3.51-3.48 (m, 2H), 3.38-3.370 (m, 2H), 2.90 (t, *J* = 7.9 Hz, 2H), 2.68 (dd, *J* = 4.8, 12.5 Hz, 1H), 2.01 (s, 3H), 1.99 (s, 3H), 1.96 (s, 3H), 1.95 (s, 3H), 1.73 (t, *J* = 8.6 Hz,

1H), 1.61-1.56 (m, 2H), 1.54-1.46 (m, 2H), 1.34-1.33 (m, 2H); ^{13}CNMR (150 MHz, D_2O) : δ 171.94, 171.81, 171.37, 170.80, 113.44, 99.86, 99.53, 99.27, 98.42, 97.99, 97.38, 97.08, 96.74, 96.21, 75.74, 75.66, 75.52, 73.56, 72.85, 72.41, 72.10, 71.62, 71.45, 71.36, 70.27, 69.81, 69.62, 69.28, 69.14, 69.02, 68.90, 68.69, 67.91, 67.82, 67.50, 67.20, 67.08, 66.87, 66.36, 65.46, 65.29, 65.01, 64.39, 64.32, 63.68, 62.47, 62.09, 61.02, 59.50, 59.39, 58.64, 57.96, 57.87, 57.10, 56.91, 52.12, 51.91, 48.60, 42.85, 40.32, 36.54, 36.25, 35.04, 25.27, 24.98, 23.34, 20.60, 19.53, 19.13, 19.03, 18.95, 13.70; ESI-MS (negative mode) : *m/z* calcd for $C_{76}H_{129}N_5O_{54}$; 1975.7418 found 1974.7671 (M - H)$^-$.

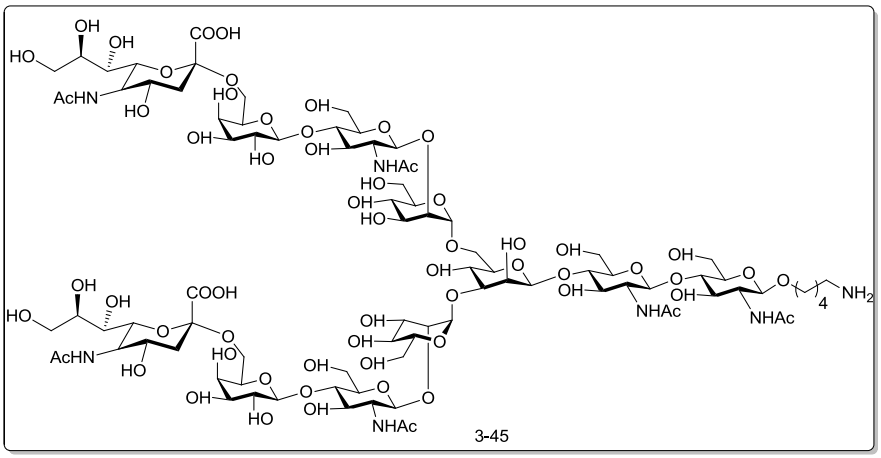

5-Aminopentyl-di-[5-Acetamido-3,5-dideoxy-D-glycero-α-D-galacto-2-nonulopyranosylo-nate-(2→6)-β-D-galactopyranosyl-(1→4)-2-acetamido-2-deoxy-β-D-glucopyranosyl-(1→2)-α-D-mannopyranosyl]-(1→3),(1→6)-β-D-mannopyranosyl-(1→4)-2-acetamido-2-deoxy-β-D-glucopyranosyl-(1→4)-2-acetamido-2-deoxy-β-D-glucopyranoside (3-45): Compound **3-30** (15 mg, 0.010 mmol) was sialylated with α-2,6-sialyltransferase for 2 d by following general procedure 2 to get desired title compound **3-45** (14.1 mg, 72%) as white solid. ^{1}HNMR (600 MHz, D_2O) : δ 4.95 (d, J = 12.3 Hz, 1H), 4.54 (d, J = 12.2 Hz, 1H), 4.42 (d, J = 10.3 Hz, 1H), 4.38-4.35 (m, 2H), 4.25-4.18 (m, 3H), 4.38-3.25 (m, 70H), 2.91 (t, J = 8.6 Hz, 2H), 3.63-3.58 (m, 2H), 2.00 (s, 6H), 2.00 (s, 3H), 1.96 (s, 6H), 1.96 (s, 3H), 1.66-1.61 (m, 4H), 1.54-1.49 (m, 2H), 1.35-1.30 (m, 2H) ; ^{13}CNMR (150 MHz, D_2O) : δ 177.71, 177.53, 177.45, 177.14, 176.24, 176.19, 106.27, 106.10, 104.11, 103.79, 103.54, 103.14, 102.98, 102.90, 99.53, 83.6683.14, 82.28, 82.14, 81.77, 79.43, 79.12, 78.92, 77.34, 77.22, 76.86, 76.42, 75.32, 75.17, 74.88, 74.58, 73.57, 73.47, 72.81, 71.28, 70.93, 70.08, 67.62, 66.09, 65.68, 65.40, 64.50, 62.83, 57.70, 57.30, 55.03, 54.62, 54.07, 42.80, 42.38,

42.06, 41.78, 30.77, 30.57; ESI-MS (negative mode) : *m/z* calcd for $C_{89}H_{149}N_7O_{62}$; 2309.8670 found 2307.8578 $(M\text{-}2H)^-$.

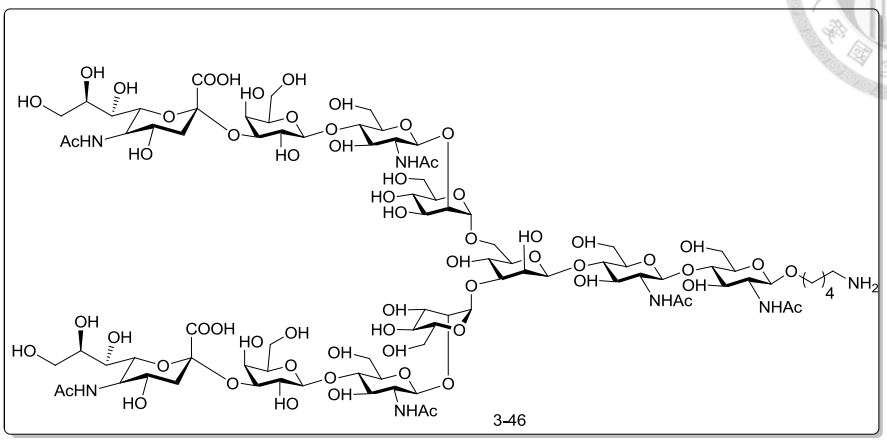

5-Aminopentyl-di-[5-Acetamido-3,5-dideoxy-D-glycero-α-D-galacto-2-nonulopyrano-sylo-nate-(2→3)-β-D-galactopyranosyl-(1→4)-2-acetamido-2-deoxy-β-D-glucopyranosyl-(1→2)-α-D-mannopyranosyl]-(1→3),(1→6)-β-D-mannopyranosyl-(1→4)-2-acetamido-2-deoxy-β-D-glucopyranosyl-(1→4)-2-acetamido-2-deoxy-β-D-glucopyran oside (3-46): Compound **3-30** (4 mg, 0.0023 mmol) was sialylated with α-2,3-sialyltransferase by following general procedure 2 for 8 d to get desired title compound **3-46** (4.02 mg, 75%) as white solid. ^{1}HNMR (600 MHz, D_2O) : δ 5.04 (d, *J* = 8.4 Hz, 1H), 4.64 (d, *J* = 7.9 Hz, 1H), 4.58-4.56 (m, 2H), 4.53-4.49 (m, 1H), 4.32 (d, *J* = 3.2 Hz, 1H), 4.29 (d, *J* = 4.5 Hz, 2H), 4.26 (d, *J* = 3.5 Hz, 1H), 4.14 (dt, *J* = 7.8, 3.5 Hz, 2H), 4.02-3.45 (m, 68H), 3.00 (t, *J* = 7.8 Hz, 2H), 2.79 (dd, *J* = 3.1, 8.4 Hz, 2H), 2.15 (s, 3H), 2.14 (s, 3H), 2.13 (s, 3H), 2.07 (s, 9H), 1.85-1.80 (m, 2H), 1.71-1.66 (m, 2H), 1.63-1.59 (m, 2H), 1.44-1.40 (m, 2H); ^{13}CNMR (150 MHz, D_2O) : δ 177.7, 177.5, 177.1, 176.6, 105.8, 105.6, 105.3, 104.1, 103.9, 103.7, 103.2, 102.9, 102.5, 99.6, 82.1, 82.0, 81.7, 81.5, 81.2, 80.4, 79.4, 79.2, 79.1, 79.0, 78.2, 78.0, 77.9, 77.4, 77.2, 75.6, 75.2, 75.1, 75.0, 74.8, 74.5, 74.4, 73.6, 72.8, 72.1, 70.8, 70.2, 70.1, 69.4, 67.5, 65.2, 64.4, 64.3, 63.7, 62.8, 62.6, 58.0, 57.9, 57.8, 57.7, 84.4, 64.4, 63.7, 62.8, 62.6, 58.0, 57.9, 57.8, 57.7, 54.4, 42.3, 42.3, 42.0, 30.7, 29.1, 25.3, 25.2, 24.9, 24.90, 24.8, 24.7; ESI-MS (negative mode) : *m/z* calcd for $C_{89}H_{149}N_7O_{62}$; 2309.8670 found 1152.9341 $(M\text{-}2H)^{2-}$.

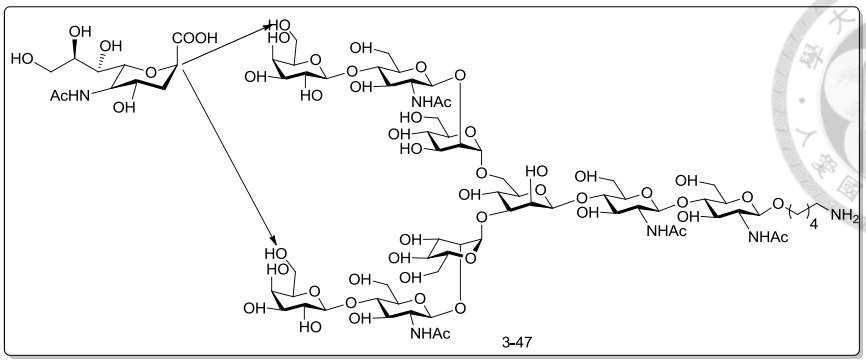

5-Aminopentyl-[5-Acetamido-3,5-dideoxy-D-glycero-α-D-galacto-2-nonulopyranosylonate-(2→6)-β-D-galactopyranosyl-(1→4)-2-acetamido-2-deoxy-β-D-glucopyranosyl-(1→2)-α-D-mannopyranosyl]-(1→3)/(1→6)-β-D-galactopyranosyl-(1→4)-2-acetamido-2-deoxy-β-D-gl-ucopyranosyl-(1→2)-α-D-mannopyranosyl]-(1→3)/(1→6)-β-D-mannopyranosyl-(1→4)-2-acetamido-2-deoxy-β-D-glucopyranosyl-(1→4)-2-acetamido-2-deoxy-β-D-glucopyranoside (3-47): Compound **3-30** (3 mg, 0.002 mmol) was sialylated with α-2,6-Sialyltransferase for 24 h by following general procedure 2 to get desired title compound **3-47** (1.8 mg, 31%) as white solid. ^{1}HNMR (600 MHz, D_2O) : δ 5.03 (d, *J* = 8.5 Hz, 1H), 4.61 (d, 1H, *J* = 8.6 Hz), 4.50 (d, *J* = 9.3 Hz, 1H), 4.45 (t, *J* = 10.2 Hz, 2H), 4.31-4.26 (m, 3H), 4.04-3.32 (m, 64H), 2.99 (t, *J* = 10.2 Hz, 2H), 2.69 (dd, *J* = 3.8 , 10.8 Hz, 1H), 2.08 (s, 9H), 2.03 (s, 6H), 1.74-1.65 (m, 3H), 1.62-1.56 (m, 2H), 1.42-1.37 (m, 2H); ^{13}CNMR (150 MHz, D_2O) : δ 177.53, 177.14, 106.27, 104.12, 103.79, 103.55, 103.14, 102.98, 99.54, 83.67, 83.13, 79.12, 78.07, 77.23, 77.16, 76.42, 75.31, 75.16, 74.88, 74.81, 74.45, 73.56, 73.48, 72.81, 71.13, 70.95, 70.17, 67.62, 66.10, 66.01, 65.41, 64.50, 64.33, 63.11, 62.82, 62.67, 57.89, 57.70, 54.62, 42.88, 42.81, 42.05, 30.77, 29.08, 26.47, 25.45, 25.41, 24.99, 24.87, 24.81; ESI-MS (negative mode) : *m/z* calcd for $C_{78}H_{132}N_6O_{54}$; 2017.8905 found 2016.7166 $(M-H)^-$.

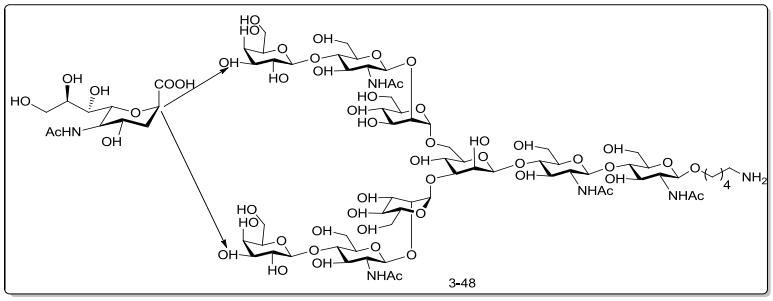

5-Aminopentyl-[5-Acetamido-3,5-dideoxy-D-glycero-α-D-galacto-2-nonulopyranosylonate-(2→3)-β-D-galactopyranosyl-(1→4)-2-acetamido-2-deoxy-β-D-glucopyranosyl-(1→2)-α-D-mannopyranosyl]-(1→3)/(1→6)-β-D-galactopyranosyl-(1→4)-2-acetamido-2-deoxy-β-D-glucopyranosyl-(1→2)-α-D-mannopyranosyl]-(1→3)/(1→6)-β-D-mannopyranosyl-(1→4)-2-acetamido-2-deoxy-β-D-glucopyranosyl-(1→4)-2-acetamido-2-deoxy-β-D-glucopyranoside (3-48): Compound **3-30** (3 mg, 0.010 mmol) was sialylated with α-2,3-sialyltransferase by following general procedure B for 2 d to get desired title compound **3-48** (1.3 mg, 21%) as white solid. ^{1}HNMR (600 MHz, D_2O) : δ 4.96 (d, *J* = 8.6 Hz, 1H), 4.52 (d, *J* = 8.3 Hz, 1H), 4.47 (dd, *J* = 3.2, 8.1 Hz, 1H), 4.43-4.39 (m, 2H), 4.22-4.16 (m,4H), 4.05 (dd, *J* = 2.6, 8.9 Hz, 1H), 3.95-3.26 (m, 62H), 2.91 (t, *J* = 10.6 Hz, 2H), 2.72 (dd, *J* = 4.3, 11.8 Hz, 1H), 1.99 (s, 3H), 1.96 (s, 3H), 1.94 (s, 9H), 1.75-1.70 (m, 1H), 1.62-1.57 (m, 2H), 1.54-1.45 (m, 2H), 1.34-1.27 (m, 2H); ^{13}CNMR (150 MHz, D_2O) : δ 174.96, 174.71, 174.38, 107.30, 103.03, 102.53, 101.23, 101.13, 101.01, 100.49, 100.21, 99.78, 79.28, 79.00, 78.69, 75.38, 72.46, 71.94, 70.91, 69.33, 66.81, 64.70, 64.22, 62.52, 61.61, 60.88, 60.03, 59.89, 55.14, 54.94, 51.61, 39.55, 39.26, 29.52, 28.24, 28.00, 26.32, 23.63, 22.60, 22.12, 21.98; ESI-MS (negative mode) : *m/z* calcd for $C_{78}H_{132}N_6O_{54}$; 2017.8905 found 2016.7890 (*M* -H)$^-$.

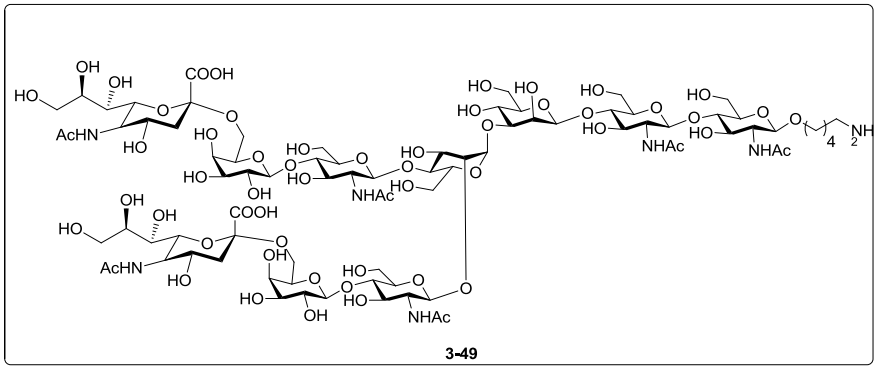

3-49

5-Aminopentyl-di-{[5-Acetamido-3,5-dideoxy-D-glycero-α-D-galacto-2-nonulopyranosylonate-(2→6)-β-D-galactopyranosyl-(1→4)-2-acetamido-2-deoxy-β-D-glucopyranosyl]-(1→2),(1→4)-α-D-mannopyranosyl}-(1→3)-β-D-mannopyranosyl-(1→4)-2-acetamido-2-deoxy-β-D-glucopyranosyl-(1→4)-2-acetamido-2-deoxy-β-D-glucopyranoside (3-49): Compound **3-35** (2 mg, 0.0012 mmol) was sialylated with α–2,6-sialyltransferase by following general procedure 2 for 2 days to get the desired title compound **3-49** (1.5 mg,

55%) as white solid. ^{1}HNMR (600 MHz, D_2O): δ 5.16 (s, 1H), 4.62 (d, *J* = 7.8 Hz, 1H), 5.58 (d, *J* = 8.4 Hz, 1H), 4.51 (d, *J* = 8.4 Hz, 1H), 4.47 (dd, *J* = 3.6 Hz, 8.4 Hz, 2H), 4.23 (dd, *J* = 3.6 Hz, 8.2 Hz, 2H), 4.03-3.40 (m, 64H), 2.99 (t, *J* = 8.2 Hz, 2H), 2.70 (dd, *J* = 4.8 Hz, 12.2 Hz, 2H), 2.12 (s, 3H), 2.11 (s, 3H), 2.09 (s, 3H), 2.05 (s, 9H), 1.76-1.67 (m, 3H), 1.62-1.59 (m, 2H), 1.44-1.40 (m, 2H); ^{13}CNMR (150 MHz, D_2O) : δ 177.6, 177.4, 177.3, 177.2, 177.1, 176.2, 106.3, 104.2, 104.1, 103.7, 102.9, 102.8, 102.6, 102.1, 101.8, 83.5, 83.0, 83.0, 82.0, 81.4, 80.9, 78.9, 78.7, 72.2, 76.4, 75.2, 75.1, 75.1, 75.0, 74.8, 74.7, 74.8, 74.4, 73.4, 73.2, 72.9, 72.8, 71.1, 70.9, 70.8, 68.7, 66.0, 65.3, 64.0, 63.5, 63.1, 62.8, 57.7, 57.3, 54.6, 42.8, 42.0, 32.9, 30.7, 29.1, 25.2, 25.0, 24.8, 24.7, 24.6; ESI-MS (negative mode) : *m/z* calcd for $C_{83}H_{139}N_7O_{57}$ 2145.8193; found 1071.9093 $(M-H)^{2-}$.

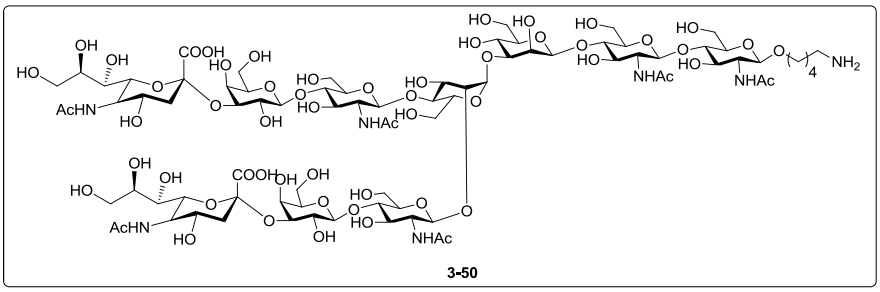

5-Aminopentyl-di-{[5-Acetamido-3,5-dideoxy-D-glycero-α-D-galacto-2-nonulopyranosylonate-(2→3)-β-D-galactopyranosyl-(1→4)-2-acetamido-2-deoxy-β-D-glucopyranosyl]-(1→2),(1→4)-α-D-mannopyranosyl}-(1→3)-β-D-mannopyranosyl-(1→4)-2-acetamido-2-deoxy-β-D-glucopyranosyl-(1→4)-2-acetamido-2-deoxy-β-D-glucopyranoside(3-50): Compound **3-35** (2 mg, 0.0012 mmol) was sialylated with α–2,3-sialyltransferase by following general procedure 2 for 8 days to get the desired title compound **3-50** (2.0 mg, 70%) as white solid. ^{1}HNMR (600 MHz, D_2O): δ 5.14 (s, 1H), 4.61 (d, *J* = 7.8 Hz, 1H), 4.58-4.56 (m, 5H), 4.51 (d, *J* = 8.4 Hz, 1H), 4.23 (dd, *J* = 2.4 Hz, *J* = 12.2 Hz, 2H), 4.13 (dd, *J* = 3.0 Hz, *J* = 12.0 Hz, 2H), 4.10-3.98 (m, 58H), 3.00 (t, *J* = 12.6 Hz, 2H), 2.78 (dd, *J* = 4.8 Hz, *J* = 12.2 Hz, 2H), 2.12 (s, 3H), 2.09 (s, 3H), 2.08 (s, 3H), 2.05 (s, 9H), 1.82 (t, *J* = 12Hz, 2H), 1.71-1.66 (m, 2H), 1.62-1.60 (m, 2H), 1.44-1.40 (m, 2H); ^{13}CNMR (150 MHz, D_2O) : δ 177.7, 177.3, 177.3, 177.2, 177.1, 176.6, 176.5, 105.6, 105.3, 104.2, 104.1, 103.7, 102.6, 102.5, 102.4, 102.3, 101.8, 99.1, 82.9, 82.0, 81.4, 81.2, 81.0, 80.9, 90.6, 78.9, 78.7, 78.1, 78.0, 77.8, 77.5, 77.2, 75.6, 75.2, 75.1, 74.8, 74.6, 74.5, 73.6, 73.1, 73.0, 72.9,

71.8, 71.2, 71.1, 70.8, 70.2, 70.0, 68.9, 66.0, 65.3, 64.0, 63.7, 63.5, 62.8, 62.6, 57.8, 57.7, 57.5, 54.9, 54.5, 54.4, 30.7, 29.0, 24.1, 24.8, 24.7, 24.5, 24.4; ESI-MS (negative mode): *m/z* calcd for $C_{83}H_{139}N_7O_{57}$ 2145.8193; found 1071.8075 $(M\text{-H})^{2-}$.

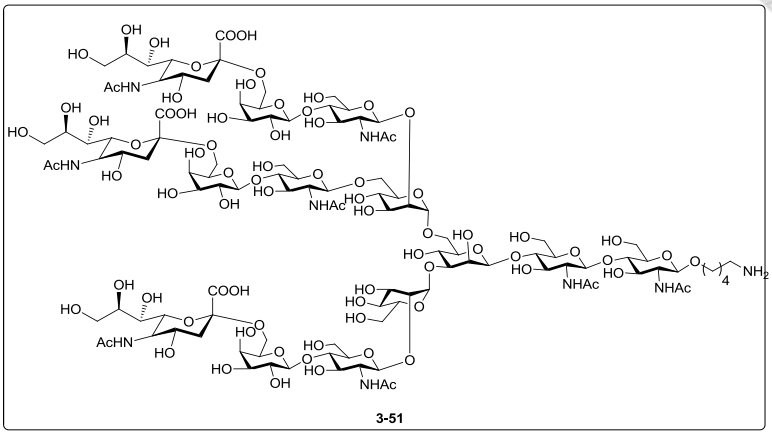

5-Aminopentyl-[5-Acetamido-3,5-dideoxy-D-glycero-α-D-galacto-2-nonulopyranosyl onate -(2→6)-β-D-galactopyranosyl-(1→4)-2-acetamido-2-deoxy-β-D-glucopyranosyl-(1→2)-α-D-mannopyranosyl]-(1→3)]-di-{[5-Acetamido-3,5-dideoxy-D-glycero-α-D-galacto-2-nonulop-yrano-sylonate-(2→6)-β-D-galactopyranosyl-(1→4)-2-acetamido-2-deoxy-β-D-glucopyran-osyl]-(1→2),(1→6)-α-D-mannopyranosyl}-(1→6)-β-D-manno pyranosyl-(1→4)-2-acetamido-2-deoxy-β-D-glucopyranosyl-(1→4)-2-acetamido-2-deoxy-β-D-glucopyranoside (3-51): Compound **3-32** (3 mg, 0.0014 mmol) was sialylated with α–2,6-sialyltransferase by following general procedure 2 for 2 days to get desired title compound **3-51** (2.8 mg, 66%) as white solid. ^{1}HNMR (600 MHz, D_2O): δ 5.07 (d, *J* = 7.8 Hz, 1H), 4.94 (d, *J* = 7.8 Hz, 1H), 4.86 (s, 2H), 4.69 (s, 1H), 4.62 (t, *J* = 8.4 Hz, 2H), 4.51 (d, *J* = 7.8 Hz, 1H), 4.48-4.44 (m, 3H), 4.32-4.24 (m, 4H), 4.03-3.90 (m, 86H), 3.00 (t, *J* = 12 Hz, 2H), 2.76-2.68 (m, 3H), 2.16 (s, 3H), 2.15 (s, 3H), 2.14 (s, 3H), 2.10 (s, 3H), 2.09 (s, 3H), 2.07 (s, 9H), 1.76-1.66 (m, 5H), 1.63-1.59 (m, 2H), 1.44-1.40 (m, 2H); ^{13}CNMR (150 MHz, D_2O): δ 175.0, 174.99, 174.90, 174.8, 174.5, 174.3, 174.0, 173.6, 173.5, 173.4, 103.4, 103.41, 103.3, 101.5, 101.3, 100.9, 100.6, 100.5, 100.3, 100.2, 100.20, 100.1, 96.9, 80.5, 80.4, 79.6, 78.2, 77.7, 76.6, 75.9, 75.4, 75.0, 74.5, 74.5, 73.6, 73.4, 72.6, 72.5, 72.3, 72.1, 71.9, 71.6, 70.8, 70.7, 70.5, 70.4, 70.2, 69.7, 68.3, 68.2, 68.1, 67.7, 66.6, 65.1, 65.0, 64.1, 63.2, 63.0, 62.6, 62.5, 62.4, 62.3, 61.7, 60.3, 60.2, 60.1, 59.9, 55.3, 55.2, 54.9, 54.8,

51.8, 40.1, 40.10, 40.0, 39.2, 30.1, 28.0, 26.3, 22.7, 22.6, 22.4, 22.3, 22.1, 22.0, 21.9; ESI-MS (negative mode) : *m/z* calcd for $C_{114}H_{189}N_9O_{80}$ 2964.0998; found 1481.0471 $(M\text{-H})^{2-}$.

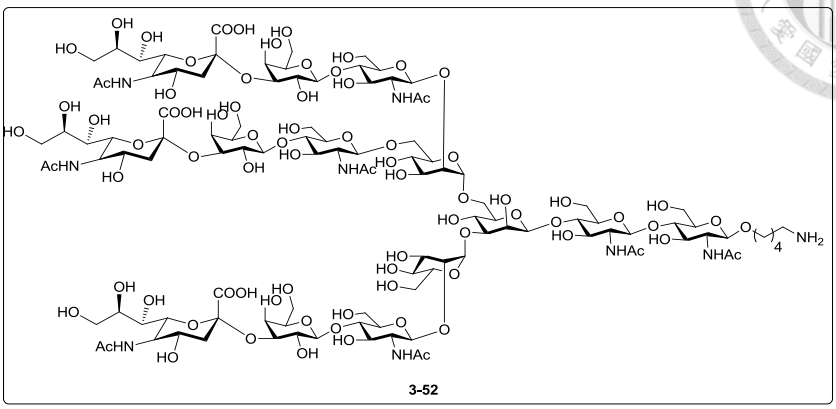

3-52

5-Aminopentyl-[5-Acetamido-3,5-dideoxy-D-glycero-α-D-galacto-2-nonulopyranosyl onate -(2→3)-β-D-galactopyranosyl-(1→4)-2-acetamido-2-deoxy-β-D-glucopyranosyl-(1→2)-α-D-mannopyranosyl]-(1→3)]-di-{[5-Acetamido-3,5-dideoxy-D-glycero-α-D-galacto-2-nonulop-yrano-sylonate-(2→3)-β-D-galactopyranosyl-(1→4)-2-acetamido-2-deoxy-β-D-glucopyran-osyl]-(1→2),(1→6)-α-D-mannopyranosyl}-(1→6)-β-D-manno pyranosyl-(1→4)-2-acetamid-o-2-deoxy-β-D-glucopyranosyl-(1→4)-2-acetamido-2-deoxy-β-D-glucopyranoside (3-52) : Compound **3-32** (4 mg, 0.0019 mmol) was sialylated with α–2,3-sialyltransferase by following general procedure 2 for 8 days to get the desired title compound **3-52** (3.7 mg, 66%) as white solid. ^{1}HNMR (600 MHz, D_2O): δ 5.03 (d, *J* = 7.9 Hz, 1H), 4.89 (d, *J* = 7.2 Hz, 1H), 4.85 (d, *J* = 13.2 Hz, 1H), 4.64 (s, 1H), 4.62 (d, *J* = 7.2 Hz, 1H), 4.57-4.53 (m, 3H), 4.49 (d, *J* = 7.8 Hz, 2H), 4.30 (s, 1H), 4.27 (d, *J* = 3.2 Hz, 1H), 4.24-4.23 (m,, 2H), 4.17-4.10 (m,7H), 4.01-3.89 (m, 8H), 4.88-3.80 (m, 14H), 3.79-3.50 (m, 57H), 2.98 (t, *J* = 8.4 Hz, 2H), 2.75 (dd, *J* = 4.8, 12 Hz, 3H), 2.07 (s, 3H), 2.06 (s, 3H), 2.02 (s, 18H), 1080 (t, *J* = 12.2 Hz, 3H), 1.69-1.64 (m, 2H), 1.60-1.57 (m, 2H), 1.42-1.38 (m, 2H); ^{13}CNMR (150 MHz, D_2O) : δ 177.7, 177.5, 177.1, 177.0, 176.6, 105.5, 105.3, 105.30, 104.1, 103.9, 103.8, 10.7, 103.2, 102.6, 102.5, 82.0, 81.3, 81.0, 79.3, 79.0, 78.1, 77.8, 77.6, 77.3, 77.2, 77.1, 75.6, 75.2, 75.1, 74.9, 74.8, 74.6, 74.5, 74.4, 72.8, 71.1, 70.8, 70.5, 70.2, 65.3, 64.8, 63.7, 62.8, 62.7, 58.0, 57.9, 57.8, 57.7, 54.5, 54.4, 42.6, 42.0, 30.7, 29.1, 29.4, 25.3, 25.1, 24.9, 24.8, 24.81, 24.7; ESI-MS (negative mode): *m/z* calcd for $C_{114}H_{189}N_9O_{80}$ 2964.0998; found 1481.0535 $(M\text{-H})^{2-}$.

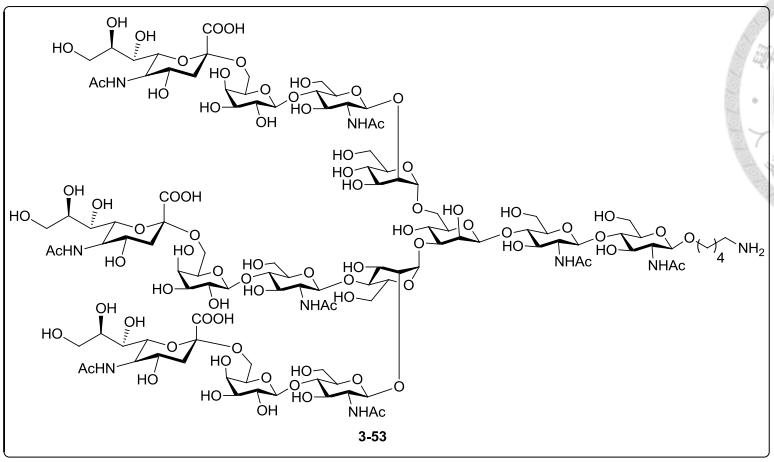

5-Aminopentyl-di-{[5-Acetamido-3,5-dideoxy-D-glycero-α-D-galacto-2-nonulopyrano sylonate-(2→6)-β-D-galactopyranosyl-(1→4)-2-acetamido-2-deoxy-β-D-glucopyra nosyl]-(1→2),(1→4)-α-D-mannopyranosyl}-(1→3)-[5-Acetamido-3,5-dideoxy-D-gly cero-α-D-galacto-2-nonulopyrano-sylonate-(2→6)-β-D-galactopyranosyl-(1→4)-2-acetamido-2-deoxy-β-D-glu-copyranosyl]-(1→2)-α-D-mannopyranosyl]-(1→6)-β-D-mannopyranosyl-(1→4)-2-acetami-do-2-deoxy-β-D-glucopyranosyl-(1→4)-2-acetami do-2-deoxy-β-D-glucopyranoside (3-53) : Compound **3-38** (5.3 mg, 0.0025 mmol) was sialylated with α–2,6-sialyltransferase by following general procedure 2 for 2 days to get the desired title compound **3-53** (4.8 mg, 64%) as white solid. ^{1}HNMR (600 MHz, D_2O): 5.16 (s, 1H), 4.96 (s, 1H), 4.62 (d, *J* = 7.2 Hz, 2H), 4.59 (d, *J* = 7.8 Hz, 2H), 4.51 (d, *J* = 8.4 Hz, 1H), 4.45 (t, *J* = 12.1 Hz, 3H), 4.24 (s, 2H), 4.14 (s, 1H), 4.02-3.48 (m, 87H), 3.01 (t, *J* = 7.8 Hz, 2H), 2.70-2.68 (m, 3H), 2.16 (s, 3H), 2.15 (s, 3H), 2.14 (s, 3H), 2.12 (s, 3H), 2.07 (s, 12H), 1.76-1.69 (m, 5H), 1.62-1.60 (m, 2H), 1.44-1.40 (m, 2H); ^{13}CNMR (150 MHz, D_2O): δ 177.6, 177.45, 177.44, 177.38, 177.35, 177.15, 176.2, 106.3, 104.1, 104.10, 103.7, 103.0, 102.9, 102.8, 102.4, 101.9, 101.8, 99.7, 83.5, 83.3, 83.1, 83.0, 82.3, 82.0, 80.0, 78.9, 78.7, 77.2, 77.1, 77.0, 76.4, 75.5, 75.2, 75.1, 75.0, 74.8, 74.81, 74.0, 73.4, 73.4, 73.1, 72.1, 7.8, 70.0, 68.9, 69.5, 67.8, 65.3, 65.2, 64.3, 64.0, 63.0, 62.9, 62.8, 62.6, 57.7, 57.6, 57.5, 57.3, 57.2, 54.6, 42.8, 42.0, 30.7, 29.0, 25.2, 25.1, 25.0, 24.9, 24.8, 24.7; ESI-MS (negative mode): *m/z* calcd for $C_{114}H_{189}N_9O_{80}$ 2964.0998; found 1481.5483 $(M-H)^{2-}$.

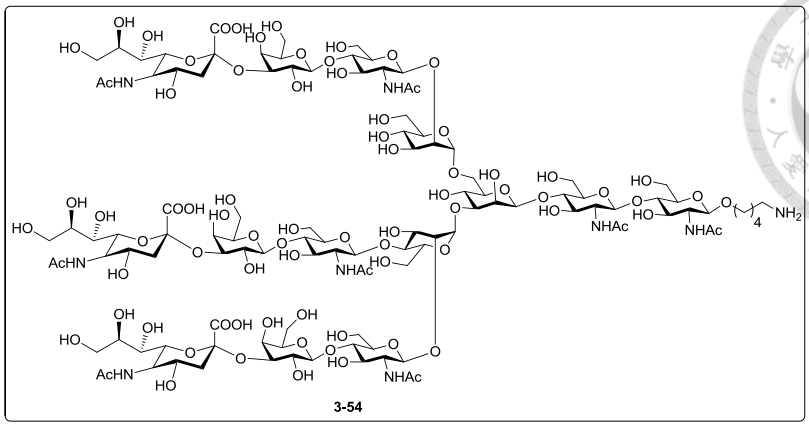

3-54

5-Aminopentyl-di-{[5-Acetamido-3,5-dideoxy-D-glycero-α-D-galacto-2-nonulopyranosylonate-(2→3)-β-D-galactopyranosyl-(1→4)-2-acetamido-2-deoxy-β-D-glucopyranosyl]-(1→2),(1→4)-α-D-mannopyranosyl}-(1→3)-[5-Acetamido-3,5-dideoxy-D-glycero-α-D-gal-acto-2-nonulopyrano-sylonate-(2→3)-β-D-galactopyranosyl-(1→4)-2-acetamido-2-deoxy-β-D-gl-ucopyranosyl]-(1→2)-α-D-mannopyranosyl]-(1→6)-β-D-mannopyranosyl-(1→4)-2-acetam-ido-2-deoxy-β-D-glucopyranosyl-(1→4)-2-acetamido-2-deoxy-β-D-glucopyranoside (3-54): Compound **3-38** (4 mg, 0.0019 mmol) was sialylated with α–2,3-sialyltransferase by following general procedure B for 8 days to get the desired title compound **3-54** (3.7 mg, 66%) as white solid. ^{1}HNMR (600 MHz, D_2O): δ 5.13 (s, 1H), 4.93 (s, 1H), 4.62-4.56 (m, 7H), 4.51 (d, *J* = 7.2 Hz, 1H), 4.23 (s, 2H), 4.13 (d, *J* = 8.4 Hz, 4H), 4.10-3.79 (m, 84H), 3.00 (t, *J* = 8.4 Hz, 2H), 2.77 (dd, *J* = 3.2 Hz, *J* = 7.8 Hz, 3H), 2.19 (s, 3H), 2.5 (s, 3H), 2.10 (s, 9H), 2.06 (s, 9H), 1.82 (t, *J* = 8.4 Hz, 3H), 1.71-1.66 (m, 2H), 1.62-1.60 (m, 2H), 1.44-1.40 (m, 2H); ^{13}CNMR (150 MHz, D_2O) : δ 175.0, 174.6, 174.4, 102.6, 102.5, 102.3, 101.5, 101.0, 99.8, 99.5, 99.4, 99.0, 97.0, 80.2, 79.4, 79.2, 78.2, 77.9, 76.2, 76.0, 75.4, 74.8, 74.6, 74.3, 72.8, 72.3, 72.1, 72.0, 71.9, 71.7, 70.0, 69.3, 68.3, 68.0, 67.4, 67.3, 65.7, 62.5, 61.6, 61.2, 60.0, 59.9, 55.1, 54.9, 54.8, 51.6, 39.6, 39.3, 28.0, 26.3, 22.3, 22.2, 22.1; ESI-MS (negative mode): *m/z* calcd for $C_{114}H_{189}N_9O_{80}$ 2964.0998; found 1481.0524 $(M-H)^{2-}$.

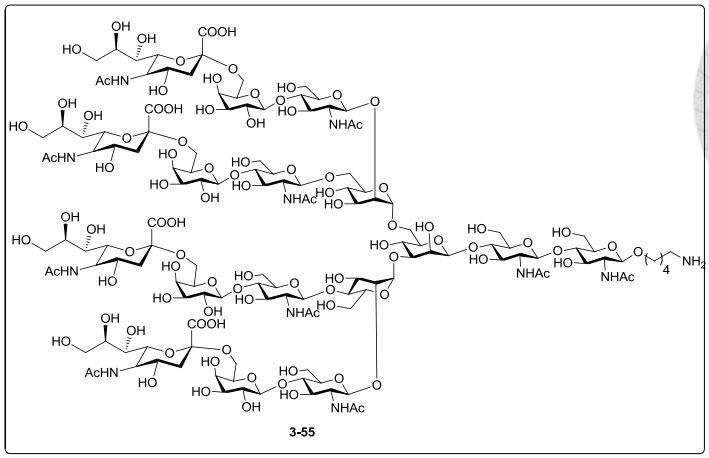

5-Aminopentyl-di-{[5-Acetamido-3,5-dideoxy-D-glycero-α-D-galacto-2-nonulopyrano-syl-onate-(2→6)-β-D-galactopyranosyl-(1→4)-2-acetamido-2-deoxy-β-D-glucopyrano syl]-(1→2),(1→4)-α-D-mannopyranosyl}-(1→3)- di-{[5-Acetamido-3,5-dideoxy-D-glycero-α-D-galacto-2-nonulopyrano-sylonate-(2→6)-β-D-galactopyranosyl-(1→4)-2-acetamido-2-deoxy -β-D-glucopyranosyl]-(1→2),(1→6)-α-D-mannopyranosyl}-(1→6)-β-D-mannopyranosyl(1→4)-2-acetamido-2-deoxy-β-D-glucopyranosyl-(1→4)-2-aceta mido-2-deoxy-β-D-glucop-yranoside (3-55): Compound **3-40** (4.0 mg, 0.0016 mmol) was sialylated with α–2,6-sialyltransferase by following general procedure 2 for 2 days to get the desired title compound **32** (3.5 mg, 60%) as white solid. ^{1}HNMR (600 MHz, D_2O): δ 5.16 (s, 1H), 4.92 (s, 1H), 4.61-4.56 (m, 5H), 4.50 (d, *J* = 12.2 Hz, 1H), 5.48-4.45 (m, 4H), 4.25-1.24 (m, 2H), 4.12-3.51 (m, 107H), 3.00 (t, *J* = 7.5 Hz, 2H), 2.70 (dd, *J* = 4.2 Hz, *J* = 12.6 Hz, 4H), 2.12 (s, 3H), 2.11 (s, 3H), 2.09 (s, 3H), 2.05 (s, 6H), 2.03 (s, 15H), 1.76-1.66 (m, 6H), 1.62-1.59 (m, 2H), 1.44-1.41 (m, 2H); ^{13}CNMR (150 MHz, D_2O) : δ 177.6, 177.4, 177.3, 177.1, 176.2, 173.7, 106.3, 104.2, 104.1, 103.7, 102.9, 102.1, 101.8, 99.9, 98.9, 83.6, 83.1, 82.0, 79.0, 77.2, 77.1, 75.2, 75.1, 74.8, 74.6, 74.4, 73.4, 72.9, 72.7, 71.1, 70.9, 68.3, 66.0, 65.3, 63.1, 63.0, 62.8, 62.7, 57.6, 57.5, 57.4, 56.9, 54.6, 46.5, 42.8, 42.0, 30.7, 29.0, 25.3, 25.2, 25.0, 24.8, 24.8, 24.7, 20.6; ESI-MS (negative mode): *m/z* calcd for $C_{139}H_{229}N_{11}O_{98}$ 3620.3274; found 1809.6702 $(M-H)^{2-}$.

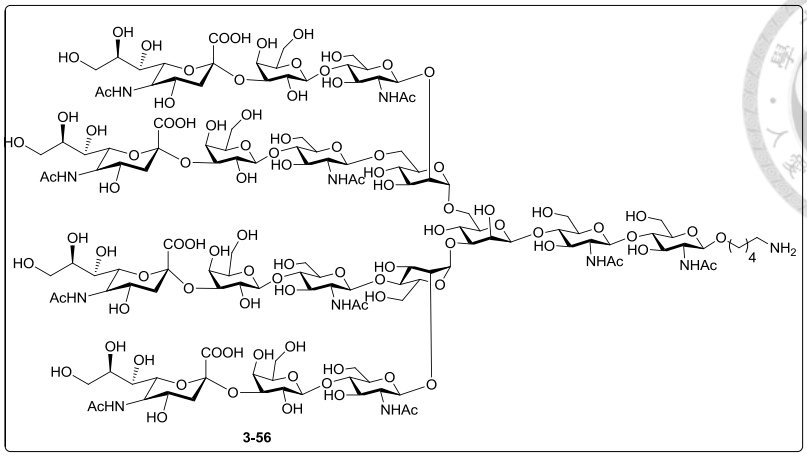

5-Aminopentyl-di-{[5-Acetamido-3,5-dideoxy-D-glycero-α-D-galacto-2-nonulopyrano-syl-onate-(2→3)-β-D-galactopyranosyl-(1→4)-2-acetamido-2-deoxy-β-D-glucopyrano syl]-(1→2),(1→4)-α-D-mannopyranosyl}-(1→3)- di-{[5-Acetamido-3,5-dideoxy-D-glycero-α-D-galac-to-2-nonulopyrano-sylonate-(2→3)-β-D-galactopyranosyl-(1→4)-2-acetamido-2-deoxy-β-D -glucopyranosyl]-(1→2),(1→6)-α-D-mannopyranosyl}-(1→6)-β-D-mannopyranosyl-(1→4)-2-acetamido-2-deoxy-β-D-glucopyranosyl-(1→4)-2-acetamido-2-deoxy-β-D-glucopyranoside (3-56) : Compound **3-40** (4.0 mg, 0.0016 mmol) was sialylated with α–2,6-sialyltransferase by following general procedure 2 for 8 days to get the desired title compound **3-56** (4.1 mg, 70%) as white solid. ^{1}HNMR (600 MHz, D_2O): δ 5.13 (s, 1H), 4.60-4.51(m, 6H), 5.48-4.45 (m, 7H), 4.25-3.45 (m, 107H), 2.98 (t, *J* = 7.8 Hz, 2H), 2.65 (dd, *J* = 4.0 Hz, *J* = 12.0 Hz, 4H), 2.09 (s, 3H), 2.05 (s, 6H), 2.03 (s, 21H), 1.76-1.70 (m, 4H), 1.66-1.64 (m, 2H), 1.62-1.59 (m, 2H), 1.44-1.41 (m, 2H); ^{13}CNMR (150 MHz, D_2O) : δ 177.3, 177.2, 177.0, 176.8, 176.2, 173.6, 106.0, 105.2, 104.1, 103.7, 102.9, 102.1, 101.8, 99.9, 98.9, 83.6, 83.1, 82.0, 79.0, 77.2, 77.1, 75.2, 75.1, 74.8, 74.6, 74.4, 73.4, 72.9, 72.7, 71.1, 70.9, 68.3, 66.0, 65.3, 63.1, 63.0, 62.8, 62.7, 57.6, 57.5, 57.4, 56.9, 54.6, 46.5, 42.8, 42.0, 31.0, 25.1, 24.9, 24.8, 24.7; ESI-MS (negative mode): *m/z* calcd for $C_{139}H_{229}N_{11}O_{98}$ 3620.3274; found 1809.1649 $(M\text{-H})^{2-}$ and 1205.7736 $(M\text{-H})^{3-}$.

6.4. Experimental for Chapter 4

Synthesis of Glycans with Phosphonic Acid Tails.

General Procedure 3:

To a solution of sugars with amine tail **2-22**, **2-27**, **2-30**, **2-32**, **2-35**, **2-48**, **3-33**, **3-28**, **3-41**, **3-44**, and **3-45** (3 µmol) in DMF (400 µl) was added linker [2(2(2(bis(benzyloxy)phosphoryl)ethoxy ethoxy)ethyl(2,5-dioxopyrrolidin-1-yl)carbonate] (15 µmol), resulting reaction mixture was stirred at room temperature for 5 h. DMF was removed by using high vacuum and product was purified was purified by using Bio-Gel P-2 chromatography (eluent H_2O). Solid was dissolved in 2 mL of H_2O , added $Pd(OH)_2$ (50% by weight) and hydrogenate for overnight. Reaction mixture was filtered through celite and concentrated in *vacuo*. The residue was purified by Bio-Gel P-2 (BIO-RAD) column chromatography using water as eluent. Product was the lypholysed to get desired sugars **4-1** to **4-11** with phosphonic acid tail as white color powder.

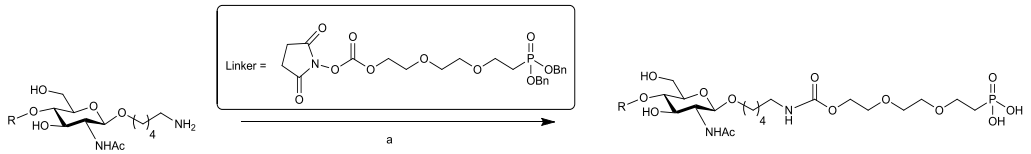

Scheme 6.1: Preparation of sugars with phosphonic acid linker. a, (1) Linker, DMF, r t, 5h; (2) $Pd(OH)_2$, H_2O , room temperature, overnight

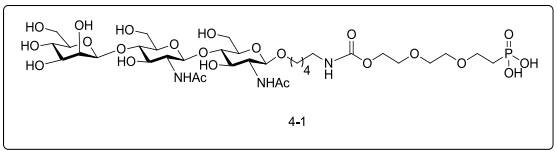

β-D-mannopyranosyl-(1→4)-2-acetamido-2-deoxy-β-D-glucopyranosyl-(1→4)-2-acetamido -2-deoxy-β-D-glucopyranoside (4-1): Compound **2-22** (3.5 mg, 5.4 µmol) was undergone reducing end transformation by following procedure 3 to afford compound **4-1** (2.2 mg, 61%), as white solid. TLC (MeOH : EA : AcOH : H_2O, 7/1/1/1, v/v). ^{1}HNMR (600 MHz, D_2O) : δ 4.60 (d, *J* = 8.4 Hz, 1H), 4.48 (d, *J* = 7.8 Hz, 1H), 4.19 (s, 2H), 4.05 (d, *J* = 3.2 Hz, 1H), 3.93-3.49 (m, 33H), 1.75 (t, *J* = 7.8 Hz, 2H), 2.06 (s, 3H), 1.95 (s, 3H),

1.95-1.92 (m, 2H), 1.58-1.54 (m, 2H), 1.50-1.47 (m, 2H), 1.33-1.30 (m, 2H). HRMS (MALDI-TOF) : *m/z* calcd for $C_{34}H_{59}N_3O_{23}PNa_2$; 954.3067 found 954.3099 (M+2Na).

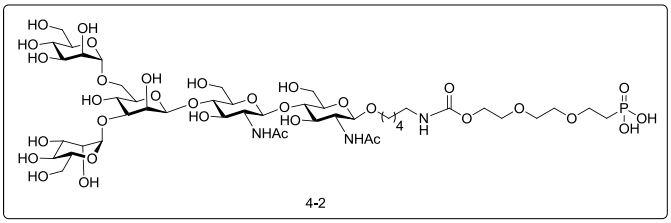

(Phosphonate-tri-(ethyleneglycol)-carbonyl-amino)-pentyl-α-D-mannopyranosyl(1→3)-α-D-mannopyranosyl]-(1→6)-β-D-mannopyranosyl-(1→4)-2-acetamido-2-deoxy-β-D-gluco-pyranosyl-(1→4)-2-acetamido-2-deoxy-β-D-glucopyranoside (4-2): Compound **2-27** (4 mg, 2.3 μmol) was undergone reducing end transformation by following procedure 3 to afford compound **4-2** (3.2 mg, 71%), as white solid. TLC (MeOH : EA : AcOH : H_2O, 7/1/1/1, v/v). ^{1}HNMR (600 MHz, D_2O) : δ 5.01 (s, 1H), 4.83 (s, 1H), 4.51 (d, *J* = 6.1 Hz, 1H), 4.40 (d, *J* = 6.2 Hz, 1H), 4.17 (s, 1H), 4.11 (s, 2H), 3.98 (s, 1H), 3.88-3.39 (m, 52H), 3.03 (t, *J* = 7.8 Hz, 2H), 1.99 (s, 3H), 1.95 (s, 3H), 1.95-1.91 (m, 2H), 1.50-1.45 (m, 2H), 1.42-1.38 (m, 2H), 1.26-1.22 (m, 2H). HRMS (MALDI-TOF) Negative mode : *m/z* calcd for $C_{58}H_{102}N_3O_{43}PNa_2$; 1280.4484 found 1278.5001 $(M+2Na-2H)^-$.

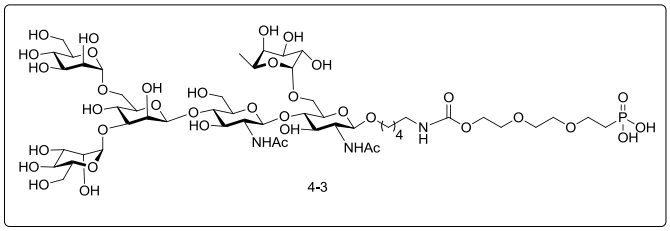

(Phosphonate-tri-(ethyleneglycol)-carbonyl-amino)-pentyl-α-D-mannopyranosyl(1→3)-α-D-mannopyranosyl]-(1→6)-β-D-mannopyranosyl-(1→4)-2-acetamido-2-deoxy-β-D-glucop-yranosyl-(1→4)-)-(α-L-fucopyranosyl-(1→6)-2-acetamido-2-deoxy-β-D-gluco pyranoside) (4-3): Compound **2-48** (1.2 mg, 1.0 μmol) was undergone reducing end transformation by following procedure 3 to afford compound **4-3** (1.0mg, 91%), as white solid. TLC (MeOH : EA : AcOH : H_2O, 7/1/1/1, v/v). ^{1}HNMR (600 MHz, D_2O) : δ 5.09 (s, 1H), 4.90 (s, 1H), 4.88 (d, *J* = 7.4 Hz, 1H), 4.66 (d, *J* = 7.5 Hz, 1H), 4.48 (d, *J* = 7.2 Hz, 1H), 4.25 (s, 1H), 4.19 (s, 2H), 4.12-4.10 (m, 1H), 4.06 (s, 1H), 3.95 (s, 1H), 3.92-3.84 (m, 10H), 3.79-3.69 (m, 31H), 3.11-3.09 (m, 2H), 2.08 (s, 3H), 2.02 (s, 3H), 1.99-1.93 (m, 2H),

1.58-1.53 (m, 2H), 1.49-1.47 (m, 2H), 1.34-1.30 (m, 2H), 1.22 (d, 3H). HRMS (MALDI-TOF) : *m/z* calcd for $C_{34}H_{59}N_3O_{23}PNa_3$; 1450.5709.3067 found 1450.5709 (M+3Na).

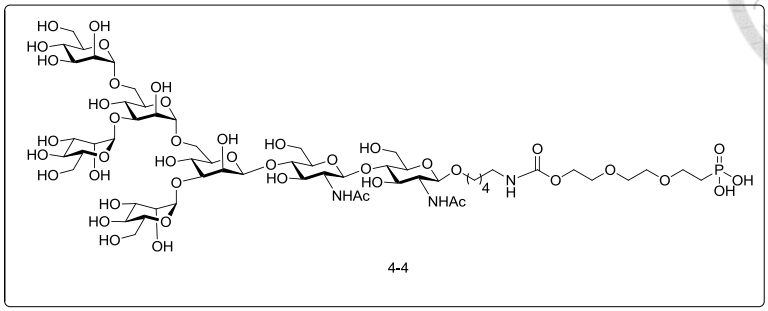

***(Phosphonate-tri-(ethyleneglycol)-carbonyl-amino)-pentyl-α-D-manno-pyranosyl (1→3), [di-(α-D-mannopyranosyl)-(1→3),(1→6)-α-D-mannopyranosyl]-(1→6)-β-D-mannopyranosyl -(1→4)-2-acetamido-2-deoxy-β-D-glucopyranosyl-(1→4)-2-acetamido-2-deoxy-β-D-glucop-yranoside (4-4)* :** Compound **2-30** (4 mg, 3.1 μmol) was undergone reducing end transformation by following procedure 3 to afford compound **4-4** (3.7 mg, 78%), as white solid. TLC (MeOH : EA : AcOH: H_2O, 7/1/1/1, v/v). ^{1}HNMR (600 MHz, D_2O): δ 5.10 (d, *J* = 9.6 Hz, 2H), 4.93 (s, 1H), 4.70 (s, 1H), 4.57 (d, *J* = 7.2 Hz, 1H), 4.48 (d, *J* = 7.8 Hz, 1H), 4.24 (d, *J* = 3.2 Hz, 2H), 4.19-4.13 (m, 4H), 4.06-4.04 (m, 3H), 3.95-3.40 (m, 45H), 3.38-3.37 (m, 1H), 2.10 (t, *J* = 7.8 Hz, 2H), 2.07 (s, 6H), 2.02 (s, 6H), 1.98-1.93 (m, 2H), 1.58-1.47 (m, 2H), 1.34-1.29 (m, 2H), 1.27-1.25 (m, 2H); HRMS (MALDI-TOF) : *m/z* calcd for $C_{58}H_{102}N_3O_{43}PNa_2$; 1606.3985 found 1607.0452 $(M+2Na+H)^+$.

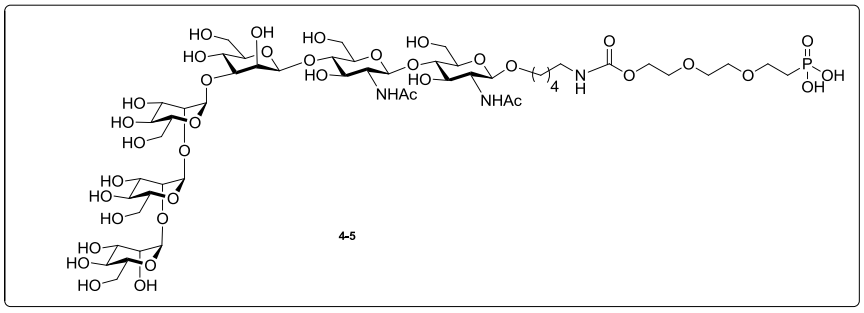

(Phosphonate-tri-(ethylene glycol)-carbonyl-amino)-pentyl-α-D-mannopyranosyl-(1→2)-α-D-mannopyranosyl-(1→2)-α-D-mannopyranosyl-(1→3)-β-D-mannopyranosyl-(1→4)-2-acetamido-2-deoxy-β-D-glucopyranosyl-(1→4)-2-acetamido-2-deoxy-β-D-glucopyranoside (4-5): Compound **2-32** (5 mg, 4.4 μmol) was undergone reducing end transformation by following procedure 3 to afford compound **4-5** (3.5 mg, 58%), as white

solid. TLC (MeOH : EA : AcOH : H_2O, 7/1/1/1, v/v). ^{1}HNMR (600 MHz, D_2O) : δ 5.34 (s, 1H), 5.29 (s, 1H), 5.03 (s, 1H), 4.58 (d, J = 7.8 Hz, 1H), 4.47 (d, J = 7.8 Hz, 1H), 4.20 (bs, 3H), 4.09-4.05 (m, 3H), 3.90-3.20 (m, 41H), 3.10 (t, J = 7.8 Hz, 2H), 2.05 (s, 3H), 2.01 (s, 3H), 2.00-1.92 (m, 2H), 1.56-1.53 (m, 2H), 1.49-1.46 (m, 2H), 1.33-1.30 (m, 2H); HRMS (MALDI-TOF) : *m/z* calcd for $C_{52}H_{92}N_3O_{38}PNa_2$; 1444.2579 found 1444.5470 $(M + 2Na)^+$.

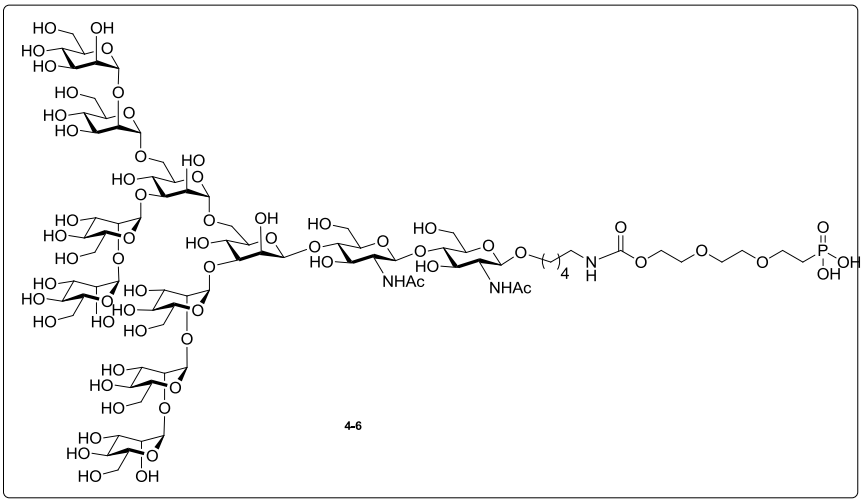

(Phosphonate-tri-(ethyleneglycol)-carbonyl-amino)-pentyl-α-D-mannopyranosyl-(1→2)-α-D-mannopyranosyl-(1→2)-α-D-manno-pyranosyl-(1→3)-{α-D-mannopyranosyl-(1→2)-α-D-mannopyranosyl-(1→3)-[α-D-manno-pyranosyl-(1→2)-α-D-mannopyranosyl-(1→6)]-α-D-mannopyranosyl-(1→6)}-β-D-manno-pyranosyl-(1→4)-2-acetamido-2-deoxy-β-D-glucopyranosyl-(1→4)-2-acetamido-2-deoxy-β-D-glucopyranoside (4-6): Compound **2-35** (4 mg, 2.0 μmol) was undergone reducing end transformation by following procedure 3 to afford compound **4-6** (3.7 mg, 66%), as white solid. TLC (MeOH : EA : AcOH : H_2O, 7/1/1/1, v/v). ^{1}HNMR (600 MHz, D_2O) : δ 5.53 (s, 1H), 5.39 (d, *J* = 10.2 Hz, 1H), 5.26 (d, *J* = 9.8 Hz, 1H), 5.23 (s, 1H), 5.16 (d, *J* = 4.8 Hz, 1H), 5.08-5.05 (m, 5H), 4.60 (d, *J* = 7.8 Hz, 1H), 4.50 (d, *J* = 7.8 Hz, 1H), 2.08 (s, 3H), 2.02 (s, 3H), 1.38-1.03 (m, 2H), 1.58-1.56 (m, 2H), 1.52-1.48 (m, 2H), 1.35-1.32 (m, 2H); HRMS (MALDI-TOF) : *m/z* calcd for $C_{82}H_{142}N_3O_{63}PNa_2$; 2255.0310 found 2257.0812 $(M + 2Na+H)^+$.

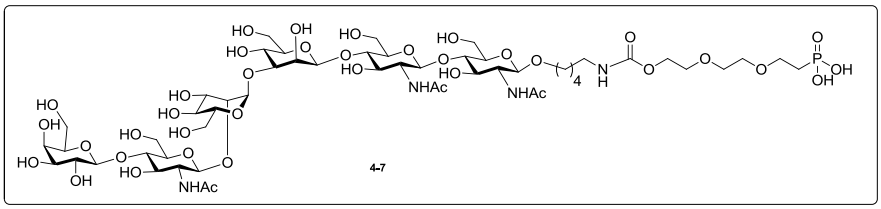

(Phosphonate-tri-(ethyleneglycol)-carbonyl-amino)-pentyl-β-D-galactopyranosyl-(1→4)-2-acetamido-2-deoxy-β-D-glucopyranosyl-(1→2)-α-D-mannopyranosyl]-(1→3)-β-D-mannop-yranosyl-(1→4)-2-acetamido-2-deoxy-β-D-glucopyranosyl-(1→4)-2-acetamido-2-deoxy-β-D -glucopyranoside (4-7): Compound **3-33** (6 mg, 5.1 μmol) was undergone reducing end transformation by following procedure 3 to afford compound **4-7** (3.5 mg, 50%), as white solid. TLC (MeOH : EA : AcOH : H_2O, 7/1/1/1, v/v). ^{1}HNMR (600 MHz, D_2O) : δ 5.03 (d, *J* = 8.4 Hz, 2H), 4.58 (d, *J* = 7.2 Hz, 1H), 4.48 (d, *J* = 7.2 Hz, 1H), 4.45 (d, *J* = 7.8 Hz, 1H), 4.26 (dd, *J* = 3, 9.2Hz, 2H), 4.19 (bs, 2H), 4.00-3.38 (m, 48H), 3.11 (t, *J* = 7.8 Hz, 2H), 2.06 (s, 3H), 2.05 (s, 3H), 2.02 (s, 3H), 1.99-1.93 (m, 2H), 1.56-1.54 (m, 2H), 1.50-1.48 (m, 2H), 1.31-1.27 (m, 2H); HRMS (MALDI-TOF) : *m/z* calcd for $C_{54}H_{92}N_4O_{38}PNa_2$; 1481.4917 found 1481.5069 $(M + 2Na)^+$.

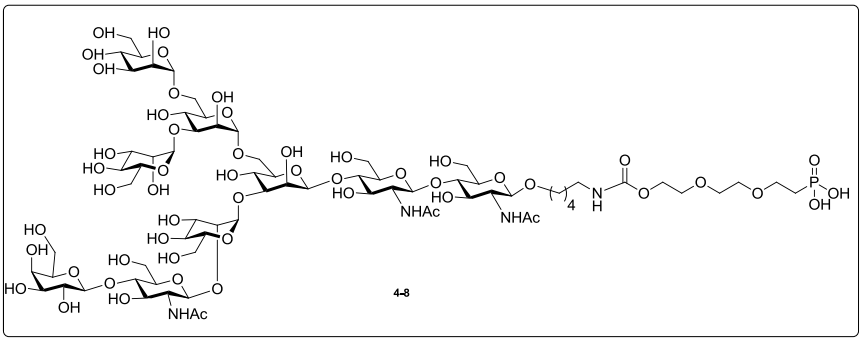

(Phosphonate-tri-(ethyleneglycol)-carbonyl-amino)-pentyl-β-D-galactopyranosyl-(1→4)-[2-acetamido-2-deoxy-β-D-gluco-pyranosyl-(1→2)-α-D-mannopyranosyl-(1→3),[di-(α-D-ma-nnopyranosyl)-(1→3),(1→6)-α-D-manno-pyranosyl](1→6)-β-D-manno pyranosyl-(1→4)-2-acetamido-2-deoxy-β-D-gluco-pyranosyl-(1→4)-2-acetamido-2-deoxy-β-D-glucopyranoside (4-8): Compound **3-28** (5 mg, 3.0 μmol) was undergone reducing end transformation by following procedure 3 to afford compound **4-8** (3.1 mg, 54%), as white solid. TLC (MeOH : EA : AcOH : H_2O, 7/1/1/1, v/v). ^{1}HNMR (600 MHz, D_2O): δ 5.11 (s, 2H), 5.02 (d, *J* = 7.8 Hz, 2H), 4.68 (d, *J* = 3.2 Hz, 2H), 4.48 (d, *J* = 7.2 Hz, 1H), 4.45 (d, *J* = 7.2 Hz, 1H), 4.27 (s, 2H), 4.22 (s, 2H), 4.15 (s, 1H), 4.08 (s, 2H), 4.00-3.30 (m, 60H), 3.10 (t, *J* = 7.8 Hz, 2H), 2.08 (s, 3H), 2.05 (s, 3H), 2.02 (s, 3H), 1.93-1.87 (m, 2H), 1.56-1.54 (m, 2H), 1.51-1.47 (m, 2H), 1.33-1.30 (m, 2H); HRMS (MALDI-TOF) : *m/z* calcd for $C_{72}H_{122}N_4O_{53}PNa_2$; 1967.6502 found 1967.6622 $(M + 2Na)^+$.

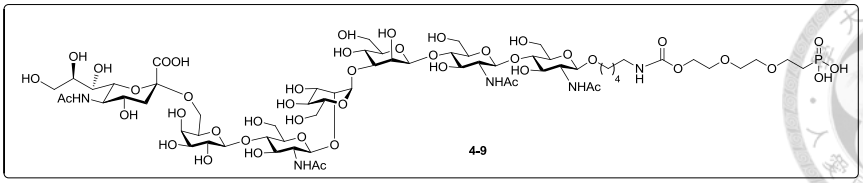

Phosphonate-tri-(ethyleneglycol)-carbonyl-amino)-pentyl-[5-Acetamido-3,5-dideoxy-D-glycero-α-D-galacto-2-nonulopyrano-sylonate-(2→6)-β-D-galactopyranosyl-(1→4)-2-acet-amido-2-deoxy-β-D-glucopyranosyl-(1→2)-α-D-mannopyranosyl]-(1→3)-β-D-mannopyranosyl-(1→4)-2-acetamido-2-deoxy-β-D-gluco-pyranosyl-(1→4)-2-acetamido-2-deoxy-β-D-glucopyranoside (4-9)S: Compound **3-41** (5 mg, 2.5 μmol) was undergone reducing end transformation by following procedure 3 to afford compound **4-9** (3.8 mg, 63%), as white solid. TLC (MeOH : EA : AcOH : H_2O, 7/1/1/1, v/v). ^{1}HNMR (600 MHz, D_2O) : δ 5.08 (d, *J* = 8.4 Hz, 2H), 4.93 (s, 1H), 4.62 (d, *J* = 7.2 Hz, 1H), 4.51 (d, *J* = 7.8 Hz, 1H), 4.45 (d, *J* = 7.8Hz, 1H), 4.30 (d, *J* = 3.2Hz, 1H), 4.28 (s, 1H), 4.22 (s, 2H), 4.02-3.30 (m, 53H), 3.13 (t, *J* = 7.8 Hz, 2H), 2.68 (dd, *J* = 3.2 & 7.8 Hz, 1H), 2.09 (s, 6H), 2.05 (s, 6H), 2.01-1.93 (m, 2H), 1.74 (t, *J* = 12.1 Hz, 1H), 1.60-1.57 (m, 2H), 1.54-1.51 (m, 2H), 1.35-1.32 (m, 2H); HRMS (MALDI-TOF) : *m/z* calcd for $C_{65}H_{109}N_5O_{46}PNa_2$; 1772.5871 found 1772.5817 $(M + 2Na)^+$.

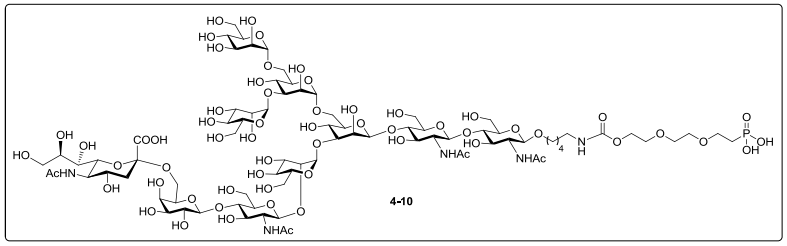

(Phosphonate-tri-(ethyleneglycol)-carbonyl-amino)-pentyl-5-Acetamido-3,5-dideoxy-D-glycero-α-D-galacto-2-nonulopyrano-sylonate-(2→6)-β-D-galactopyranosyl-(1→4)-[2-aceta-mido-2-deoxy-β-D-glucopyranosyl-(1→2)-α-D-mannopyranosyl-(1→3),[di-(α-D-mannopy-ranosyl)-(1→3),(1→6)-α-D-manno-pyranosyl](1→6)-β-D-mannopyranosyl-(1→4)-2-acetam-ido-2-deoxy-β-D-glucopyranosyl-(1→4)-2-acetamido-2-deoxy-β-D-glucopyranoside (4-10): Compound **3-45** (4 mg, 2.3 μmol) was undergone reducing end transformation by following procedure 3 to afford compound **4-10** (3.2 mg, 71%), as white solid. TLC (MeOH : EA : AcOH : H_2O, 7/1/1/1, v/v). ^{1}HNMR (600 MHz, D_2O) : δ 5.08 (d, *J* = 12.2 Hz, 1H), 5.03 (s, 1H), 4.94 (s, 2H), 4.91 (s, 1H), 4.62 (s, 1H), 4.51 (d, *J* = 6.6 Hz,

1H), 4.46 (d, *J* = 7.8 Hz, 1H), 4.30 (s, 2H), 4.25 (s, 2H), 4.17 (s, 1H), 4.06 (s, 1H), 4.00-3.20 (m, 70H), 2.70 (dd, *J* = 3.2, 7.8 Hz, 1H), 2.11 (s, 6H), 2.05 (s, 6H), 2.03-1.97 (m, 2H), 1.14 (t, *J* = 12.6 Hz, 1H), 1.58-1.51 (m, 4H), 1.36-1.31 (m, 2H). HRMS (MALDI-TOF) : *m/z* calcd for $C_{83}H_{144}N_5O_{61}PNa_2$; $(M+2Na-5H)^{2-}$ 1148.2301 found 1148.2946.

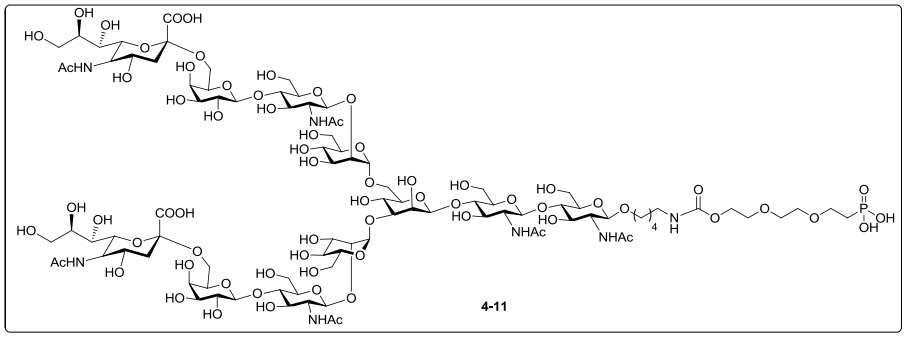

Phosphonate-tri-(ethyleneglycol)-carbonyl-amino)-pentyl-di-[5-Acetamido-3,5-dideoxy-D-glycero-α-D-galacto-2-nonulopyrano-sylonate-(2→6)-β-D-galactopyranosyl-(1→4)-2-acet-amido-2-deoxy-β-D-glucopyranosyl-(1→2)-α-D-mannopyranosyl]-(1→3),(1→6)-β-D-mann-opyranosyl-(1→4)-2-acetamido-2-deoxy-β-D-glucopyranosyl-(1→4)-2-acetamido-2-deoxy-β -D-glucopyranoside (4-11): Compound **3-45** (3.5 mg, 1.5 μmol) was undergone reducing end transformation by following procedure **3** to afford compound **4-11** (2.6 mg, 69%), as white solid. TLC (MeOH : AcOH : H_2O, 8/1/1, v/v). ^{1}HNMR (600 MHz, D_2O) : δ 5.05 (d, *J* = 8.4 Hz, 1H), 4.63 (d, *J* = 6.6 Hz, 1H), 4.51 (s, 1H), 4.46 (t, *J* = 7.8 Hz, 2H), 4.32 (s, 1H), 4.29 (s, 2H), 4.22 (s, 2H), 4.09-3.48 (m, 79H), 3.13 (t, *J* = 7.8 Hz, 2H), 2.74-2.68 (m, 2H), 2.10 (s, 9H), 2.05 (s, 9H), 2.12-2.00 (m, 2H), 1.76-1.73 (m, 2H), 1.58-1.55 (m, 2H), 1.51-1.50 (m, 2H), 1.35-1.29 (m, 2H); HRMS (MALDI-TOF negative mode) : *m/z* calcd for $C_{96}H_{162}N_7O_{69}PNa$; 2570.9096 found 1294.9685 $(M+Na-2H)^{2-}$.

6.5. Experimental for Chapter 5

Preparation of Oligosaccharide Half Esters:

For conjugation to carrier protein, hybrid type structure 5-4 was activated by forming p-nitophenyl half ester using general procedure 4.

General Procedure 4:

Pentyl amine equipped 5-**4** (4-5 μmol) was dissolved in anhydrous dimethylformamide (DMF) solution. Then, *p*-nitrophenyl ester linker (20-25 μmol) was added and stirred for 5 h at room temperature. The reaction was monitored by thin layer chromatography (TLC) (5:3:1:1, MeOH/EtOAc/H2O/AcOH) and cerium test. The disappearance of free amine indicated the completion of the reaction. The reaction mixture was evaporated under reduced pressure without heating to remove DMF. Reaction mixture was dissolved in 500 μl H_2O, insoluble excess of linker was separated by filtration and water soluble fraction was purified by P2 BIO-GEL (Bio-Rad) column chromatography and gradually eluted with H2O.The solution was then lyophilized to afford a light yellow colored solid.

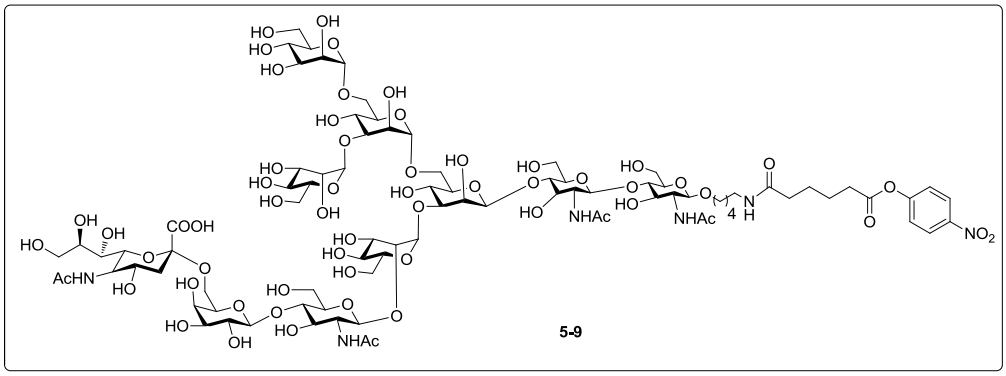

p-Nitro phenyl half ester of hybrid series glycan 5-9:

Compound **5-4** (5.5 mg, 2.8 μmol) was activated using general procedure **4** to afford compound **5-12** (3.8 mg, 61%), as pale yellow solid. TLC (MeOH : EtOAc : AcOH : H_2O, 6/2/1/1, v/v). ^{1}HNMR (600 MHz, D_2O) : δ 8.34 (d, *J* = 9 Hz, 2H), 7.37 (d, *J*= 9 Hz, 2H), 5.07 (s, 1H), 5.04 (s, 1H), 4.90 (d, *J*= 3.4 Hz, 1H), 4.88 (d, *J*= 3.2 Hz, 1H), 4.55 (d, *J*= 7.8 Hz, 1H), 4.42 (dd, *J*= 2.4 , 8.4Hz, 2H), 4.27 (dd, *J* = 2.4, 8.2 Hz, 2H), 4.14 (s, 1H), 4.06-4.04 (m, 1H), 2.72 (t, *J*= 7.8 Hz, 2H), 2.67 (dd, *J*= 4.8, 12 Hz, 1H), 2.29 (t, *J* = 7.8 Hz, 2H),

2.07 (s, 3H), 2.06 (s, 3H), 2.01 (s, 3H), 2.00 (s, 3H), 1.75-1.68 (m, 5H), 1.58-1.47 (m, 6H), 1.33-1.25 (m, 2H); HRMS (MALDI-TOF) : *m/z* calcd for $C_{88}H_{140}N_6O_{59}$; 2223.8120 found 1224.8358 $(M + H)^+$.

Preparation of Glycoconjugate 1:

General Procedure 5:

Diphtheria toxoid cross-reactive material $(CRM)_{197}$-DT protein (purchased from Merck) was dissolved in 100 mM phosphate buffer, pH 8.1 (~5 mg/mL), and 40–50 equivalents of half ester (**5-9**) was added to the solution. The mixture was stirred gently for 24 h at room temperature. The mixture was then diluted with deionized water and dialyzed against five changes of deionized water. The solution was then lyophilized to a white powder. The obtained glycan–protein conjugate **1**, was characterized by MALDI-TOF analysis to determine the carbohydrate incorporation rate and bicinchoninic acid (BCA) assay was done to calculate the amount of protein.

Selective Modification of DT-CRM_{197} with Maleimide Linker:

The salt of commercial CRM197 (1.0 mg) was removed by dissolving in water and dialyzing (10 kDa, Ultra-0.5; Amicon) for 3-4 times. The residue was dissolved in PBS buffer (pH 6.5, 1.0 mL) and transferred into a sample vial. Sulfo-EMCS (1.0 mg, 8.22 × 10−6 mol) was added to the solution, and then, the reaction was kept stirring at room temperature for 2 h. The mixture was purified by Amicon Ultra-0.5 (10 kDa). MALDI-TOF MS analysis was performed to determine the molecular and the bicinchoninic acid (BCA) assay was done to calculate the amount of protein. The difference between the molecular weights of $DTCRM_{197}$ before and after the modification was used to determine the number of linkers conjugated. The $DTCRM_{197}$-maleimid conjugate was stored in PBS buffer (pH 7.2, 1.0 mg/mL) for further use at 4°C.

Preparation of Oligosaccharides with Thiol Linker:

General Procedure 6:

To a solution of glycans **5-2, 5-3, 5-5, 5-7**, and **5-8 (~**5 μmol**)** in PBS buffer (pH 7.4, 1.0 mL) was added 3,3'-dithiobis[sulfosuccinimidylpropionate] (DTSSP) (10 μmol) at room

temperature. The pH of reaction mixture was adjusted to 7.4 by addition of 1N NaOH slowly. After the reaction was stirred for overnight, DTT (40 μmol) was added to the solution and kept stirring at 40°C for 2h. The solvent was then evaporated under reduced pressure and reside was purified by Bio-Gel P2 chromatography using water as eluent to afford the desired compounds **5-11, 5-12, 5-13, 5-14**, and **5-15** respectively as white color power.

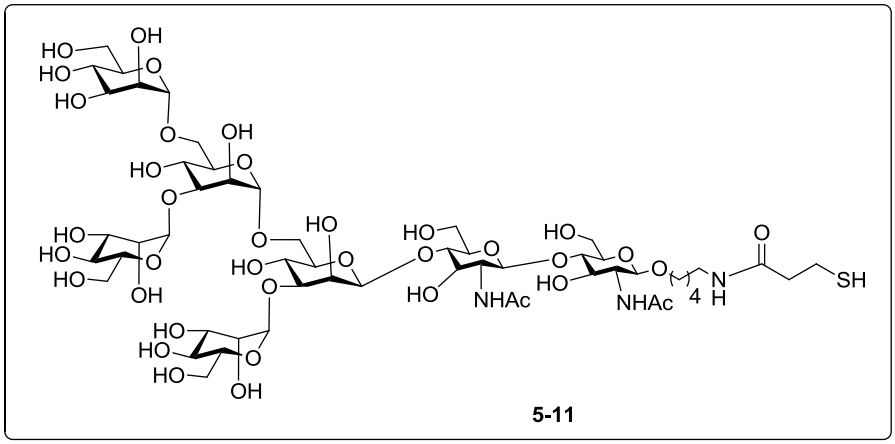

5-11

Preparation of Compound 5-11:

Compound **5-2** (5mg, 3.9 μmol) was modified by using general procedure 6 to get desired product (4mg, 75%), as a white solid.TLC (MeOH : EtOAc : AcOH : H_2O, 5/3/1/1, v/v). ^{1}HNMR (600 MHz, D_2O) : δ 5.08 (dd, *J* =1.2, 3.6 Hz, 2H), 4.89 (d, *J* = 1.8 Hz, 1H), 4.86 (dd, *J* = 2.0Hz, 1H), 4.57 (d, *J* = 7.8 Hz, 1H), 4.47 (d, *J* = 8.4 Hz, 1H), 4.24 (d, *J* = 2.4 Hz, 1H), 4.14-4.13 (m, 1H), 4.07-4.03 (m, 2H), 3.95-3.57 (m, 40H), 3.47-3.43 (m, 1H), 3.20-3.17 (m, 2H), 2.76 (t, *J* = 7.2Hz, 2H), 2.52 (t, *J* = 7.3 Hz, 2H), 2.07 (s, 3H), 2.02 (s, 3H), 1.56-1.50 (m, 4H), 1.35-1.32 (m, 2H); HRMS (MALDI-TOF) : *m/z* calcd for $C_{54}H_{93}N_3O_{37}S$; 1407.5287 found 1408.5312 $(M + H)^+$.

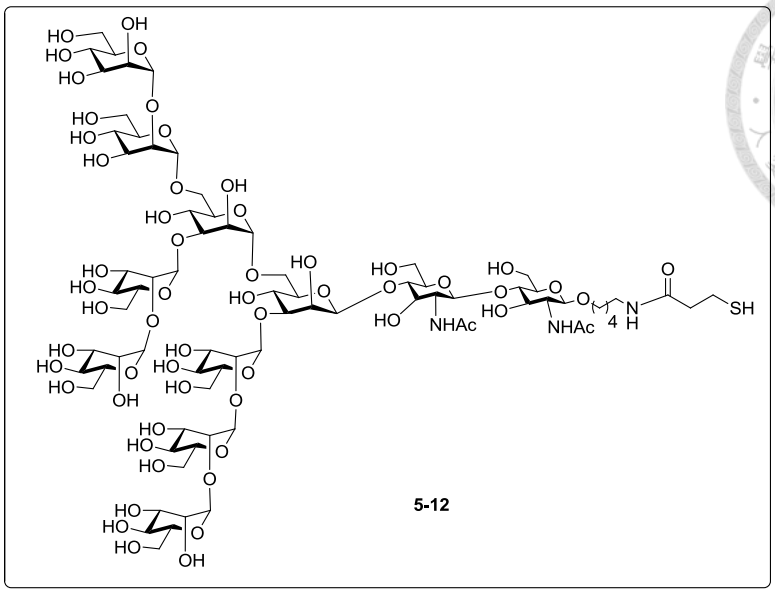

Preparation of Compound 5-12:

Compound **5-3** (6mg, 3.1 μmol) was modified by using general procedure 6 to get desired product (4.8mg, 77%), as a white solid.TLC (MeOH : EtOAc : AcOH : H_2O, 5/3/1/1, v/v). ^{1}HNMR (600 MHz, D_2O) : δ 5.40-5.27 (m, 2H), 5.21-5.12 (m, 1H), 5.06-5.01 (m, 5H), 4.58 (d, *J* = 7.8 Hz, 1H), 4.48 (d, *J* = 7.9 Hz, 1H), 4.25 (d, *J* = 3.4 Hz, 1H), 4.17-4.06 (m, 11H), 4.40-3.94 (m, 57H), 3.21-3.16 (m, 2H), 2.76 (t, *J* = 7.2Hz, 2H), 2.52 (t, *J* = 7.3 Hz, 2H), 2.07 (s, 3H), 2.00 (s, 3H), 1.52-1.49 (m, 4H), 1.36-1.32 (m, 2H); HRMS (MALDI-TOF) : *m/z* calcd for $C_{78}H_{133}N_3O_{57}SNa$; 2078.7214 found 2078.7310 $(M + Na)^+$.

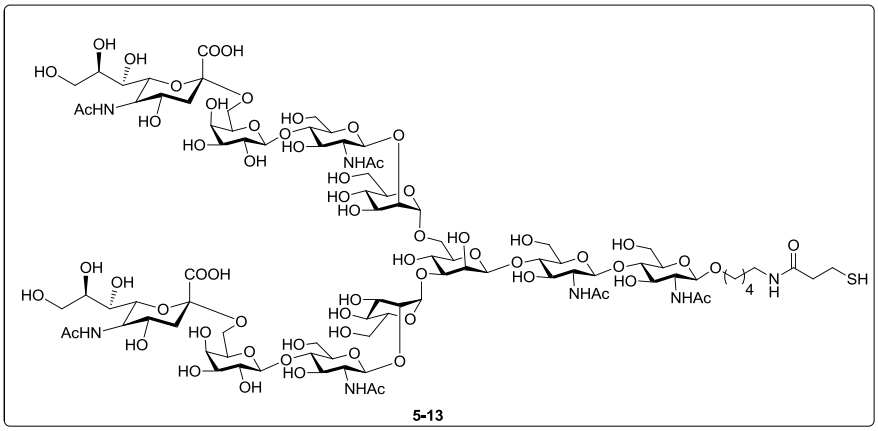

Preparation of Compound 5-13:

Compound **5-5** (5mg, 2.1 μmol) was modified by using general procedure 6 to get desired product (4.2mg, 94%), as a white solid.TLC (MeOH : EtOAc : AcOH : H_2O, 7/1/1/1, v/v).

^{1}HNMR (600 MHz, D_2O) : δ 5.02 (d, *J* = 7.8 Hz, 2H), 4.60 (d, *J* = 7.8 Hz, 1H), 4.49-4.42 (m, 3H), 4.29-4.25 (m, 3H), 4.10-3.48 (m, 70H), 3.20-3.17 (m, 2H), 2.78 (t, *J* = 7.2 Hz, 2H), 2.68 (m, 2H), 2.53 (t, *J* = 7.4 Hz, 2H), 2.08 (s, 3H), 2.06 (s, 3H), 2.05 (s, 3H), 2.03 (s, 6H), 2.02 (s, 3H), 1.73-1.68 (m, 2H), 1.57-1.49 (m, 4H), 1.35-1.32 (m, 2H); HRMS (MALDI-TOF negative mode) : *m/z* calcd for $C_{92}H_{153}N_7O_{63}SNa$; 2419.8654 found 2417.8938 $(M + Na\text{-}2H)^-$.

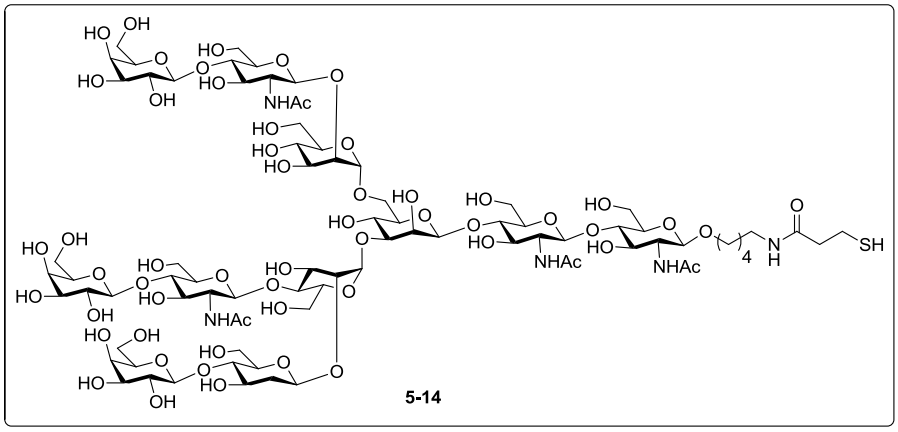

Preparation of Compound 5-14:

Compound **5-7** (7mg, 3.5 μmol) was modified by using general procedure 6 to get desired product (5.5mg, 72%), as a white solid.TLC (MeOH : EtOAc : AcOH : H_2O, 6/2/1/1, v/v). ^{1}HNMR (600 MHz, D_2O) : δ 5.10 (s, 1H), 4.91 (s, 1H), 4.59-4.52 (m, 4H), 4.49-4.45 (m, 4H), 4.20 (t, *J* = 4.8 Hz, 2H), 4.10 (d, *J* = 3.2 Hz, 1H), 4.10-3.47 (s, 66H), 3.20-3.17 (m, 2H), 2.75 (t, *J* = 7.2 Hz, 2H), 2.52 (t, *J* = 7.2 Hz, 2H), 2.11 (s, 3H), 2.10 (s, 3H), 2.07 (s, 3H), 2.04 (s, 3H), 2.02 (s, 3H), 1.56-1.50 (m, 4H), 1.35-1.32 (m, 2H); HRMS (MALDI-TOF) : *m/z* calcd for $C_{84}H_{142}N_6O_{57}SNa$; 2201.8010 found 2202.8184 $(M + Na + H)^+$.

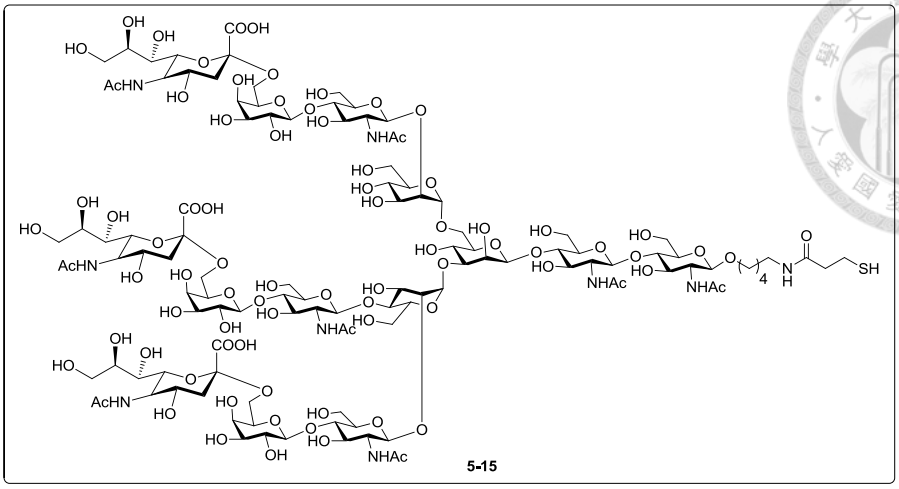

Preparation of Compound 5-15:

Compound **5-8** (3mg, 1.5 μmol) was modified by using general procedure 6 to get desired product (2.5mg, 85%), as a white solid.TLC (MeOH : EtOAc : AcOH : H_2O, 7/1/1/1, v/v). ^{1}HNMR (600 MHz, D_2O) : δ 5.12 (s, 1H), 4.93 (s, 1H), 4.60-4.55 (m, 4H), 4.48-4.42 (m, 5H), 4.21 (s, 2H), 4.10 (s, 1H), 4.05-3.47 (m, 102H), 3.20-3.17 (m, 2H), 2.76 (t, *J* = 7.2 Hz, 2H), 2.67-2.64 (m, 3H), 2.53 (t, *J* =7.3 Hz, 2H), 2.22 (s, 3H), 2.13 (s, 3H), 2.11 (s, 3H), 2.09 (s, 3H), 2.02 (s, 12H), 1.73-1.68 (m, 3H), 1.56-1.50 (m, 4H), 1.35-1.32 (m, 2H). HRMS (MALDI-TOF negative mode) : *m/z* calcd for $C_{117}H_{194}N_9O_{81}S$; 3053.7813 found 3050.5487 $(M - 3H)^-$.

Preparation of Glycoconjugates 6 and 7:

To a solution of maleimide modified DT-CRM_{197} **5-14** (1 mg/mL) in PBS buffer (pH 7.2) was added 10 equivalents of **5-15** and **5-16.** The mixtures were stirred at room temperature for 2 h. The glycans-CRM197 conjugates were purified by using Amicon Ultra-0.5 (10 kDa) to remove the nonreactive carbohydrates and sodium phosphate salt by dialysis. The obtained glycoproteins were underwent MALDI TOF MS analysis to determine incorporation rate. Glycoconjugates intermediates were dissolved in PBS buffer (pH 7.2, the concentration 1.0 mg/mL), and 10 equivalent of 2-mercaptoethanol (5 mg/mL, PBS buffer, pH 7.2) was added to the solution. The mixtures were stirred at room temperature for overnight. The final conjugates **6** and **7** were purified using Amicon Ultra-0.5 (10 kDa) to re-

move the nonreactive 2-mercaptoethanol and sodium phosphate salt by dialysis and then lyphophilized to a white powder.

Preparation of Glycoconjugates 2:

To a solution of maleimide modified DT-CRM_{197} **5-10** (1 mg/mL) in PBS buffer (pH 7.2) was added 10 equivalents of **5-11.** The mixtures were stirred at room temperature for overnight. The Man_5-CRM_{197} conjugates were purified by using Amicon Ultra-0.5 (10 kDa) to remove the nonreactive $Man_5GlcNAc_2$-SH and sodium phosphate salt by dialysis. The intermediate **5-16** underwent MALDI TOF MS analysis to determine incorporation rate. Conjugate **5-16** was dissolved in PBS buffer (pH 7.2, the concentration 1.0 mg/mL), and 20 equivalent of **5-13** was added and the resulting mixture was stirred at room temperature for overnight. The $(Man_5)_6$-CTG-CRM197 conjugates was purified by using Amicon Ultra-0.5 (10 kDa) to remove the nonreactive **5-13** and sodium phosphate salt by dialysis and glycan conjugation was confirmed by MS. To the solution of $(Man_5)_6$-$(CTG)_4$-CRM_{197} conjugates in PBS buffer was added 10 equivalents of 2-mercaptoethanol (5 mg/mL, PBS buffer, pH 7.2). The mixture were stirred at room temperature for overnight. The finally conjugates **2** was purified using Amicon Ultra-0.5 (10 kDa) to remove the nonreactive 2-mercaptoethanol and sodium phosphate salt by dialysis and then lyphophilized to a white powder.

Preparation of Glycoconjugates 3 and 4:

To a solution of maleimide modified DT-CRM_{197} **5-17** (1 mg/mL) in PBS buffer (pH 7.2) was added 10 equivalents of **5-14** or **5-15.** The mixtures were stirred at room temperature for overnight. The glycan-CRM_{197} conjugates were purified by using Amicon Ultra-0.5 (10 kDa) to remove the nonreactive thiolated oligosaccharides and sodium phosphate salt by dialysis. The glycoconjugates underwent MALDI TOF MS analysis to determine incorporation rate. To the solution of conjugates in PBS buffer was added 10 equivalents of 2-mercaptoethanol (5 mg/mL, PBS buffer, pH 7.2). The mixture was stirred at room temperature for overnight. The finally conjugates **3** and **4** were purified using Amicon Ultra-0.5 (10 kDa) to remove the nonreactive 2-mercaptoethanol and sodium phosphate salt by dialysis and then lyphophilized to a white powder.

Preparation of Glycoconjugates 5:

The experimental protocol for preparation of glycoconjugate was exactly same as described for glycoconjugate **1**.

MALDI-TOF MS Analysis for Glycoconjugates 1-5:

The glycoconjugates **1-5** and primary carrier protein DT, maleimide modified DT were re-constituted with ddH2O (~1 μg/μL). The matrix, sinapinic acid, was freshly prepared with acetonitrile and deionized water 1:1, making a final matrix concentration in 10 mg/mL including 0.1% TFA. Matrix solution and glycoconjugates were gently loaded, mixed, and air dried in the plate. Calibration was imperative using BSA before measurement. Each glycoconjugate and primary protein sample was detected under linear positive mode. The average molecular weight allows calculation of the average numbers of carbohydrate incorporated on the carrier protein.

Mice Immunization Schedule:

To investigate HIV-1 antigenicity of various glycoconjugates groups of five mice (6-wk-old female C57BL/6 mice; BioLASCO) were injected s.c. to abdomen region with glycoconjugates **1-5**, with or without C1. Three immunizations were given at 2-wk intervals. Each vaccination contained 2 μg carbohydrates with or without 2 μg adjuvant. Control mice were injected with PBS only. Mice were bled two weeks after second and third immunization. All of the sera were obtained by centrifugation at 4,000 × g for 10 min. The serologic responses were analyzed by glycan microarray.

Serologic Assay with Glycan Microarray of *N*-glycans:

Mouse sera were diluted with 3% BSA/PBS buffer (pH 7.4). The glycan microarray was blocked with 50 mM ethanolamine for 1 h and washed two times with 0.05% Tween-20 in PBS buffer (PBST buffer) before use. The serum dilutions were then introduced to the glycan microarray and incubated at room temperature for 1 h. The microarray slides were further washed three times with PBST. Next, Cy3-conjugated goat anti-mouse IgG (H + L), or antimouse IgM was added to the microarray slide and then sealed for 1-h incubation at room temperature. Finally, the slides were washed three times with PBST. The microarray slides were dried before being scanned at 532 nm with a microarray fluorescence chip reader (4000B; Genepix). Data were analyzed by the software GenePix Pro-6.0 (Axon Instruments). The local background was subtracted from the signal at each glycan spot. The spots with obvious defects or no detectable signal were omitted.

Selected Spectras

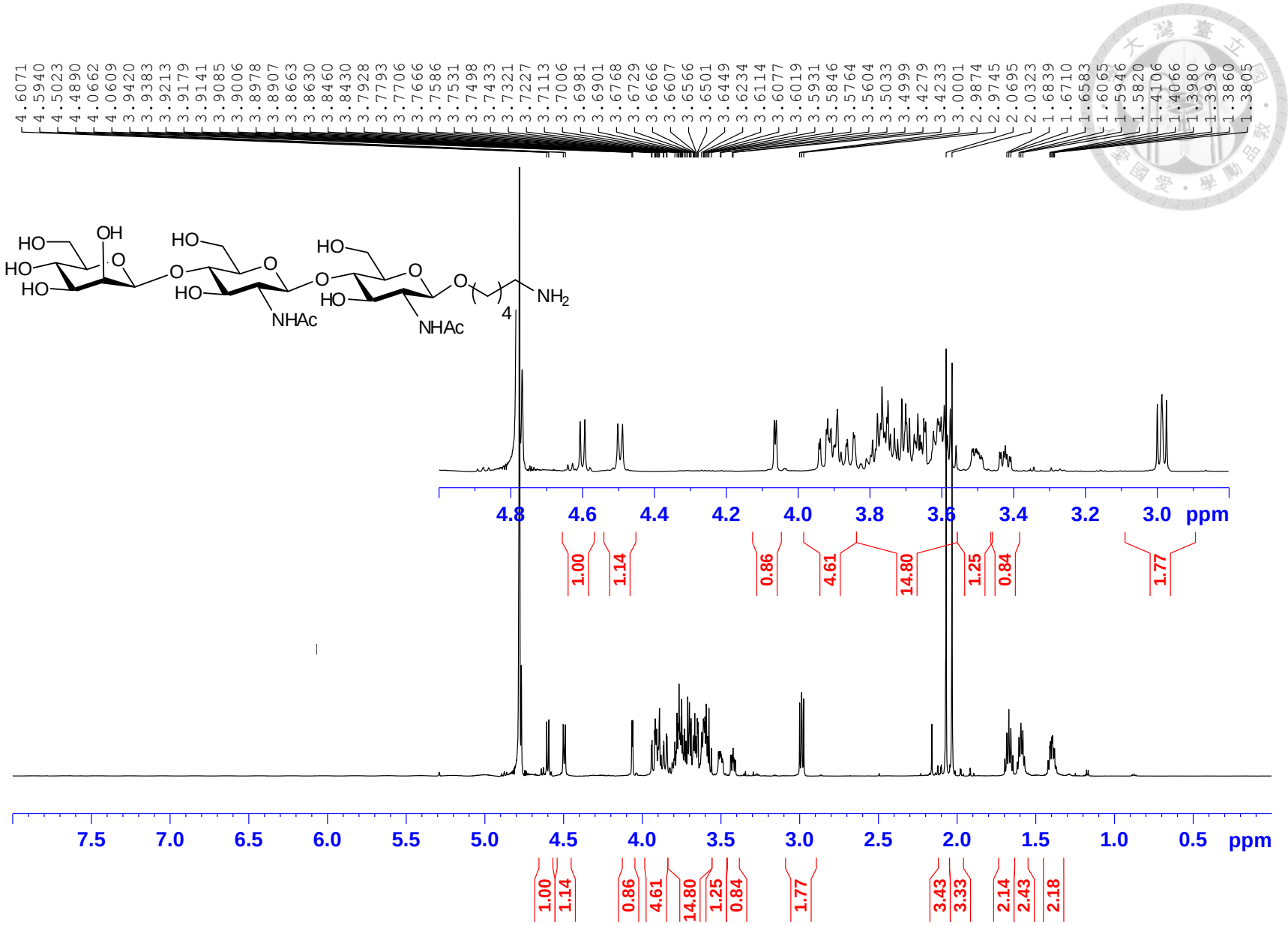
4.6071
4.5940
4.5023
4.4890
4.0662
4.0609
3.9420
3.9383
3.9213
3.9179
3.9141
3.9085
3.9006
3.8978
3.8907
3.8663
3.8630
3.8460
3.8430
3.7928
3.7793
3.7706
3.7666
3.7586
3.7531
3.7498
3.7433
3.7321
3.7227
3.7113
3.7006
3.6981
3.6901
3.6768
3.6729
3.6666
3.6607
3.6566
3.6501
3.6449
3.6234
3.6114
3.6077
3.6019
3.5931
3.5846
3.5764
3.5604
3.5033
3.4999
3.4279
3.4233
3.0001
2.9874
2.9745
2.0695
2.0323
1.6839
1.6710
1.6583
1.6065
1.5946
1.5820
1.4106
1.4066
1.3980
1.3936
1.3860
1.3805
HO
OH
O
HO
HO
O
HO
O
HO
NHAc
O
HO
HO
O
HO
NHAc
O
4
NH2
4.8
4.6
4.4
4.2
4.0
3.8
3.6
3.4
3.2
3.0
ppm
1.00
1.14
0.86
4.61
14.80
1.25
0.84
1.77
7.5
7.0
6.5
6.0
5.5
5.0
4.5
4.0
3.5
3.0
2.5
2.0
1.5
1.0
0.5
ppm
1.00
1.14
0.86
4.61
14.80
1.25
0.84
1.77
3.43
3.33
2.14
2.43
2.18

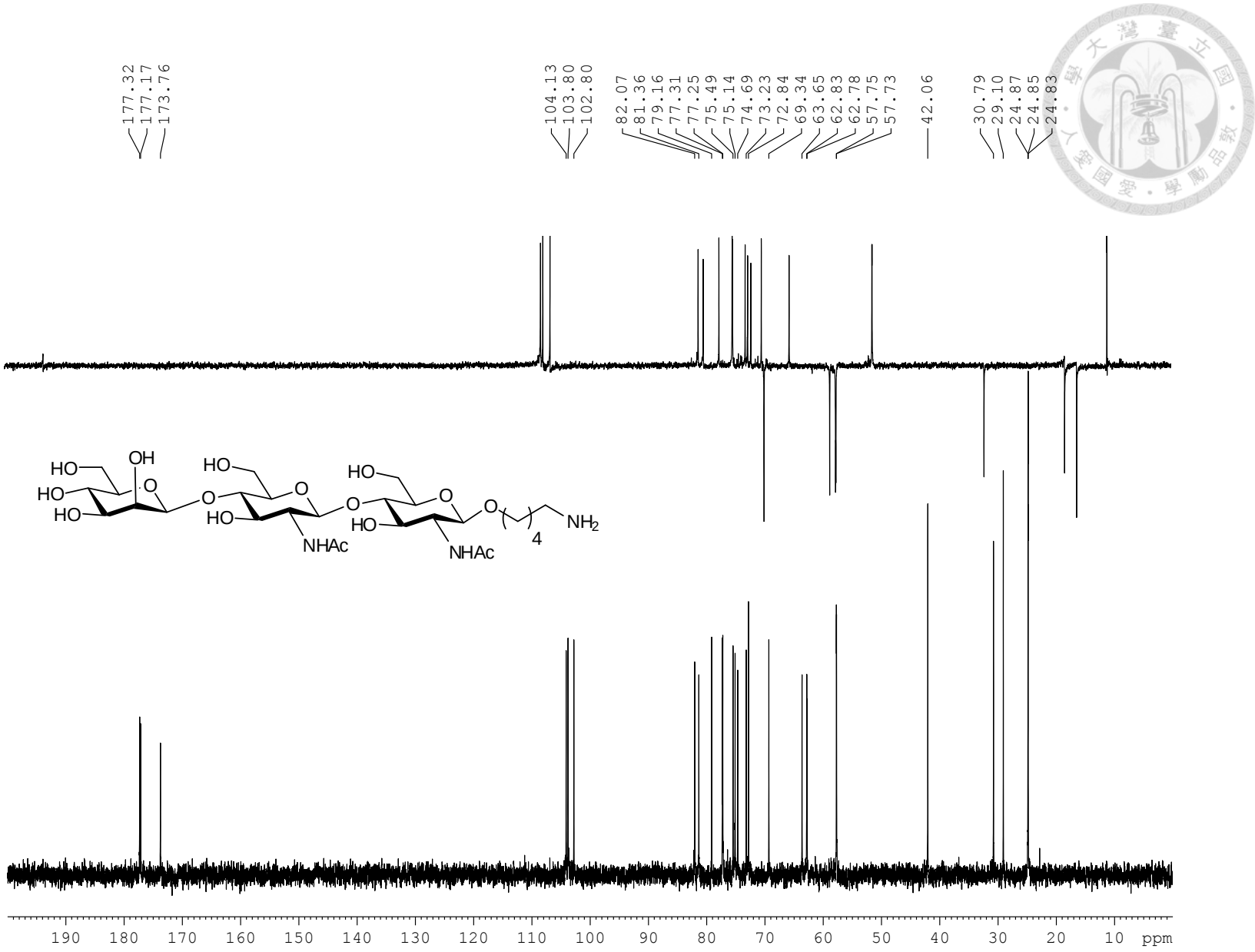
177.32
177.17
173.76
104.13
103.80
102.80
82.07
81.36
79.16
77.31
77.25
75.49
75.14
74.69
73.23
72.84
69.34
63.65
62.83
62.78
57.75
57.73
42.06
30.79
29.10
24.87
24.85
24.83
HO
OH
HO
HO
O
O
HO
O
HO
NHAc
O
HO
O
HO
NHAc
O
4
NH2
190
180
170
160
150
140
130
120
110
100
90
80
70
60
50
40
30
20
10
ppm

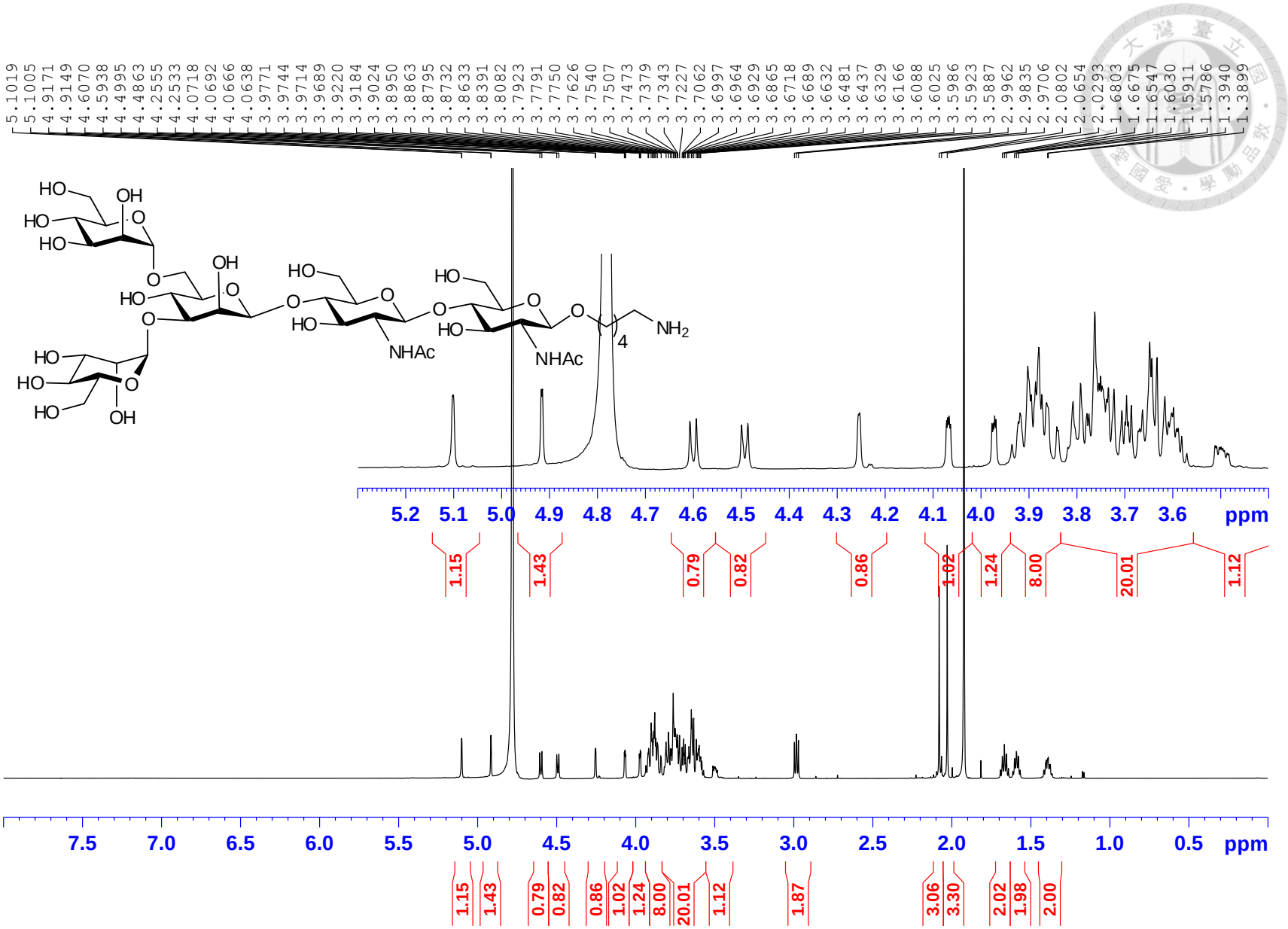
5.1019
5.1005
4.9171
4.9149
4.6070
4.5938
4.4995
4.4863
4.2555
4.2533
4.0718
4.0692
4.0666
4.0638
3.9771
3.9744
3.9714
3.9689
3.9220
3.9184
3.9024
3.8950
3.8863
3.8795
3.8732
3.8633
3.8391
3.8082
3.7923
3.7791
3.7750
3.7626
3.7540
3.7507
3.7473
3.7379
3.7343
3.7227
3.7062
3.6997
3.6964
3.6929
3.6865
3.6718
3.6689
3.6632
3.6481
3.6437
3.6329
3.6166
3.6088
3.6025
3.5986
3.5923
3.5887
2.9962
2.9835
2.9706
2.0802
2.0654
2.0293
1.6803
1.6675
1.6547
1.6030
1.5911
1.5786
1.3940
1.3899
HO
OH
O
HO
HO
O
OH
O
HO
O
HO
NHAc
HO
O
O
HO
NHAc
O
4
NH2
HO
HO
O
HO
OH
5.2 5.1 5.0 4.9 4.8 4.7 4.6 4.5 4.4 4.3 4.2 4.1 4.0 3.9 3.8 3.7 3.6 ppm
1.15
1.43
0.79
0.82
0.86
1.02
1.24
8.00
20.01
1.12
7.5 7.0 6.5 6.0 5.5 5.0 4.5 4.0 3.5 3.0 2.5 2.0 1.5 1.0 0.5 ppm
1.15
1.43
0.79
0.82
0.86
1.02
1.24
8.00
20.01
1.12
1.87
3.06
3.30
2.02
1.98
2.00

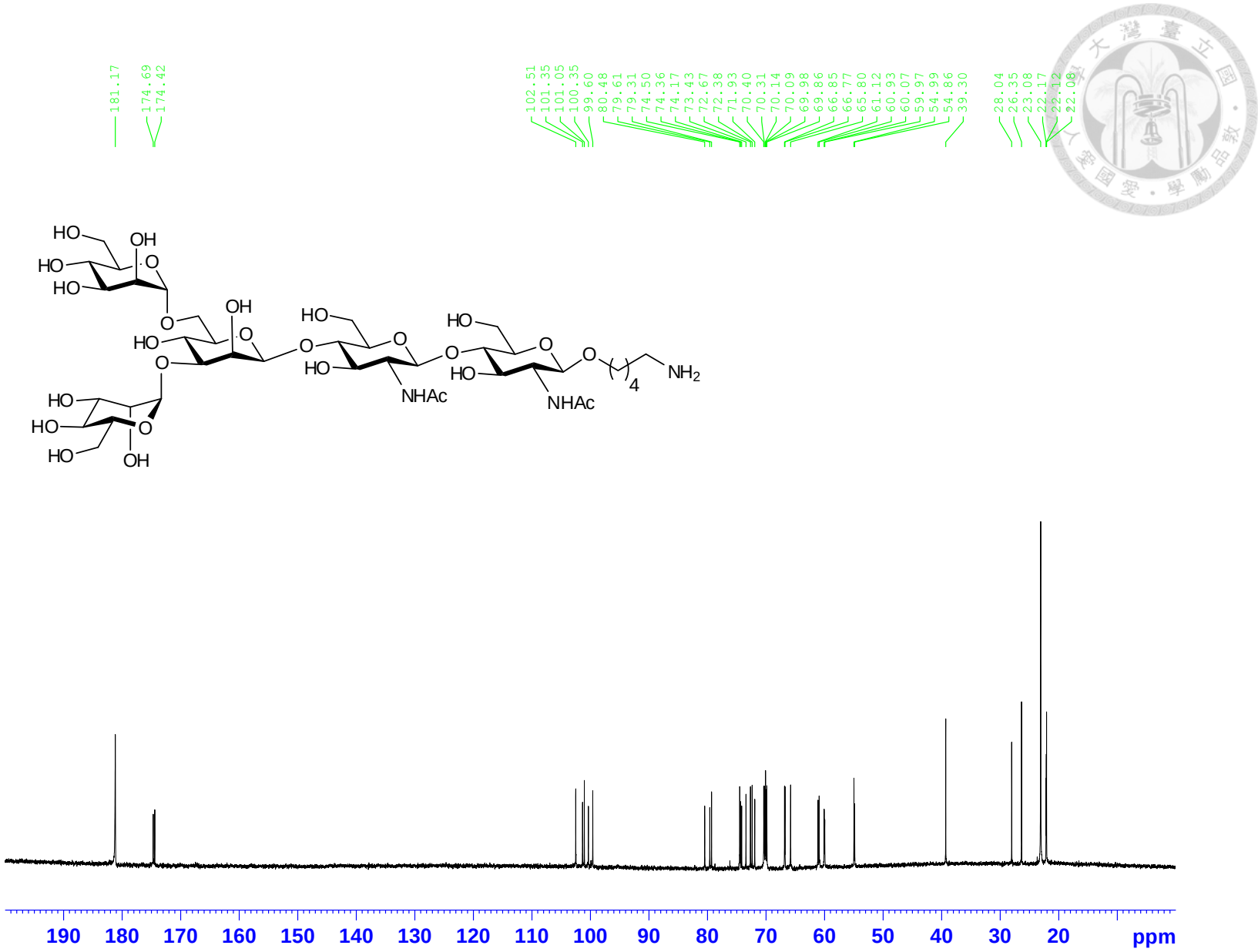
181.17
174.69
174.42
102.51
101.35
101.05
100.35
99.60
80.48
79.61
79.31
74.50
74.36
74.17
73.43
72.67
72.38
71.93
70.40
70.31
70.14
70.09
69.98
69.86
66.85
66.77
65.80
61.12
60.93
60.07
59.97
54.99
54.86
39.30
28.04
26.35
23.08
22.17
22.12
22.08
HO
OH
O
NHAc
NH2
4
190
180
170
160
150
140
130
120
110
100
90
80
70
60
50
40
30
20
ppm

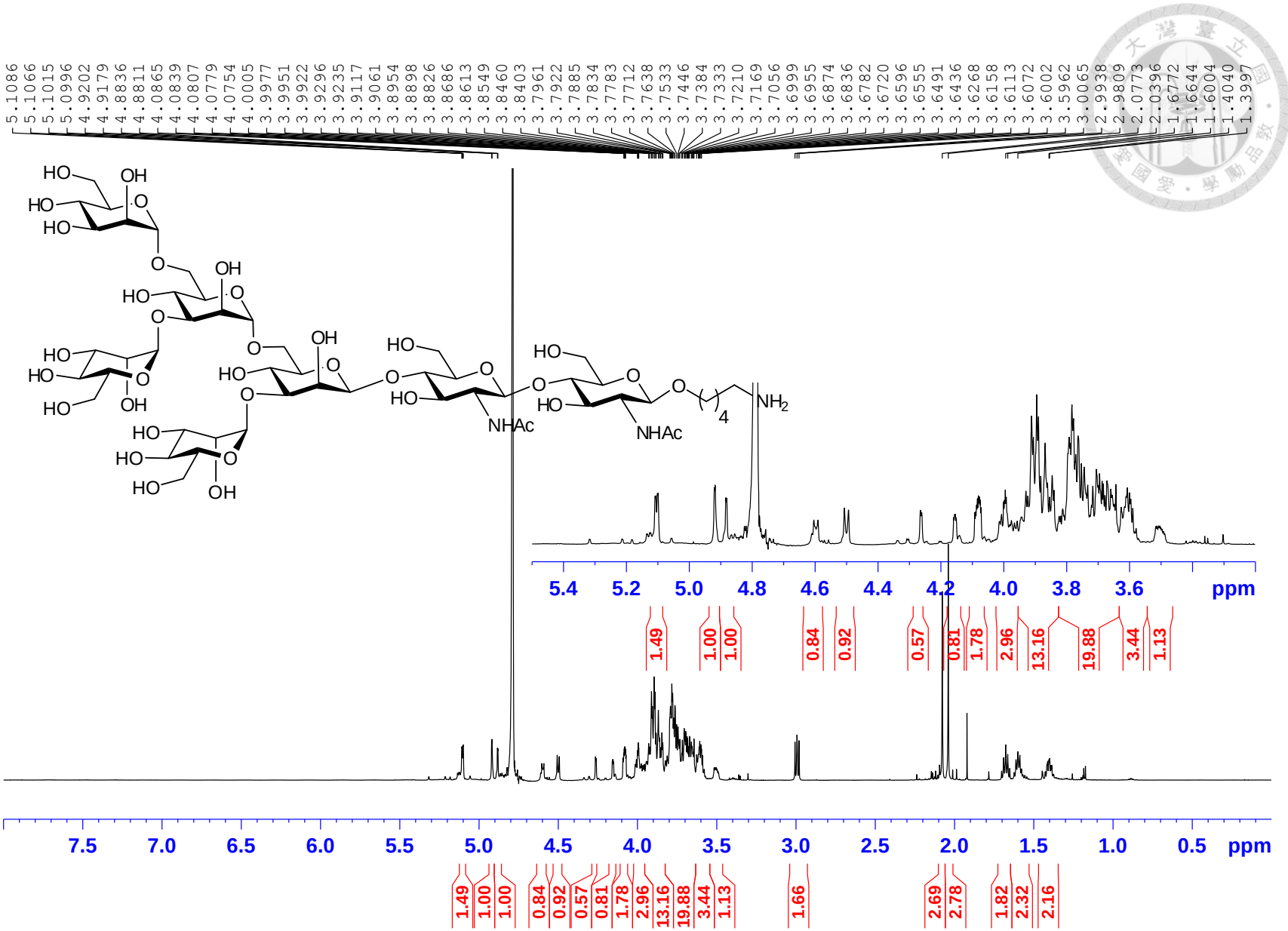
5.1086 5.1066 5.1015 5.0996 4.9202 4.9179 4.8836 4.8811 4.0865 4.0839 4.0807 4.0779 4.0754 4.0005 3.9977 3.9951 3.9922 3.9296 3.9235 3.9117 3.9061 3.8954 3.8898 3.8826 3.8686 3.8613 3.8549 3.8460 3.8403 3.7961 3.7922 3.7885 3.7834 3.7783 3.7712 3.7638 3.7533 3.7446 3.7384 3.7333 3.7210 3.7169 3.7056 3.6999 3.6955 3.6874 3.6836 3.6782 3.6720 3.6596 3.6555 3.6491 3.6436 3.6268 3.6158 3.6113 3.6072 3.6002 3.5962 3.0065 2.9938 2.9809 2.0773 2.0396 1.6772 1.6644 1.6004 1.4040 1.3997
HO
OH
O
NHAc
NH2
4
5.4 5.2 5.0 4.8 4.6 4.4 4.2 4.0 3.8 3.6 ppm
1.49 1.00 1.00 0.84 0.92 0.57 0.81 1.78 2.96 13.16 19.88 3.44 1.13
7.5 7.0 6.5 6.0 5.5 5.0 4.5 4.0 3.5 3.0 2.5 2.0 1.5 1.0 0.5 ppm
1.49 1.00 1.00 0.84 0.92 0.57 0.81 1.78 2.96 13.16 19.88 3.44 1.13 1.66 2.69 2.78 1.82 2.32 2.16

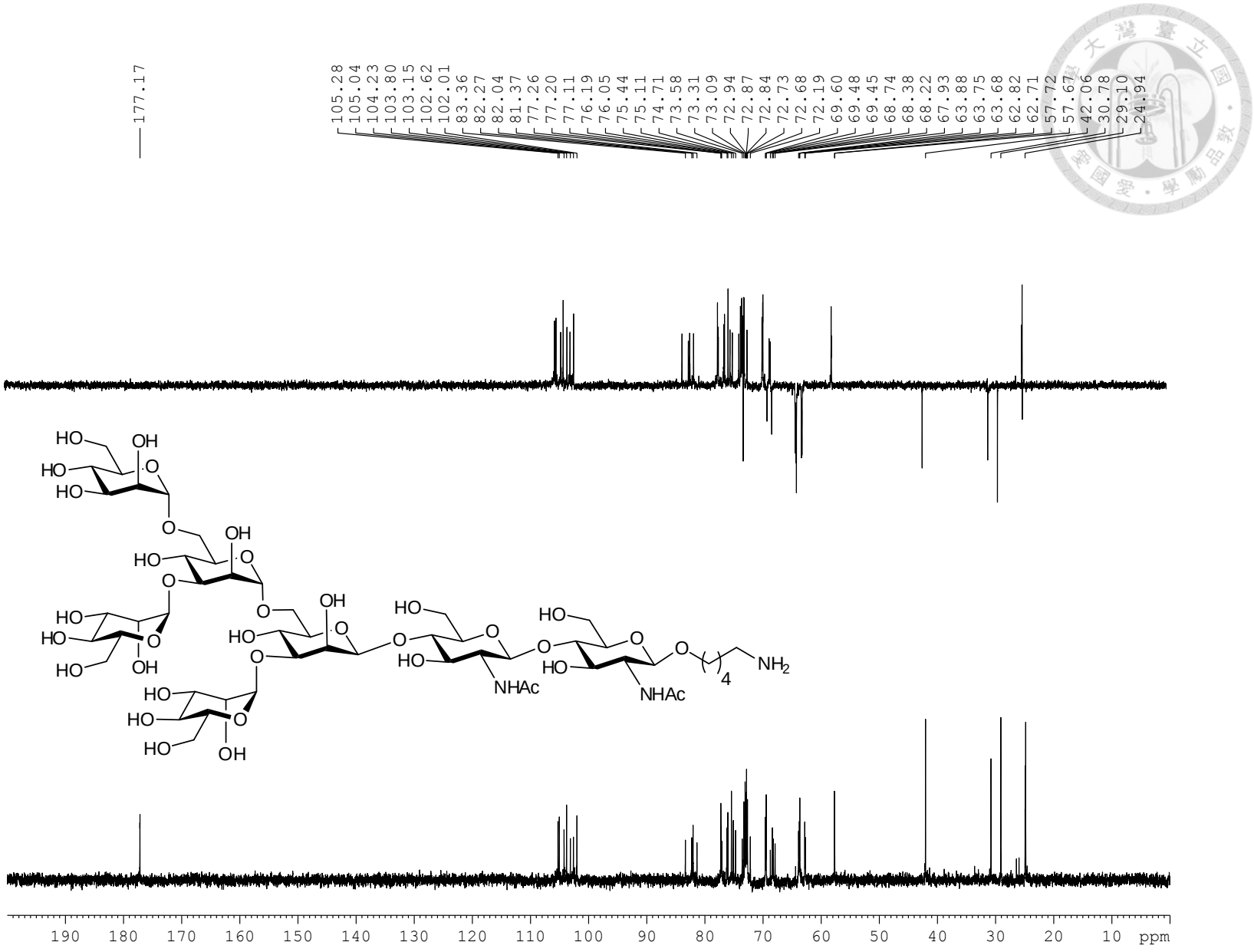
177.17
105.28
105.04
104.23
103.80
103.15
102.62
102.01
83.36
82.27
82.04
81.37
77.26
77.20
77.11
76.19
76.05
75.44
75.11
74.71
73.58
73.31
73.09
72.94
72.87
72.84
72.73
72.68
72.19
69.60
69.48
69.45
68.74
68.38
68.22
67.93
63.88
63.75
63.68
62.82
62.71
57.72
57.67
42.06
30.78
29.10
24.94
HO
OH
O
NHAc
NH2
4
190
180
170
160
150
140
130
120
110
100
90
80
70
60
50
40
30
20
10
ppm

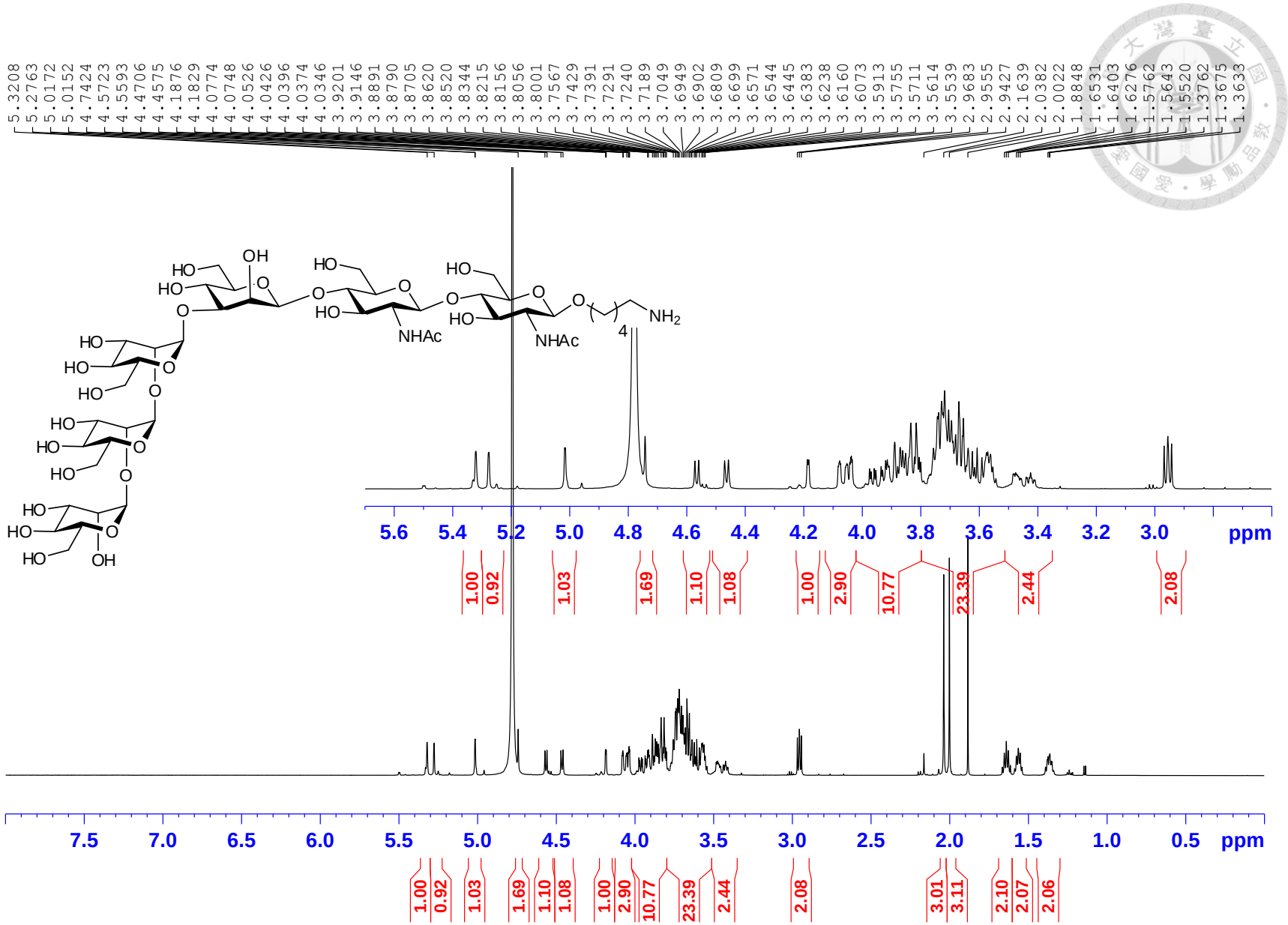
5.3208
5.2763
5.0172
5.0152
4.7424
4.5723
4.5593
4.4706
4.4575
4.1876
4.1829
4.0774
4.0748
4.0526
4.0426
4.0396
4.0374
4.0346
3.9201
3.9146
3.8891
3.8790
3.8705
3.8620
3.8520
3.8344
3.8215
3.8156
3.8056
3.8001
3.7567
3.7429
3.7391
3.7291
3.7240
3.7189
3.7049
3.6949
3.6902
3.6809
3.6699
3.6571
3.6544
3.6445
3.6383
3.6238
3.6160
3.6073
3.5913
3.5755
3.5711
3.5614
3.5539
2.9683
2.9555
2.9427
2.1639
2.0382
2.0022
1.8848
1.6531
1.6403
1.6276
1.5762
1.5643
1.5520
1.3762
1.3675
1.3633
NHAc
NHAc
NH2
4
5.6 5.4 5.2 5.0 4.8 4.6 4.4 4.2 4.0 3.8 3.6 3.4 3.2 3.0 ppm
1.00 0.92 1.03 1.69 1.10 1.08 1.00 2.90 10.77 23.39 2.44 2.08
7.5 7.0 6.5 6.0 5.5 5.0 4.5 4.0 3.5 3.0 2.5 2.0 1.5 1.0 0.5 ppm
1.00 0.92 1.03 1.69 1.10 1.08 1.00 2.90 10.77 23.39 2.44 2.08 3.01 3.11 2.10 2.07 2.06

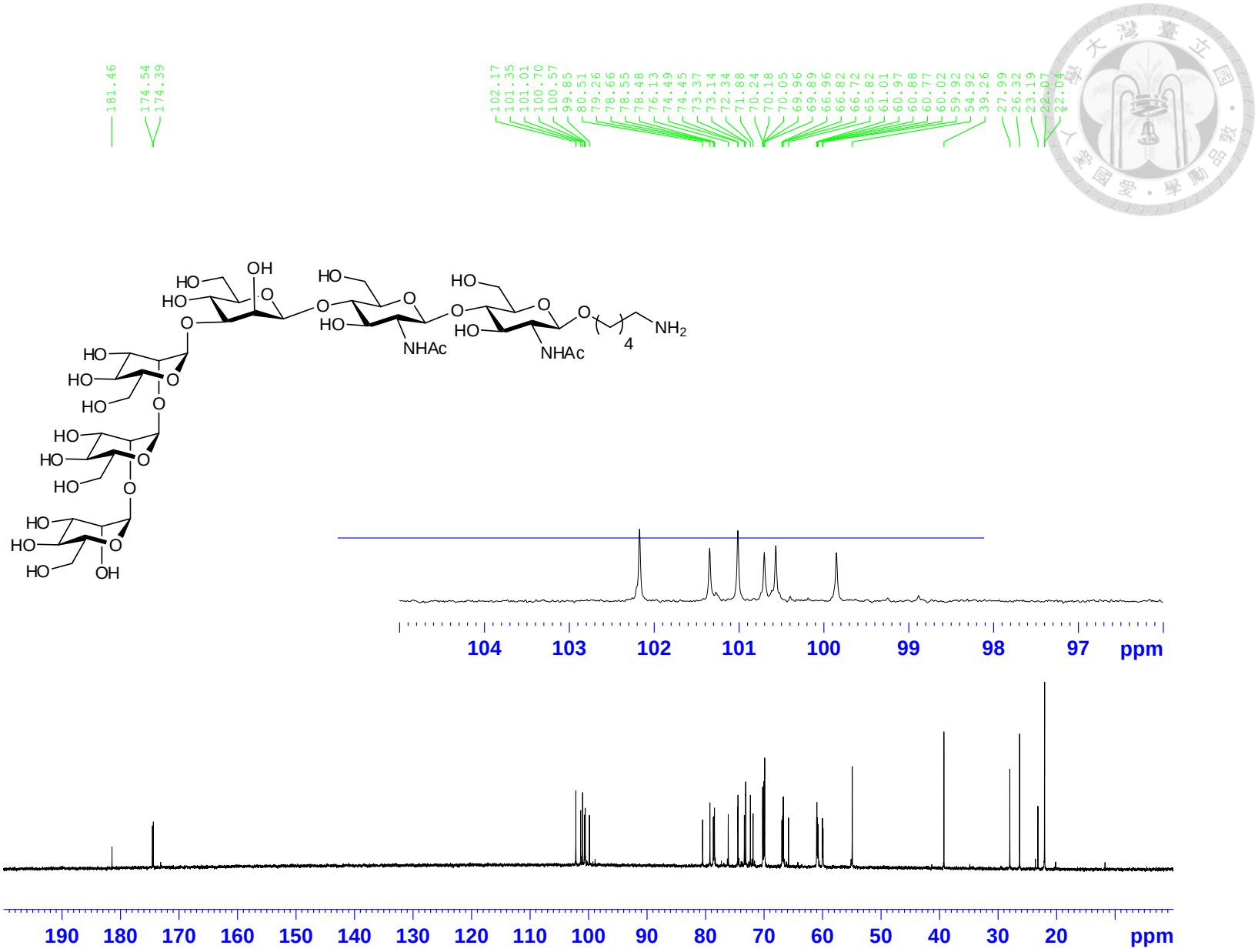
181.46
174.54
174.39
102.17
101.35
101.01
100.70
100.57
99.85
80.51
79.26
78.66
78.55
78.48
76.13
74.49
74.45
73.37
73.14
72.34
71.88
70.24
70.18
70.05
69.96
69.89
66.96
66.82
66.72
65.82
61.01
60.97
60.88
60.77
60.02
59.92
54.92
39.26
27.99
26.32
23.19
22.07
22.04
HO
OH
NHAc
NH2
4
104
103
102
101
100
99
98
97
ppm
190
180
170
160
150
140
130
120
110
100
90
80
70
60
50
40
30
20
ppm

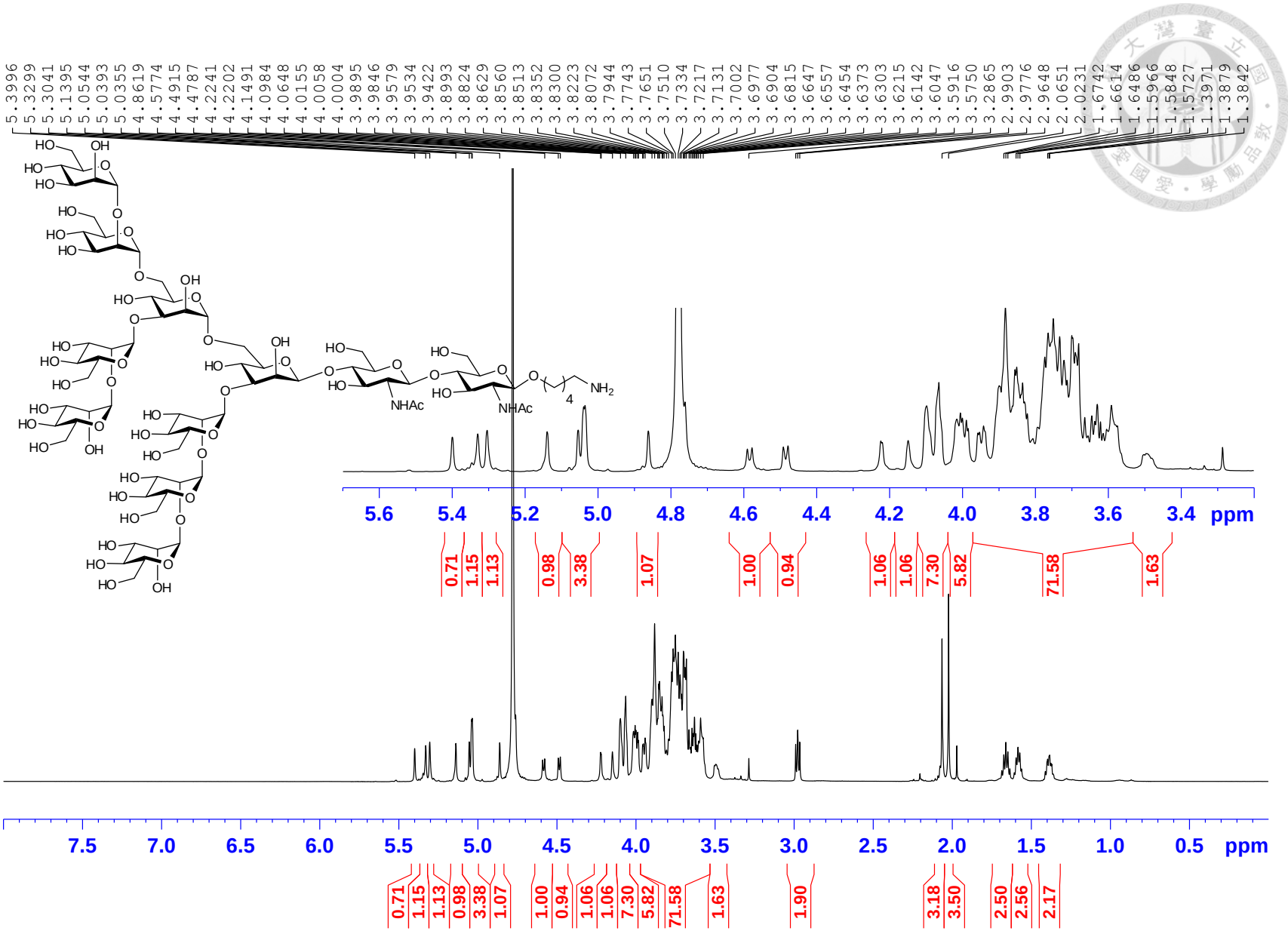
5.3996 5.3299 5.3041 5.1395 5.0544 5.0393 5.0355 4.8619 4.5774 4.4915 4.4787 4.2241 4.2202 4.1491 4.0984 4.0648 4.0155 4.0058 4.0004 3.9895 3.9846 3.9579 3.9534 3.9422 3.8993 3.8824 3.8629 3.8560 3.8513 3.8352 3.8300 3.8223 3.8072 3.7944 3.7743 3.7651 3.7510 3.7334 3.7217 3.7131 3.7002 3.6977 3.6904 3.6815 3.6647 3.6557 3.6454 3.6373 3.6303 3.6215 3.6142 3.6047 3.5916 3.5750 3.2865 2.9903 2.9776 2.9648 2.0651 2.0231 1.6742 1.6614 1.6486 1.5966 1.5848 1.5727 1.3971 1.3879 1.3842
HO OH O NHAc NH2 4
5.6 5.4 5.2 5.0 4.8 4.6 4.4 4.2 4.0 3.8 3.6 3.4 ppm
0.71 1.15 1.13 0.98 3.38 1.07 1.00 0.94 1.06 1.06 7.30 5.82 71.58 1.63
7.5 7.0 6.5 6.0 5.5 5.0 4.5 4.0 3.5 3.0 2.5 2.0 1.5 1.0 0.5 ppm
0.71 1.15 1.13 0.98 3.38 1.07 1.00 0.94 1.06 1.06 7.30 5.82 71.58 1.63 1.90 3.18 3.50 2.50 2.56 2.17

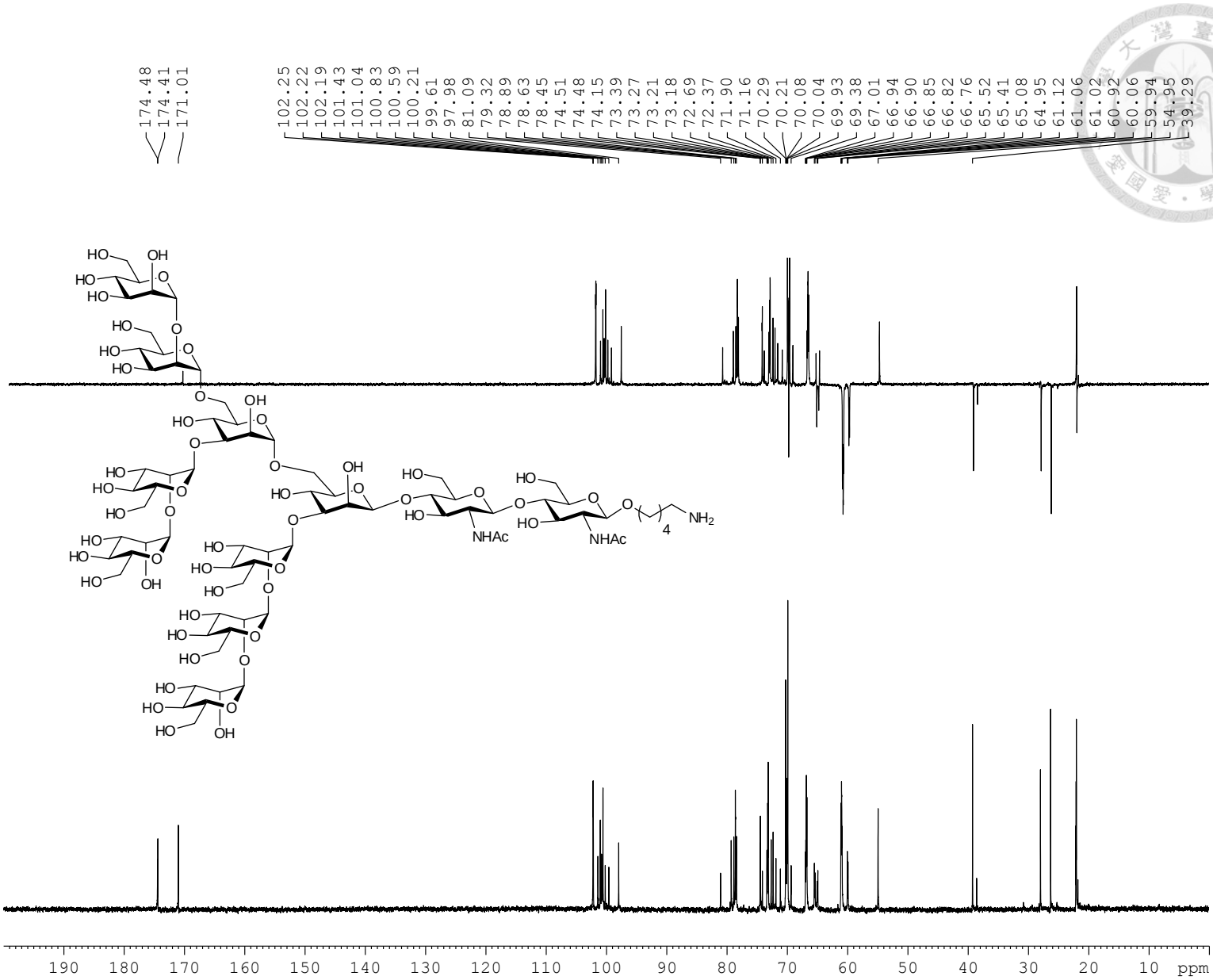
174.48
174.41
171.01
102.25
102.22
102.19
101.43
101.04
100.83
100.59
100.21
99.61
97.98
81.09
79.32
78.89
78.63
78.45
74.51
74.48
74.15
73.39
73.27
73.21
73.18
72.69
72.37
71.90
71.16
70.29
70.21
70.08
70.04
69.93
69.38
67.01
66.94
66.90
66.85
66.82
66.76
65.52
65.41
65.08
64.95
61.12
61.06
61.02
60.92
60.06
59.94
54.95
39.29
NHAc
NHAc
NH2
4
190
180
170
160
150
140
130
120
110
100
90
80
70
60
50
40
30
20
10
ppm

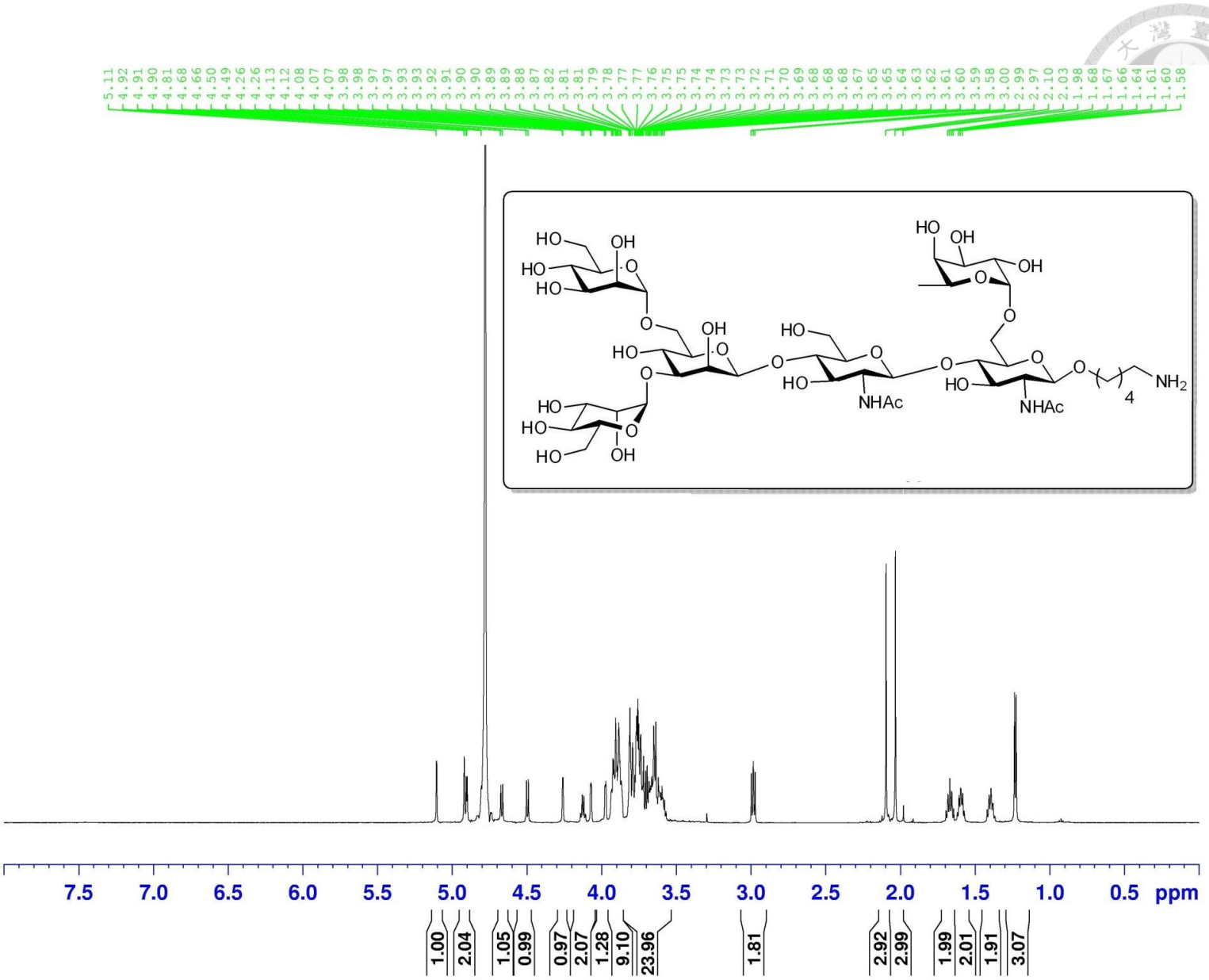
5.11 4.92 4.91 4.90 4.81 4.68 4.66 4.50 4.49 4.26 4.13 4.12 4.08 4.07 4.07 3.98 3.98 3.97 3.97 3.93 3.93 3.92 3.91 3.90 3.90 3.89 3.89 3.88 3.87 3.82 3.81 3.81 3.79 3.78 3.77 3.77 3.76 3.75 3.75 3.74 3.74 3.73 3.73 3.72 3.71 3.70 3.69 3.68 3.68 3.68 3.67 3.65 3.65 3.64 3.63 3.62 3.61 3.60 3.59 3.58 3.00 2.99 2.97 2.10 2.03 1.98 1.68 1.67 1.66 1.64 1.61 1.60 1.58
HO
OH
O
NHAc
NH2
4
7.5 7.0 6.5 6.0 5.5 5.0 4.5 4.0 3.5 3.0 2.5 2.0 1.5 1.0 0.5 ppm
1.00 2.04 1.05 0.99 0.97 2.07 1.28 9.10 23.96 1.81 2.92 2.99 1.99 2.01 1.91 3.07

177.43
177.15
173.76

105.26
103.87
103.81
103.14
102.36
102.15
83.22
82.48
81.38
77.09
76.92
76.18
75.41
75.06
74.71
74.56
73.13
73.06
72.88
72.76
72.73
72.61
72.23
70.89
69.59
69.52
69.18
68.61
68.56
63.88
63.69
62.73
57.80
57.62
42.05
30.81
29.13
25.04
24.87
18.11

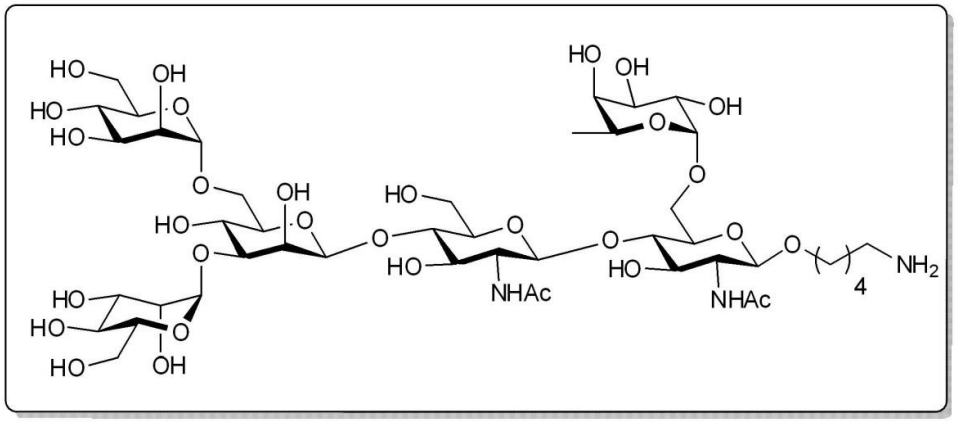

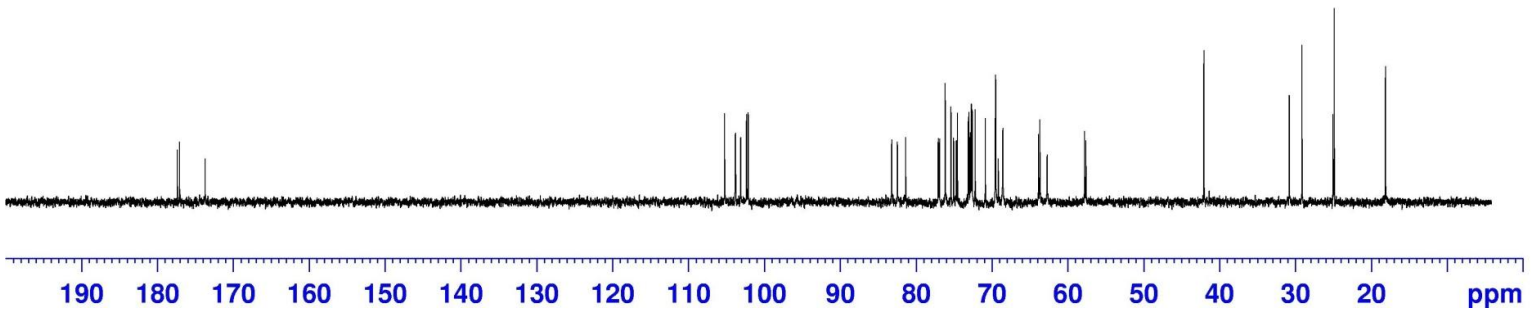

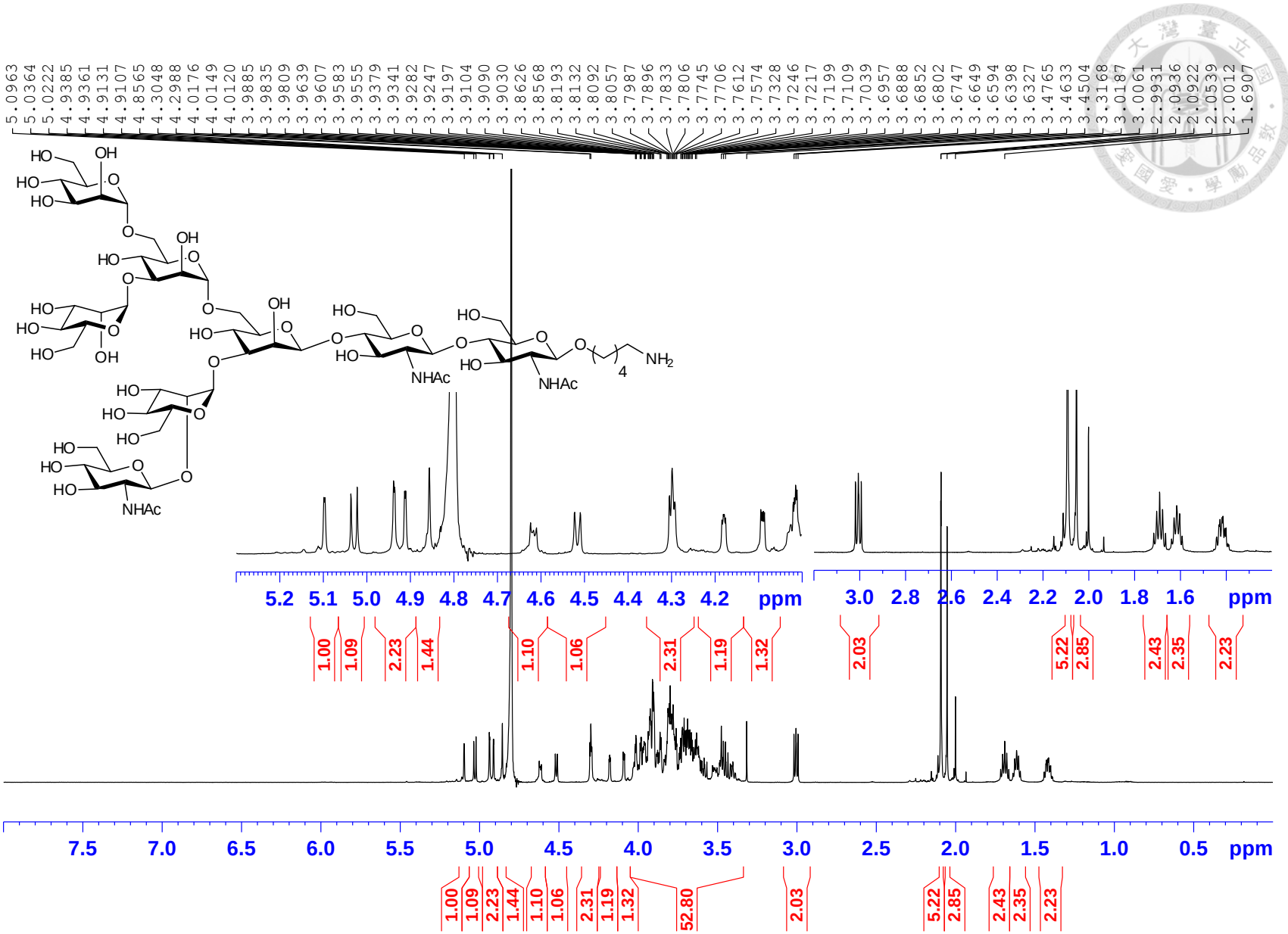
5.0963 5.0364 5.0222 4.9385 4.9361 4.9131 4.9107 4.8565 4.3048 4.2988 4.0176 4.0149 4.0120 3.9885 3.9835 3.9809 3.9639 3.9607 3.9583 3.9555 3.9379 3.9341 3.9282 3.9247 3.9197 3.9104 3.9090 3.9030 3.8626 3.8568 3.8193 3.8132 3.8092 3.8057 3.7987 3.7896 3.7833 3.7806 3.7745 3.7706 3.7612 3.7574 3.7328 3.7246 3.7217 3.7199 3.7109 3.7039 3.6957 3.6888 3.6852 3.6802 3.6747 3.6649 3.6594 3.6398 3.6327 3.4765 3.4633 3.4504 3.3168 3.0187 3.0061 2.9931 2.0936 2.0922 2.0539 2.0012 1.6907
NHAc
NHAc
NH2
4
5.2 5.1 5.0 4.9 4.8 4.7 4.6 4.5 4.4 4.3 4.2 ppm
3.0 2.8 2.6 2.4 2.2 2.0 1.8 1.6 ppm
1.00 1.09 2.23 1.44 1.10 1.06 2.31 1.19 1.32 2.03 5.22 2.85 2.43 2.35 2.23
7.5 7.0 6.5 6.0 5.5 5.0 4.5 4.0 3.5 3.0 2.5 2.0 1.5 1.0 0.5 ppm
1.00 1.09 2.23 1.44 1.10 1.06 2.31 1.19 1.32 52.80 2.03 5.22 2.85 2.43 2.35 2.23

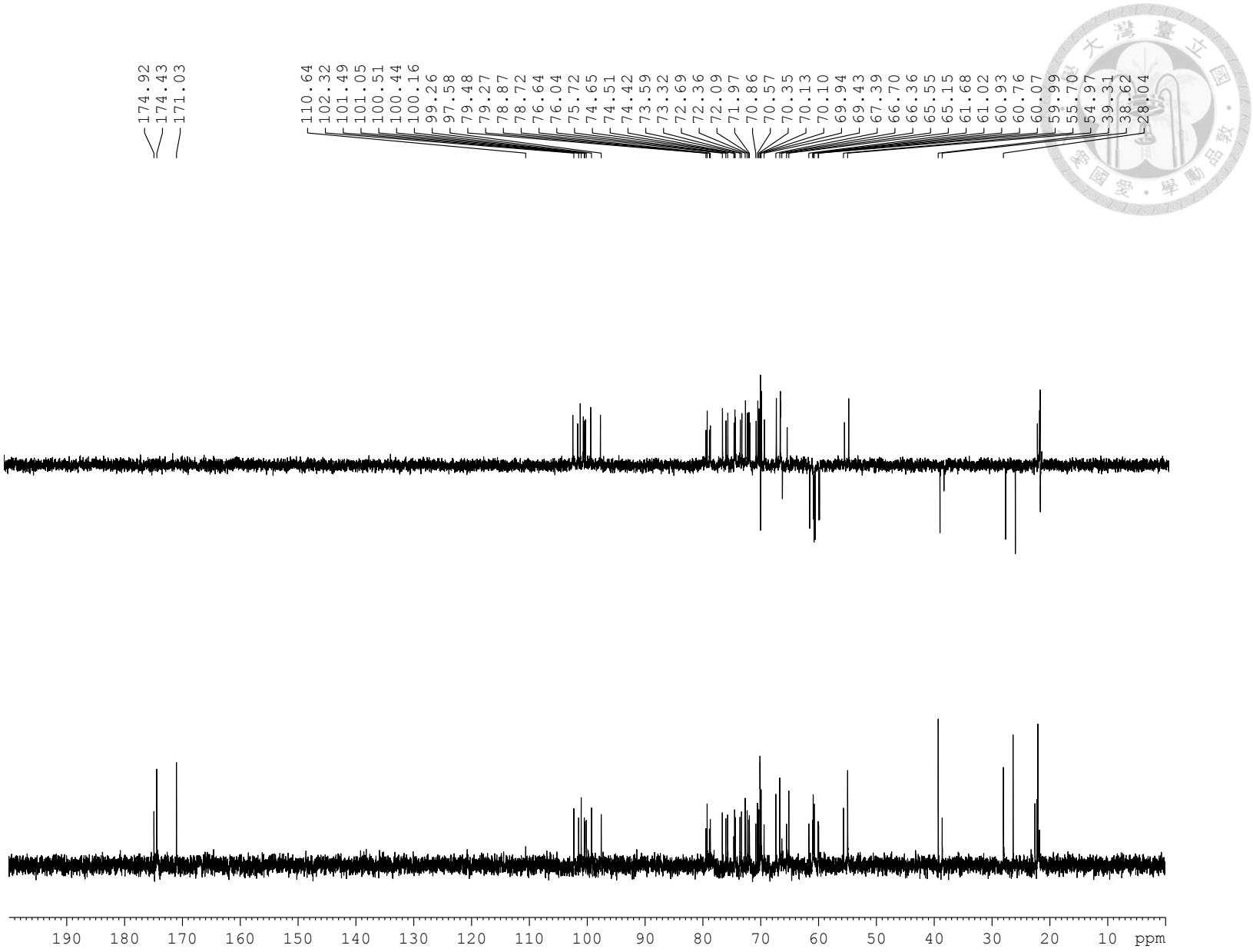
174.92
174.43
171.03
110.64
102.32
101.49
101.05
100.51
100.44
100.16
99.26
97.58
79.48
79.27
78.87
78.72
76.64
76.04
75.72
74.65
74.51
74.42
73.59
73.32
72.69
72.36
72.09
71.97
70.86
70.57
70.35
70.13
70.10
69.94
69.43
67.39
66.70
66.36
65.55
65.15
61.68
61.02
60.93
60.76
60.07
59.99
55.70
54.97
39.31
38.62
28.04
190 180 170 160 150 140 130 120 110 100 90 80 70 60 50 40 30 20 10 ppm

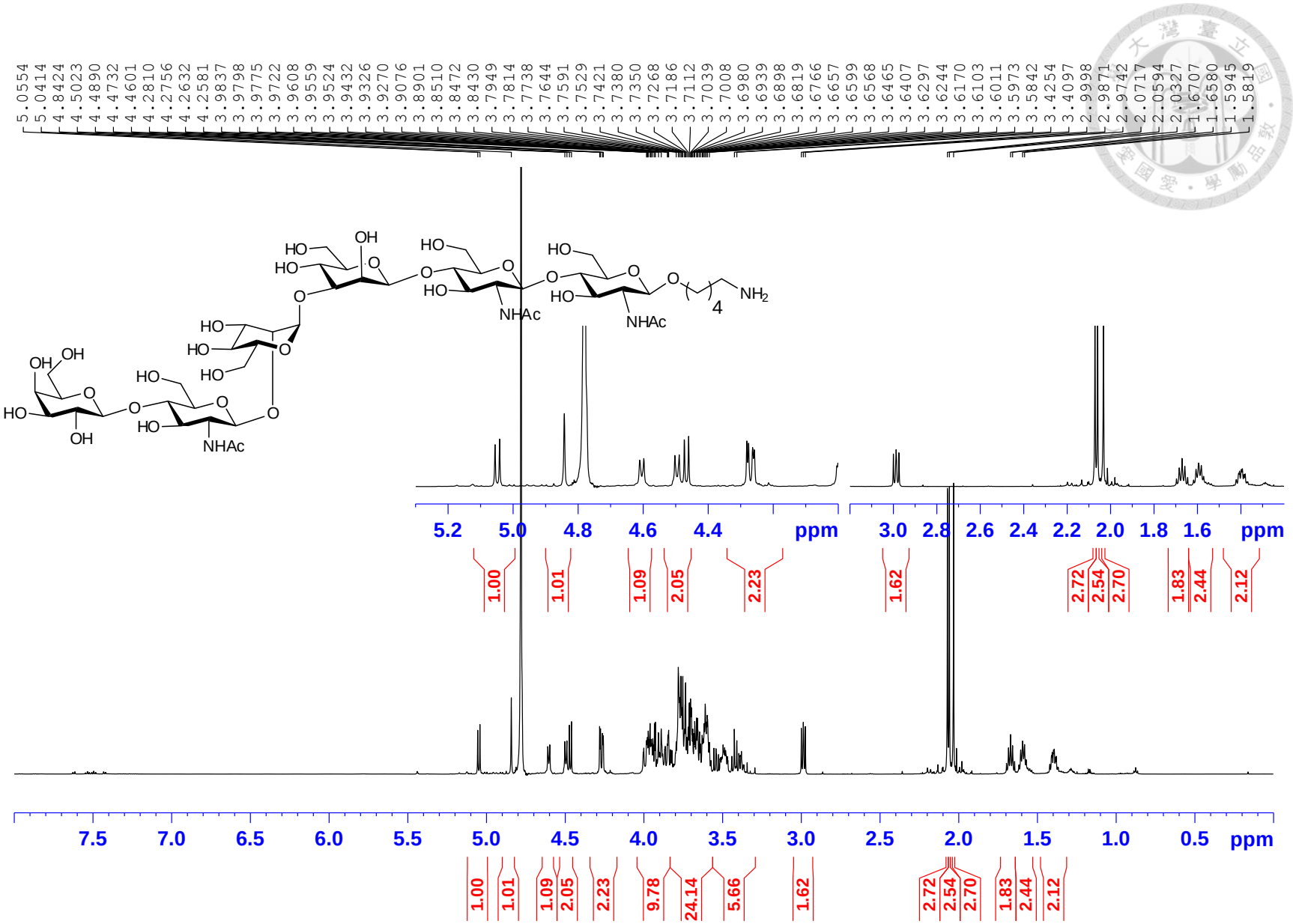
5.0554
5.0414
4.8424
4.5023
4.4890
4.4732
4.4601
4.2810
4.2756
4.2632
4.2581
3.9837
3.9798
3.9775
3.9722
3.9608
3.9559
3.9524
3.9432
3.9326
3.9270
3.9076
3.8901
3.8510
3.8472
3.8430
3.7949
3.7814
3.7738
3.7644
3.7591
3.7529
3.7421
3.7380
3.7350
3.7268
3.7186
3.7112
3.7039
3.7008
3.6980
3.6939
3.6898
3.6819
3.6766
3.6657
3.6599
3.6568
3.6465
3.6407
3.6297
3.6244
3.6170
3.6103
3.6011
3.5973
3.5842
3.4254
3.4097
2.9998
2.9871
2.9742
2.0717
2.0594
2.0327
1.6707
1.6580
1.5945
1.5819
HO
OH
O
NHAc
NH2
4
5.2
5.0
4.8
4.6
4.4
ppm
3.0
2.8
2.6
2.4
2.2
2.0
1.8
1.6
ppm
1.00
1.01
1.09
2.05
2.23
1.62
2.72
2.54
2.70
1.83
2.44
2.12
7.5
7.0
6.5
6.0
5.5
5.0
4.5
4.0
3.5
3.0
2.5
2.0
1.5
1.0
0.5
ppm
1.00
1.01
1.09
2.05
2.23
9.78
24.14
5.66
1.62
2.72
2.54
2.70
1.83
2.44
2.12

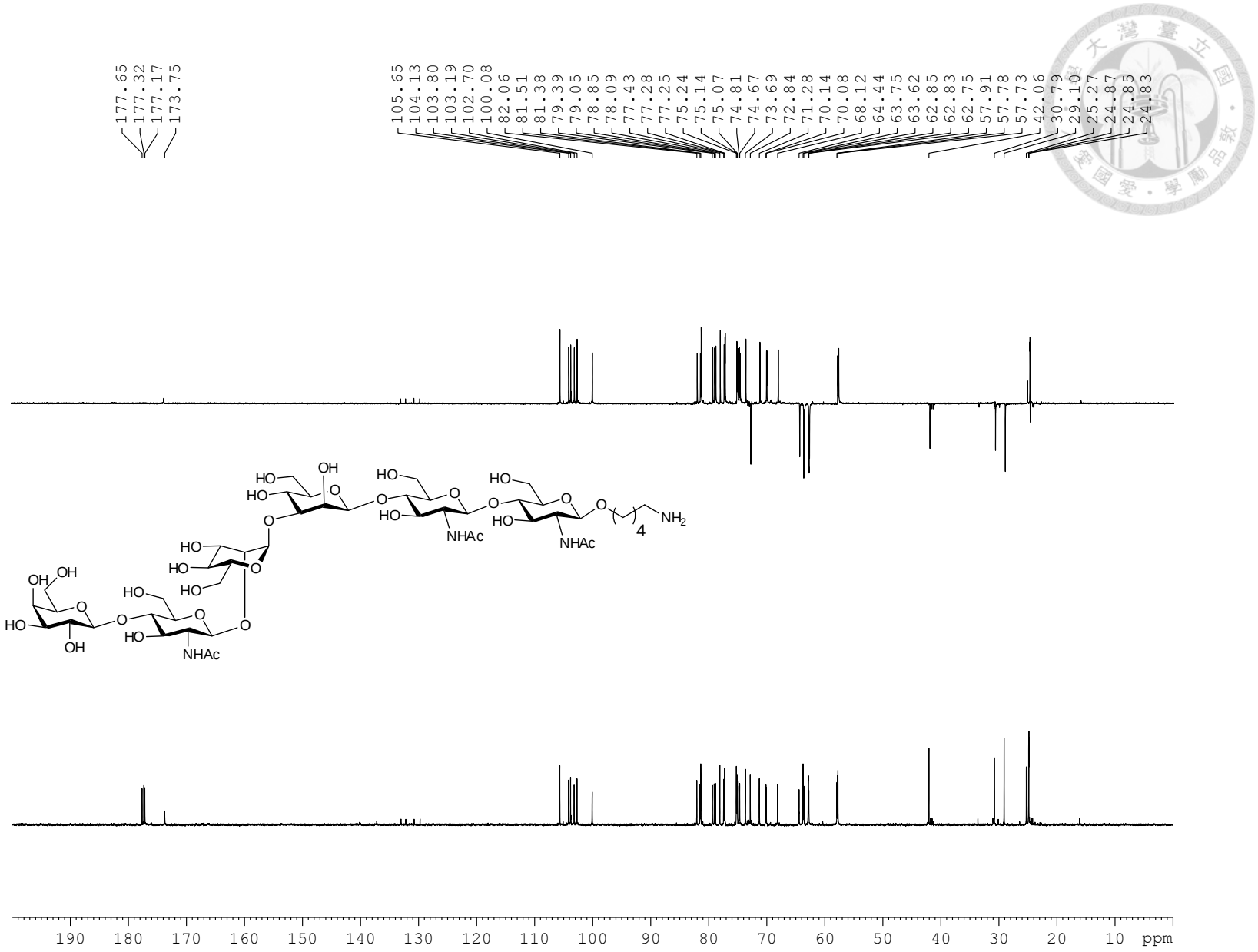
177.65
177.32
177.17
173.75
105.65
104.13
103.80
103.19
102.70
100.08
82.06
81.51
81.38
79.39
79.05
78.85
78.09
77.43
77.28
77.25
75.24
75.14
75.07
74.81
74.67
73.69
72.84
71.28
70.14
70.08
68.12
64.44
63.75
63.62
62.85
62.83
62.75
57.91
57.78
57.73
42.06
30.79
29.10
25.27
24.87
24.85
24.83
HO
OH
O
NHAc
NH2
4
190
180
170
160
150
140
130
120
110
100
90
80
70
60
50
40
30
20
10
ppm

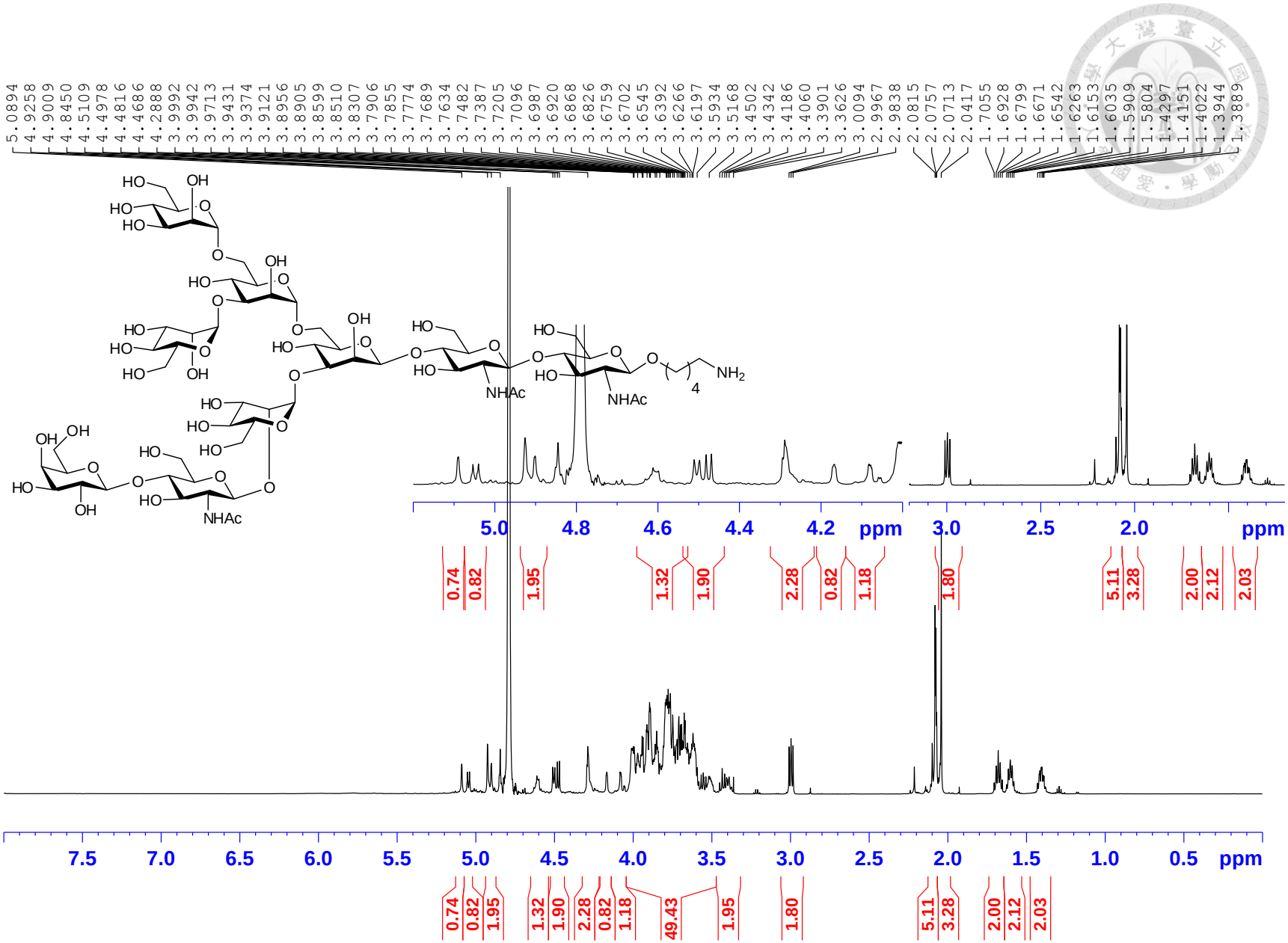
5.0894
4.9258
4.9009
4.8450
4.5109
4.4978
4.4816
4.4686
4.2888
3.9992
3.9942
3.9713
3.9431
3.9374
3.9121
3.8956
3.8905
3.8599
3.8510
3.8307
3.7906
3.7855
3.7774
3.7689
3.7634
3.7482
3.7387
3.7205
3.7096
3.6987
3.6920
3.6868
3.6826
3.6759
3.6702
3.6545
3.6392
3.6266
3.6197
3.5934
3.5168
3.4502
3.4342
3.4186
3.4060
3.3901
3.3626
3.0094
2.9967
2.9838
2.0815
2.0757
2.0713
2.0417
1.7055
1.6928
1.6799
1.6671
1.6542
1.6263
1.6153
1.6035
1.5909
1.5804
1.4297
1.4151
1.4022
1.3944
1.3889
NHAc
NHAc
NH2
4
5.0
4.8
4.6
4.4
4.2
ppm
3.0
2.5
2.0
ppm
0.74
0.82
1.95
1.32
1.90
2.28
0.82
1.18
1.80
5.11
3.28
2.00
2.12
2.03
7.5
7.0
6.5
6.0
5.5
5.0
4.5
4.0
3.5
3.0
2.5
2.0
1.5
1.0
0.5
ppm
0.74
0.82
1.95
1.32
1.90
2.28
0.82
1.18
49.43
1.95
1.80
5.11
3.28
2.00
2.12
2.03

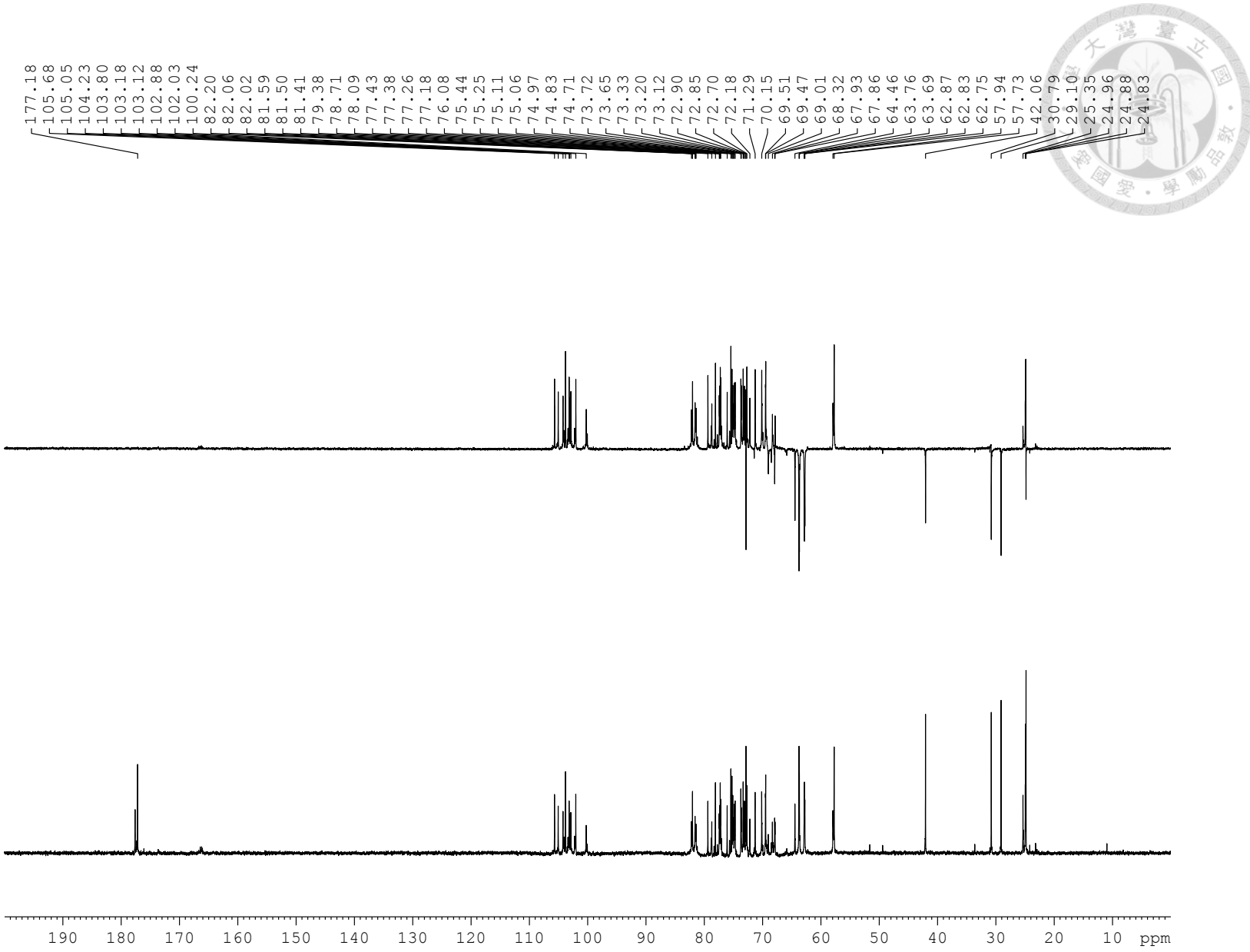
177.18
105.68
105.05
104.23
103.80
103.18
103.12
102.88
102.03
100.24
82.20
82.06
82.02
81.59
81.50
81.41
79.38
78.71
78.09
77.43
77.38
77.26
77.18
76.08
75.44
75.25
75.11
75.06
74.97
74.83
74.71
73.72
73.65
73.33
73.20
73.12
72.90
72.85
72.70
72.18
71.29
70.15
69.51
69.47
69.01
68.32
67.93
67.86
64.46
63.76
63.69
62.87
62.83
62.75
57.94
57.73
42.06
30.79
29.10
25.35
24.96
24.88
24.83
190 180 170 160 150 140 130 120 110 100 90 80 70 60 50 40 30 20 10 ppm

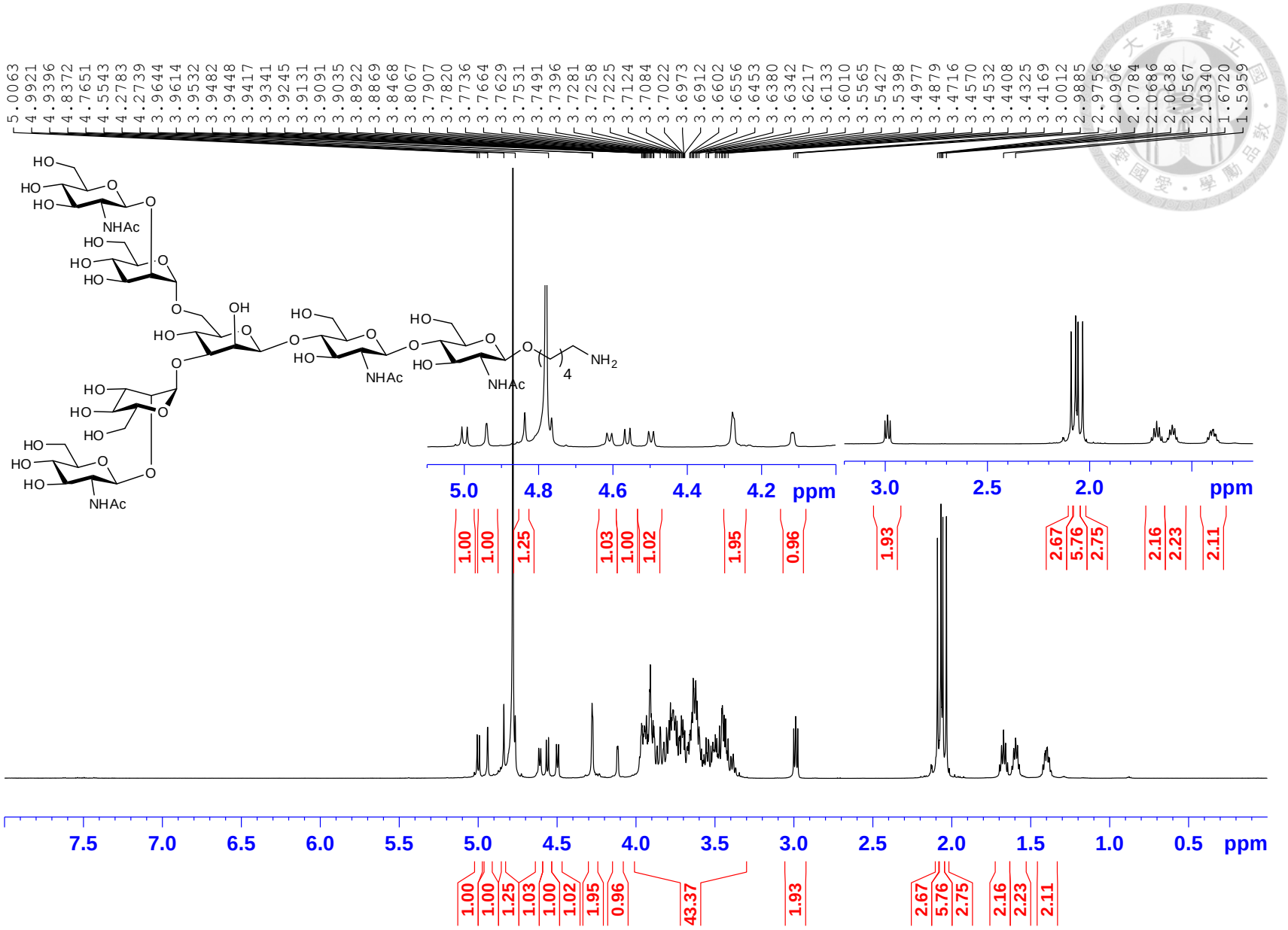
5.0063 4.9921 4.9396 4.8372 4.7651 4.5543 4.2783 4.2739 3.9644 3.9614 3.9532 3.9482 3.9448 3.9417 3.9341 3.9245 3.9131 3.9091 3.9035 3.8922 3.8869 3.8468 3.8067 3.7907 3.7820 3.7736 3.7664 3.7629 3.7531 3.7491 3.7396 3.7281 3.7258 3.7225 3.7124 3.7084 3.7022 3.6973 3.6912 3.6602 3.6556 3.6453 3.6380 3.6342 3.6217 3.6133 3.6010 3.5565 3.5427 3.5398 3.4977 3.4879 3.4716 3.4570 3.4532 3.4408 3.4325 3.4169 3.0012 2.9885 2.9756 2.0906 2.0784 2.0686 2.0638 2.0567 2.0340 1.6720 1.5959
HO
NHAc
OH
NH2
4
5.0 4.8 4.6 4.4 4.2 ppm
3.0 2.5 2.0 ppm
1.00 1.00 1.25 1.03 1.00 1.02 1.95 0.96 1.93 2.67 5.76 2.75 2.16 2.23 2.11
7.5 7.0 6.5 6.0 5.5 5.0 4.5 4.0 3.5 3.0 2.5 2.0 1.5 1.0 0.5 ppm
1.00 1.00 1.25 1.03 1.00 1.02 1.95 0.96 43.37 1.93 2.67 5.76 2.75 2.16 2.23 2.11

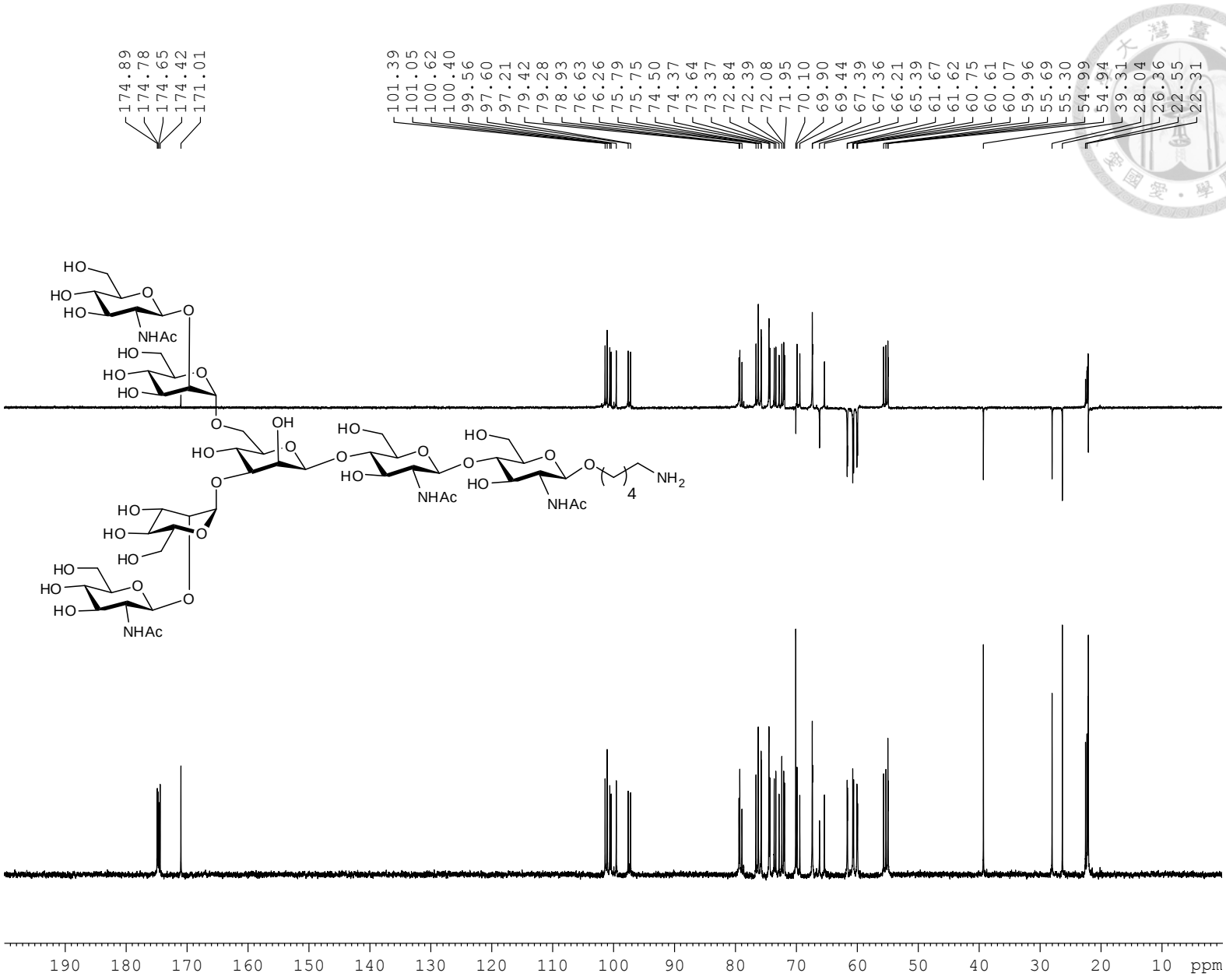
174.89
174.78
174.65
174.42
171.01
101.39
101.05
100.62
100.40
99.56
97.60
97.21
79.42
79.28
78.93
76.63
76.26
75.79
75.75
74.50
74.37
73.64
73.37
72.84
72.39
72.08
71.95
70.10
69.90
69.44
67.39
67.36
66.21
65.39
61.67
61.62
60.75
60.61
60.07
59.96
55.69
55.30
54.99
54.94
39.31
28.04
26.36
22.55
22.31
HO
O
NHAc
OH
NH2
4
190
180
170
160
150
140
130
120
110
100
90
80
70
60
50
40
30
20
10
ppm

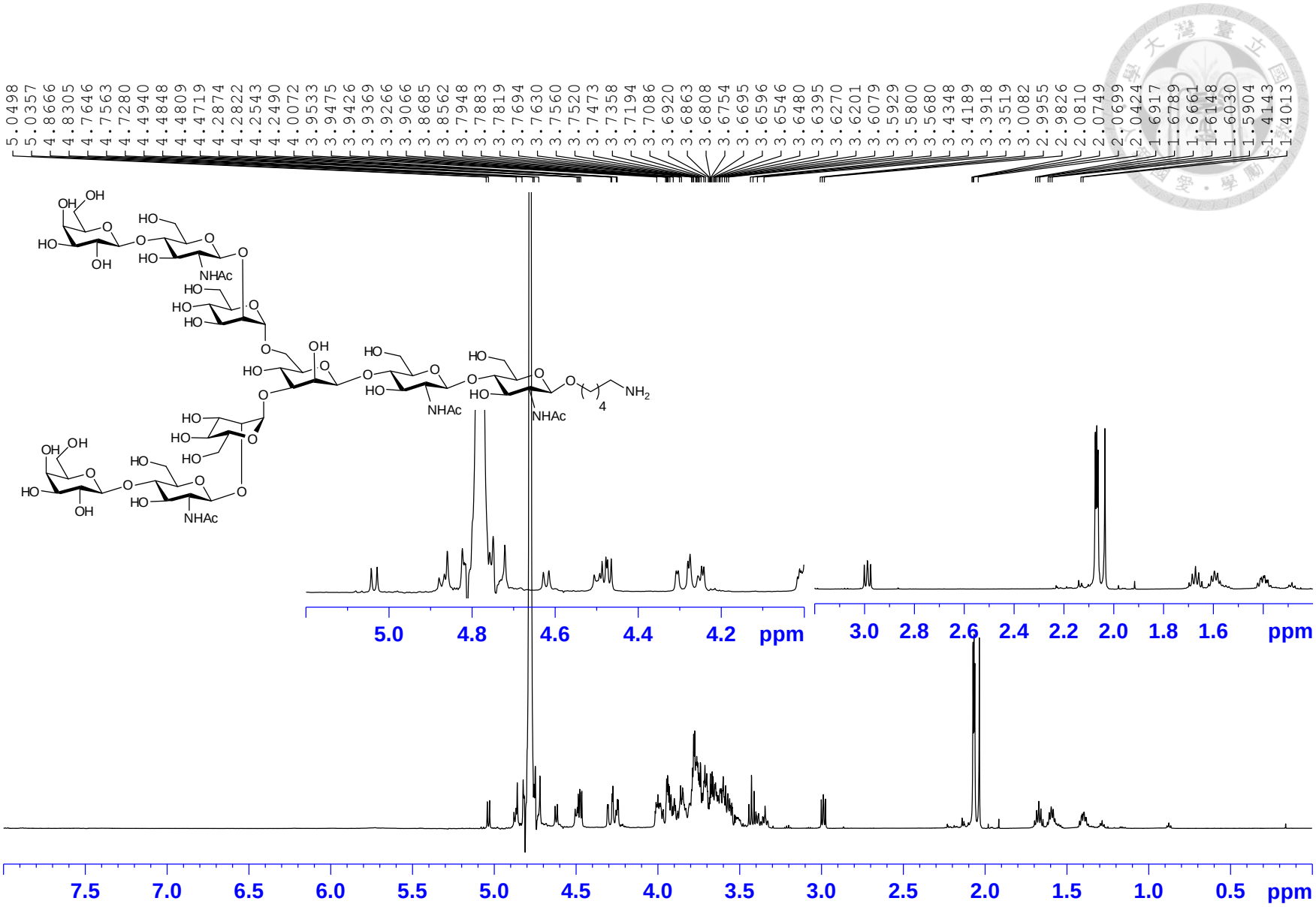
5.0498
5.0357
4.8666
4.8305
4.7646
4.7563
4.7280
4.4940
4.4848
4.4809
4.4719
4.2874
4.2822
4.2543
4.2490
4.0072
3.9533
3.9475
3.9426
3.9369
3.9266
3.9066
3.8685
3.8562
3.7948
3.7883
3.7819
3.7694
3.7630
3.7560
3.7520
3.7473
3.7358
3.7194
3.7086
3.6920
3.6863
3.6808
3.6754
3.6695
3.6596
3.6546
3.6480
3.6395
3.6270
3.6201
3.6079
3.5929
3.5800
3.5680
3.4348
3.4189
3.3918
3.3519
3.0082
2.9955
2.9826
2.0810
2.0749
2.0699
2.0424
1.6917
1.6789
1.6661
1.6148
1.6030
1.5904
1.4143
1.4013
NHAc
NHAc
NHAc
NH2
4
5.0
4.8
4.6
4.4
4.2
ppm
3.0
2.8
2.6
2.4
2.2
2.0
1.8
1.6
ppm
7.5
7.0
6.5
6.0
5.5
5.0
4.5
4.0
3.5
3.0
2.5
2.0
1.5
1.0
0.5
ppm

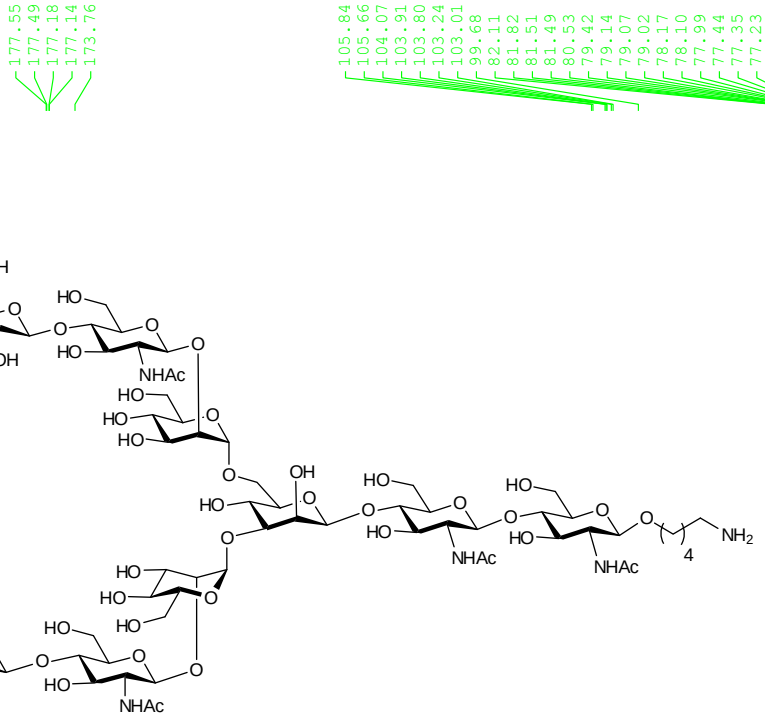

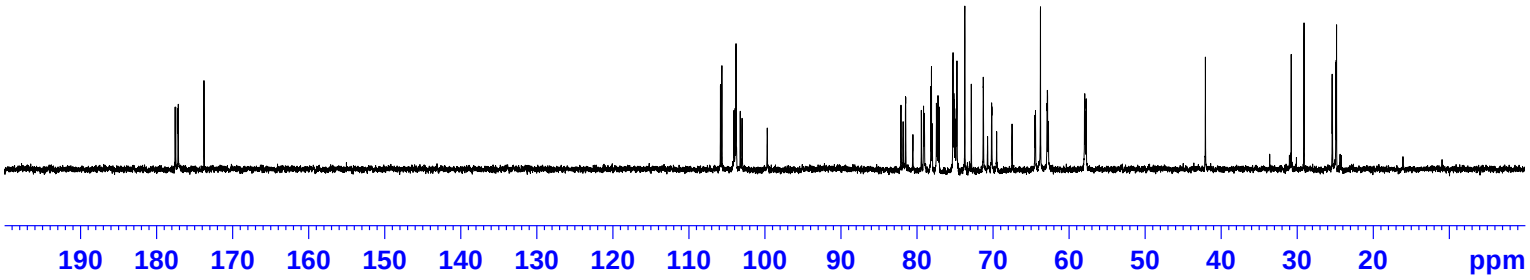
190
180
170
160
150
140
130
120
110
100
90
80
70
60
50
40
30
20
ppm

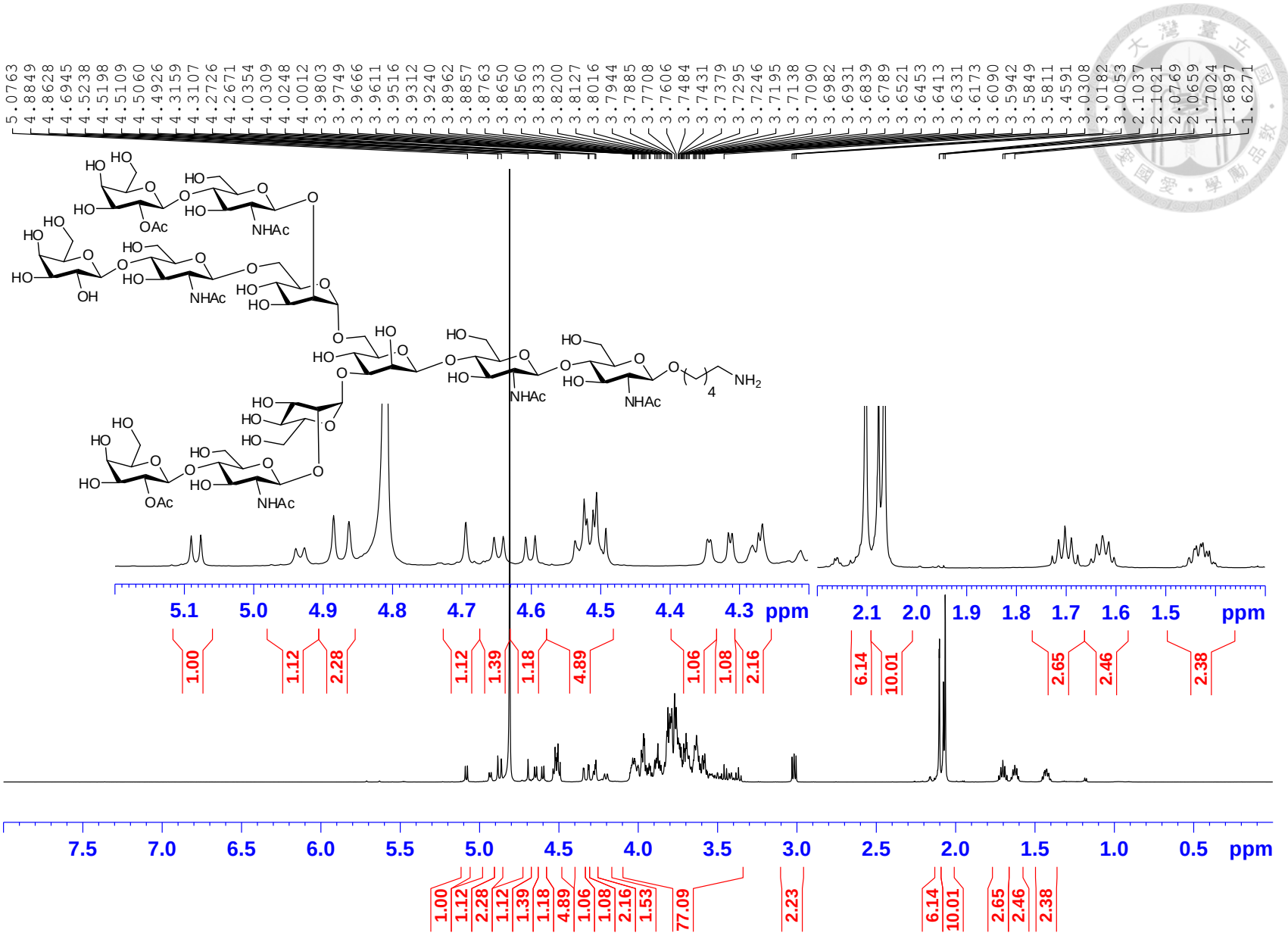
5.0763
4.8849
4.8628
4.6945
4.5238
4.5198
4.5109
4.5060
4.4926
4.3159
4.3107
4.2726
4.2671
4.0354
4.0309
4.0248
4.0012
3.9803
3.9749
3.9666
3.9611
3.9516
3.9312
3.9240
3.8962
3.8857
3.8763
3.8650
3.8560
3.8333
3.8200
3.8127
3.8016
3.7944
3.7885
3.7708
3.7606
3.7484
3.7431
3.7379
3.7295
3.7246
3.7195
3.7138
3.7090
3.6982
3.6931
3.6839
3.6789
3.6521
3.6453
3.6413
3.6331
3.6173
3.6090
3.5942
3.5849
3.5811
3.4591
3.0308
3.0182
3.0053
2.1037
2.1021
2.0769
2.0659
1.7024
1.6897
1.6271
5.1 5.0 4.9 4.8 4.7 4.6 4.5 4.4 4.3 ppm
2.1 2.0 1.9 1.8 1.7 1.6 1.5 ppm
1.00 1.12 2.28 1.12 1.39 1.18 4.89 1.06 1.08 2.16 6.14 10.01 2.65 2.46 2.38
7.5 7.0 6.5 6.0 5.5 5.0 4.5 4.0 3.5 3.0 2.5 2.0 1.5 1.0 0.5 ppm
1.00 1.12 2.28 1.12 1.39 1.18 4.89 1.06 1.08 2.16 1.53 77.09 2.23 6.14 10.01 2.65 2.46 2.38

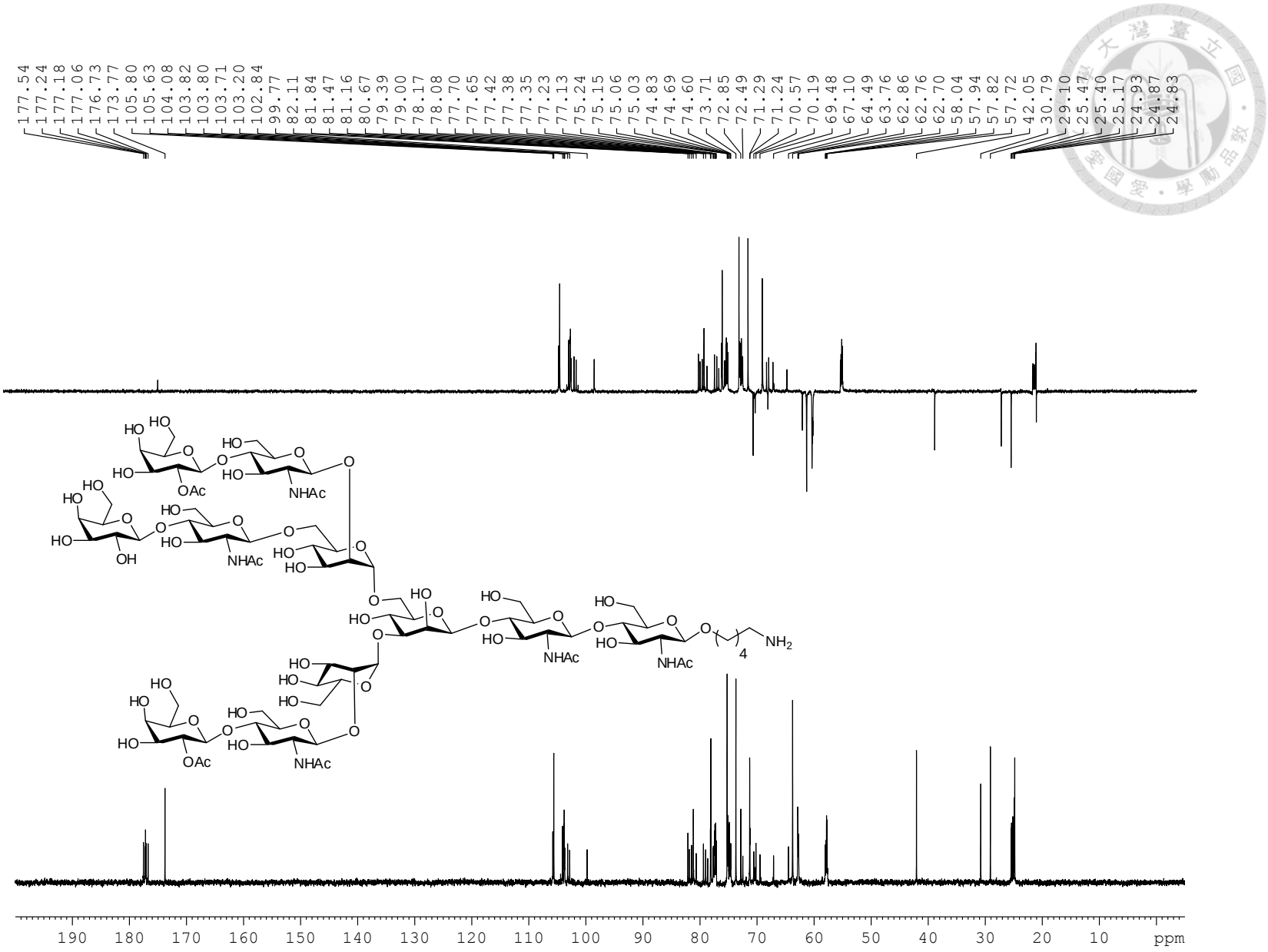
177.54
177.24
177.18
177.06
176.73
173.77
105.80
105.63
104.08
103.82
103.80
103.71
103.20
102.84
99.77
82.11
81.84
81.47
81.16
80.67
79.39
79.00
78.17
78.08
77.70
77.65
77.42
77.38
77.35
77.23
77.13
75.24
75.15
75.06
75.03
74.83
74.69
74.60
73.71
72.85
72.49
71.29
71.24
70.57
70.19
69.48
67.10
64.49
63.76
62.86
62.76
62.70
58.04
57.94
57.82
57.72
42.05
30.79
29.10
25.47
25.40
25.17
24.93
24.87
24.83
HO
OAc
NHAc
OH
NH2
4
O
190
180
170
160
150
140
130
120
110
100
90
80
70
60
50
40
30
20
10
ppm

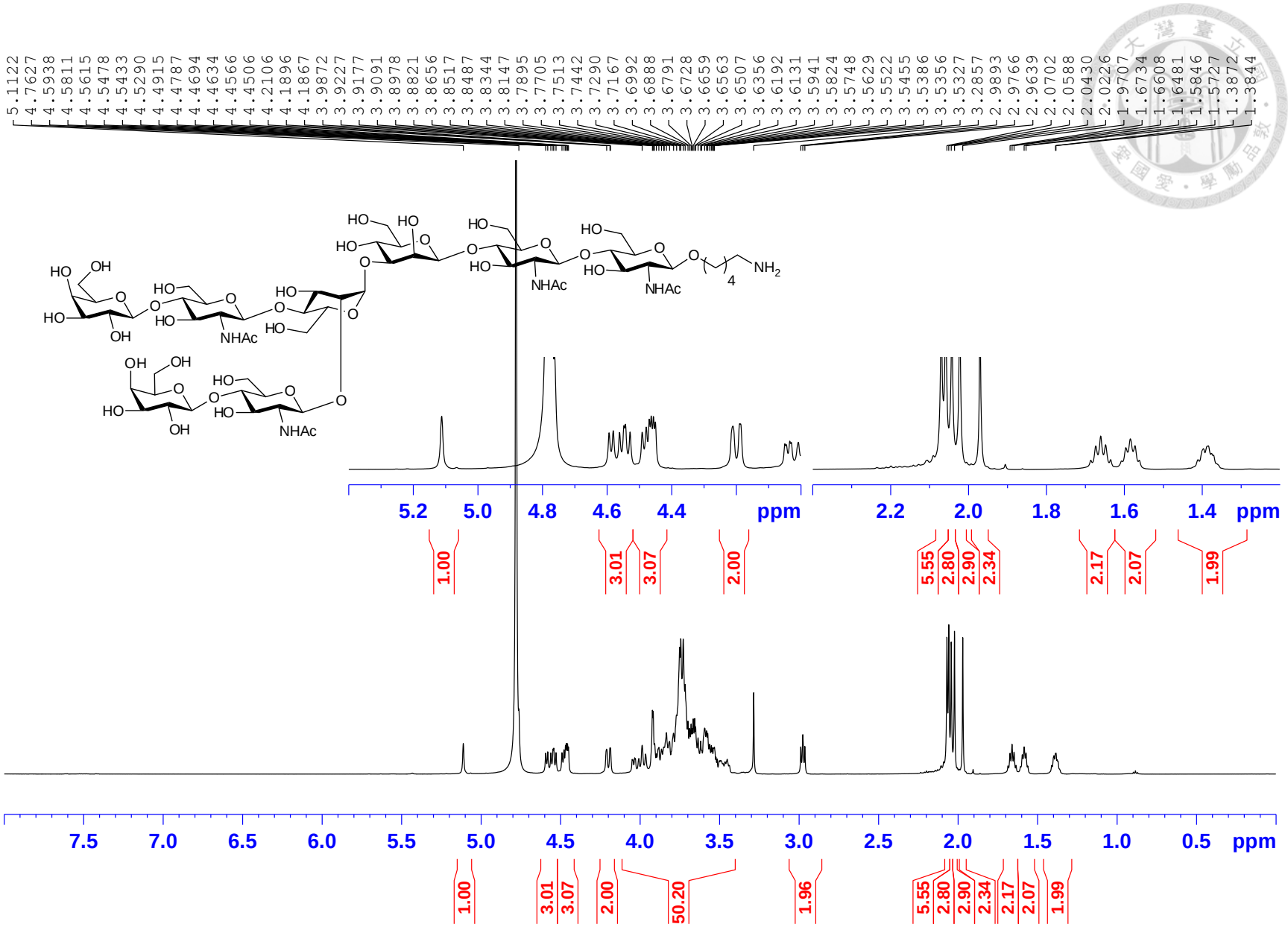
5.1122
4.7627
4.5938
4.5811
4.5615
4.5478
4.5433
4.5290
4.4915
4.4787
4.4694
4.4634
4.4566
4.4506
4.2106
4.1896
4.1867
3.9872
3.9227
3.9177
3.9091
3.8978
3.8821
3.8656
3.8517
3.8487
3.8344
3.8147
3.7895
3.7705
3.7513
3.7442
3.7290
3.7167
3.6992
3.6888
3.6791
3.6728
3.6659
3.6563
3.6507
3.6356
3.6192
3.6131
3.5941
3.5824
3.5748
3.5629
3.5522
3.5455
3.5386
3.5356
3.5327
3.2857
2.9893
2.9766
2.9639
2.0702
2.0588
2.0430
2.0226
1.9707
1.6734
1.6608
1.6481
1.5846
1.5727
1.3872
1.3844
NHAc
NHAc
NHAc
NHAc
NH2
4
5.2
5.0
4.8
4.6
4.4
ppm
2.2
2.0
1.8
1.6
1.4
ppm
1.00
3.01
3.07
2.00
5.55
2.80
2.90
2.34
2.17
2.07
1.99
7.5
7.0
6.5
6.0
5.5
5.0
4.5
4.0
3.5
3.0
2.5
2.0
1.5
1.0
0.5
ppm
1.00
3.01
3.07
2.00
50.20
1.96
5.55
2.80
2.90
2.34
2.17
2.07
1.99

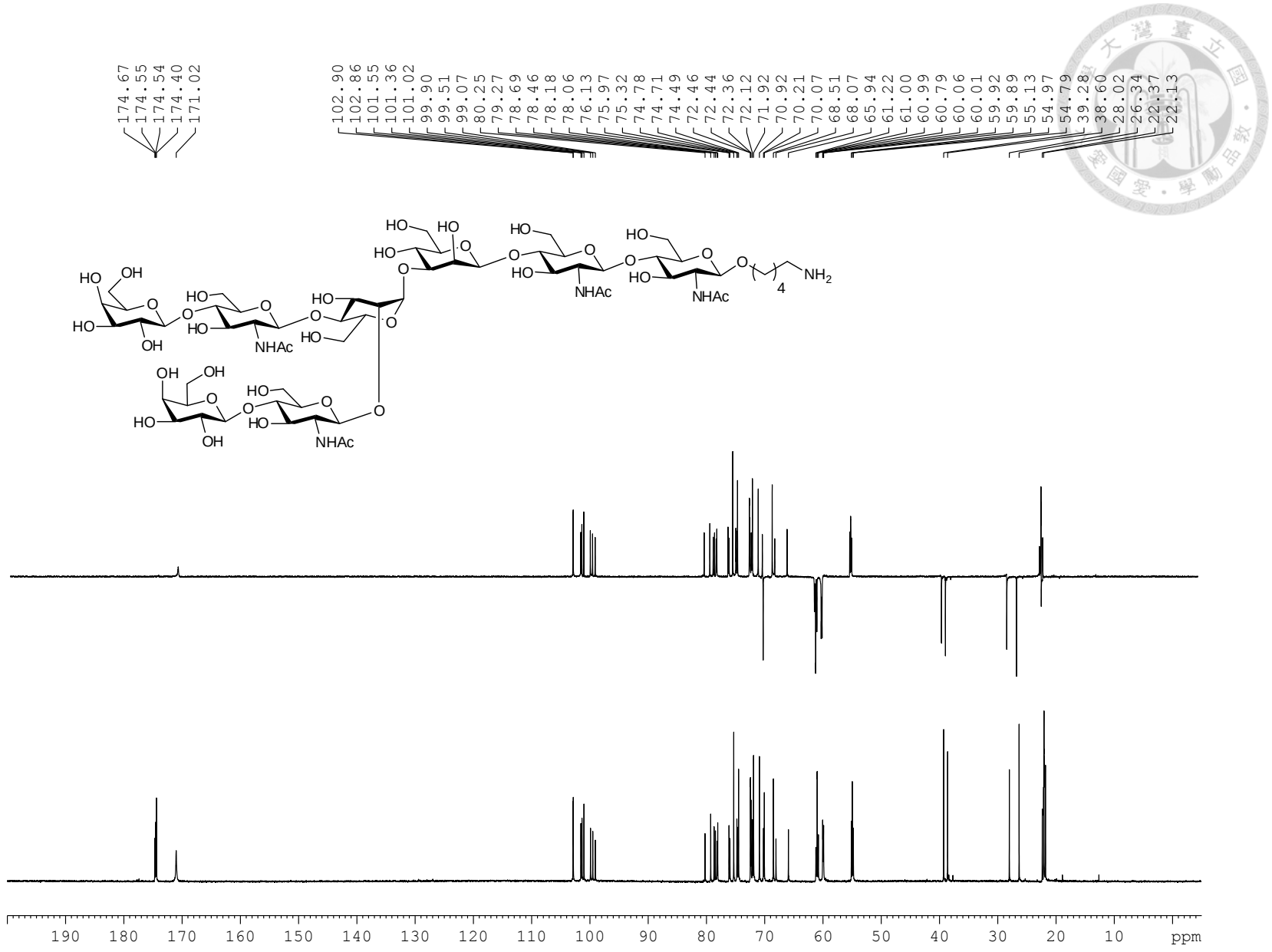
174.67
174.55
174.54
174.40
171.02
102.90
102.86
101.55
101.36
101.02
99.90
99.51
99.07
80.25
79.27
78.69
78.46
78.18
78.06
76.13
75.97
75.32
74.78
74.71
74.49
72.46
72.44
72.36
72.12
71.92
70.92
70.21
70.07
68.51
68.07
65.94
61.22
61.00
60.99
60.79
60.06
60.01
59.92
59.89
55.13
54.97
54.79
39.28
38.60
28.02
26.34
22.37
22.13
NHAc
NHAc
NHAc
NH2
4
190
180
170
160
150
140
130
120
110
100
90
80
70
60
50
40
30
20
10
ppm

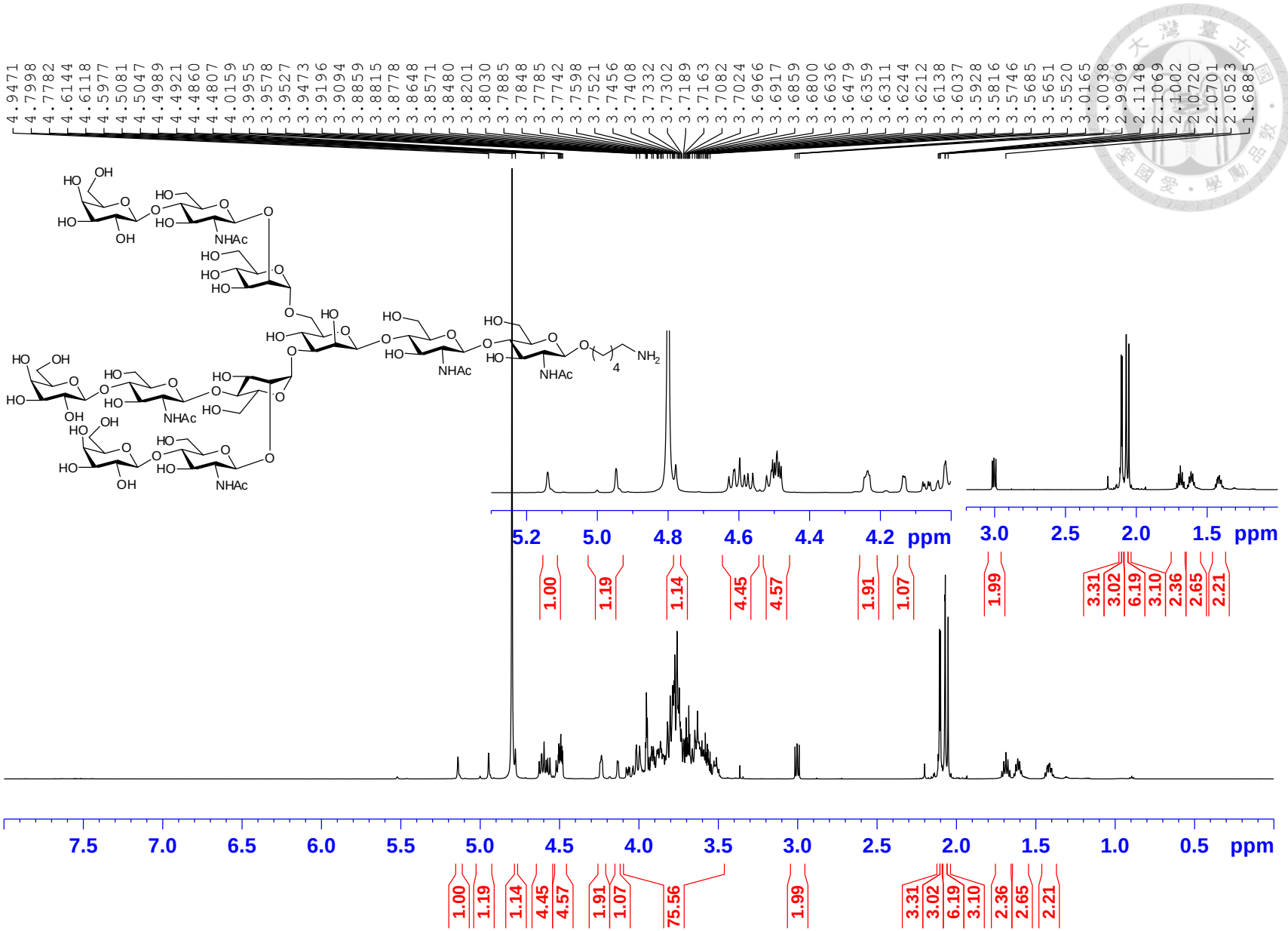
4.9471 4.7998 4.7782 4.6144 4.6118 4.5977 4.5081 4.5047 4.4989 4.4921 4.4860 4.4807 4.0159 3.9955 3.9578 3.9527 3.9473 3.9196 3.9094 3.8859 3.8815 3.8778 3.8648 3.8571 3.8480 3.8201 3.8030 3.7885 3.7848 3.7785 3.7742 3.7598 3.7521 3.7456 3.7408 3.7332 3.7302 3.7189 3.7163 3.7082 3.7024 3.6966 3.6917 3.6859 3.6800 3.6636 3.6479 3.6359 3.6311 3.6244 3.6212 3.6138 3.6037 3.5928 3.5816 3.5746 3.5685 3.5651 3.5520 3.0165 3.0038 2.9909 2.1148 2.1069 2.1002 2.0720 2.0701 2.0523 1.6885
NHAc
NHAc
NHAc
NHAc
NH2
4
5.2 5.0 4.8 4.6 4.4 4.2 ppm
3.0 2.5 2.0 1.5 ppm
1.00 1.19 1.14 4.45 4.57 1.91 1.07 1.99 3.31 3.02 6.19 3.10 2.36 2.65 2.21
7.5 7.0 6.5 6.0 5.5 5.0 4.5 4.0 3.5 3.0 2.5 2.0 1.5 1.0 0.5 ppm
1.00 1.19 1.14 4.45 4.57 1.91 1.07 75.56 1.99 3.31 3.02 6.19 3.10 2.36 2.65 2.21

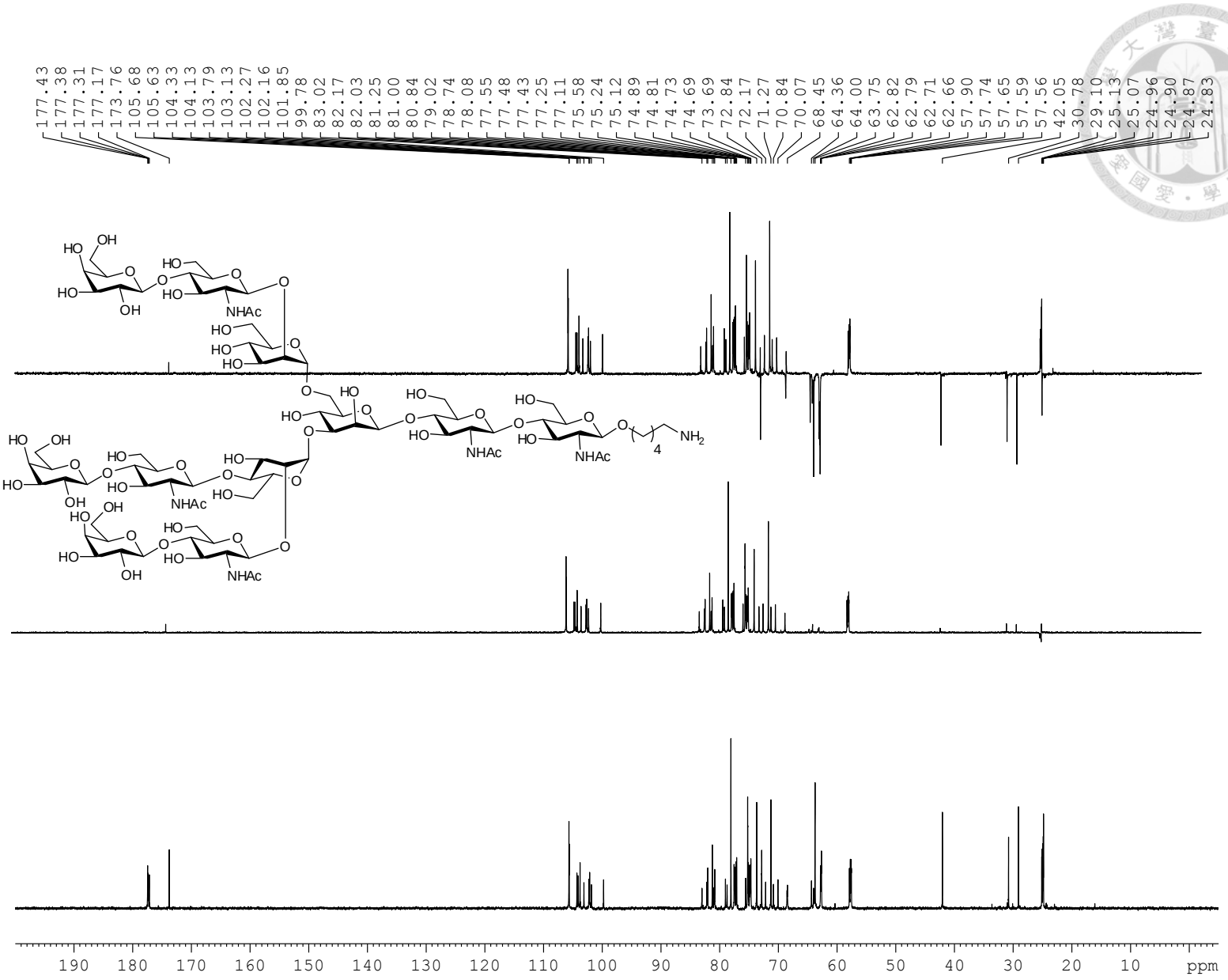
177.43
177.38
177.31
177.17
173.76
105.68
105.63
104.33
104.13
103.79
103.13
102.27
102.16
101.85
99.78
83.02
82.17
82.03
81.25
81.00
80.84
79.02
78.74
78.08
77.55
77.48
77.43
77.25
77.11
75.58
75.24
75.12
74.89
74.81
74.73
74.69
73.69
72.84
72.17
71.27
70.84
70.07
68.45
64.36
64.00
63.75
62.82
62.79
62.71
62.66
57.90
57.74
57.65
57.59
57.56
42.05
30.78
29.10
25.13
25.07
24.96
24.90
24.87
24.83
190
180
170
160
150
140
130
120
110
100
90
80
70
60
50
40
30
20
10
ppm

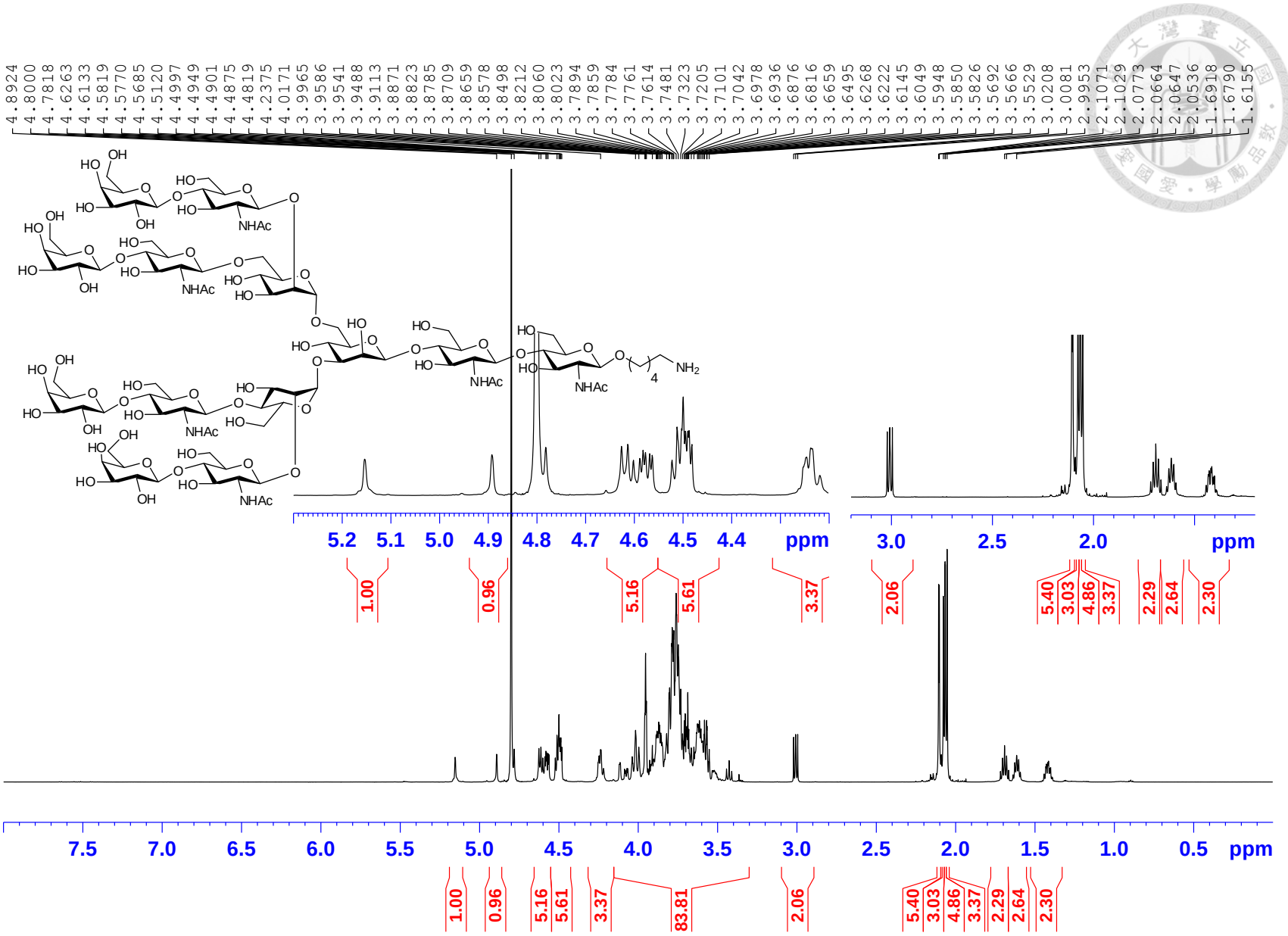
4.8924 4.8000 4.7818 4.6263 4.6133 4.5819 4.5770 4.5685 4.5120 4.4997 4.4949 4.4901 4.4875 4.4819 4.2375 4.0171 3.9965 3.9586 3.9541 3.9488 3.9113 3.8871 3.8823 3.8785 3.8709 3.8659 3.8578 3.8498 3.8212 3.8060 3.8023 3.7894 3.7859 3.7784 3.7761 3.7614 3.7481 3.7323 3.7205 3.7101 3.7042 3.6978 3.6936 3.6876 3.6816 3.6659 3.6495 3.6268 3.6222 3.6145 3.6049 3.5948 3.5850 3.5826 3.5692 3.5666 3.5529 3.0208 3.0081 2.9953 2.1071 2.1029 2.0773 2.0664 2.0647 2.0536 1.6918 1.6790 1.6155
5.2 5.1 5.0 4.9 4.8 4.7 4.6 4.5 4.4 ppm
3.0 2.5 2.0 ppm
1.00 0.96 5.16 5.61 3.37 2.06 5.40 3.03 4.86 3.37 2.29 2.64 2.30
7.5 7.0 6.5 6.0 5.5 5.0 4.5 4.0 3.5 3.0 2.5 2.0 1.5 1.0 0.5 ppm
1.00 0.96 5.16 5.61 3.37 83.81 2.06 5.40 3.03 4.86 3.37 2.29 2.64 2.30

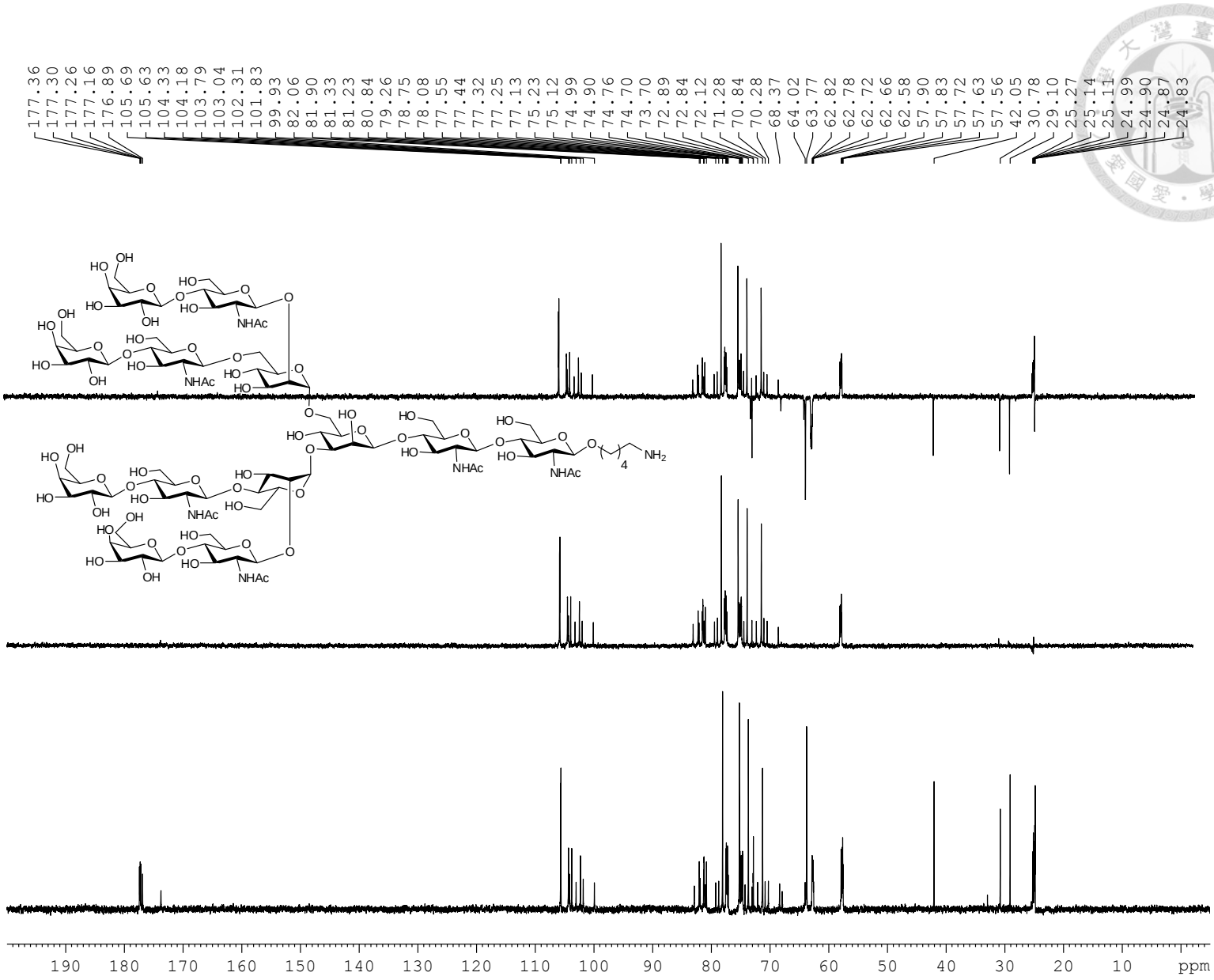
177.36
177.30
177.26
177.16
176.89
105.69
105.63
104.33
104.18
103.79
103.04
102.31
101.83
99.93
82.06
81.90
81.33
81.23
80.84
79.26
78.75
78.08
77.55
77.44
77.32
77.25
77.13
75.23
75.12
74.99
74.90
74.76
74.70
73.70
72.89
72.84
72.12
71.28
70.84
70.28
68.37
64.02
63.77
62.82
62.78
62.72
62.66
62.58
57.90
57.83
57.72
57.63
57.56
42.05
30.78
29.10
25.27
25.14
25.11
24.99
24.90
24.87
24.83
190
180
170
160
150
140
130
120
110
100
90
80
70
60
50
40
30
20
10
ppm

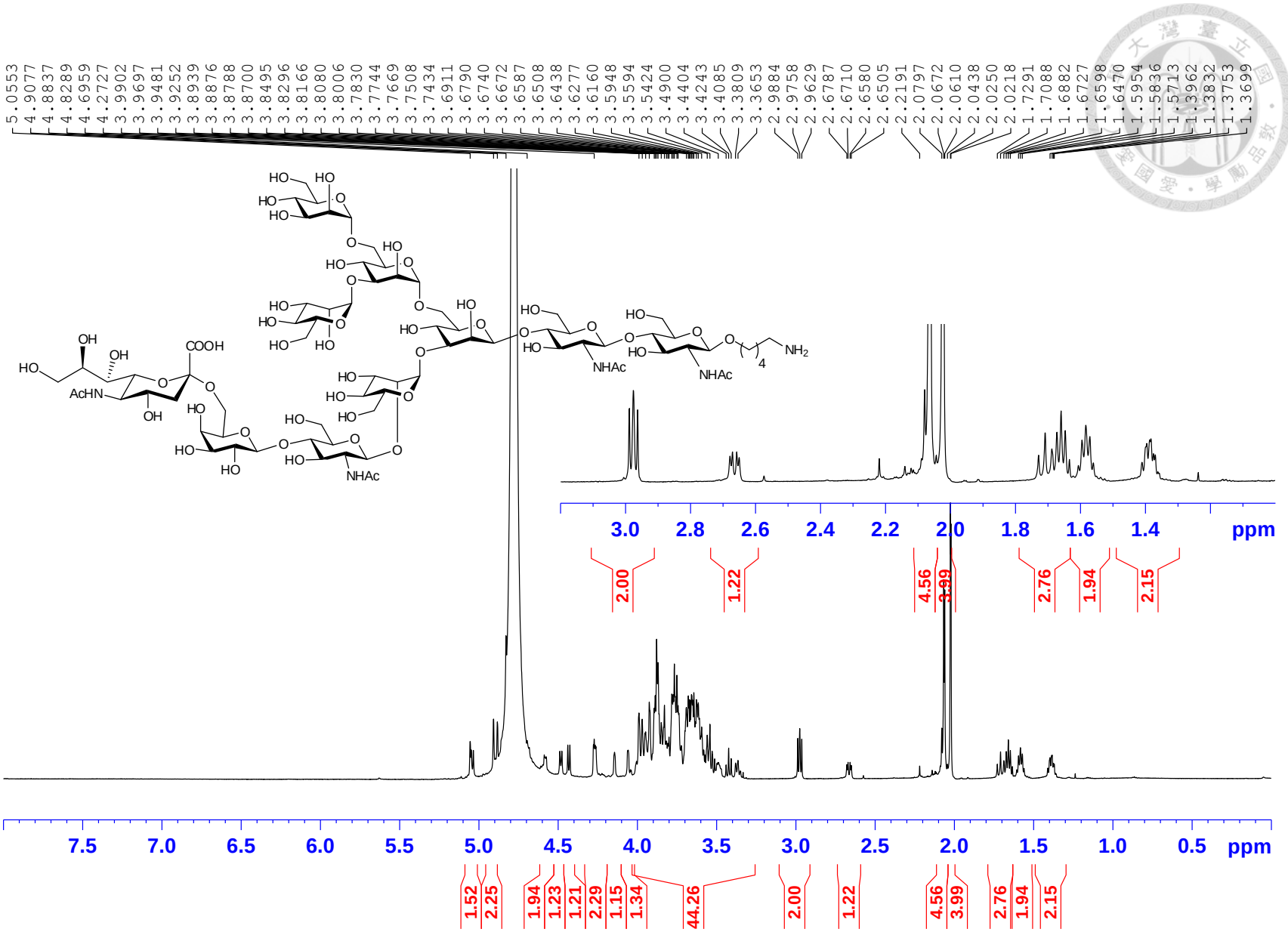
5.0553
4.9077
4.8837
4.8289
4.6959
4.2727
3.9902
3.9697
3.9481
3.9252
3.8939
3.8876
3.8788
3.8700
3.8495
3.8296
3.8166
3.8080
3.8006
3.7830
3.7744
3.7669
3.7508
3.7434
3.6911
3.6790
3.6740
3.6672
3.6587
3.6508
3.6438
3.6277
3.6160
3.5948
3.5594
3.5424
3.4900
3.4404
3.4243
3.4085
3.3809
3.3653
2.9884
2.9758
2.9629
2.6787
2.6710
2.6580
2.6505
2.2191
2.0797
2.0672
2.0610
2.0438
2.0250
2.0218
1.7291
1.7088
1.6882
1.6727
1.6598
1.6470
1.5954
1.5836
1.5713
1.3962
1.3832
1.3753
1.3699
3.0
2.8
2.6
2.4
2.2
2.0
1.8
1.6
1.4
ppm
2.00
1.22
4.56
3.99
2.76
1.94
2.15
7.5
7.0
6.5
6.0
5.5
5.0
4.5
4.0
3.5
3.0
2.5
2.0
1.5
1.0
0.5
ppm
1.52
2.25
1.94
1.23
1.21
2.29
1.15
1.34
44.26
2.00
1.22
4.56
3.99
2.76
1.94
2.15

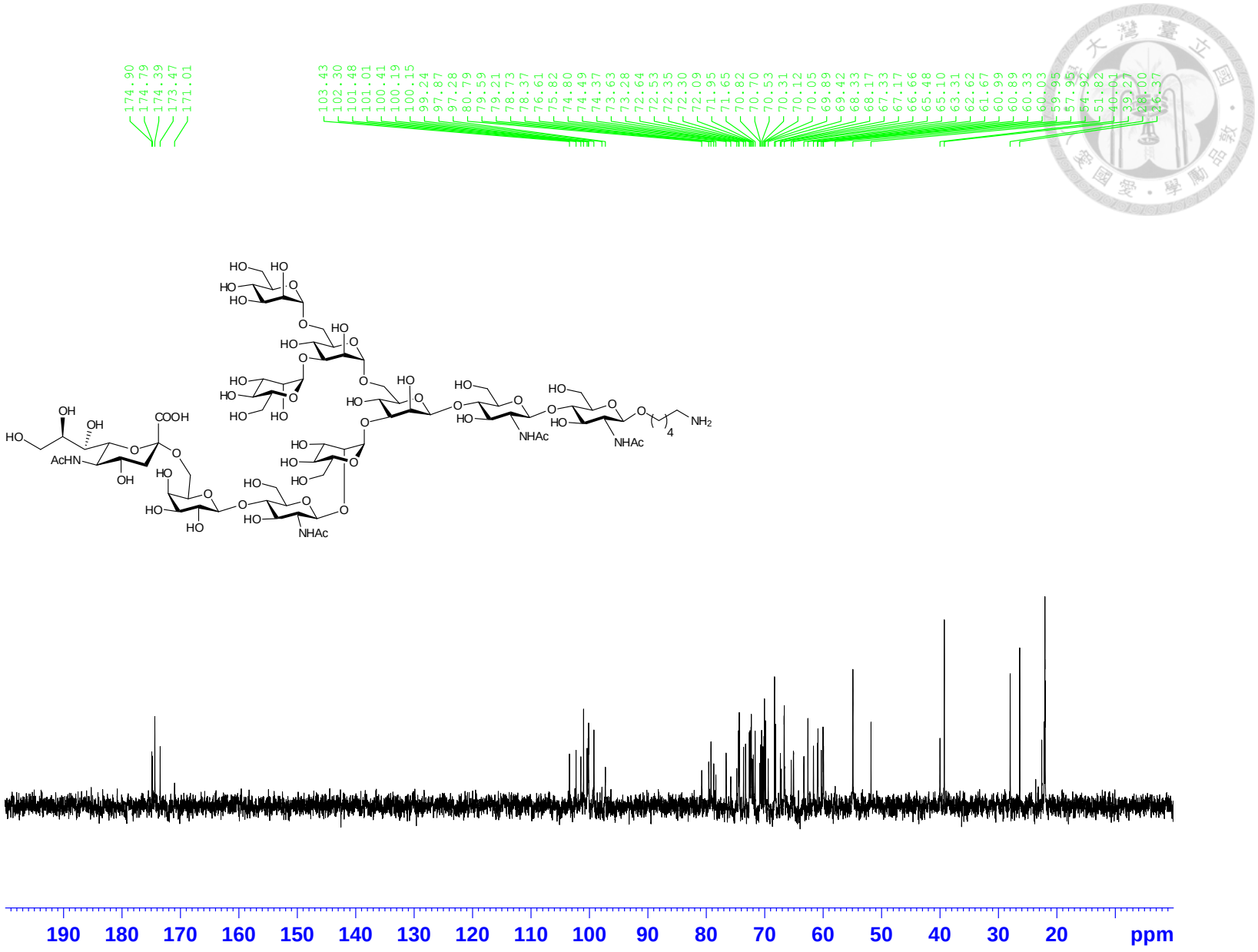
174.90
174.79
174.39
173.47
171.01
103.43
102.30
101.48
101.01
100.41
100.19
100.15
99.24
97.87
97.28
80.79
79.59
79.21
78.73
78.37
76.61
75.82
74.80
74.49
74.37
73.63
73.28
72.64
72.53
72.35
72.30
72.09
71.95
71.65
70.82
70.70
70.53
70.31
70.12
70.05
69.89
69.42
68.33
68.17
67.33
67.17
66.66
65.48
65.10
63.31
62.62
61.67
60.99
60.89
60.33
60.03
59.95
57.95
54.92
51.82
40.01
39.27
28.00
26.37
HO
OH
AcHN
COOH
NHAc
NH2
4
190
180
170
160
150
140
130
120
110
100
90
80
70
60
50
40
30
20
ppm

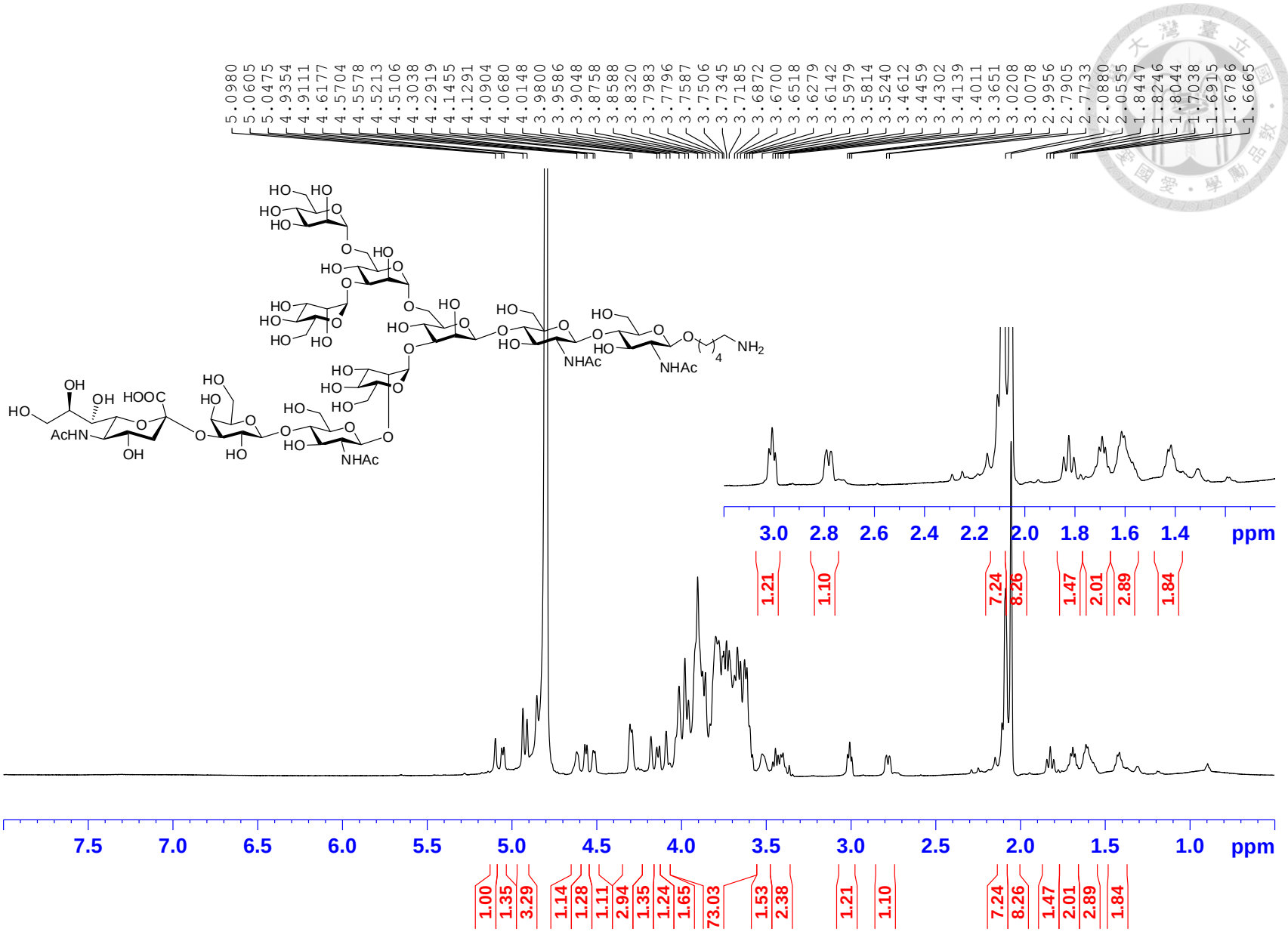
5.0980
5.0605
5.0475
4.9354
4.9111
4.6177
4.5704
4.5578
4.5213
4.5106
4.3038
4.2919
4.1455
4.1291
4.0904
4.0680
4.0148
3.9800
3.9586
3.9048
3.8758
3.8588
3.8320
3.7983
3.7796
3.7587
3.7506
3.7345
3.7185
3.6872
3.6700
3.6518
3.6279
3.6142
3.5979
3.5814
3.5240
3.4612
3.4459
3.4302
3.4139
3.4011
3.3651
3.0208
3.0078
2.9956
2.7905
2.7733
2.0880
2.0555
1.8447
1.8246
1.8044
1.7038
1.6915
1.6786
1.6665
HO
HOOC
AcHN
NHAc
NH2
3.0 2.8 2.6 2.4 2.2 2.0 1.8 1.6 1.4 ppm
1.21 1.10 7.24 8.26 1.47 2.01 2.89 1.84
7.5 7.0 6.5 6.0 5.5 5.0 4.5 4.0 3.5 3.0 2.5 2.0 1.5 1.0 ppm
1.00 1.35 3.29 1.14 1.28 1.11 2.94 1.35 1.24 1.65 73.03 1.53 2.38 1.21 1.10 7.24 8.26 1.47 2.01 2.89 1.84

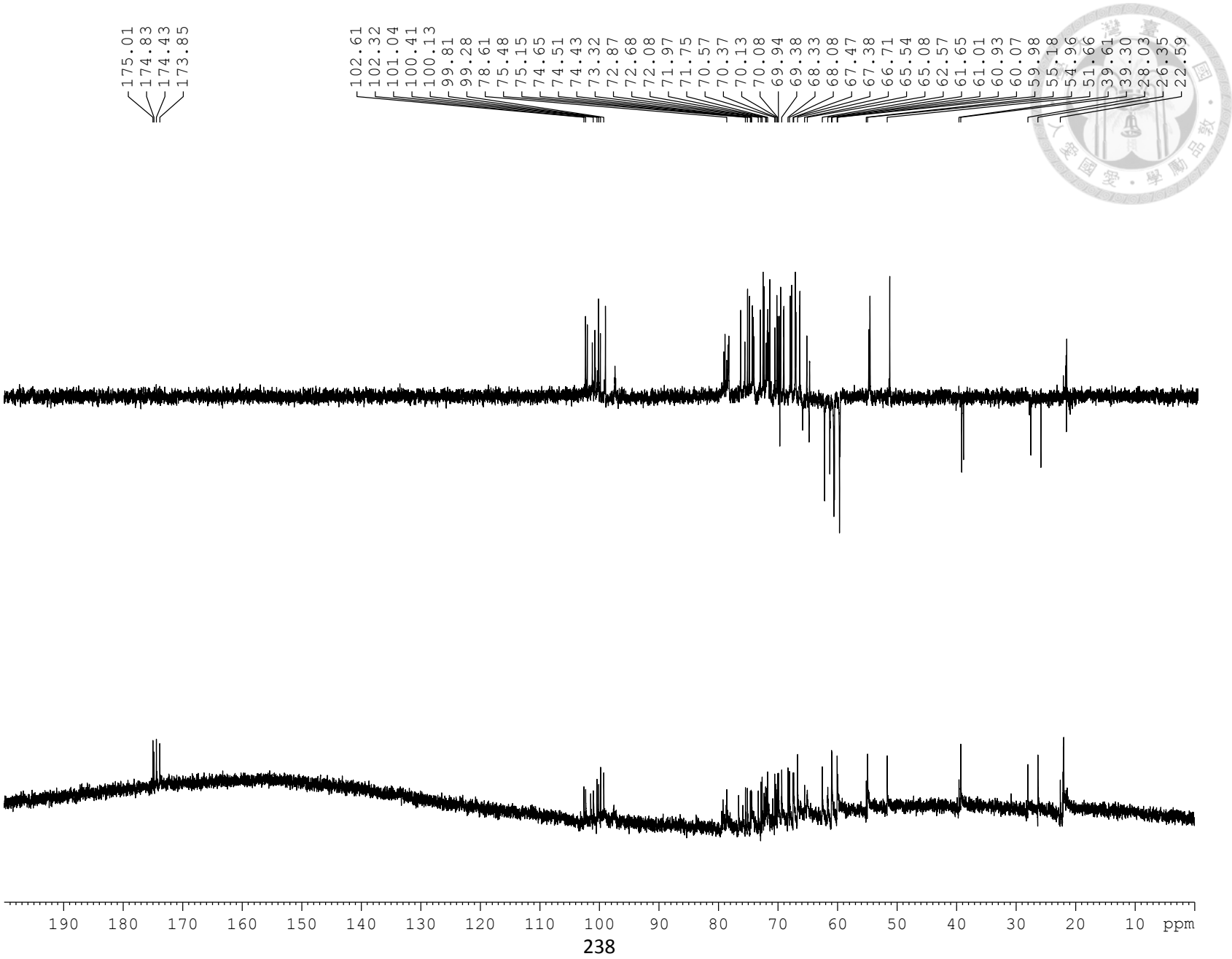
175.01
174.83
174.43
173.85
102.61
102.32
101.04
100.41
100.13
99.81
99.28
78.61
75.48
75.15
74.65
74.51
74.43
73.32
72.87
72.68
72.08
71.97
71.75
70.57
70.37
70.13
70.08
69.94
69.38
68.33
68.08
67.47
67.38
66.71
65.54
65.08
62.57
61.65
61.01
60.93
60.07
59.98
55.18
54.96
51.66
39.61
39.30
28.03
26.35
22.59
190 180 170 160 150 140 130 120 110 100 90 80 70 60 50 40 30 20 10 ppm

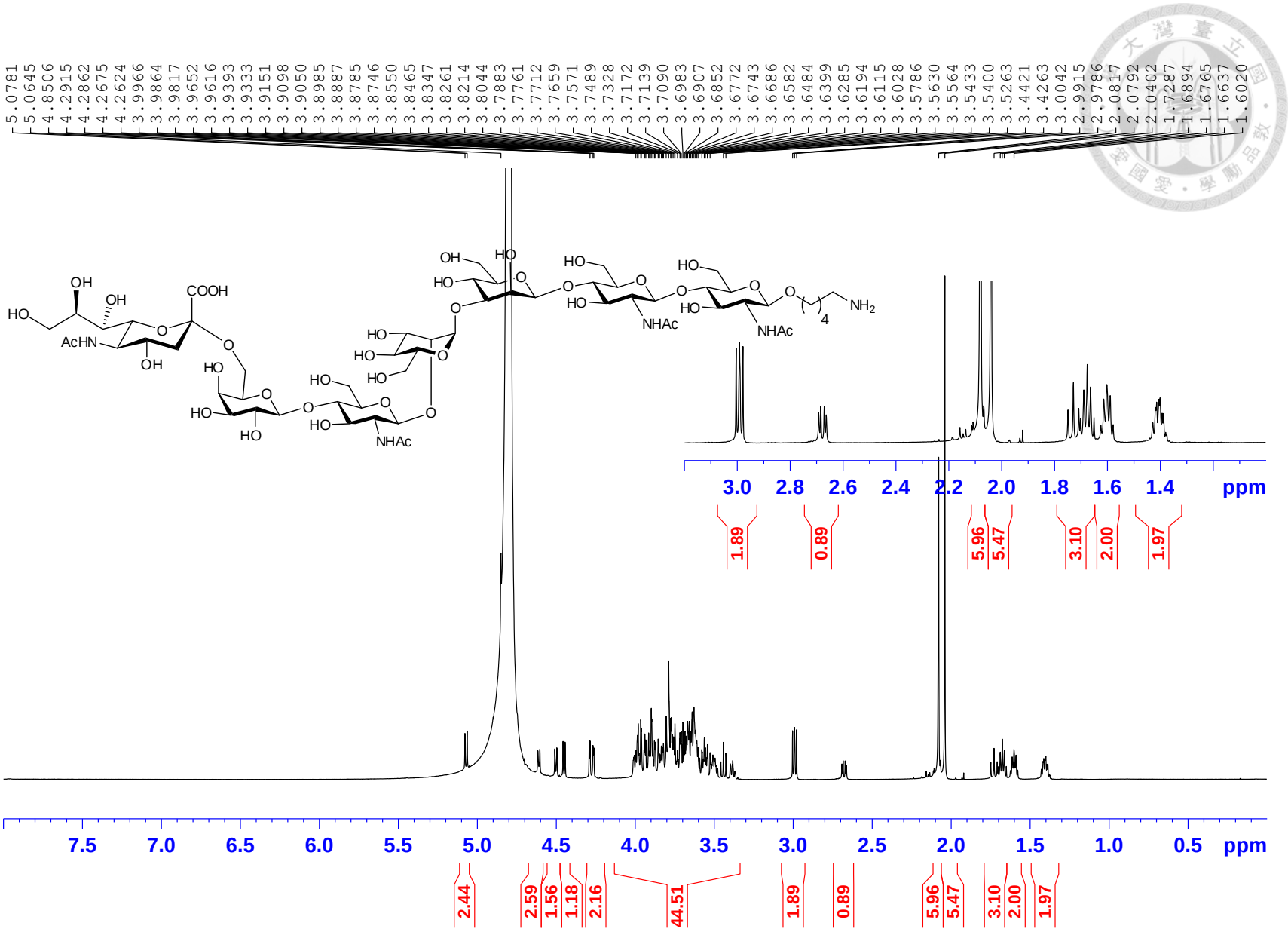
5.0781
5.0645
4.8506
4.2915
4.2862
4.2675
4.2624
3.9966
3.9864
3.9817
3.9652
3.9616
3.9393
3.9333
3.9151
3.9098
3.9050
3.8985
3.8887
3.8785
3.8746
3.8550
3.8465
3.8347
3.8261
3.8214
3.8044
3.7883
3.7761
3.7712
3.7659
3.7571
3.7489
3.7328
3.7172
3.7139
3.7090
3.6983
3.6907
3.6852
3.6772
3.6743
3.6686
3.6582
3.6484
3.6399
3.6285
3.6194
3.6115
3.6028
3.5786
3.5630
3.5564
3.5433
3.5400
3.5263
3.4421
3.4263
3.0042
2.9915
2.9786
2.0817
2.0792
2.0402
1.7287
1.6894
1.6765
1.6637
1.6020
OH
HO
OH
COOH
AcHN
OH
O
HO
HO
HO
HO
HO
HO
HO
HO
HO
HO
HO
HO
HO
HO
HO
NHAc
NHAc
NHAc
NH2
4
3.0
2.8
2.6
2.4
2.2
2.0
1.8
1.6
1.4
ppm
1.89
0.89
5.96
5.47
3.10
2.00
1.97
7.5
7.0
6.5
6.0
5.5
5.0
4.5
4.0
3.5
3.0
2.5
2.0
1.5
1.0
0.5
ppm
2.44
2.59
1.56
1.18
2.16
44.51
1.89
0.89
5.96
5.47
3.10
2.00
1.97

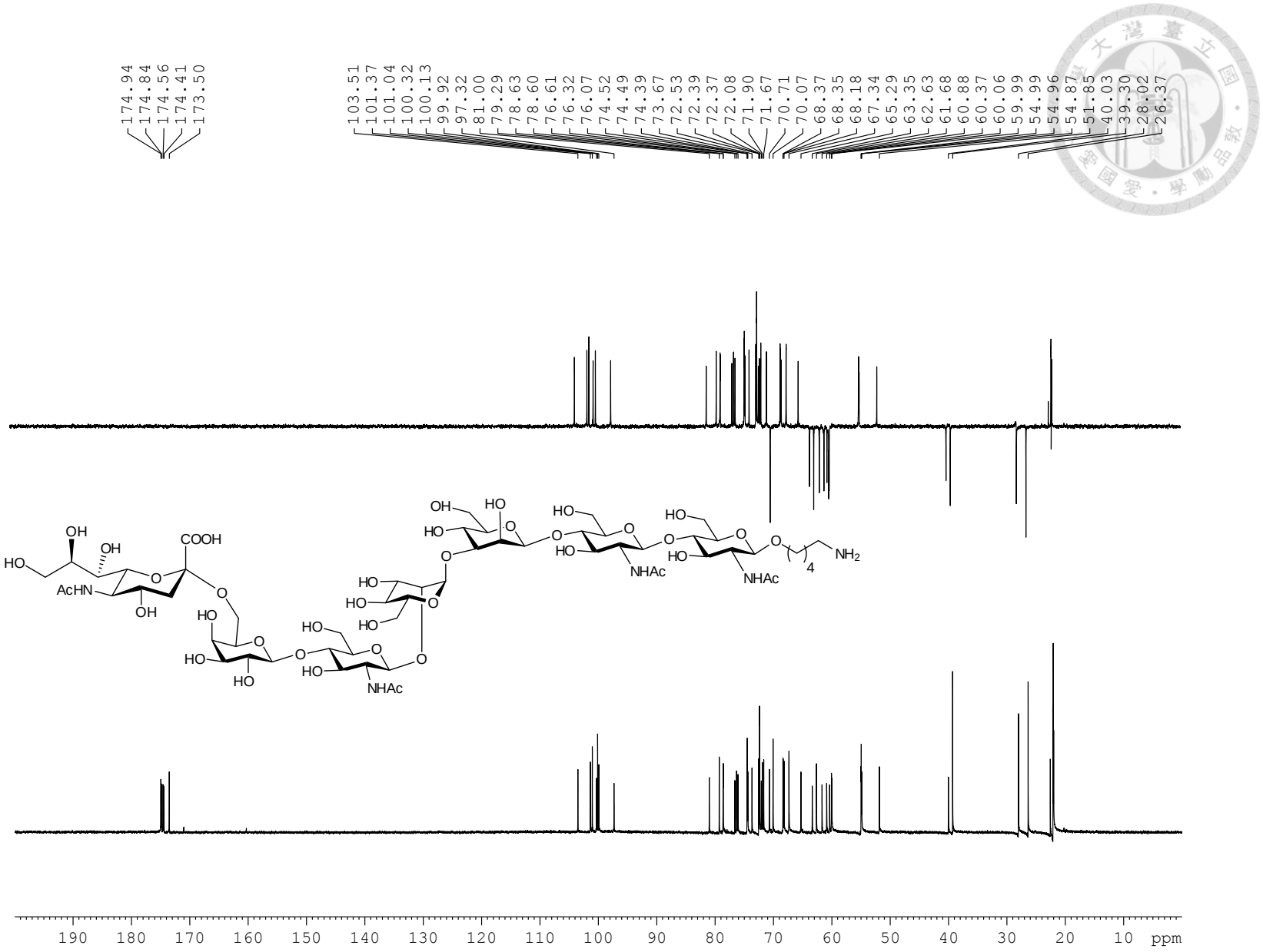
174.94
174.84
174.56
174.41
173.50
103.51
101.37
101.04
100.32
100.13
99.92
97.32
81.00
79.29
78.63
78.60
76.61
76.32
76.07
74.52
74.49
74.39
73.67
72.53
72.39
72.37
72.08
71.90
71.67
70.71
70.07
68.37
68.35
68.18
67.34
65.29
63.35
62.63
61.68
60.88
60.37
60.06
59.99
54.96
54.87
51.85
40.03
39.30
28.02
26.37
190
180
170
160
150
140
130
120
110
100
90
80
70
60
50
40
30
20
10
ppm

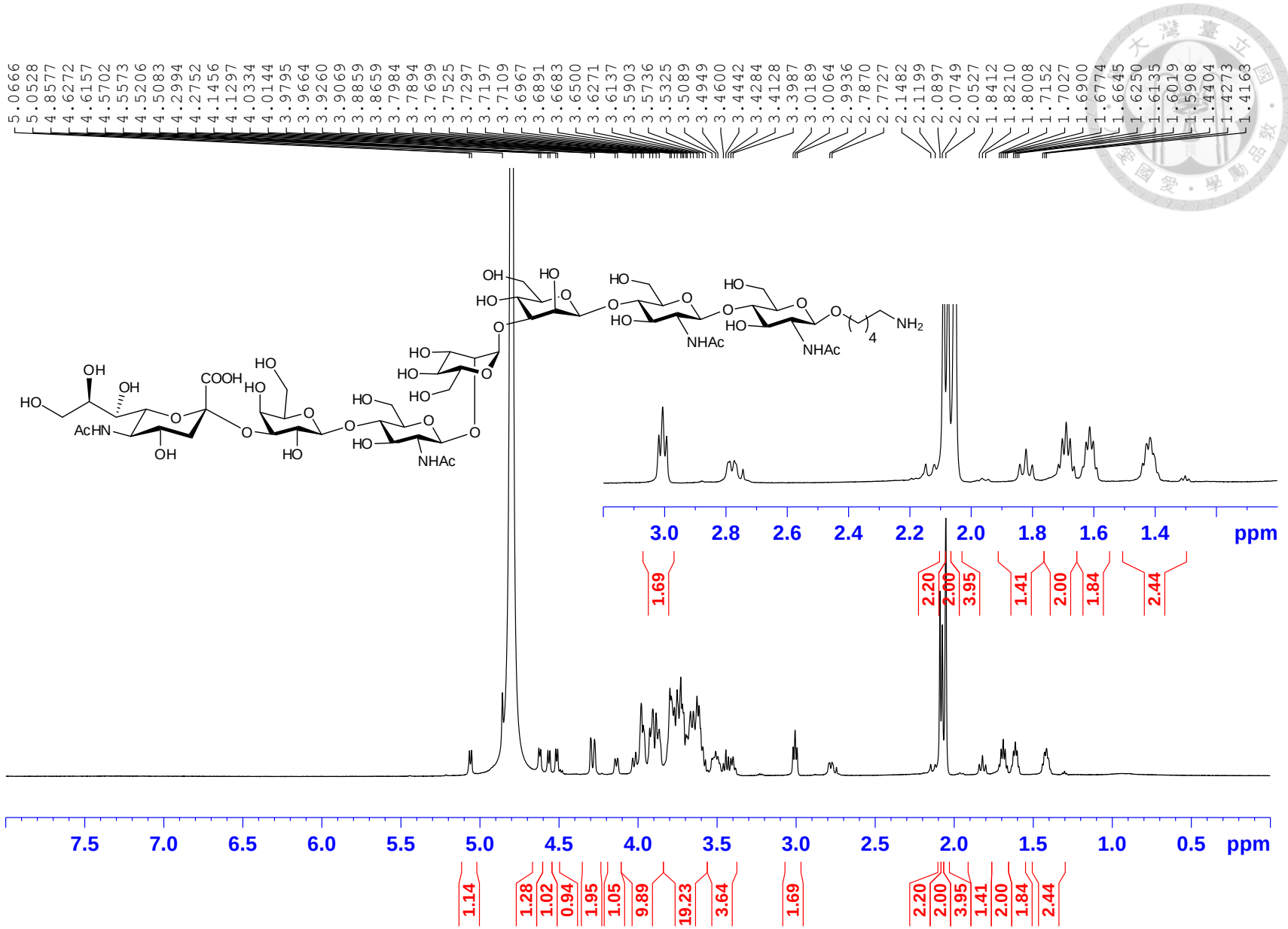
5.0666
5.0528
4.8577
4.6272
4.6157
4.5702
4.5573
4.5206
4.5083
4.2994
4.2752
4.1456
4.1297
4.0334
4.0144
3.9795
3.9664
3.9260
3.9069
3.8859
3.8659
3.7984
3.7894
3.7699
3.7525
3.7297
3.7197
3.7109
3.6967
3.6891
3.6683
3.6500
3.6271
3.6137
3.5903
3.5736
3.5325
3.5089
3.4949
3.4600
3.4442
3.4284
3.4128
3.3987
3.0189
3.0064
2.9936
2.7870
2.7727
2.1482
2.1199
2.0897
2.0749
2.0527
1.8412
1.8210
1.8008
1.7152
1.7027
1.6900
1.6774
1.6645
1.6250
1.6135
1.6019
1.5908
1.4404
1.4273
1.4163
3.0
2.8
2.6
2.4
2.2
2.0
1.8
1.6
1.4
ppm
1.69
2.20
2.00
3.95
1.41
2.00
1.84
2.44
7.5
7.0
6.5
6.0
5.5
5.0
4.5
4.0
3.5
3.0
2.5
2.0
1.5
1.0
0.5
ppm
1.14
1.28
1.02
0.94
1.95
1.05
9.89
19.23
3.64
1.69
2.20
2.00
3.95
1.41
2.00
1.84
2.44

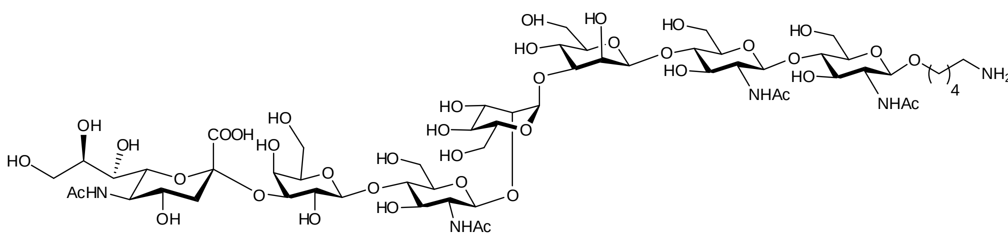
OH
HO
OH
COOH
HO
HO
AcHN
OH
HO
HO
HO
HO
NHAc
HO
HO
HO
OH
HO
HO
HO
NHAc
HO
HO
NHAc
4
NH2

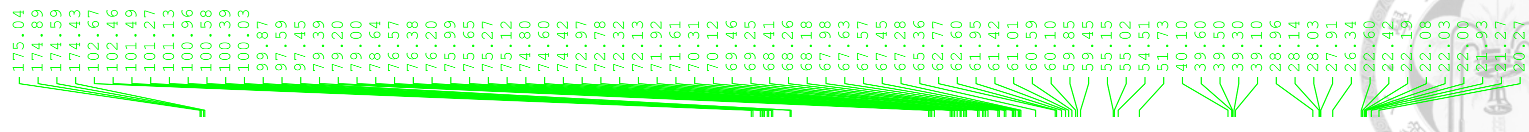
175.04
174.89
174.59
174.43
102.67
102.46
101.49
101.27
101.13
100.96
100.58
100.39
100.03
99.87
97.59
97.45
79.39
79.20
79.00
78.64
76.57
76.38
76.20
75.99
75.65
75.27
75.12
74.80
74.60
74.42
72.97
72.78
72.32
72.13
71.92
71.61
70.31
70.12
69.46
69.25
68.41
68.26
68.18
67.98
67.63
67.57
67.45
67.28
65.36
62.77
62.60
61.95
61.42
61.01
60.59
60.10
59.85
59.45
55.15
55.02
54.51
51.73
40.10
39.60
39.50
39.30
39.10
28.96
28.14
28.03
27.91
26.34
22.60
22.42
22.19
22.08
22.03
22.00
21.93
21.27
20.27

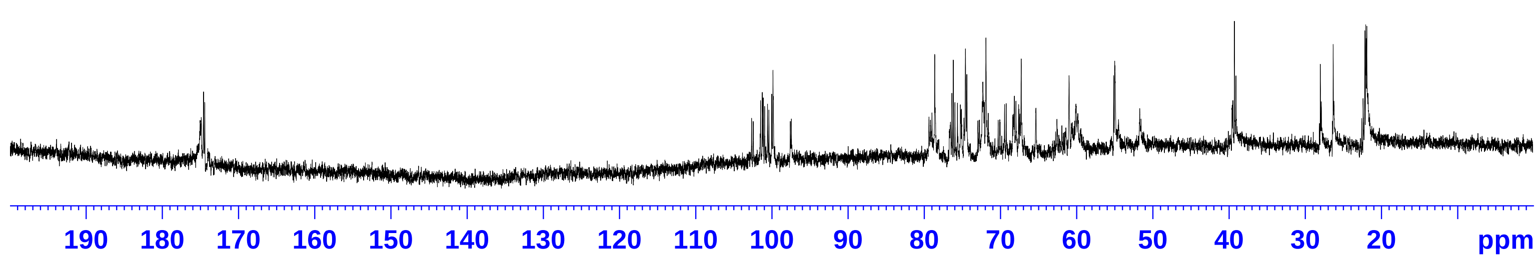
190
180
170
160
150
140
130
120
110
100
90
80
70
60
50
40
30
20
ppm

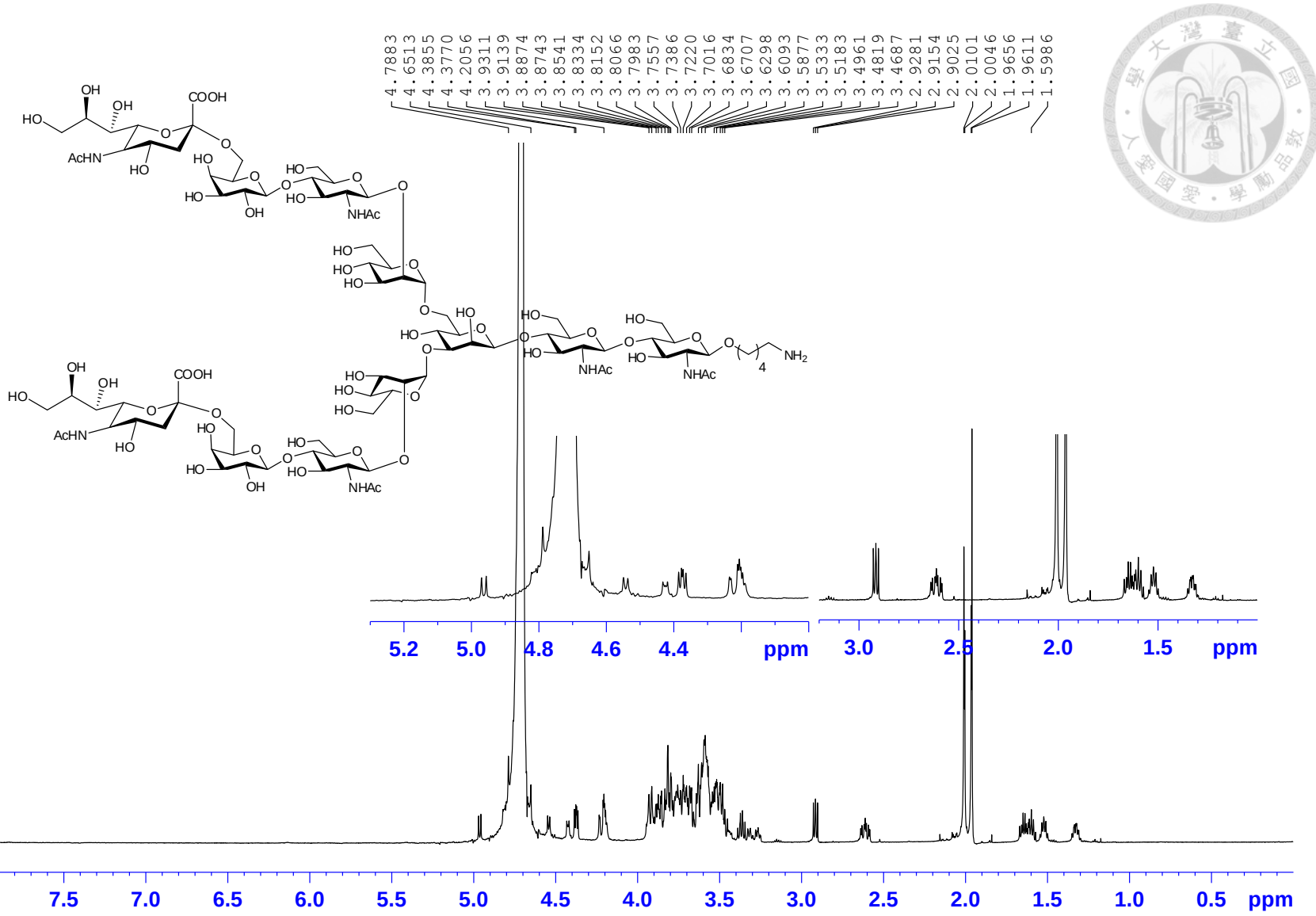
4.7883
4.6513
4.3855
4.3770
4.2056
3.9311
3.9139
3.8874
3.8743
3.8541
3.8334
3.8152
3.8066
3.7983
3.7557
3.7386
3.7220
3.7016
3.6834
3.6707
3.6298
3.6093
3.5877
3.5333
3.5183
3.4961
3.4819
3.4687
3.9281
2.9154
2.9025
2.0101
2.0046
1.9656
1.9611
1.5986
5.2
5.0
4.8
4.6
4.4
ppm
3.0
2.5
2.0
1.5
ppm
7.5
7.0
6.5
6.0
5.5
5.0
4.5
4.0
3.5
3.0
2.5
2.0
1.5
1.0
0.5
ppm

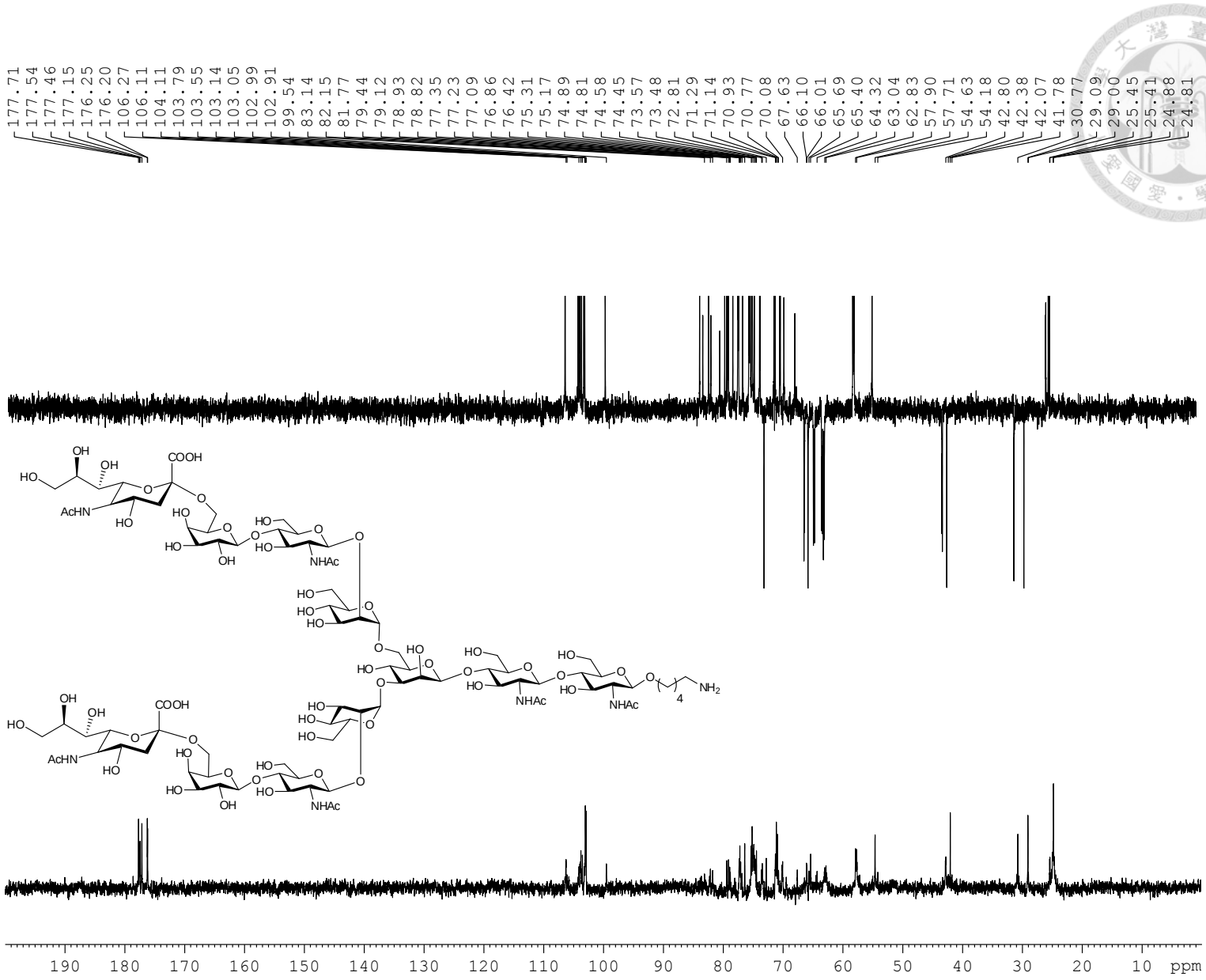
177.71
177.54
177.46
177.15
176.25
176.20
106.27
106.11
104.11
103.79
103.55
103.14
103.05
102.99
102.91
99.54
83.14
82.15
81.77
79.44
79.12
78.93
78.82
77.35
77.23
77.09
76.86
76.42
75.31
75.17
74.89
74.81
74.58
74.45
73.57
73.48
72.81
71.29
71.14
70.93
70.77
70.08
67.63
66.10
66.01
65.69
65.40
64.32
63.04
62.83
57.90
57.71
54.63
54.18
42.80
42.38
42.07
41.78
30.77
29.09
29.00
25.45
25.41
24.88
24.81
190
180
170
160
150
140
130
120
110
100
90
80
70
60
50
40
30
20
10
ppm

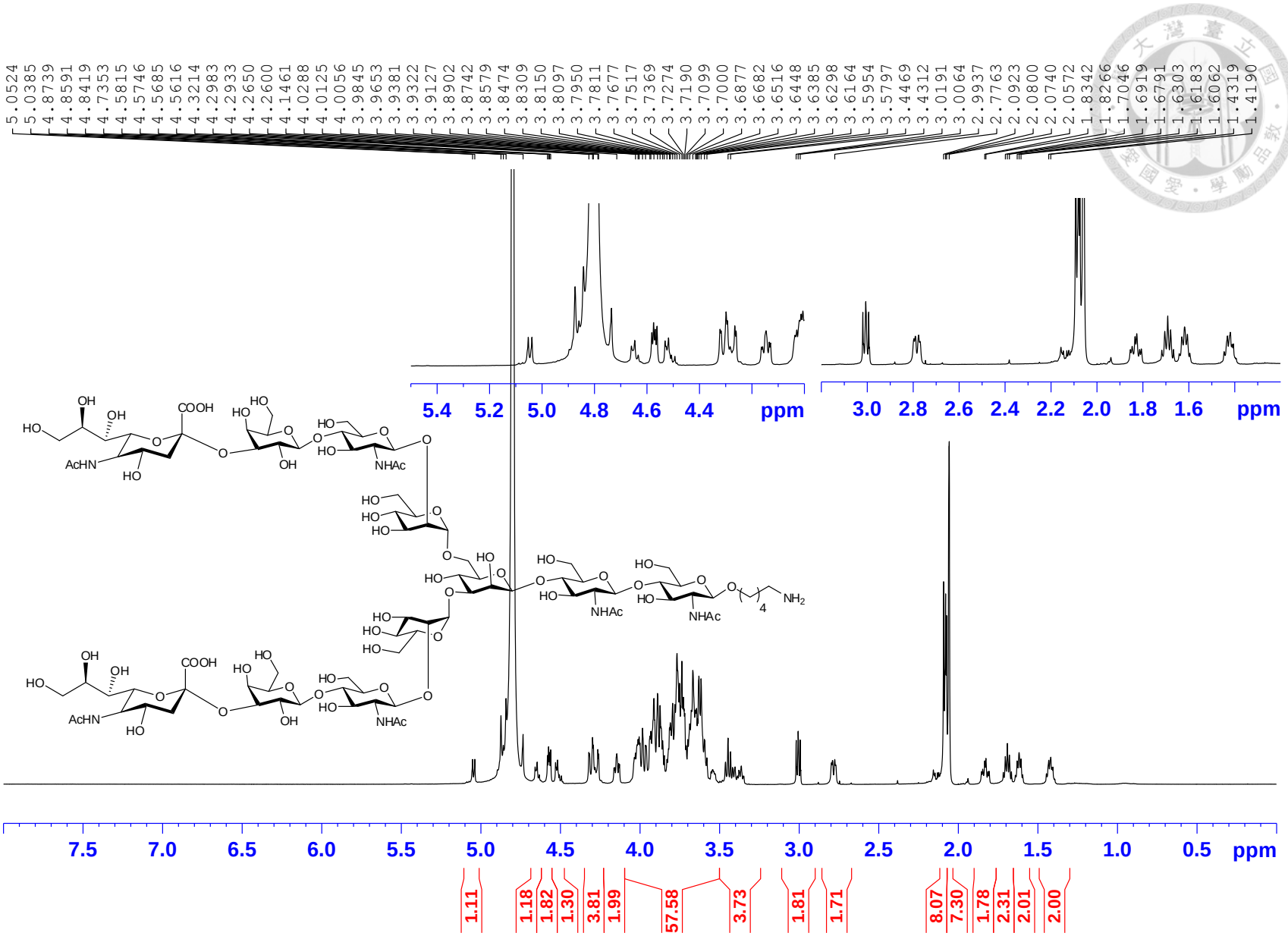
5.0524
5.0385
4.8739
4.8591
4.8419
4.7353
4.5815
4.5746
4.5685
4.5616
4.3214
4.2983
4.2933
4.2650
4.2600
4.1461
4.0288
4.0125
4.0056
3.9845
3.9653
3.9381
3.9322
3.9127
3.8902
3.8742
3.8579
3.8474
3.8309
3.8150
3.8097
3.7950
3.7811
3.7677
3.7517
3.7369
3.7274
3.7190
3.7099
3.7000
3.6877
3.6682
3.6516
3.6448
3.6385
3.6298
3.6164
3.5954
3.5797
3.4469
3.4312
3.0191
3.0064
2.9937
2.7763
2.0923
2.0800
2.0740
2.0572
1.8342
1.8266
1.7046
1.6919
1.6791
1.6303
1.6183
1.6062
1.4319
1.4190
5.4 5.2 5.0 4.8 4.6 4.4 ppm
3.0 2.8 2.6 2.4 2.2 2.0 1.8 1.6 ppm
7.5 7.0 6.5 6.0 5.5 5.0 4.5 4.0 3.5 3.0 2.5 2.0 1.5 1.0 0.5 ppm
1.11
1.18
1.82
1.30
3.81
1.99
57.58
3.73
1.81
1.71
8.07
7.30
1.78
2.31
2.01
2.00

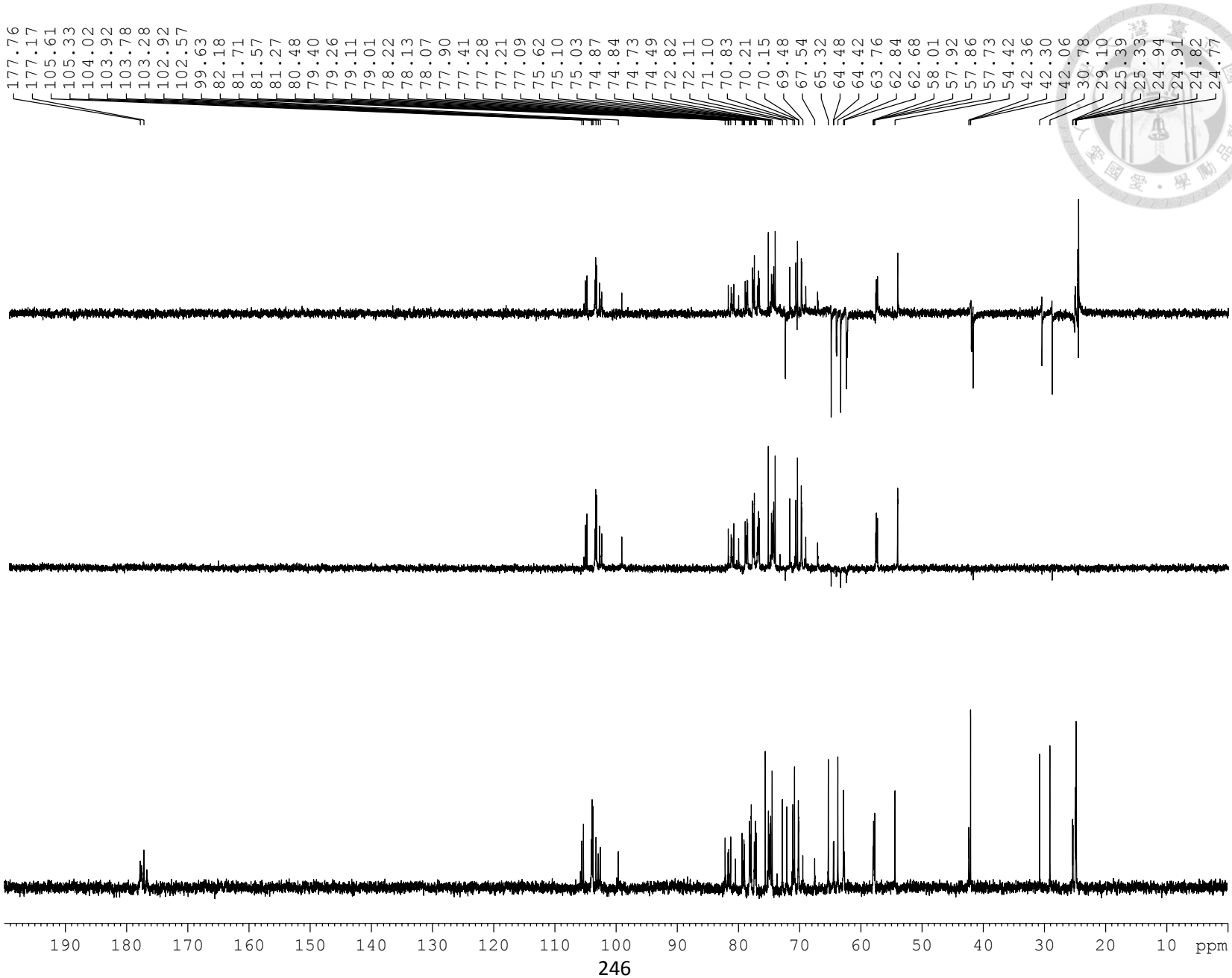
177.76
177.17
105.61
105.33
104.02
103.92
103.78
103.28
102.92
102.57
99.63
82.18
81.71
81.57
81.27
80.48
79.40
79.26
79.11
79.01
78.22
78.13
78.07
77.90
77.41
77.28
77.21
77.09
75.62
75.10
75.03
74.87
74.84
74.73
74.49
72.82
72.11
71.10
70.83
70.21
70.15
69.48
67.54
65.32
64.48
64.42
63.76
62.84
62.68
58.01
57.92
57.86
57.73
54.42
42.36
42.30
42.06
30.78
29.10
25.39
25.33
24.94
24.91
24.82
24.77
190
180
170
160
150
140
130
120
110
100
90
80
70
60
50
40
30
20
10
ppm

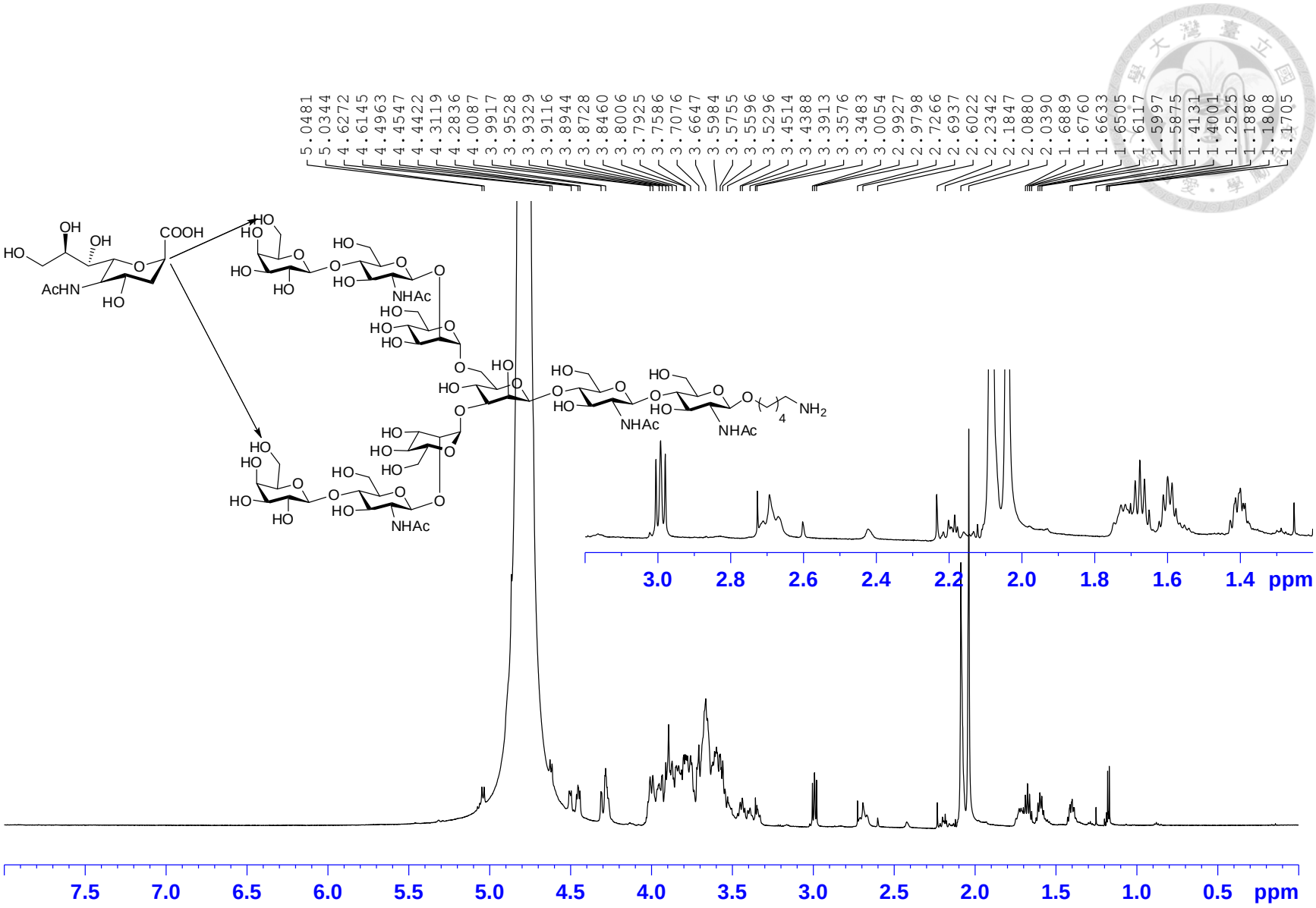
5.0481
5.0344
4.6272
4.6145
4.4963
4.4547
4.4422
4.3119
4.2836
4.0087
3.9917
3.9528
3.9329
3.9116
3.8944
3.8728
3.8460
3.8006
3.7925
3.7586
3.7076
3.6647
3.5984
3.5755
3.5596
3.5296
3.4514
3.4388
3.3913
3.3576
3.3483
3.0054
2.9927
2.9798
2.7266
2.6937
2.6022
2.2342
2.1847
2.0880
2.0390
1.6889
1.6760
1.6633
1.6505
1.6117
1.5997
1.5875
1.4131
1.4001
1.2525
1.1886
1.1808
1.1705
COOH
AcHN
NHAc
NH2
3.0
2.8
2.6
2.4
2.2
2.0
1.8
1.6
1.4
ppm
7.5
7.0
6.5
6.0
5.5
5.0
4.5
4.0
3.5
3.0
2.5
2.0
1.5
1.0
0.5
ppm

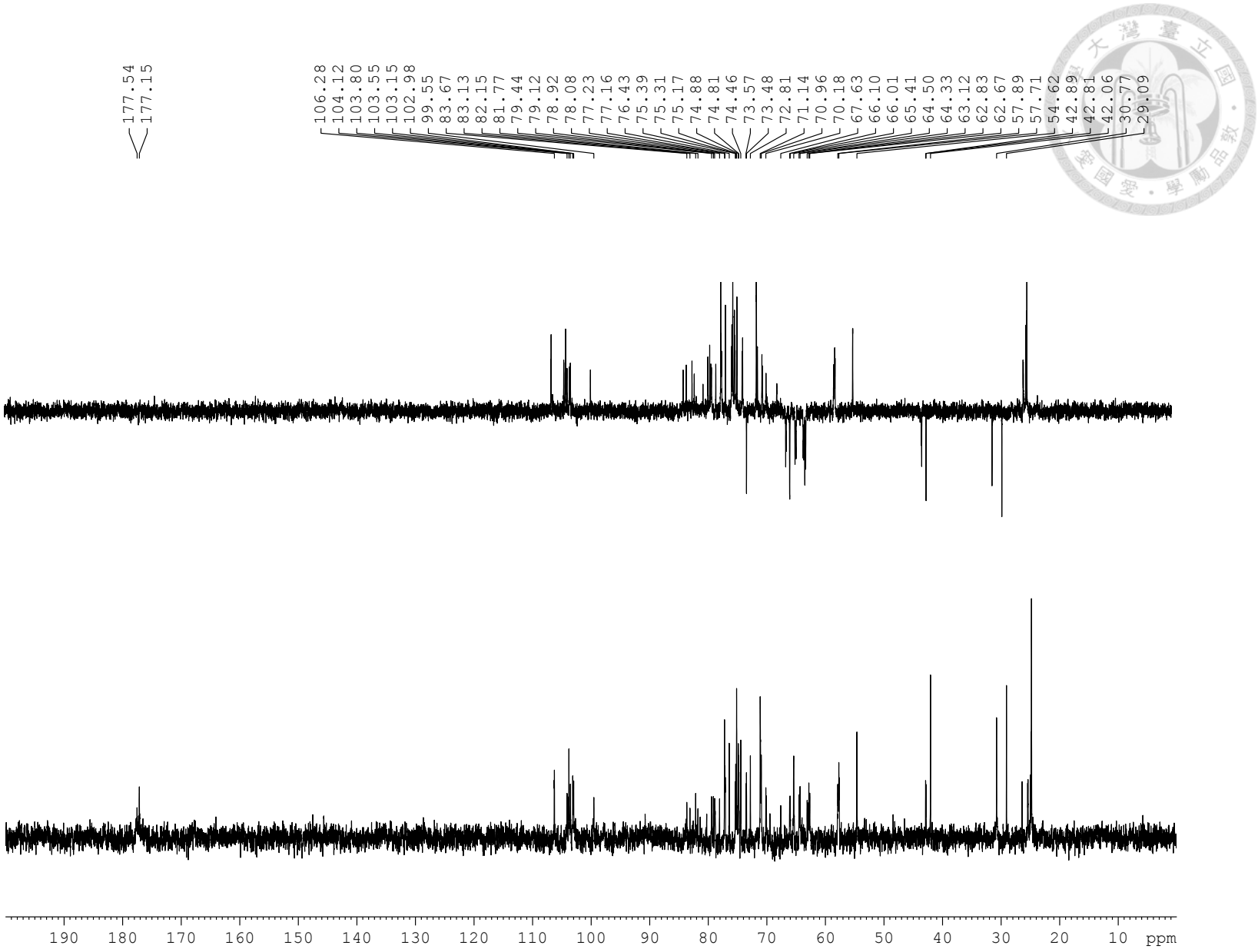
177.54
177.15
106.28
104.12
103.80
103.55
103.15
102.98
99.55
83.67
83.13
82.15
81.77
79.44
79.12
78.92
78.08
77.23
77.16
76.43
75.39
75.31
75.17
74.88
74.81
74.46
73.57
73.48
72.81
71.14
70.96
70.18
67.63
66.10
66.01
65.41
64.50
64.33
63.12
62.83
62.67
57.89
57.71
54.62
42.89
42.81
42.06
30.77
29.09
190 180 170 160 150 140 130 120 110 100 90 80 70 60 50 40 30 20 10 ppm

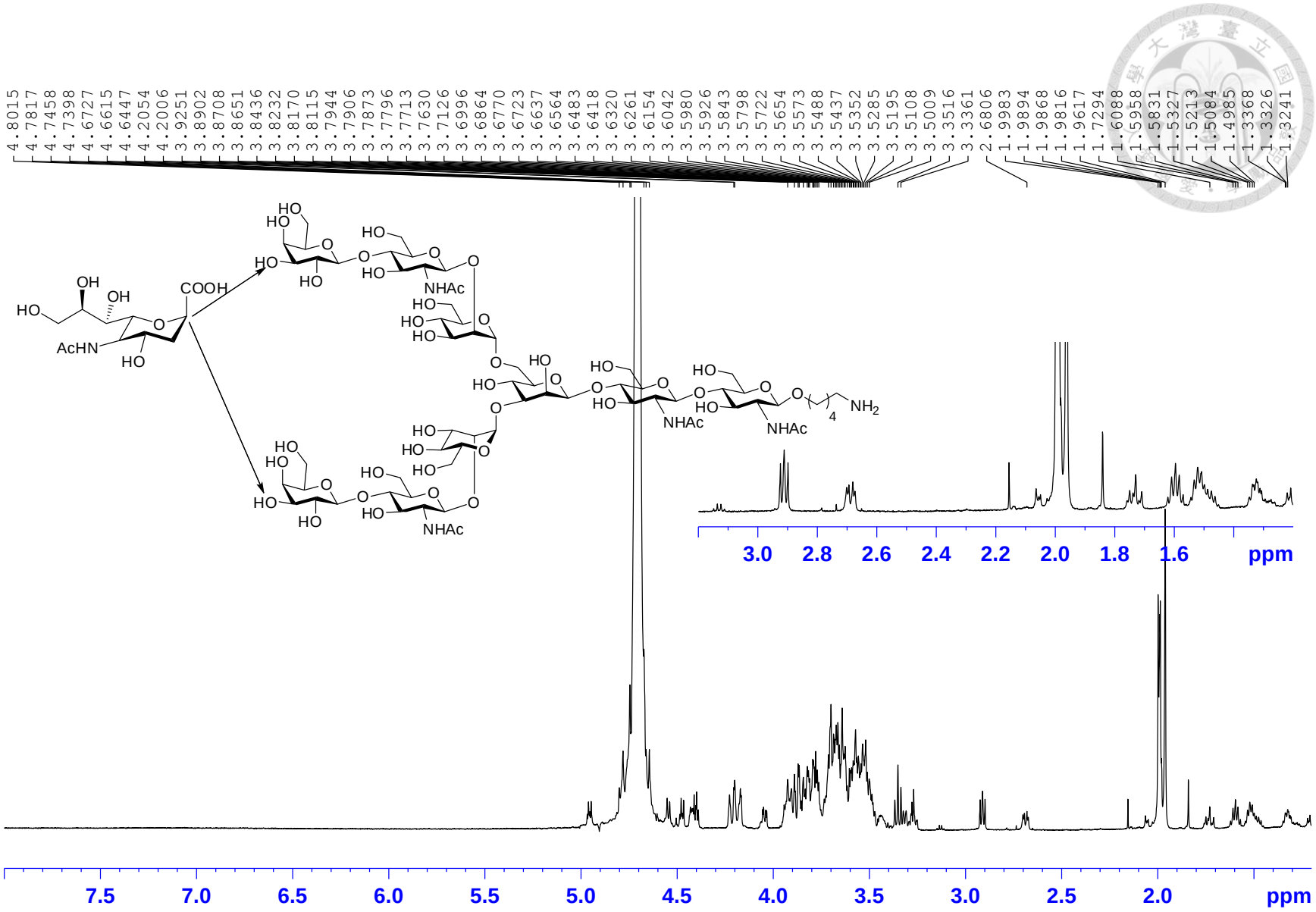
4.8015
4.7817
4.7458
4.7398
4.6727
4.6615
4.6447
4.2054
4.2006
3.9251
3.8902
3.8708
3.8651
3.8436
3.8232
3.8170
3.8115
3.7944
3.7906
3.7873
3.7796
3.7713
3.7630
3.7126
3.6996
3.6864
3.6770
3.6723
3.6637
3.6564
3.6483
3.6418
3.6320
3.6261
3.6154
3.6042
3.5980
3.5926
3.5843
3.5798
3.5722
3.5654
3.5573
3.5488
3.5437
3.5352
3.5285
3.5195
3.5108
3.5009
3.3516
3.3361
2.6806
1.9983
1.9894
1.9868
1.9816
1.9617
1.7294
1.6088
1.5958
1.5831
1.5327
1.5213
1.5084
1.4985
1.3368
1.3326
1.3241
COOH
OH
OH
HO
AcHN
HO
NHAc
NHAc
NHAc
NHAc
NH2
4
3.0
2.8
2.6
2.4
2.2
2.0
1.8
1.6
ppm
7.5
7.0
6.5
6.0
5.5
5.0
4.5
4.0
3.5
3.0
2.5
2.0
ppm

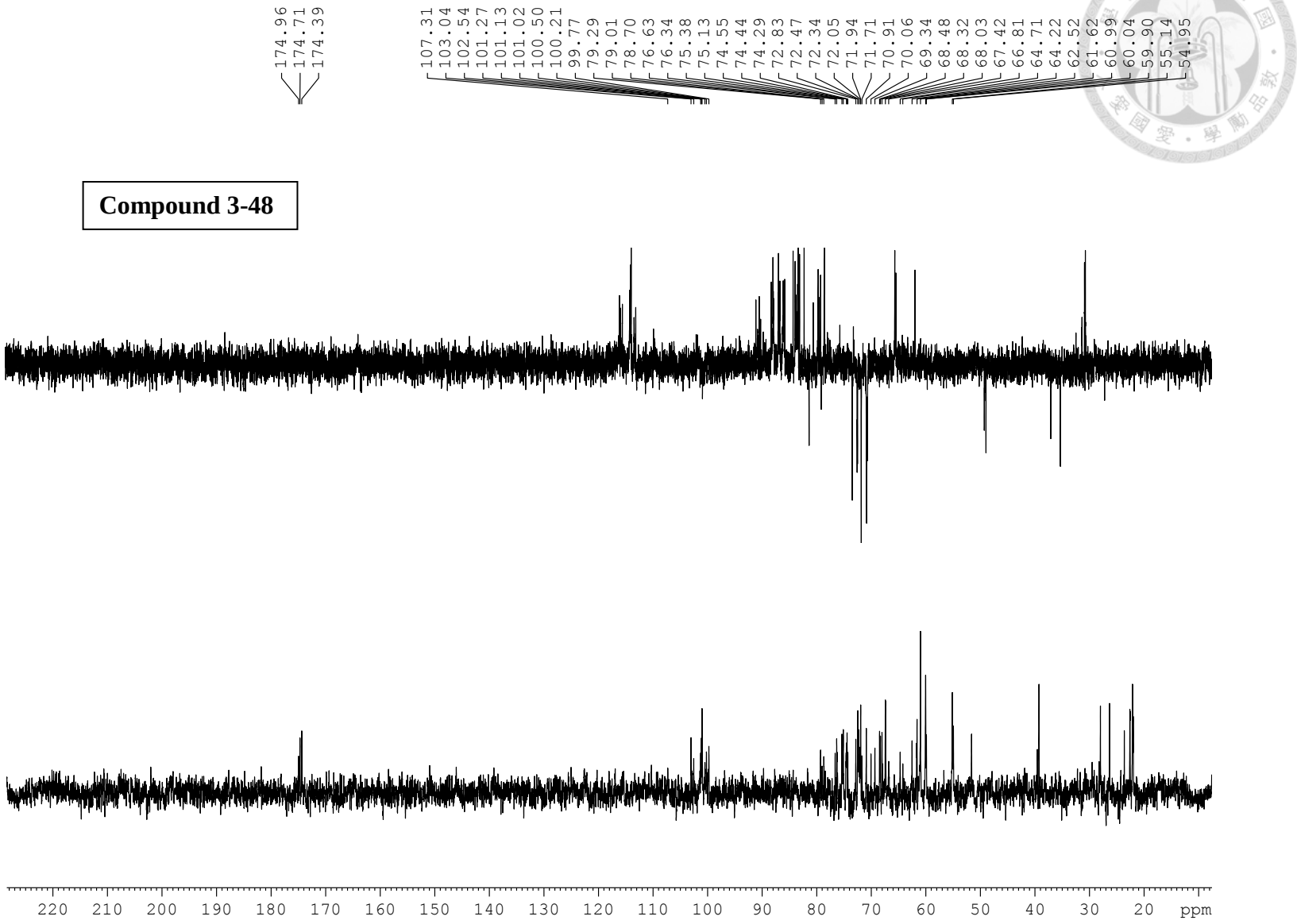
174.96
174.71
174.39
107.31
103.04
102.54
101.27
101.13
101.02
100.50
100.21
99.77
79.29
79.01
78.70
76.63
76.34
75.38
75.13
74.55
74.44
74.29
72.83
72.47
72.34
72.05
71.94
71.71
70.91
70.06
69.34
68.48
68.32
68.03
67.42
66.81
64.71
64.22
62.52
61.62
60.99
60.04
59.90
55.14
54.95
Compound 3-48
220 210 200 190 180 170 160 150 140 130 120 110 100 90 80 70 60 50 40 30 20 ppm

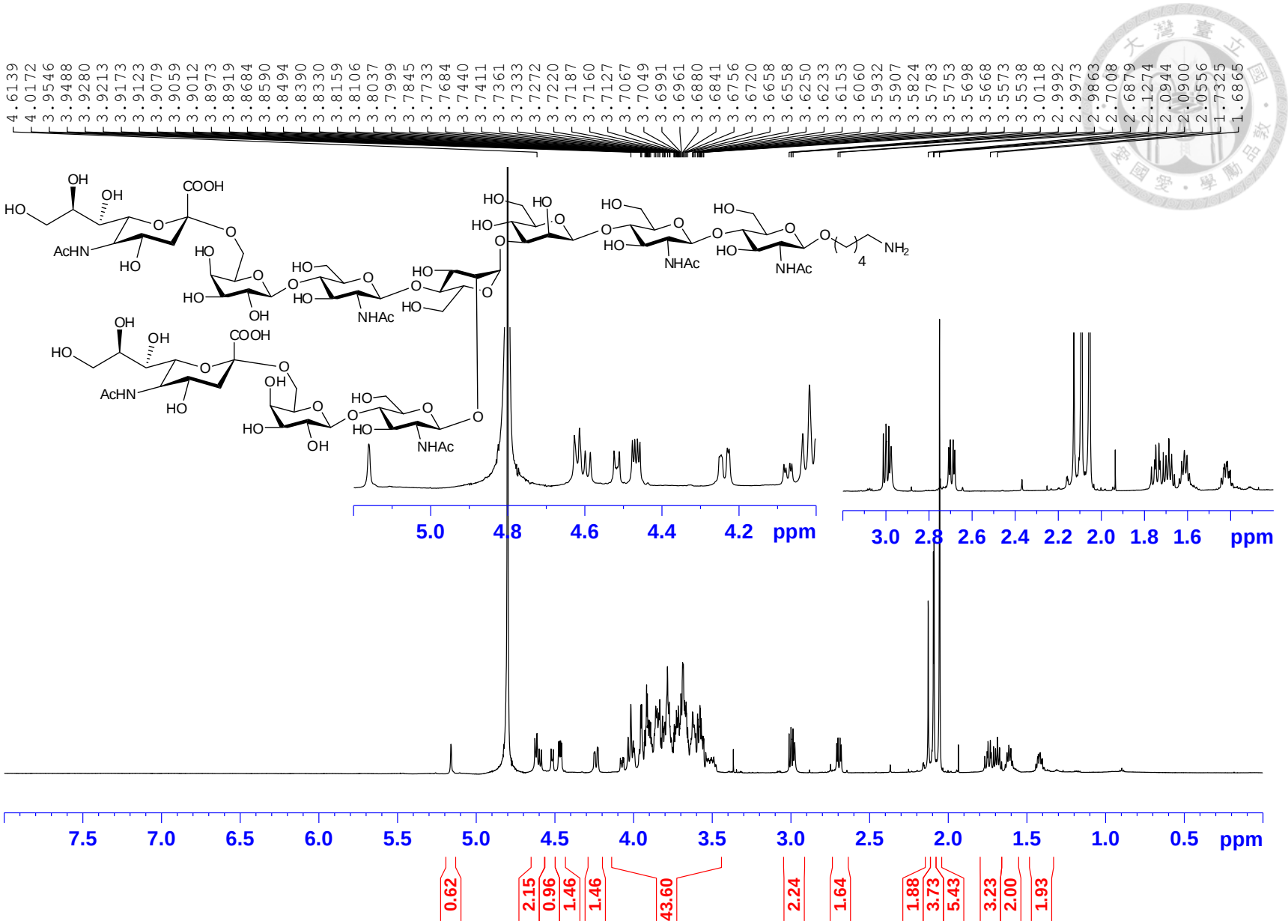
4.6139
4.0172
3.9546
3.9488
3.9280
3.9213
3.9173
3.9123
3.9079
3.9059
3.9012
3.8973
3.8919
3.8684
3.8590
3.8494
3.8390
3.8330
3.8159
3.8106
3.8037
3.7999
3.7845
3.7733
3.7684
3.7440
3.7411
3.7361
3.7333
3.7272
3.7220
3.7187
3.7160
3.7127
3.7067
3.7049
3.6991
3.6961
3.6880
3.6841
3.6756
3.6720
3.6658
3.6558
3.6250
3.6233
3.6153
3.6060
3.5932
3.5907
3.5824
3.5783
3.5753
3.5698
3.5668
3.5573
3.5538
3.0118
2.9992
2.9973
2.9863
2.7008
2.6879
2.1274
2.0944
2.0900
2.0556
1.7325
1.6865
5.0
4.8
4.6
4.4
4.2
ppm
3.0
2.8
2.6
2.4
2.2
2.0
1.8
1.6
ppm
7.5
7.0
6.5
6.0
5.5
5.0
4.5
4.0
3.5
3.0
2.5
2.0
1.5
1.0
0.5
ppm
0.62
2.15
0.96
1.46
1.46
43.60
2.24
1.64
1.88
3.73
5.43
3.23
2.00
1.93

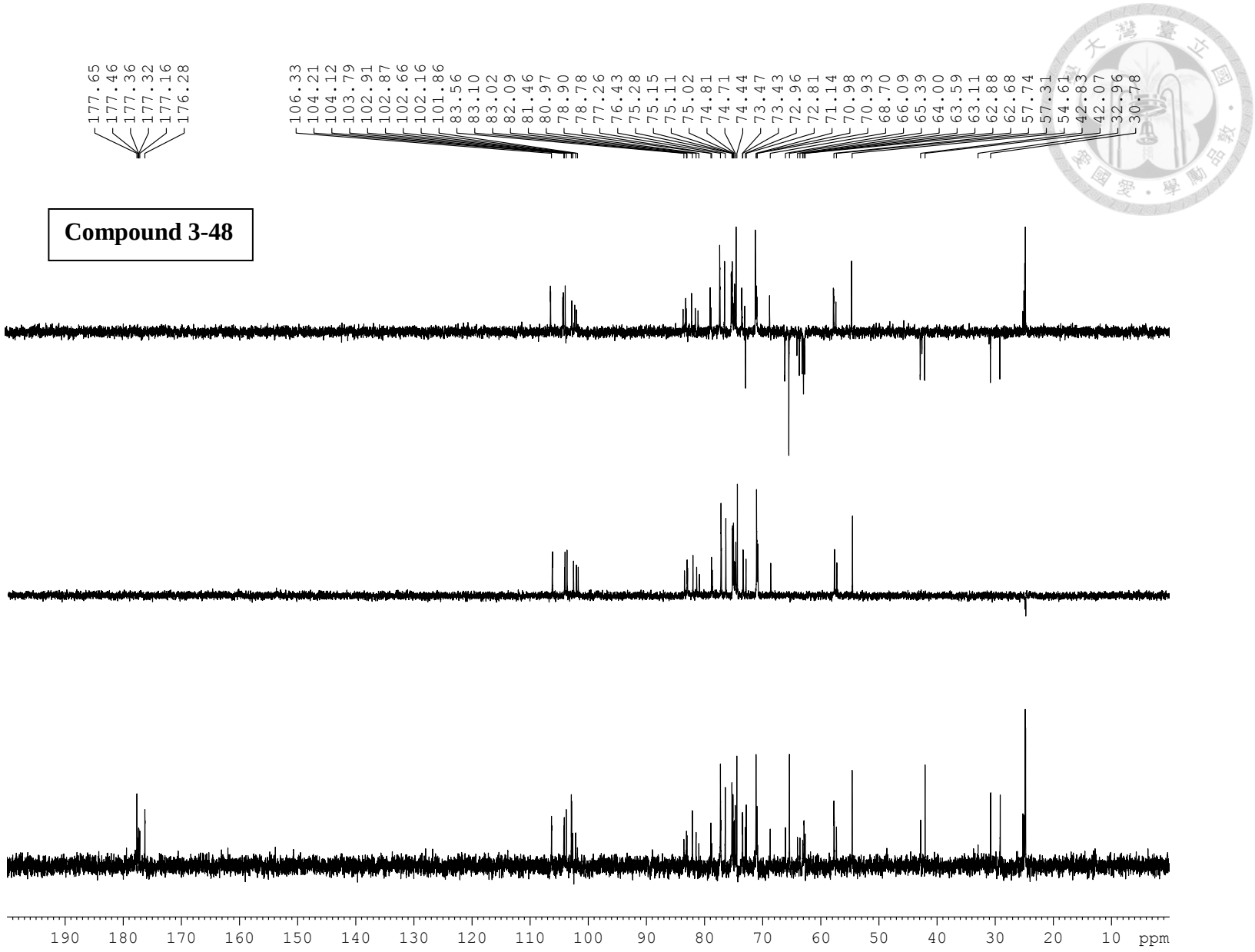
177.65
177.46
177.36
177.32
177.16
176.28
106.33
104.21
104.12
103.79
102.91
102.87
102.66
102.16
101.86
83.56
83.10
83.02
82.09
81.46
80.97
78.90
78.78
77.26
76.43
75.28
75.15
75.11
75.02
74.81
74.71
74.44
73.47
73.43
72.96
72.81
71.14
70.98
70.93
68.70
66.09
65.39
64.00
63.59
63.11
62.88
62.68
57.74
57.31
54.61
42.83
42.07
32.96
30.78
Compound 3-48
190
180
170
160
150
140
130
120
110
100
90
80
70
60
50
40
30
20
10
ppm

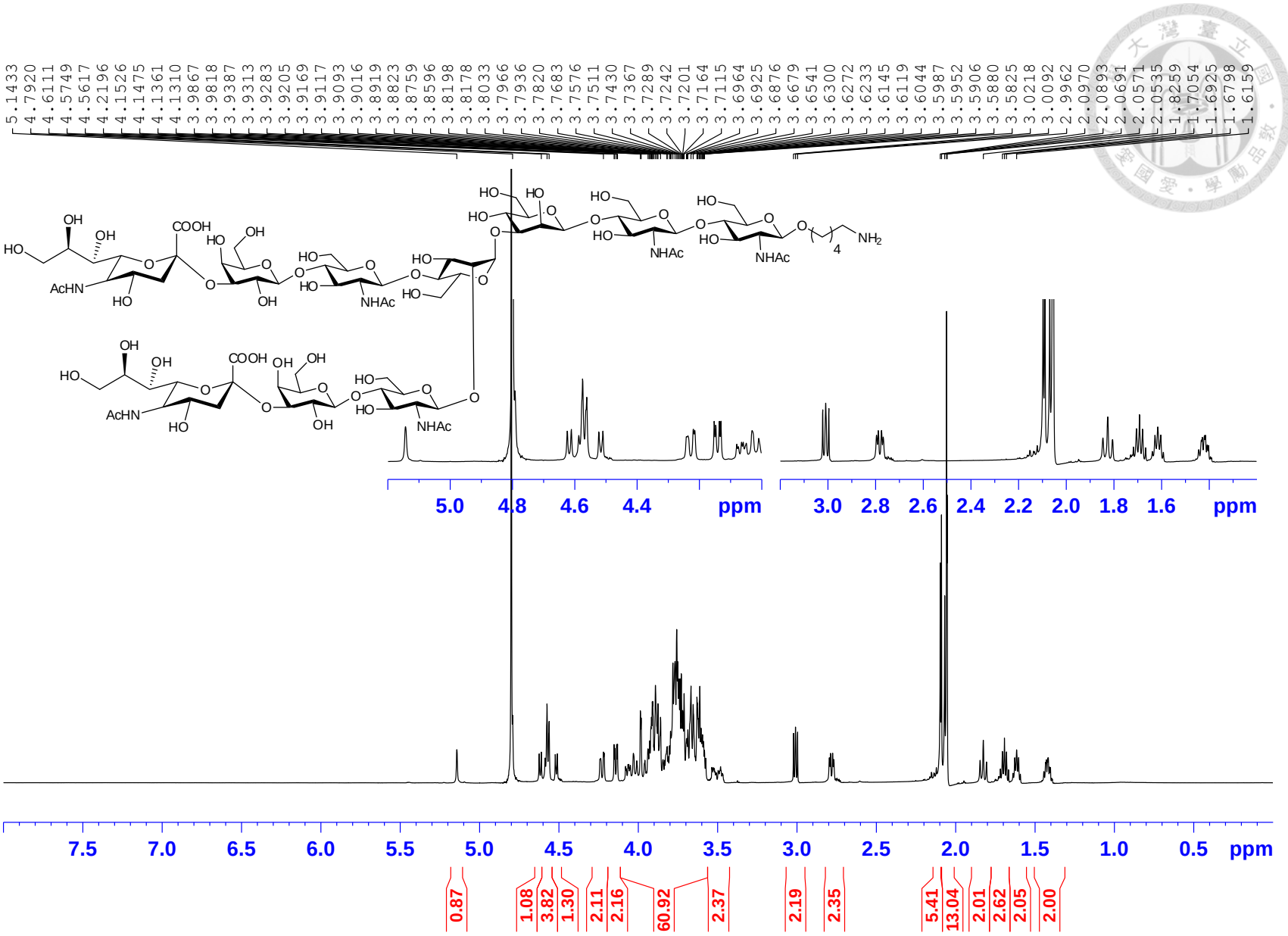
5.1433
4.7920
4.6111
4.5749
4.5617
4.2196
4.1526
4.1475
4.1361
4.1310
3.9867
3.9818
3.9387
3.9313
3.9283
3.9205
3.9169
3.9117
3.9093
3.9016
3.8919
3.8823
3.8759
3.8596
3.8198
3.8178
3.8033
3.7966
3.7936
3.7820
3.7683
3.7576
3.7511
3.7430
3.7367
3.7289
3.7242
3.7201
3.7164
3.7115
3.6964
3.6925
3.6876
3.6679
3.6541
3.6300
3.6272
3.6233
3.6145
3.6119
3.6044
3.5987
3.5952
3.5906
3.5880
3.5825
3.0218
3.0092
2.9962
2.0970
2.0893
2.0691
2.0571
2.0535
1.8259
1.7054
1.6925
1.6798
1.6159
5.0
4.8
4.6
4.4
ppm
3.0
2.8
2.6
2.4
2.2
2.0
1.8
1.6
ppm
7.5
7.0
6.5
6.0
5.5
5.0
4.5
4.0
3.5
3.0
2.5
2.0
1.5
1.0
0.5
ppm
0.87
1.08
3.82
1.30
2.11
2.16
60.92
2.37
2.19
2.35
5.41
13.04
2.01
2.62
2.05
2.00

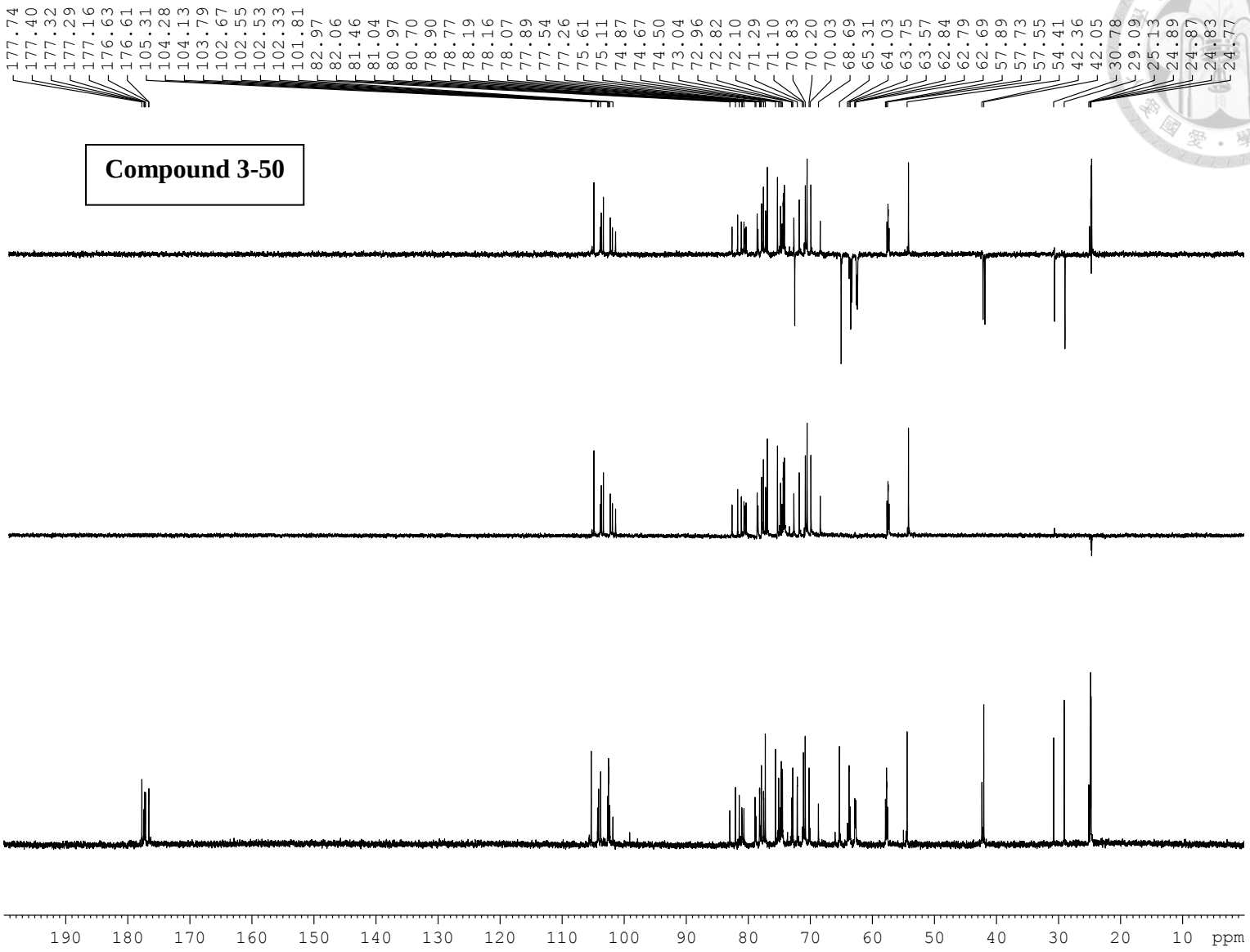
177.74
177.40
177.32
177.29
177.16
176.63
176.61
105.31
104.28
104.13
103.79
102.67
102.55
102.53
102.33
101.81
82.97
82.06
81.46
81.04
80.97
80.70
78.90
78.77
78.19
78.16
78.07
77.89
77.54
77.26
75.61
75.11
74.87
74.67
74.50
73.04
72.96
72.82
72.10
71.29
71.10
70.83
70.20
70.03
68.69
65.31
64.03
63.75
63.57
62.84
62.79
62.69
57.89
57.73
57.55
54.41
42.36
42.05
30.78
29.09
25.13
24.89
24.87
24.83
24.77
Compound 3-50
190
180
170
160
150
140
130
120
110
100
90
80
70
60
50
40
30
20
10
ppm

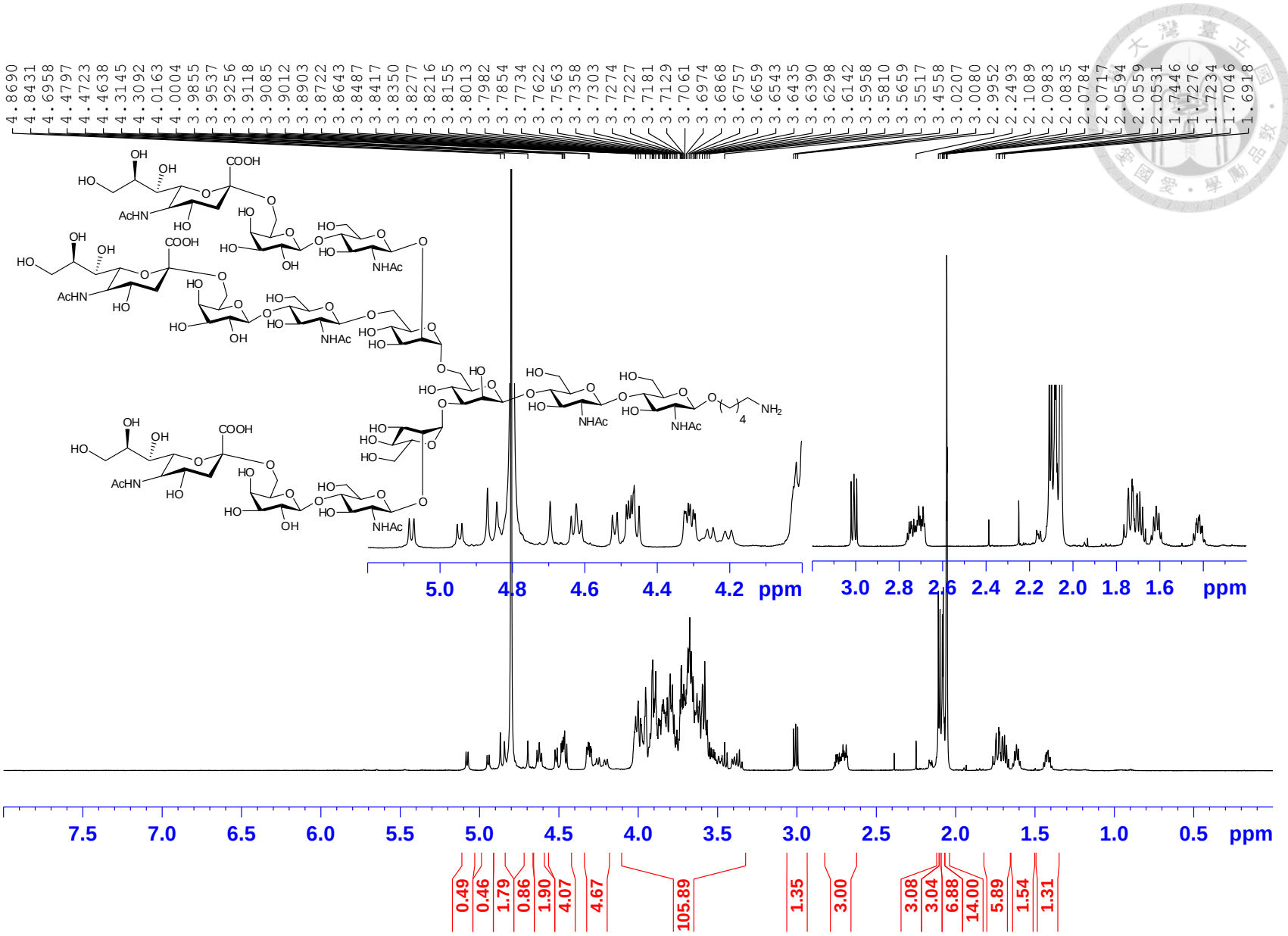
4.8690 4.8431 4.6958 4.4797 4.4723 4.4638 4.3145 4.3092 4.0163 4.0004 3.9855 3.9537 3.9256 3.9118 3.9085 3.9012 3.8903 3.8722 3.8643 3.8487 3.8417 3.8350 3.8277 3.8216 3.8155 3.8013 3.7982 3.7854 3.7734 3.7622 3.7563 3.7358 3.7303 3.7274 3.7227 3.7181 3.7129 3.7061 3.6974 3.6868 3.6757 3.6659 3.6543 3.6435 3.6390 3.6298 3.6142 3.5958 3.5810 3.5659 3.5517 3.4558 3.0207 3.0080 2.9952 2.2493 2.1089 2.0983 2.0835 2.0784 2.0717 2.0594 2.0559 2.0531 1.7446 1.7276 1.7234 1.7046 1.6918
5.0 4.8 4.6 4.4 4.2 ppm
3.0 2.8 2.6 2.4 2.2 2.0 1.8 1.6 ppm
7.5 7.0 6.5 6.0 5.5 5.0 4.5 4.0 3.5 3.0 2.5 2.0 1.5 1.0 0.5 ppm
0.49 0.46 1.79 0.86 1.90 4.07 4.67 105.89 1.35 3.00 3.08 3.04 6.88 14.00 5.89 1.54 1.31

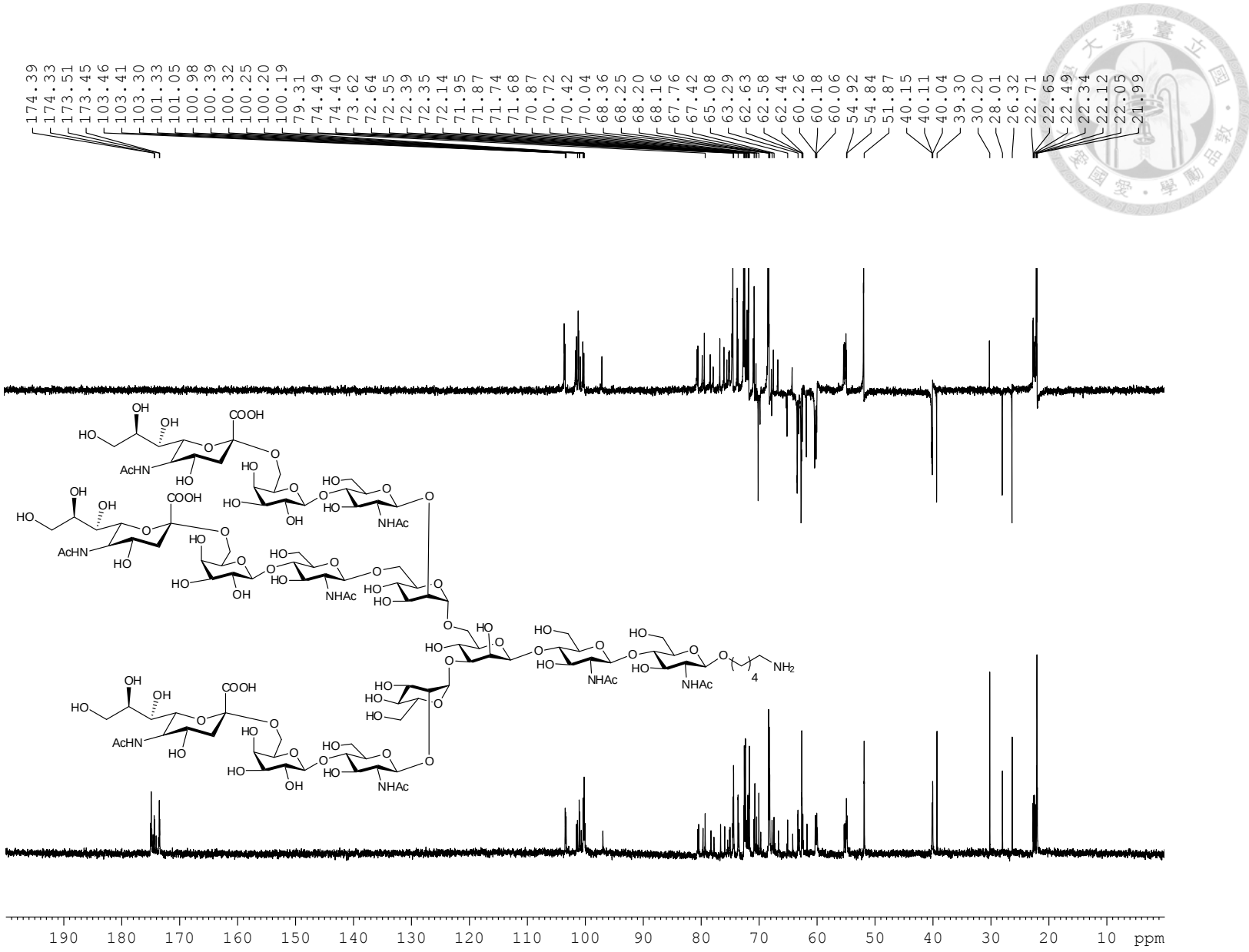
174.39
174.33
173.51
173.45
103.46
103.41
103.30
101.33
101.05
100.98
100.39
100.32
100.25
100.20
100.19
79.31
74.49
74.40
73.62
72.64
72.55
72.39
72.35
72.14
71.95
71.87
71.74
71.68
70.87
70.72
70.42
70.04
68.36
68.25
68.20
68.16
67.76
67.42
65.08
63.29
62.63
62.58
62.44
60.26
60.18
60.06
54.92
54.84
51.87
40.15
40.11
40.04
39.30
30.20
28.01
26.32
22.71
22.65
22.49
22.34
22.12
22.05
21.99
190 180 170 160 150 140 130 120 110 100 90 80 70 60 50 40 30 20 10 ppm

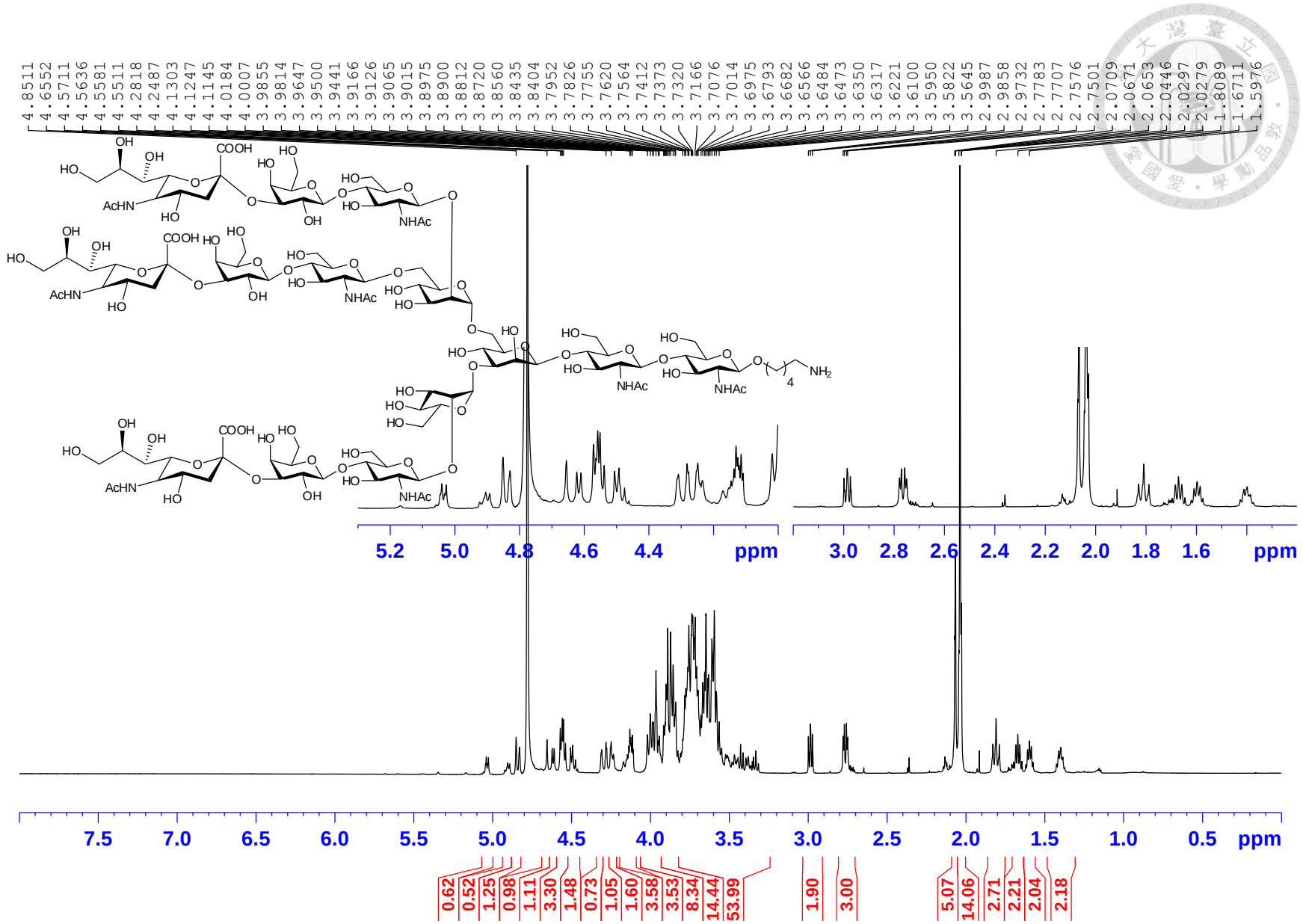
4.8511 4.6552 4.5711 4.5636 4.5581 4.5511 4.2818 4.2487 4.1303 4.1247 4.1145 4.0184 4.0007 3.9855 3.9814 3.9647 3.9500 3.9441 3.9166 3.9126 3.9065 3.9015 3.8975 3.8900 3.8812 3.8720 3.8560 3.8435 3.8404 3.7952 3.7826 3.7755 3.7620 3.7564 3.7412 3.7373 3.7320 3.7166 3.7076 3.7014 3.6975 3.6793 3.6682 3.6566 3.6484 3.6473 3.6350 3.6317 3.6221 3.6100 3.5950 3.5822 3.5645 2.9987 2.9858 2.9732 2.7783 2.7707 2.7576 2.7501 2.0709 2.0671 2.0653 2.0446 2.0297 2.0279 1.8089 1.6711 1.5976
5.2 5.0 4.8 4.6 4.4 ppm
3.0 2.8 2.6 2.4 2.2 2.0 1.8 1.6 ppm
7.5 7.0 6.5 6.0 5.5 5.0 4.5 4.0 3.5 3.0 2.5 2.0 1.5 1.0 0.5 ppm
0.62 0.52 1.25 0.98 1.11 3.30 1.48 0.73 1.05 1.60 3.58 3.53 8.34 14.44 53.99 1.90 3.00 5.07 14.06 2.71 2.21 2.04 2.18

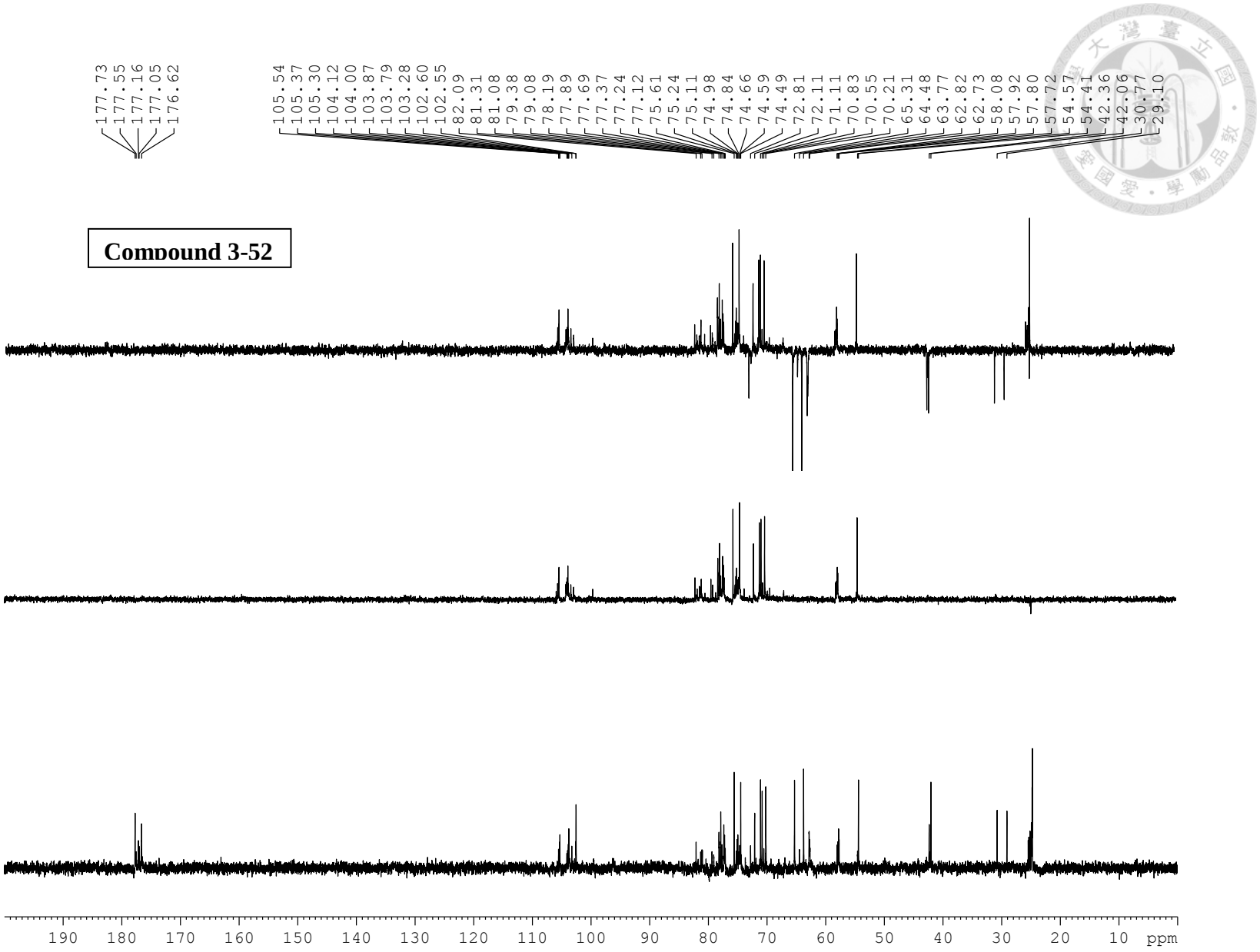
177.73
177.55
177.16
177.05
176.62
105.54
105.37
105.30
104.12
104.00
103.87
103.79
103.28
102.60
102.55
82.09
81.31
81.08
79.38
79.08
78.19
77.89
77.69
77.37
77.24
77.12
75.61
75.24
75.11
74.98
74.84
74.66
74.59
74.49
72.81
72.11
71.11
70.83
70.55
70.21
65.31
64.48
63.77
62.82
62.73
58.08
57.92
57.80
57.72
54.57
54.41
42.36
42.06
30.77
29.10
Compound 3-52
190
180
170
160
150
140
130
120
110
100
90
80
70
60
50
40
30
20
10
ppm

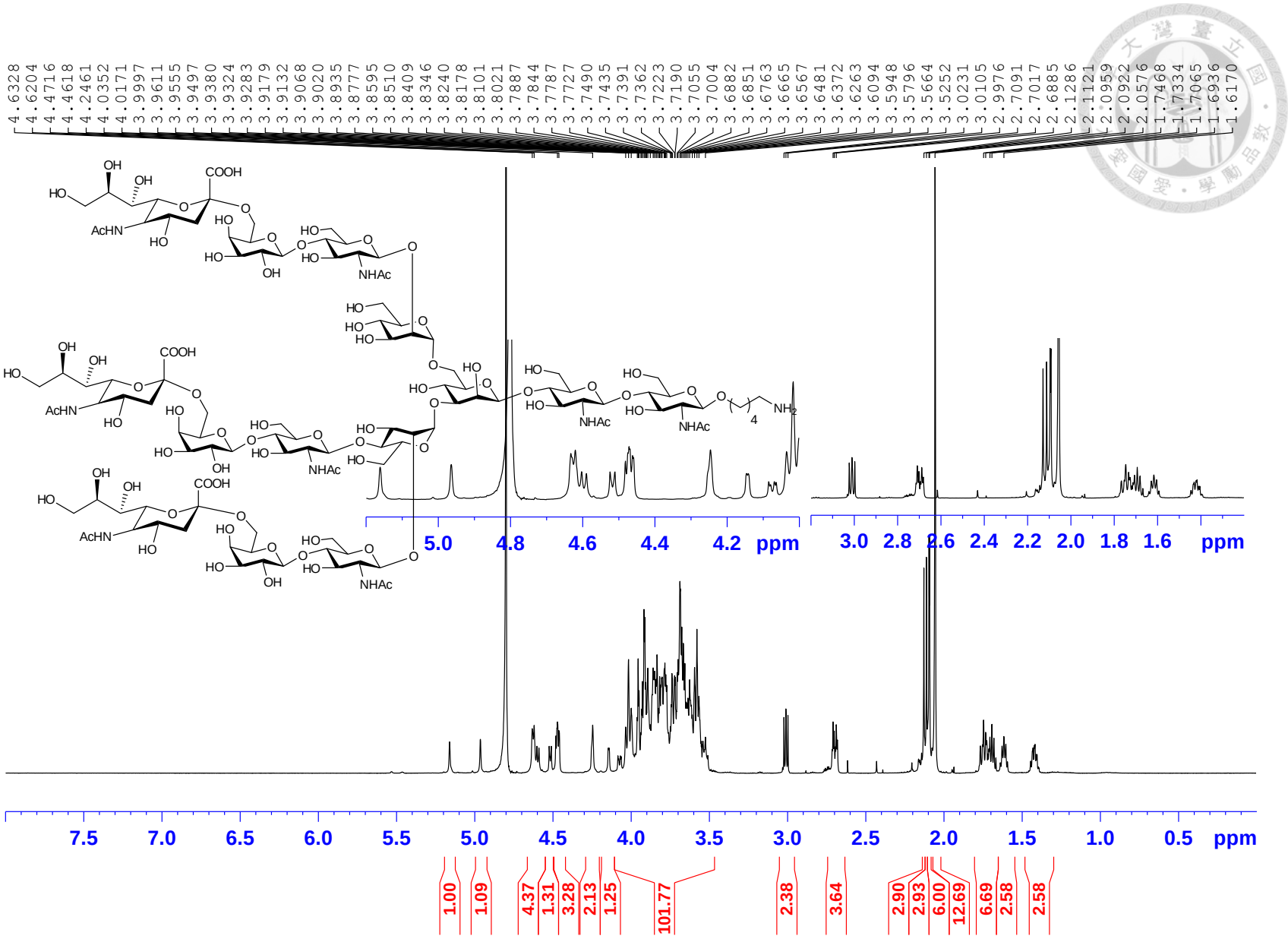
4.6328
4.6204
4.4716
4.4618
4.2461
4.0352
4.0171
3.9997
3.9611
3.9555
3.9497
3.9380
3.9324
3.9283
3.9179
3.9132
3.9068
3.9020
3.8935
3.8777
3.8595
3.8510
3.8409
3.8346
3.8240
3.8178
3.8101
3.8021
3.7887
3.7844
3.7787
3.7727
3.7490
3.7435
3.7391
3.7362
3.7223
3.7190
3.7055
3.7004
3.6882
3.6851
3.6763
3.6665
3.6567
3.6481
3.6372
3.6263
3.6094
3.5948
3.5796
3.5664
3.5252
3.0231
3.0105
2.9976
2.7091
2.7017
2.6885
2.1286
2.1121
2.0959
2.0922
2.0576
1.7468
1.7334
1.7065
1.6936
1.6170
5.0 4.8 4.6 4.4 4.2 ppm
3.0 2.8 2.6 2.4 2.2 2.0 1.8 1.6 ppm
7.5 7.0 6.5 6.0 5.5 5.0 4.5 4.0 3.5 3.0 2.5 2.0 1.5 1.0 0.5 ppm
1.00
1.09
4.37
1.31
3.28
2.13
1.25
101.77
2.38
3.64
2.90
2.93
6.00
12.69
6.69
2.58
2.58

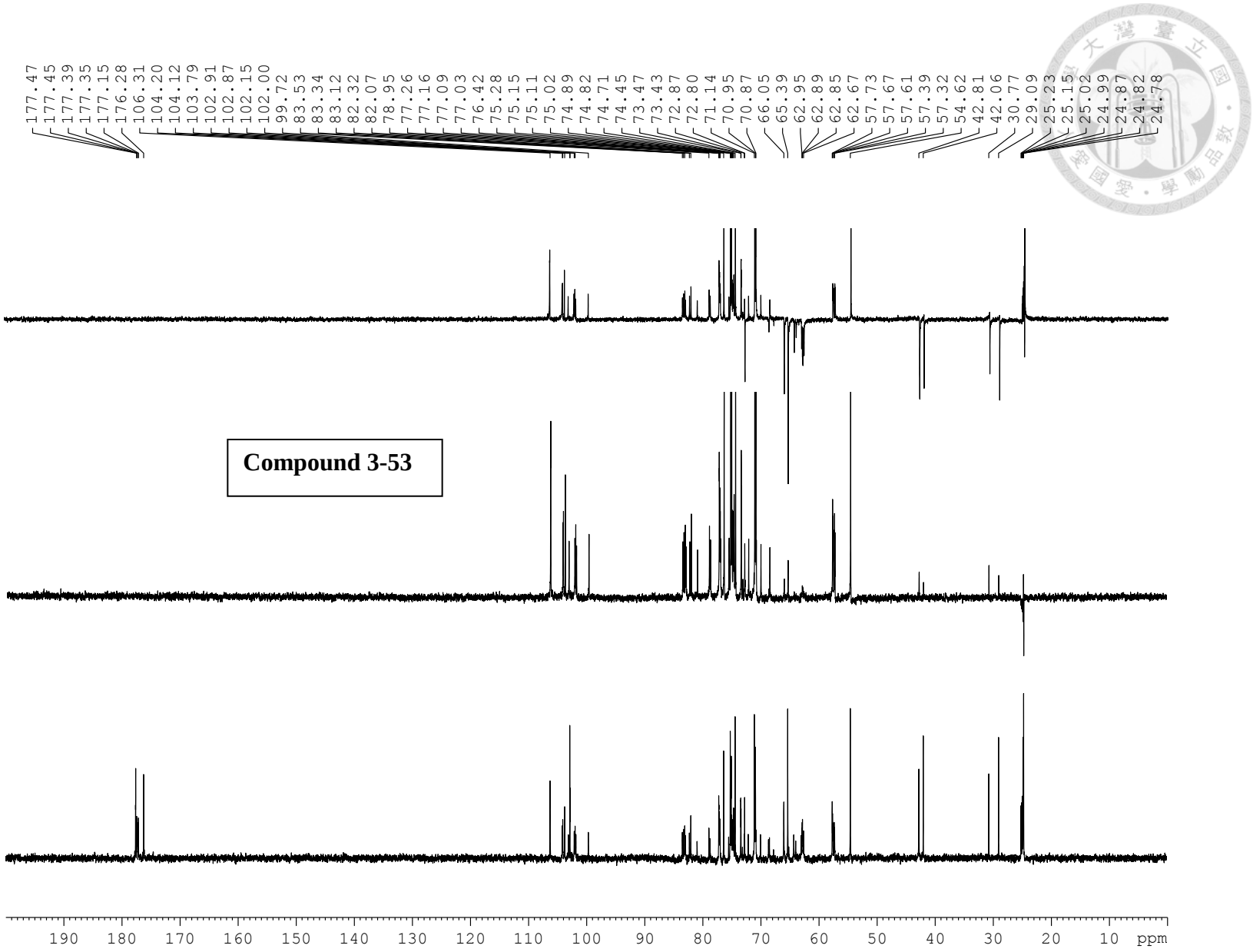
177.47
177.45
177.39
177.35
177.15
176.28
106.31
104.20
104.12
103.79
102.91
102.87
102.15
102.00
99.72
83.53
83.34
83.12
82.32
82.07
78.95
77.26
77.16
77.09
77.03
76.42
75.28
75.15
75.11
75.02
74.89
74.82
74.71
74.45
73.47
73.43
72.87
72.80
71.14
70.95
70.87
66.05
65.39
62.95
62.89
62.85
62.67
57.73
57.67
57.61
57.39
57.32
54.62
42.81
42.06
30.77
29.09
25.23
25.15
25.02
24.99
24.87
24.82
24.78
Compound 3-53
190
180
170
160
150
140
130
120
110
100
90
80
70
60
50
40
30
20
10
ppm

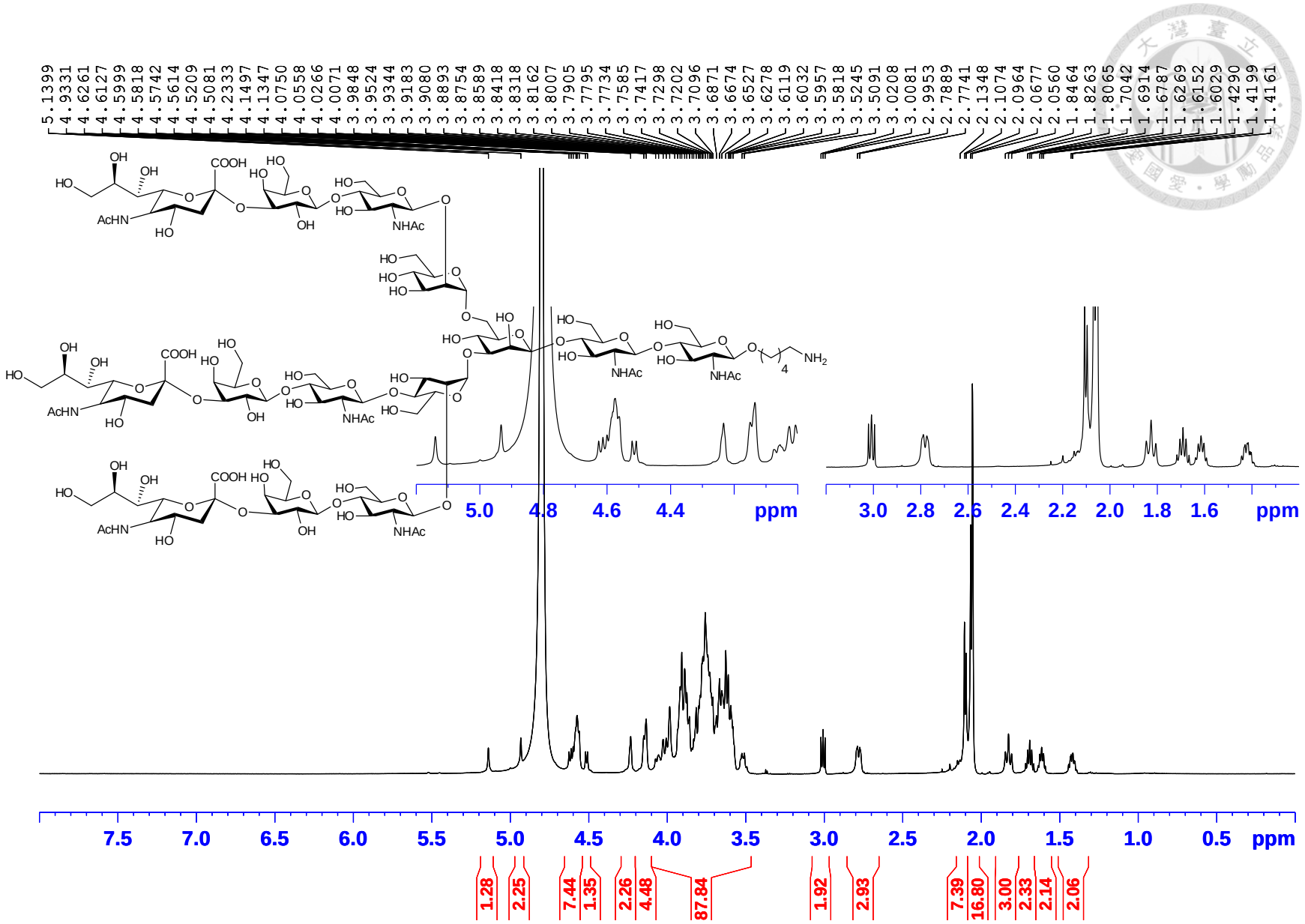
5.1399 4.9331 4.6261 4.6127 4.5999 4.5818 4.5742 4.5614 4.5209 4.5081 4.2333 4.1497 4.1347 4.0750 4.0558 4.0266 4.0071 3.9848 3.9524 3.9344 3.9183 3.9080 3.8893 3.8754 3.8589 3.8418 3.8318 3.8162 3.8007 3.7905 3.7795 3.7734 3.7585 3.7417 3.7298 3.7202 3.7096 3.6871 3.6674 3.6527 3.6278 3.6119 3.6032 3.5957 3.5818 3.5245 3.5091 3.0208 3.0081 2.9953 2.7889 2.7741 2.1348 2.1074 2.0964 2.0677 2.0560 1.8464 1.8263 1.8065 1.7042 1.6914 1.6787 1.6269 1.6152 1.6029 1.4290 1.4199 1.4161
5.0 4.8 4.6 4.4 ppm
3.0 2.8 2.6 2.4 2.2 2.0 1.8 1.6 ppm
7.5 7.0 6.5 6.0 5.5 5.0 4.5 4.0 3.5 3.0 2.5 2.0 1.5 1.0 0.5 ppm
1.28 2.25 7.44 1.35 2.26 4.48 87.84 1.92 2.93 7.39 16.80 3.00 2.33 2.14 2.06

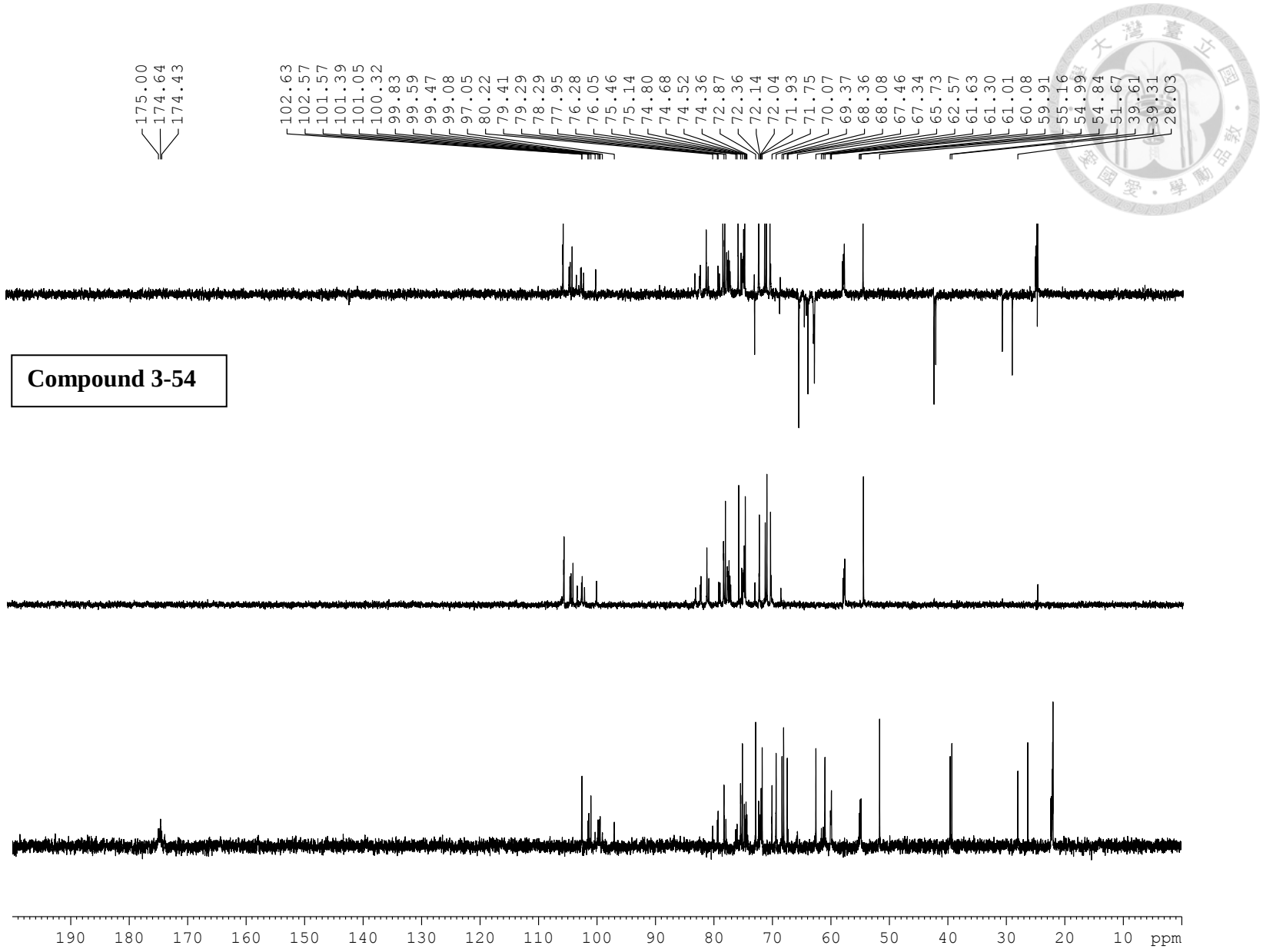
175.00
174.64
174.43
102.63
102.57
101.57
101.39
101.05
100.32
99.83
99.59
99.47
99.08
97.05
80.22
79.41
79.29
78.29
77.95
76.28
76.05
75.46
75.14
74.80
74.68
74.52
74.36
72.87
72.36
72.14
72.04
71.93
71.75
70.07
69.37
68.36
68.08
67.46
67.34
65.73
62.57
61.63
61.30
61.01
60.08
59.91
55.16
54.99
54.84
51.67
39.61
39.31
28.03
Compound 3-54
190
180
170
160
150
140
130
120
110
100
90
80
70
60
50
40
30
20
10
ppm

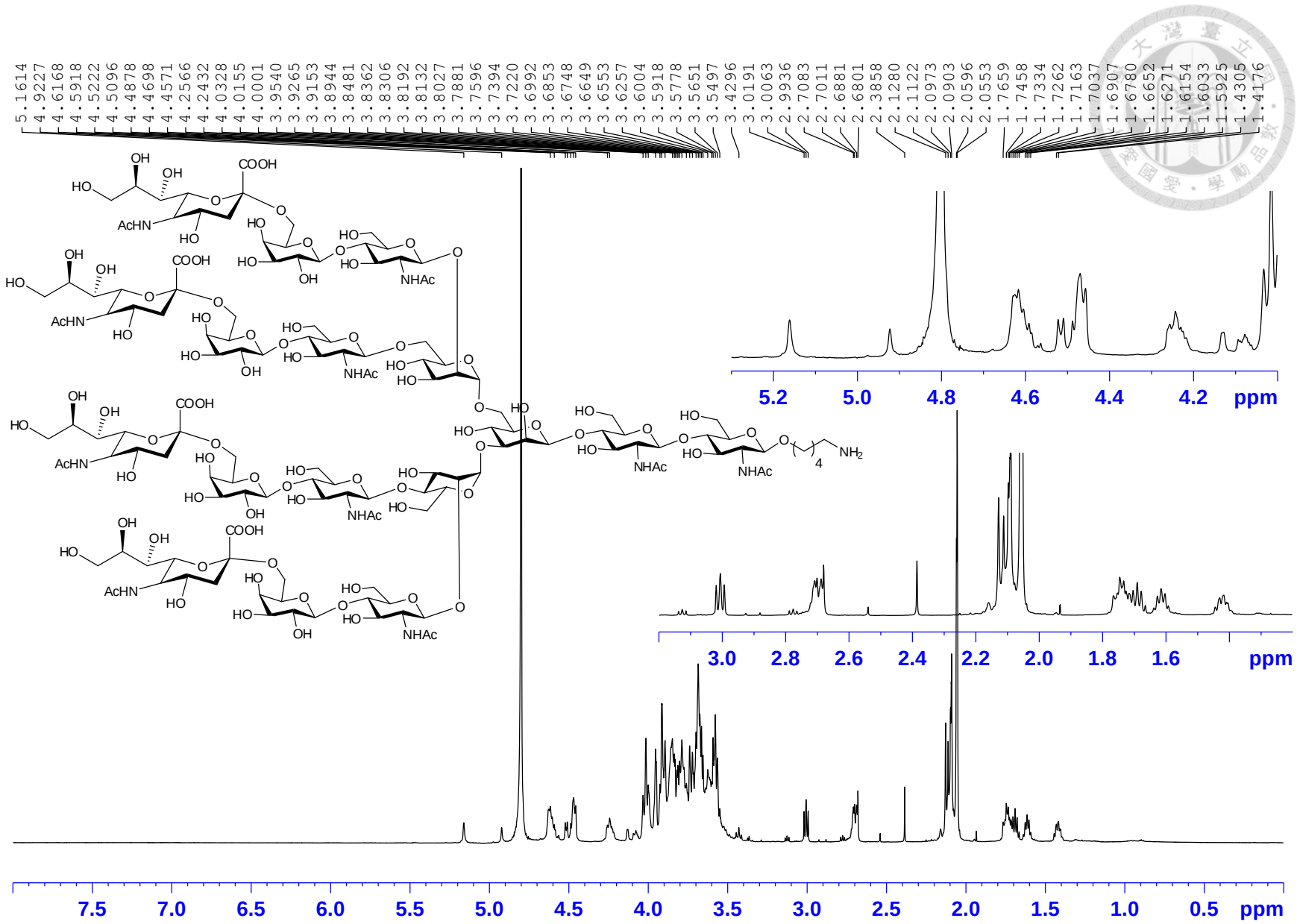
5.1614
4.9227
4.6168
4.5918
4.5222
4.5096
4.4878
4.4698
4.4571
4.2566
4.2432
4.0328
4.0155
4.0001
3.9540
3.9265
3.9153
3.8944
3.8481
3.8362
3.8306
3.8192
3.8132
3.8027
3.7881
3.7596
3.7394
3.7220
3.6992
3.6853
3.6748
3.6649
3.6553
3.6257
3.6004
3.5918
3.5778
3.5651
3.5497
3.4296
3.0191
3.0063
2.9936
2.7083
2.7011
2.6881
2.6801
2.3858
2.1280
2.1122
2.0973
2.0903
2.0596
2.0553
1.7659
1.7458
1.7334
1.7262
1.7163
1.7037
1.6907
1.6780
1.6652
1.6271
1.6154
1.6033
1.5925
1.4305
1.4176
5.2 5.0 4.8 4.6 4.4 4.2 ppm
3.0 2.8 2.6 2.4 2.2 2.0 1.8 1.6 ppm
7.5 7.0 6.5 6.0 5.5 5.0 4.5 4.0 3.5 3.0 2.5 2.0 1.5 1.0 0.5 ppm

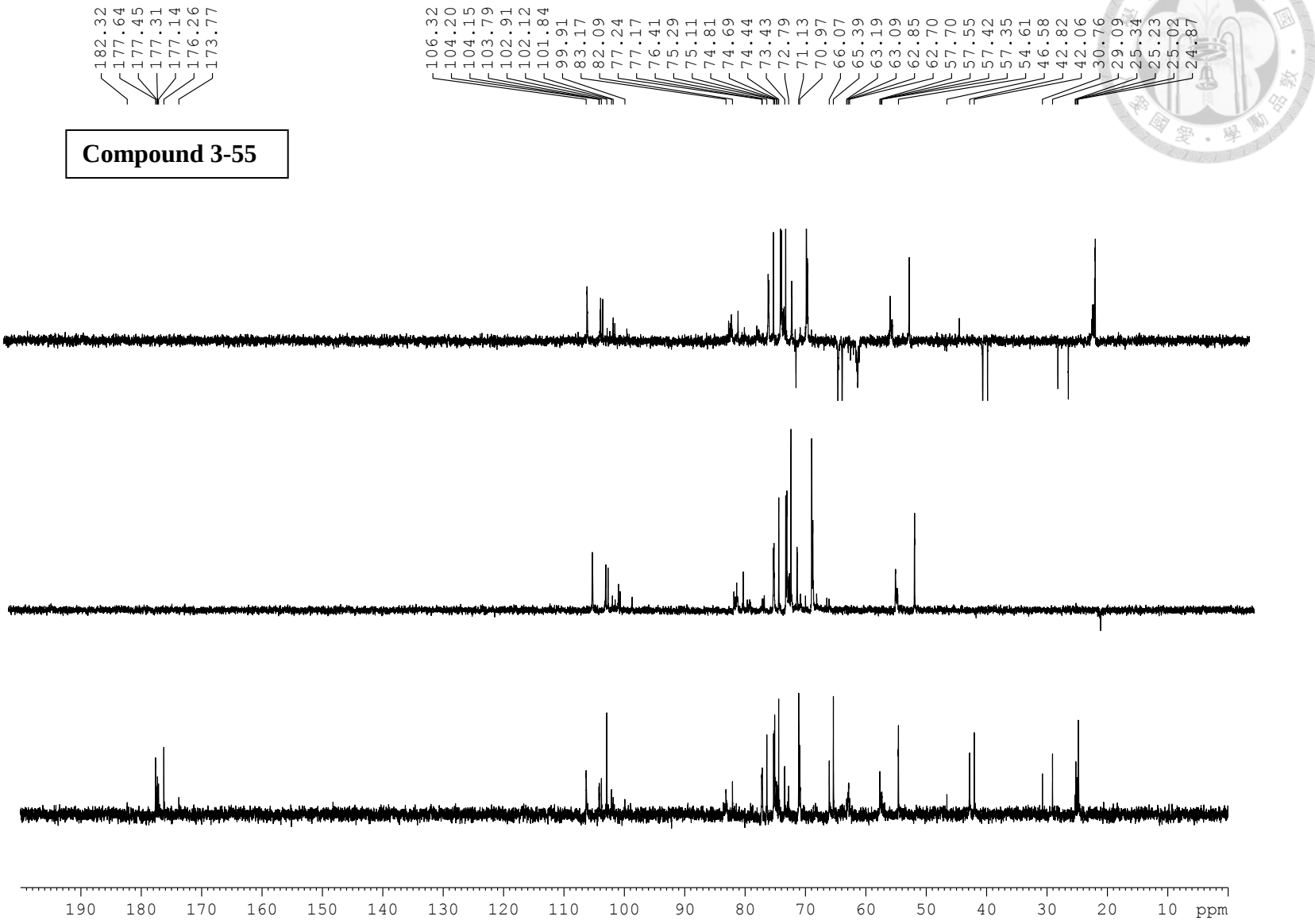
182.32
177.64
177.45
177.31
177.14
176.26
173.77
106.32
104.20
104.15
103.79
102.91
102.12
101.84
99.91
83.17
82.09
77.24
77.17
76.41
75.29
75.11
74.81
74.69
74.44
73.43
72.79
71.13
70.97
66.07
65.39
63.19
63.09
62.85
62.70
57.70
57.55
57.42
57.35
54.61
46.58
42.82
42.06
30.76
29.09
25.34
25.23
25.02
24.87
Compound 3-55
190
180
170
160
150
140
130
120
110
100
90
80
70
60
50
40
30
20
10
ppm

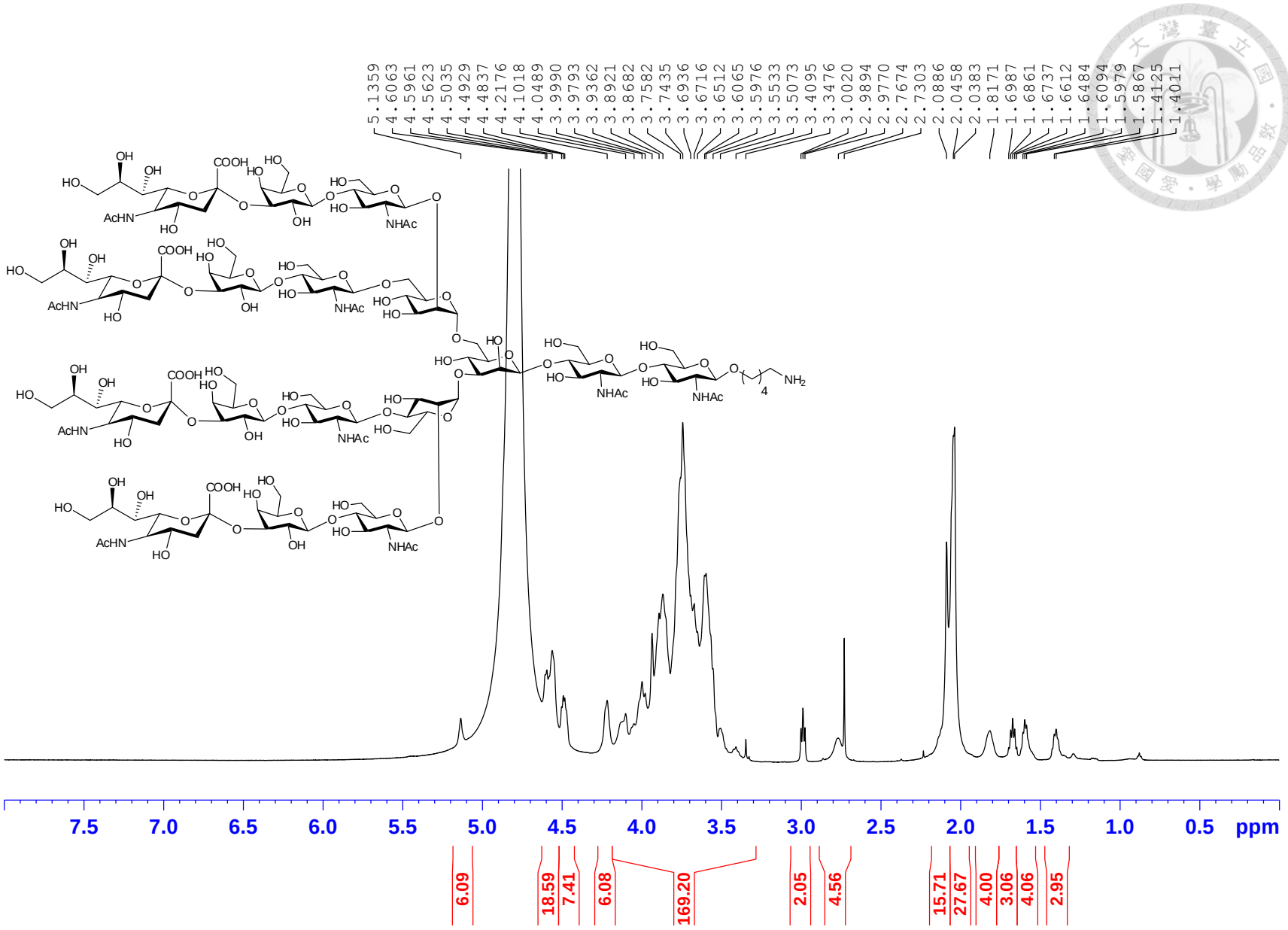
5.1359
4.6063
4.5961
4.5623
4.5035
4.4929
4.4837
4.2176
4.1018
4.0489
3.9990
3.9793
3.9362
3.8921
3.8682
3.7582
3.7435
3.6936
3.6716
3.6512
3.6065
3.5976
3.5533
3.5073
3.4095
3.3476
3.0020
2.9894
2.9770
2.7674
2.7303
2.0886
2.0458
2.0383
1.8171
1.6987
1.6861
1.6737
1.6612
1.6484
1.6094
1.5979
1.5867
1.4125
1.4011
7.5
7.0
6.5
6.0
5.5
5.0
4.5
4.0
3.5
3.0
2.5
2.0
1.5
1.0
0.5
ppm
6.09
18.59
7.41
6.08
169.20
2.05
4.56
15.71
27.67
4.00
3.06
4.06
2.95

Compound 3-56

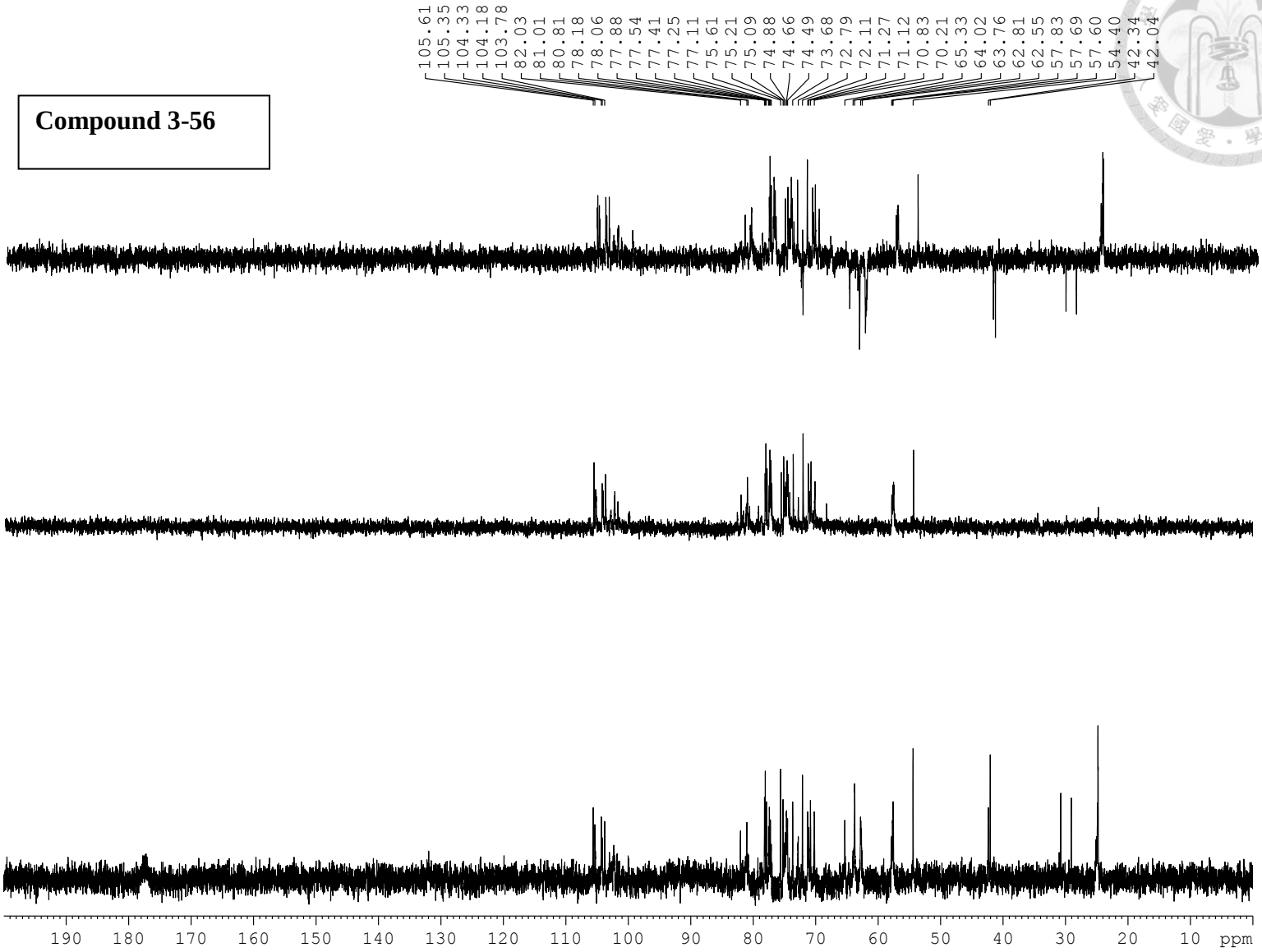

MALDI-TOF MS Spectra

for Glycoconjugates 1-5

(Chapter 5)

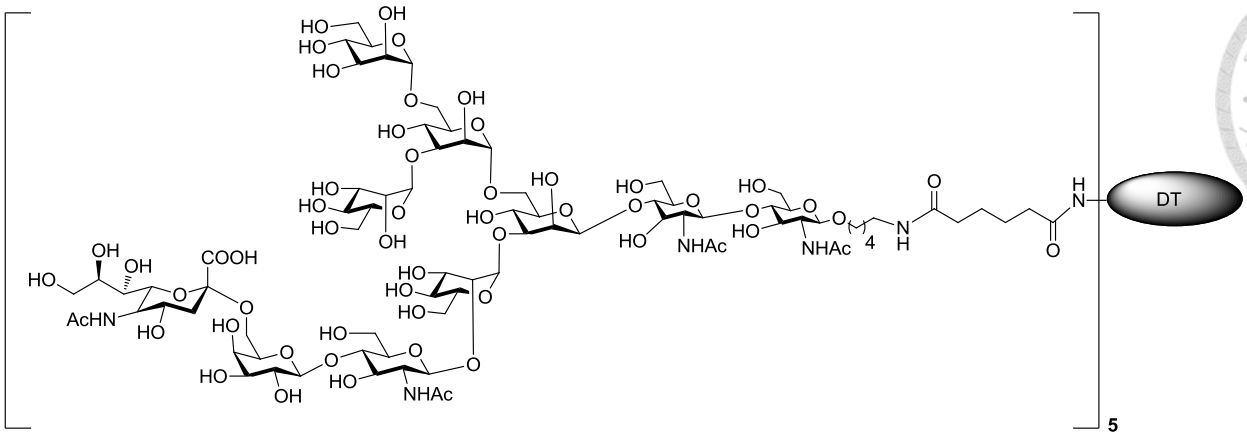

Glycoconjugate 1

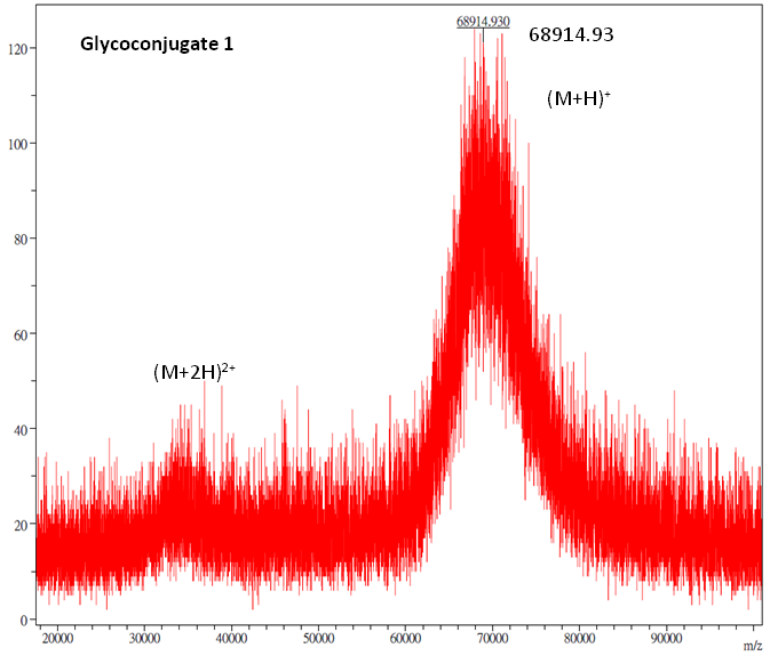

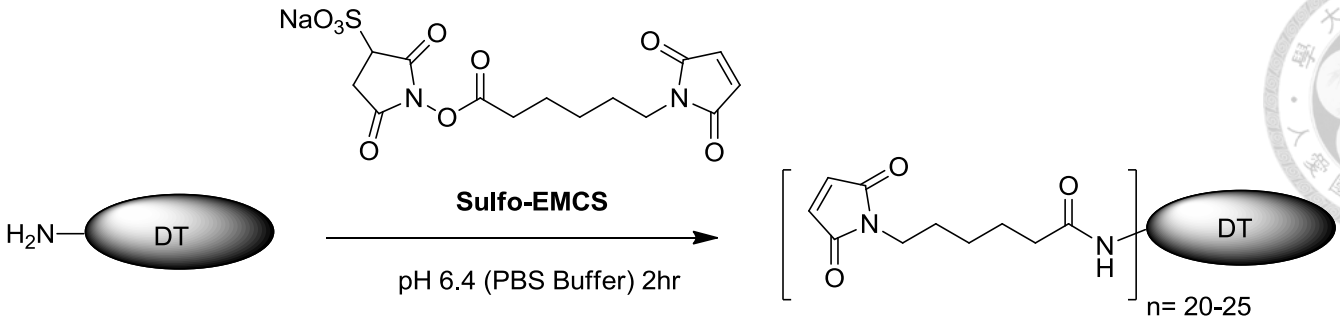
NaO3S
Sulfo-EMCS
H2N
DT
pH 6.4 (PBS Buffer) 2hr
DT
n= 20-25

5-10

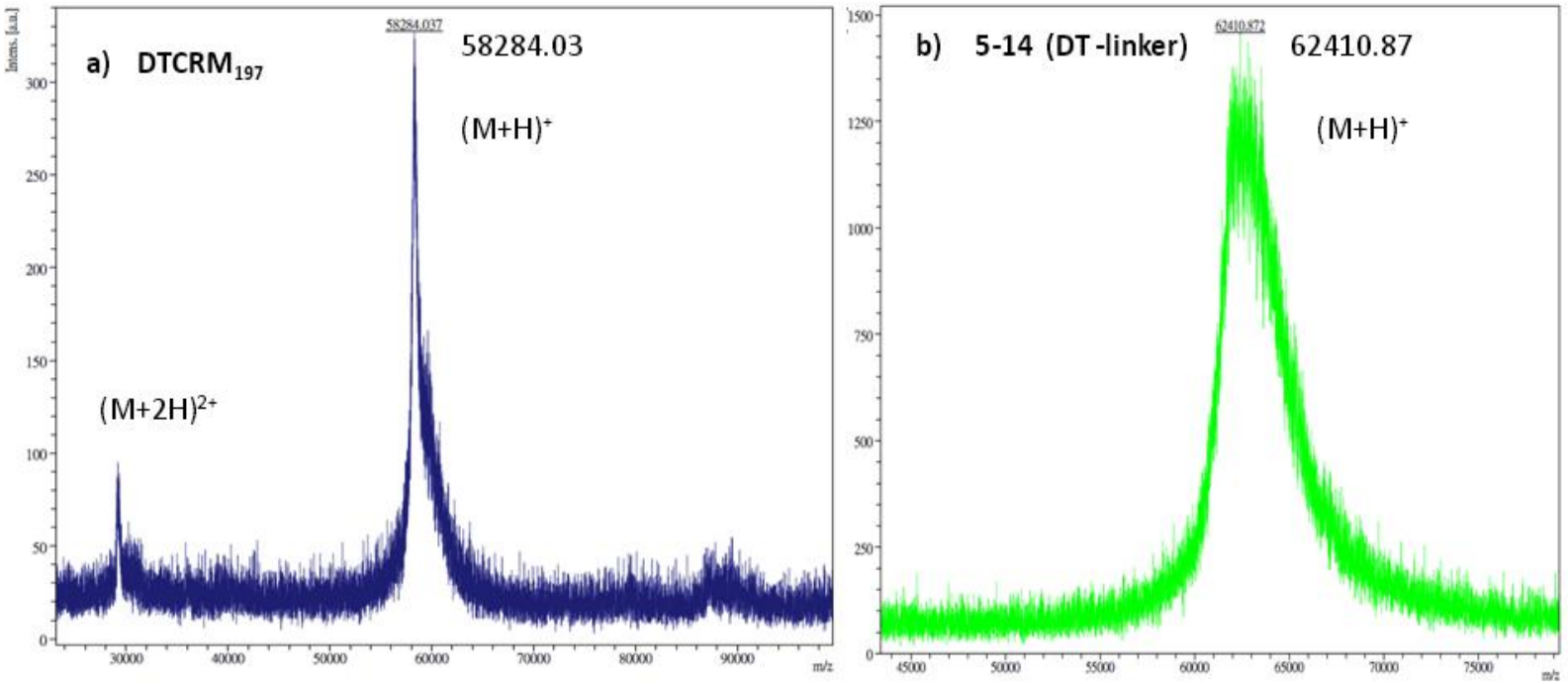
a) DTCRM197
58284.03
(M+H)+
(M+2H)2+
b) 5-14 (DT-linker)
62410.87
(M+H)+

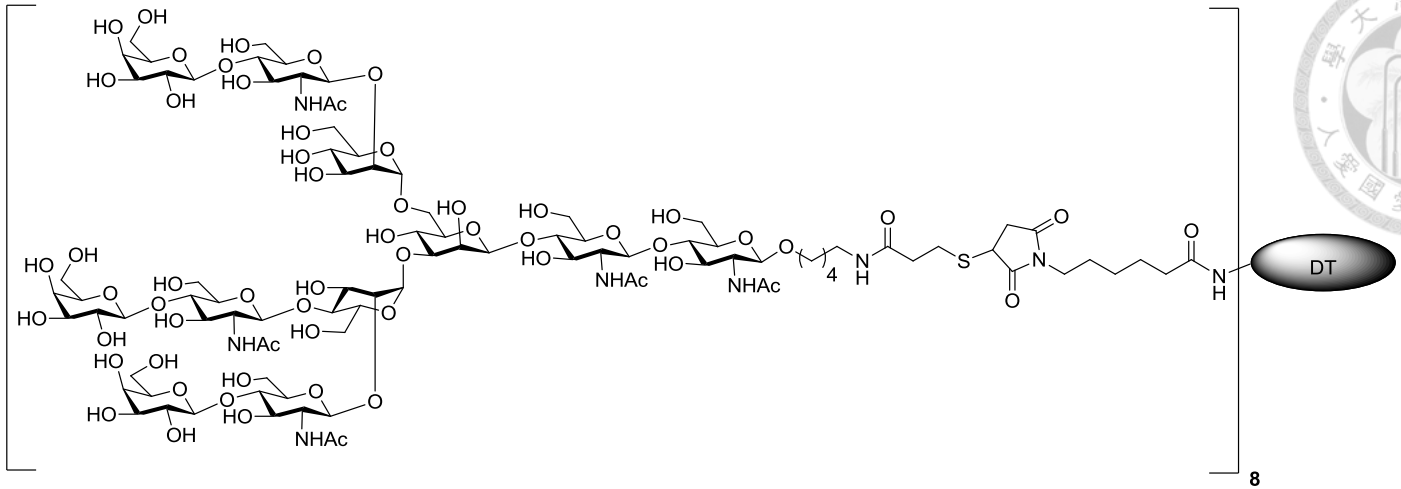

Glycoconjugate 3

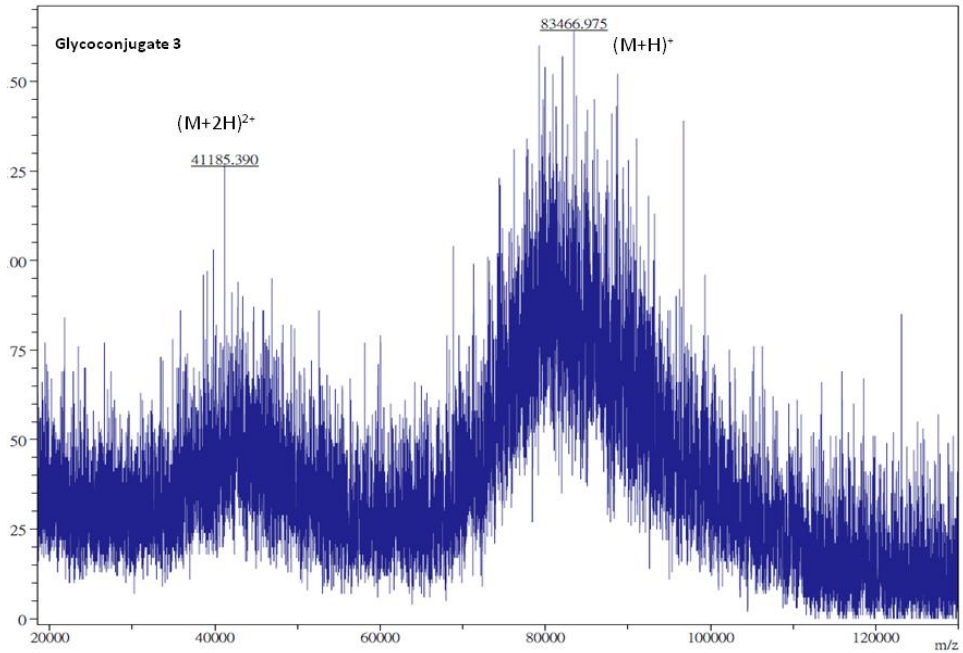

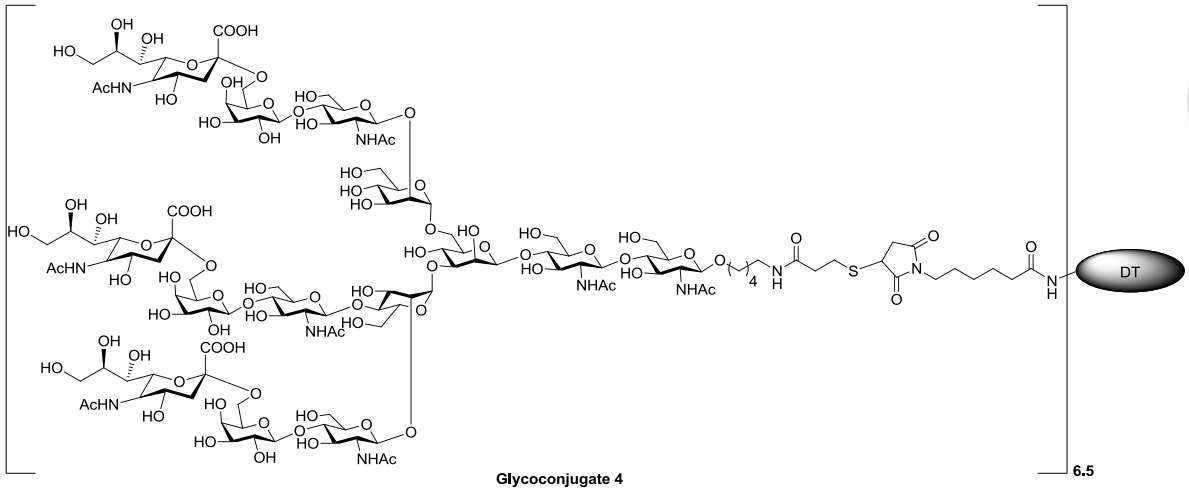

Glycoconjugate 4

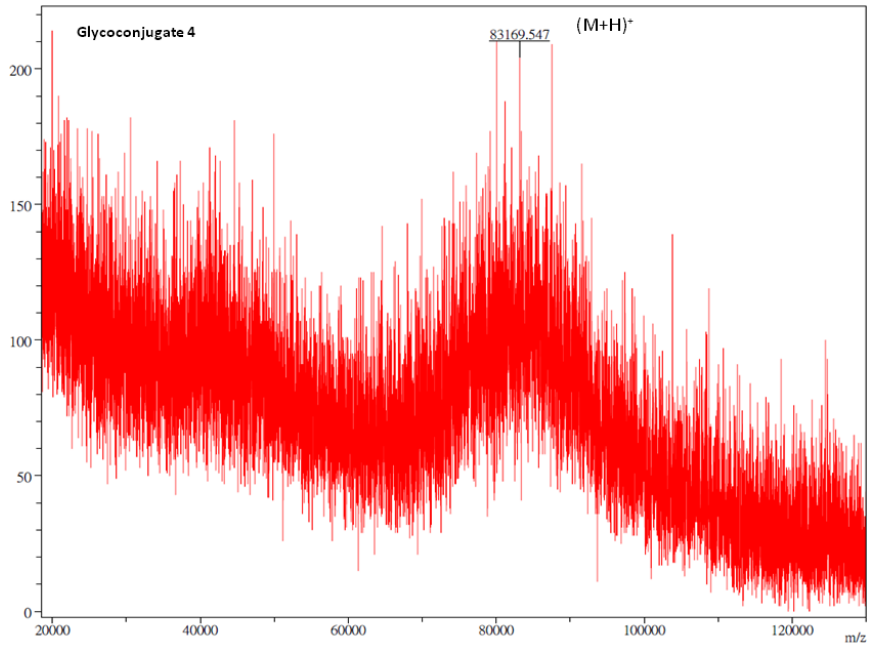

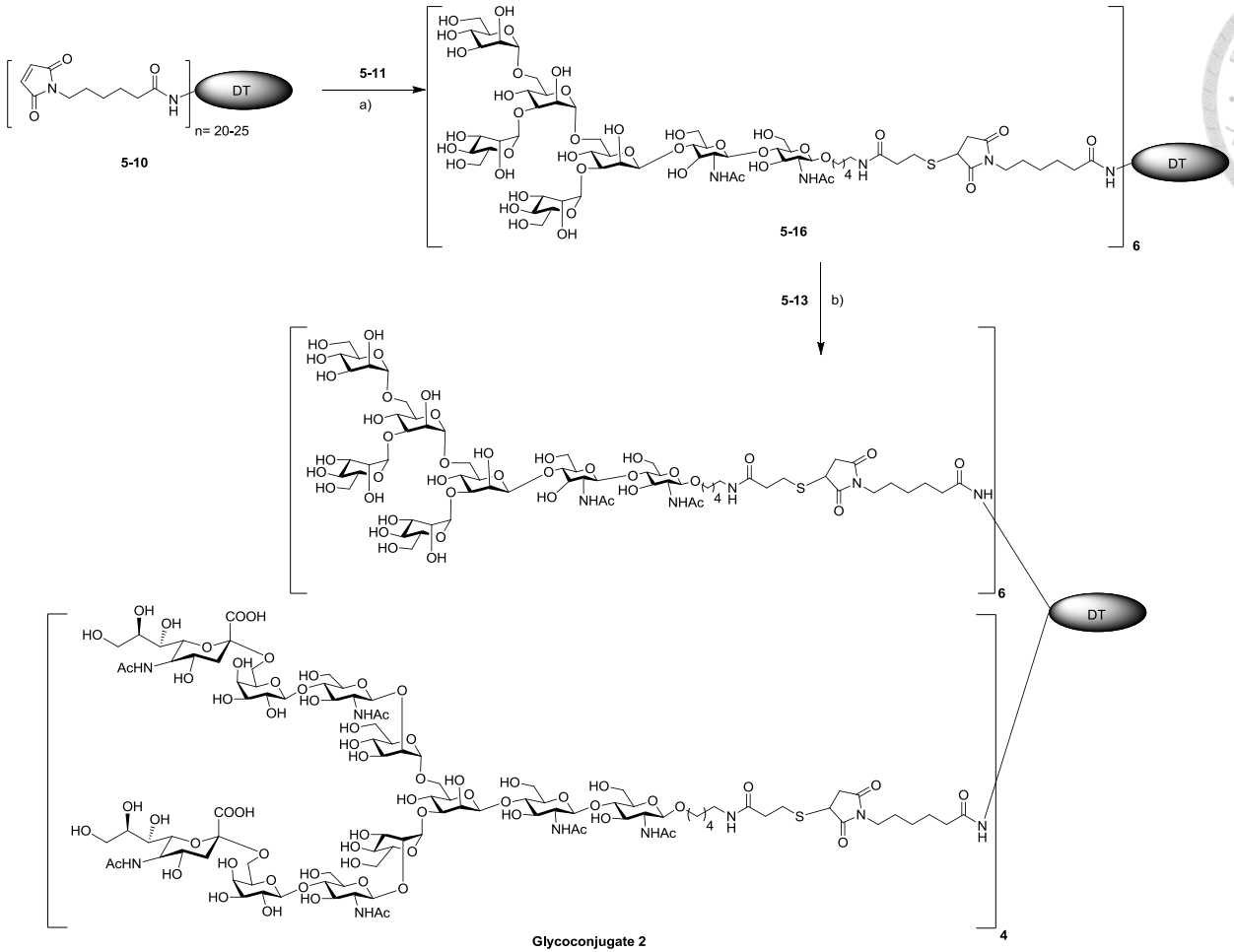
DT
n= 20-25
5-10
5-11
a)
5-16
6
5-13
b)
6
DT
4
Glycoconjugate 2

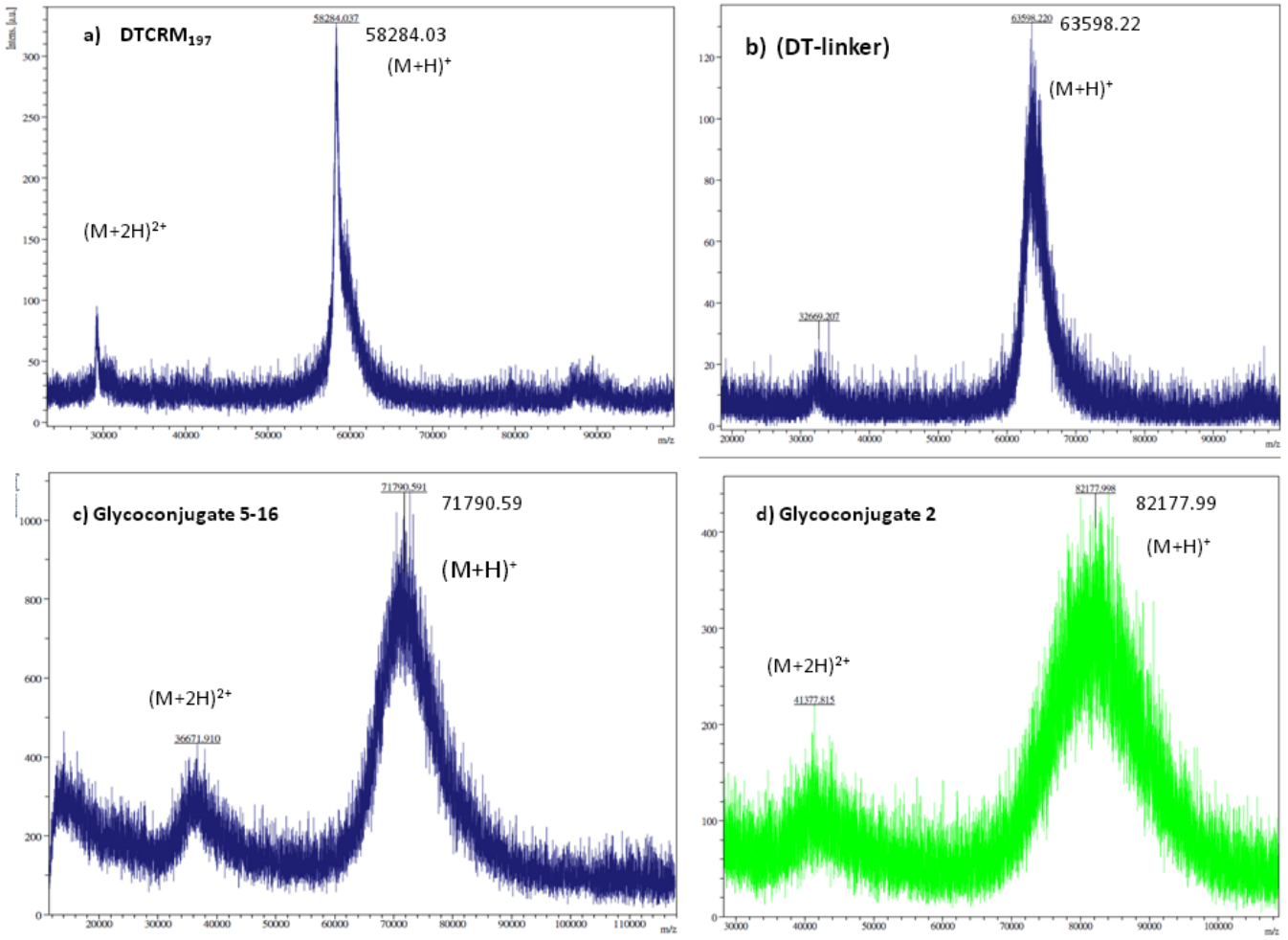
a) DTCRM197
58284.037
58284.03
(M+H)+
(M+2H)2+
b) (DT-linker)
63598.220
63598.22
(M+H)+
32669.207
c) Glycoconjugate 5-16
71790.591
71790.59
(M+H)+
(M+2H)2+
36671.910
d) Glycoconjugate 2
82177.998
82177.99
(M+H)+
(M+2H)2+
41377.815

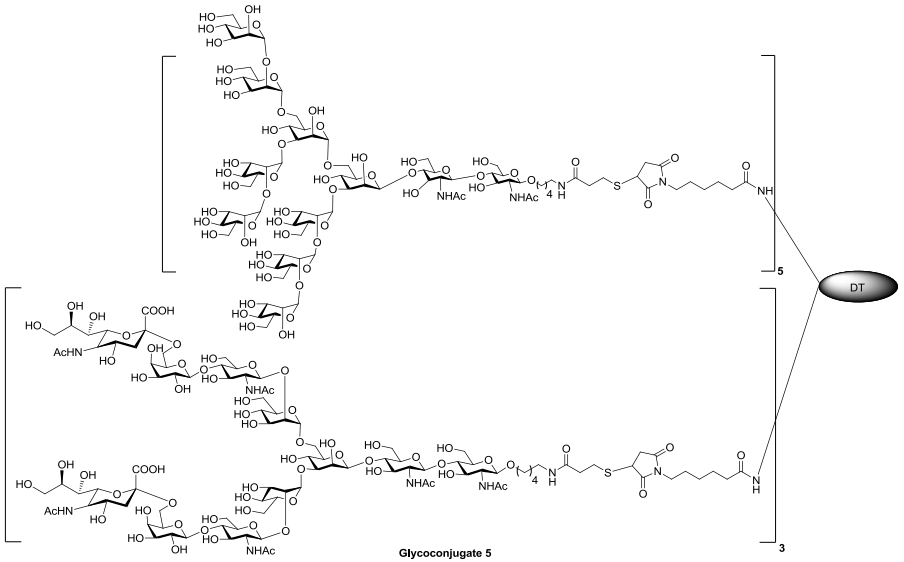

Glycoconjugate 5

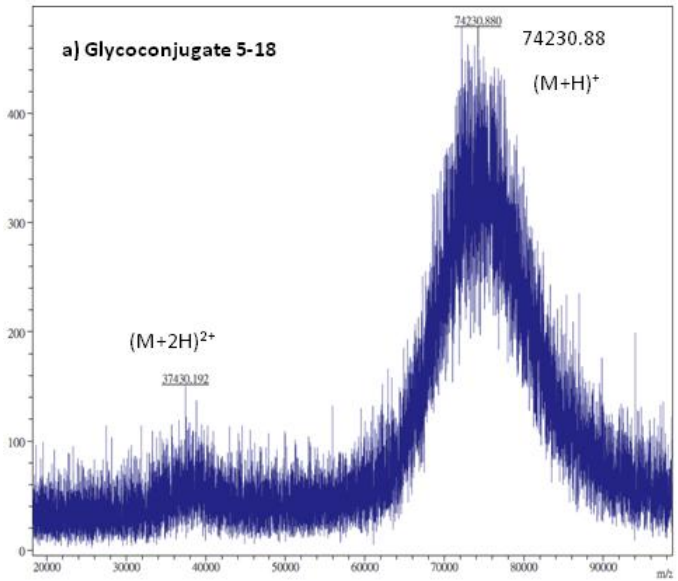

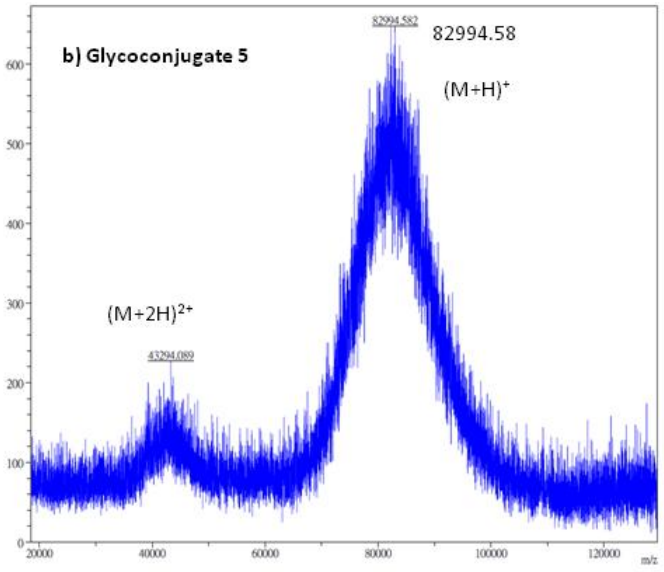

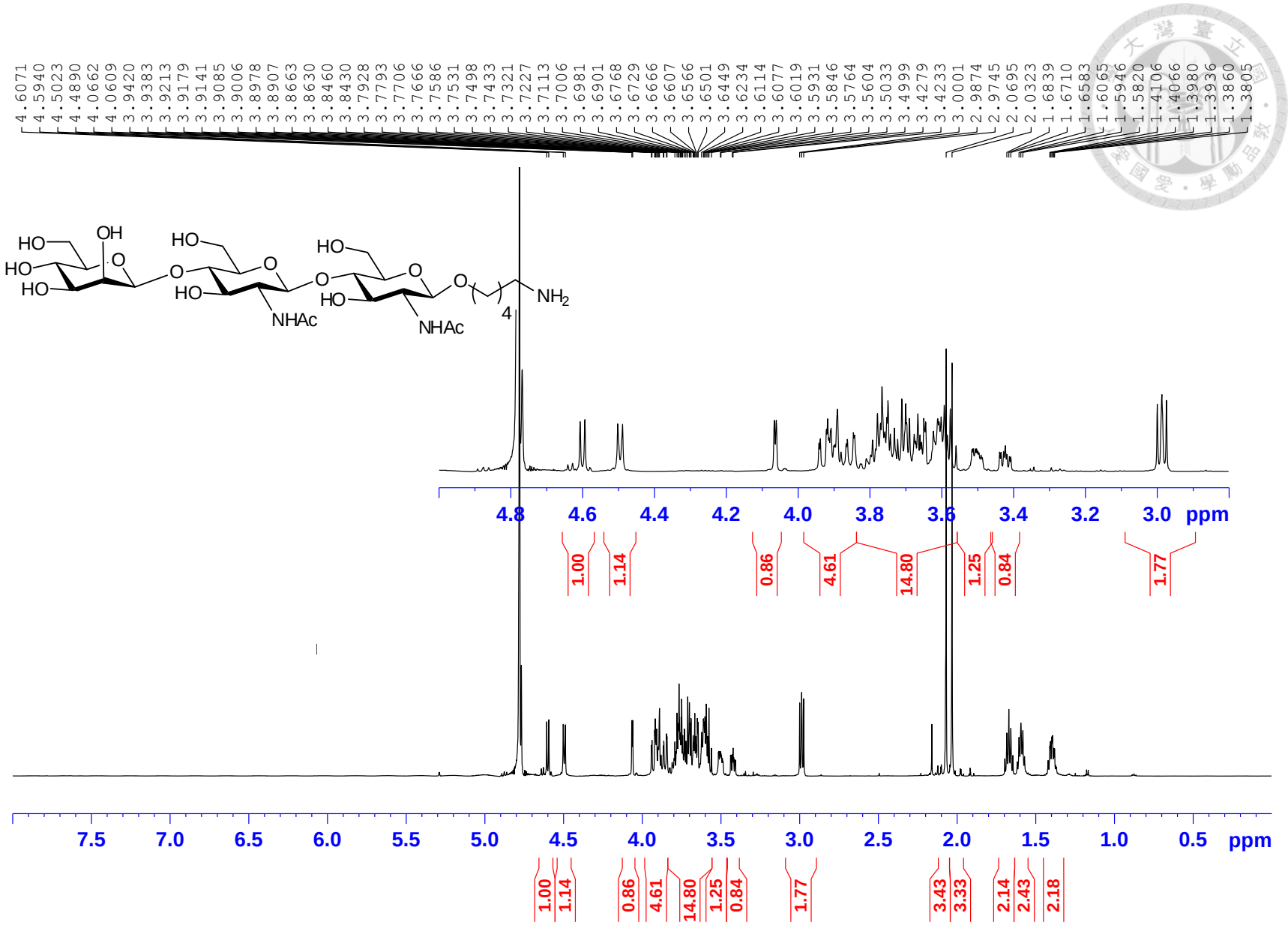
4.6071
4.5940
4.5023
4.4890
4.0662
4.0609
3.9420
3.9383
3.9213
3.9179
3.9141
3.9085
3.9006
3.8978
3.8907
3.8663
3.8630
3.8460
3.8430
3.7928
3.7793
3.7706
3.7666
3.7586
3.7531
3.7498
3.7433
3.7321
3.7227
3.7113
3.7006
3.6981
3.6901
3.6768
3.6729
3.6666
3.6607
3.6566
3.6501
3.6449
3.6234
3.6114
3.6077
3.6019
3.5931
3.5846
3.5764
3.5604
3.5033
3.4999
3.4279
3.4233
3.0001
2.9874
2.9745
2.0695
2.0323
1.6839
1.6710
1.6583
1.6065
1.5946
1.5820
1.4106
1.4066
1.3980
1.3936
1.3860
1.3805
HO
OH
O
HO
HO
O
HO
O
HO
NHAc
O
HO
HO
O
HO
NHAc
O
4
NH2
4.8
4.6
4.4
4.2
4.0
3.8
3.6
3.4
3.2
3.0
ppm
1.00
1.14
0.86
4.61
14.80
1.25
0.84
1.77
7.5
7.0
6.5
6.0
5.5
5.0
4.5
4.0
3.5
3.0
2.5
2.0
1.5
1.0
0.5
ppm
1.00
1.14
0.86
4.61
14.80
1.25
0.84
1.77
3.43
3.33
2.14
2.43
2.18

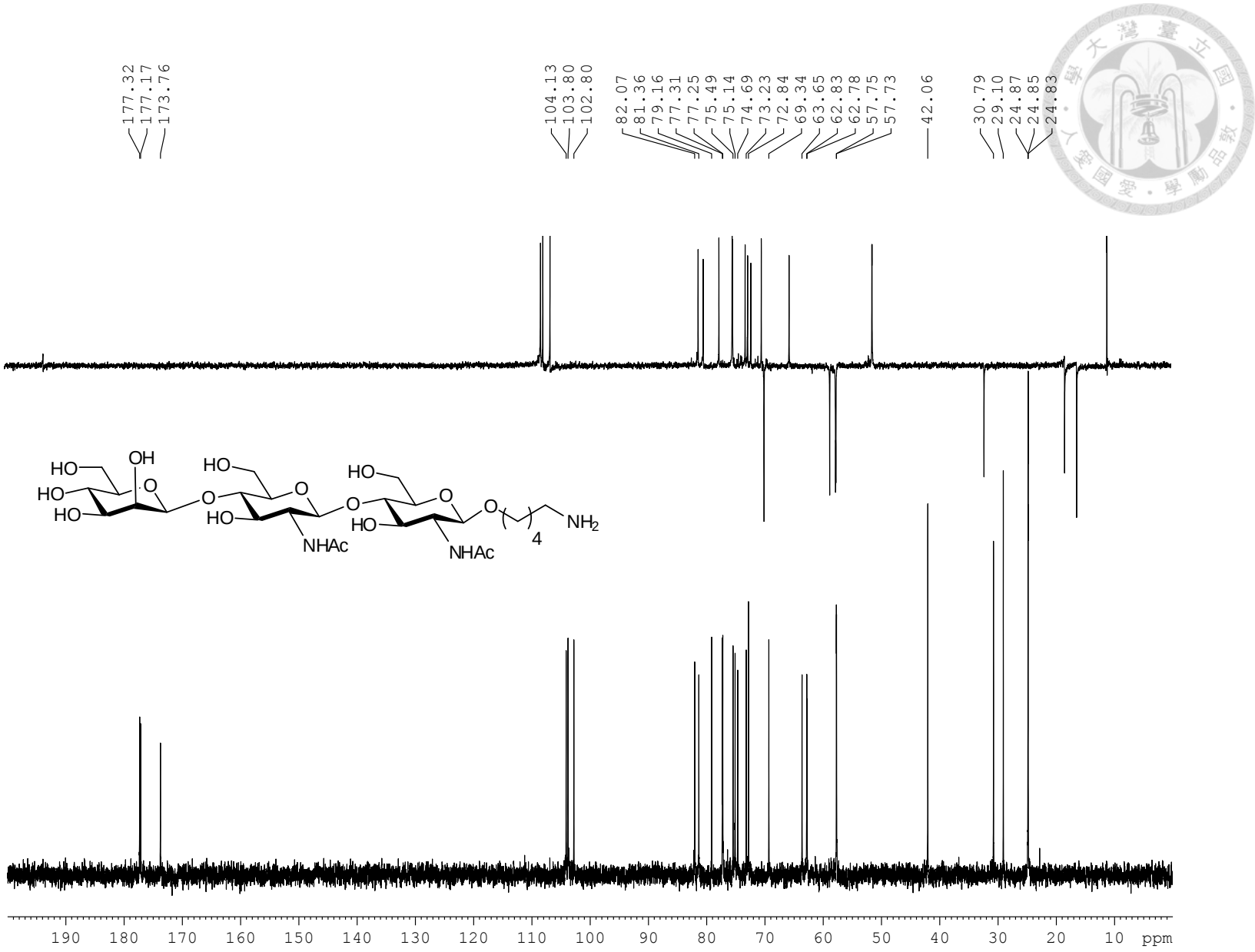
177.32
177.17
173.76
104.13
103.80
102.80
82.07
81.36
79.16
77.31
77.25
75.49
75.14
74.69
73.23
72.84
69.34
63.65
62.83
62.78
57.75
57.73
42.06
30.79
29.10
24.87
24.85
24.83
HO
OH
HO
HO
O
O
HO
O
HO
NHAc
O
HO
O
HO
NHAc
O
4
NH2
190
180
170
160
150
140
130
120
110
100
90
80
70
60
50
40
30
20
10
ppm

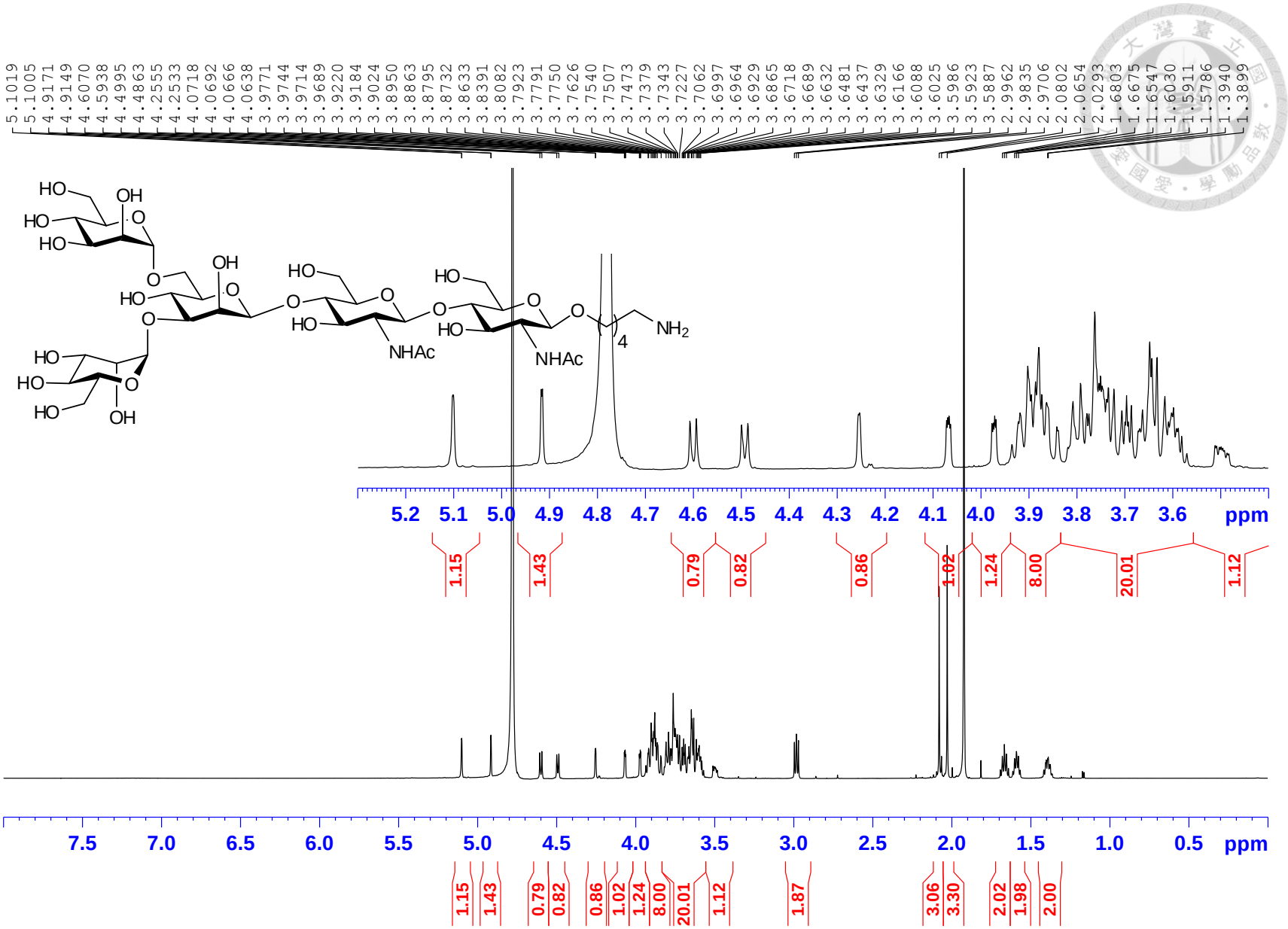
5.1019
5.1005
4.9171
4.9149
4.6070
4.5938
4.4995
4.4863
4.2555
4.2533
4.0718
4.0692
4.0666
4.0638
3.9771
3.9744
3.9714
3.9689
3.9220
3.9184
3.9024
3.8950
3.8863
3.8795
3.8732
3.8633
3.8391
3.8082
3.7923
3.7791
3.7750
3.7626
3.7540
3.7507
3.7473
3.7379
3.7343
3.7227
3.7062
3.6997
3.6964
3.6929
3.6865
3.6718
3.6689
3.6632
3.6481
3.6437
3.6329
3.6166
3.6088
3.6025
3.5986
3.5923
3.5887
2.9962
2.9835
2.9706
2.0802
2.0654
2.0293
1.6803
1.6675
1.6547
1.6030
1.5911
1.5786
1.3940
1.3899
HO
OH
O
HO
HO
O
OH
O
HO
O
HO
NHAc
HO
O
O
HO
NHAc
O
4
NH2
HO
HO
O
HO
OH
5.2 5.1 5.0 4.9 4.8 4.7 4.6 4.5 4.4 4.3 4.2 4.1 4.0 3.9 3.8 3.7 3.6 ppm
1.15
1.43
0.79
0.82
0.86
1.02
1.24
8.00
20.01
1.12
7.5 7.0 6.5 6.0 5.5 5.0 4.5 4.0 3.5 3.0 2.5 2.0 1.5 1.0 0.5 ppm
1.15
1.43
0.79
0.82
0.86
1.02
1.24
8.00
20.01
1.12
1.87
3.06
3.30
2.02
1.98
2.00

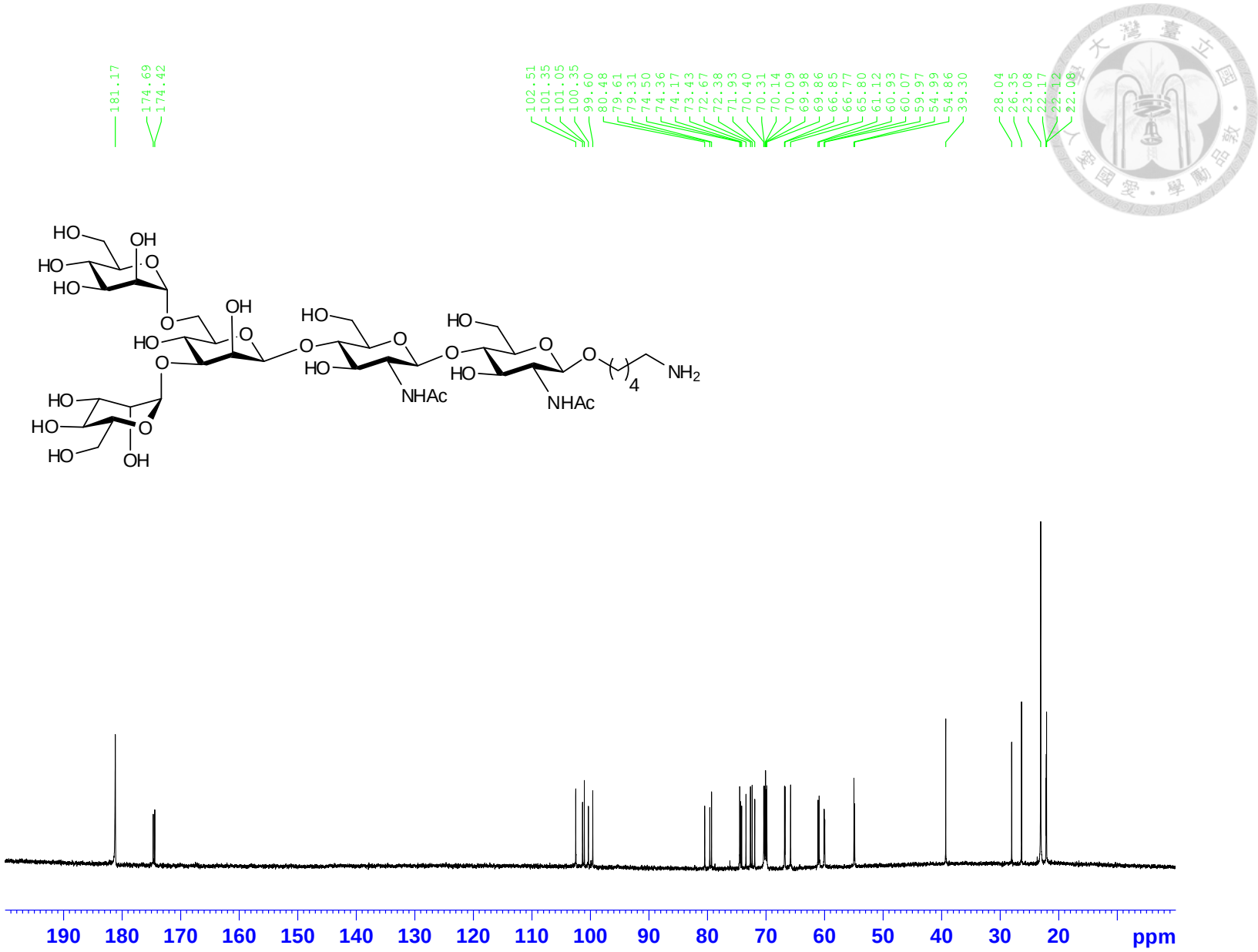
181.17
174.69
174.42
102.51
101.35
101.05
100.35
99.60
80.48
79.61
79.31
74.50
74.36
74.17
73.43
72.67
72.38
71.93
70.40
70.31
70.14
70.09
69.98
69.86
66.85
66.77
65.80
61.12
60.93
60.07
59.97
54.99
54.86
39.30
28.04
26.35
23.08
22.17
22.12
22.08
HO
OH
O
NHAc
NH2
4
190
180
170
160
150
140
130
120
110
100
90
80
70
60
50
40
30
20
ppm

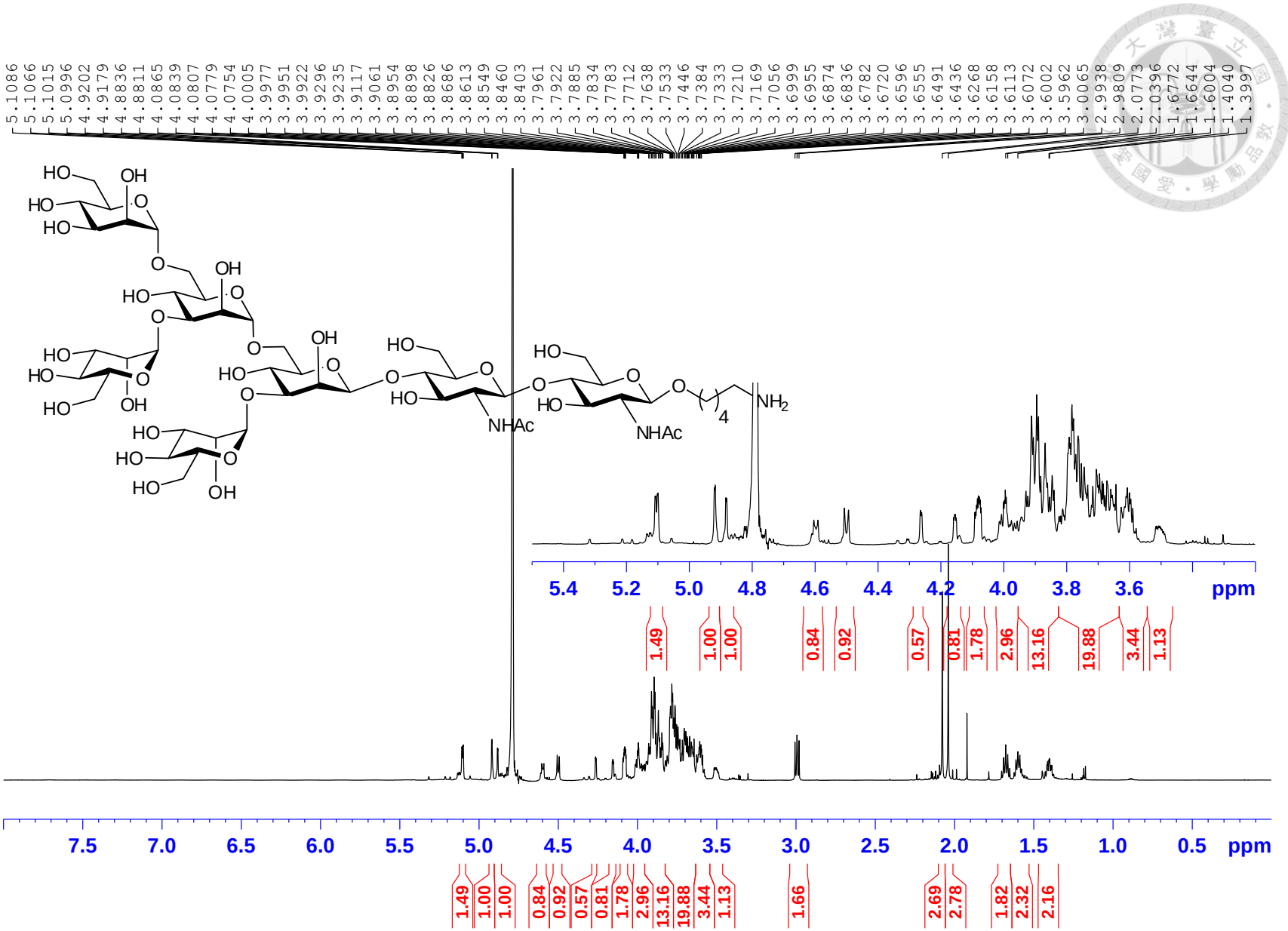
5.1086 5.1066 5.1015 5.0996 4.9202 4.9179 4.8836 4.8811 4.0865 4.0839 4.0807 4.0779 4.0754 4.0005 3.9977 3.9951 3.9922 3.9296 3.9235 3.9117 3.9061 3.8954 3.8898 3.8826 3.8686 3.8613 3.8549 3.8460 3.8403 3.7961 3.7922 3.7885 3.7834 3.7783 3.7712 3.7638 3.7533 3.7446 3.7384 3.7333 3.7210 3.7169 3.7056 3.6999 3.6955 3.6874 3.6836 3.6782 3.6720 3.6596 3.6555 3.6491 3.6436 3.6268 3.6158 3.6113 3.6072 3.6002 3.5962 3.0065 2.9938 2.9809 2.0773 2.0396 1.6772 1.6644 1.6004 1.4040 1.3997
HO
OH
O
NHAc
NH2
4
5.4 5.2 5.0 4.8 4.6 4.4 4.2 4.0 3.8 3.6 ppm
1.49 1.00 1.00 0.84 0.92 0.57 0.81 1.78 2.96 13.16 19.88 3.44 1.13
7.5 7.0 6.5 6.0 5.5 5.0 4.5 4.0 3.5 3.0 2.5 2.0 1.5 1.0 0.5 ppm
1.49 1.00 1.00 0.84 0.92 0.57 0.81 1.78 2.96 13.16 19.88 3.44 1.13 1.66 2.69 2.78 1.82 2.32 2.16

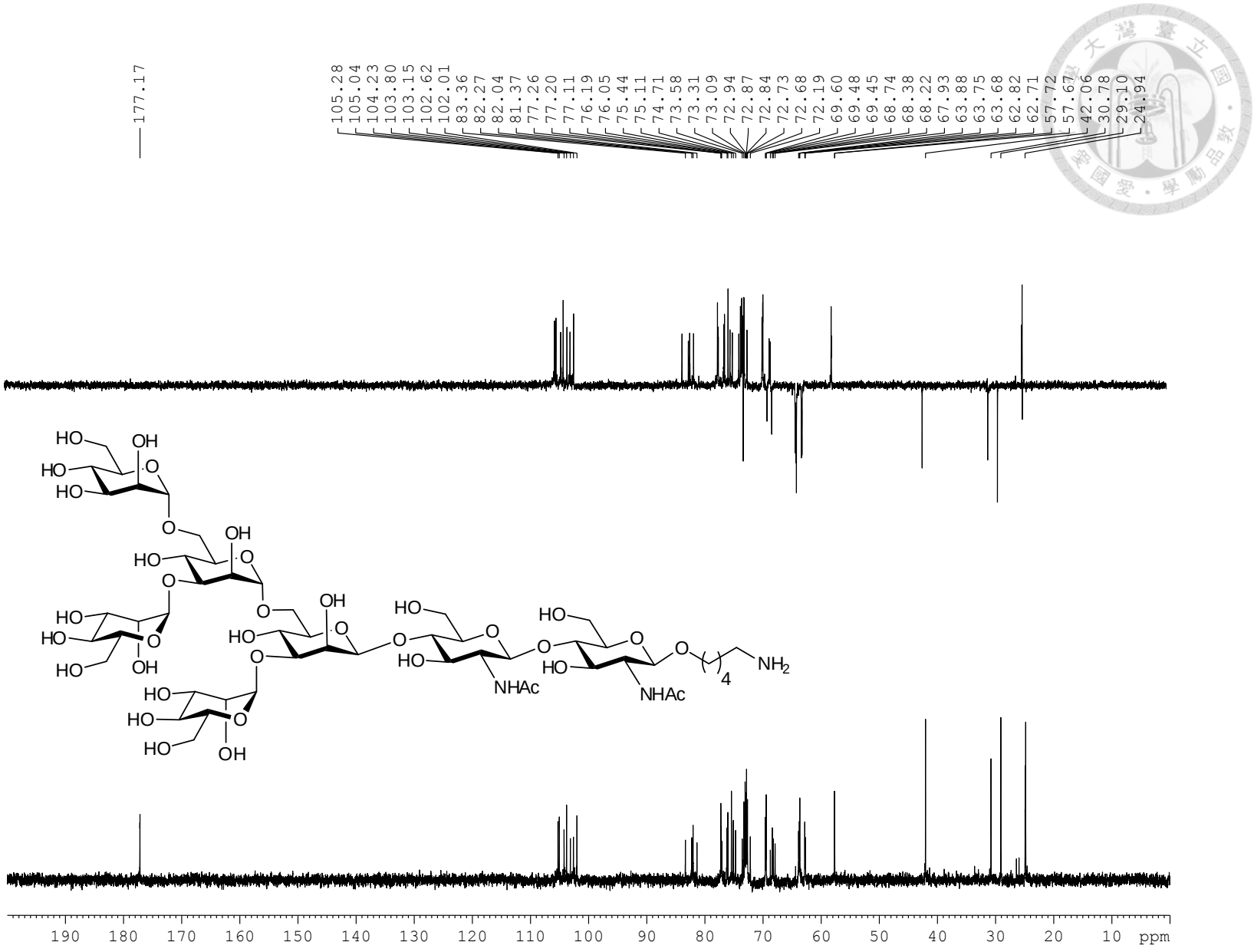
177.17
105.28
105.04
104.23
103.80
103.15
102.62
102.01
83.36
82.27
82.04
81.37
77.26
77.20
77.11
76.19
76.05
75.44
75.11
74.71
73.58
73.31
73.09
72.94
72.87
72.84
72.73
72.68
72.19
69.60
69.48
69.45
68.74
68.38
68.22
67.93
63.88
63.75
63.68
62.82
62.71
57.72
57.67
42.06
30.78
29.10
24.94
HO
OH
O
NHAc
NH2
4
190
180
170
160
150
140
130
120
110
100
90
80
70
60
50
40
30
20
10
ppm

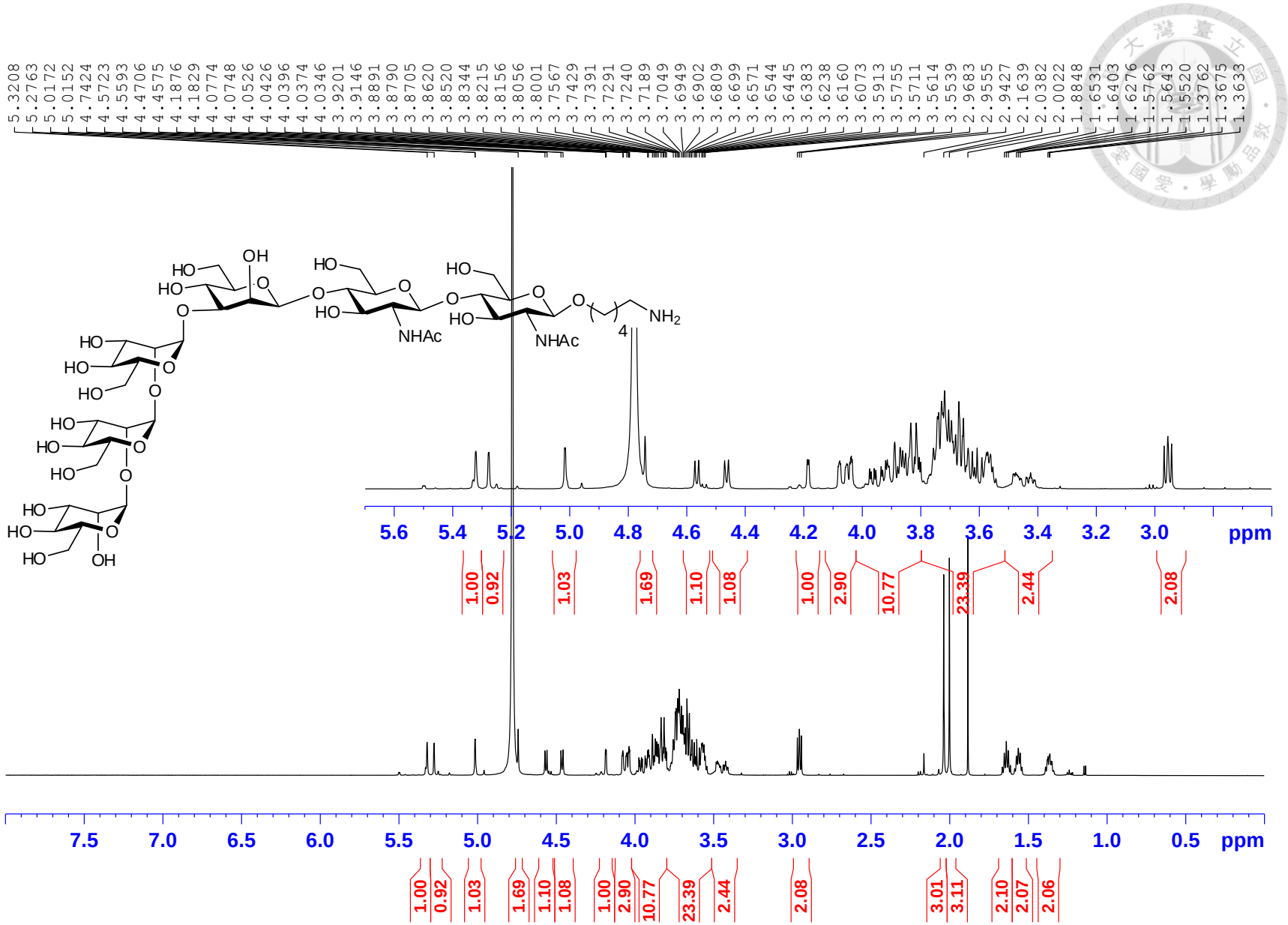
5.3208
5.2763
5.0172
5.0152
4.7424
4.5723
4.5593
4.4706
4.4575
4.1876
4.1829
4.0774
4.0748
4.0526
4.0426
4.0396
4.0374
4.0346
3.9201
3.9146
3.8891
3.8790
3.8705
3.8620
3.8520
3.8344
3.8215
3.8156
3.8056
3.8001
3.7567
3.7429
3.7391
3.7291
3.7240
3.7189
3.7049
3.6949
3.6902
3.6809
3.6699
3.6571
3.6544
3.6445
3.6383
3.6238
3.6160
3.6073
3.5913
3.5755
3.5711
3.5614
3.5539
2.9683
2.9555
2.9427
2.1639
2.0382
2.0022
1.8848
1.6531
1.6403
1.6276
1.5762
1.5643
1.5520
1.3762
1.3675
1.3633
NHAc
NHAc
NH2
4
5.6 5.4 5.2 5.0 4.8 4.6 4.4 4.2 4.0 3.8 3.6 3.4 3.2 3.0 ppm
1.00 0.92 1.03 1.69 1.10 1.08 1.00 2.90 10.77 23.39 2.44 2.08
7.5 7.0 6.5 6.0 5.5 5.0 4.5 4.0 3.5 3.0 2.5 2.0 1.5 1.0 0.5 ppm
1.00 0.92 1.03 1.69 1.10 1.08 1.00 2.90 10.77 23.39 2.44 2.08 3.01 3.11 2.10 2.07 2.06

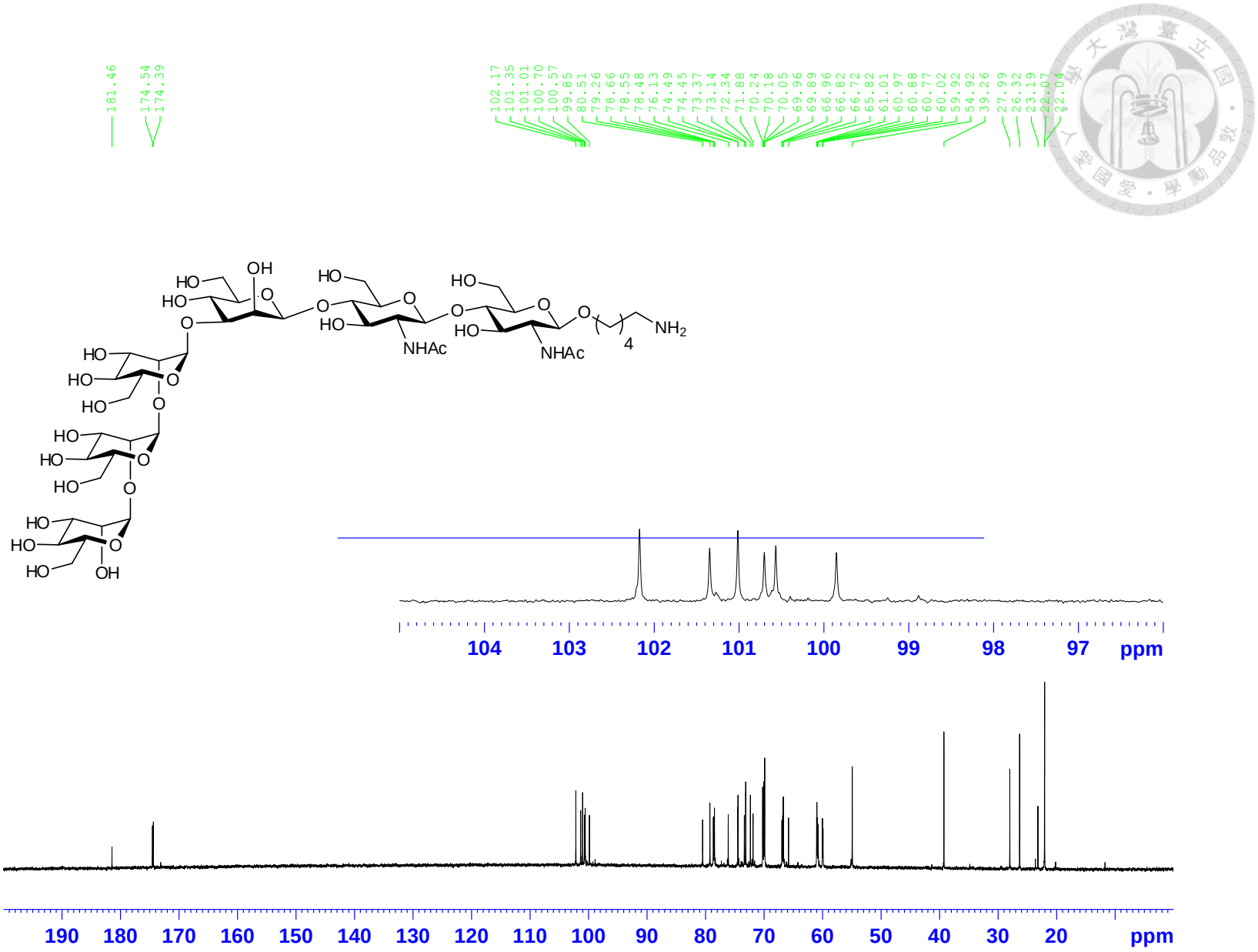
181.46
174.54
174.39
102.17
101.35
101.01
100.70
100.57
99.85
80.51
79.26
78.66
78.55
78.48
76.13
74.49
74.45
73.37
73.14
72.34
71.88
70.24
70.18
70.05
69.96
69.89
66.96
66.82
66.72
65.82
61.01
60.97
60.88
60.77
60.02
59.92
54.92
39.26
27.99
26.32
23.19
22.07
22.04
HO
OH
NHAc
NH2
4
104
103
102
101
100
99
98
97
ppm
190
180
170
160
150
140
130
120
110
100
90
80
70
60
50
40
30
20
ppm

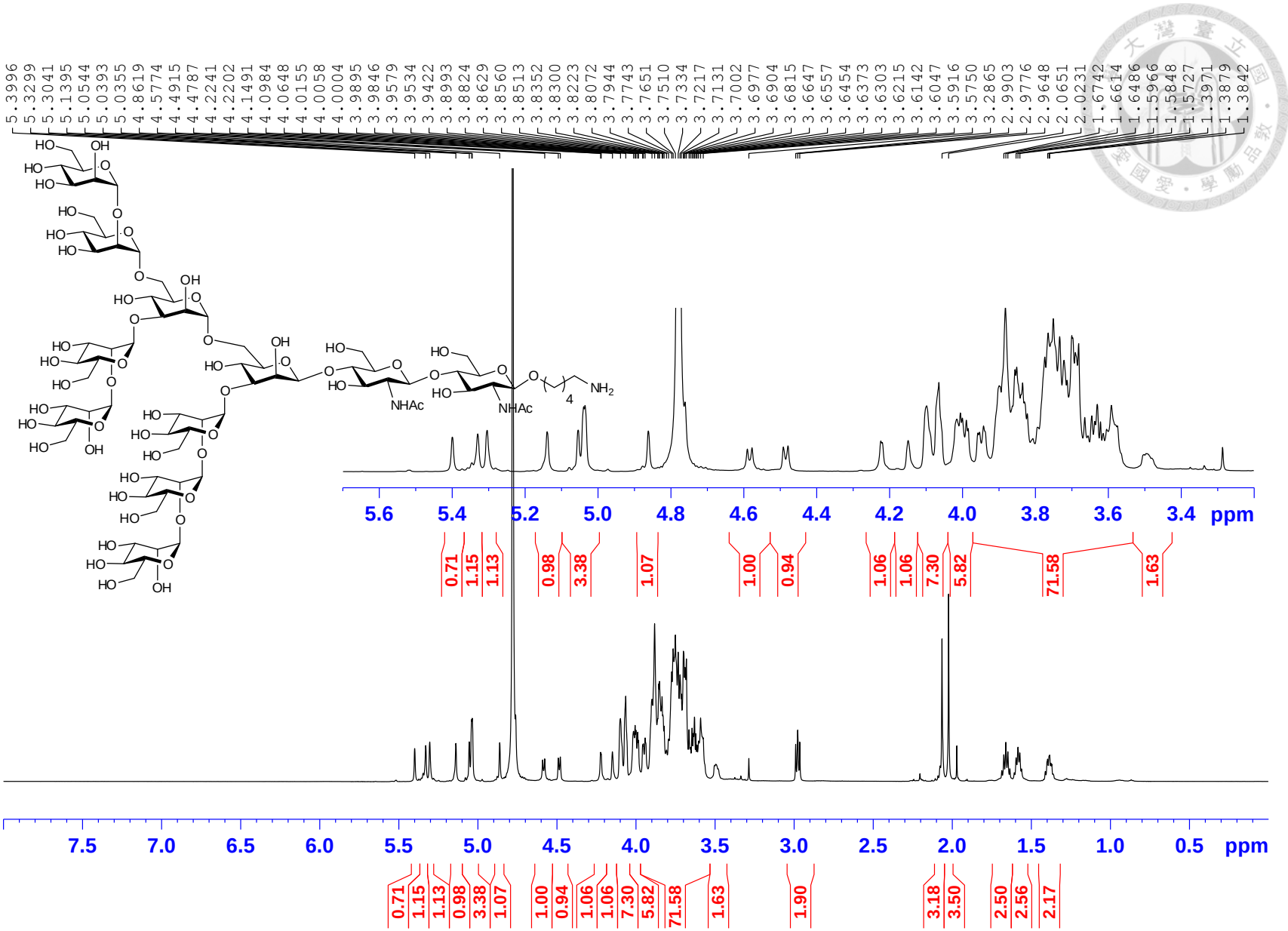
5.3996 5.3299 5.3041 5.1395 5.0544 5.0393 5.0355 4.8619 4.5774 4.4915 4.4787 4.2241 4.2202 4.1491 4.0984 4.0648 4.0155 4.0058 4.0004 3.9895 3.9846 3.9579 3.9534 3.9422 3.8993 3.8824 3.8629 3.8560 3.8513 3.8352 3.8300 3.8223 3.8072 3.7944 3.7743 3.7651 3.7510 3.7334 3.7217 3.7131 3.7002 3.6977 3.6904 3.6815 3.6647 3.6557 3.6454 3.6373 3.6303 3.6215 3.6142 3.6047 3.5916 3.5750 3.2865 2.9903 2.9776 2.9648 2.0651 2.0231 1.6742 1.6614 1.6486 1.5966 1.5848 1.5727 1.3971 1.3879 1.3842
HO OH O NHAc NH2 4
5.6 5.4 5.2 5.0 4.8 4.6 4.4 4.2 4.0 3.8 3.6 3.4 ppm
0.71 1.15 1.13 0.98 3.38 1.07 1.00 0.94 1.06 1.06 7.30 5.82 71.58 1.63
7.5 7.0 6.5 6.0 5.5 5.0 4.5 4.0 3.5 3.0 2.5 2.0 1.5 1.0 0.5 ppm
0.71 1.15 1.13 0.98 3.38 1.07 1.00 0.94 1.06 1.06 7.30 5.82 71.58 1.63 1.90 3.18 3.50 2.50 2.56 2.17

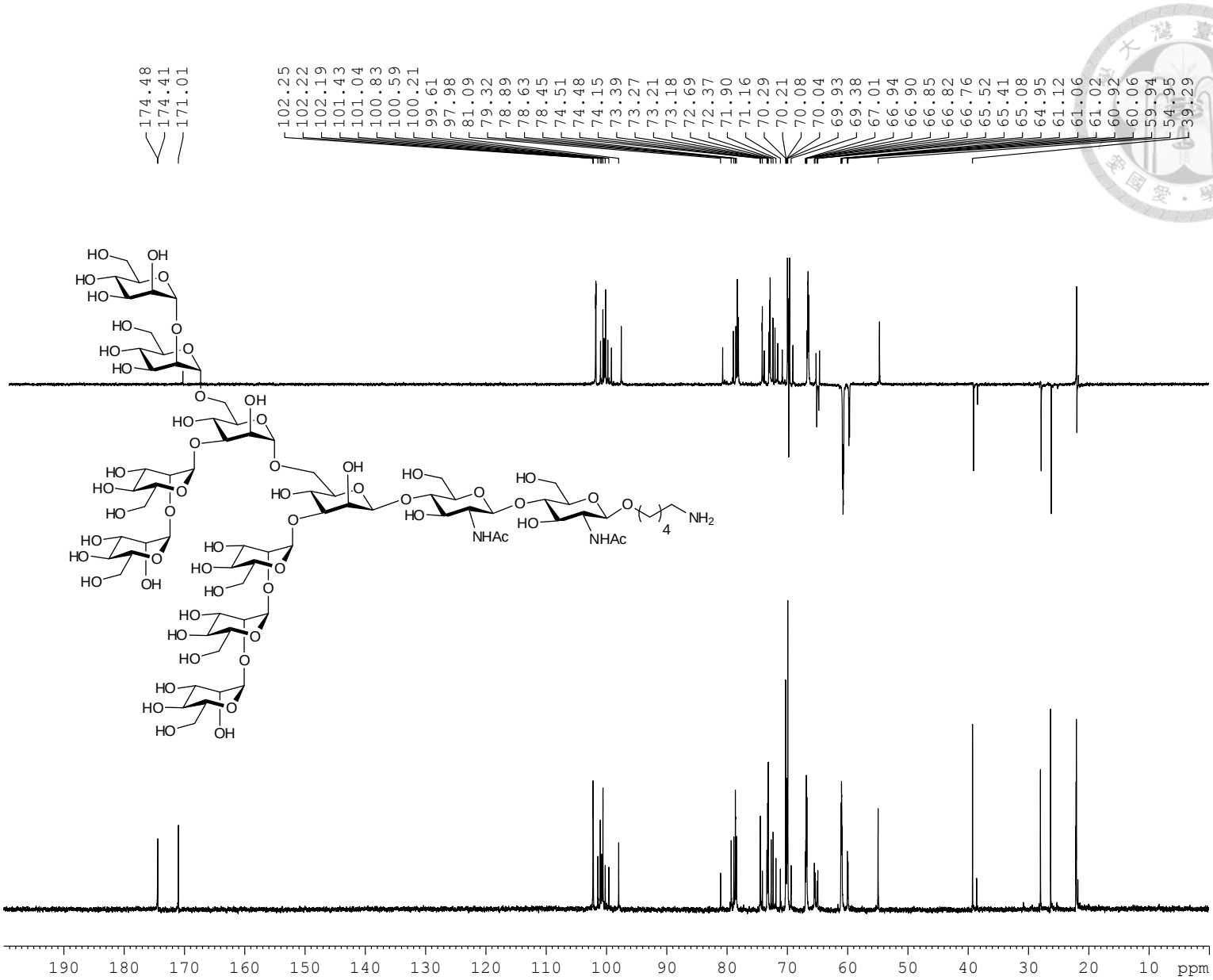
174.48
174.41
171.01
102.25
102.22
102.19
101.43
101.04
100.83
100.59
100.21
99.61
97.98
81.09
79.32
78.89
78.63
78.45
74.51
74.48
74.15
73.39
73.27
73.21
73.18
72.69
72.37
71.90
71.16
70.29
70.21
70.08
70.04
69.93
69.38
67.01
66.94
66.90
66.85
66.82
66.76
65.52
65.41
65.08
64.95
61.12
61.06
61.02
60.92
60.06
59.94
54.95
39.29
NHAc
NHAc
NH2
4
190
180
170
160
150
140
130
120
110
100
90
80
70
60
50
40
30
20
10
ppm

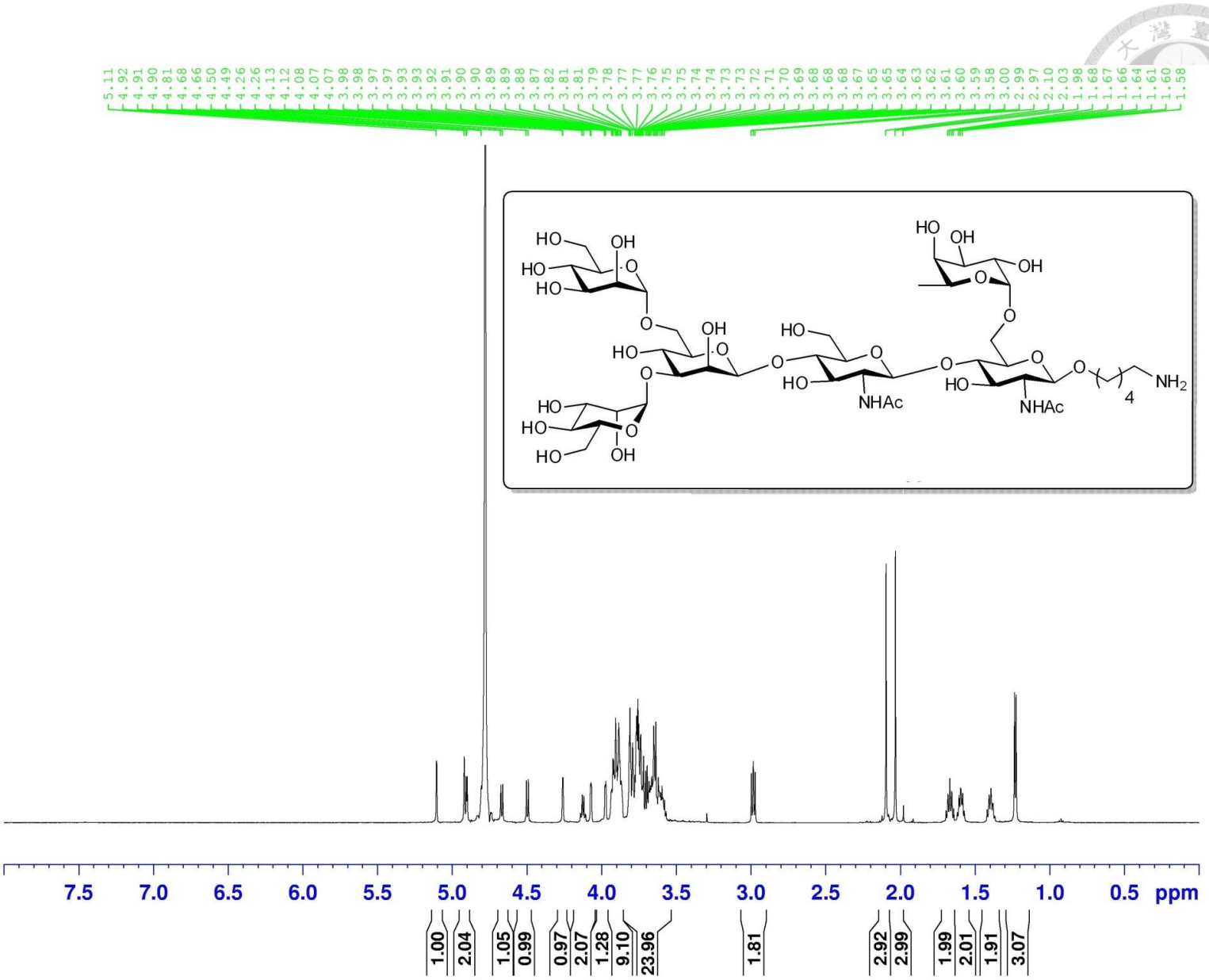
5.11 4.92 4.91 4.90 4.81 4.68 4.66 4.50 4.49 4.26 4.13 4.12 4.08 4.07 4.07 3.98 3.98 3.97 3.97 3.93 3.93 3.92 3.91 3.90 3.90 3.89 3.89 3.88 3.87 3.82 3.81 3.81 3.79 3.78 3.77 3.77 3.76 3.75 3.75 3.74 3.74 3.73 3.73 3.72 3.71 3.70 3.69 3.68 3.68 3.68 3.67 3.65 3.65 3.64 3.63 3.62 3.61 3.60 3.59 3.58 3.00 2.99 2.97 2.10 2.03 1.98 1.68 1.67 1.66 1.64 1.61 1.60 1.58
HO
OH
O
NHAc
NH2
4
7.5 7.0 6.5 6.0 5.5 5.0 4.5 4.0 3.5 3.0 2.5 2.0 1.5 1.0 0.5 ppm
1.00 2.04 1.05 0.99 0.97 2.07 1.28 9.10 23.96 1.81 2.92 2.99 1.99 2.01 1.91 3.07

177.43
177.15
173.76

105.26
103.87
103.81
103.14
102.36
102.15
83.22
82.48
81.38
77.09
76.92
76.18
75.41
75.06
74.71
74.56
73.13
73.06
72.88
72.76
72.73
72.61
72.23
70.89
69.59
69.52
69.18
68.61
68.56
63.88
63.69
62.73
57.80
57.62
42.05
30.81
29.13
25.04
24.87
18.11

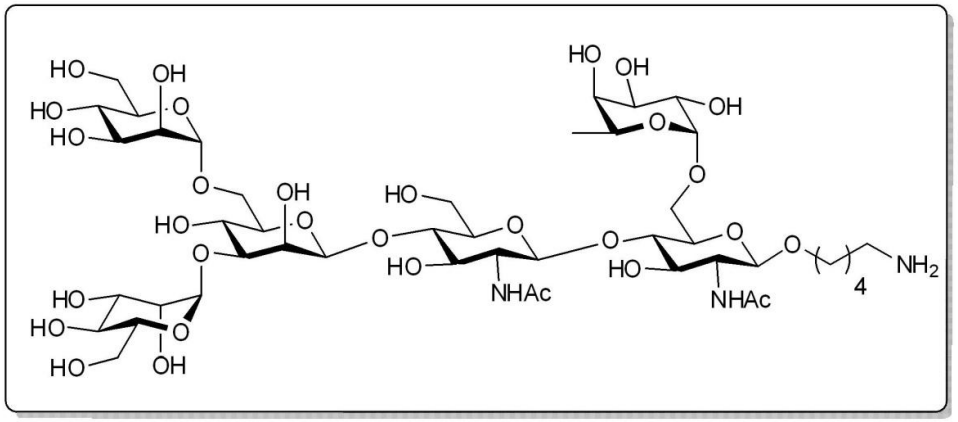

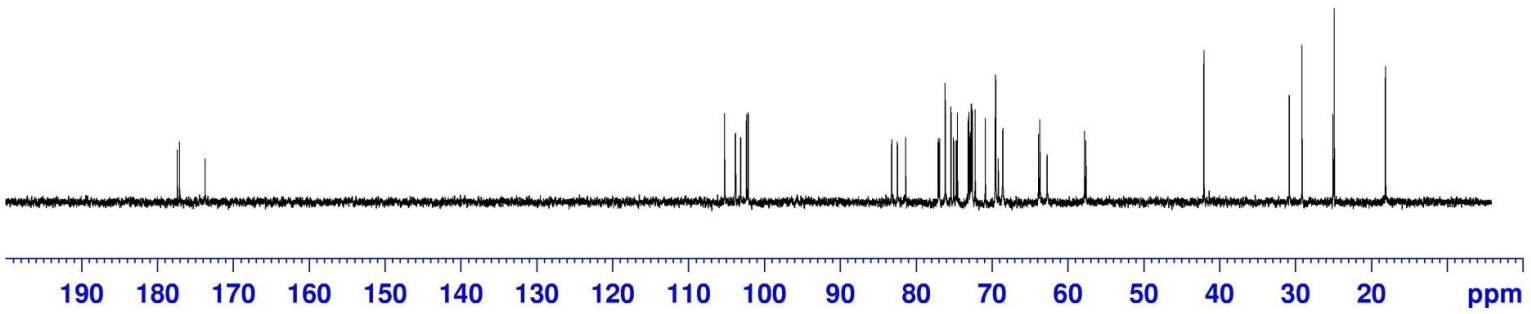

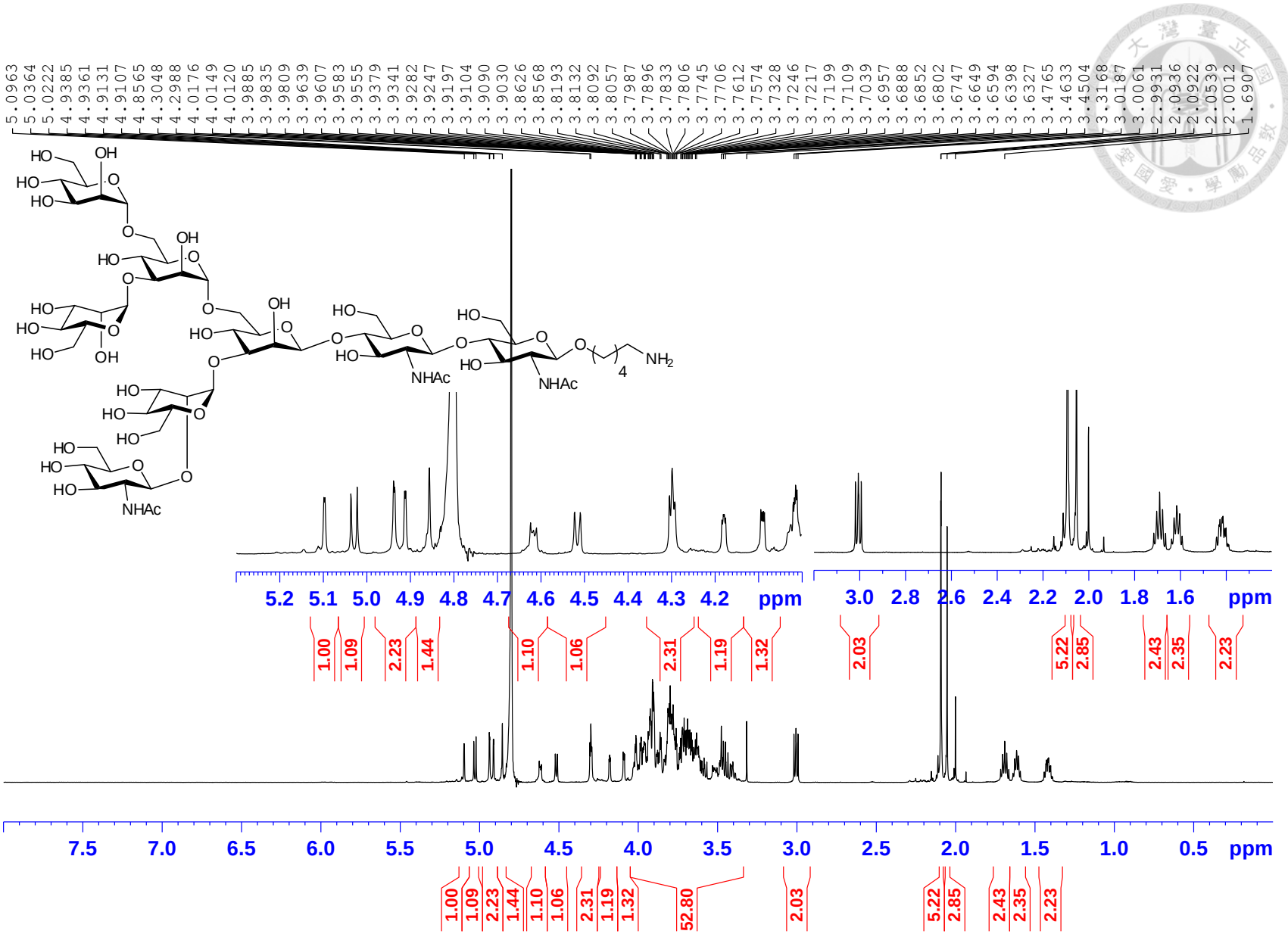
5.0963 5.0364 5.0222 4.9385 4.9361 4.9131 4.9107 4.8565 4.3048 4.2988 4.0176 4.0149 4.0120 3.9885 3.9835 3.9809 3.9639 3.9607 3.9583 3.9555 3.9379 3.9341 3.9282 3.9247 3.9197 3.9104 3.9090 3.9030 3.8626 3.8568 3.8193 3.8132 3.8092 3.8057 3.7987 3.7896 3.7833 3.7806 3.7745 3.7706 3.7612 3.7574 3.7328 3.7246 3.7217 3.7199 3.7109 3.7039 3.6957 3.6888 3.6852 3.6802 3.6747 3.6649 3.6594 3.6398 3.6327 3.4765 3.4633 3.4504 3.3168 3.0187 3.0061 2.9931 2.0936 2.0922 2.0539 2.0012 1.6907
NHAc
NHAc
NH2
4
5.2 5.1 5.0 4.9 4.8 4.7 4.6 4.5 4.4 4.3 4.2 ppm
3.0 2.8 2.6 2.4 2.2 2.0 1.8 1.6 ppm
1.00 1.09 2.23 1.44 1.10 1.06 2.31 1.19 1.32 2.03 5.22 2.85 2.43 2.35 2.23
7.5 7.0 6.5 6.0 5.5 5.0 4.5 4.0 3.5 3.0 2.5 2.0 1.5 1.0 0.5 ppm
1.00 1.09 2.23 1.44 1.10 1.06 2.31 1.19 1.32 52.80 2.03 5.22 2.85 2.43 2.35 2.23

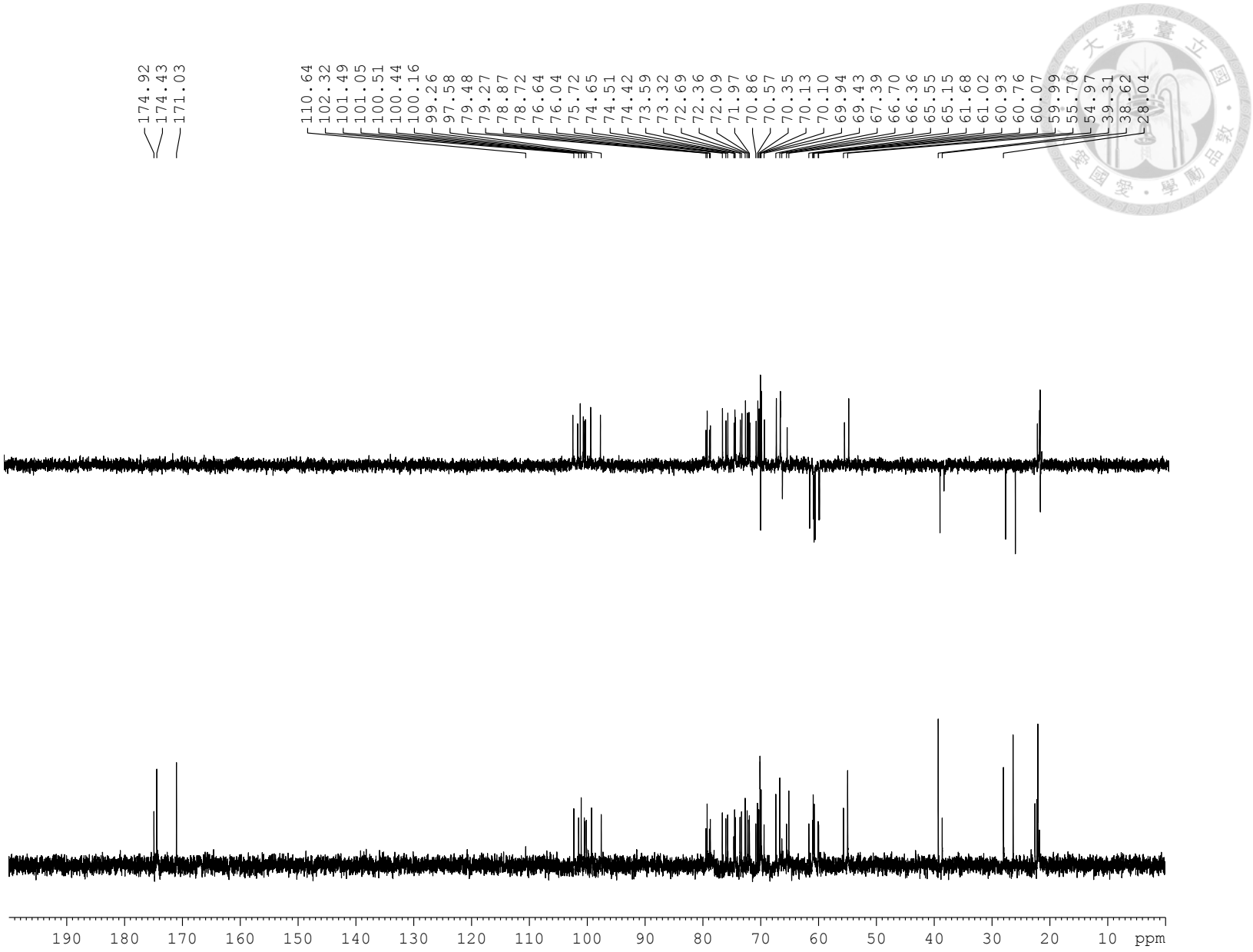
174.92
174.43
171.03
110.64
102.32
101.49
101.05
100.51
100.44
100.16
99.26
97.58
79.48
79.27
78.87
78.72
76.64
76.04
75.72
74.65
74.51
74.42
73.59
73.32
72.69
72.36
72.09
71.97
70.86
70.57
70.35
70.13
70.10
69.94
69.43
67.39
66.70
66.36
65.55
65.15
61.68
61.02
60.93
60.76
60.07
59.99
55.70
54.97
39.31
38.62
28.04
190 180 170 160 150 140 130 120 110 100 90 80 70 60 50 40 30 20 10 ppm

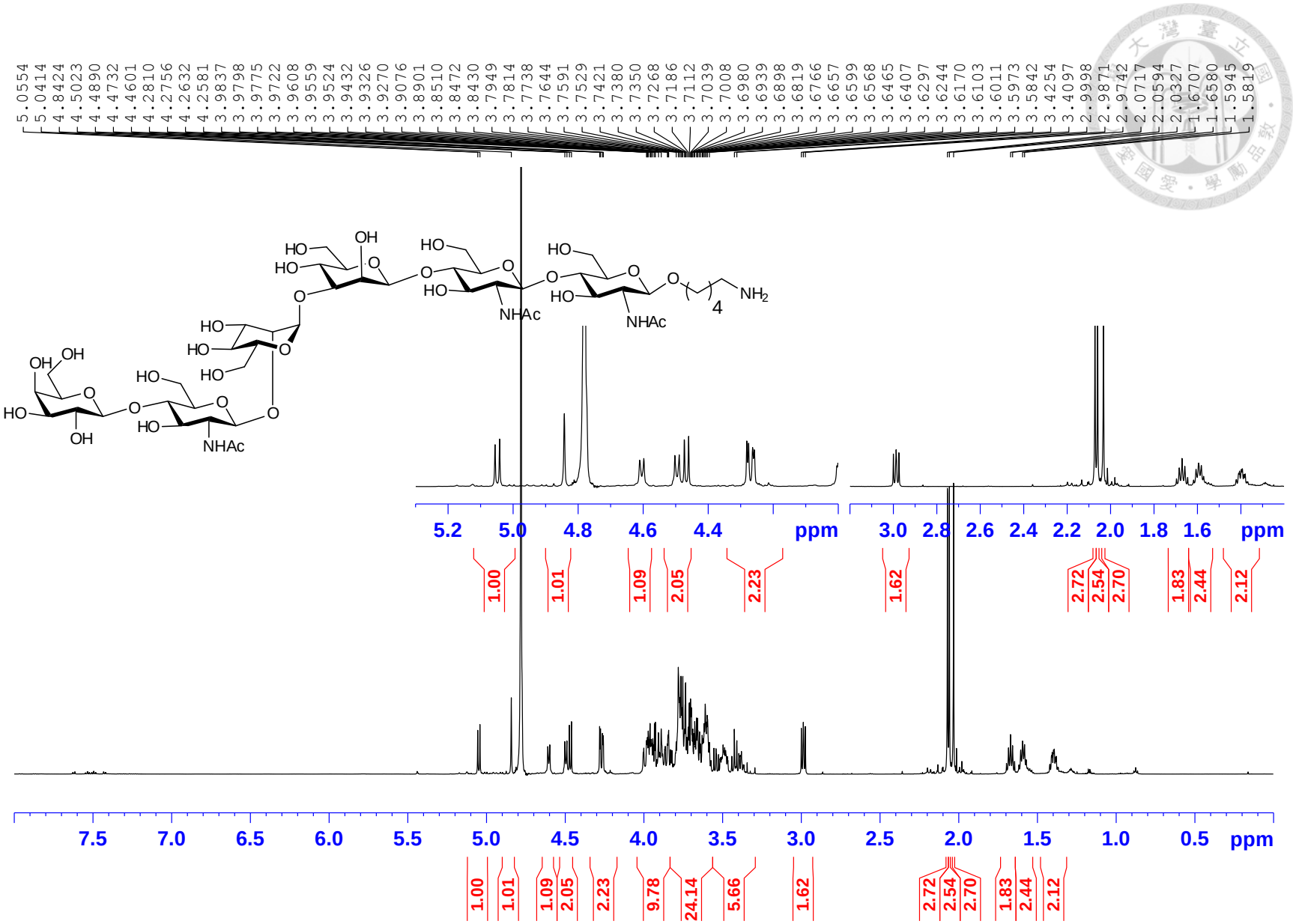
5.0554
5.0414
4.8424
4.5023
4.4890
4.4732
4.4601
4.2810
4.2756
4.2632
4.2581
3.9837
3.9798
3.9775
3.9722
3.9608
3.9559
3.9524
3.9432
3.9326
3.9270
3.9076
3.8901
3.8510
3.8472
3.8430
3.7949
3.7814
3.7738
3.7644
3.7591
3.7529
3.7421
3.7380
3.7350
3.7268
3.7186
3.7112
3.7039
3.7008
3.6980
3.6939
3.6898
3.6819
3.6766
3.6657
3.6599
3.6568
3.6465
3.6407
3.6297
3.6244
3.6170
3.6103
3.6011
3.5973
3.5842
3.4254
3.4097
2.9998
2.9871
2.9742
2.0717
2.0594
2.0327
1.6707
1.6580
1.5945
1.5819
HO
OH
O
NHAc
NH2
4
5.2
5.0
4.8
4.6
4.4
ppm
3.0
2.8
2.6
2.4
2.2
2.0
1.8
1.6
ppm
1.00
1.01
1.09
2.05
2.23
1.62
2.72
2.54
2.70
1.83
2.44
2.12
7.5
7.0
6.5
6.0
5.5
5.0
4.5
4.0
3.5
3.0
2.5
2.0
1.5
1.0
0.5
ppm
1.00
1.01
1.09
2.05
2.23
9.78
24.14
5.66
1.62
2.72
2.54
2.70
1.83
2.44
2.12

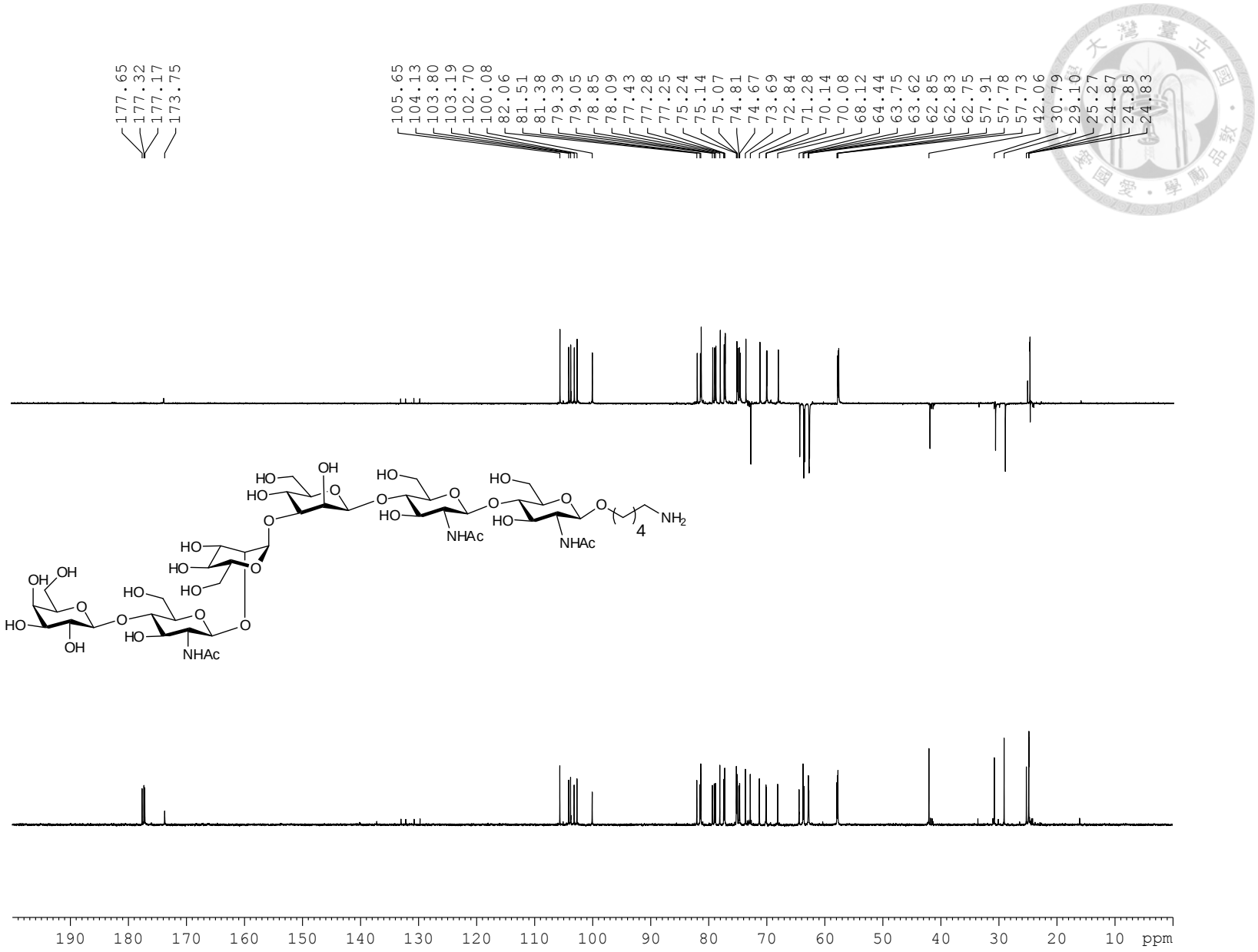
177.65
177.32
177.17
173.75
105.65
104.13
103.80
103.19
102.70
100.08
82.06
81.51
81.38
79.39
79.05
78.85
78.09
77.43
77.28
77.25
75.24
75.14
75.07
74.81
74.67
73.69
72.84
71.28
70.14
70.08
68.12
64.44
63.75
63.62
62.85
62.83
62.75
57.91
57.78
57.73
42.06
30.79
29.10
25.27
24.87
24.85
24.83
HO
OH
O
NHAc
NH2
4
190
180
170
160
150
140
130
120
110
100
90
80
70
60
50
40
30
20
10
ppm

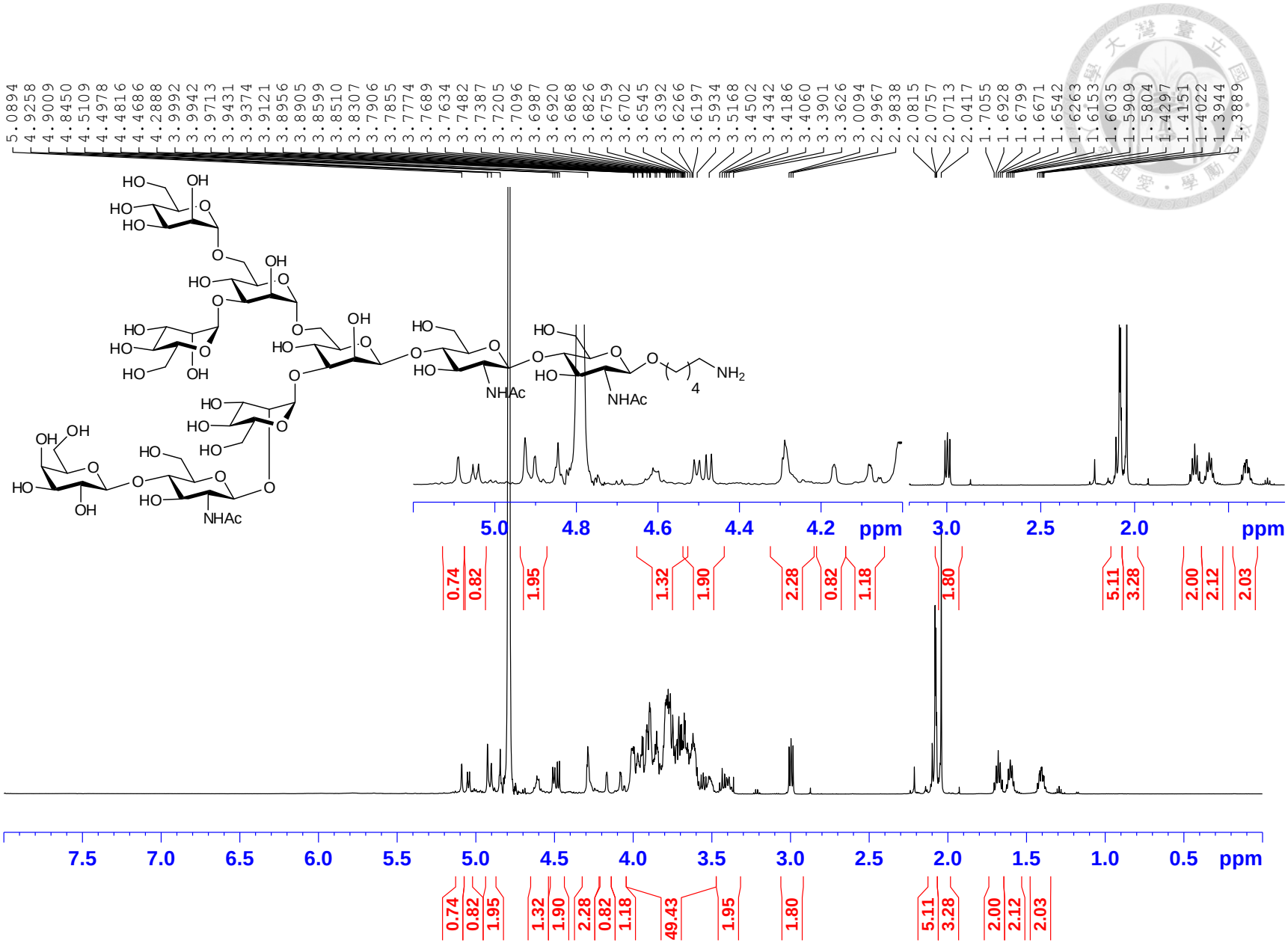
5.0894
4.9258
4.9009
4.8450
4.5109
4.4978
4.4816
4.4686
4.2888
3.9992
3.9942
3.9713
3.9431
3.9374
3.9121
3.8956
3.8905
3.8599
3.8510
3.8307
3.7906
3.7855
3.7774
3.7689
3.7634
3.7482
3.7387
3.7205
3.7096
3.6987
3.6920
3.6868
3.6826
3.6759
3.6702
3.6545
3.6392
3.6266
3.6197
3.5934
3.5168
3.4502
3.4342
3.4186
3.4060
3.3901
3.3626
3.0094
2.9967
2.9838
2.0815
2.0757
2.0713
2.0417
1.7055
1.6928
1.6799
1.6671
1.6542
1.6263
1.6153
1.6035
1.5909
1.5804
1.4297
1.4151
1.4022
1.3944
1.3889
NHAc
NHAc
NH2
4
5.0
4.8
4.6
4.4
4.2
ppm
3.0
2.5
2.0
ppm
0.74
0.82
1.95
1.32
1.90
2.28
0.82
1.18
1.80
5.11
3.28
2.00
2.12
2.03
7.5
7.0
6.5
6.0
5.5
5.0
4.5
4.0
3.5
3.0
2.5
2.0
1.5
1.0
0.5
ppm
0.74
0.82
1.95
1.32
1.90
2.28
0.82
1.18
49.43
1.95
1.80
5.11
3.28
2.00
2.12
2.03

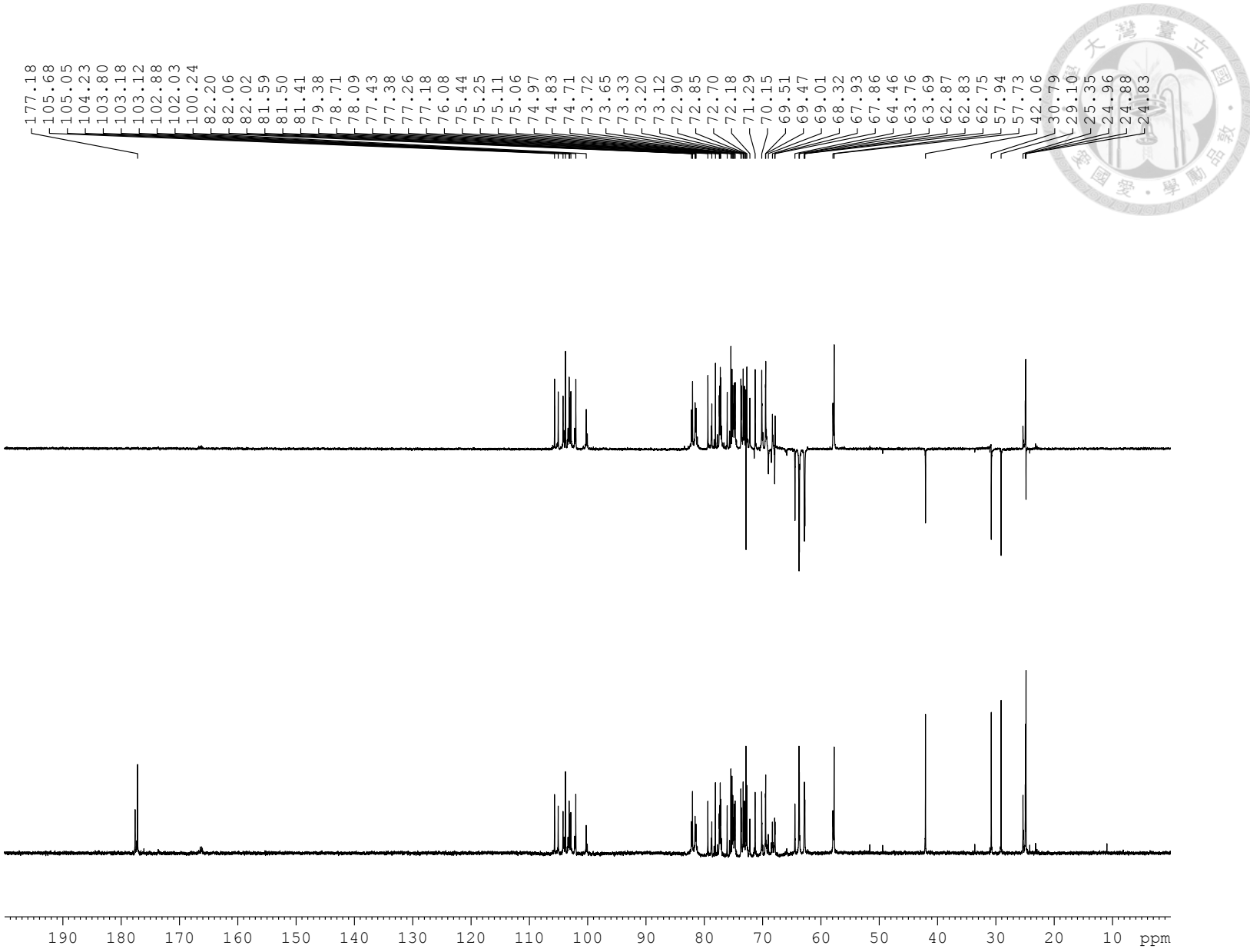
177.18
105.68
105.05
104.23
103.80
103.18
103.12
102.88
102.03
100.24
82.20
82.06
82.02
81.59
81.50
81.41
79.38
78.71
78.09
77.43
77.38
77.26
77.18
76.08
75.44
75.25
75.11
75.06
74.97
74.83
74.71
73.72
73.65
73.33
73.20
73.12
72.90
72.85
72.70
72.18
71.29
70.15
69.51
69.47
69.01
68.32
67.93
67.86
64.46
63.76
63.69
62.87
62.83
62.75
57.94
57.73
42.06
30.79
29.10
25.35
24.96
24.88
24.83
190 180 170 160 150 140 130 120 110 100 90 80 70 60 50 40 30 20 10 ppm

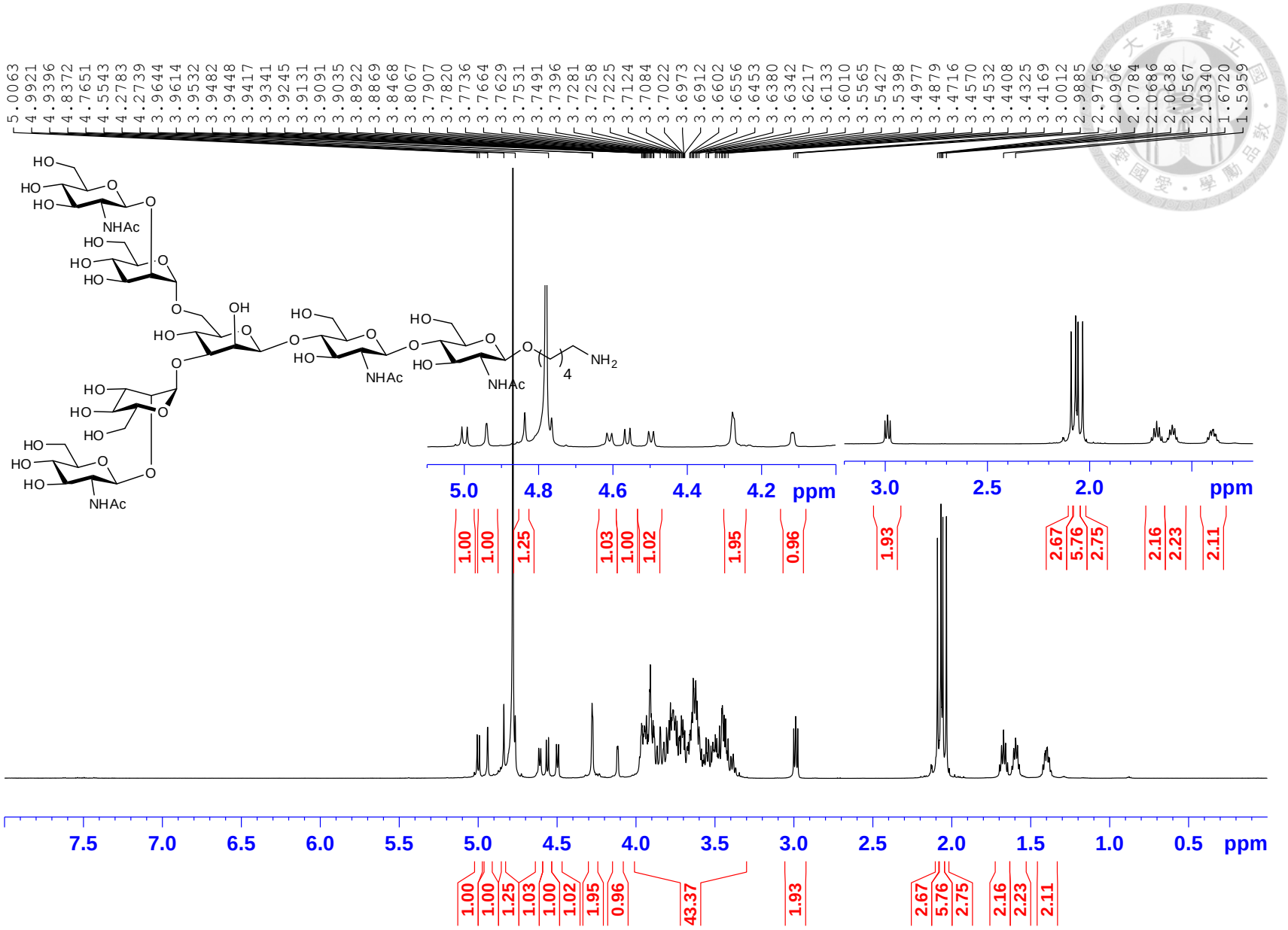
5.0063 4.9921 4.9396 4.8372 4.7651 4.5543 4.2783 4.2739 3.9644 3.9614 3.9532 3.9482 3.9448 3.9417 3.9341 3.9245 3.9131 3.9091 3.9035 3.8922 3.8869 3.8468 3.8067 3.7907 3.7820 3.7736 3.7664 3.7629 3.7531 3.7491 3.7396 3.7281 3.7258 3.7225 3.7124 3.7084 3.7022 3.6973 3.6912 3.6602 3.6556 3.6453 3.6380 3.6342 3.6217 3.6133 3.6010 3.5565 3.5427 3.5398 3.4977 3.4879 3.4716 3.4570 3.4532 3.4408 3.4325 3.4169 3.0012 2.9885 2.9756 2.0906 2.0784 2.0686 2.0638 2.0567 2.0340 1.6720 1.5959
HO
NHAc
OH
NH2
4
5.0 4.8 4.6 4.4 4.2 ppm
3.0 2.5 2.0 ppm
1.00 1.00 1.25 1.03 1.00 1.02 1.95 0.96 1.93 2.67 5.76 2.75 2.16 2.23 2.11
7.5 7.0 6.5 6.0 5.5 5.0 4.5 4.0 3.5 3.0 2.5 2.0 1.5 1.0 0.5 ppm
1.00 1.00 1.25 1.03 1.00 1.02 1.95 0.96 43.37 1.93 2.67 5.76 2.75 2.16 2.23 2.11

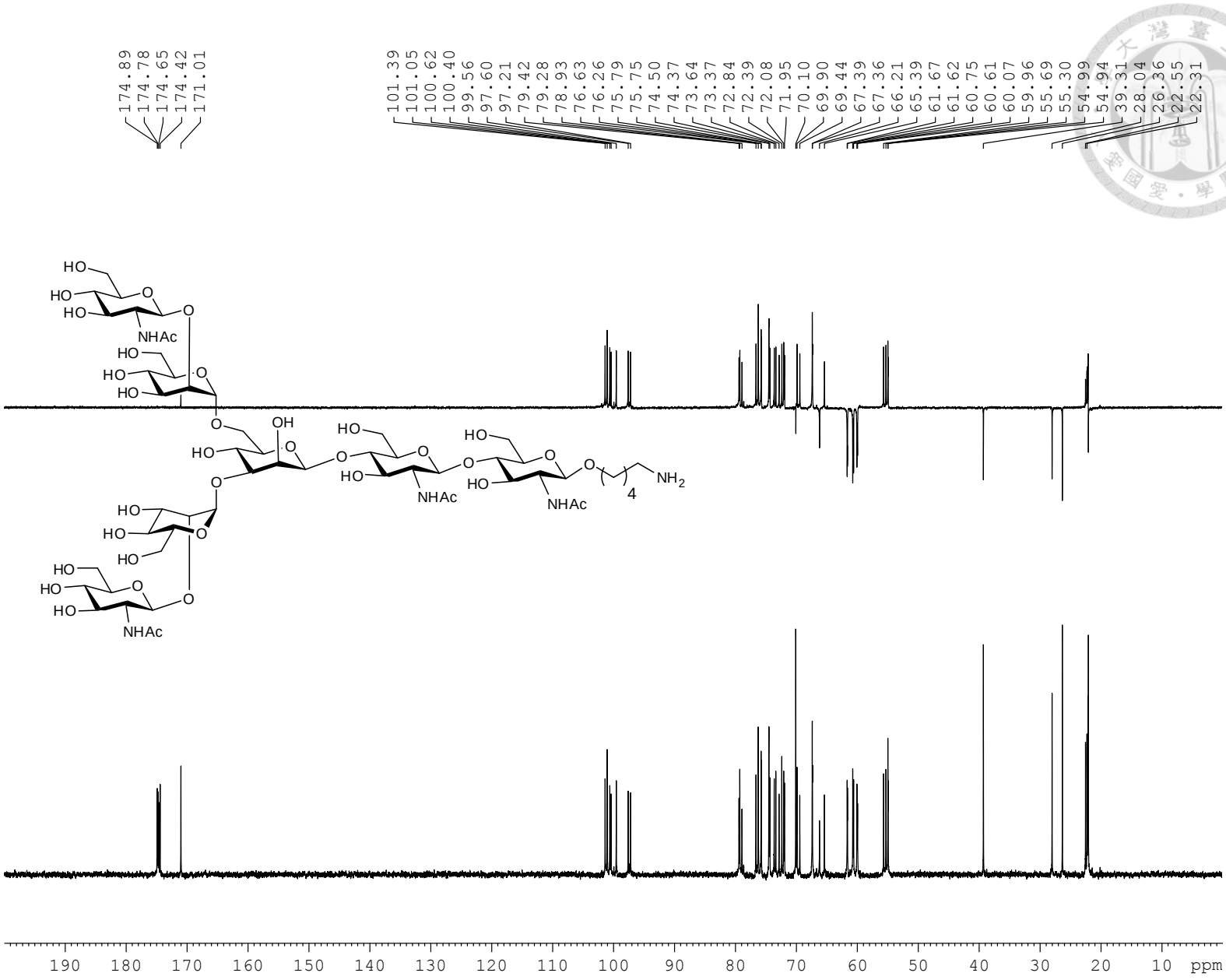
174.89
174.78
174.65
174.42
171.01
101.39
101.05
100.62
100.40
99.56
97.60
97.21
79.42
79.28
78.93
76.63
76.26
75.79
75.75
74.50
74.37
73.64
73.37
72.84
72.39
72.08
71.95
70.10
69.90
69.44
67.39
67.36
66.21
65.39
61.67
61.62
60.75
60.61
60.07
59.96
55.69
55.30
54.99
54.94
39.31
28.04
26.36
22.55
22.31
HO
O
NHAc
OH
NH2
4
190
180
170
160
150
140
130
120
110
100
90
80
70
60
50
40
30
20
10
ppm

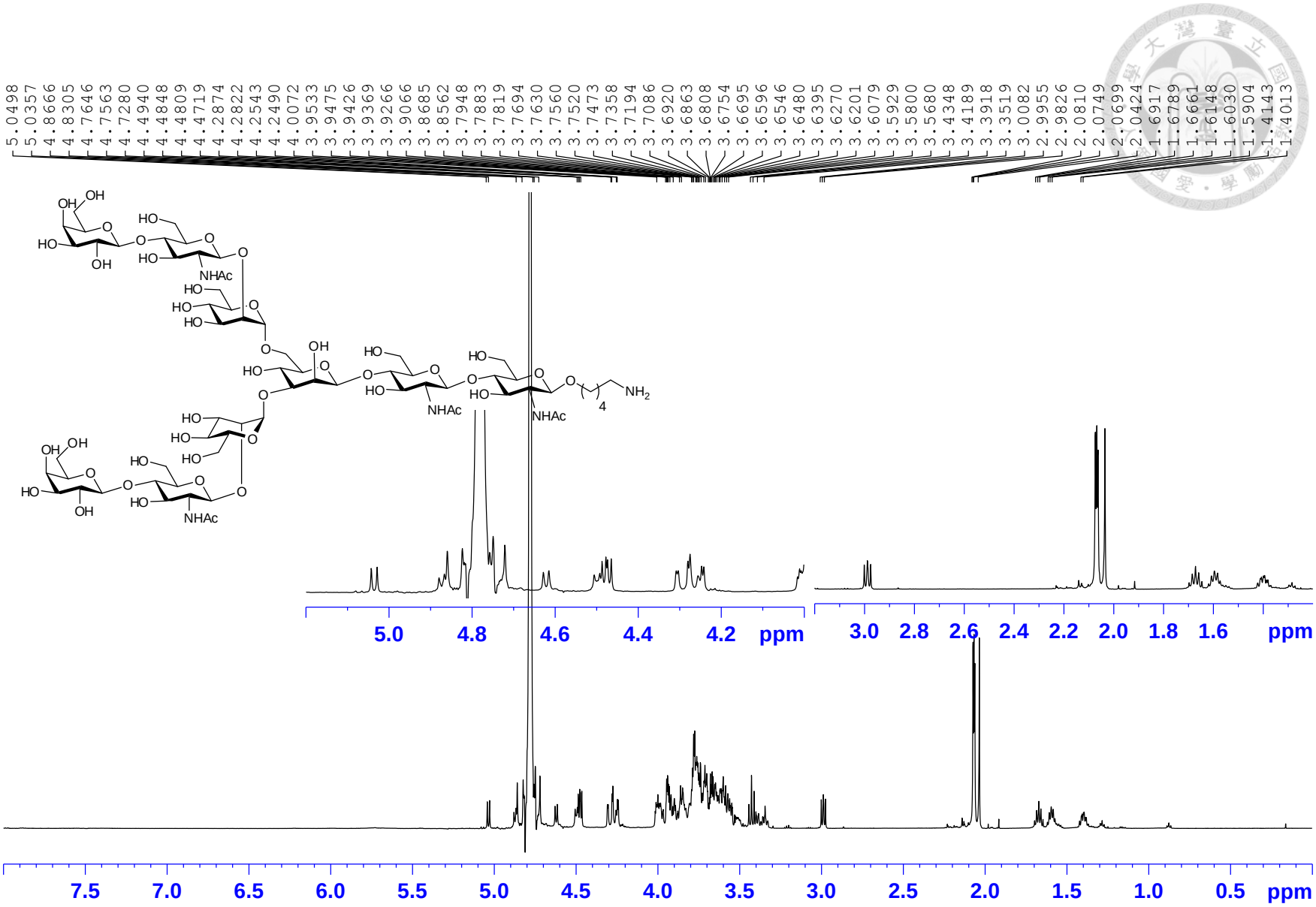
5.0498
5.0357
4.8666
4.8305
4.7646
4.7563
4.7280
4.4940
4.4848
4.4809
4.4719
4.2874
4.2822
4.2543
4.2490
4.0072
3.9533
3.9475
3.9426
3.9369
3.9266
3.9066
3.8685
3.8562
3.7948
3.7883
3.7819
3.7694
3.7630
3.7560
3.7520
3.7473
3.7358
3.7194
3.7086
3.6920
3.6863
3.6808
3.6754
3.6695
3.6596
3.6546
3.6480
3.6395
3.6270
3.6201
3.6079
3.5929
3.5800
3.5680
3.4348
3.4189
3.3918
3.3519
3.0082
2.9955
2.9826
2.0810
2.0749
2.0699
2.0424
1.6917
1.6789
1.6661
1.6148
1.6030
1.5904
1.4143
1.4013
NHAc
NHAc
NHAc
NH2
4
5.0
4.8
4.6
4.4
4.2
ppm
3.0
2.8
2.6
2.4
2.2
2.0
1.8
1.6
ppm
7.5
7.0
6.5
6.0
5.5
5.0
4.5
4.0
3.5
3.0
2.5
2.0
1.5
1.0
0.5
ppm

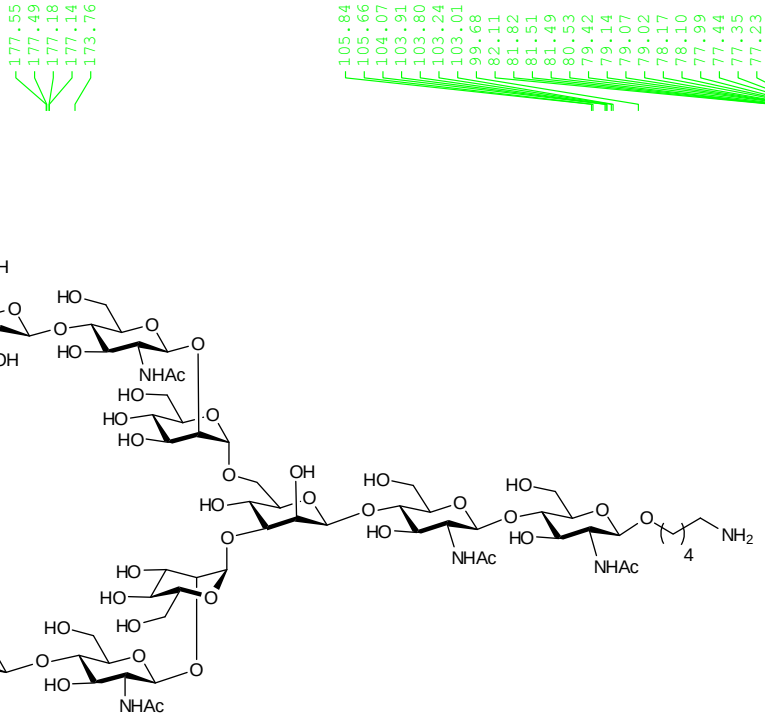

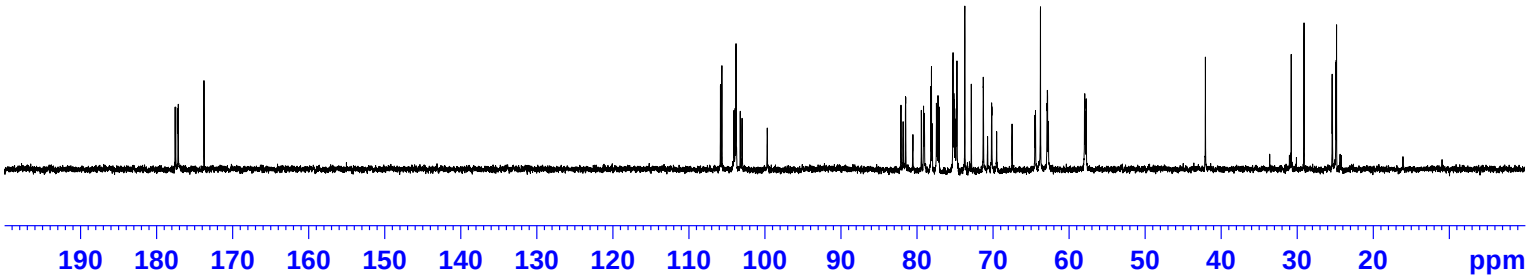
190
180
170
160
150
140
130
120
110
100
90
80
70
60
50
40
30
20
ppm

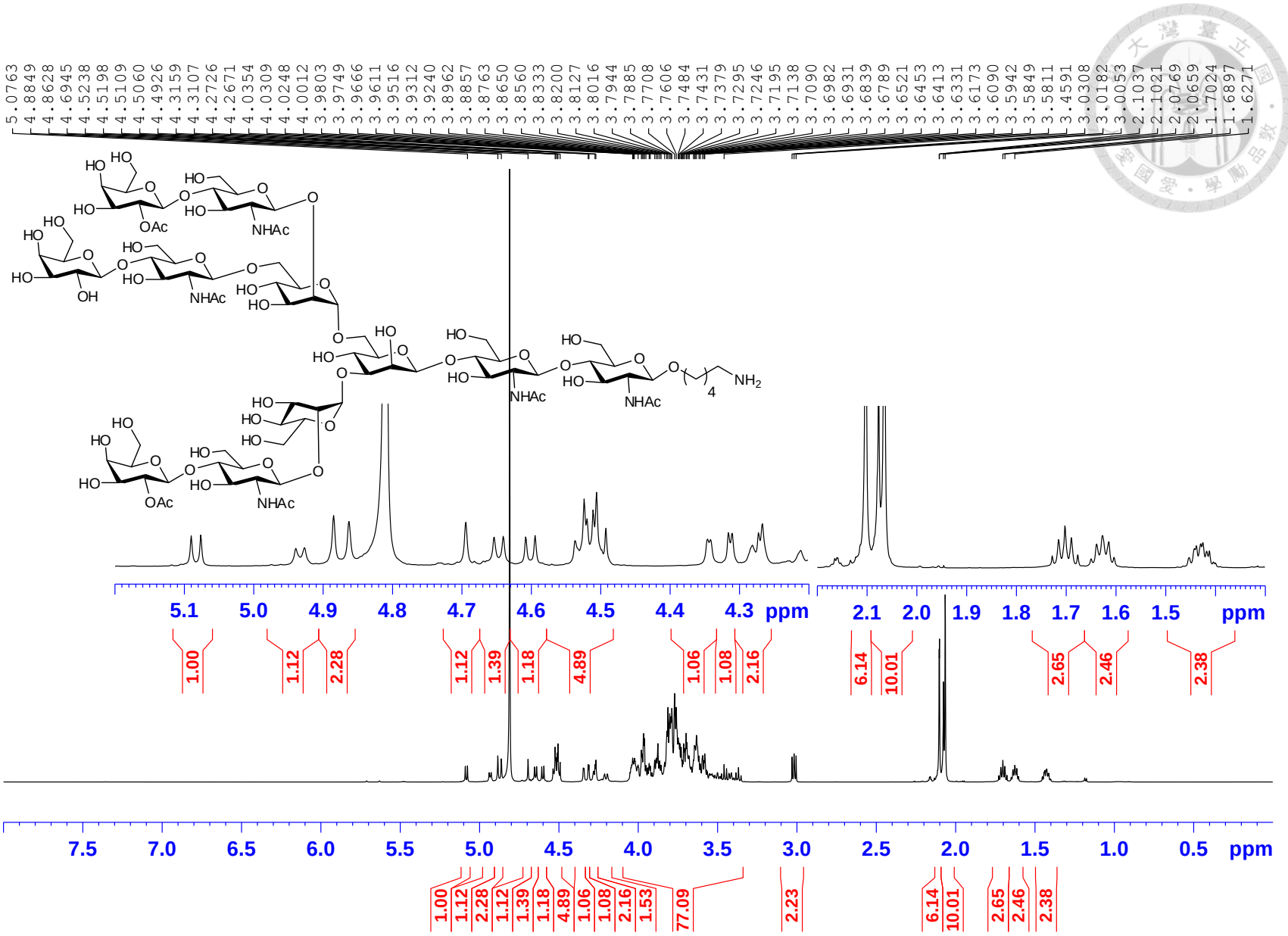
5.0763
4.8849
4.8628
4.6945
4.5238
4.5198
4.5109
4.5060
4.4926
4.3159
4.3107
4.2726
4.2671
4.0354
4.0309
4.0248
4.0012
3.9803
3.9749
3.9666
3.9611
3.9516
3.9312
3.9240
3.8962
3.8857
3.8763
3.8650
3.8560
3.8333
3.8200
3.8127
3.8016
3.7944
3.7885
3.7708
3.7606
3.7484
3.7431
3.7379
3.7295
3.7246
3.7195
3.7138
3.7090
3.6982
3.6931
3.6839
3.6789
3.6521
3.6453
3.6413
3.6331
3.6173
3.6090
3.5942
3.5849
3.5811
3.4591
3.0308
3.0182
3.0053
2.1037
2.1021
2.0769
2.0659
1.7024
1.6897
1.6271
5.1 5.0 4.9 4.8 4.7 4.6 4.5 4.4 4.3 ppm
2.1 2.0 1.9 1.8 1.7 1.6 1.5 ppm
1.00 1.12 2.28 1.12 1.39 1.18 4.89 1.06 1.08 2.16 6.14 10.01 2.65 2.46 2.38
7.5 7.0 6.5 6.0 5.5 5.0 4.5 4.0 3.5 3.0 2.5 2.0 1.5 1.0 0.5 ppm
1.00 1.12 2.28 1.12 1.39 1.18 4.89 1.06 1.08 2.16 1.53 77.09 2.23 6.14 10.01 2.65 2.46 2.38

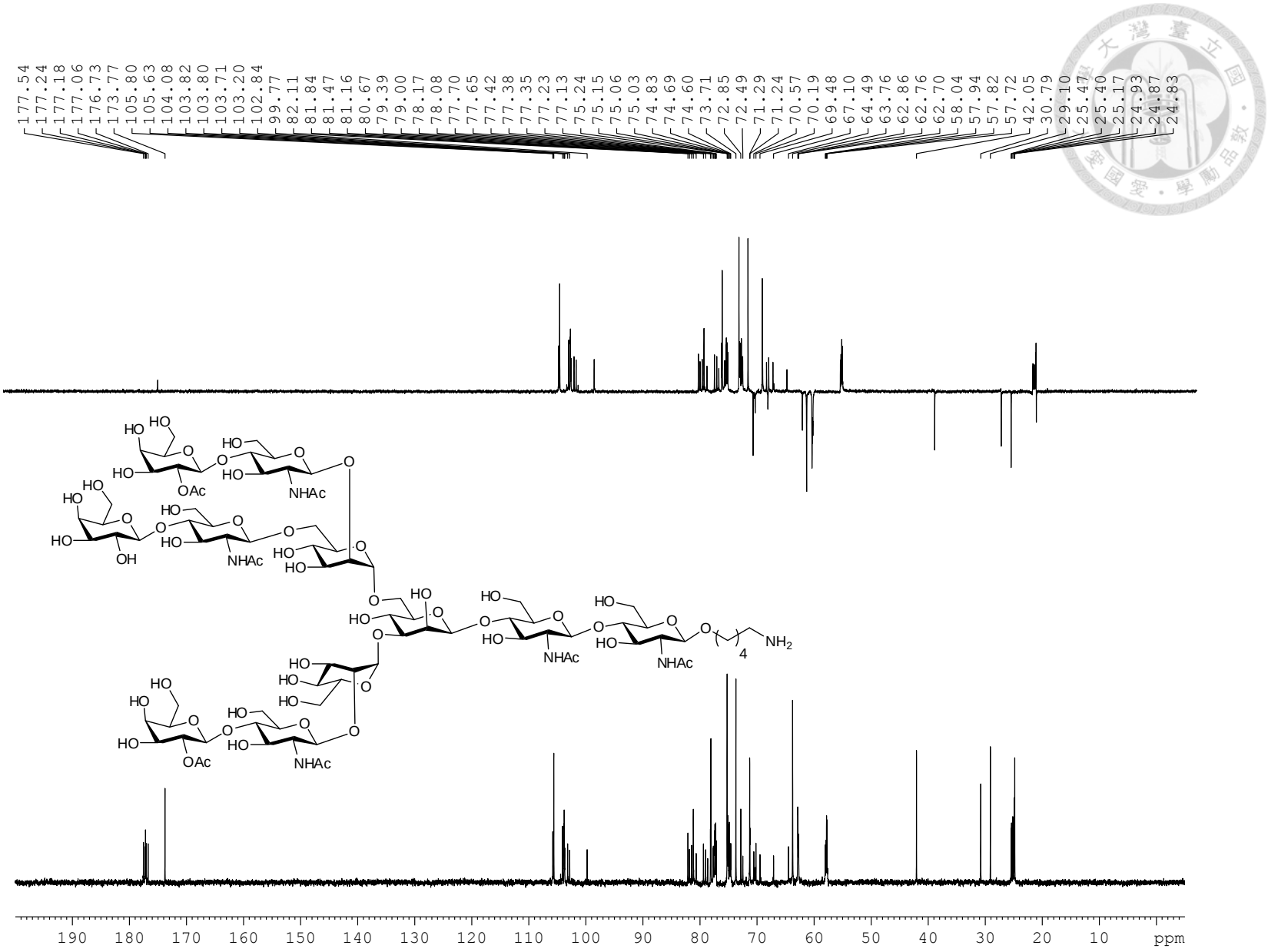
177.54
177.24
177.18
177.06
176.73
173.77
105.80
105.63
104.08
103.82
103.80
103.71
103.20
102.84
99.77
82.11
81.84
81.47
81.16
80.67
79.39
79.00
78.17
78.08
77.70
77.65
77.42
77.38
77.35
77.23
77.13
75.24
75.15
75.06
75.03
74.83
74.69
74.60
73.71
72.85
72.49
71.29
71.24
70.57
70.19
69.48
67.10
64.49
63.76
62.86
62.76
62.70
58.04
57.94
57.82
57.72
42.05
30.79
29.10
25.47
25.40
25.17
24.93
24.87
24.83
HO
OAc
NHAc
OH
NH2
4
O
190
180
170
160
150
140
130
120
110
100
90
80
70
60
50
40
30
20
10
ppm

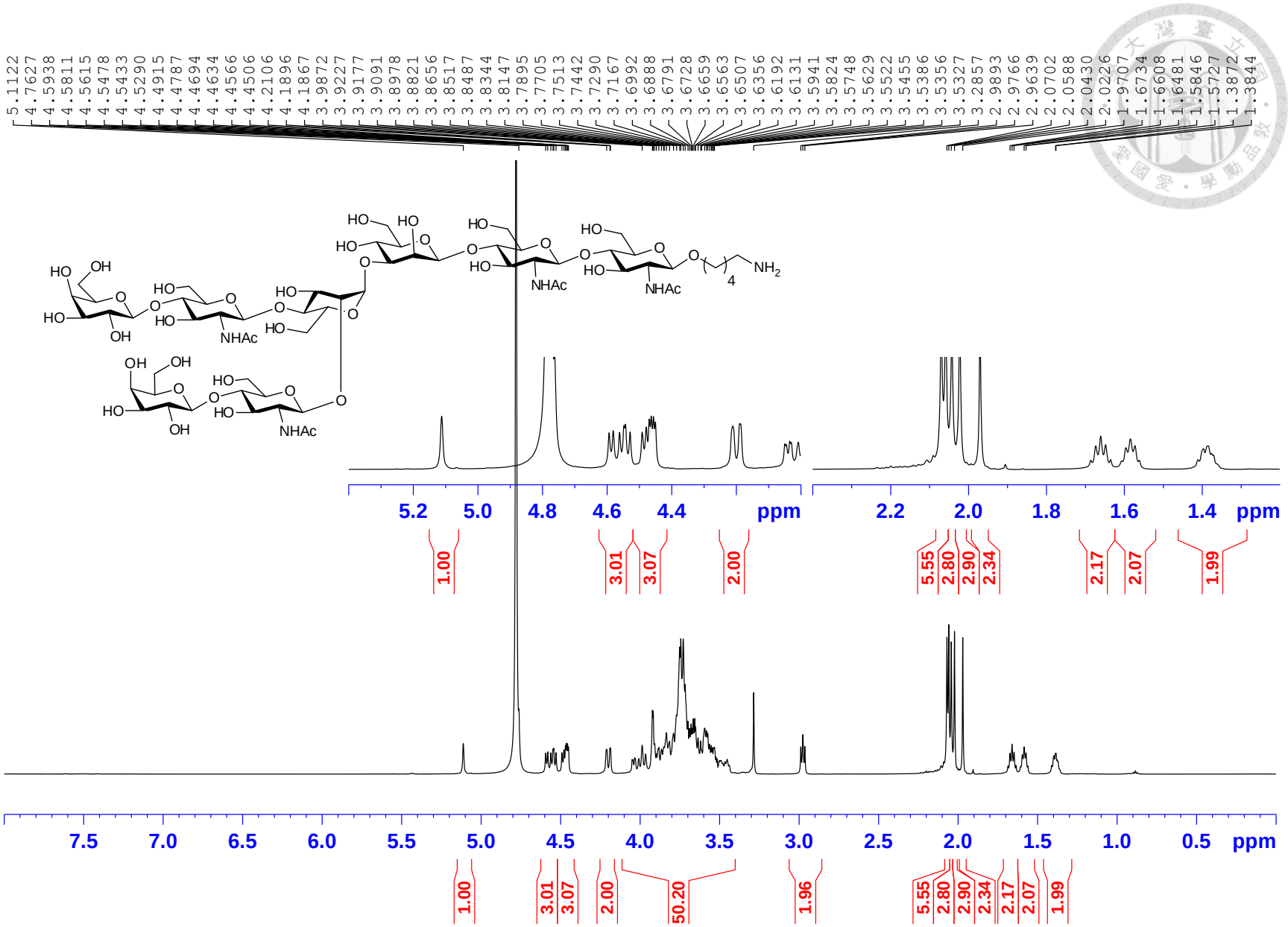
5.1122
4.7627
4.5938
4.5811
4.5615
4.5478
4.5433
4.5290
4.4915
4.4787
4.4694
4.4634
4.4566
4.4506
4.2106
4.1896
4.1867
3.9872
3.9227
3.9177
3.9091
3.8978
3.8821
3.8656
3.8517
3.8487
3.8344
3.8147
3.7895
3.7705
3.7513
3.7442
3.7290
3.7167
3.6992
3.6888
3.6791
3.6728
3.6659
3.6563
3.6507
3.6356
3.6192
3.6131
3.5941
3.5824
3.5748
3.5629
3.5522
3.5455
3.5386
3.5356
3.5327
3.2857
2.9893
2.9766
2.9639
2.0702
2.0588
2.0430
2.0226
1.9707
1.6734
1.6608
1.6481
1.5846
1.5727
1.3872
1.3844
NHAc
NHAc
NHAc
NHAc
NH2
4
5.2
5.0
4.8
4.6
4.4
ppm
2.2
2.0
1.8
1.6
1.4
ppm
1.00
3.01
3.07
2.00
5.55
2.80
2.90
2.34
2.17
2.07
1.99
7.5
7.0
6.5
6.0
5.5
5.0
4.5
4.0
3.5
3.0
2.5
2.0
1.5
1.0
0.5
ppm
1.00
3.01
3.07
2.00
50.20
1.96
5.55
2.80
2.90
2.34
2.17
2.07
1.99

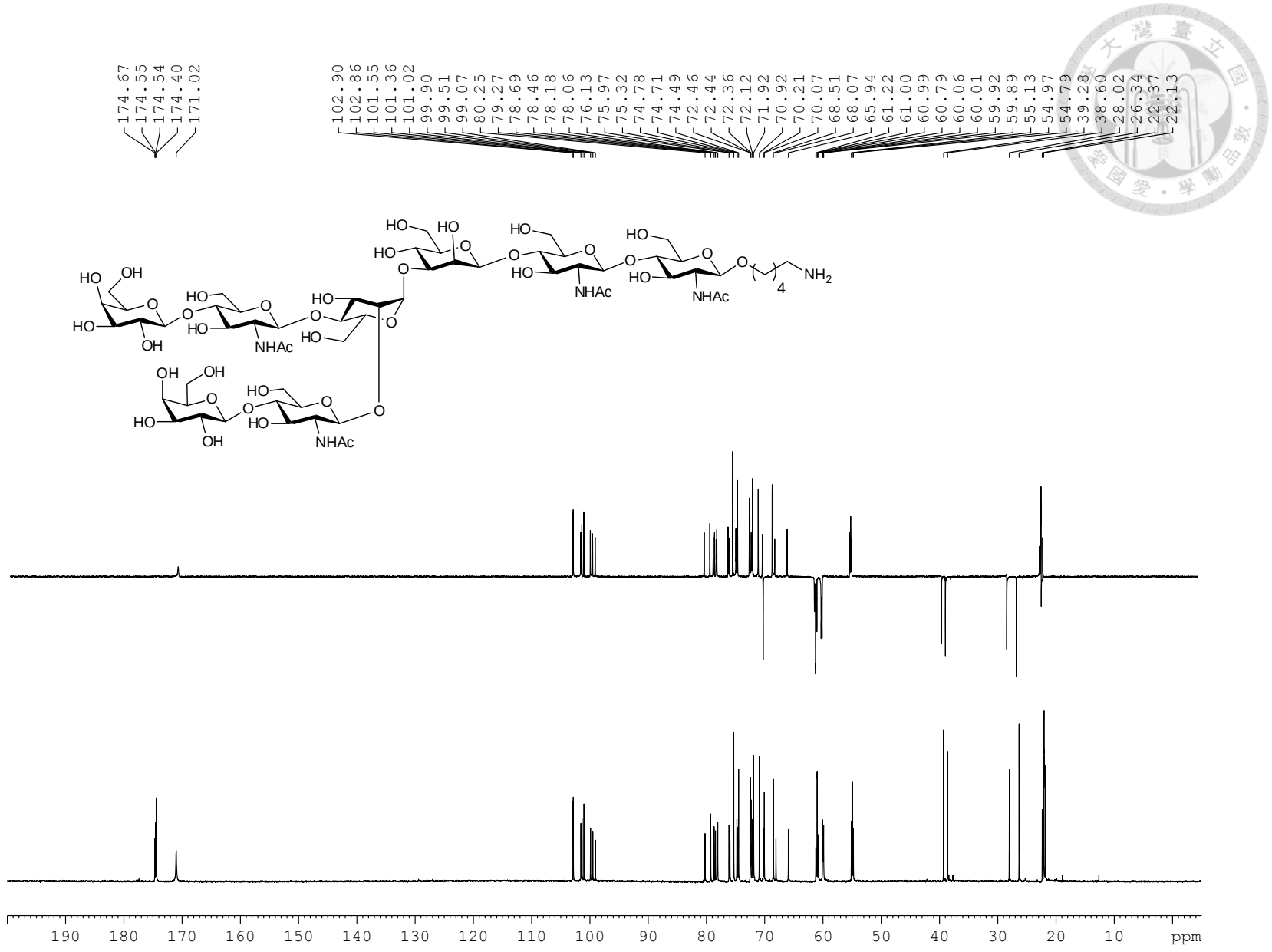
174.67
174.55
174.54
174.40
171.02
102.90
102.86
101.55
101.36
101.02
99.90
99.51
99.07
80.25
79.27
78.69
78.46
78.18
78.06
76.13
75.97
75.32
74.78
74.71
74.49
72.46
72.44
72.36
72.12
71.92
70.92
70.21
70.07
68.51
68.07
65.94
61.22
61.00
60.99
60.79
60.06
60.01
59.92
59.89
55.13
54.97
54.79
39.28
38.60
28.02
26.34
22.37
22.13
NHAc
NHAc
NHAc
NH2
4
190
180
170
160
150
140
130
120
110
100
90
80
70
60
50
40
30
20
10
ppm

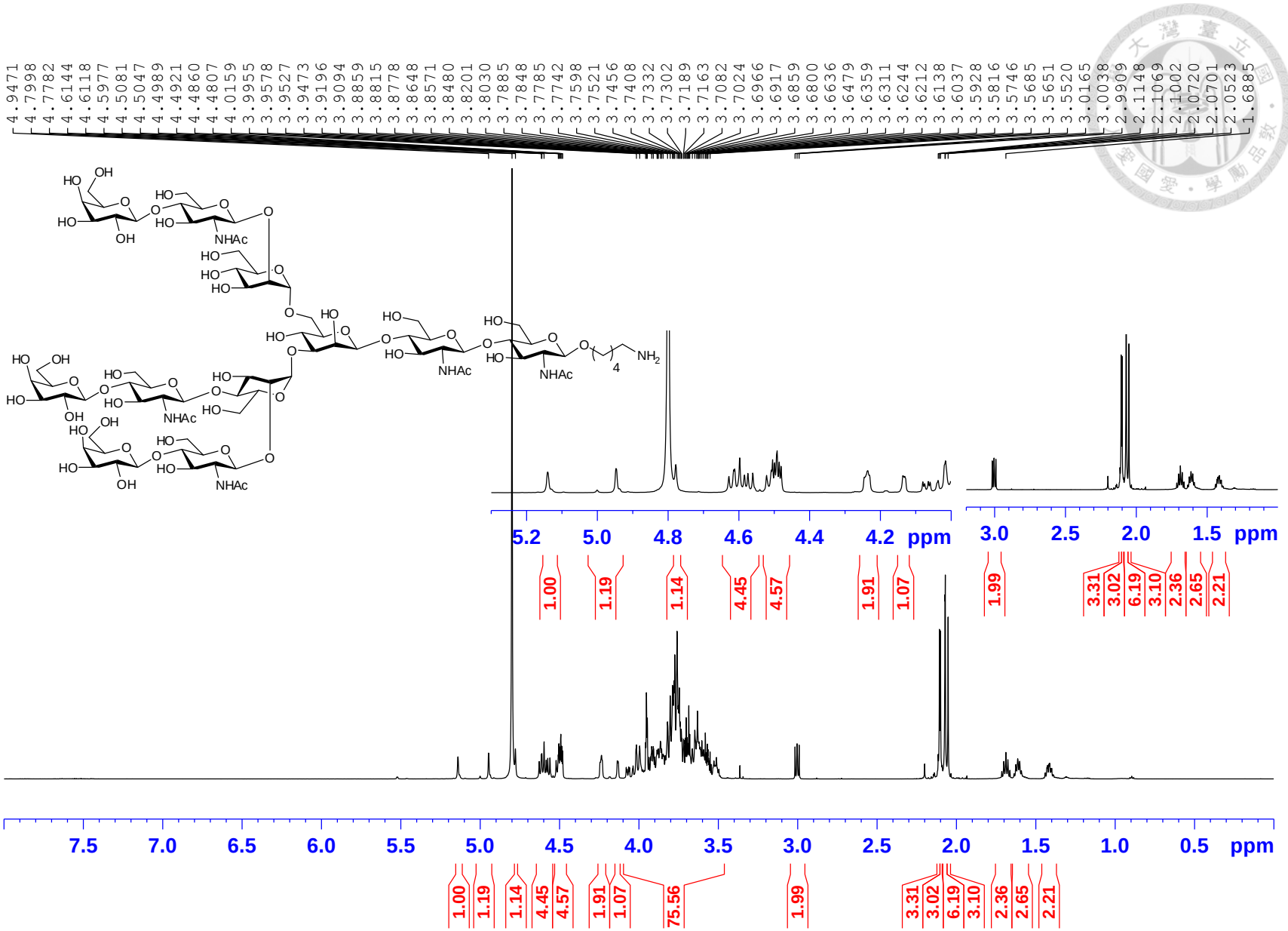
4.9471 4.7998 4.7782 4.6144 4.6118 4.5977 4.5081 4.5047 4.4989 4.4921 4.4860 4.4807 4.0159 3.9955 3.9578 3.9527 3.9473 3.9196 3.9094 3.8859 3.8815 3.8778 3.8648 3.8571 3.8480 3.8201 3.8030 3.7885 3.7848 3.7785 3.7742 3.7598 3.7521 3.7456 3.7408 3.7332 3.7302 3.7189 3.7163 3.7082 3.7024 3.6966 3.6917 3.6859 3.6800 3.6636 3.6479 3.6359 3.6311 3.6244 3.6212 3.6138 3.6037 3.5928 3.5816 3.5746 3.5685 3.5651 3.5520 3.0165 3.0038 2.9909 2.1148 2.1069 2.1002 2.0720 2.0701 2.0523 1.6885
NHAc
NHAc
NHAc
NHAc
NH2
4
5.2 5.0 4.8 4.6 4.4 4.2 ppm
3.0 2.5 2.0 1.5 ppm
1.00 1.19 1.14 4.45 4.57 1.91 1.07 1.99 3.31 3.02 6.19 3.10 2.36 2.65 2.21
7.5 7.0 6.5 6.0 5.5 5.0 4.5 4.0 3.5 3.0 2.5 2.0 1.5 1.0 0.5 ppm
1.00 1.19 1.14 4.45 4.57 1.91 1.07 75.56 1.99 3.31 3.02 6.19 3.10 2.36 2.65 2.21

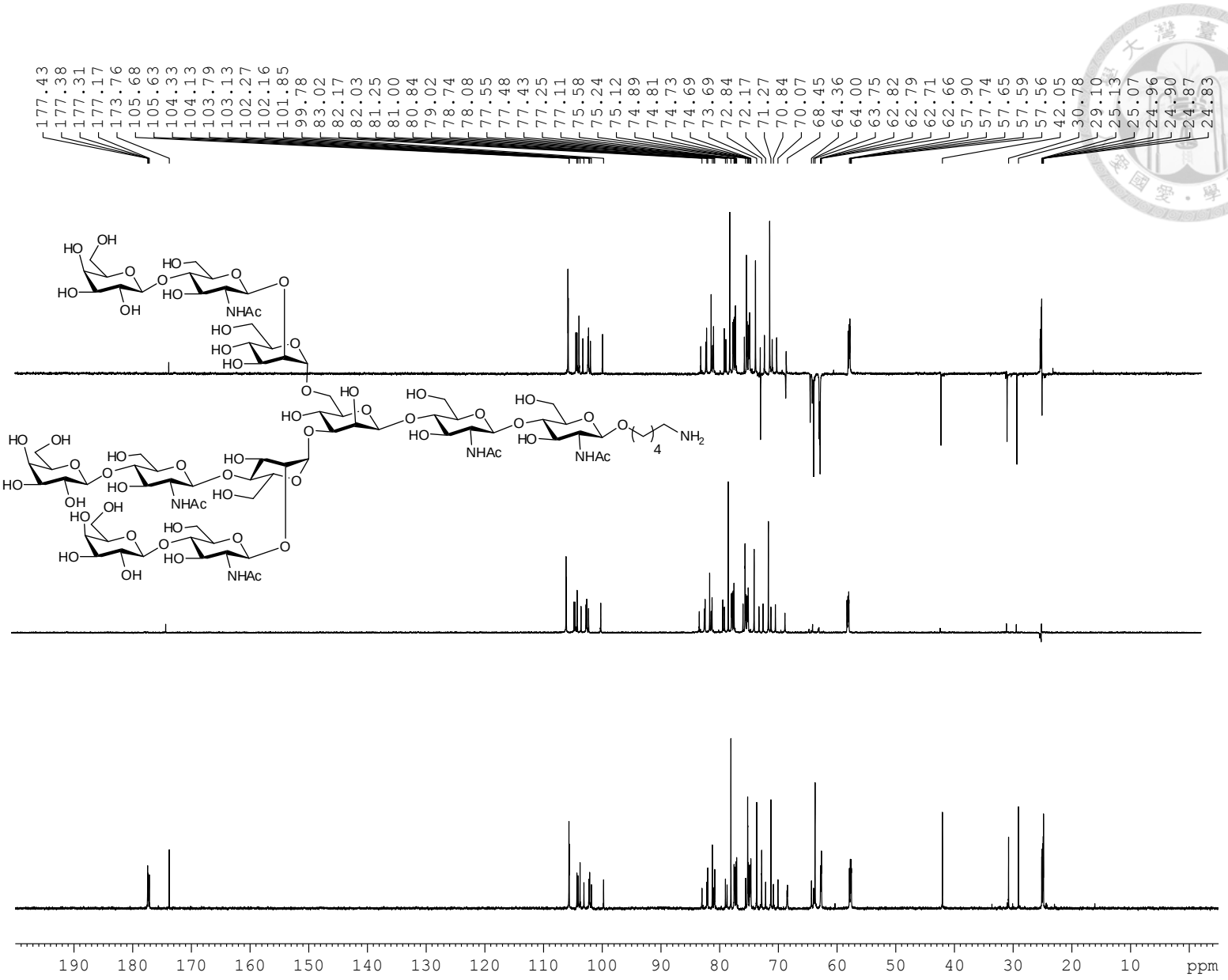
177.43
177.38
177.31
177.17
173.76
105.68
105.63
104.33
104.13
103.79
103.13
102.27
102.16
101.85
99.78
83.02
82.17
82.03
81.25
81.00
80.84
79.02
78.74
78.08
77.55
77.48
77.43
77.25
77.11
75.58
75.24
75.12
74.89
74.81
74.73
74.69
73.69
72.84
72.17
71.27
70.84
70.07
68.45
64.36
64.00
63.75
62.82
62.79
62.71
62.66
57.90
57.74
57.65
57.59
57.56
42.05
30.78
29.10
25.13
25.07
24.96
24.90
24.87
24.83
190
180
170
160
150
140
130
120
110
100
90
80
70
60
50
40
30
20
10
ppm

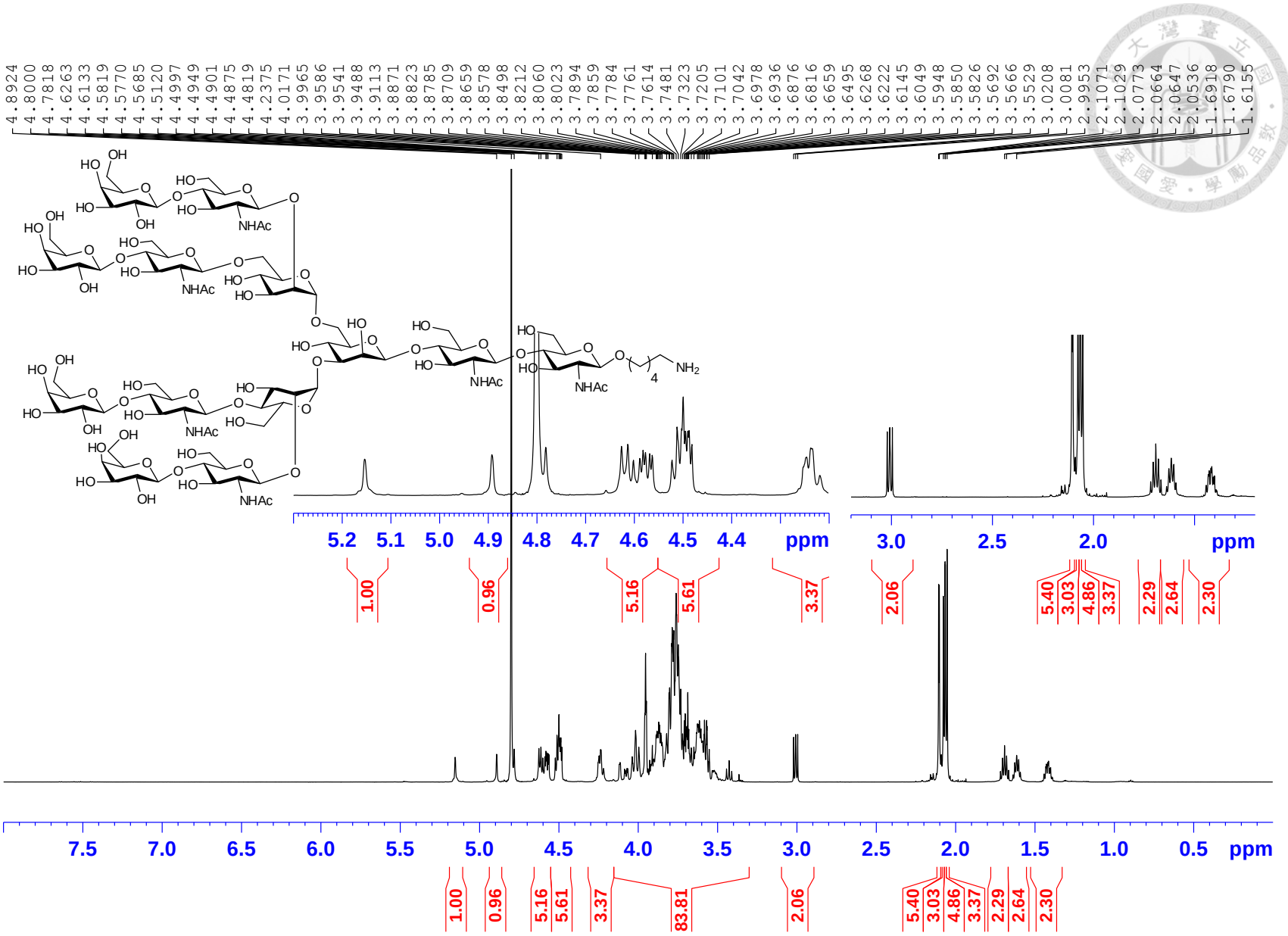
4.8924 4.8000 4.7818 4.6263 4.6133 4.5819 4.5770 4.5685 4.5120 4.4997 4.4949 4.4901 4.4875 4.4819 4.2375 4.0171 3.9965 3.9586 3.9541 3.9488 3.9113 3.8871 3.8823 3.8785 3.8709 3.8659 3.8578 3.8498 3.8212 3.8060 3.8023 3.7894 3.7859 3.7784 3.7761 3.7614 3.7481 3.7323 3.7205 3.7101 3.7042 3.6978 3.6936 3.6876 3.6816 3.6659 3.6495 3.6268 3.6222 3.6145 3.6049 3.5948 3.5850 3.5826 3.5692 3.5666 3.5529 3.0208 3.0081 2.9953 2.1071 2.1029 2.0773 2.0664 2.0647 2.0536 1.6918 1.6790 1.6155
5.2 5.1 5.0 4.9 4.8 4.7 4.6 4.5 4.4 ppm
3.0 2.5 2.0 ppm
1.00 0.96 5.16 5.61 3.37 2.06 5.40 3.03 4.86 3.37 2.29 2.64 2.30
7.5 7.0 6.5 6.0 5.5 5.0 4.5 4.0 3.5 3.0 2.5 2.0 1.5 1.0 0.5 ppm
1.00 0.96 5.16 5.61 3.37 83.81 2.06 5.40 3.03 4.86 3.37 2.29 2.64 2.30

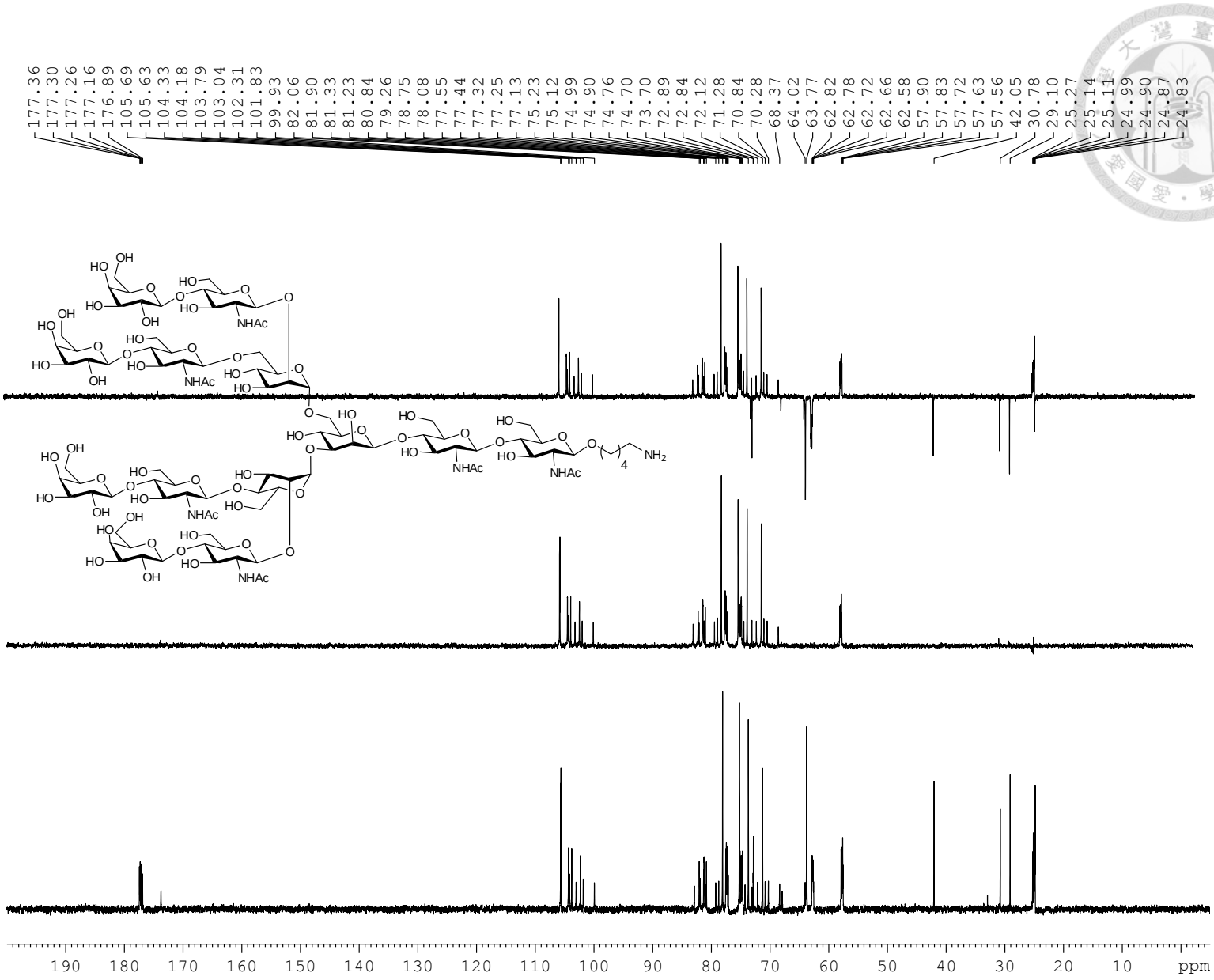
177.36
177.30
177.26
177.16
176.89
105.69
105.63
104.33
104.18
103.79
103.04
102.31
101.83
99.93
82.06
81.90
81.33
81.23
80.84
79.26
78.75
78.08
77.55
77.44
77.32
77.25
77.13
75.23
75.12
74.99
74.90
74.76
74.70
73.70
72.89
72.84
72.12
71.28
70.84
70.28
68.37
64.02
63.77
62.82
62.78
62.72
62.66
62.58
57.90
57.83
57.72
57.63
57.56
42.05
30.78
29.10
25.27
25.14
25.11
24.99
24.90
24.87
24.83
190
180
170
160
150
140
130
120
110
100
90
80
70
60
50
40
30
20
10
ppm

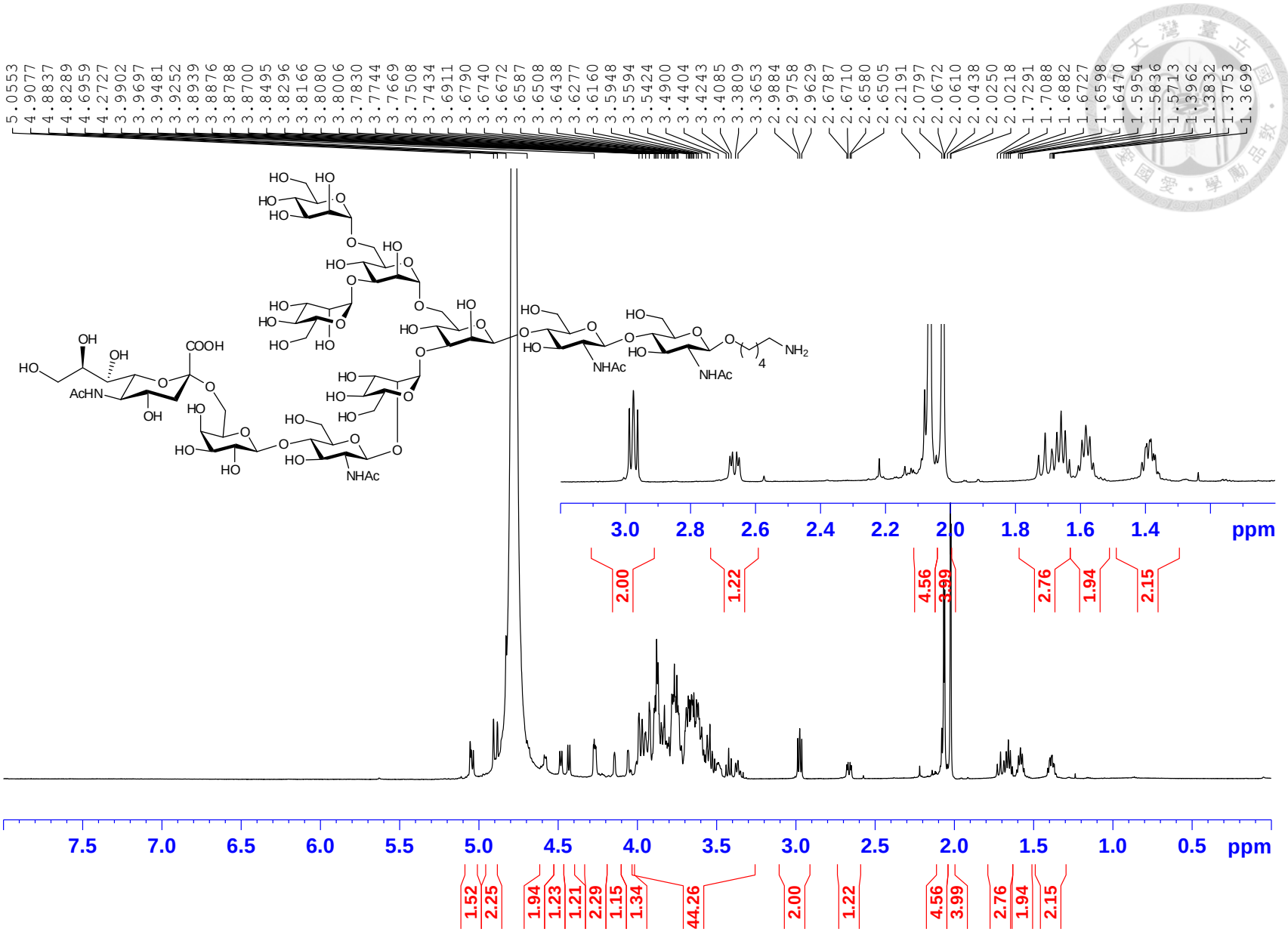
5.0553
4.9077
4.8837
4.8289
4.6959
4.2727
3.9902
3.9697
3.9481
3.9252
3.8939
3.8876
3.8788
3.8700
3.8495
3.8296
3.8166
3.8080
3.8006
3.7830
3.7744
3.7669
3.7508
3.7434
3.6911
3.6790
3.6740
3.6672
3.6587
3.6508
3.6438
3.6277
3.6160
3.5948
3.5594
3.5424
3.4900
3.4404
3.4243
3.4085
3.3809
3.3653
2.9884
2.9758
2.9629
2.6787
2.6710
2.6580
2.6505
2.2191
2.0797
2.0672
2.0610
2.0438
2.0250
2.0218
1.7291
1.7088
1.6882
1.6727
1.6598
1.6470
1.5954
1.5836
1.5713
1.3962
1.3832
1.3753
1.3699
3.0
2.8
2.6
2.4
2.2
2.0
1.8
1.6
1.4
ppm
2.00
1.22
4.56
3.99
2.76
1.94
2.15
7.5
7.0
6.5
6.0
5.5
5.0
4.5
4.0
3.5
3.0
2.5
2.0
1.5
1.0
0.5
ppm
1.52
2.25
1.94
1.23
1.21
2.29
1.15
1.34
44.26
2.00
1.22
4.56
3.99
2.76
1.94
2.15

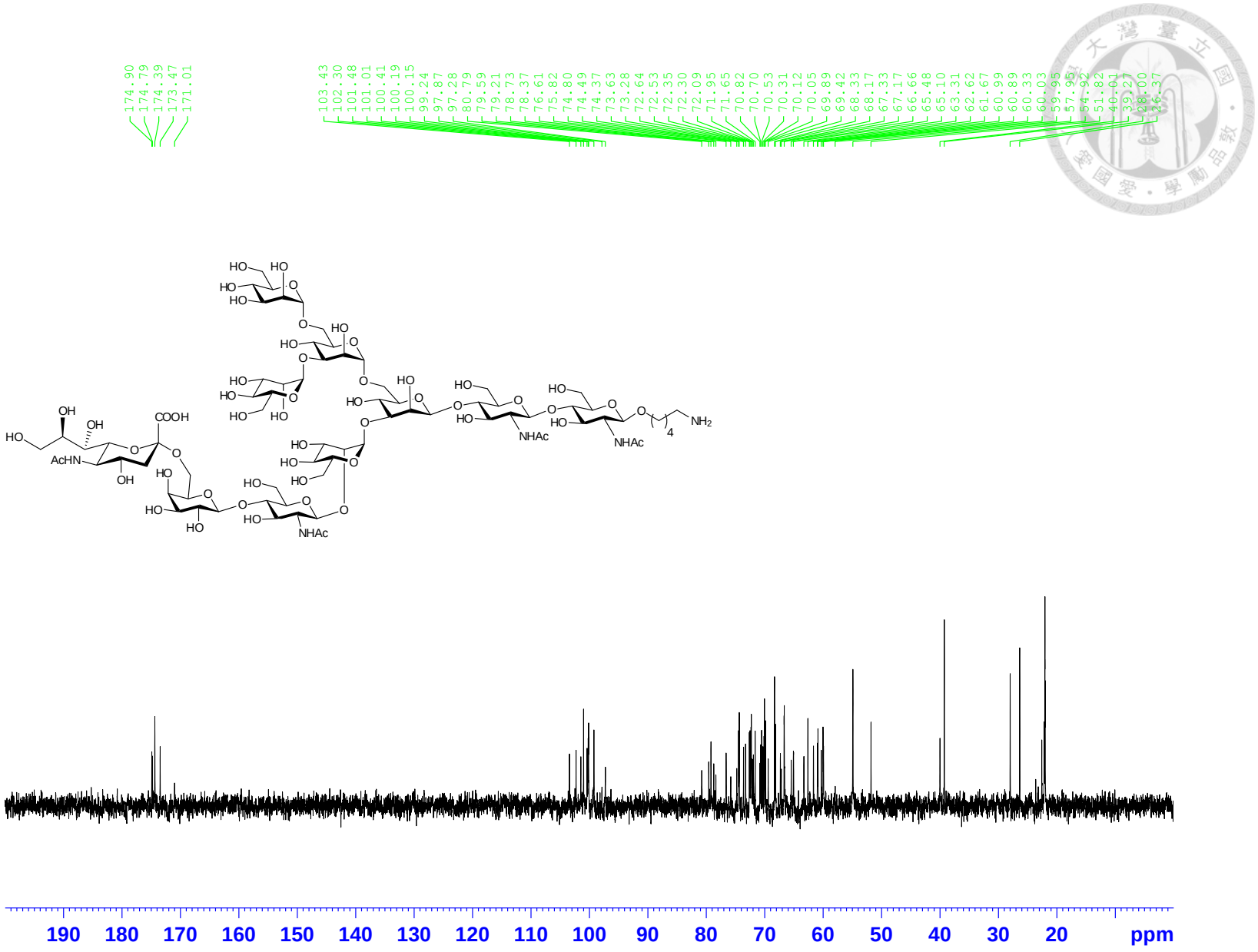
174.90
174.79
174.39
173.47
171.01
103.43
102.30
101.48
101.01
100.41
100.19
100.15
99.24
97.87
97.28
80.79
79.59
79.21
78.73
78.37
76.61
75.82
74.80
74.49
74.37
73.63
73.28
72.64
72.53
72.35
72.30
72.09
71.95
71.65
70.82
70.70
70.53
70.31
70.12
70.05
69.89
69.42
68.33
68.17
67.33
67.17
66.66
65.48
65.10
63.31
62.62
61.67
60.99
60.89
60.33
60.03
59.95
57.95
54.92
51.82
40.01
39.27
28.00
26.37
HO
OH
AcHN
COOH
NHAc
NH2
4
190
180
170
160
150
140
130
120
110
100
90
80
70
60
50
40
30
20
ppm

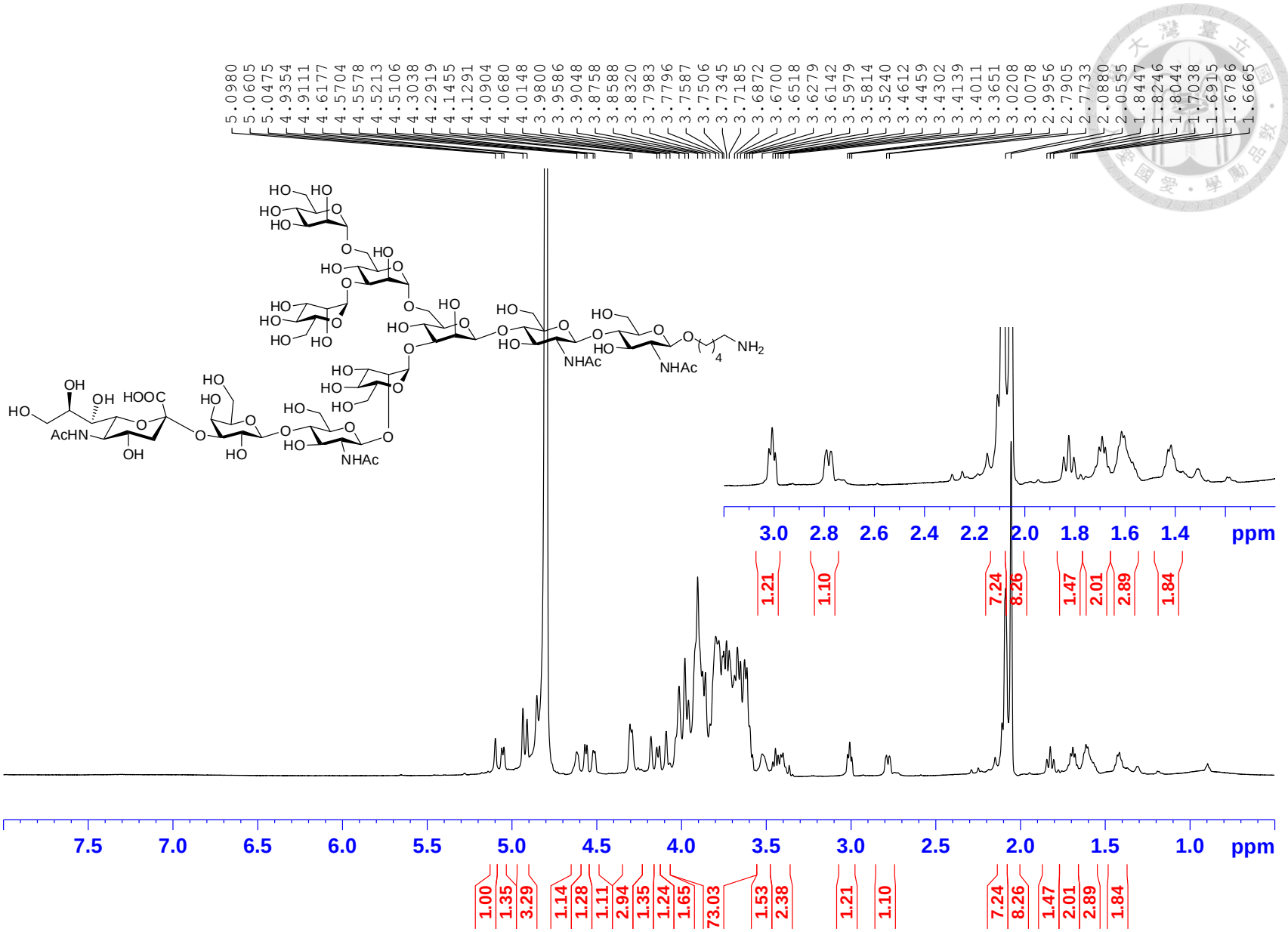
5.0980
5.0605
5.0475
4.9354
4.9111
4.6177
4.5704
4.5578
4.5213
4.5106
4.3038
4.2919
4.1455
4.1291
4.0904
4.0680
4.0148
3.9800
3.9586
3.9048
3.8758
3.8588
3.8320
3.7983
3.7796
3.7587
3.7506
3.7345
3.7185
3.6872
3.6700
3.6518
3.6279
3.6142
3.5979
3.5814
3.5240
3.4612
3.4459
3.4302
3.4139
3.4011
3.3651
3.0208
3.0078
2.9956
2.7905
2.7733
2.0880
2.0555
1.8447
1.8246
1.8044
1.7038
1.6915
1.6786
1.6665
HO
HOOC
AcHN
NHAc
NH2
3.0 2.8 2.6 2.4 2.2 2.0 1.8 1.6 1.4 ppm
1.21 1.10 7.24 8.26 1.47 2.01 2.89 1.84
7.5 7.0 6.5 6.0 5.5 5.0 4.5 4.0 3.5 3.0 2.5 2.0 1.5 1.0 ppm
1.00 1.35 3.29 1.14 1.28 1.11 2.94 1.35 1.24 1.65 73.03 1.53 2.38 1.21 1.10 7.24 8.26 1.47 2.01 2.89 1.84

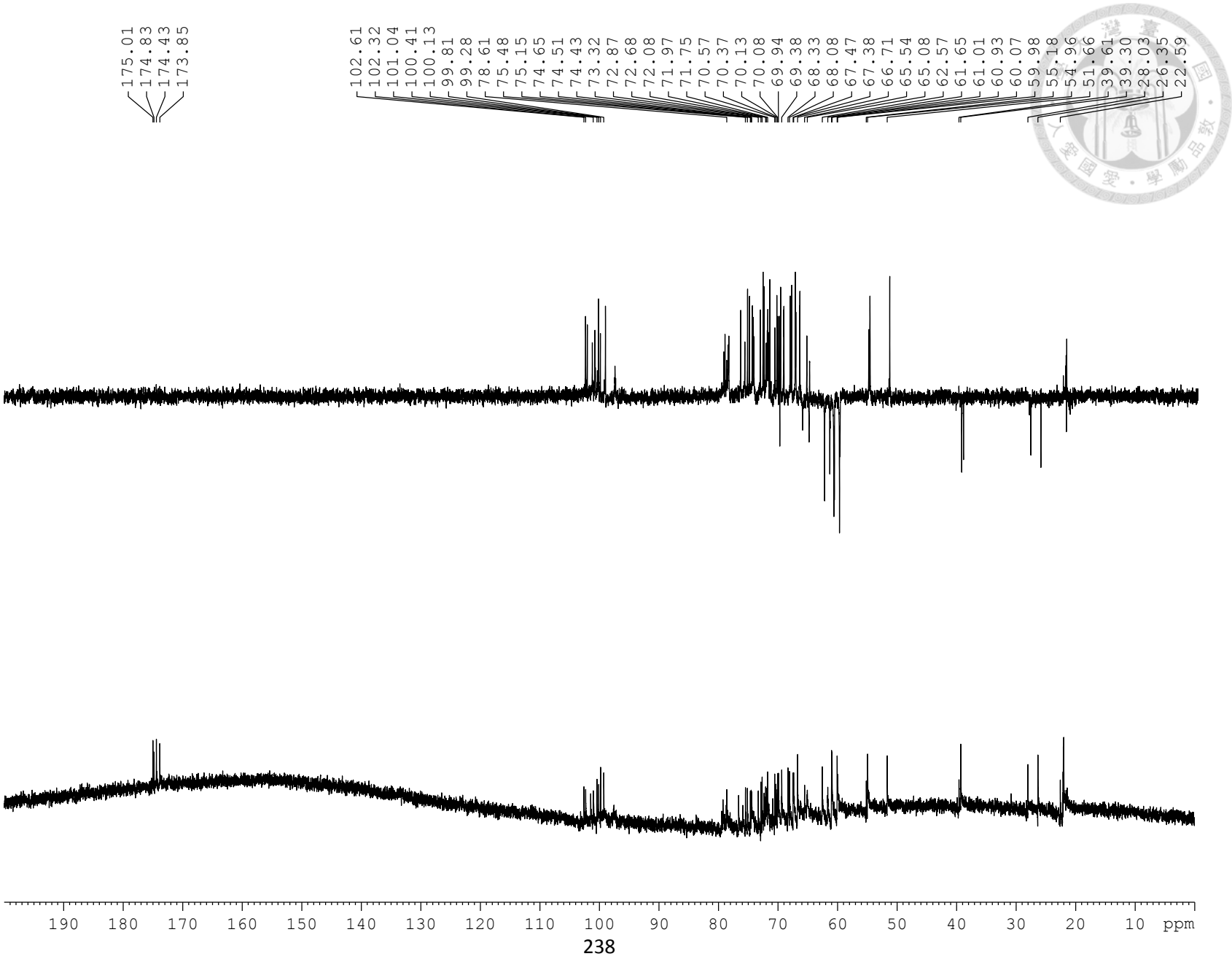
175.01
174.83
174.43
173.85
102.61
102.32
101.04
100.41
100.13
99.81
99.28
78.61
75.48
75.15
74.65
74.51
74.43
73.32
72.87
72.68
72.08
71.97
71.75
70.57
70.37
70.13
70.08
69.94
69.38
68.33
68.08
67.47
67.38
66.71
65.54
65.08
62.57
61.65
61.01
60.93
60.07
59.98
55.18
54.96
51.66
39.61
39.30
28.03
26.35
22.59
190 180 170 160 150 140 130 120 110 100 90 80 70 60 50 40 30 20 10 ppm

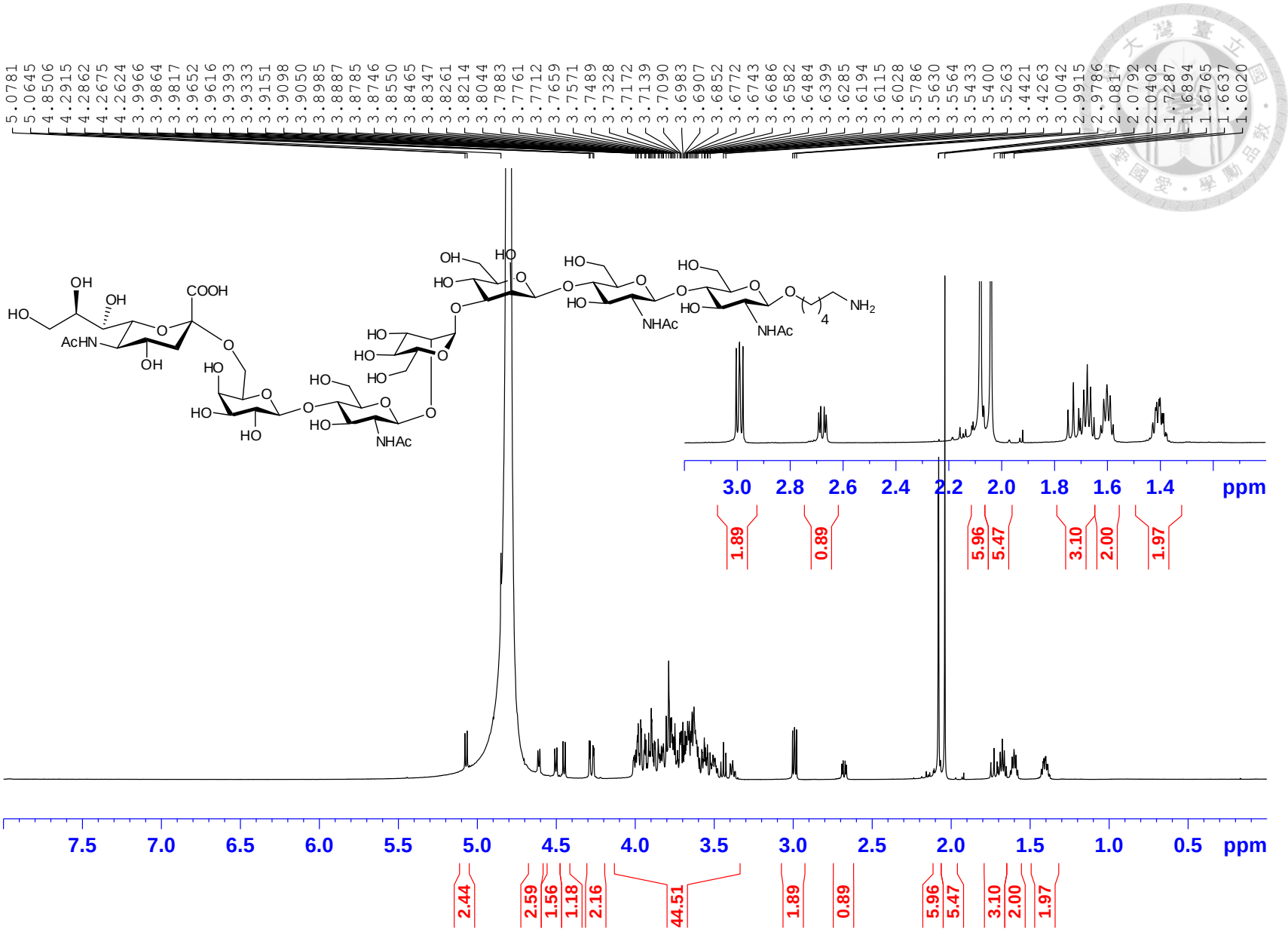
5.0781
5.0645
4.8506
4.2915
4.2862
4.2675
4.2624
3.9966
3.9864
3.9817
3.9652
3.9616
3.9393
3.9333
3.9151
3.9098
3.9050
3.8985
3.8887
3.8785
3.8746
3.8550
3.8465
3.8347
3.8261
3.8214
3.8044
3.7883
3.7761
3.7712
3.7659
3.7571
3.7489
3.7328
3.7172
3.7139
3.7090
3.6983
3.6907
3.6852
3.6772
3.6743
3.6686
3.6582
3.6484
3.6399
3.6285
3.6194
3.6115
3.6028
3.5786
3.5630
3.5564
3.5433
3.5400
3.5263
3.4421
3.4263
3.0042
2.9915
2.9786
2.0817
2.0792
2.0402
1.7287
1.6894
1.6765
1.6637
1.6020
OH
HO
OH
COOH
AcHN
OH
O
HO
HO
HO
HO
HO
HO
HO
HO
HO
HO
HO
HO
HO
HO
HO
NHAc
NHAc
NHAc
NH2
4
3.0
2.8
2.6
2.4
2.2
2.0
1.8
1.6
1.4
ppm
1.89
0.89
5.96
5.47
3.10
2.00
1.97
7.5
7.0
6.5
6.0
5.5
5.0
4.5
4.0
3.5
3.0
2.5
2.0
1.5
1.0
0.5
ppm
2.44
2.59
1.56
1.18
2.16
44.51
1.89
0.89
5.96
5.47
3.10
2.00
1.97

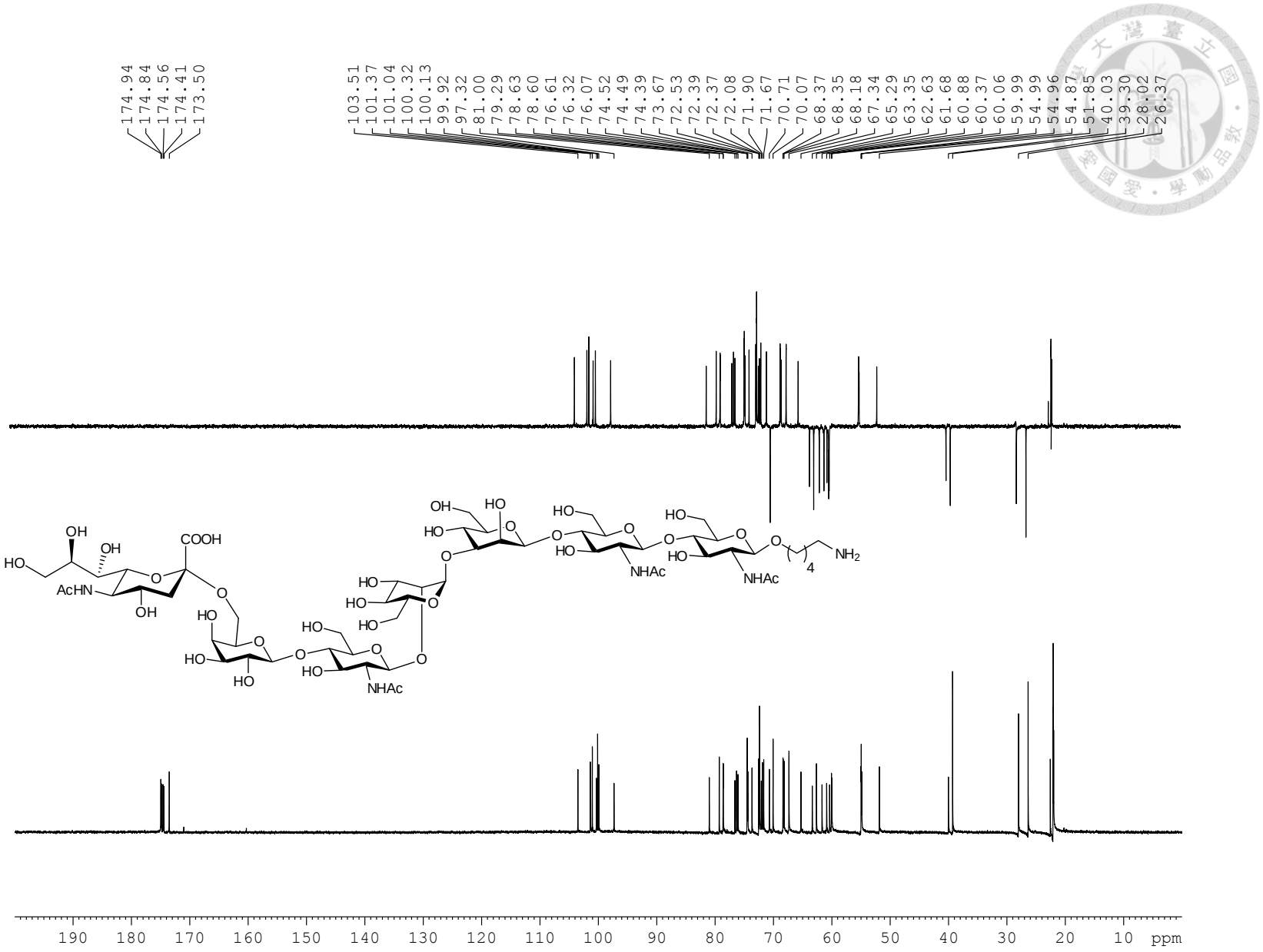
174.94
174.84
174.56
174.41
173.50
103.51
101.37
101.04
100.32
100.13
99.92
97.32
81.00
79.29
78.63
78.60
76.61
76.32
76.07
74.52
74.49
74.39
73.67
72.53
72.39
72.37
72.08
71.90
71.67
70.71
70.07
68.37
68.35
68.18
67.34
65.29
63.35
62.63
61.68
60.88
60.37
60.06
59.99
54.96
54.87
51.85
40.03
39.30
28.02
26.37
190
180
170
160
150
140
130
120
110
100
90
80
70
60
50
40
30
20
10
ppm

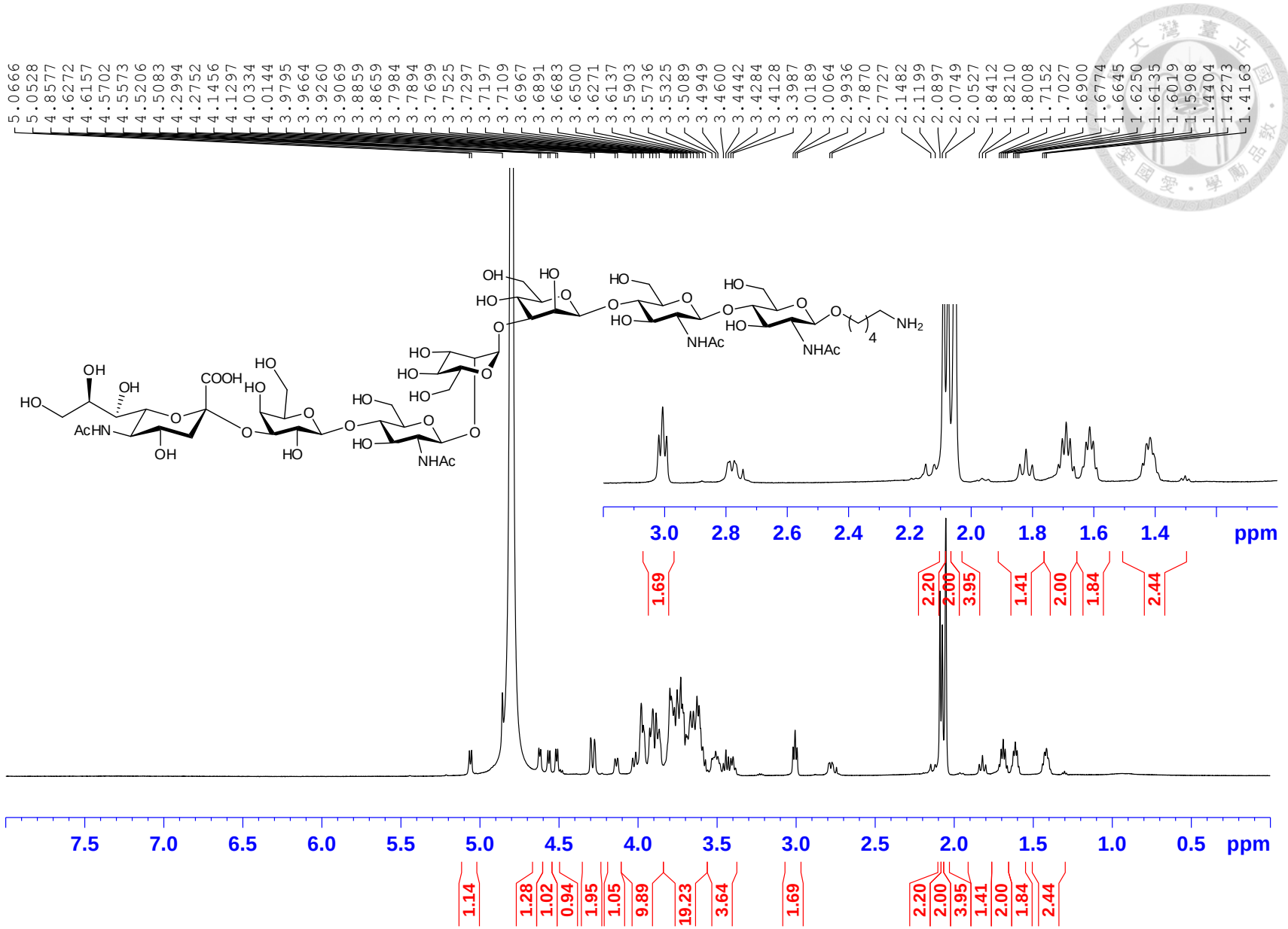
5.0666
5.0528
4.8577
4.6272
4.6157
4.5702
4.5573
4.5206
4.5083
4.2994
4.2752
4.1456
4.1297
4.0334
4.0144
3.9795
3.9664
3.9260
3.9069
3.8859
3.8659
3.7984
3.7894
3.7699
3.7525
3.7297
3.7197
3.7109
3.6967
3.6891
3.6683
3.6500
3.6271
3.6137
3.5903
3.5736
3.5325
3.5089
3.4949
3.4600
3.4442
3.4284
3.4128
3.3987
3.0189
3.0064
2.9936
2.7870
2.7727
2.1482
2.1199
2.0897
2.0749
2.0527
1.8412
1.8210
1.8008
1.7152
1.7027
1.6900
1.6774
1.6645
1.6250
1.6135
1.6019
1.5908
1.4404
1.4273
1.4163
3.0
2.8
2.6
2.4
2.2
2.0
1.8
1.6
1.4
ppm
1.69
2.20
2.00
3.95
1.41
2.00
1.84
2.44
7.5
7.0
6.5
6.0
5.5
5.0
4.5
4.0
3.5
3.0
2.5
2.0
1.5
1.0
0.5
ppm
1.14
1.28
1.02
0.94
1.95
1.05
9.89
19.23
3.64
1.69
2.20
2.00
3.95
1.41
2.00
1.84
2.44

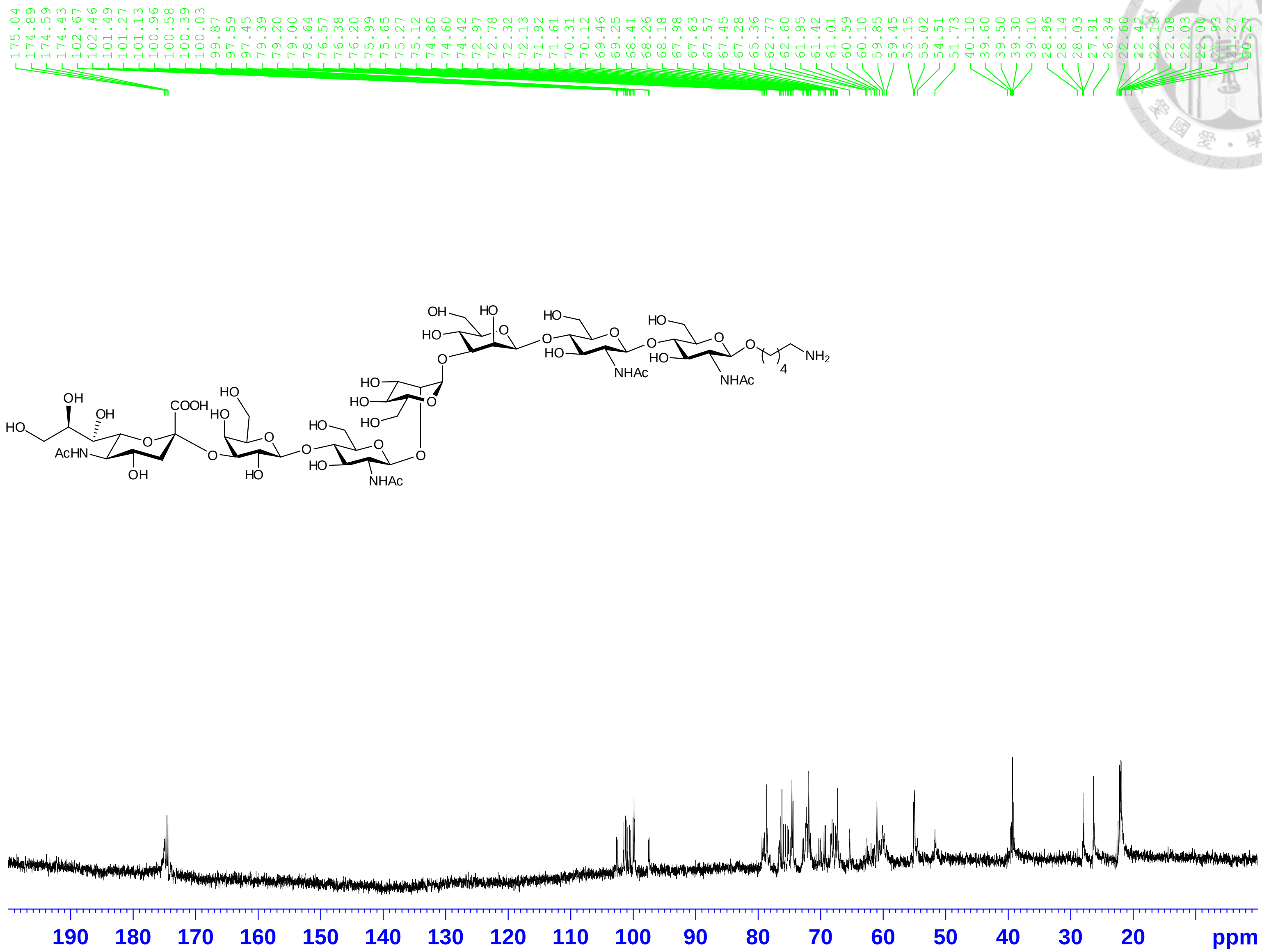
175.04
174.89
174.59
174.43
102.67
102.46
101.49
101.27
101.13
100.96
100.58
100.39
100.03
99.87
97.59
97.45
79.39
79.20
79.00
78.64
76.57
76.38
76.20
75.99
75.65
75.27
75.12
74.80
74.60
74.42
72.97
72.78
72.32
72.13
71.92
71.61
70.31
70.12
69.46
69.25
68.41
68.26
68.18
67.98
67.63
67.57
67.45
67.28
65.36
62.77
62.60
61.95
61.42
61.01
60.59
60.10
59.85
59.45
55.15
55.02
54.51
51.73
40.10
39.60
39.50
39.30
39.10
28.96
28.14
28.03
27.91
26.34
22.60
22.42
22.19
22.08
22.03
22.00
21.93
21.27
20.27
OH
HO
HO
O
HO
O
HO
O
HO
O
O
NH2
HO
HO
NHAc
NHAc
4
HO
HO
O
HO
OH
COOH
HO
HO
OH
O
HO
HO
O
O
O
AcHN
O
O
HO
O
OH
HO
NHAc
190
180
170
160
150
140
130
120
110
100
90
80
70
60
50
40
30
20
ppm

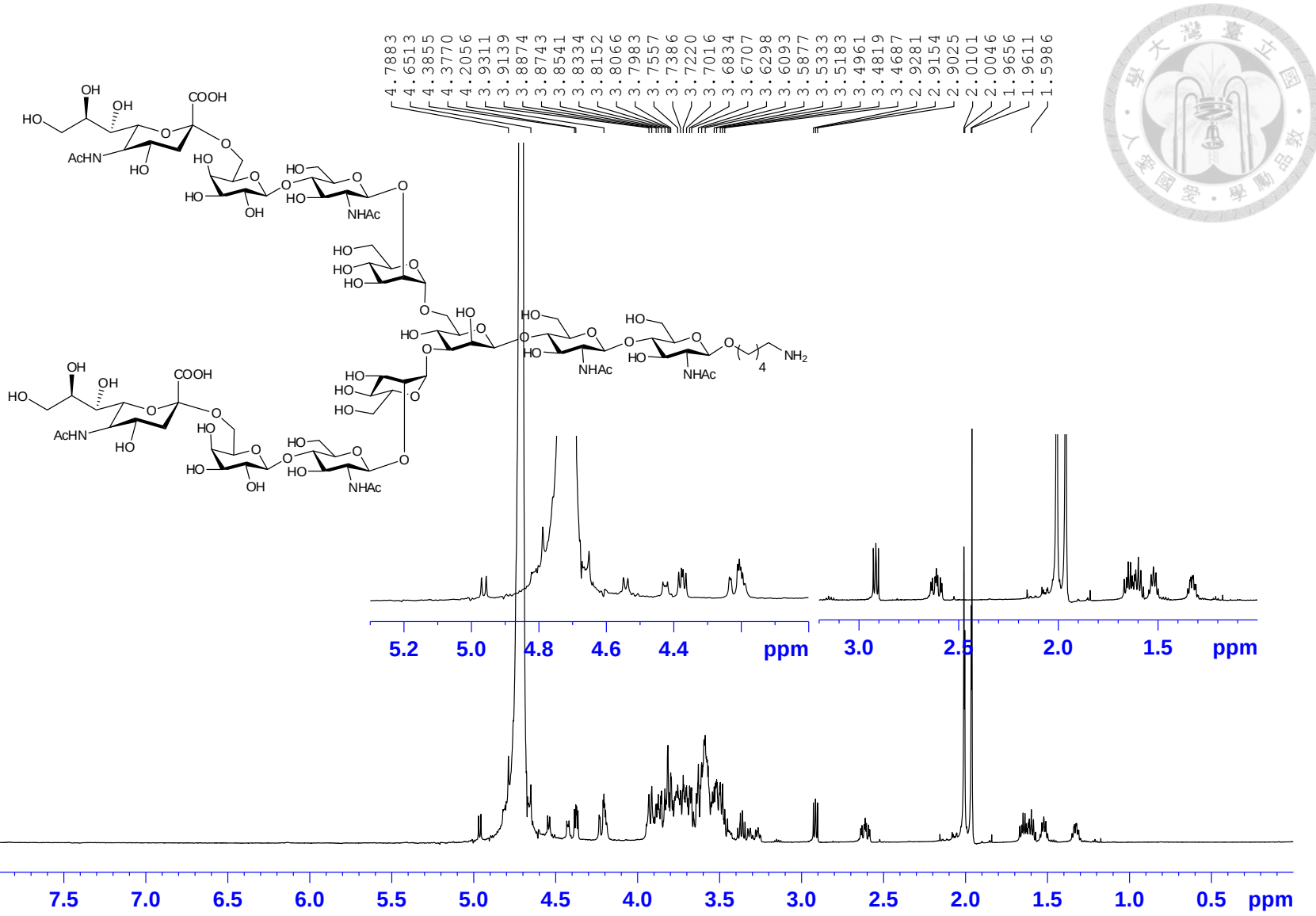
4.7883
4.6513
4.3855
4.3770
4.2056
3.9311
3.9139
3.8874
3.8743
3.8541
3.8334
3.8152
3.8066
3.7983
3.7557
3.7386
3.7220
3.7016
3.6834
3.6707
3.6298
3.6093
3.5877
3.5333
3.5183
3.4961
3.4819
3.4687
3.9281
2.9154
2.9025
2.0101
2.0046
1.9656
1.9611
1.5986
5.2
5.0
4.8
4.6
4.4
ppm
3.0
2.5
2.0
1.5
ppm
7.5
7.0
6.5
6.0
5.5
5.0
4.5
4.0
3.5
3.0
2.5
2.0
1.5
1.0
0.5
ppm

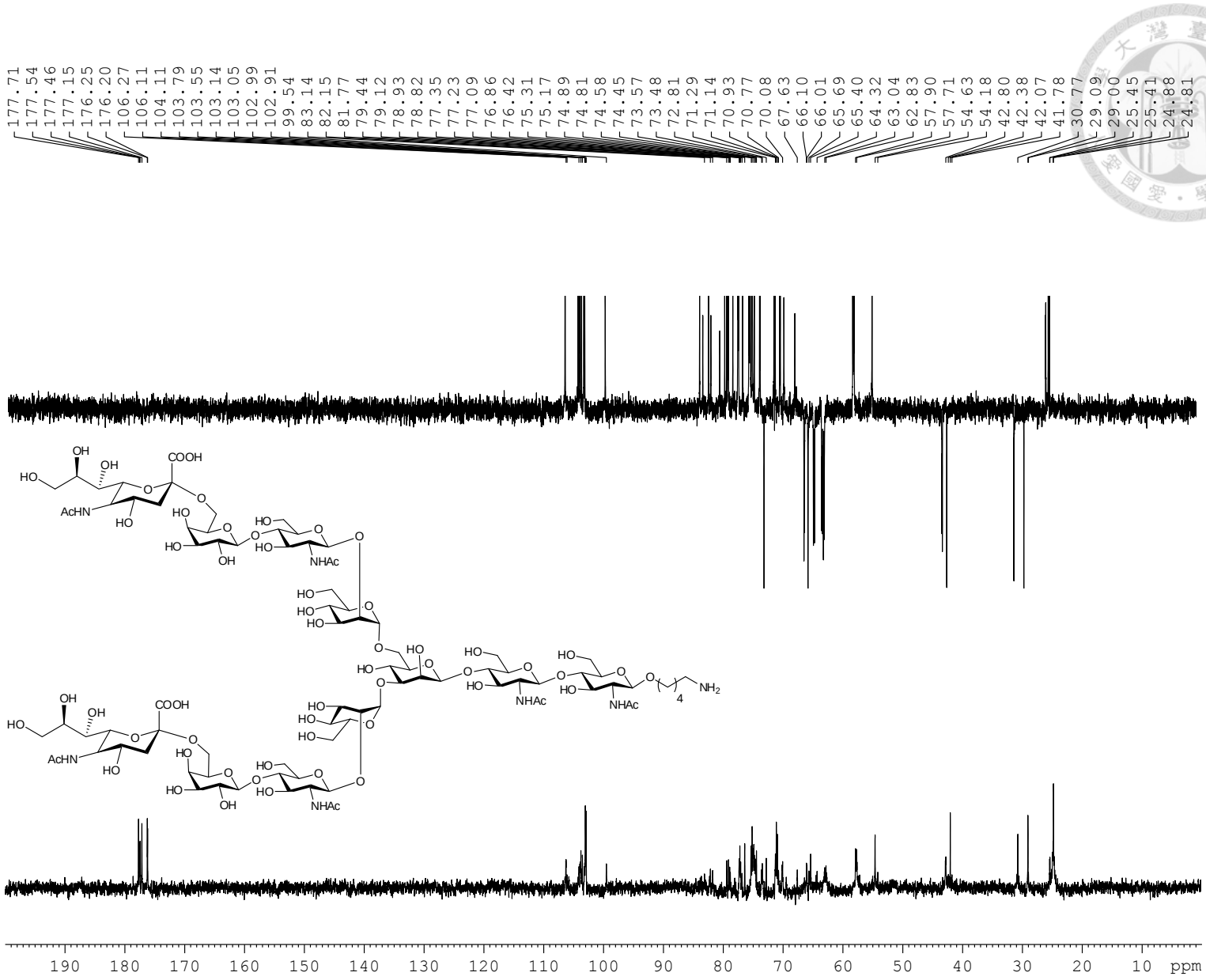
177.71
177.54
177.46
177.15
176.25
176.20
106.27
106.11
104.11
103.79
103.55
103.14
103.05
102.99
102.91
99.54
83.14
82.15
81.77
79.44
79.12
78.93
78.82
77.35
77.23
77.09
76.86
76.42
75.31
75.17
74.89
74.81
74.58
74.45
73.57
73.48
72.81
71.29
71.14
70.93
70.77
70.08
67.63
66.10
66.01
65.69
65.40
64.32
63.04
62.83
57.90
57.71
54.63
54.18
42.80
42.38
42.07
41.78
30.77
29.09
29.00
25.45
25.41
24.88
24.81
190
180
170
160
150
140
130
120
110
100
90
80
70
60
50
40
30
20
10
ppm

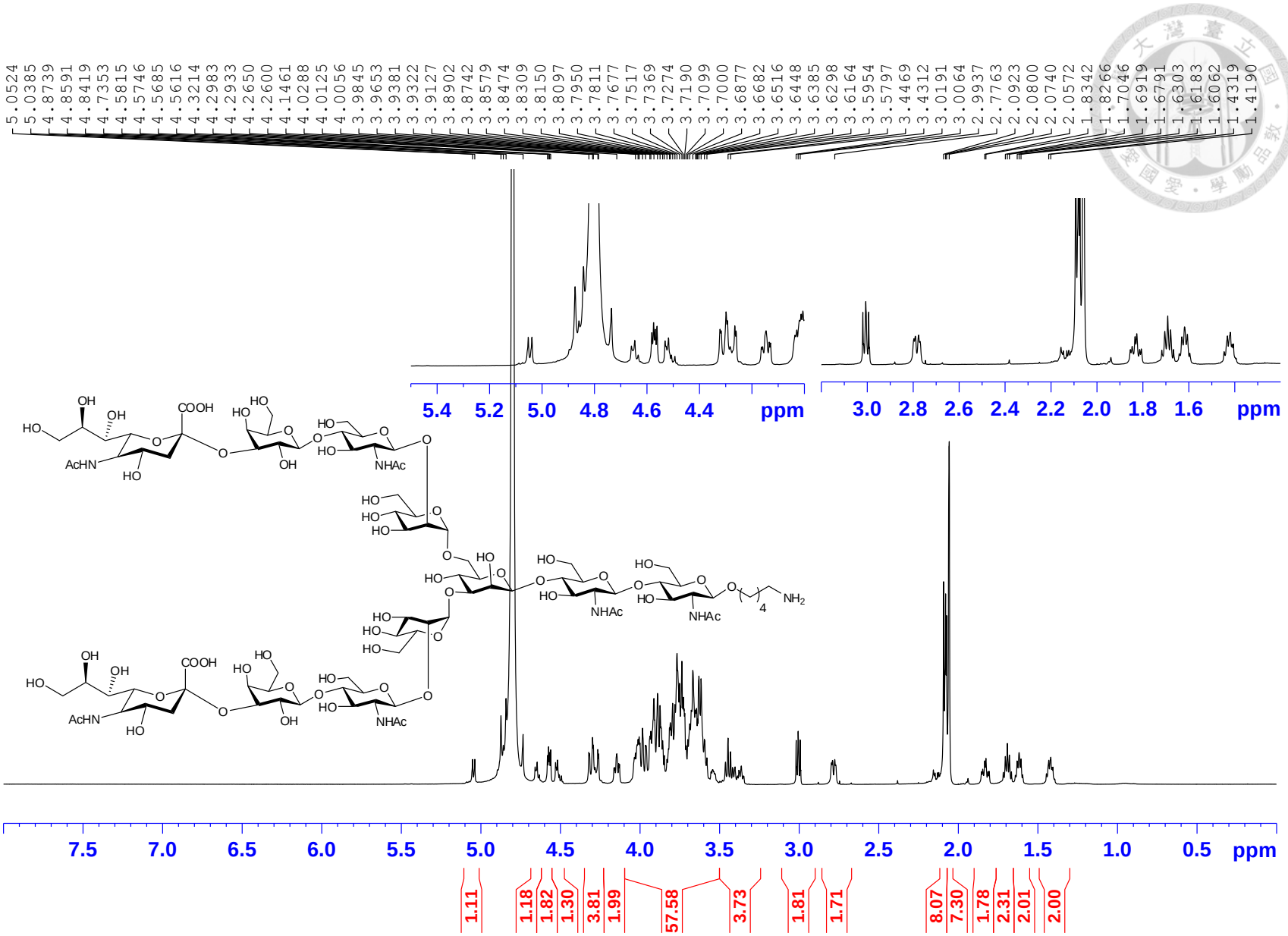
5.0524
5.0385
4.8739
4.8591
4.8419
4.7353
4.5815
4.5746
4.5685
4.5616
4.3214
4.2983
4.2933
4.2650
4.2600
4.1461
4.0288
4.0125
4.0056
3.9845
3.9653
3.9381
3.9322
3.9127
3.8902
3.8742
3.8579
3.8474
3.8309
3.8150
3.8097
3.7950
3.7811
3.7677
3.7517
3.7369
3.7274
3.7190
3.7099
3.7000
3.6877
3.6682
3.6516
3.6448
3.6385
3.6298
3.6164
3.5954
3.5797
3.4469
3.4312
3.0191
3.0064
2.9937
2.7763
2.0923
2.0800
2.0740
2.0572
1.8342
1.8266
1.7046
1.6919
1.6791
1.6303
1.6183
1.6062
1.4319
1.4190
5.4 5.2 5.0 4.8 4.6 4.4 ppm
3.0 2.8 2.6 2.4 2.2 2.0 1.8 1.6 ppm
7.5 7.0 6.5 6.0 5.5 5.0 4.5 4.0 3.5 3.0 2.5 2.0 1.5 1.0 0.5 ppm
1.11
1.18
1.82
1.30
3.81
1.99
57.58
3.73
1.81
1.71
8.07
7.30
1.78
2.31
2.01
2.00

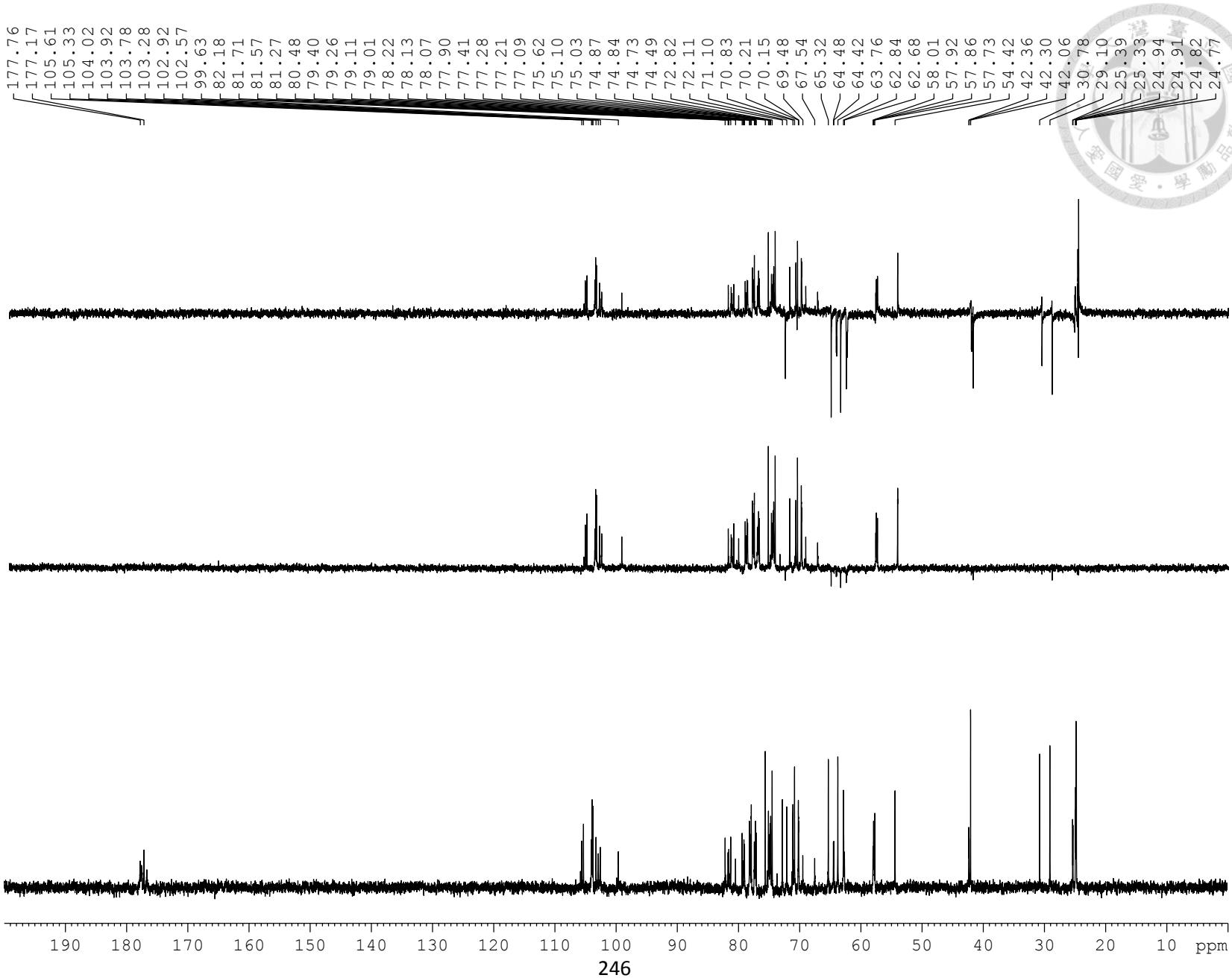
177.76
177.17
105.61
105.33
104.02
103.92
103.78
103.28
102.92
102.57
99.63
82.18
81.71
81.57
81.27
80.48
79.40
79.26
79.11
79.01
78.22
78.13
78.07
77.90
77.41
77.28
77.21
77.09
75.62
75.10
75.03
74.87
74.84
74.73
74.49
72.82
72.11
71.10
70.83
70.21
70.15
69.48
67.54
65.32
64.48
64.42
63.76
62.84
62.68
58.01
57.92
57.86
57.73
54.42
42.36
42.30
42.06
30.78
29.10
25.39
25.33
24.94
24.91
24.82
24.77
190
180
170
160
150
140
130
120
110
100
90
80
70
60
50
40
30
20
10
ppm

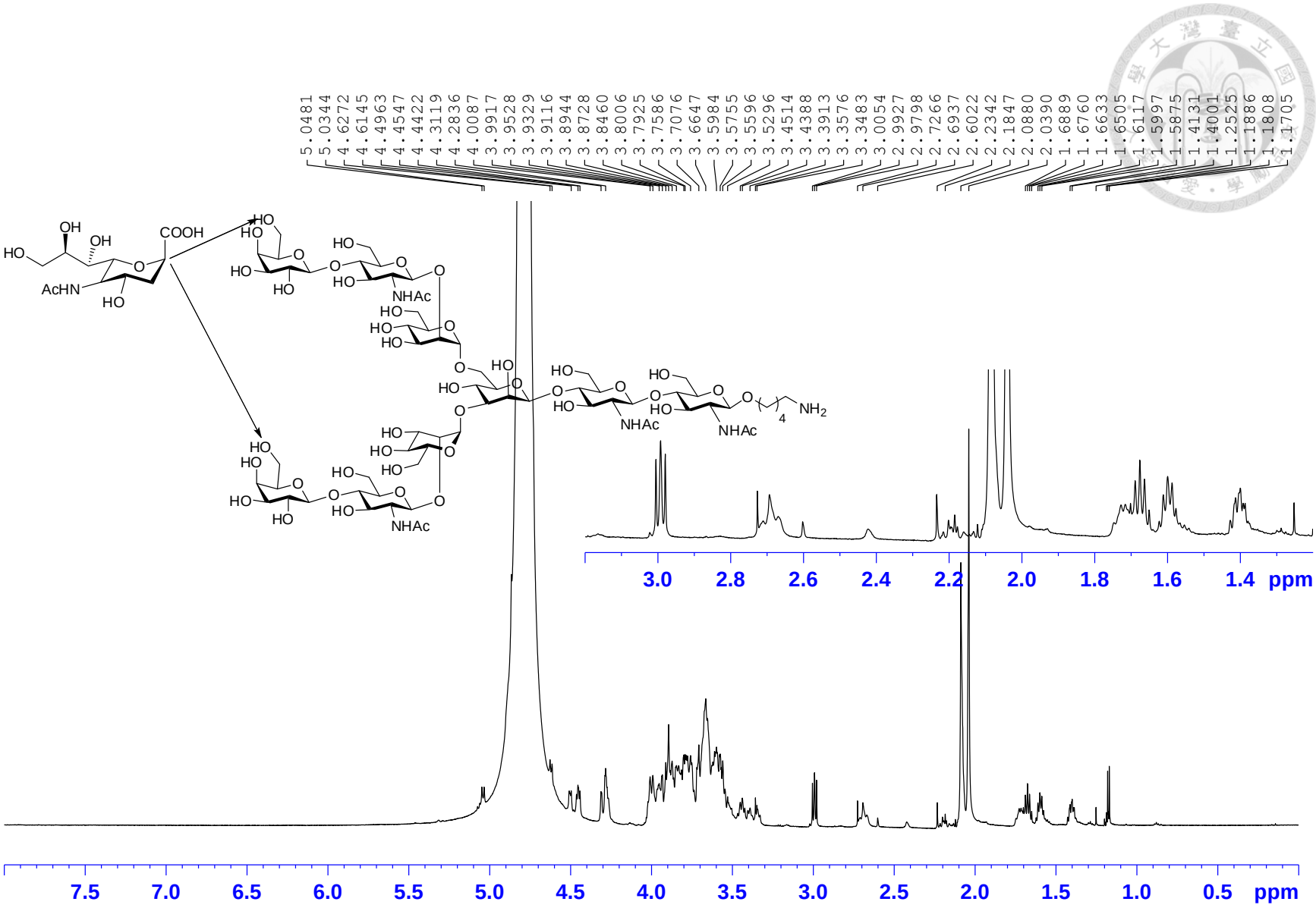
5.0481
5.0344
4.6272
4.6145
4.4963
4.4547
4.4422
4.3119
4.2836
4.0087
3.9917
3.9528
3.9329
3.9116
3.8944
3.8728
3.8460
3.8006
3.7925
3.7586
3.7076
3.6647
3.5984
3.5755
3.5596
3.5296
3.4514
3.4388
3.3913
3.3576
3.3483
3.0054
2.9927
2.9798
2.7266
2.6937
2.6022
2.2342
2.1847
2.0880
2.0390
1.6889
1.6760
1.6633
1.6505
1.6117
1.5997
1.5875
1.4131
1.4001
1.2525
1.1886
1.1808
1.1705
COOH
AcHN
NHAc
NH2
3.0
2.8
2.6
2.4
2.2
2.0
1.8
1.6
1.4
ppm
7.5
7.0
6.5
6.0
5.5
5.0
4.5
4.0
3.5
3.0
2.5
2.0
1.5
1.0
0.5
ppm

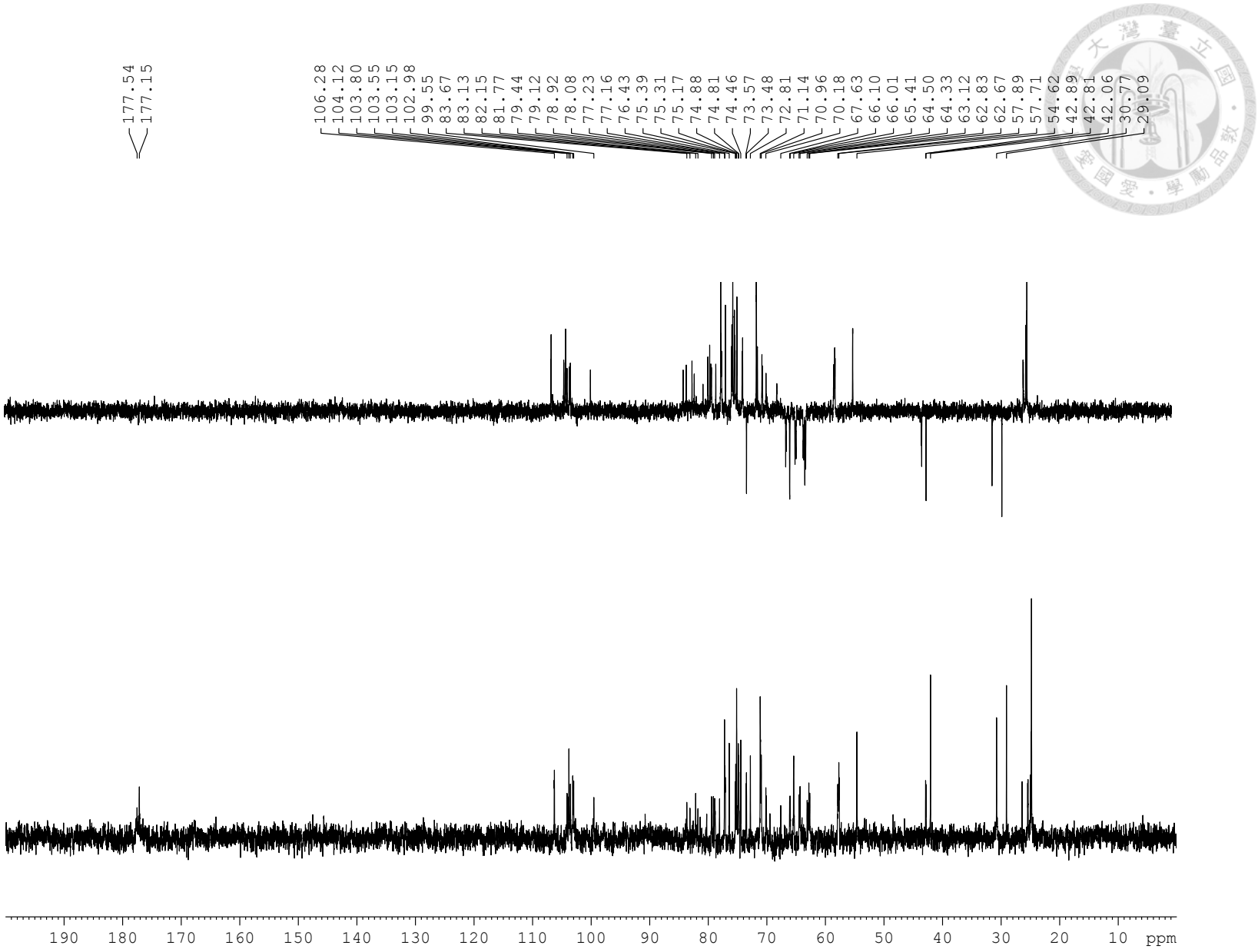
177.54
177.15
106.28
104.12
103.80
103.55
103.15
102.98
99.55
83.67
83.13
82.15
81.77
79.44
79.12
78.92
78.08
77.23
77.16
76.43
75.39
75.31
75.17
74.88
74.81
74.46
73.57
73.48
72.81
71.14
70.96
70.18
67.63
66.10
66.01
65.41
64.50
64.33
63.12
62.83
62.67
57.89
57.71
54.62
42.89
42.81
42.06
30.77
29.09
190 180 170 160 150 140 130 120 110 100 90 80 70 60 50 40 30 20 10 ppm

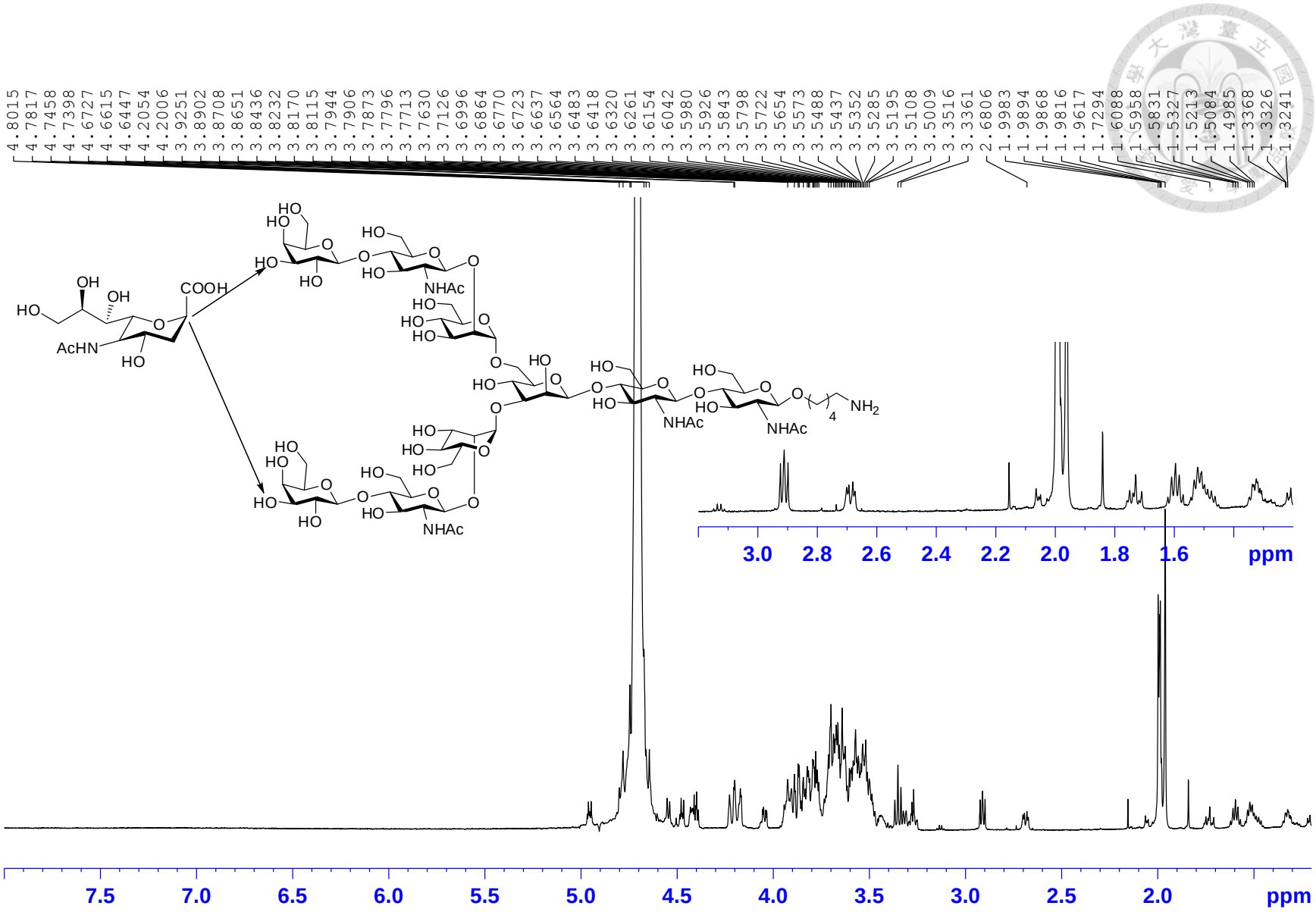
4.8015
4.7817
4.7458
4.7398
4.6727
4.6615
4.6447
4.2054
4.2006
3.9251
3.8902
3.8708
3.8651
3.8436
3.8232
3.8170
3.8115
3.7944
3.7906
3.7873
3.7796
3.7713
3.7630
3.7126
3.6996
3.6864
3.6770
3.6723
3.6637
3.6564
3.6483
3.6418
3.6320
3.6261
3.6154
3.6042
3.5980
3.5926
3.5843
3.5798
3.5722
3.5654
3.5573
3.5488
3.5437
3.5352
3.5285
3.5195
3.5108
3.5009
3.3516
3.3361
2.6806
1.9983
1.9894
1.9868
1.9816
1.9617
1.7294
1.6088
1.5958
1.5831
1.5327
1.5213
1.5084
1.4985
1.3368
1.3326
1.3241
COOH
OH
OH
HO
AcHN
HO
NHAc
NHAc
NHAc
NHAc
NH2
4
3.0
2.8
2.6
2.4
2.2
2.0
1.8
1.6
ppm
7.5
7.0
6.5
6.0
5.5
5.0
4.5
4.0
3.5
3.0
2.5
2.0
ppm

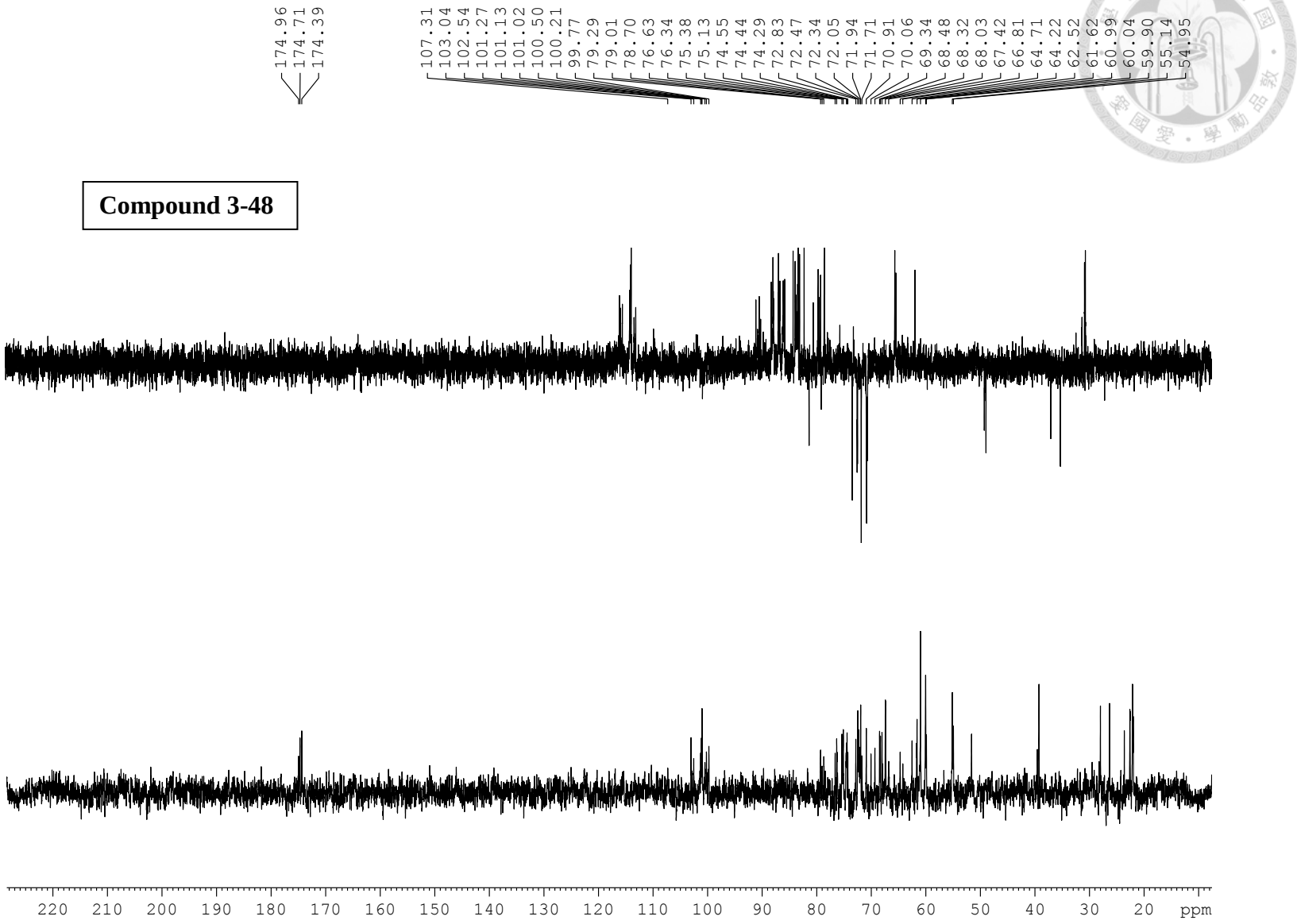
174.96
174.71
174.39
107.31
103.04
102.54
101.27
101.13
101.02
100.50
100.21
99.77
79.29
79.01
78.70
76.63
76.34
75.38
75.13
74.55
74.44
74.29
72.83
72.47
72.34
72.05
71.94
71.71
70.91
70.06
69.34
68.48
68.32
68.03
67.42
66.81
64.71
64.22
62.52
61.62
60.99
60.04
59.90
55.14
54.95
Compound 3-48
220 210 200 190 180 170 160 150 140 130 120 110 100 90 80 70 60 50 40 30 20 ppm

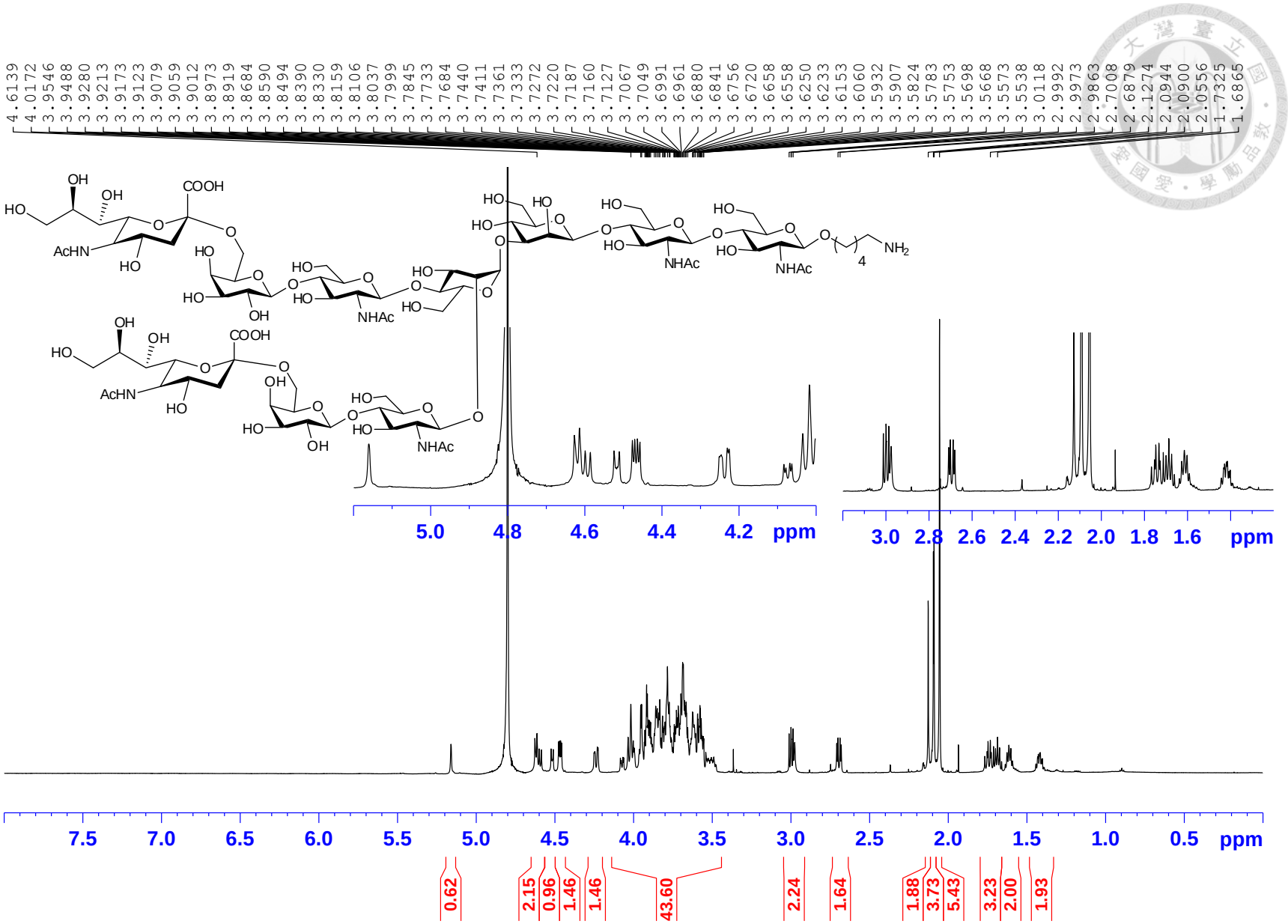
4.6139
4.0172
3.9546
3.9488
3.9280
3.9213
3.9173
3.9123
3.9079
3.9059
3.9012
3.8973
3.8919
3.8684
3.8590
3.8494
3.8390
3.8330
3.8159
3.8106
3.8037
3.7999
3.7845
3.7733
3.7684
3.7440
3.7411
3.7361
3.7333
3.7272
3.7220
3.7187
3.7160
3.7127
3.7067
3.7049
3.6991
3.6961
3.6880
3.6841
3.6756
3.6720
3.6658
3.6558
3.6250
3.6233
3.6153
3.6060
3.5932
3.5907
3.5824
3.5783
3.5753
3.5698
3.5668
3.5573
3.5538
3.0118
2.9992
2.9973
2.9863
2.7008
2.6879
2.1274
2.0944
2.0900
2.0556
1.7325
1.6865
5.0
4.8
4.6
4.4
4.2
ppm
3.0
2.8
2.6
2.4
2.2
2.0
1.8
1.6
ppm
7.5
7.0
6.5
6.0
5.5
5.0
4.5
4.0
3.5
3.0
2.5
2.0
1.5
1.0
0.5
ppm
0.62
2.15
0.96
1.46
1.46
43.60
2.24
1.64
1.88
3.73
5.43
3.23
2.00
1.93

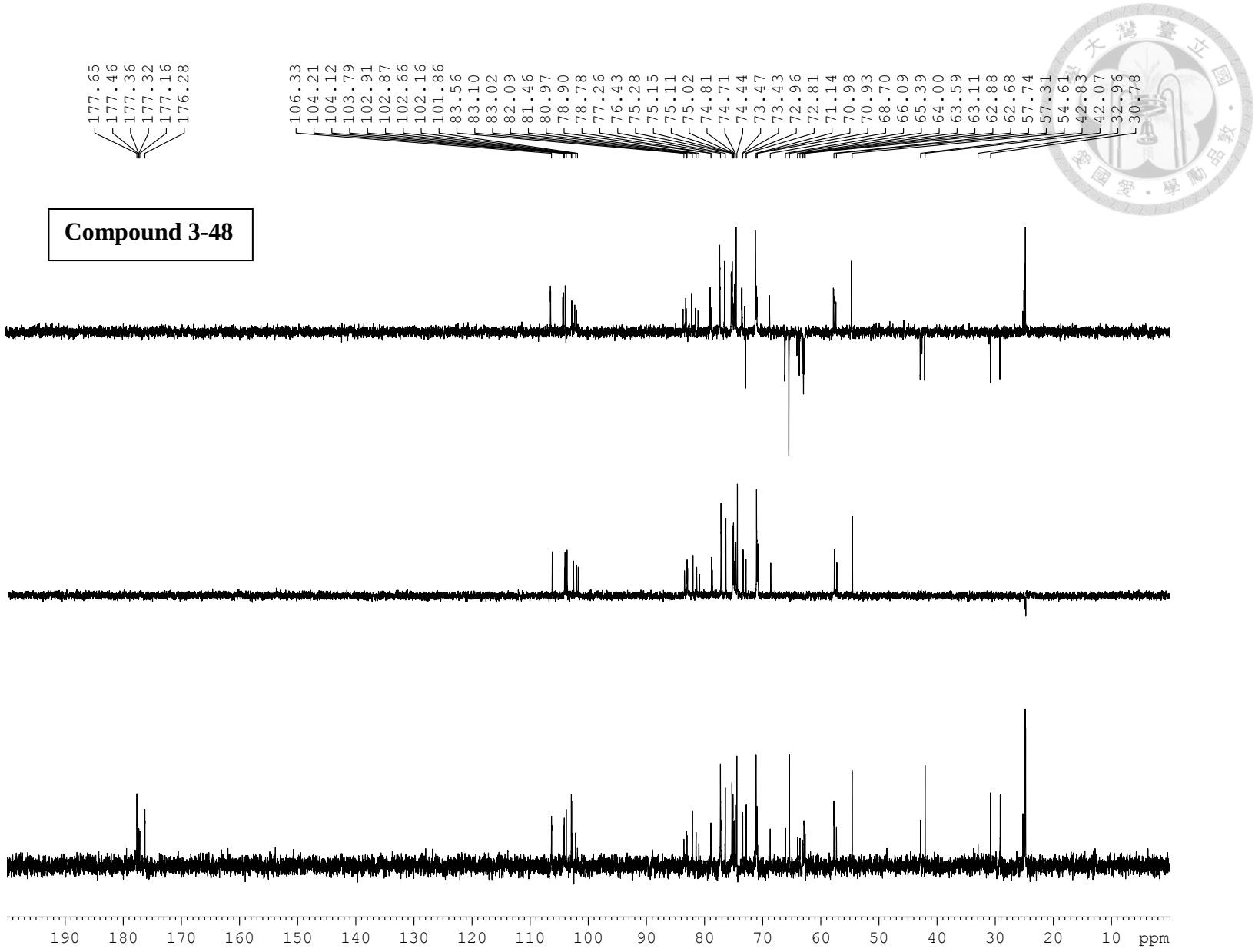
177.65
177.46
177.36
177.32
177.16
176.28
106.33
104.21
104.12
103.79
102.91
102.87
102.66
102.16
101.86
83.56
83.10
83.02
82.09
81.46
80.97
78.90
78.78
77.26
76.43
75.28
75.15
75.11
75.02
74.81
74.71
74.44
73.47
73.43
72.96
72.81
71.14
70.98
70.93
68.70
66.09
65.39
64.00
63.59
63.11
62.88
62.68
57.74
57.31
54.61
42.83
42.07
32.96
30.78
Compound 3-48
190
180
170
160
150
140
130
120
110
100
90
80
70
60
50
40
30
20
10
ppm

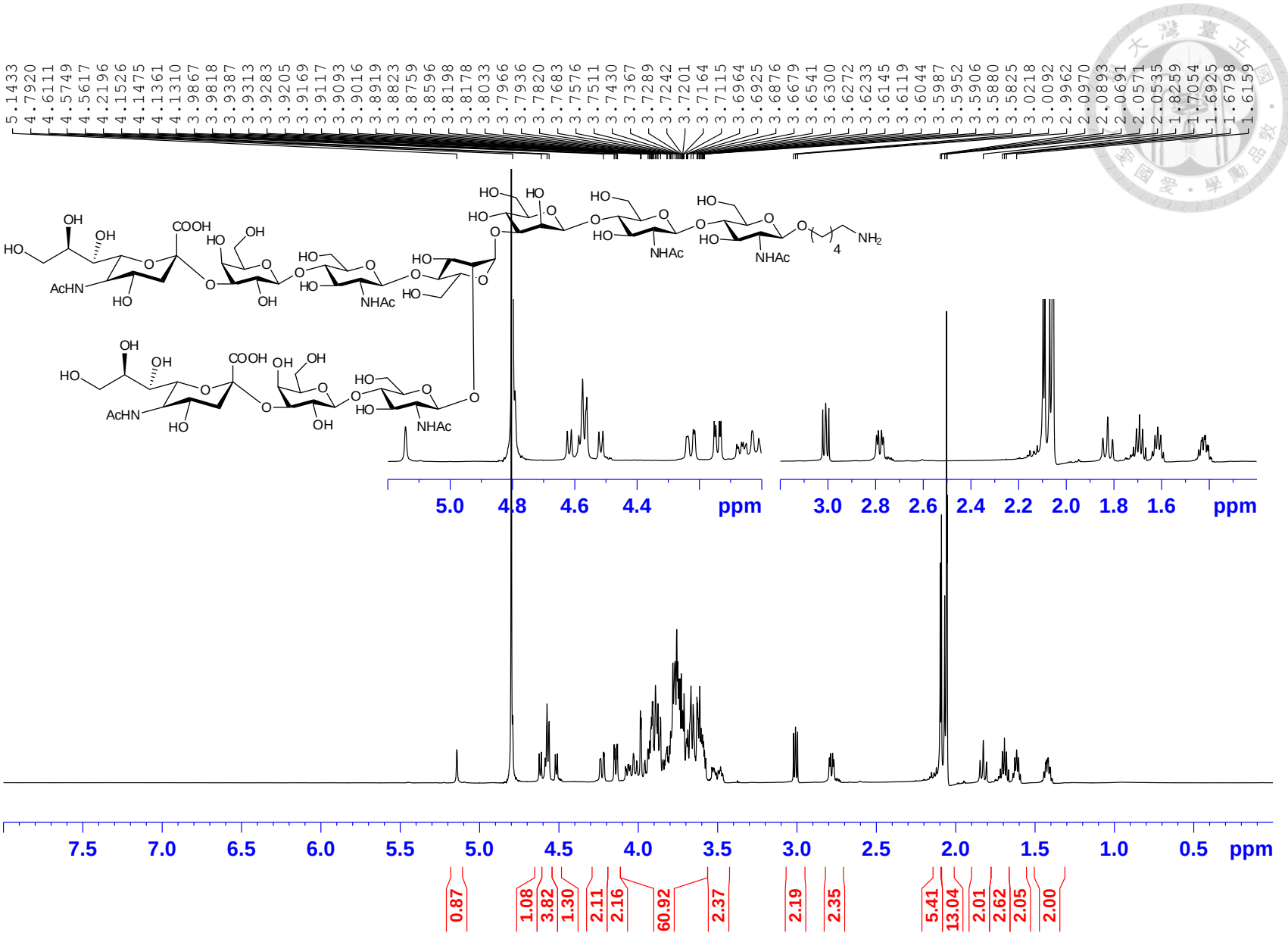
5.1433
4.7920
4.6111
4.5749
4.5617
4.2196
4.1526
4.1475
4.1361
4.1310
3.9867
3.9818
3.9387
3.9313
3.9283
3.9205
3.9169
3.9117
3.9093
3.9016
3.8919
3.8823
3.8759
3.8596
3.8198
3.8178
3.8033
3.7966
3.7936
3.7820
3.7683
3.7576
3.7511
3.7430
3.7367
3.7289
3.7242
3.7201
3.7164
3.7115
3.6964
3.6925
3.6876
3.6679
3.6541
3.6300
3.6272
3.6233
3.6145
3.6119
3.6044
3.5987
3.5952
3.5906
3.5880
3.5825
3.0218
3.0092
2.9962
2.0970
2.0893
2.0691
2.0571
2.0535
1.8259
1.7054
1.6925
1.6798
1.6159
5.0
4.8
4.6
4.4
ppm
3.0
2.8
2.6
2.4
2.2
2.0
1.8
1.6
ppm
7.5
7.0
6.5
6.0
5.5
5.0
4.5
4.0
3.5
3.0
2.5
2.0
1.5
1.0
0.5
ppm
0.87
1.08
3.82
1.30
2.11
2.16
60.92
2.37
2.19
2.35
5.41
13.04
2.01
2.62
2.05
2.00

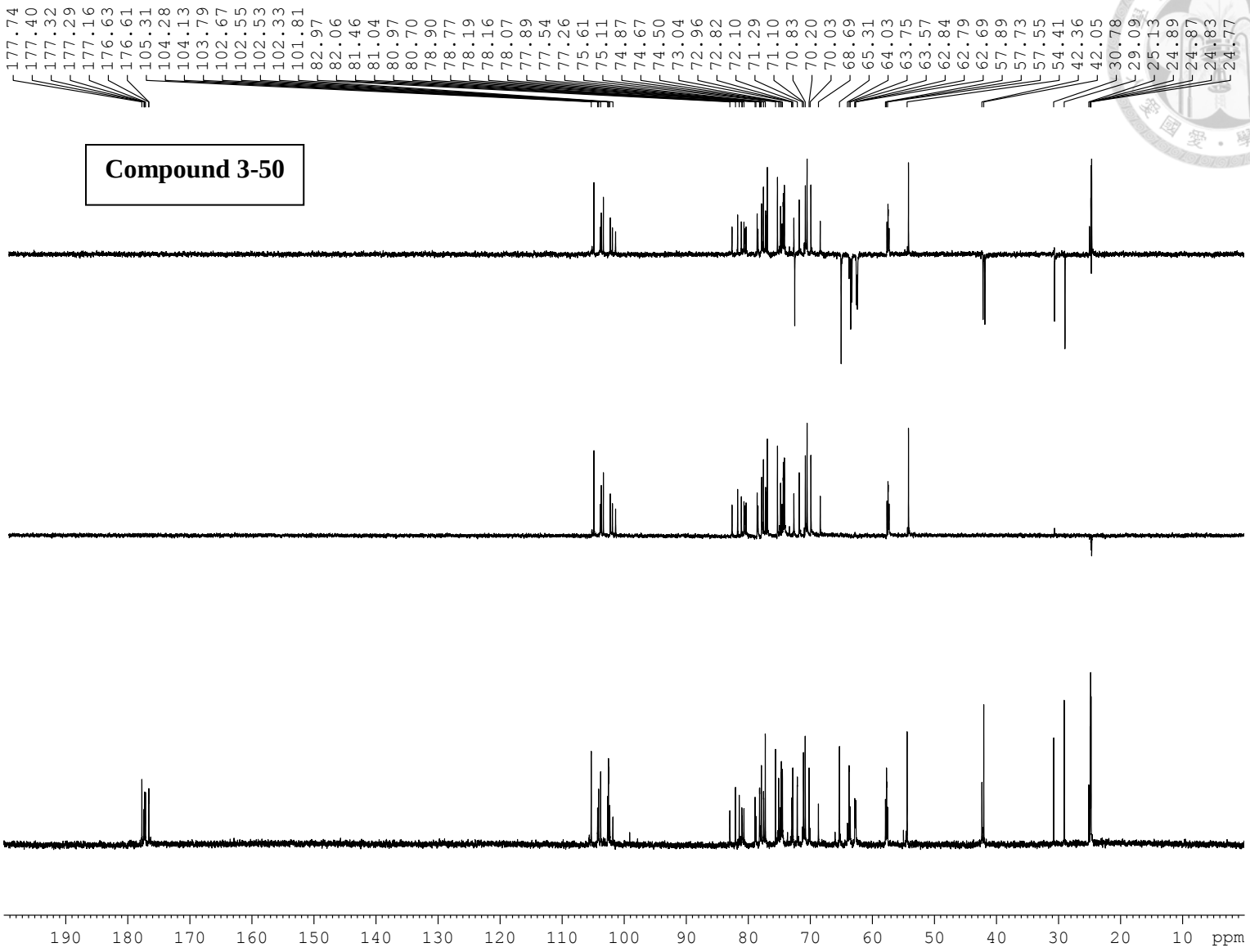
177.74
177.40
177.32
177.29
177.16
176.63
176.61
105.31
104.28
104.13
103.79
102.67
102.55
102.53
102.33
101.81
82.97
82.06
81.46
81.04
80.97
80.70
78.90
78.77
78.19
78.16
78.07
77.89
77.54
77.26
75.61
75.11
74.87
74.67
74.50
73.04
72.96
72.82
72.10
71.29
71.10
70.83
70.20
70.03
68.69
65.31
64.03
63.75
63.57
62.84
62.79
62.69
57.89
57.73
57.55
54.41
42.36
42.05
30.78
29.09
25.13
24.89
24.87
24.83
24.77
Compound 3-50
190
180
170
160
150
140
130
120
110
100
90
80
70
60
50
40
30
20
10
ppm

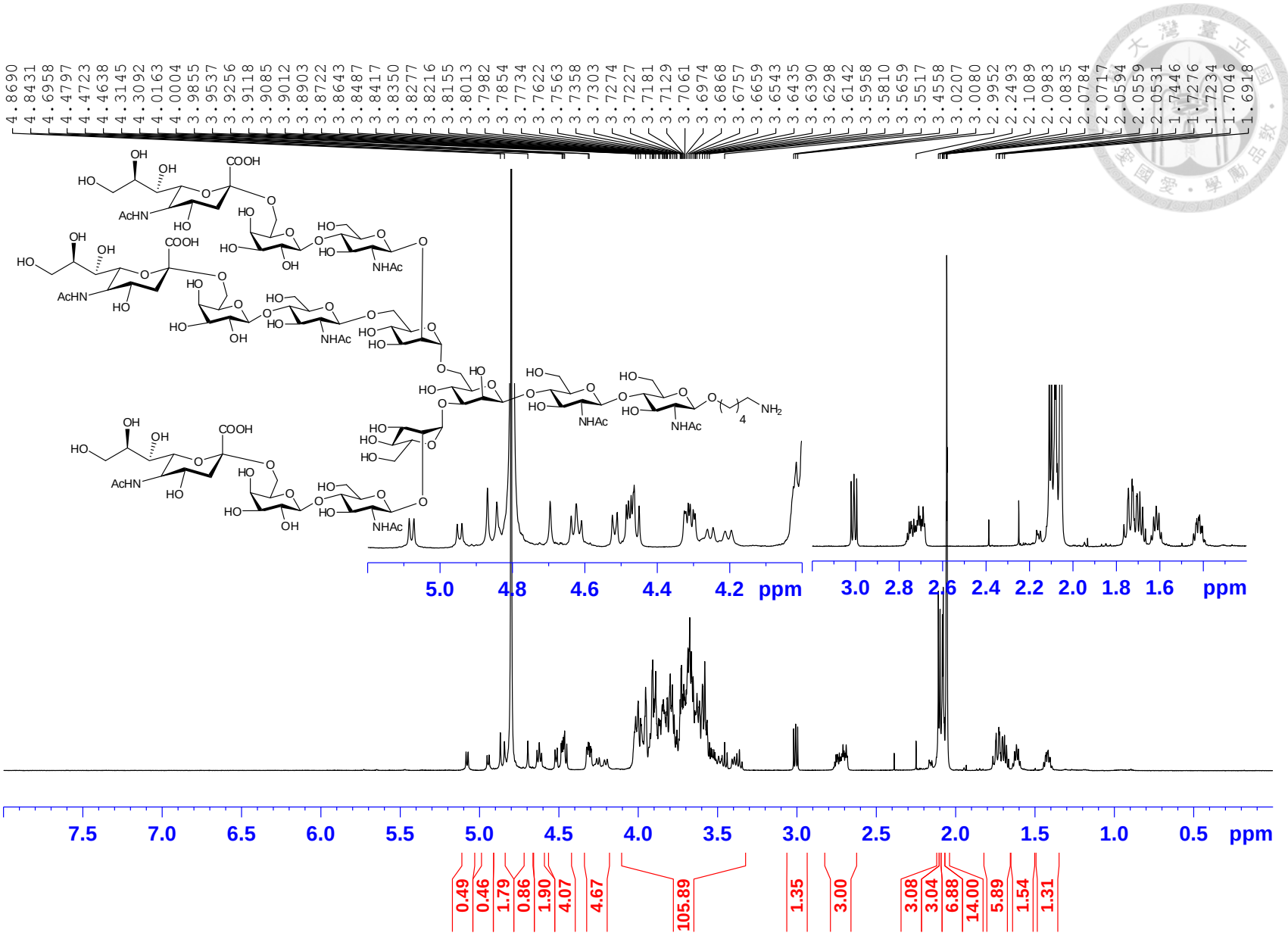
4.8690 4.8431 4.6958 4.4797 4.4723 4.4638 4.3145 4.3092 4.0163 4.0004 3.9855 3.9537 3.9256 3.9118 3.9085 3.9012 3.8903 3.8722 3.8643 3.8487 3.8417 3.8350 3.8277 3.8216 3.8155 3.8013 3.7982 3.7854 3.7734 3.7622 3.7563 3.7358 3.7303 3.7274 3.7227 3.7181 3.7129 3.7061 3.6974 3.6868 3.6757 3.6659 3.6543 3.6435 3.6390 3.6298 3.6142 3.5958 3.5810 3.5659 3.5517 3.4558 3.0207 3.0080 2.9952 2.2493 2.1089 2.0983 2.0835 2.0784 2.0717 2.0594 2.0559 2.0531 1.7446 1.7276 1.7234 1.7046 1.6918
5.0 4.8 4.6 4.4 4.2 ppm
3.0 2.8 2.6 2.4 2.2 2.0 1.8 1.6 ppm
7.5 7.0 6.5 6.0 5.5 5.0 4.5 4.0 3.5 3.0 2.5 2.0 1.5 1.0 0.5 ppm
0.49 0.46 1.79 0.86 1.90 4.07 4.67 105.89 1.35 3.00 3.08 3.04 6.88 14.00 5.89 1.54 1.31

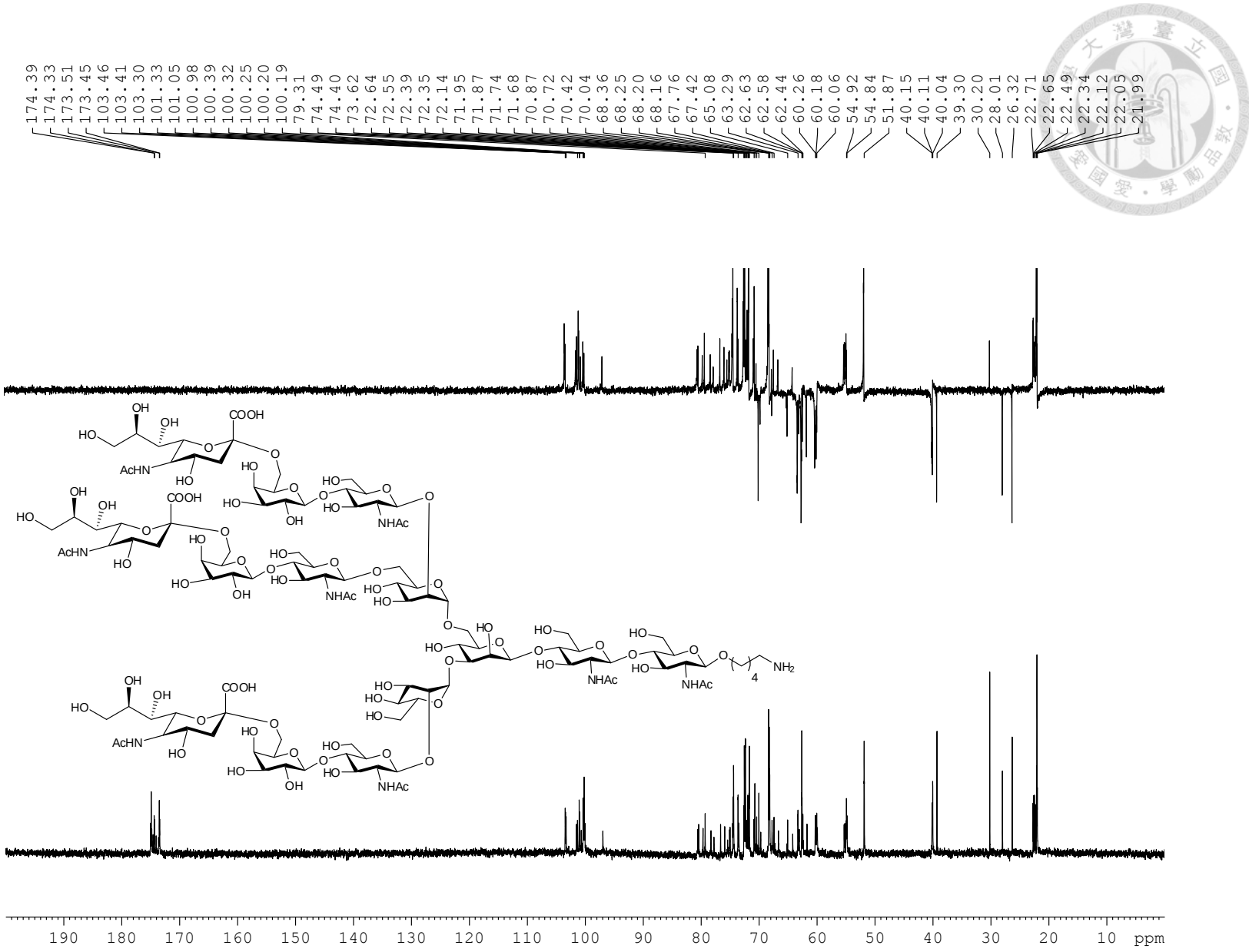
174.39
174.33
173.51
173.45
103.46
103.41
103.30
101.33
101.05
100.98
100.39
100.32
100.25
100.20
100.19
79.31
74.49
74.40
73.62
72.64
72.55
72.39
72.35
72.14
71.95
71.87
71.74
71.68
70.87
70.72
70.42
70.04
68.36
68.25
68.20
68.16
67.76
67.42
65.08
63.29
62.63
62.58
62.44
60.26
60.18
60.06
54.92
54.84
51.87
40.15
40.11
40.04
39.30
30.20
28.01
26.32
22.71
22.65
22.49
22.34
22.12
22.05
21.99
190 180 170 160 150 140 130 120 110 100 90 80 70 60 50 40 30 20 10 ppm

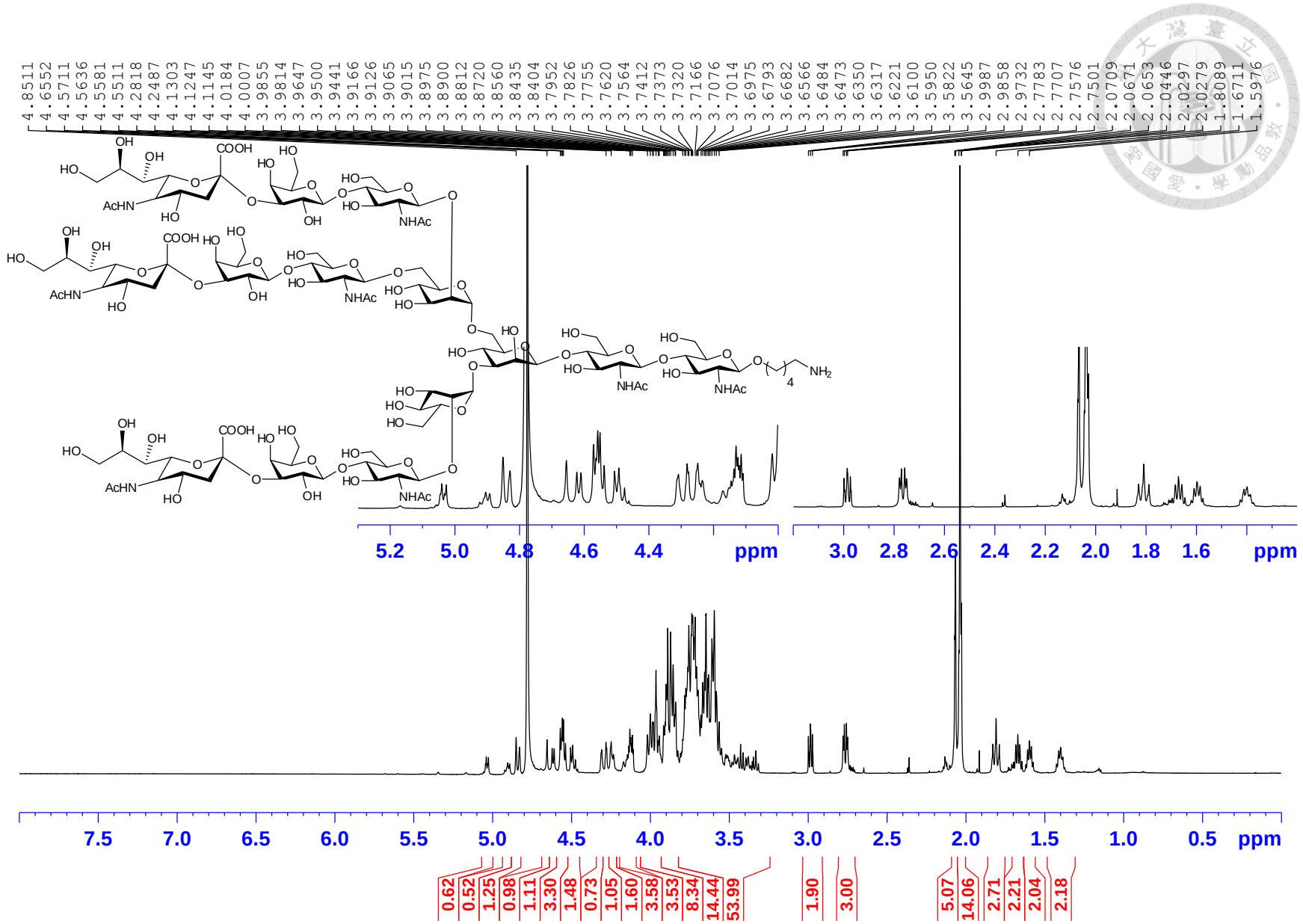
4.8511 4.6552 4.5711 4.5636 4.5581 4.5511 4.2818 4.2487 4.1303 4.1247 4.1145 4.0184 4.0007 3.9855 3.9814 3.9647 3.9500 3.9441 3.9166 3.9126 3.9065 3.9015 3.8975 3.8900 3.8812 3.8720 3.8560 3.8435 3.8404 3.7952 3.7826 3.7755 3.7620 3.7564 3.7412 3.7373 3.7320 3.7166 3.7076 3.7014 3.6975 3.6793 3.6682 3.6566 3.6484 3.6473 3.6350 3.6317 3.6221 3.6100 3.5950 3.5822 3.5645 2.9987 2.9858 2.9732 2.7783 2.7707 2.7576 2.7501 2.0709 2.0671 2.0653 2.0446 2.0297 2.0279 1.8089 1.6711 1.5976
5.2 5.0 4.8 4.6 4.4 ppm
3.0 2.8 2.6 2.4 2.2 2.0 1.8 1.6 ppm
7.5 7.0 6.5 6.0 5.5 5.0 4.5 4.0 3.5 3.0 2.5 2.0 1.5 1.0 0.5 ppm
0.62 0.52 1.25 0.98 1.11 3.30 1.48 0.73 1.05 1.60 3.58 3.53 8.34 14.44 53.99 1.90 3.00 5.07 14.06 2.71 2.21 2.04 2.18

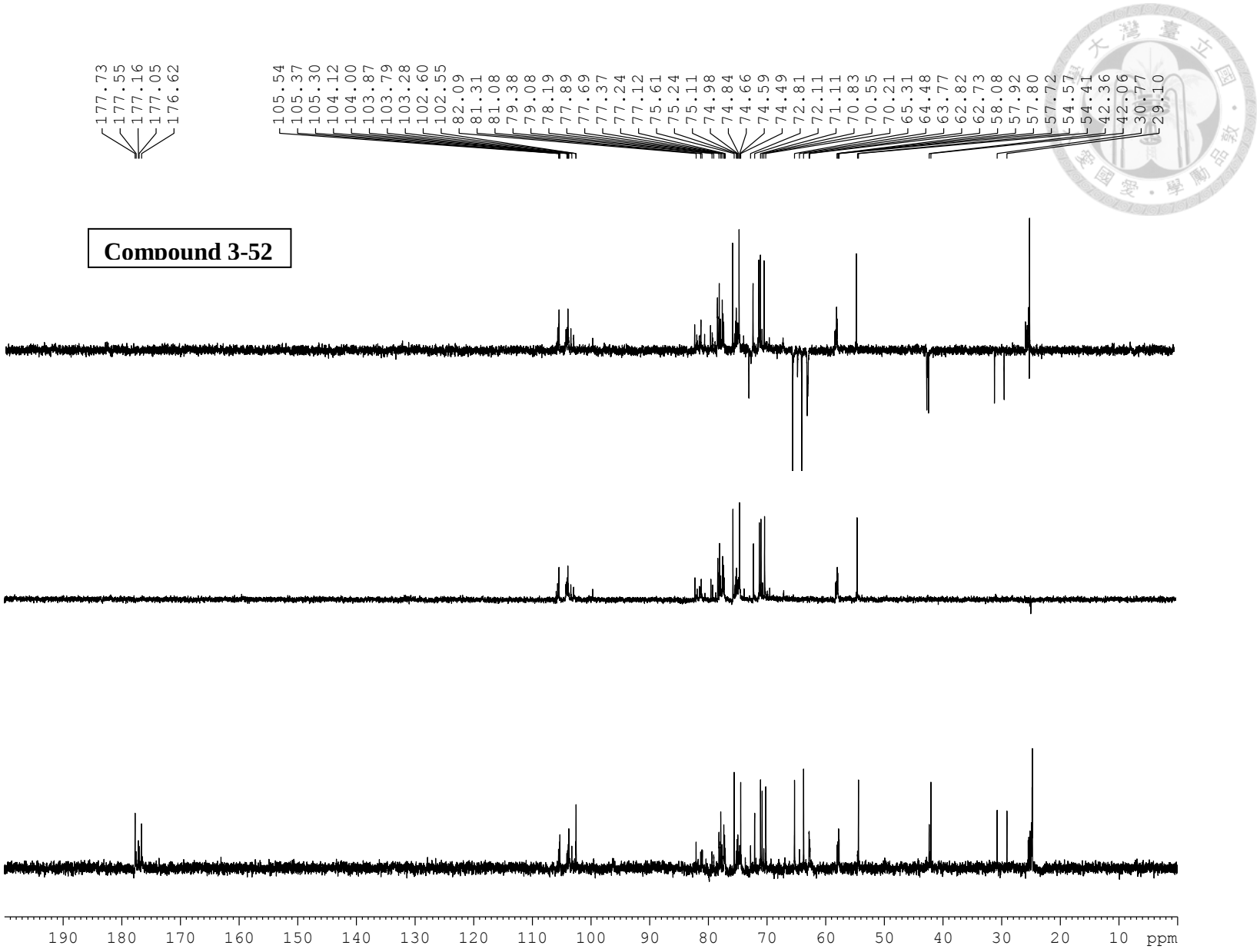
177.73
177.55
177.16
177.05
176.62
105.54
105.37
105.30
104.12
104.00
103.87
103.79
103.28
102.60
102.55
82.09
81.31
81.08
79.38
79.08
78.19
77.89
77.69
77.37
77.24
77.12
75.61
75.24
75.11
74.98
74.84
74.66
74.59
74.49
72.81
72.11
71.11
70.83
70.55
70.21
65.31
64.48
63.77
62.82
62.73
58.08
57.92
57.80
57.72
54.57
54.41
42.36
42.06
30.77
29.10
Compound 3-52
190
180
170
160
150
140
130
120
110
100
90
80
70
60
50
40
30
20
10
ppm

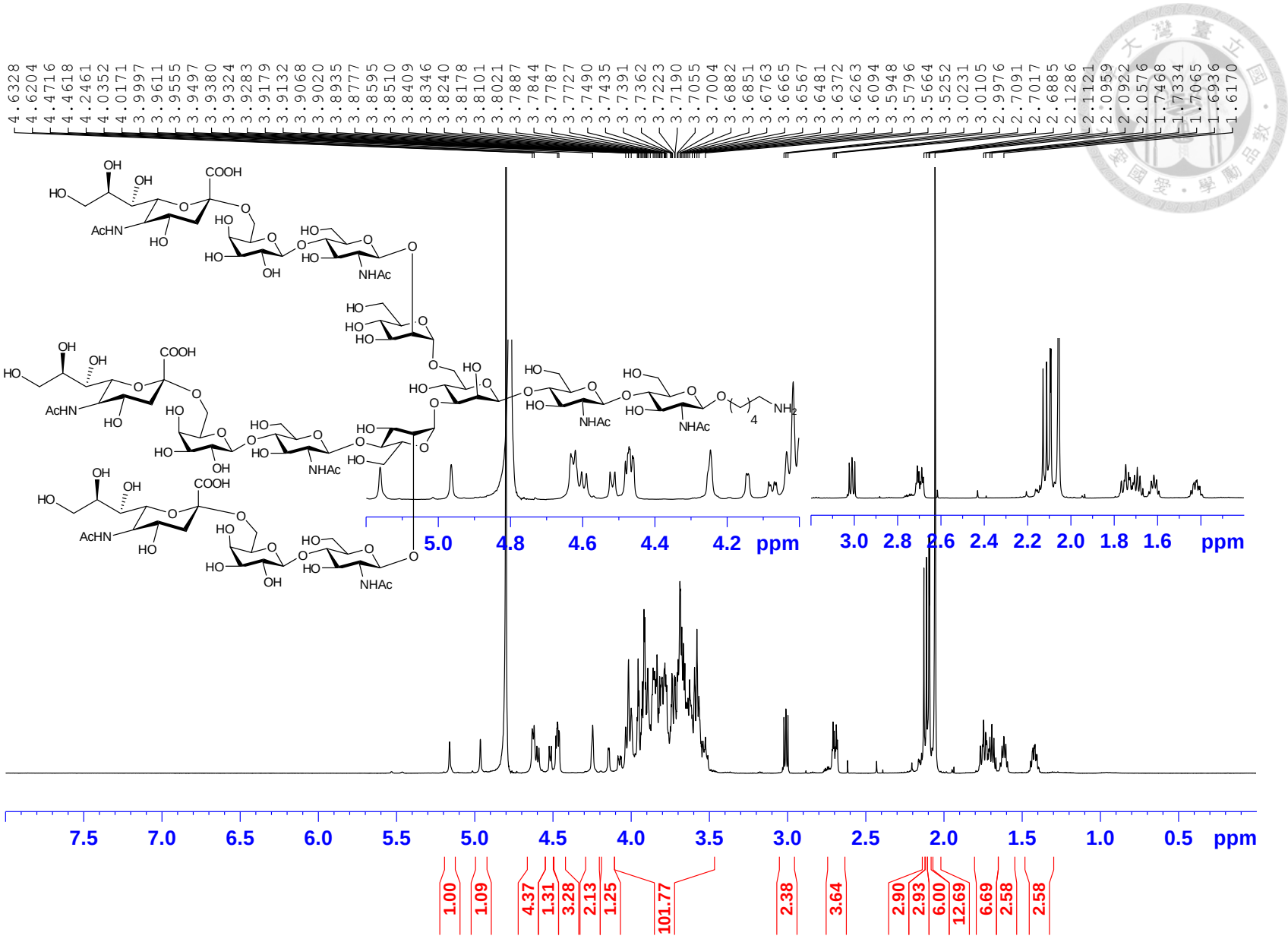
4.6328
4.6204
4.4716
4.4618
4.2461
4.0352
4.0171
3.9997
3.9611
3.9555
3.9497
3.9380
3.9324
3.9283
3.9179
3.9132
3.9068
3.9020
3.8935
3.8777
3.8595
3.8510
3.8409
3.8346
3.8240
3.8178
3.8101
3.8021
3.7887
3.7844
3.7787
3.7727
3.7490
3.7435
3.7391
3.7362
3.7223
3.7190
3.7055
3.7004
3.6882
3.6851
3.6763
3.6665
3.6567
3.6481
3.6372
3.6263
3.6094
3.5948
3.5796
3.5664
3.5252
3.0231
3.0105
2.9976
2.7091
2.7017
2.6885
2.1286
2.1121
2.0959
2.0922
2.0576
1.7468
1.7334
1.7065
1.6936
1.6170
5.0 4.8 4.6 4.4 4.2 ppm
3.0 2.8 2.6 2.4 2.2 2.0 1.8 1.6 ppm
7.5 7.0 6.5 6.0 5.5 5.0 4.5 4.0 3.5 3.0 2.5 2.0 1.5 1.0 0.5 ppm
1.00
1.09
4.37
1.31
3.28
2.13
1.25
101.77
2.38
3.64
2.90
2.93
6.00
12.69
6.69
2.58
2.58

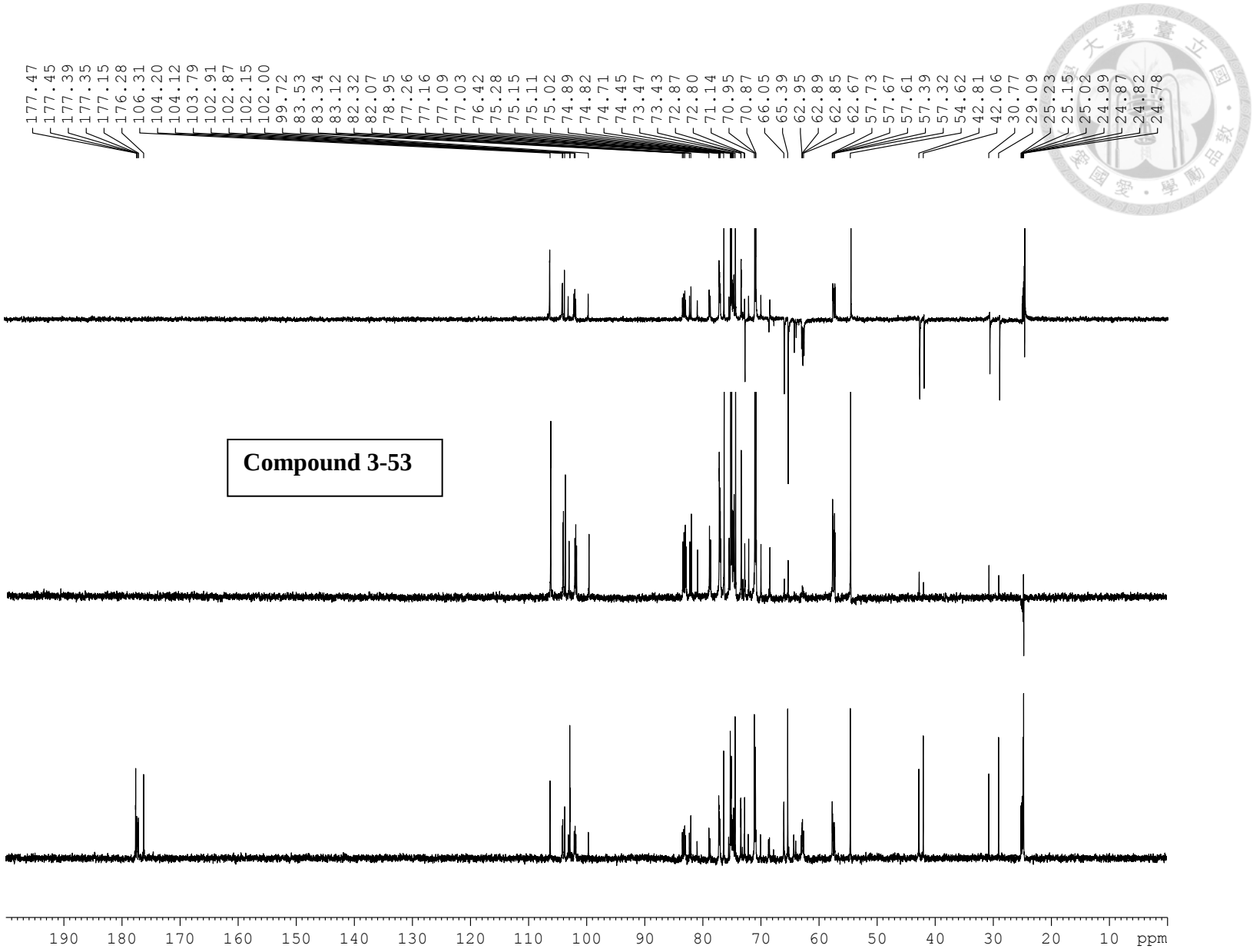
177.47
177.45
177.39
177.35
177.15
176.28
106.31
104.20
104.12
103.79
102.91
102.87
102.15
102.00
99.72
83.53
83.34
83.12
82.32
82.07
78.95
77.26
77.16
77.09
77.03
76.42
75.28
75.15
75.11
75.02
74.89
74.82
74.71
74.45
73.47
73.43
72.87
72.80
71.14
70.95
70.87
66.05
65.39
62.95
62.89
62.85
62.67
57.73
57.67
57.61
57.39
57.32
54.62
42.81
42.06
30.77
29.09
25.23
25.15
25.02
24.99
24.87
24.82
24.78
Compound 3-53
190
180
170
160
150
140
130
120
110
100
90
80
70
60
50
40
30
20
10
ppm

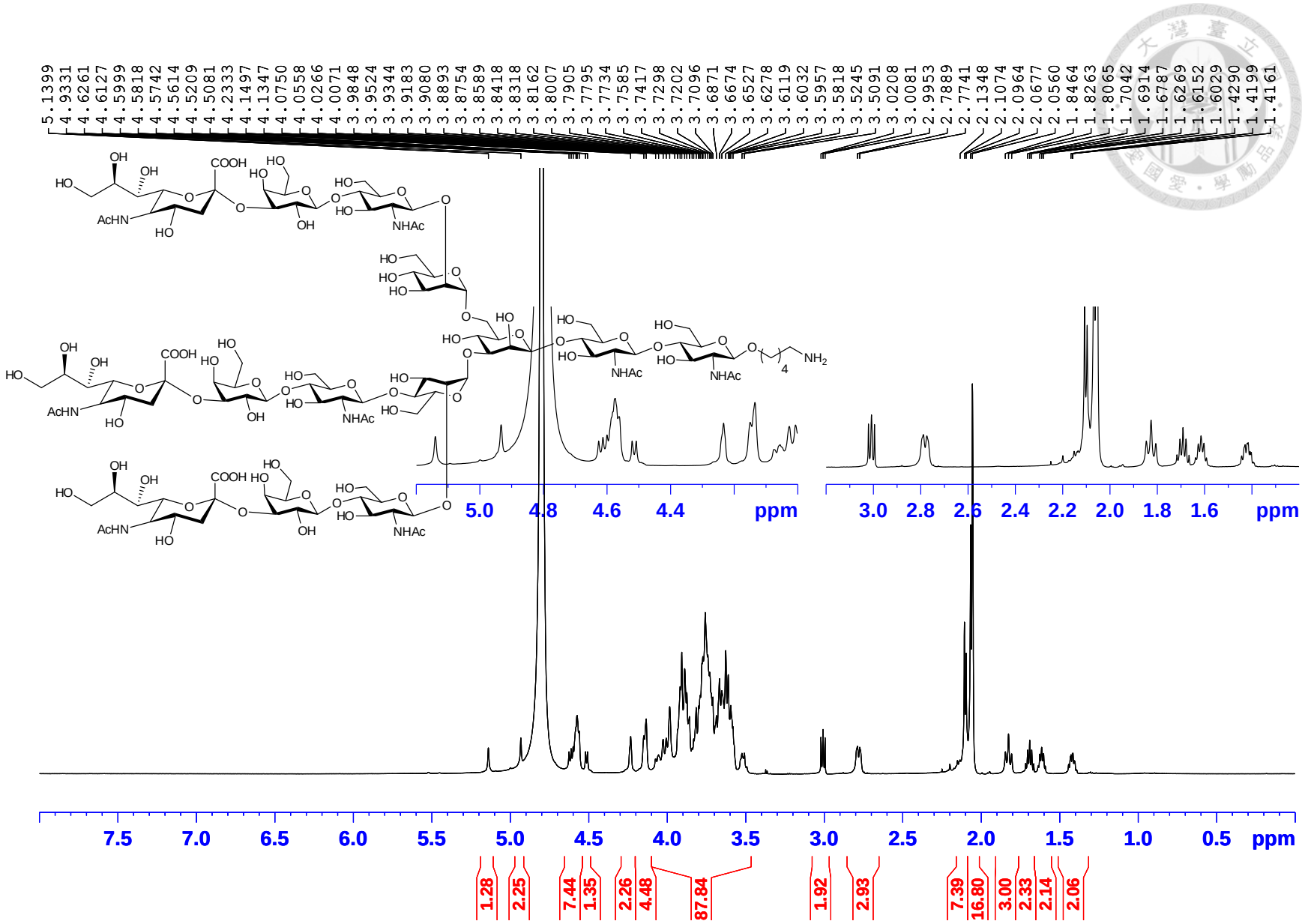
5.1399 4.9331 4.6261 4.6127 4.5999 4.5818 4.5742 4.5614 4.5209 4.5081 4.2333 4.1497 4.1347 4.0750 4.0558 4.0266 4.0071 3.9848 3.9524 3.9344 3.9183 3.9080 3.8893 3.8754 3.8589 3.8418 3.8318 3.8162 3.8007 3.7905 3.7795 3.7734 3.7585 3.7417 3.7298 3.7202 3.7096 3.6871 3.6674 3.6527 3.6278 3.6119 3.6032 3.5957 3.5818 3.5245 3.5091 3.0208 3.0081 2.9953 2.7889 2.7741 2.1348 2.1074 2.0964 2.0677 2.0560 1.8464 1.8263 1.8065 1.7042 1.6914 1.6787 1.6269 1.6152 1.6029 1.4290 1.4199 1.4161
5.0 4.8 4.6 4.4 ppm
3.0 2.8 2.6 2.4 2.2 2.0 1.8 1.6 ppm
7.5 7.0 6.5 6.0 5.5 5.0 4.5 4.0 3.5 3.0 2.5 2.0 1.5 1.0 0.5 ppm
1.28 2.25 7.44 1.35 2.26 4.48 87.84 1.92 2.93 7.39 16.80 3.00 2.33 2.14 2.06

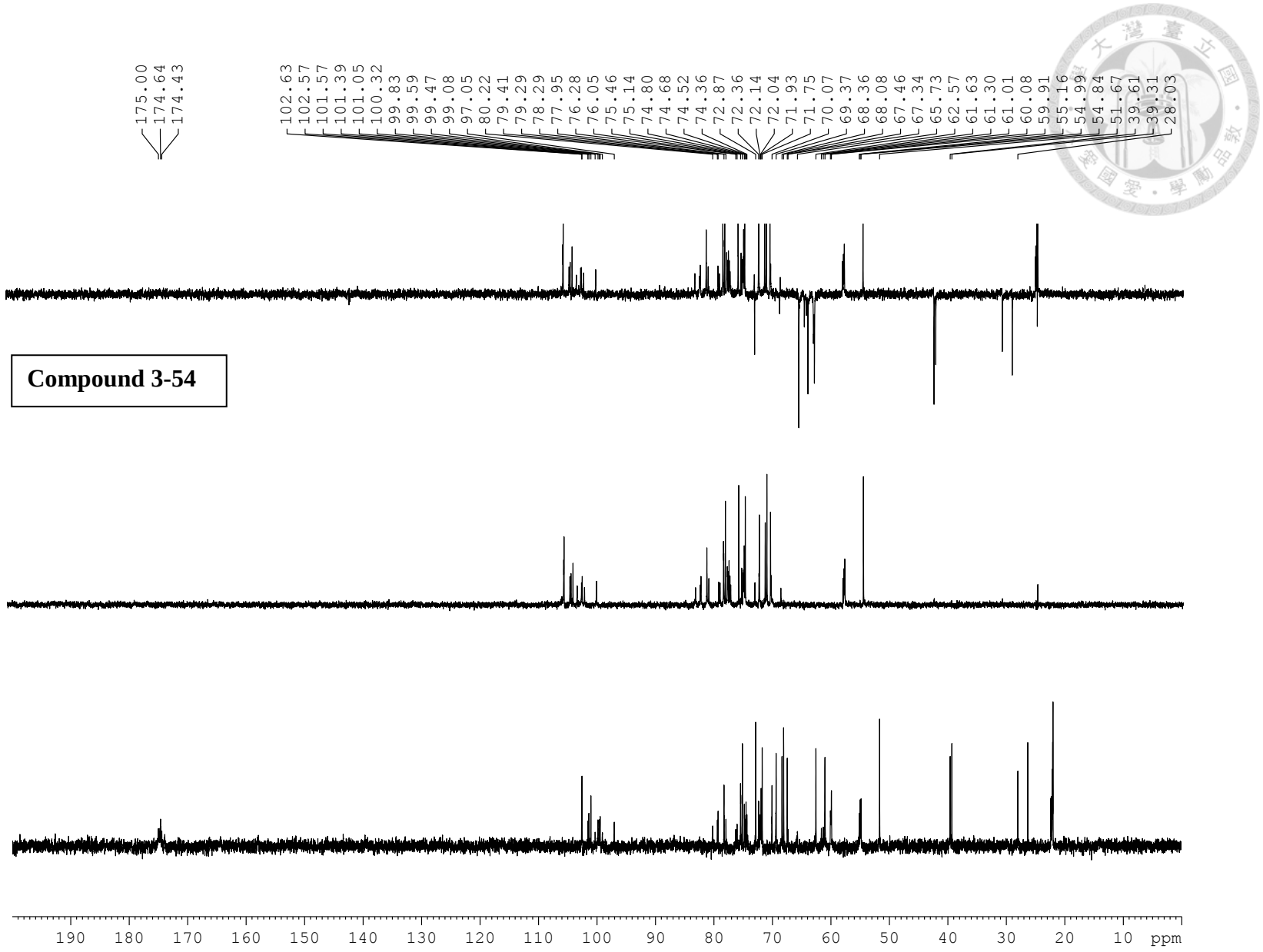
175.00
174.64
174.43
102.63
102.57
101.57
101.39
101.05
100.32
99.83
99.59
99.47
99.08
97.05
80.22
79.41
79.29
78.29
77.95
76.28
76.05
75.46
75.14
74.80
74.68
74.52
74.36
72.87
72.36
72.14
72.04
71.93
71.75
70.07
69.37
68.36
68.08
67.46
67.34
65.73
62.57
61.63
61.30
61.01
60.08
59.91
55.16
54.99
54.84
51.67
39.61
39.31
28.03
Compound 3-54
190
180
170
160
150
140
130
120
110
100
90
80
70
60
50
40
30
20
10
ppm

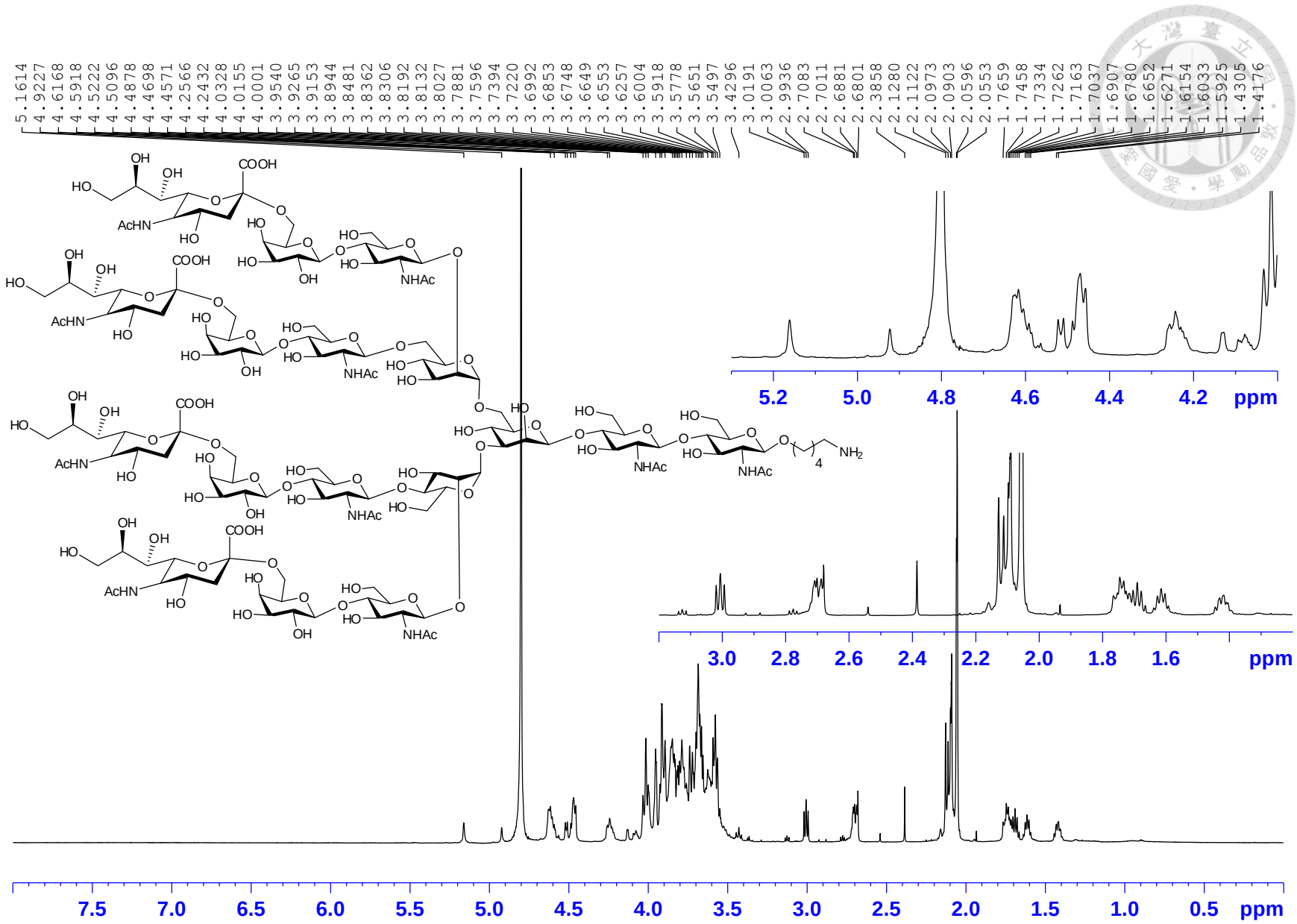
5.1614
4.9227
4.6168
4.5918
4.5222
4.5096
4.4878
4.4698
4.4571
4.2566
4.2432
4.0328
4.0155
4.0001
3.9540
3.9265
3.9153
3.8944
3.8481
3.8362
3.8306
3.8192
3.8132
3.8027
3.7881
3.7596
3.7394
3.7220
3.6992
3.6853
3.6748
3.6649
3.6553
3.6257
3.6004
3.5918
3.5778
3.5651
3.5497
3.4296
3.0191
3.0063
2.9936
2.7083
2.7011
2.6881
2.6801
2.3858
2.1280
2.1122
2.0973
2.0903
2.0596
2.0553
1.7659
1.7458
1.7334
1.7262
1.7163
1.7037
1.6907
1.6780
1.6652
1.6271
1.6154
1.6033
1.5925
1.4305
1.4176
5.2 5.0 4.8 4.6 4.4 4.2 ppm
3.0 2.8 2.6 2.4 2.2 2.0 1.8 1.6 ppm
7.5 7.0 6.5 6.0 5.5 5.0 4.5 4.0 3.5 3.0 2.5 2.0 1.5 1.0 0.5 ppm

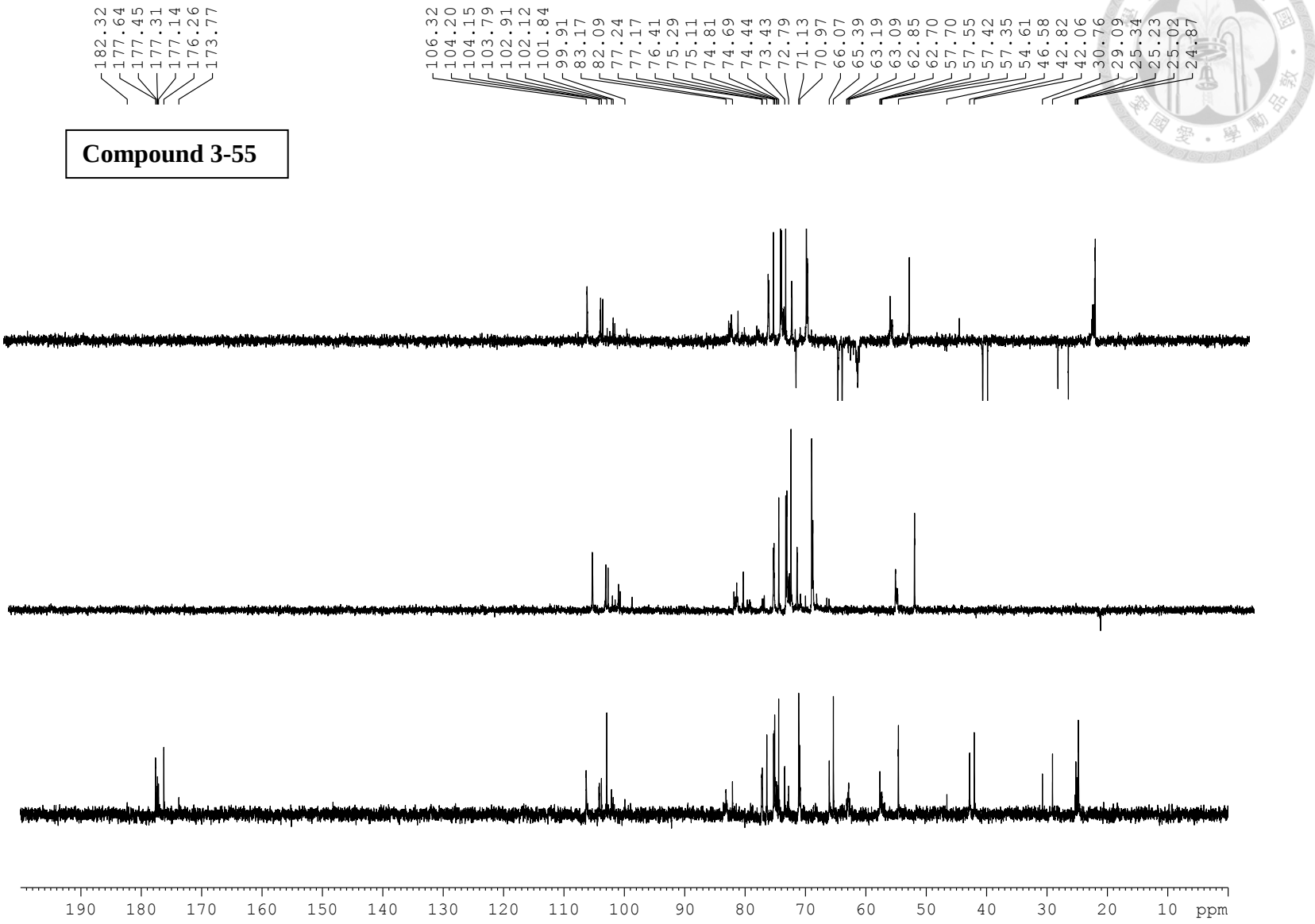
182.32
177.64
177.45
177.31
177.14
176.26
173.77
106.32
104.20
104.15
103.79
102.91
102.12
101.84
99.91
83.17
82.09
77.24
77.17
76.41
75.29
75.11
74.81
74.69
74.44
73.43
72.79
71.13
70.97
66.07
65.39
63.19
63.09
62.85
62.70
57.70
57.55
57.42
57.35
54.61
46.58
42.82
42.06
30.76
29.09
25.34
25.23
25.02
24.87
Compound 3-55
190
180
170
160
150
140
130
120
110
100
90
80
70
60
50
40
30
20
10
ppm

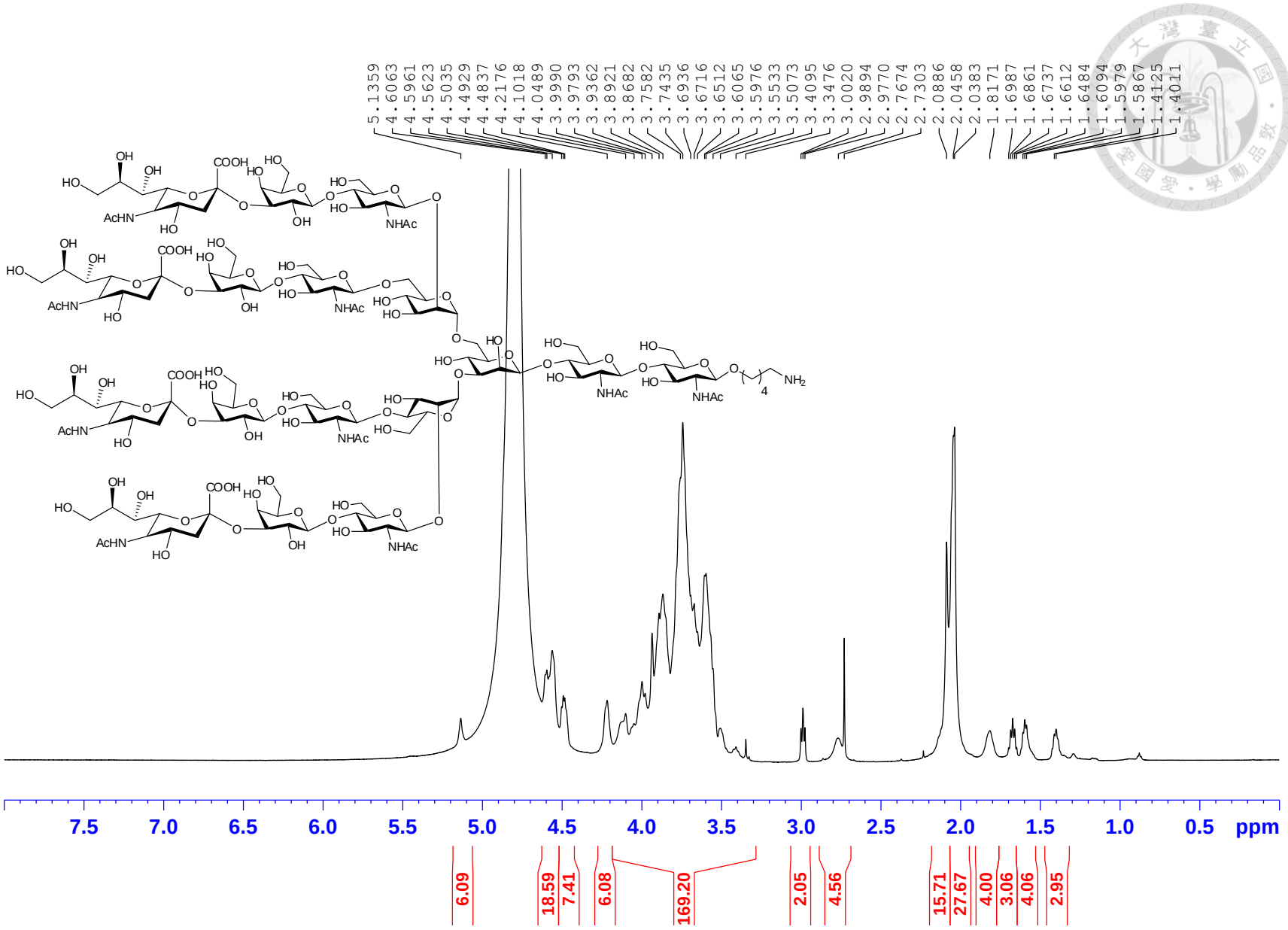
5.1359
4.6063
4.5961
4.5623
4.5035
4.4929
4.4837
4.2176
4.1018
4.0489
3.9990
3.9793
3.9362
3.8921
3.8682
3.7582
3.7435
3.6936
3.6716
3.6512
3.6065
3.5976
3.5533
3.5073
3.4095
3.3476
3.0020
2.9894
2.9770
2.7674
2.7303
2.0886
2.0458
2.0383
1.8171
1.6987
1.6861
1.6737
1.6612
1.6484
1.6094
1.5979
1.5867
1.4125
1.4011
7.5
7.0
6.5
6.0
5.5
5.0
4.5
4.0
3.5
3.0
2.5
2.0
1.5
1.0
0.5
ppm
6.09
18.59
7.41
6.08
169.20
2.05
4.56
15.71
27.67
4.00
3.06
4.06
2.95

Compound 3-56

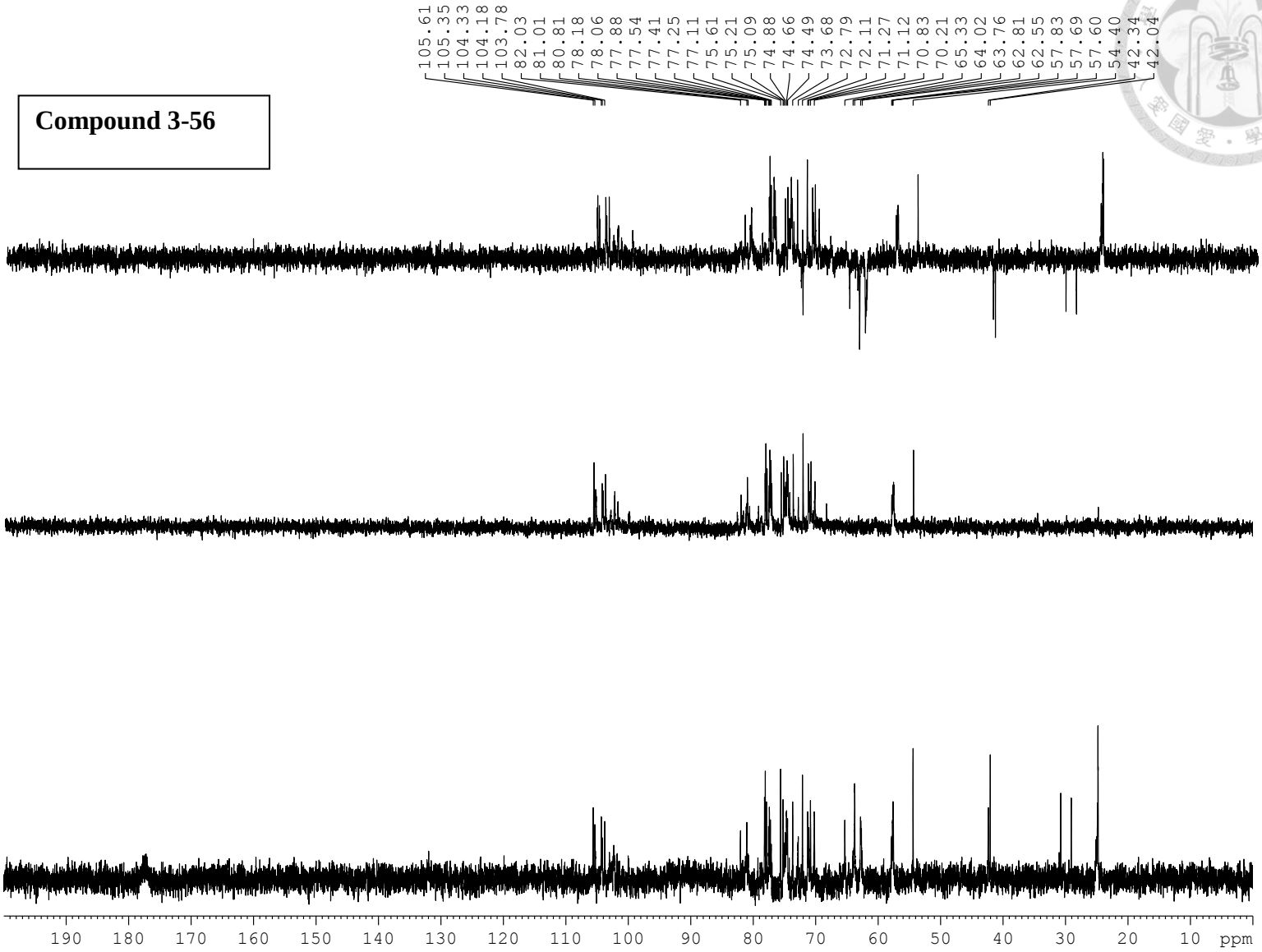

MALDI-TOF MS Spectra

for Glycoconjugates 1-5

(Chapter 5)

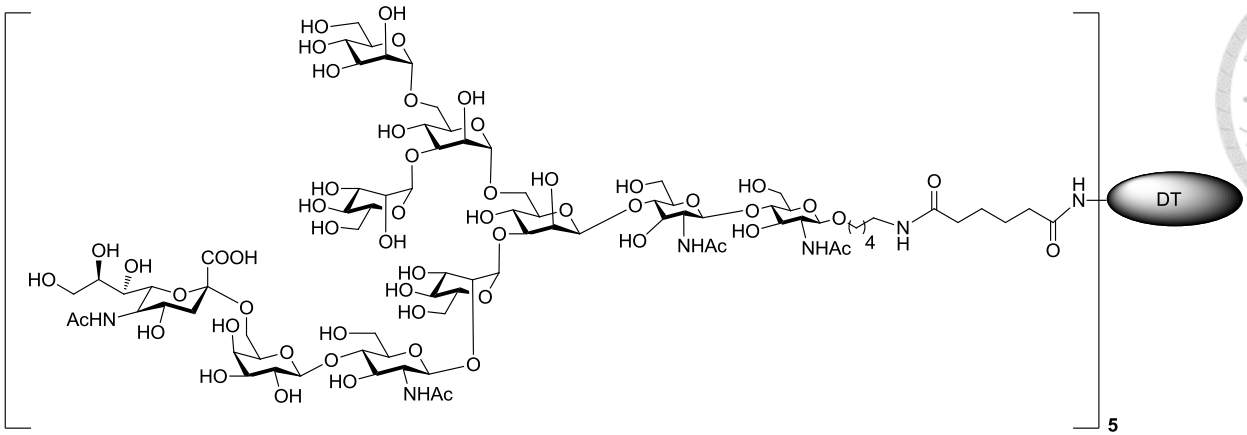

Glycoconjugate 1

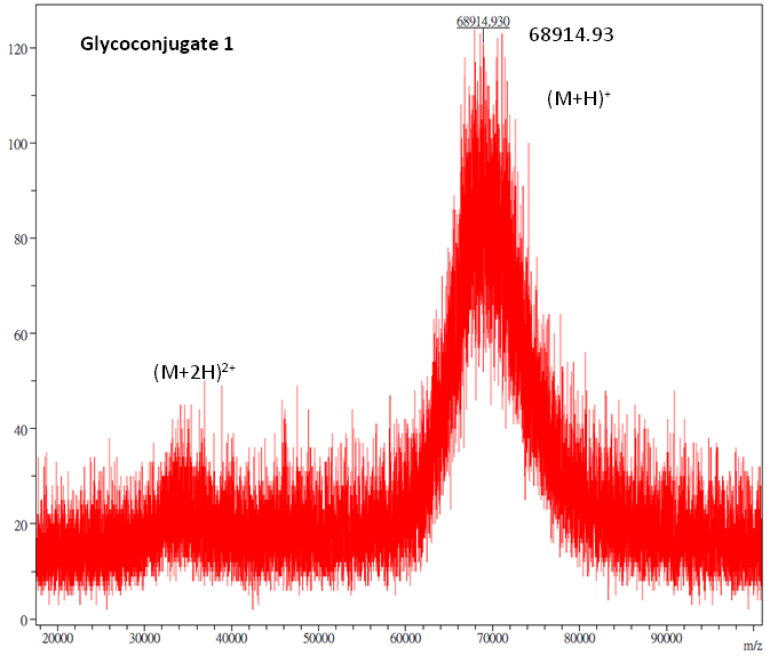

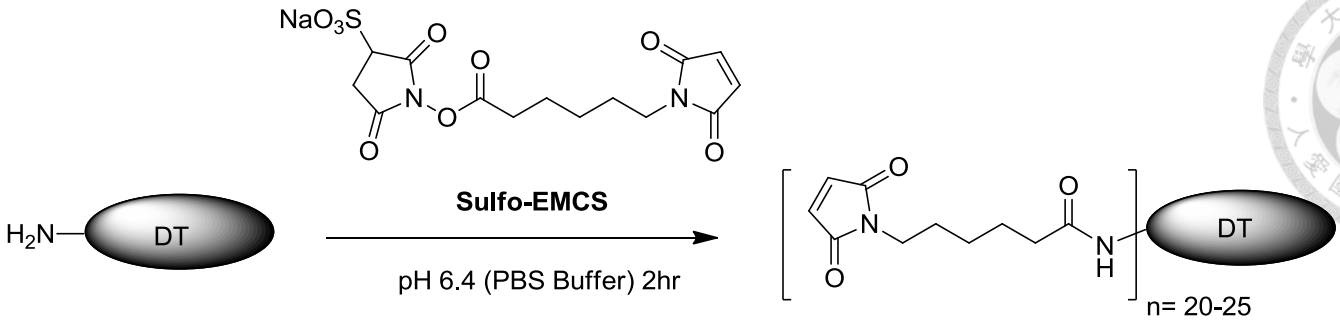
NaO3S
Sulfo-EMCS
H2N
DT
pH 6.4 (PBS Buffer) 2hr
DT
n= 20-25

5-10

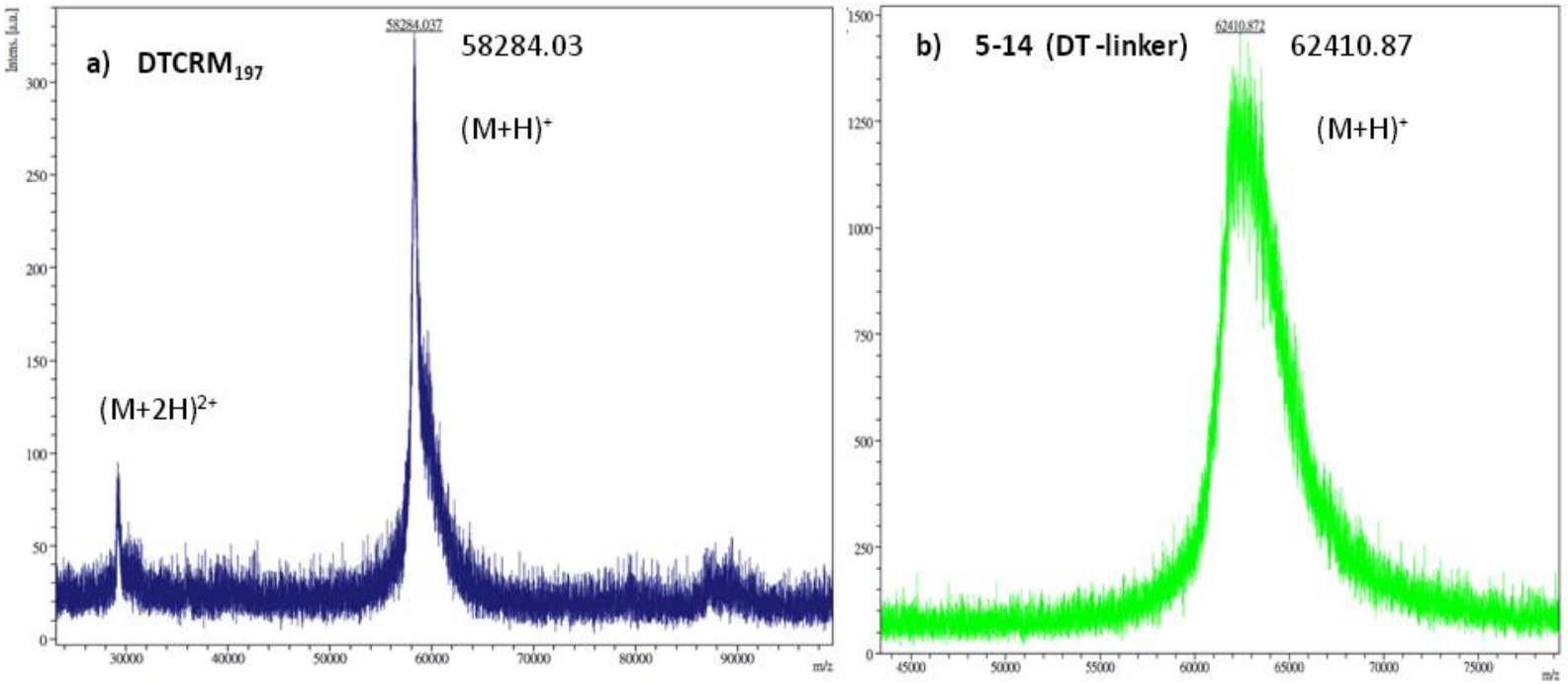
a) DTCRM197
58284.03
(M+H)+
(M+2H)2+
b) 5-14 (DT-linker)
62410.87
(M+H)+

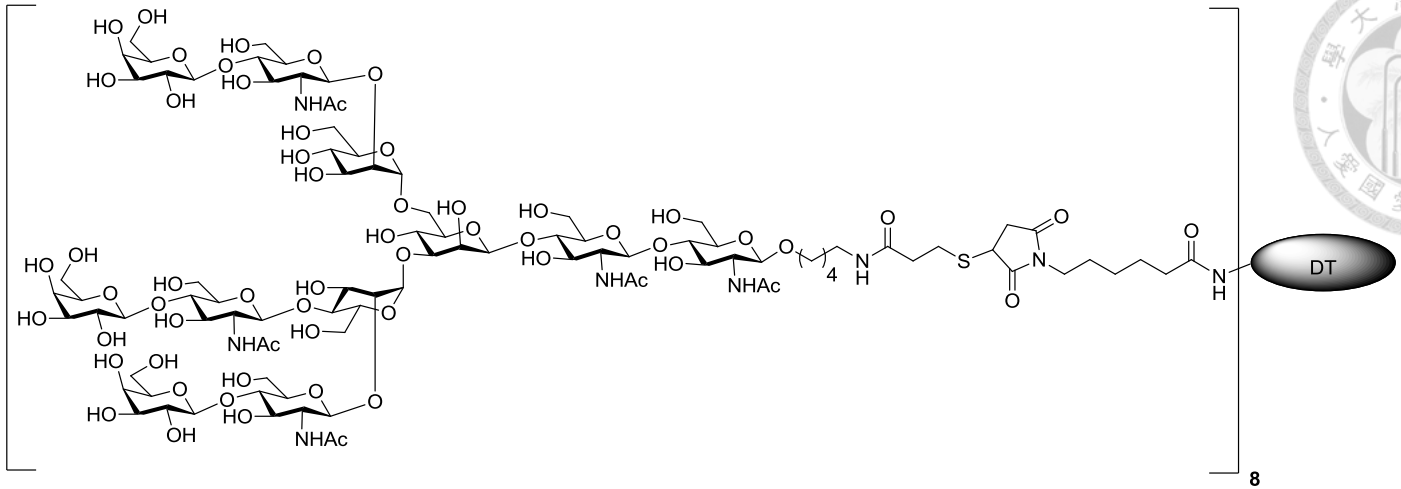

Glycoconjugate 3

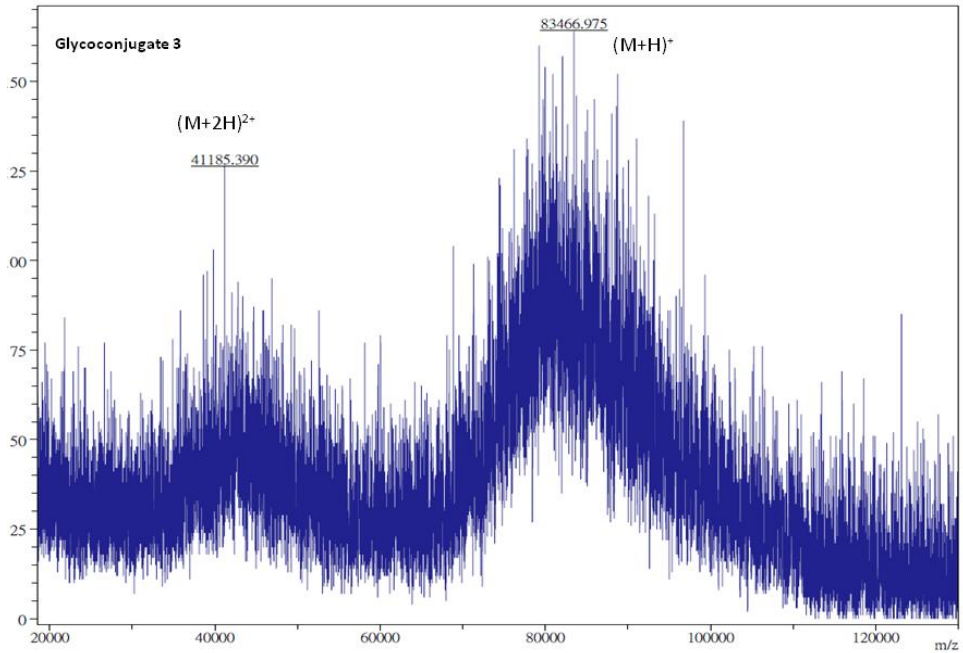

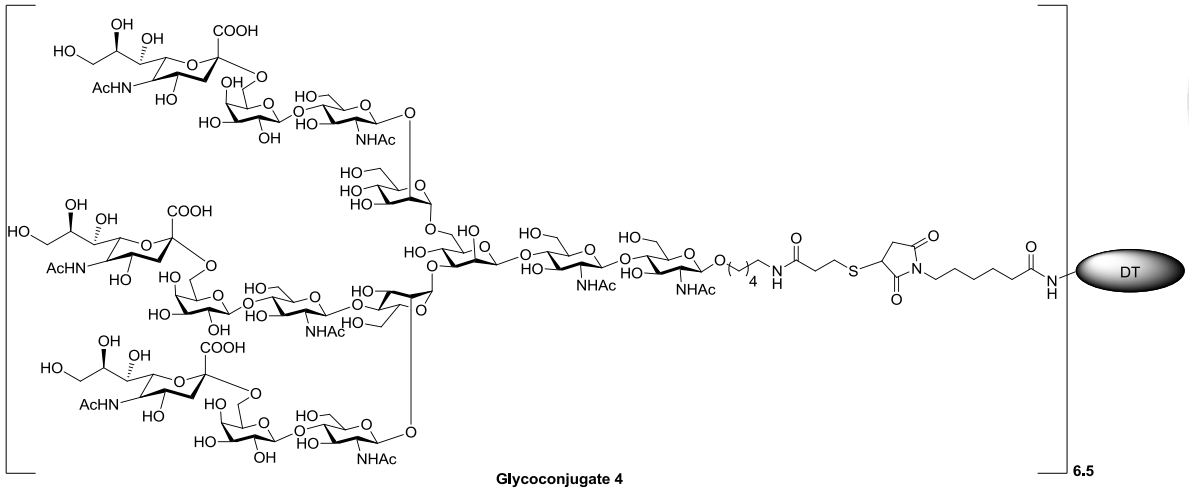

Glycoconjugate 4

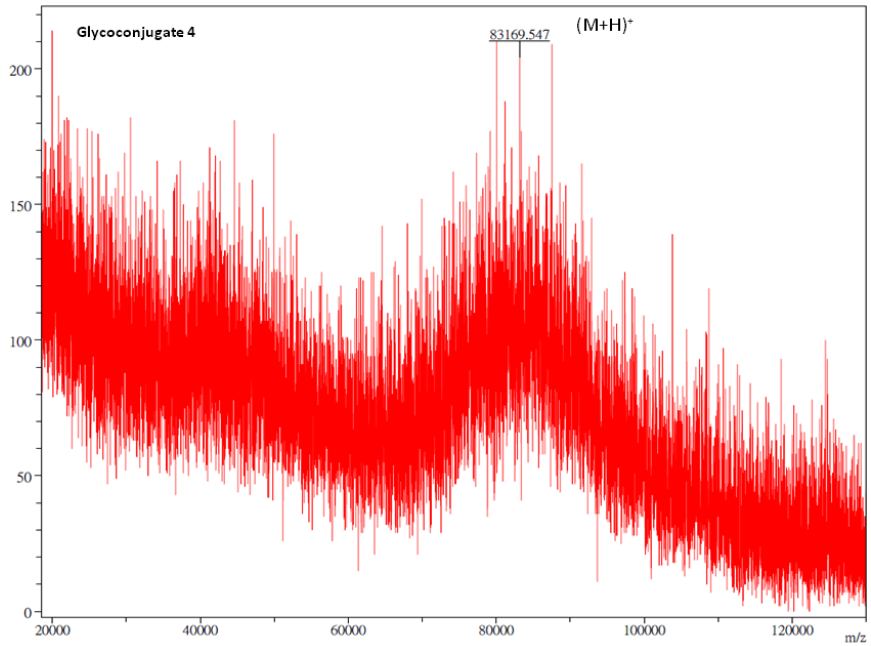

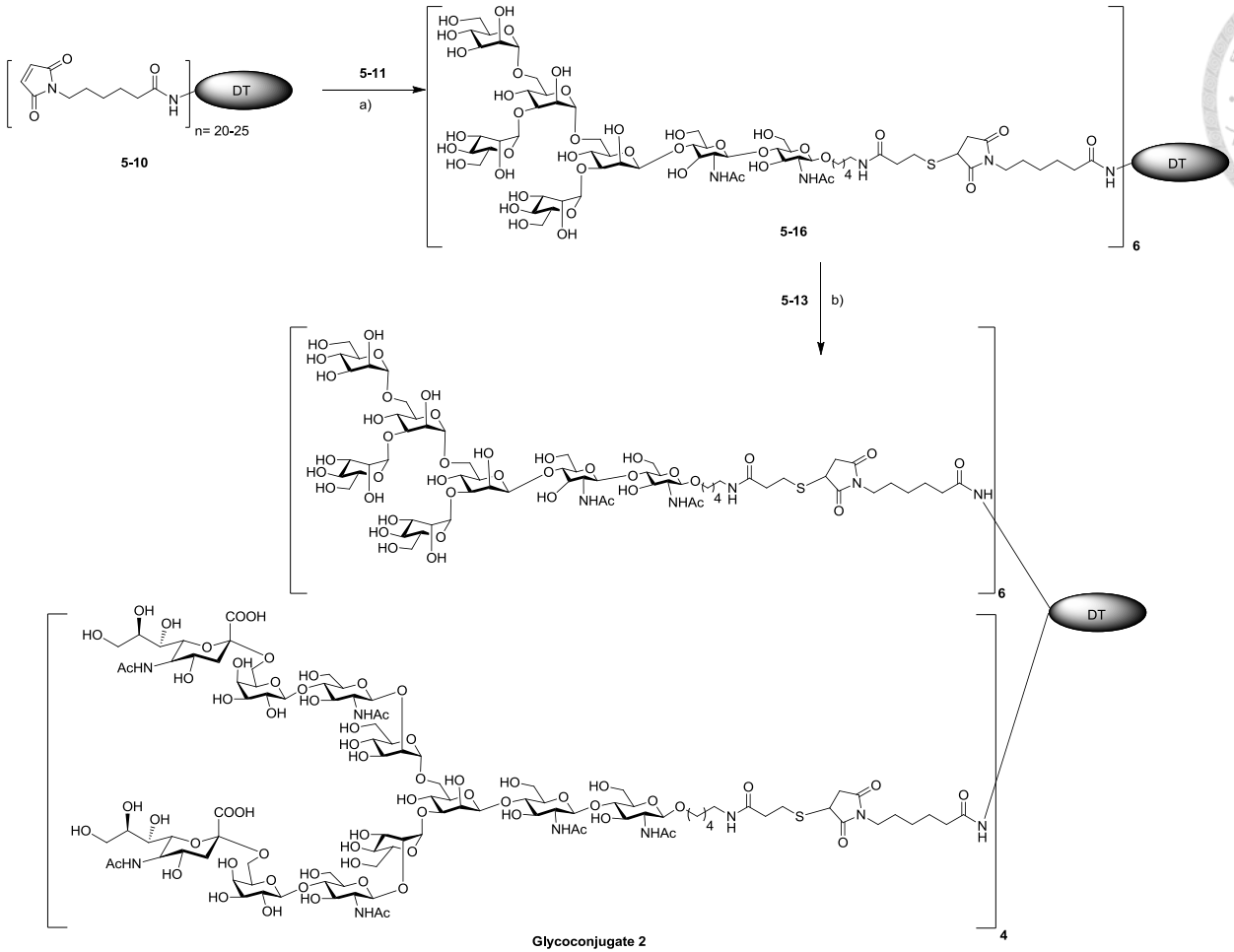
DT
n= 20-25
5-10
5-11
a)
5-16
6
5-13
b)
6
DT
4
Glycoconjugate 2

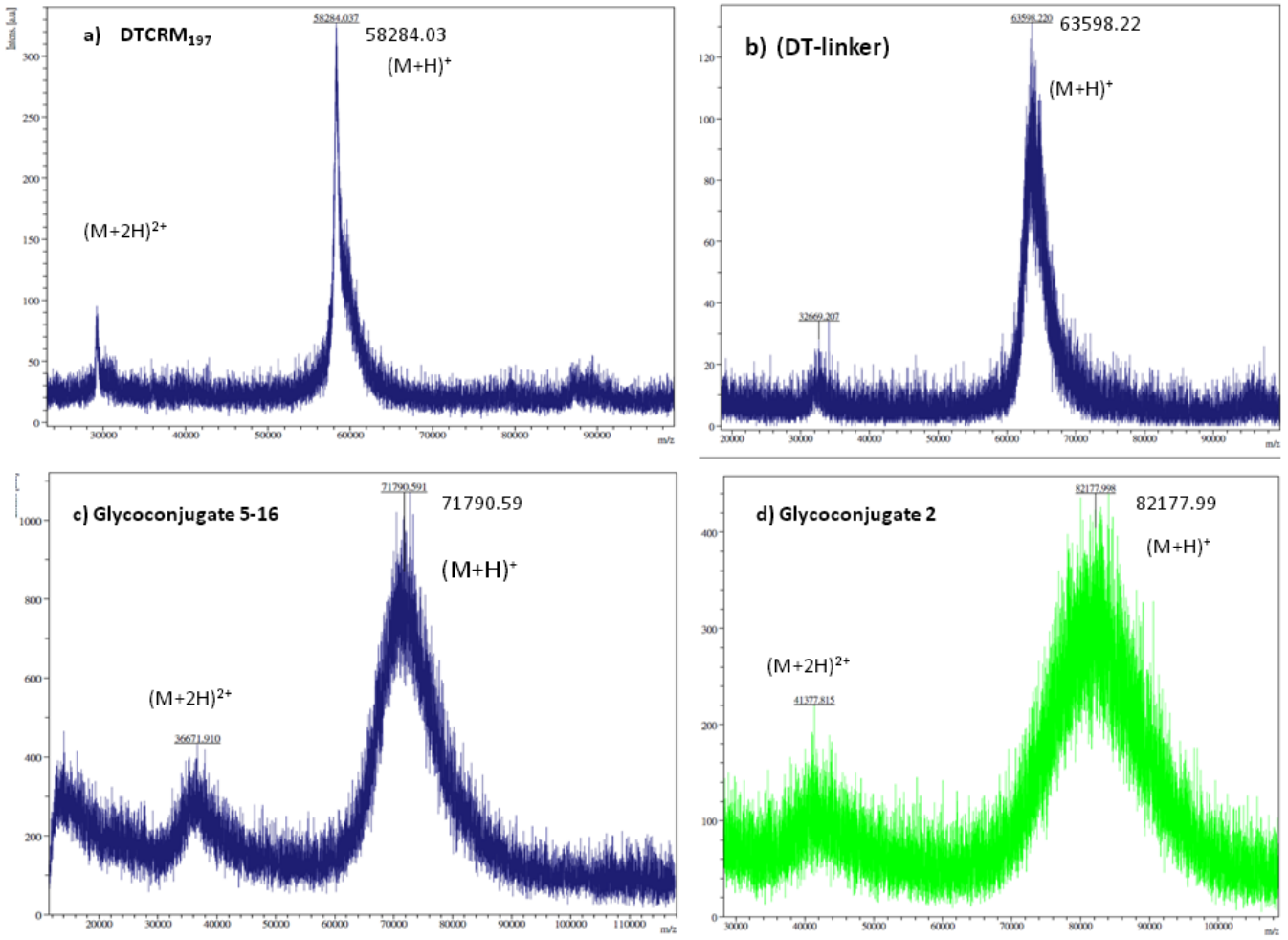
a) DTCRM197
58284.037
58284.03
(M+H)+
(M+2H)2+
b) (DT-linker)
63598.220
63598.22
(M+H)+
32669.207
c) Glycoconjugate 5-16
71790.591
71790.59
(M+H)+
(M+2H)2+
36671.910
d) Glycoconjugate 2
82177.998
82177.99
(M+H)+
(M+2H)2+
41377.815

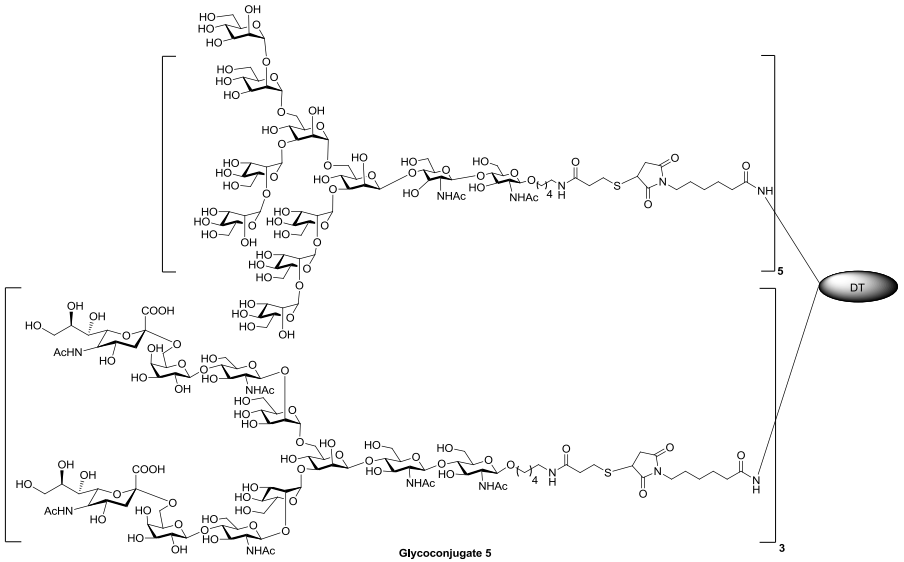

Glycoconjugate 5